



Mummy Portraits of Roman Egypt

Volume 2

Emerging
Research
from
the APPEAR
Project



Edited by
Marie Svoboda
and
Caroline R. Cartwright

Mummy Portraits of Roman Egypt, Volume 2

Mummy Portraits of Roman Egypt, Volume 2: Emerging Research from the APPEAR Project

Edited by Marie Svoboda and Caroline R. Cartwright

J. PAUL GETTY MUSEUM, LOS ANGELES

This publication was created using Quire™, a multiformat publishing tool from Getty.

The free online edition of this open-access publication is available at getty.edu/publications/mummy-portraits-2/ and includes zoomable illustrations and graphs. Free PDF and EPUB downloads of the book are also available.

© 2026 J. Paul Getty Trust



The text of this work is licensed under a Creative Commons Attribution-NonCommercial 4.0 International License. All images are reproduced with the permission of the rights holders acknowledged in the captions and are expressly excluded from the CC BY-NC license covering the rest of this publication. These images may not be reproduced, copied, transmitted, or manipulated without consent from the owners, who reserve all rights. To view a copy of this license, visit <https://creativecommons.org/licenses/by-nc/4.0/>.

First edition 2026

Any revisions or corrections made to this publication after the first edition date will be listed here and in the project repository at <https://github.com/thegetty/mummy-portraits-2>, where a more detailed version history is available. The revisions branch of the project repository, when present, will show any changes currently under consideration but not yet published here.

Published by the J. Paul Getty Museum, Los Angeles

Getty Publications
1200 Getty Center Drive, Suite 500
Los Angeles, California 90049-1682
getty.edu/publications

Rachel Barth, *Project Editor*

Katrina Posner, Amanda Sparrow, Courtney Johnson Thomas, and Leslie Tilley,
Manuscript Editors

Greg Albers, *Digital Publications Manager*

Erin Cecele Dunigan, *Digital Project Lead*

Jenny Park, *Digital Production*

Alex Hallenbeck, *Digital Assistant*

Jeffrey Cohen, *Cover Design*

Victoria Gallina, *Production*

Danielle Brink, *Image and Rights Acquisition*

Distributed in the United States and Canada by
the University of Chicago Press

Distributed outside the United States and Canada by
Yale University Press, London

Library of Congress Cataloging-in-Publication Data

Names: APPEAR (Project), author. | Svoboda, Marie, editor. <https://id.oclc.org/worldcat/entity/E39PCjxBrwpcypqprDtxxJmWpd> | Cartwright, Caroline, editor. <https://id.oclc.org/worldcat/entity/E39PCjxVxPC6MTTKdB78BDyJRX> | J. Paul Getty Museum, issuing body.

Title: Mummy portraits of Roman Egypt, Volume 2: emerging research from the APPEAR Project / edited by Marie Svoboda and Caroline R. Cartwright.

Description: First edition. | Los Angeles : J. Paul Getty Museum, 2026. | Proceedings of a conference held at the Allard Pierson in Amsterdam in 2022. | Includes bibliographical references. | Summary: "Publishes the papers delivered at the 2022 APPEAR (Ancient Panel Paintings: Examination, Analysis, and Research) conference, which present research on and discoveries about ancient Romano-Egyptian funerary portraits preserved in international collections"—Provided by publisher.

Identifiers: LCCN 2025018648 | ISBN 9781606069967 (paperback) | ISBN 9781606069998 (epub) | ISBN 9781606069981 (adobe pdf) | ISBN 9781606069974

Subjects: LCSH: Mummy portraits—Expertising—Congresses. | Mummy portraits—Egypt—Congresses. | Portraits, Roman—Egypt—Congresses. | Portraits, Egyptian—Congresses. | Egypt—Antiquities, Roman—Congresses. | LCGFT: Conference papers and proceedings.

Classification: LCC ND1327.E3 A673 2026 | DDC 757.0932/09015—dc23/eng/20250619

LC record available at <https://lccn.loc.gov/2025018648>

Front cover: Mummy portrait of a man, Greek/Roman/Egyptian, second century CE (detail, fig. 13.6)

Illustration Credits

Every effort has been made to contact the owners and photographers of illustrations reproduced here whose names do not appear in the captions. Anyone having further information concerning copyright holders is asked to contact Getty Publications so this information can be included in future printings.

All papers collected in this work were peer reviewed through a single-masked process in which the reviewers remained anonymous.

Authorized Product Safety Representative in the European Union: Easy Access System Europe, Mustamäe tee 50, 10621 Tallinn, Estonia, gpsr.requests@easproject.com

Contents

Foreword — <i>Timothy Potts</i>	viii
Introduction — <i>Marie Svoboda and Caroline R. Cartwright</i>	1
1. The Histories They Hold: On Making Mummy Portraits Matter — <i>Jan M. van Daal</i>	5
2. Roman-Egyptian Mummy Portraits and Panels of Gods from the Louvre: Renewed Historical and Material Knowledge — <i>Lucile Brunel-Duverger, Caroline Thomas, Anne-Solenn Le Hô, Michel Menu, Christine Andraud, Maria Victoria Asensi Amorós, Thomas Calligaro, Anne Michelin, Raphaël Moreau, Laurent Pichon, and Aurélie Tournié</i>	15
3. Three Romano-Egyptian Panel Paintings in the Ny Carlsberg Glyptotek — <i>Jens Stenger, Cecilie Brøns, Richard Newman, and Caroline R. Cartwright</i>	28
4. Between the Linen and the Overpaint: Understanding the Materials and Techniques Used on Two Romano-Egyptian Funerary Portrait Shrouds — <i>William J. Mastandrea, Kate Clive-Powell, Evelyn (Eve) Mayberger, Richard Newman, Lawrence M. Berman, and Daniel P. Kirby</i>	39
5. Non-Invasive Investigations on Three Ancient Mummy Portraits at the National Archaeological Museum in Athens: Challenges and Benefits — <i>Peppy Tsakri and Ioannis Panagakos</i>	51
6. Learning from Lemons: Mummy Portrait Forgeries in the Menil Collection — <i>Corina E. Rogge and Caroline R. Cartwright</i>	62
7. Mummy Portraits and Painted Panels from Roman Egypt: Seeing the Wood for the Trees — <i>Caroline R. Cartwright</i>	73

8. Egg on Their Faces: Investigation of an Unusual Surface Coating Observed on Egyptian Funerary Portraits — <i>Marie Svoboda, Daniel P. Kirby, Joy Mazurek, Lin Rosa Spaabæk, and John Southon</i>	82
9. Insights from a Collaborative Study of Beeswax Paint from Romano-Egyptian Mummy Portraits — <i>Joy Mazurek and Lin Rosa Spaabæk</i>	93
10. Calculated Viewing Angles in the Presentation of Romano-Egyptian Mummy Portraits — <i>Jevon Thistlewood</i>	99
11. The Saint Louis Painter's Artistic Circle — <i>Branko F. van Oppen de Ruiter</i>	105
12. Exploring Artistic Practice in Roman Egypt: A Study of Nine Portraits at The Metropolitan Museum of Art — <i>Dorothy Mahon, Silvia A. Centeno, Marsha Hill, Charlotte Hale, Louisa Smieska, Clara Granzotto, Julie Arslanoglu, and Anna Serotta</i>	122
13. <i>Umbras dividendas ab lumine</i> : Pigments, Their Mixtures, and Distribution on Mummy Portraits in Relation to Primary Sources — <i>Giovanni Verri, Marc Vermeulen, Alicia McGeachy, Ken Sutherland, Clara Granzotto, Federica Pozzi, Rachel Sabino, Laura A. D'Alessandro, Alison Whyte, and Marc Walton</i>	139
14. Insights into the Materials and Technique of a Roman Egyptian Funerary Portrait Obtained from Elemental Mapping and Luminescence Imaging — <i>Stephanie Spence and John Twilley</i>	153
15. Linked Histories: Understanding the Making and Remaking of a Roman Egyptian Portrait at the Detroit Institute of Arts Through Comparison to a Funerary Portrait at the Walters Art Museum, Baltimore — <i>Christina Bisulca, Ellen Hanspach-Bernal, and Aaron Steele</i>	162
16. Mummy Portrait of a Boy from the National Museum in Warsaw: Investigation of Its History and Technology — <i>Agnieszka Kijowska, Aleksandra Sulikowska-Belczowska, Magdalena Wróbel-Szypula, Barbara Wagner, and Justyna Kwiatkowska</i>	172
17. Funerary Portraits from Roman Egypt: Facing Forward—An Exhibition and Inter-Institutional Collaboration Looking for the Artists of Ancient Philadelphia — <i>Kate Smith, Susanne Ebbinghaus, Katherine Eremin, Georgina Rayner, Jen Thum, Courtney Books, Richard Hark, Irma Passeri, and Marcie Wiggins</i>	182
Glossary	193
Bibliography	203
APPEAR Participants	225

Contributors	227
Acknowledgments — <i>Marie Svoboda and Caroline R. Cartwright</i>	238

Foreword

In 2013 the Getty Museum initiated Ancient Panel Painting: Examination, Analysis, and Research (APPEAR) as an international collaborative project to collect technical information on ancient panel paintings, specifically funerary mummy portraits produced in Egypt during the Roman era, as a platform for comparative research and conservation of this important archaeological and art historical corpus. Through the participation of museums around the world, APPEAR has shed much light on the sourcing, materiality, and function of ancient Egyptian panel painting production, and it will continue to advance this research as more works are analyzed and documented on this platform. Already the project has done much to elucidate how the ancient artists worked and the pivotal contributions they made to the development of panel painting over the following millennium. In these portraits we see how people lived, worked, worshipped, and died in ancient Egypt, providing fascinating insights into one of the most dynamic periods of artistic cross-fertilization in antiquity.

APPEAR began as a study of the sixteen Romano-Egyptian panel paintings in the Getty Museum's collection. Through the participation of institutions and colleagues around the world, it has since grown to encompass a third of the known panel paintings—currently residing in more than sixty museums and collections. The opportunity to study such a large body of material dating from the first through third centuries CE, reflecting a wide diversity of religious, cultural, artistic, and funerary traditions, is unique.

There is still much to discover, and further progress will depend on continuing collaboration between museums and scholars via a participant-led database. The dissemination of this information is facilitated by Getty's support of the database, as well as conferences and publications.

With this publication, we are delighted to make available online and by print-on-demand the proceedings of the second APPEAR conference, held in 2022, *Mummy Portraits of Roman Egypt, Volume 2: Emerging Research from the APPEAR Project*. The papers in this publication and in the first volume, from the first conference in 2020 (<https://www.getty.edu/publications/mummyportraits/>), together with numerous exhibitions and technical and interpretive investigations that have evolved from the APPEAR project, are a tribute to the growing interest in cross-cultural research on the

peoples and cultures of the ancient Mediterranean and beyond. Finally, thanks for initiating and stewarding this project, along with its many dedicated collaborators, are due to Marie Svoboda, conservator of antiquities at the Getty Villa.

Timothy Potts
Maria Hummer-Tuttle and Robert Tuttle Director
J. Paul Getty Museum

Introduction

Marie Svoboda
Caroline R. Cartwright

Launched in 2013 by the Getty, the Ancient Panel Painting, Examination, Analysis, and Research (APPEAR) project is a collaborative platform that allows participating institutions to study ancient funerary panel painting from Roman Egypt. From the onset, APPEAR has sought to increase our understanding of the materials and techniques employed in the production of artifacts with the best-preserved evidence of ancient painting. The project is made possible through the collaboration and support of more than sixty partner institutions. Their valuable contributions include information obtained from visible and technical examinations and scientific analyses; this data, along with historic archives of the artworks from their collections, are stored in a shared database. The consolidated information allows for comparison and enables the discovery of trends, unique features, and working methodologies, shedding light on artistic practice, material sourcing, and function. The data contributed by collaborators offer a unique window into our understanding of painted works in antiquity and their important influence in future artistic endeavors.

This current volume—the proceedings from the 2022 APPEAR conference, held at the Allard Pierson in Amsterdam—presents the results of nine years of international partnerships and complements the first published volume: *Mummy Portraits of Roman Egypt: Emerging Research from the APPEAR Project*. Over a three-day period, the Allard Pierson and Getty hosted more than one hundred attendees from around the world, representing nine countries and twenty-six institutions. Seventeen speakers and a keynote address covered the

latest research on the history, provenance, materials, methods, imaging, and analyses inspired by the APPEAR project. Speakers and attendees contributed expertise in art conservation, science, Egyptology, classics, art history, or simply a passion for the subject.



The APPEAR conference was launched with a keynote lecture that reviewed the status of the field. Heavily illustrated and with new discoveries that impact the broader technical study of antiquities, “Ancient Relationships: Bridging Mummy Portraiture to Its Past and Future” (not reproduced here) addressed the intersections of artistic production and meaning. Bringing recent investigations to light by exploring the complex production, function, and history of Romano-Egyptian painted funerary portraits, the lecture by Giovanni Verri set the stage for the broad range of topics that followed.

We must not underestimate the pivotal importance of the stories these funerary panel paintings tell. “The Histories They Hold: On Making Mummy Portraits Matter” presents an overview of mummy-portrait studies, examined through a series of questions that have inspired and engaged scholars for over a century. Beginning with the analytical investigation of four mummy portraits in the Allard Pierson collection, this chapter then takes a cross-disciplinary approach that examines alchemical meaning and nineteenth-century principles of exploration and connoisseurship.

Bridging the gap between historical and material information is “Roman-Egyptian Mummy Portraits and

Panels of Gods from the Louvre: Renewed Historical and Material Knowledge.” Here the in-depth investigation of thirty-one mummy portraits and two panel paintings of gods in the Musée du Louvre collection, in collaboration with the Centre de Recherche et de Restauration des Musées de France, allows for a renewed understanding of this group. Using both the existing historical data and the latest developments in non-invasive and non-destructive material analyses, the authors explore the works’ artistic production; the chapter discusses the deliberate use of pigments to represent garments, flesh, and backgrounds and how they relate to iconography, style, and media.

Another interdisciplinary survey conducts a technical analysis of three rare funerary panel paintings and examines their function. “Three Romano-Egyptian Panel Paintings in the Ny Carlsberg Glyptotek” explores a rare but intriguing group of funerary panel paintings with a very different role than that of the portraits secured to mummified remains. This specific group portrays different subjects (gods and goddesses) and possibly served a purpose as cultic works for display in temples or domestic settings. Technical and scientific analysis deepens the understanding of their production, allowing for comparison within the larger corpus of funerary panel paintings and providing a unique and broader insight into the materials and techniques employed during the Roman period in Egypt.

Two papers explore thoughtful studies of funerary portraits painted on panels and textile shrouds. The first, “Between the Linen and the Overpaint: Understanding the Materials and Techniques Used on Two Romano-Egyptian Funerary Portrait Shrouds,” takes an interdepartmental look at two linen mummy shrouds at the Museum of Fine Arts, Boston. The study of these unique funerary paintings, which have never been systematically examined, aims to fill a gap in technical and art history research. As a unique investigation, this scholarship lays the groundwork for future comparative studies of funerary shrouds from the so-called Soter group.

The second, “Non-Invasive Investigations on Three Ancient Mummy Portraits at the National Archaeological Museum in Athens: Challenges and Benefits,” focuses on the non-invasive findings of three portraits of similar manufacture and style; the authors’ approach during the challenging period of COVID 19 is a model for any institution without technical resources. The research conducted not only shows what cultural heritage conservation professions can achieve during less-than-ideal circumstances but also demonstrates a successful research model that can be reproduced in similar variable and rich collections.

The connoisseurship of mummy portraits is the focus in “Learning from Lemons: Mummy Portrait Forgeries in the Menil Collection.” Acknowledging that demand often outweighs supply, the authors address how forgers sometimes found creative ways to deliver the sought-after mummy portraits that were in fashion during the nineteenth century. An existing knowledge of mummy portrait material and manufacture lays the foundation for forgery detection. The prime message in this special paper is how important it is to combine scientific analyses and collection history with comparative study. Once a neglected topic—works of dubious origin were often ignored and stored in museum basements—the issue of forgeries is important not only to the APPEAR database but also to the greater study of ancient works.

Four essays continue research from the 2020 publication. A significant study identifies the woods used as the primary support for panel paintings. “Mummy Portraits and Painted Panels from Roman Egypt: Seeing the Wood for the Trees” is the culminating summary of wooden panels, conducted through the complex and precise scientific identification of wood species. This scientific research has afforded a comprehensive data set of the underlying processes involved in woods selection. The interpretation of data collected is not only valuable in understanding what woods were used for panel painting in antiquity; it also speaks to access, sourcing, production, recycling, and how ancient artists truly understood the quality and benefits of a material that was not readily available in ancient Egypt. Access to and samples of wooden panels provided by APPEAR participants—and the reliable and consistent scientific approach to their identification—has led to valuable insight into our understanding of ancient wood selection and trade.

Both scientific analysis and forensic methodologies have seen major developments in the detection and interpretation of complex materials used to create ancient paintings. These advancements are a direct result of more sensitive analytical instrumentation requiring little or even no sampling to obtain results, or of keen observation. Peptide mass fingerprinting, carbon-14 dating, and gas chromatography/mass spectrometry are sensitive microsampling techniques for organic analysis. Two papers follow up on the analyses of organic materials used on panel paintings from diverse collections; both essays take a deeper dive into the very complex topic of organic material identification.

“Egg on Their Faces: Investigation of an Unusual Surface Coating Observed on Egyptian Funerary Portraits” calls attention to a unique fluorescence captured with

ultraviolet radiation on painted panels. This feature led the essay's authors to identify a similar coating on six paintings; radiocarbon dating confirmed that two had their coatings applied during the time of manufacture. This finding allows for a better understanding of the function of surface coatings. It also opens the possibility for further discovery on other panels through diagnostic observation. "Insights from a Collaborative Study of Beeswax Paint from Romano-Egyptian Mummy Portraits" addresses the ongoing investigation of binding media, taking a closer look at the ancient beeswax identified on eight panel paintings from the Ny Carlsberg Glyptotek and National Museum of Denmark. The relationship of lead-based pigments and their interaction with beeswax to produce lead soaps is explored and raises the question of whether modified wax media are the result of intentional influences—i.e., "Punic wax"—as was previously believed, or the result of pigment interaction over time. This little-understood process illustrates how certain pigments can affect paint chemistry and encourages further discussion and debate.

"Calculated Viewing Angles in the Presentation of Romano-Egyptian Mummy Portraits" looks at how portraits were designed/laid out and intended to be viewed. Here, the author takes an extended look into how artists worked when painting funerary mummy portraits from human faces. After reviewing more than two hundred portraits within the APPEAR database, the author finds many considerations (proportion, angle, intention) that affected an artist's approach to produce a portrait balanced with the intended funerary context.

A goal of the APPEAR project has always been use of the database as a source for exploring viable artist workshops. Recognition of visually comparable groups, corroboration of data, and access to the APPEAR institutional network have shed light on how artists worked, revealing comparable groupings of portraits. "The Saint Louis Painter's Artistic Circle" presents a distinct collection of portraits that are housed in several museums yet exhibit similar technical, stylistic, and design features. These observations possibly support production in a workshop or even the hand of one artist. Such evident clues and the systematic approach to looking at painted portraits will no doubt lead to the identification of other groupings and provide a better understanding of ancient artist workshops.

A similar, though more technical, approach is undertaken in "Exploring Artistic Practice in Roman Egypt: A Study of Nine Portraits at The Metropolitan Museum of Art." This essay examines nine funerary portraits, most of which first

entered The Metropolitan Museum of Art's collection before the twentieth century. The study breaks down the various unique techniques used in their production, revealing hidden features within the Met's collection. This in-depth investigation has offered valuable clues about artistic practice and methodologies, visualized through technical imaging, non-invasive analyses, and comparison.

"Umbras dividendas ab lumine: Pigments, Their Mixtures, and Distribution on Mummy Portraits in Relation to Primary Sources" explores seven funerary portraits from three Chicago collections—the Art Institute, Institute for the Study of Ancient Cultures, and Field Museum—and from a private collection, the majority of which have never been systematically studied. The authors carried out the technical investigation of these painted panels through various analytical approaches that focused on the distribution and stratigraphy of paint materials. Comparing the methodologies of this group with data within the APPEAR project and using keen observation, the authors found new information on the complex nature of producing flesh tones. The interpretation of these obtained data benefits the ongoing corpus of existing scholarship.

Unique to this publication is the implementation of specialized analytical methodology in the study of ancient panel paintings. Bridging visual techniques is a non-destructive analytical tool that has immensely improved our understanding of materials, by producing elemental maps, effectively illustrated in the Met's study as well as in the in-depth investigation of one portrait in the Nelson Atkins Museum of Art. "Insights into the Materials and Technique of a Roman Egyptian Funerary Portrait Obtained from Elemental Mapping and Luminescence Imaging" addresses a portrait with an Antinoöpolis provenience in the Nelson Atkins collection. Material characterization and imaging techniques aid in the identification of Egyptian blue by revealing its use as an underdrawing or when combined with other pigments to alter shades and color. Additionally, these methodologies can help shed light on the alteration of pigments as a result of unique environmental conditions.

Another intimate examination of a single portrait, with parallels to the study of the Nelson Atkins work, is presented in "Linked Histories: Understanding the Making and Remaking of a Roman Egyptian Portrait at the Detroit Institute of Arts Through Comparison to a Funerary Portrait at the Walters Art Museum, Baltimore." All three mummy portraits, suspected to come from Antinoöpolis, feature the addition of gilded jewelry painted in raised relief. The technical examination of the portrait at the

Detroit Institute of Art relays a journey through the various contexts of this portrait, including its collection history, material identification, direct comparison with the Walters Art Museum portrait, and post-antique treatment.

The conservation of a mummy portrait with a complex provenance and treatment history is the focus of “Mummy Portrait of a Boy from the National Museum in Warsaw: Investigation of Its History and Technology.” Recognized for its compelling rendering of a young boy and the unique addition of a rearing horse on the sitter’s proper-right shoulder, the once heavily damaged portrait was restored with the addition of a fragment from a similar ancient portrait and overpainted to disguise the invasive repair. An in-depth historical and technical study to better understand the authenticity, origin, and condition of the various fragments helped guide this work’s de-restoration. This chapter addresses collecting history and practices, restoration approaches at the turn of the nineteenth and twentieth centuries, and the challenging treatment choices made in preparation for the panel’s display in the ancient art gallery of the National Museum in Warsaw.

Outreach via exhibitions, lectures, and publications has grown extensively in recent years—mostly due to the interest and appeal among scholars for the study of ancient mummy portraits and the issues surrounding the ethical and intelligent display of this material to the public. This work is summarized in “Funerary Portraits from Roman Egypt: Facing Forward—An Exhibition and Inter-Institutional Collaboration Looking for the Artists of Ancient Philadelphia,” which describes how a curated exhibition at the Harvard Art Museums thoughtfully addressed the various issues surrounding the study of funerary portraits. The exhibition involved a large team of collaborators bringing together for the first time portraits that share common traits (possibly linking them to a

common workshop). In addition to raising important questions about production, ancient practices, and visual connoisseurship, and presenting the main perspectives surrounding the presentation of funerary portraits, the exhibition was a catalyst for public lectures and outreach around the practice, study, and appreciation of mummy portraits from Roman Egypt.

Similarly, an exhibition (2023/24) at the Allard Pierson—*Face to Face, the People Behind Mummy Portraits*—featured thirty-eight portraits with the aim of exploring the artists, descendants, followers, collectors, archaeologists, and researchers connected to these works. Meant to coincide with the APPEAR conference hosted by the Allard Pierson but delayed due to COVID, this exhibition brought together a complementary group of portraits, highlighting artistic similarities and their relationship to modern culture. The technical study of twelve portraits, never previously examined, carried out by the Netherlands Institute for Conservation + Art + Science (NICAS) has further contributed to the growing database and increased our understanding of these significant and engaging ancient artworks.

Independent research and multiple resources give direction for the development of new tools and technologies in the study of ancient materials. These resources, mainly borrowed from other disciplines, are constantly evolving; they are now more accessible than ever and require simpler methodologies and equipment. This volume’s editors hope that the momentum behind the APPEAR project endures and that future collaborations occur, so that all of us—scholars, conservators, scientists, and the public—can better understand the artist’s mind, and so museums, united to benefit from collective knowledge, can create new avenues for sharing and disseminating information.

The Histories They Hold: On Making Mummy Portraits Matter

Jan M. van Daal

In *Love's Jewelled Fetter* (1895), the Dutch painter Sir Lawrence Alma-Tadema situated an ancient Mediterranean romantic fantasy against a backdrop of a cerulean sea and a cool marble interior where a lover's portrait hangs—unmistakably modeled on a funerary portrait from Roman Egypt.¹ The 1896 exhibition poster for antiquities dealer Theodor Graf's collection of Romano-Egyptian mummy portraits presents them as "ancient Greek" portraits. The poster's iconography stages these portraits between orientalizing motifs and a toolkit typical for Western European old master painters: a palette, maulstick, and a set of brushes.² In the early twentieth century, German expressionist painter Paula Modersohn-Becker emulated the technique and composition of mummy portraits to paint a series of self-portraits. Modersohn-Becker had studied mummy portraits at the Louvre and through reproductions, two of which survive as part of her estate.³

These are three early examples of people inspired by mummy portraits who used them to tell stories and to paint pictures.⁴ The inspirational effect of mummy portraits has not waned since. With a thousand-odd portraits and fragments surviving worldwide, the corpus is not vast; yet since the late nineteenth century, researchers have continued to investigate how mummy portraits were made and to endeavor to better understand their state of preservation. The APPEAR project has proven to be a catalyst for this type of material-technical research in the

last decade. The conferences sparked a variety of new research directions, and the database makes it possible for collaborators to share and compare the results of their research.

Identifying a pigment or binding medium can tell us more than just what the ancient painter had on their palette; it embeds mummy portraits in histories of trade, art technology, and artistic choices. This paper advocates the use of the Morellian method as a structuring tool in composing such histories. This method consists of a structured analysis of isolated details in an artwork to draw conclusions about its making. The method emerged in the late nineteenth century from the work of the Italian art connoisseur Giovanni Morelli as a scientifically informed process for attributing paintings to schools, workshops, and individual artists. This paper, however, argues for extending the Morellian method beyond attribution and authentication, the typical purviews of connoisseurship. It aims to demonstrate the value of the method as a conceptual tool in mummy portrait studies and as a means to facilitate composing histories along the lines of material-technical findings.

The storytelling potential of technical examination shines most brightly when illuminated by a case study. Hence, the technical examination of four mummy portraits from the Allard Pierson collection in Amsterdam forms the stage on

which this paper presents a Morellian, story-based approach to mummy portrait studies. This case study commences with an introduction to the research project and the portraits. Two vignettes of themes follow—ones that emerged from compiling the research results in the light of a Morellian gaze—the choices of materials and their meanings, and conservation-restoration interventions as the physical evidence of these portraits' second lives as part of collections. First, however, the next section looks more closely at the Morellian method and its adaptation for this research project.

MORELLI AND MUMMIES?

Long after Alma-Tadema and Modersohn-Becker, passionate twenty-first-century researchers continue to tell stories about mummy portraits. Expertise and creativity still abound among those researchers, but modern analytical techniques have paved the way to compose studies to investigate mummy portraits using a palette that is virtually boundless. Macro X-ray fluorescence (MA-XRF) spectroscopy mapping detects the distribution of elements in mummy portraits. Gas chromatography/mass spectrometry (GC/MS) can identify binding media in sampled areas. Infrared reflectography and X-radiography can penetrate paint layers in the quest for underdrawings and modern additions.

Those familiar with the work of the Italian art connoisseur Giovanni Morelli may also associate his name with images. Diagrams of hands and ears have become nearly synonymous with the Morellian method. In the late nineteenth century, Morelli developed a method to structurally analyze habitually depicted details in a painting.⁵ Morelli's purviews were those of the traditional connoisseur: attribution and authentication. His method served to provide a more solid ground for identifying the hand of a painter or workshop.

Jaynie Anderson, Morelli's biographer, captures the essence of his method as "focusing on highly characteristic details of all kinds which he considered of high value for an artist."⁶ Hands and ears were favorite case studies of "high-value" details for Morelli. His works contain anatomical diagrams of hands and ears, and publications that discuss Morelli often refer to those diagrams. However, although they are essential, anatomical diagrams should not be equated with the Morellian method; Morelli advocated drawing conclusions through object-based examination that takes into account anatomical details, materials, and conservation history.⁷

Morelli did not study mummy portraits, but his approach has the potential to utilize the material-technical data of emerging mummy portrait research to their fullest potential. As van Oppen de Ruiter has published in this volume, the attribution of mummy portraits requires careful consideration of their cultural-historical, stylistic, and material-technical features. In this light, it bears repeating that this paper does not discuss the Morellian method as an aid to authenticating and attributing mummy portraits. Rather, it aims to illustrate how viewing mummy portraits with a Morellian gaze enriches their histories—histories that contribute to a better understanding of the meanings behind ancient painters' choices of specific materials and techniques.

Looking at mummy portraits in a Morellian fashion begins with identifying high-value details in the material-technical data acquired during a mummy portrait examination. Here, the high-value details are those that have a strong storytelling potential, going beyond diagnostic criteria for attributions. Within this study, they are the materials that can be connected to documentary sources: those the ancient painter used, in specific locations; those that are relatively uncommon either in the portrait under investigation or in the broader mummy portrait corpus; and those that reveal more about a mummy portrait's post-acquisition afterlife. Discussing mummy portraits along the lines of single, evocative materials contributes to the understanding of how they were made in ancient Egypt and how they were treated after discovery and helps us understand why certain choices were made.

Some analytical methods frequently used within APPEAR diverge in the answers that they provide; others overlap. A specific question like the nature of a binding medium requires use of a specialized technique to obtain a result, and this illustrates the approach taken in the case study this paper describes. However, it is important to emphasize that any of the analytical techniques used within APPEAR hold the potential to aid in shedding new light on the study of ancient painting. While many analytical results in this paper rely on spectroscopic techniques, such advanced analytical methods are sometimes unavailable for cultural heritage institutions due to lack of access to equipment, required expertise, or funds. Fortunately, preliminary characterization of materials can be achieved through more accessible methods, such as technical imaging. Magnified images captured with a digital microscope are equally indispensable. In addition, in their contributions to this volume, Thistlewood and van Oppen de Ruiter show the analytical power of diagrams produced after careful observation. The methodological possibilities available in

the material-technical analysis of mummy portraits resonate with the many high-value details that Morelli used to compose art histories of Renaissance paintings.

In addition to being an art historian, Morelli was a storyteller, and that is what makes his approach so attractive for mummy portrait studies. The archaeological context of most mummy portraits is irrevocably lost, so their history must be pieced together through small clues. Morelli's structural, detail-oriented way of looking facilitates asking pertinent questions that enable mummy portraits to reveal their own histories. Morelli chose to tell stories of attribution, but he approached it as someone who was at once politician and patriot, scientist and socialite.⁸

EXAMINING FOUR MUMMY PORTRAITS FROM THE ALLARD PIERSON COLLECTION

In June 2018 and in the spring of 2019, four mummy portraits from the Allard Pierson collection were the subject of a technical examination campaign: a portrait of a young girl (fig. 1.1), referred to hereafter as "the Girl";⁹ a piece of the portrait of an older lady (fig. 1.2), hereafter "the Fragment"; a portrait of a young lady (fig. 1.3), hereafter "the Lady"; and a portrait of a bearded man (fig. 1.4), hereafter "the Man."



Figure 1.1 Romano-Egyptian funerary portrait of a young girl with a gold wreath in her hair, wearing a red tunic (the Girl). Allard Pierson, University of Amsterdam, APM00724. Photo: Jan van Daal



Figure 1.2 Fragmentary Romano-Egyptian funerary portrait of a lady with gray hair wearing a pink tunic (the Fragment). Allard Pierson, University of Amsterdam, APM08654. Photo: Jan van Daal



Figure 1.3 Romano-Egyptian funerary portrait of a young lady wearing a pink tunic (the Lady). Allard Pierson, University of Amsterdam, APM14232. Photo: Jan van Daal

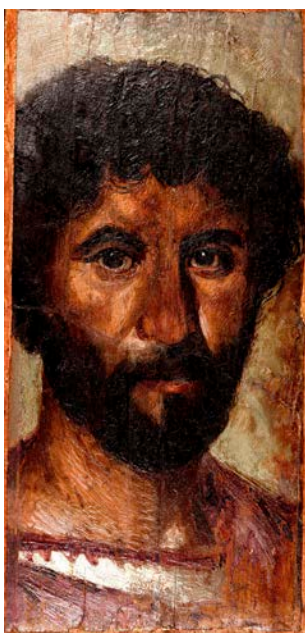


Figure 1.4 Romano-Egyptian funerary portrait of a bearded man wearing a purple cloak (the Man). Allard Pierson, University of Amsterdam, APM14498. Photo: Jan van Daal

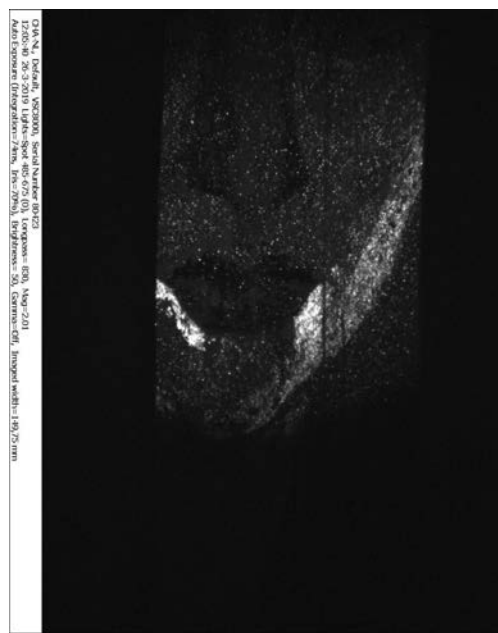


Figure 1.5 VIL image of the Fragment (lower half of the face). Allard Pierson, University of Amsterdam, APM08654. Photo: VIL image acquired by Luc Megens with the VSC8000 imaging system

Analyses of the portraits took place at the Rijksmuseum conservation laboratories in Amsterdam. None of the portraits had undergone technical examination before. The aim of this project was broad: to characterize the ancient painter's palette, to catalogue characteristic painterly techniques, and to understand historical conservation-restoration treatments.

The project employed a wide array of analytical and imaging techniques. Methods discussed in this paper are: digital microscopy; MA-XRF; photography using visible, infrared (IR), and ultraviolet (UV) radiation; visible-induced infrared luminescence (VIL); and X-ray diffraction spectroscopy (XRD).¹⁰

MATERIALS: CHOICES AND MEANING

In her study on the copper-based pigment Egyptian blue (cuprorivaite, $\text{CaCuSi}_4\text{O}_{10}$) used in mummy portraits, Gabrielle Thiboutot argues that the way ancient artists employed Egyptian blue reveals that they understood both the material and the symbolic properties the pigment affords.¹¹ Within the Allard Pierson group, only the Fragment (see fig. 1.2) exhibited a convincing match for Egyptian blue.¹² It showed up distinctly with VIL imaging (figs. 1.5–1.6). XRD analysis in an area where Egyptian blue's presence was expected confirmed those findings.¹³ Furthermore, MA-XRF yielded an elemental distribution



Figure 1.6 VIL image of the Fragment (forehead and hairline). Allard Pierson, University of Amsterdam, APM08654. Photo: VIL image acquired by Luc Megens with the VSC8000 imaging system

map for copper that corresponded with the VIL results, confirming the use of Egyptian blue in the Fragment.¹⁴

The copper map shows that Egyptian blue is present throughout the Fragment, yet blue is not visible as a

distinct color. The ancient painter used Egyptian blue in the gray hair, the entire neck area, and forehead. The MA-XRF copper map and VIL images also reveal Egyptian blue in the corners of the mouth and along the jawline. The chin and the lower forehead are devoid of Egyptian blue.

A female portrait in the collection of the Phoebe A. Hearst Museum shows a similar use of Egyptian blue in the contours of the face.¹⁵ Ganio et al. interpret the function of Egyptian blue here as either an underdrawing or a modulating pigment,¹⁶ and Verri et al. in this volume argue that the use of Egyptian blue as a modulating pigment is, in fact, a key facet of artisanal practice in many mummy portraits.

The Egyptian blue in the Fragment suggests that the painter strongly grasped the modulating properties of the pigment. Both the VIL images and the copper map clearly show how the painter also varied the quantity of Egyptian blue. The corners of the mouth and the foremost lock of hair received more of the pigment than the rest of the portrait. Egyptian blue here tells the story of a skilled painter who understood how to benefit from its optical properties in a mixture with other pigments and modified the mix to produce a stronger or weaker effect.

One particular pigment in the Allard Pierson group still retains some of its original brilliance: arsenic yellow. This yellow pigment was detected only on the Lady (see fig. 1.3). The MA-XRF map for arsenic (fig. 1.7) identifies arsenic in the tiny golden bar that connects the pearls of the earrings and in the green stones of the necklace. A heightened concentration of sulfur overlaps with the arsenic map. The pigment that was used to suggest gold and to produce green is likely the yellow arsenic sulfide, orpiment (As_2S_3) or pararealgar (As_4S_4). Arsenic sulfides are notoriously toxic and not native to Egypt.

Why did the painter of the Lady choose an arsenic yellow for specific areas of the portrait? The alchemical Leyden and Stockholm papyri may provide the answer to this question.¹⁷ Written in Greek and dating to around 300 CE, they contain a wealth of information on art technology in Roman Egypt in the form of short recipes.¹⁸ The papyri mention arsenic sulfides several times. Orpiment regularly appears in recipes related to imitating or working with gold. Moreover, the adjective “golden” accompanies both orpiment and realgar to describe their color.¹⁹ A recipe in the Leyden papyrus for “writing in gold” even lists orpiment as the single colorant for this “golden” ink.²⁰ The Stockholm papyrus also mentions orpiment as an ingredient mixed with dyes, such as high-quality Tyrian purple, sometimes referred to as “scarlet of Galatia.”²¹ (Galatia was a region in Anatolia adjacent to and



Figure 1.7 False-color MA-XRF map of the Lady showing the signals for As-K (red), Ti-K (green), and Pb-M (blue). Acquisition and processing of the MA-XRF maps by Erma Hermens, Annelies van Loon, Victor Gonzalez, and Francesca Gabrieli. Photo: False-color imaging by Jan van Daal

southwest of Pontus, where arsenic sulfides were mined intensively.)

The alchemical papyri present arsenic sulfides as materials associated with gold and imported materials. This supports the idea that arsenic sulfides carried symbolic value as prestigious materials in Roman Egypt. The visual impact of orpiment, in particular, affords a conspicuous presentation of this symbolic value.

The visual impact of the orpiment in the Lady's earrings is still perceptible with the naked eye. When viewed under magnification, the golden hue of this arsenic yellow remains vivid (fig. 1.8). Furthermore, the plate-like crystal structure of orpiment causes it to vividly sparkle in the light and thus to appear as lustrous gold on painted surfaces.²² Figure 1.9 shows these crystals in the proper right earring at high magnification. The relatively large crystals in this small area suggest that the ancient painter did not attempt to grind the pigment as fine as possible. The sparkling quality of orpiment appears to have been essential to the Lady. The painter applied the pigment thickly and unmixed with other pigments, unlike in the green stones, where they mixed the arsenic yellow with a



Figure 1.8 Zeiss stereomicroscope VIS photomicrograph at 2.6x magnification showing the Lady's proper left earring. Photo: Jan van Daal



Figure 1.10 Dino-Lite digital microscope VIS photomicrograph at 8.8x magnification showing the Girl's proper left earring. Photo: Jan van Daal



Figure 1.9 HIROX RH-2000 VIS photomicrograph at 160x magnification showing yellow pigment crystals in the Lady's proper right earring. Photo: Jan van Daal

still unidentified blue colorant.²³ In the earrings, arsenic yellow was meant to be seen and emphasizes the jewelry as a focal area of prestige, with the emphasis reinforced by the use of a pigment that counted as a prestigious material in itself.

Another yellow pigment used was yellow ochre, which was also sometimes employed to depict gold. Yellow ochre was native to Roman Egypt and commercially available in large quantities, as suggested by the inventory of a pharmacist, Aurelios Neoptolemeos, preserved on a papyrus dated May 18, 259 CE,²⁴ which lists three talents (approximately 25–30 kg) of yellow ochre.²⁵ The painter of the Girl (see fig. 1.1) used yellow ochre to create her golden earrings (fig. 1.10), as suggested by the MA-XRF map for iron (fig. 1.11). Romano-Egyptian painters also used actual gold leaf to depict golden jewelry, and this is the case for the Girl's



Figure 1.11 False-color MA-XRF map of the Girl showing the signals for Mn-K (red), Fe-K (green), and Au-L (blue). Acquisition and processing of the MA-XRF maps by Erma Hermens, Annelies van Loon, Victor Gonzalez and Francesca Gabrieli. Photo: False-color imaging by Jan van Daal

wreath (see fig. 1.11). As Spence and Twilley discuss in this volume, the painter of the woman in the Nelson Atkins Museum used gold leaf for the earrings, as did the painter of the well-known portrait in the Getty collection, where gold leaf was used for the subject's earrings, necklace, and wreath.²⁶

The pearls in the Lady (see fig. 1.3) are one of the portrait's defining features, not only because they have survived the test of time relatively well but also because the ancient painter depicted them so prominently, in a brilliant white (fig. 1.12). The MA-XRF results suggest that lead white pigment is present in the pearls (see fig. 1.7). The Stockholm papyrus may have something to reveal about the aesthetic ideal that underlaid the painter's choice of materials. The papyrus refers to pearls on numerous occasions and provides recipes for making imitation pearls and bringing out their white luster.²⁷ One recipe is especially thought-provoking. It explains how to clean real pearls that have become dirtied through extended use, so they regain a "whiteness not inferior to the original."²⁸

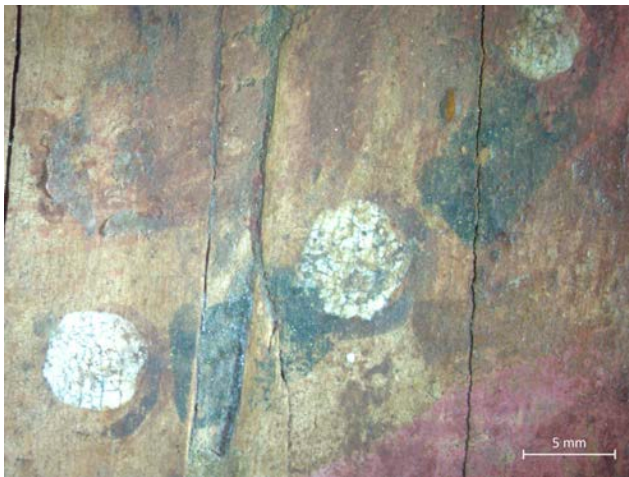


Figure 1.12 Zeiss stereomicroscope VIS photomicrograph at 2.6x magnification showing part of the proper-left side of the Lady's necklace. Photo: Jan van Daal

Perhaps the brilliant lead white of the Lady's pearls and the recipe in the Stockholm papyrus reflect the aesthetics that people in Roman Egypt valued in pearls. It also raises questions of how pearls were worn in real life: how often and for how long. Like the choice of pure arsenic yellow to represent gold, this choice for pure white is a high-value detail conveying meaning in mummy portraits.²⁹

AFTERLIVES: CONSERVATION AND RESTORATION

The traces of the portraits' post-acquisition afterlives manifest in the form of conservation-restoration treatments and aesthetic interventions. The four portraits all underwent at least one treatment following their acquisition. Documentation of this accompanies only the Fragment (see fig. 1.2), noting W. F. Meijer van Cassel as

the conservator at the Allard Pierson who treated the painting in 1975. A four-page conservation report on the nature and the underlying motivation for the treatment is on file. The adhesion of the Fragment's paint layers was in poor condition, so the painted surface required consolidation.³⁰

The Man (see fig. 1.4) underwent treatment around the same time. The portrait is witness to a different conservation approach, however. A sticker on the back of the Man's modern support identifies L. D. Vercouteren as the conservator and indicates that he treated the portrait in his studio in Scheveningen, the Netherlands. Vercouteren's curriculum vitae places him in Scheveningen in the early 1970s.

Documentation of the Man's treatment is not on file; however, interventions are clearly visible. The portrait had broken down into at least three large fragments. Vercouteren reassembled the fragments onto a cloth-covered panel with a simple wooden frame. A large, rectangular strip on the portrait's left side has been painted to reconstruct the missing portion of the Man's head. It is clearly distinguishable in the infrared photograph (fig. 1.13). The painting style and the direction of brushstrokes in the background of the modern addition imitate the original paint. The restored section visually produces a complete portrait. It is unknown whether Vercouteren created this infill or whether it dates from a previous intervention.

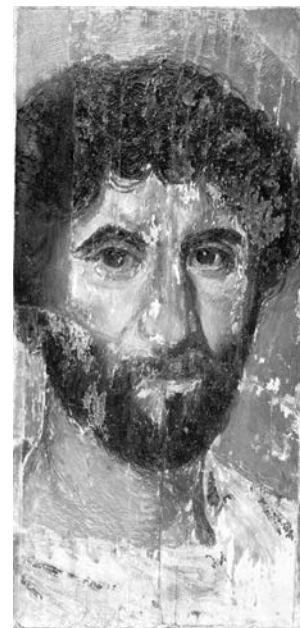


Figure 1.13 IR reflectance photograph of the Man. Photo: Jan van Daal

Whereas Meijer van Cassel deemed a glossy surface objectionable for a mummy portrait, Vercouteren arguably did not. A glossy varnish completely covers the Man and fluoresces strongly under UV radiation (fig. 1.14). The Girl (see fig. 1.1) was also varnished at some point in its history, and has darkened over time, giving the portrait a significant brown cast, and like the Man it was restored to look like a complete painting. Several additions to the panel serve this purpose. The oldest of these are the infills of the panel's original angled corners; these corners were already present in the 1909 Lunsingh Scheurleer catalogue photo of the Girl.³¹ The Man features the same type of added corner at the top right of the panel, distinguishable from the rest of the painting in both IR and UV radiation (see figs. 1.13–1.14). The corner matches the ancient background in color but is distinct from it—and from the rectangular infill—in terms of texture.

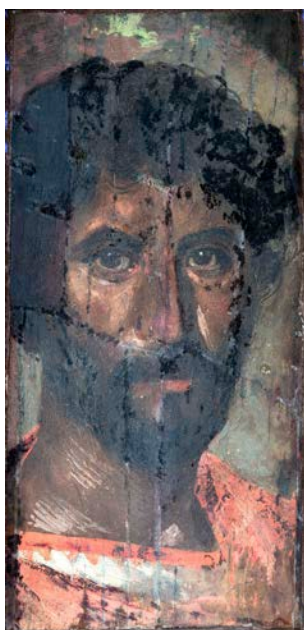


Figure 1.14 UV fluorescence photograph of the Man. Photo: Jan van Daal

These corners in both portraits both contain manganese (see fig. 1.11). This is noteworthy, as manganese is not present in the ancient paint. Analysis of these modern materials may reveal whether similar or identical pigments are present in these added corners, and this might lead in turn to an estimated dating for these additions based on the documentary evidence of the Girl and the exact composition of the pigments used.

The dating of modern materials also tells more about the second life of the Lady (see fig. 1.3). At some point, the portrait received a modern secondary support consisting

of three wooden panels with a cradle affixed to the back. On the front, these panels are painted white. MA-XRF revealed the principal pigment here to be titanium white (see fig. 1.7). Titanium white was developed in the late 1910s but became popular only in the 1930s.³² This narrows the date range for the secondary support and yields an image of how the Lady was presented before the mid-twentieth century.

The cradle itself testifies to sophisticated artisanship. The wood is smooth and the edges of the fixed vertical slats carefully beveled. The effort put into this cradle makes it clear that the secondary support was to remain affixed to the ancient panel for an extensive period of time, if not indefinitely. Rather than merely a structural aid, it was an integral part of the object. The cradle reveals two further aspects of the Lady's afterlife: warping and deformation potentially threatened the panel, and the Lady's custodians of the time dealt with it no differently than a European old master painting would have been treated.

These observations about past conservation treatments contribute to the stories of individual portraits' post-acquisition lives. They illustrate how people interacted with mummy portraits; the mode of engagement reflects the value of mummy portraits to people and institutions in different locations and periods of time. Furthermore, deconstructing conservation histories makes it possible to visualize how individual mummy portraits appeared as they moved through circles of collectors and dealers.

In the first APPEAR volume, Judith Barr emphasized that studying conservation histories informs provenance studies, and vice versa.³³ Indeed, as Kijowska et al. contribute in this volume, examining conservation materials and practices can yield invaluable information about the earliest selling and collecting practices in mummy portrait history. There always remains the possibility of historical conservation materials disappearing as they fall out of fashion or are deemed harmful.

CONCLUSION: MUMMY PORTRAITS MATTER

The APPEAR project has provided an impetus to uncover stories about mummy portraits. Continuing with the metaphor of composing histories as painted pictures, modern analytical techniques provide scholars with the palette and the tools to tell those histories. This paper has shown the power of a Morellian approach for the study of mummy portraits. Examining their production may

deconstruct mummy portraits into individual materials and techniques; these then serve as the anchor points for the histories that one wishes to compose.

Expanding the notion of the Morellian method to include storytelling strengthens technical examination as a way to understand the meaning of mummy portraits. The Allard Pierson portraits discussed here reveal the potential of this approach.

ACKNOWLEDGMENTS

This kind of research can only blossom through collaboration, and a great many people made it possible for me to dive into this project. For the arrangements and infrastructure to examine the Allard Pierson portraits, I thank Branko F. van Oppen de Ruiters, Wim Hupperetz, Willem van Haarlem, Birgit Maas, Tony Jonges, and Erma Hermens. For the acquisition and interpretation of the MA-XRF data, I thank Erma Hermens, Annelies van Loon, Victor Gonzalez, and Francesca Gabrieli. For the acquisition and interpretation of the VIL and XRD data, I thank Luc Megens. Finally, I thank Marie Svoboda and Ben van den Bercken for organizing this second APPEAR conference—it proved such fertile ground to present and test my ideas.³⁴

NOTES

1. The painting presently resides in a private collection under the care of Grant Ford Ltd.
2. The Österreichische Nationalbibliothek preserves a copy of this poster. See the Bildarchiv und Grafiksammlung, Pk 3003, 275.
3. Schneede 2021, 135–39. Also see Stamm 2007, specifically, on the connection between Modersohn-Becker and Romano-Egyptian funerary portraits.
4. See Montserrat 1998, 172–80, for the late nineteenth- and early twentieth-century enthusiasm for mummy portraits.
5. See Drimmer 2022, 416–26, for a concise overview of the history of the Morellian method, its connection to contemporary and analogue developments in paleography, and an extensive bibliography on Morelli. See Anderson 2019 for a biography of Morelli.
6. Anderson 2019, 170–71.
7. Anderson 2019, 125, 128–29, 134, 155.
8. See Anderson 2019, 89–167, for examples of how Morelli balanced his activities as a connoisseur with his friendships, political convictions, and scholarly perspectives.
9. See Barr et al. 2019 for a study of the Girl as a core piece of the Allard Pierson collection. This publication also discusses the preliminary results of the first technical examination campaign.
10. See van Daal 2019 for an extensive account of the analytical results after the second examination campaign.
11. Thiboutot 2020. For further discussions of Egyptian blue in mummy portraits, see Dyer and Newman 2020, 59–61; Ganio et al. 2015; Mayberger et al. 2020, 82; and Vak, Iannaccone, and Uhlir 2020, 137–38.
12. See van Daal 2019, 45–48, 133–52, for a full discussion of Egyptian blue in this group. The question of Egyptian blue's presence in the Lady and the Man warrants further research.
13. van Daal 2019, 146–50.
14. van Daal 2019, 45–48.
15. Inventory number 6-21375. See Ganio et al. 2015 for the analysis.
16. Ganio et al. 2015, 817.
17. For the Leyden papyrus, see Rijksmuseum van Oudheden, Leiden, AMS 66. For the Stockholm papyrus, see Sveriges nationalbibliotek, Stockholm, 2013/75.
18. See Halleux 1981 for a Greek text edition and French translation of both papyri.
19. Halleux 1981, 98r, 56, 101r, 72–73.
20. Halleux 1981, 96r, 49.
21. Halleux 1981, 150r, 156–57.
22. Smith and Ólaffson 2023, 13.
23. Identification of the blue colorant in the green stones would require further analysis. For example, VIL or false-color infrared imaging may determine whether Egyptian blue or indigo, respectively, is present.
24. P.Oxy. 31.2567. Papyrology Rooms, Bodleian Art, Archaeology and Ancient World Library, Oxford. See Totelin 2016, 83–84, for the Greek text edition and English translation of this papyrus.
25. See Totelin 2016, 77, for the conversion of a talent to kilograms.
26. J. Paul Getty Museum, 81.AP.42; see <https://www.getty.edu/art/collection/object/103QSW>.
27. See Halleux 1981, 222, for all references to pearls in the Stockholm papyrus.
28. Halleux 1981, 126r, 60.
29. See the work of Ann-Sophie Lehmann for the notion of materials shaping meaning in art. Lehmann 2012 and Lehmann 2014 are good overviews.

30. In this report, Meijer van Cassel also expressed concerns about the treatment altering the surface of the portrait, causing it to become glossy or darkened.
31. Barr et al. 2019, 105–6.
32. Eastaugh et al. 2008, 370–71.
33. Barr 2020.
34. van Daal 2019, 99–100, presents a full list of the people who were part of this project.

Roman-Egyptian Mummy Portraits and Panels of Gods from the Louvre: Renewed Historical and Material Knowledge

Lucile Brunel-Duverger

Caroline Thomas

Anne-Solenn Le Hô

Michel Menu

Christine Andraud

Maria Victoria Asensi Amorós

Thomas Calligaro

Anne Michelin

Raphaël Moreau

Laurent Pichon

Aurélie Tournié

Roman-Egyptian mummy portraits, which were probably used in a domestic context before the death of the person depicted,¹ were fixed over the face of mummies from the first to the fourth centuries CE. Created at the crossroads between Pharaonic funerary tradition and Greco-Roman memorial portraiture, these works constitute one of the rare surviving testimonies of the origins of what is now known as Western panel painting. Simultaneously, mainly in the Fayum region, another type of production expressed a complementary aspect of the religious practices of Roman Egypt's mixed population: framed painted panels representing gods. Found mainly in disturbed archaeological contexts in chapels and temples, these

panels were objects of worship for the syncretic cults characteristic of the period. The cultural and historical significance of mummy portraits has been studied in depth,² whereas the panels of gods have only recently received extensive attention.³

Until quite recently, few studies have been dedicated to the materials and technical practices used in the production of these artifacts.⁴ Although the number of studies and publications has increased, it remains difficult to link material results to archaeological information, as provenience and contexts are sparsely documented in many cases. The study of workshops (artisans and

organization) and the understanding of technical practices remain elusive despite the increasing amount of research.⁵

The Louvre collection is no exception; most of its portraits have no precise archaeological context offering secure data to cross reference with the results of material studies. The collection is composed of thirty-one mummy panel portraits and two panels of gods. Only five portraits have a secure archaeological provenience; the hypotheses for the remaining works in the collection are based on iconography, style, shape, and information about the collectors' whereabouts.

Three portraits were found by Albert Gayet in Antinoöpolis,⁶ which is a likely provenience for eight others.⁷ Seven portraits purchased from the Salt collection in 1826 are probably from Thebes.⁸ The Fayum region⁹ provides up to seven examples, only one of which is securely attached to the area,¹⁰ while six others are very plausibly from that region (five portraits acquired from Daninos Pacha in 1893 probably come from Philadelphia/er-Rubayat,¹¹ whereas Dioscorous's mummy-case, E 13044, is likely to have come from Hawara). Portrait N 2733 1 was brought from Egypt by Léon de Laborde in 1827, after being found in the Memphis necropolis. Five others are too fragmentary or damaged to even suggest a hypothetical provenience.¹² As for the panels of gods, both are said to be from the Fayum region dating back to the second century CE.¹³ The fragment representing a Dioscure¹⁴ (MND 193 - E 10815) was acquired by Georges Bénédite in 1899 in Cairo, whereas the Heron and Lycurgus panel is a 2020 acquisition from the Thierry Collection in Étampes, France (RFML.AE.2020.8.1).

Despite the relative scarcity of archaeological information, the opportunity to launch a material study on such an important corpus has been viewed as a unique occasion to deepen and refine the knowledge of this collection and of the production of these objects in general. Part of the collection had already been studied during the 1990s and 2000s, which resulted in the catalogue raisonné¹⁵ published in 2008. The APPEAR project prompted the Louvre to assess which possibilities could be offered by scientific equipment not available more than twenty years ago. Therefore, a two-year program of research was undertaken (FAYOUM Project, 2020–22),¹⁶ carried out by the Louvre and the Centre de Recherche et de Restauration des Musées de France (C2RMF) in collaboration with the Centre de Recherche sur la Conservation (CRC). The study was performed by Lucile Brunel-Duverger, physicochemist, and codirected by Caroline Thomas, curator of Egyptian art at the Louvre, and Michel Menu and Anne-Solenn Le Hô, scientists at the C2RMF. The aim was to undertake a

material study on the whole collection,¹⁷ on the widest range of questions and issues, in order to share results with the APPEAR community and to prompt discussion. The present paper aims to sum up the main results of this campaign, hoping the connection between historical and cultural information and scientific data can benefit from the comparison offered by similar studies.

MANUFACTURING STEPS

Since the latest research campaign in the early 2000s, several technical and technological advances have been made, offering new insights into the production of ancient painting. One of the main evolutions is the development of two-dimensional (2D) equipment that gives information on the entire surface of the object and provides distribution of materials (the methods and technology used are described in further detail in the Scientific Methodology section). Here we summarize the order of manufacturing steps, from the wooden support to the surface, describing the wood species, ground layers and backgrounds, underdrawings, binders, polychromy, and gilding (see the Results section for greater detail).

Wood

An exhaustive wood anatomy study of the corpus had already been carried out mainly by Maria Victoria Asensi Amorós (from Xylodata) and Pierre Détienne (CIRAD).¹⁸ Results are consistent with what has been found by Caroline R. Cartwright in the APPEAR project.¹⁹ Most mummy portraits from the Louvre are made with imported timber, with indigenous wood accounting for a third. A large majority are made of linden (*Tilia* sp., Malvaceae, nineteen examples), followed by sycomore fig (*Ficus sycomorus* L., Moraceae, seven). More rarely we encounter beech (*Fagus* sp., Fagaceae, two), cedar (*Cedrus* sp., Pinaceae, two), and tamarisk (*Tamarix* cf. *aphylla*, Tamaricaceae, one). Both panels of gods are made of willow (*Salix* sp. and *Salix* cf. *subserata* Willd., Salicaceae).²⁰

Ground Layers, Underdrawings, and Backgrounds

Different types of ground layers have been identified. Light ground layers are calcium-based; most of them have been identified as gypsum-based (both panels of gods and five of the portraits),²¹ while the composition of two could not be clarified.²² Beige layers are made of calcium-based material (sulfate or carbonate) mixed with iron yellow. The

largest number of portraits (twelve)²³ have a dark ground layer composed of a mixture of calcium-based materials and carbon black and/or iron-based pigments. Finally, three appear to have no ground layer, polychromy being directly applied on bare wood.²⁴ Doubts persist for the remaining seven.²⁵

Underdrawings have rarely been discussed in publications to date; this is mostly related to the technical difficulties faced when trying to detect them, rather than to their supposed rarity. Recent studies using modern technology have detected a variety of colors used to produce underdrawings, such as black,²⁶ white,²⁷ blue,²⁸ and mixtures of colors, possibly using madder lake-based pigments, to create preparatory sketches and add volume to faces and hair.²⁹ For dark underdrawings on light ground layers, infrared reflectography (IRR) is an efficient imaging method for revealing carbon black on white substrate. This common technique was unfortunately not carried out during the 2000s campaign. Using hyperspectral imaging (HSI) in the near-infrared range (NIR) we were able to reveal dark underdrawings on two portraits³⁰ with light ground layers and on both panels of gods. However, their composition could not be identified, as the technique reveals only the presence of carbon black and does not indicate if it is used pure or mixed. Modifications between first sketches and final result can be noted, whether it is a slight shifting of the jaw and nose outlines³¹ or the reworking of an eye (fig. 2.1).³²



Figure 2.1 (A) Panel with a Dioscure, Fayum(?), ca. 100–200 CE. Tempera on willow, 38 × 6.5 × 0.5 cm (15 × 2.5 × 0.2 in.). Photo: © C2RMF / Anne Maigret; (B) Black underdrawing (see arrows) revealed by HSI-SWIR: $\lambda = 1647.37$ nm from complete data cube (1000–2500 nm). Paris, Musée du Louvre, département des Antiquités grecques, étrusques et romaines. MND 193 - E 10815. Photo: © C2RMF / Lucile Brunel-Duverger

The most surprising result was the uncovering of white sketches on a dark ground layer that refuted earlier claims that there were none. The energy range of HSI-SWIR (short-wavelength infrared) produces signals for materials deep into the stratigraphy due to their characteristic vibrational features. Indeed, we were able to identify the main vibrational patterns of water from gypsum ($\nu_a + \delta$ OH [H₂O])³³ with specific positions at 1941 nm and a 1973 nm shoulder, sometimes associated with a lower band at 1445 nm, also attributable to the water in gypsum ($\nu_3 + 2\nu_2$ H₂O). The identification of gypsum (CaSO₄ · 2H₂O) for white underdrawings is consistent with what was found in other studies.³⁴ Those white drawings were revealed on at least seven portraits,³⁵ some of them showing changes in composition, notably redesigning the hairline or direction of garment folds (fig. 2.2).³⁶ It should be noted that the whole series that is probably from Thebes (Salt collection) exhibits this feature, pointing toward a possible criterion for a Theban workshop.³⁷



Figure 2.2 (A) Portrait of a man, Thebes(?), ca. 250 CE. Encaustic on beechwood, 41 × 14 × 0.1 cm (16 × 5.5 × 0.04 in.). Photo: © C2RMF / Anne Maigret; (B) White underdrawing revealed by HSI-SWIR. Imaging is the result of a band calculation (B2–B1), where B1 = 1941 nm ($\nu_a + \delta$ OH [H₂O]) from gypsum and B2 = 1916 nm (absence of gypsum). The bands were extracted from a resized data cube (1910–2029 nm) after application of a continuum removal. Data treatment realized with Envie software. Paris, Musée du Louvre, département des Antiquités égyptiennes, AF 6885. Photo: © C2RMF / Lucile Brunel-Duverger

The color of portrait backgrounds ranges from light beige to dark gray, passing through a multitude of shades. Background application does not seem to follow a consistent pattern: nineteen were applied after the portrait

was painted,³⁸ two may have been applied on the whole surface of the ground layer before the portrait was painted,³⁹ one shows a background applied in anticipation of the shape of the not-yet-painted portrait (E 12570), and the application steps remain unclear for seven.⁴⁰

Binders

Mummy portraits' binders have prompted a lot of research, especially on the complex question of wax-based portraits and Punic wax.⁴¹ On the Louvre corpus, we identified two specific patterns characteristic of encaustic (fig. 2.3) and tempera (fig. 2.4) using HSI-SWIR and macro X-ray fluorescence (MA-XRF) data. Most portraits are wax-based (twenty-four),⁴² whereas a smaller number (seven),⁴³ as well as both panels of gods, are water-based.⁴⁴ Because of the spectral resolution (~7 nm) we were not able to discern the nature of the protein.⁴⁵ By resizing the initial data cube (1000–2500 nm) within the area of interest (2100–2500 nm) we could map the distribution of both types of binders.



Figure 2.3 (A) Portrait of a woman, Antinoöpolis, ca. 150 CE. Encaustic on sycamore fig, 37 × 17 × 1 cm (14.5 × 6.7 × 0.4 in.). Photo: © C2RMF / Anne Maigret; (B) Distribution of the waxy binder used. HSI-SWIR: $\lambda = 2210$ nm ($\nu_s + \delta$ CH from wax), extracted from a resized data cube (2241–2360 nm) after application of a continuum removal. Data treatment realized with Envie software. Photo: © C2RMF / Lucile Brunel-Duverger; (C) MA-XRF imaging showing the distribution of lead (Pb L α) attributed to the presence of lead white. Paris, Musée du Louvre, département des Antiquités égyptiennes, E 12569. Photo: © C2RMF / Lucile Brunel-Duverger

An interesting connection was revealed between the nature of the binder and the addition of a filler. It seems that in most cases a white filler was added to the pictorial matter, thus contributing to the large range of hues characteristic of Roman-Egyptian polychromy. This filler has been identified as calcium-based for protein-based binders on the one hand (see fig. 2.4C) and as lead white

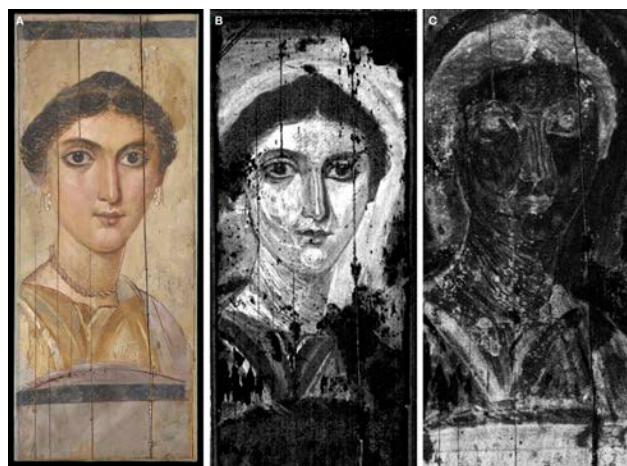


Figure 2.4 (A) Portrait of a woman, Memphis necropolis, ca. 150 CE. Tempera on linden, 46 × 19 × 0.2 cm (18 × 7.5 × 0.08 in.). Photo: © C2RMF / Anne Maigret; (B) Distribution of the proteinaceous binder used. HSI-SWIR: $\lambda = 2173$ nm (δ NH + ν_s CN from protein binder), extracted from a resized data cube (2098–2247 nm) after application of a continuum removal. Data treatment realized with Envie software. Photo: © C2RMF / Lucile Brunel-Duverger; (C) MA-XRF imaging showing the distribution of calcium (Ca K α) attributed to the presence of a white, calcium-based material identified as gypsum with HSI-SWIR. Paris, Musée du Louvre, département des Antiquités égyptiennes, N 2733 1. Photo: © C2RMF / Lucile Brunel-Duverger

for wax-based binders on the other (see fig. 2.3C). In the latter case, the addition of lead white was perhaps intended to create a saponification reaction (as in Punic wax), which would impact the texture and properties of the wax, rendering it easier to apply cold.

Two portraits seem to be exceptions among the corpus: Salt collection portraits N 2732 2 and N 2733 2, long said to be encaustic, are in fact water-based but show a coating of wax on the whole surface. Their style is indeed more characteristic of tempera-based paintings, and the shine of their surfaces was misleading for a long time. We do not know when the wax was applied.⁴⁶ Moreover, the white filler used for this tempera-based binder is lead white, adding another peculiarity to these complex portraits.

Another portrait (MNC 1695) stands out as an unusual combination of all examples: it is protein-based but shows traces of wax on the surface of certain areas, maybe to emphasize the outlines of the face and jewels. The white filler is predominantly calcium-based; however, lead white found on the face and jewels does not perfectly match the distribution of the wax. The understanding of those peculiarities could greatly benefit from comparisons outside of the Louvre collection to see if they could be clues toward workshop practices.



Figure 2.5 (A) Panel representing the gods Heron and Lycurgus, Fayum region(?), ca. 100–200 CE. Tempera on willow, 39 × 31.4 × 0.8 cm (15.3 × 12.4 × 0.3 in.). The VIL imaging shows Egyptian blue for the gods' clothing. (B) Portrait of a woman, Antinoöpolis(?), ca. 100–180 CE. Encaustic on cedar, 38 × 25 × 1.9 cm (15 × 9.8 × 0.75 in.). The VIL imaging shows Egyptian blue for the flesh tones and stripes of the clothing. (C) Portrait of a man, Thebes(?), ca. 250 CE. Encaustic on linden, 33.5 × 18.5 × 0.2 cm (13.2 × 7.3 × 0.08 in.). The VIL imaging shows Egyptian blue for the background and flesh tones. (D) Portrait of a woman, Antinoöpolis(?), ca. 130–150 CE. Encaustic on linden, 32 × 17 × 0.1 cm (12.6 × 6.7 × 0.04 in.). The VIL imaging shows Egyptian blue for the clothing. Paris, Musée du Louvre, département des Antiquités égyptiennes, RFMLAE.2020.8.1, AF 6886, N 2732 3, AF 6884. Photos: © C2RMF / Anne Maigret

Polychromy

Subsequent to Pharaonic Egypt, new pigments and techniques became available, thus material choices may provide evidence for the identification of workshops. Some materials seem to be more commonly used than others; for example, earth pigments are found on the whole collection.⁴⁷ Brown pigments were used for the hair,⁴⁸ while red and yellow are always found mixed together with a white material to depict flesh tones. Iron red is consistently found in contours and details: it corresponds to the main red pigment, mostly characterized as hematite, which in few cases is titanium-rich,⁴⁹ possibly indicating the presence of ilmenite, a natural compound frequently found in Egyptian red ochres.⁵⁰ We identified cinnabar on two male portraits, to highlight the upper lip in one case⁵¹ and possibly for the complexion in the second.⁵²

Yellow appears on female portraits to render golden jewels or hues of tinted textiles. Besides iron earth, which in some cases we were able to characterize as jarosite,⁵³ we also found arsenic-based pigment—presumably orpiment—on three protein-based portraits⁵⁴ as well as on the Dioscure panel (also protein-based).⁵⁵

Blue hues are not often found on mummy portraits, except occasionally in tunics, mantles, jewels, and eyes, although Egyptian blue and indigo are well attested to as components of the pictorial layers by the APPEAR project.⁵⁶ Among the Louvre collection, blue is not widely used. On the Heron and Lycurgus panel, Egyptian blue is used to render the clothing⁵⁷ (fig. 2.5A), while on mummy portraits, indigo is employed to depict a light blue stone in a necklace on MNC 1695 and three dark clavi.⁵⁸ In the corpus, Egyptian blue is mainly employed to render complexion (fig. 2.5B) and backgrounds (fig. 2.5C), and more rarely to create details such as white sclera.⁵⁹ Those blue pigments are also used to obtain purple shades for the tunics (fig. 2.5D), mantles, and clavi characteristic of Roman-Egyptian portraiture.

Purple was rarely depicted in Pharaonic Egypt⁶⁰ but became more popular during the Ptolemaic period, under the influence of Hellenistic Greece, where pink and mauve denoted sophistication, preciousness, and power. During the Roman period, a wide variety of hues appeared, ranging from light pink to dark purple, and were used to render both complexion⁶¹ and clothing. Despite the absence of Tyrian purple on any portrait, these shades are most probably connected to the rare and prestigious colorant/dye derived from Muricidae gastropods, reserved for emperors and circles of power.⁶² On mummy portraits, madder lake has often been used with other colored materials (indigo, Egyptian blue, or minium⁶³), mixed together or applied in overlapping layers, to add subtlety to its hue.⁶⁴ In this way, artisans were able to create a large range of shades for representing textiles, from bright red to bluish purple. The several shades of purple on the Louvre portraits were identified using hyperspectral imaging data in the visible and near infrared range (HSI-VNIR).⁶⁵ In portraits' purple clothes we found two types of mixtures: madder lake and Egyptian blue,⁶⁶ and madder lake and indigo.⁶⁷ A particular example (AF 6884; fig. 2.6A) shows a combination of both blue pigments (Egyptian blue and indigo) in conjunction with madder lake. While the main part of the tunic is rendered in a mixture of Egyptian blue and madder lake (figs. 2.6B and 2.6C), specific areas of the clothing are painted with indigo used in association with madder lake (figs. 2.6B and 2.6D), possibly to render the volume of the folds using different shades. A single portrait shows the use of orchil, a violet dye extracted from

lichen (*Rocella*) to render the purple clavis.⁶⁸ Pigment mixtures used to produce purple hues could be clues toward workshop practices and might well be addressed by the sharing of results prompted by the APPEAR project.



Figure 2.6 (A) Portrait of a woman, Antinoöpolis(?), ca. 130–150 CE. Encaustic on linden, 32 × 17 × 0.1 cm (14.6 × 6.7 × 0.04 in.). (B) The pink pixels correspond to the spectral presence of madder lake. (C) The blue pixels correspond to the spectral presence of Egyptian blue. (D) The turquoise pixels correspond to the spectral presence of indigo lake. Paris, Musée du Louvre, département des Antiquités égyptiennes, AF 6884. Photos: © C2RMF / Lucile Brunel-Duverger

Green is not the most widespread color observed on mummy portraits, even though several mixtures are purported to render this hue in the Roman period.⁶⁹ Indeed, green shades found on the Louvre portraits only depicted stones (probably emeralds) or clavi. Green stones are consistently painted with copper green materials,⁷⁰ whereas clavi can be rendered with an iron-based green called green earth.⁷¹ On the panel of gods RFML.AE.2020.8.1, green earth is mixed with Egyptian blue to depict the blades of the ax or the cnemids (shin guards).⁷²

Gilding was quite frequently used on mummy portraits to represent elements such as wreaths, hair ornaments, and jewels (e.g., MNC 1695). The so-called Européenne mummy portrait (MND 2047) shows gold on the neck and torso up to the ears; the former study concluded that the gold leaves, composed of two-thirds gold and one-third silver, were randomly applied, thus confirming the assumption of a ritualistic action rather than the depiction of a specific object.⁷³ Gilding is rare on panels of gods, but the Dioscure (see fig. 2.1) provides one example. Tiny rectangular pieces of gold cover the god's throat and mouth as well as other shining areas: nimbus, hair, cuirass, cnemids.⁷⁴ Leaf-thickness measurements have been attempted on the MA-XRF datasets; however, the values obtained from the altered leaves were less than 1 μm, which cannot be considered as representative of gold-leaf production.

A Word about Workshops

In addition to iconographic and stylistic traits, choice of materials and techniques place Roman-Egyptian painting at the crossroads between Pharaonic tradition and Greco-Roman practices. The many recent studies on this topic continuously shed light on the connection between technological characteristics and workshops. The extensive research carried out on Louvre mummy panel portraits and panels of gods provided a wide range of data that deepened our knowledge of the collection. However, the lack of precise information on provenience hampers cross-referencing material data with firmly secured archaeological contexts, which would enable workshop practices to be distinguished. A wider scope is necessary to make data speak and shed light on the context of the production of mummy portraits and panels of gods. Therefore, it is through sharing information within the APPEAR community that this data is best able to provide reliable clues regarding workshops, provenience, and dating.

Let us complete this affirmation with a cautionary tale likely to trigger discussion. Material and technical characteristics can say a lot about production, which continues to be studied from an art history point of view. Indeed, research on corpora with an attested provenience has shown without doubt the potential of intersecting material data and archaeological information. This supports the widespread hope that possible proveniences could be secured by the recognition of common material characteristics. However, some cases call for caution, and therefore we considered this otherwise useful assumption with care.

The set of seven portraits from the Salt collection, presumably from Thebes, showed some material similarities, in particular newly discovered white underdrawings. We were hoping to go further, expecting meaningful material results (potential clues of a local workshop!) for the four male portraits within the group that showed close iconographic and stylistic affinities. It turned out that their material composition presents important disparities (type of wood, use of Egyptian blue or madder lake; see the Results section). That came as a surprise, when perhaps it should not have.⁷⁵ This example testifies to the fact that technical similarities can provide important clues about mummy portraits but also suggests that disparities can coexist among an apparently cohesive group with comparable dating and provenience—another confirmation of the complexity of this remarkable production, which is still promising for research.

SCIENTIFIC METHODOLOGY

The material study included two steps, starting with the assessment of previous analysis carried out between 1967 and 2011, mostly on microsampling. From the cross sections and related scanning electron microscopy (SEM) analyses previously done on 150 samples, we obtained a significant amount of information on the stratigraphy. Starting from there, the FAYOUM Project conceived a non-invasive, non-destructive analytical protocol that aimed to get information on the entire surface of the object. This 2D methodology comprised a technical imaging campaign (ultraviolet [UV], infrared [IR], infrared-reflected false color [IRFC], visible-induced visible luminescence [VIVL], and visible-induced infrared luminescence [VIL]) associated with scientific imaging methods able to collect, on the UV–SWIR range, chemical and optical information highlighting the Egyptian painters' palette.

The MA-XRF/RIS/PL is an instrument developed in-house.⁷⁶ It delivers in a single pass five spectral data cubes containing all spectra at each pixel:

- ◆ X-ray fluorescence spectrometry (XRF)
- ◆ Photoluminescence (PL) at 250, 365, and 655 nm
- ◆ Reflectance imaging spectroscopy (RIS) at 400–1000 nm

The instrument head is scanned in front of the panel over an area measuring up to 300 mm (X) × 300 mm (Y) × 120 mm (Z) with a standard 0.5 mm step size and 80 ms dwell time per point.

For hyperspectral imaging (HSI), two different imaging devices were used for the two spectral ranges under study. The visible and near infrared (VNIR) imager was a Specim HS camera, operating at 400–1000 nm, equipped with an ImSpector V10E 2/300 spectrograph combined with an Imperx IPX-2M30 CCD detector (1600 [spatial] × 1200 [spectral] pixels).

The short-wave infrared (SWIR) system consisted of an ImSpector N25E 2/300 spectrograph coupled with a cooled, temperature-stabilized MCT detector (9.6 mm detector with 320 [spatial] × 256 [spectral] pixels), operating at 970–2500 nm. The objective lenses used were, respectively, OLES23 (23 mm f1.4) and OLES56 (56 mm f1.4) for the VNIR and SWIR cameras. Spectral samplings for the VNIR and SWIR detectors are, respectively, 3 nm and 7 nm. Spatial resolutions were fixed at 0.5 mm, to match the spatial resolution of MA-XRF/RIS/PL acquisitions.

In this way, elemental cartography by XRF can be compared to the distribution of other materials, such as madder lake, thanks to its characteristic emission under UV, or Egyptian blue under red excitation (VIL).⁷⁷ Indeed, elementary maps obtained by XRF were also correlated to the distribution of colored materials such as pigments and dyes using RIS and HSI-VNIR,⁷⁸ while HSI-SWIR allowed us to characterize white materials and binders.⁷⁹ Because of the spectral domain covered by HSI (400–2500 nm) we were also able to mimic infrared reflectance (IRR) by selecting specific wavelengths of the SWIR data cube (980 nm, 1300 nm, and 1650 nm).⁸⁰ IRR is an imaging technique that uses wavelengths in the infrared range to penetrate opaque paint layers and reveal invisible elements of the composition. It is based on the fact that infrared light is absorbed by carbon-rich materials and reflected back from light-colored elements such as a white ground.⁸¹

RESULTS

Figures 2.7, 2.8, and 2.9 detail the mummy portraits and panels of gods from the Louvre collection studied in the course of this research.

Inventory number	Gender	Estimated date based on style (CE)	Provenience	Wood	Binder	Charge	Ground layer	Underdrawing	Background (Egyptian blue)
AF 6723	M	250	Thebes (?)	<i>Fagus</i> sp.	Wax	Lead white	Dark gray Iron oxide ^a	White Gypsum	
AF 6724	F	0-100	Antinoópolis (?)	<i>Tilia</i> sp.	Wax	Lead white	None(?)	NH	
AF 6882	F	130-150	Antinoópolis (?)	<i>Tilia</i> sp.	Wax	NA	NA	NA	
AF 6883	M	190-230	Antinoópolis (?)	<i>Tilia</i> sp.	Wax	Lead white	Dark gray Ochres + iron oxide ^a	NH	
AF 6884	F	130-150	Antinoópolis (?)	<i>Tilia</i> sp.	Wax	Lead white	None	NH	
AF 6885	M	250	Thebes (?)	<i>Fagus</i> sp.	Wax	Lead white	None	White Gypsum	
AF 6886	F	100-180	Antinoópolis (?)	<i>Cedrus</i> sp.	Wax	Lead white	Beige CaSO ₄ + jarosite + Si ²	NH	
AF 6887	M	150-225	Antinoópolis (?)	<i>Ficus sycamorus</i> L.	Wax	Lead white	Light gray; CaSO ₄ + carbon black ^a	NH	
AF 6888	F	150	Antinoópolis (?)	<i>Tilia</i> sp.	Wax	Lead white	Dark gray NI	NH	
AF 6889	F	100-200	Antinoópolis	<i>Tilia</i> sp.	Wax	Lead white	Dark gray NI	White (?) Gypsum (?)	X
AF 6890	M	0-400	Unknown	<i>Tilia</i> sp.	Wax	Lead white	Dark gray CaSO ₄ + carbon black ^a	NH	
AF 6891	M	200-300	Unknown	<i>Tilia</i> sp.	Protein	Calcium-based	White Calcium-based	Red (?) Fe-based (?)	
AF 6892	(?)	0-400	Unknown	<i>Tilia</i> sp.	Wax	Lead white	NH	NH	X
AF 6893	M (?)	0-400	Unknown	<i>Ficus sycamorus</i> L.	Wax	Lead white	Black CaSO ₄ + C black + ochres ^a	NH	X
E 12569	F	150	Antinoópolis	<i>Ficus sycamorus</i> L.	Wax	Lead white	Dark red Ochres + iron oxide + Si ²	NH	
E 12570	M	175-225	Antinoópolis	<i>Ficus sycamorus</i> L.	Wax	Lead white	Dark gray CaSO ₄ + ? ^a	Blue (?) Egyptian blue (?)	
E 13044	F	250-300	Hawara (?)	<i>Tilia</i> cf. <i>europaea</i>	Wax	NA	NA	NA	
E 33650	M	0-400	unknown	<i>Tamarix</i> cf. <i>aphylla</i>	Wax	Lead white	NH	NH	X
MNC 1693	F	150-350	Er-Rubayat (?)	<i>Ficus sycamorus</i> L.	Wax	Lead white	Black CaSO ₄ + carbon black ^a	NH	
MNC 1694	F	150	Er-Rubayat (?)	<i>Tilia</i> sp.	Wax	Lead white	Black NI	NH	
MNC 1695	F	175-225	Er-Rubayat (?)	<i>Tilia</i> sp.	Protein Traces of wax	Calcium-based Traces of lead white	White Gypsum	White Gypsum	
MNC 1696	F	150-200	Er-Rubayat (?)	<i>Tilia</i> sp.	Wax	Lead white	NH	NH	X
MNC 1697	F	275-325	Er-Rubayat (?)	<i>Ficus sycamorus</i> L.	Protein	Calcium-based	White-beige Calcium-based	Red (?) Fe-based	
MND 2029	F	350	Er-Rubayat	<i>Ficus sycamorus</i> L.	Protein	Calcium-based	White CaSO ₄ ^a	Gray Carbon black	
MND 2047	F	100-150	Antinoópolis (?)	<i>Cedrus</i> sp.	Wax	Lead white	Black CaSO ₄ + carbon black ^a (soot)	NH	
N 2732.1	M	250	Thebes (?)	<i>Tilia</i> sp.	Wax	Lead white	Brown NI	White Gypsum	X
N 2732.2	M	250	Thebes (?)	<i>Tilia</i> sp.	Gum (?)	Lead white	NH	White Gypsum	X
N 2732.3	M	250	Thebes (?)	<i>Tilia</i> sp.	Wax	Lead white	None	White	X

Inventory number	Gender	Estimated date based on style (CE)	Provenience	Wood	Binder	Charge	Ground layer	Underdrawing	Background (Egyptian blue)
								Gypsum	
N 2733.1	F	150	Memphis necropolis	<i>Tilia</i> sp.	Protein	Gypsum	Light gray CaSO ₄ ^a	Black Carbon black	
N 2733.2	F	200-250	Thebes (?)	<i>Tilia</i> sp.	Gum (?)	Lead white	White (?)	White (?) Gypsum (?)	
N 2733.3	F	150-200	Thebes (?)	<i>Tilia</i> sp.	Wax	Lead white	Black or none (?)	White Gypsum	

Note:

NI = unidentified (relating to material identification: analysis conducted but without relevant results), NH = not highlighted (relating to manufacturing step: observations and analysis conducted but without relevant results), NA: not analyzed.

^a Results obtained by MEB-EDS on cross section.

Figure 2.7 Results obtained on the thirty-one mummy portraits from the Louvre collection: identification, materials, and underlayers.

Inventory number	Clavi		Clothing		Flesh tones		Noteworthy pigments	Gilding
	Color	Composition	Color	Composition	EB	ML		
AF 6723	Red	Madder lake + Egyptian blue	White	Lead white	X	X	Vermillion (upper lip)	
AF 6724	Gray	Lead white + carbon black Detail: copper	Pink	Madder lake	X		Copper green (stone), Cu-based materials (hair)	
AF 6883	Purple	Madder lake + Egyptian blue	White	Lead white	X			
AF 6884	Green	Green earth (K rich) + carbon black	Purple	Madder lake + Egyptian blue + indigo	X			
AF 6885	Red	Madder lake + Egyptian blue	White	Lead white		X		
AF 6886	Pink	Madder lake + Egyptian blue	Yellow	Iron-based material	X	X	Copper green (stone)	
AF 6887	Purple	Madder lake + indigo	White	Lead white			Ti-rich hematite	
AF 6888	Pink	Madder lake Folds: indigo	White	Lead white			Copper green (stone)	
AF 6889	Black	Carbon black	Red	Madder lake + minium Folds: hematite	X		Vermillion (complexion)	
AF 6890	NO		White	Lead white				
AF 6891	NO		NO				Ti-rich hematite	
AF 6892	NO		NO					
AF 6893	NO		NO			X		
E 12569	Green	Green earth + Egyptian blue	Purple	Iron-based material + carbon black Folds: madder lake			Jarosite, copper green (stone)	
E 12570	Purple	Madder lake + indigo	White	Lead white	X			
E 33650	NO		NO					
MNC 1693	Dark blue	Indigo	Purple	Madder lake on gray background			Jarosite	
MNC 1694	Dark purple	Orchil	Yellow	Iron-based material	X		Ti-rich hematite, copper green (stone)	
MNC 1695	Blue	Indigo + carbon black	Pink	Madder lake Folds: hematite and indigo			Orpiment (necklaces), Ti-rich hematite	X
MNC 1696	NO		Pink	Madder lake			Copper green (stone)	
MNC 1697	Black	Carbon black	Pink	Madder lake	X		Orpiment (jewelry)	
MND 2029	Dark blue	Indigo	Pink	Madder lake		X		
MND 2047	NO		Yellow	Iron-based material			Jarosite, copper green (stone)	X
N 2732 1	Pink	Madder lake on Egyptian blue	White	Lead white				
N 2732 2	Pink	Madder lake	White	Lead white		X		
N 2732 3	Pink	Madder lake	White	Lead white		X		
N 2733 1	White	Aluminum sulfate	Yellow	Iron-based material + orpiment		X	Orpiment (cloth, necklace)	

Inventory number	Clavi		Clothing		Flesh tones		Noteworthy pigments	Gilding
	Color	Composition	Color	Composition	EB	ML		
N 2733 2	Purple	Madder lake + indigo	White	Lead white		x	Jarosite, Ti-rich hematite, white As-based material (necklace)	
N 2733 3	Black	Carbon black	Purple	Madder lake + Egyptian blue Folds: iron-based material		x	Jarosite, Ti-rich hematite	

Note:

EB = Egyptian blue, ML = Madder lake, NO = not observable (e.g., fragmentary portraits).

Figure 2.8 Results obtained on the thirty-one mummy portraits from the Louvre collection: polychromy.

Characteristics	Inventory Number	
	MND 193 - E 10815	RFML.AE.2020.8.1
Date	100–200 CE	100–200 CE
Provenience	Fayum(?)	Fayum(?)
Wood	<i>Salix</i> sp.	<i>Salix cf. subserrata</i> Willd.
Binder	Protein	Protein
Charge	Gypsum	Gypsum
Ground layer	White Gypsum	White Gypsum
Underdrawing	NI Carbon black	Gray Carbon black
Egyptian blue background	X	—
Pigments	Orpiment, madder lake	Madder lake, Egyptian blue, green earth, yellow lake
Gilding	X	—

Note:

NI = unidentified

Figure 2.9 Results obtained on the two panels of gods from the Louvre collection.

NOTES

1. Borg 1997, 26–32.
2. See, for example, Parlasca 1969–2003; Corcoran 1995; Borg 1996; Walker and Bierbrier 1997.

3. Rondot 2013; Mathews and Müller 2016.
4. The greatest step made has been thanks to the APPEAR project, as the publication of the first conference testifies (Svoboda and Cartwright 2020).
5. Some studies of corpora with an attested provenience show the potential of intersecting material data and archaeological information, such as the eleven Tebtunis portraits published by Salvant et al. 2018.
6. E 12569 and E 12570 (1904–1905 excavations); AF 6889 (1909 excavations).
7. AF 6724, AF 6882, AF 6883, AF 6884, AF 6886, AF 6887, AF 6888, MND 2047.
8. N 2732 1, N 2732 2, N 2732 3, N 2733 2, N 2733 3, and AF 6885; AF 6723 is most probably the seventh portrait acquired from the Salt collection.
9. As we know, the so-called Fayum portraits got their name from the first important discoveries made in the Fayum region; however, their production is attested to be from Marina el-Alamein to Aswan.
10. MND 2029, which is also the only portrait from the Theodor Graf collection kept in the Louvre, comes from Philadelphia (Er-Rubayat).
11. MNC 1693, MNC 1694, MNC 1695, MNC 1696, MNC 1697.
12. E 33650, AF 6890, AF 6891, AF 6892, AF 6893.
13. Thomas and Brunel-Duverger 2023.
14. The Dioscuri are divine brothers from Greco-Roman mythology, often depicted in Roman Egypt as powerful armed gods.
15. Aubert and Cortopassi 2008.
16. The FAYOUM Project was supported by the Paris Seine Graduate School of Humanities, Creation, Heritage, Investissement d'Avenir ANR-17-EURE-0021 – Foundation for Cultural Heritage Science.
17. For practical reasons we had to omit two portraits still placed on their mummies (AF 6882 and E 13044). The remainder of the collection was included in the study: twenty-nine mummy panel portraits and two panels of gods.
18. Asensi Amorós et al. 2001; Asensi Amorós and Détienne 2008. Additional analysis was carried out by Asensi Amorós in 2021 and 2022 on portraits AF 6893, E 33650, and E 13044 and on panel RFML.AE.2020.8.1. CIRAD is the Centre de coopération internationale en recherche agronomique pour le développement.
19. Cartwright 2020. <https://www.getty.edu/publications/mummyportraits/part-one/2/>.
20. We have not come across other panels of gods painted on willow, but scientific data is still scarce on that production compared to mummy portraits. Providence RISD Heron panel (59.030) is made of sidr wood (*Ziziphus spina-christi*), as identified by Caroline R. Cartwright and published by Borromeo et al. 2020. In her talk at the second APPEAR Conference (“Three Romano-Egyptian Panel Paintings in the Ny Carlsberg Glyptotek”), Cecilie Brøns mentioned sidr wood (*Ziziphus spina-christi*) and tamarisk (*Tamarix* sp.) for panels of gods. That study seems to show a variety of wood species—in most cases native to Egypt—which is different from the observations made on mummy portraits. See Thomas and Brunel-Duverger 2023, 122–23.
21. AF 6886, AF 6887, MNC 1695, MND 2029, N 2733 1.
22. AF 6891 and MNC 1697. Only macro X-ray fluorescence (MAXRF) was performed.
23. AF 6723, AF 6883, AF 6888, AF 6889, AF 6890, AF 6893, E 12659, E 12570, MNC 1693, MNC 1694, MND 2047, N 2732 1.
24. AF 6884, AF 6885, N 2732 3.
25. Because there were no existing samples nor paint losses for non-invasive analysis, we were not able to get information regarding the nature of the background. These portraits are AF 6724, AF 6892, E 33650, MNC 1696, N 2732 2, N 2733 2, N 2733 3.
26. Knudsen 2017, in particular paragraph 9, footnote 9, and further developments.
27. Williams 2010; Salvant et al. 2018.
28. Ganio et al. 2015.
29. Mayberger et al. 2020, 79–89.
30. MND 2029, N 2733 1.
31. N 2733 1.
32. Dioscure panel: MND 193 - E 10815.
33. Longoni et al. 2022.
34. Salvant et al. 2018.
35. AF 6723, AF 6885, MNC 1695, N 2732 1, N 2732 2, N 2732 3, N 2733 3; strongly suggested on AF 6889 and N 2733 2.
36. N 2732 3 and AF 6885.
37. The fact that we found it on the seven portraits presumably from Thebes is worth noting. However, white underdrawings have been found on other corpora, such as the group of portraits from Tebtunis (Fayum), published by Salvant et al. 2018. Therefore it is attested to at least on one other site. It could well be a criterion for specific workshops on both sites.

38. AF 6723, AF 6883, AF 6884, AF 6885, AF 6886, AF 6887, AF 6888, AF 6890, AF 6891, AF 6892, AF 6893, E 33650, MNC 1697, MND 2047, N 2732 1, N 2732 2, N 2732 3, N 2733 1, N 2733 3.
39. AF 6724, MNC 1695; in both cases, the portrait is painted on a gray layer that serves as background. Underdrawing was noticed only on MNC 1695.
40. AF 6889, E 12569, MNC 1693, MNC 1694, MNC 1696, MND 2047, N 2733 2.
41. From the earlier studies of H. Kühn to research performed by S. Colinart in particular on the Louvre corpus; Kühn 1960; Colinart and Grappin-Wsevoljsky 1999. More recently, see Cuní et al. 2012; and Mazurek, Svoboda, and Schilling 2019, 1960–85.
42. AF 6723, AF 6724, AF 6882, AF 6883, AF 6884, AF 6885, AF 6886, AF 6887, AF 6888, AF 6889, AF 6890, AF 6892, AF 6893, E 12569, E 12570, E 13044, E 33650, MNC 1693, MNC 1694, MNC 1696, MND 2047, N 2732 1, N 2732 3, N 2733 3.
43. Protein-based: AF 6891, MNC 1695, MNC 1697, MND 2029, N 2733 1; probably sugar-based: N 2732 2, N 2733 2.
44. It should be noted that all panels of gods analyzed thus far have water-based binders (gum, glue, or egg); see the Annex B chart in Mathews and Müller 2016; also see Borromeo et al. 2020, 97; Thomas and Brunel-Duverger 2023, 122–24.
45. Vagnini et al. 2009 proposes characteristic bands for several protein binders, particularly for the (1ν C=O amide I + amide II) vibrational band positioned at 2173 nm for casein, 2176 nm for whole egg, 2176 nm for skin glue, and 2178 nm for egg white.
46. We are hoping to carry out carbon-14 dating to get more data. Evidence suggests a modern date because one of the wax drops covers a paint loss.
47. These are iron-based materials easily characterized by MA-XRF.
48. In one case (MNC 1694), observations made under binocular magnification show bright orange particles, identified with hyperspectral imaging in the visible and near infrared range (HSI-VNIR) as minium, associated with brown earth. While we detected traces of copper (without being able to be more precise) on AF 6724 to render the hair outline, eyebrows, and chin, these resemble the cursory brushstrokes outlining the figure highlighted with visible-induced visible luminescence (VIVL) imaging technique in Mayberger et al. 2020, 80–81.
49. AF 6887, AF 6891, MNC 1694, MNC 1695, N 2733 2, N 2733 3.
50. Additional in-depth structural analyses would have been necessary to be conclusive. Dandrau 1999.
51. AF 6723. For another example of use on lips, see Salvant et al. 2018.
52. AF 6893; unfortunately, the portrait is too damaged to confirm this.
53. $\text{KFe}_3(\text{SO}_4)_2(\text{OH})_6$, on AF 6882, E 12569, MNC 1693, MND 2047, N 2733 2, N 2733 3.
54. MNC 1695, MNC 1697, N 2733 1.
55. MND 193 - E 10815. All details have been revealed by MA-XRF. Arsenic-based pigment is used here for some outlines and details and to depict glittering elements, such as the cuirass and spear, and the brooch and head jewel hidden under gold leaves. See Thomas and Brunel-Duverger 2023, 124.
56. Thiboutot 2020. We observed the same correlation between the use of Egyptian blue and wax binders for mummy portraits; however, both panels of gods show Egyptian blue despite a protein-based polychromy.
57. On some areas, hyperspectral imaging in visible and near infrared range (HSI-VNIR) shows Egyptian blue mixed with green earth. See Thomas and Brunel-Duverger 2023, 124.
58. All identified as indigo by infrared false color imaging (IRFC), confirmed with HSI-VNIR. Clavi on MNC 1693, MNC 1695, and MND 2029 appear more black than blue.
59. M. Ganio found that Egyptian blue was used imperceptibly for underdrawings and highlights, and that it was mixed with white pigment to enhance specific details, such as eyes and tunics (Ganio et al. 2015); similar observations are made in Salvant et al. 2018. On portrait E 12570 we noticed a peculiar distribution of Egyptian blue, which could be used as underdrawing or mixed with other materials for outlining contours.
60. Scott 2016.
61. We found madder lake frequently used for complexion and pink accents such as lips or cheeks, on AF 6723, AF 6885, AF 6886, MND 193 - E 10815, MNC 1697, MND 2029, N 2732 2, N 2733 1, N 2733 2, RFML.AE.2020.8.1. The first three are encaustic, while others are tempera.
62. See Cardon et al. 2018 for perspective regarding the use of this dye in Greco-Roman Egyptian society, particularly in the making of cosmetics and dyed textiles.
63. Minium added to madder lake has been identified using HSI-VNIR on one case: AF 6889.
64. Mixture of madder lake and indigo for bright purple clavi: Salvant et al. 2018. Mixture of madder lake and Egyptian blue: Cartwright and Middleton 2008; Sand et al. 2017.
65. The discrimination between Egyptian blue and indigo can be challenging due to the absorbance maxima peak of their reflectance spectrum being in close range. Therefore, the Kubelka-Munk approximation was applied to every data cube containing purple to better discriminate the localization of both blue pigments, which was made possible by the linear

- unmixing algorithm of the Envie software. The Envie software Linear Spectral Unmixing tool is used to determine the relative abundance of materials that are depicted in hyperspectral data cubes based on the materials' spectral characteristics. Here it was applied on a data cube transformed with the Kubelka-Munk approximation on the 450–750 nm range, after application of a continuum removal. To increase the signal-noise ratio, pixels were aggregated 5×5. Each false color map is superposed to the RGB image (R=700 nm, G=546 nm, B=469 nm) from the entire VNIR data cube (400–1000 nm).
66. Four portraits: AF 6723, AF 6883, AF 6886, N 2733 3.
 67. Five portraits: AF 6887, AF 6888, E 12570, MNC 1695, N 2733 2.
 68. Orchil was identified by HSI-VNIR on MNC 1694 by its characteristic spectral pattern (Aceto et al. 2014).
 69. Mainly green earth, copper green, Egyptian blue and yellow, and mixtures of indigo and yellow ochre or indigo and orpiment (Roberts 2020, 34–45).
 70. AF 6724, AF 6886, AF 6888, MNC 1694, MNC 1696, MND 2047. We join J. Dyer and N. Newman (Dyer and Newman 2020, 66) in observing that copper-based organometallic greens are used only in encaustic portraits.
 71. AF 6884 and E 12569. On AF 6884, MA-XRF shows the presence of K associated with Fe-rich green, suggesting the possible use of glauconite ((K,Na)(Fe³⁺AlMg)₂(Si,Al)₄O₁₀(OH)₂). This is not obvious for E 12569, where green earth appears to be mixed with Egyptian blue. Note that E 12569 combines copper-green for rendering emeralds with green earth for the clavus.
 72. See Thomas and Brunel-Duverger 2023, 124.
 73. Colinart et al. 2001, 58–65. The gold leaf covers and hides the pearl necklace.
 74. See Thomas and Brunel-Duverger 2023, 124.
 75. N 2732 1, N 2732 3, AF 6885, AF 6723. All are wax-based, but the choice of materials differs more than one might guess from comparing similar-looking images with similar dates and provenience (in terms of wood, use of Egyptian blue, and rendering of flesh tones). N 2732 3 is painted on linden, Egyptian blue in the background and flesh tones, madder lake for clothing. N 2732 1 is also painted on linden but with no Egyptian blue, iron-based materials for flesh tones, and madder lake for clothing. AF 6885 is on beechwood with Egyptian blue for the clavus and madder lake for flesh tones and clothing. AF 6723 is also on beechwood, and a combination of madder lake and Egyptian blue is used for flesh tones and clothing and cinnabar for the upper lip.
 76. Moreau et al. 2023; Moreau et al. 2024.
 77. According to Clementi et al. 2008, madder lake has a maxima emission band between ~ 590 nm < $\lambda_{em,max}$ < ~ 605 nm, while Verri et al. 2010 identified for Egyptian blue $\lambda_{em,max} = 910$ nm.
 78. Delaney et al. 2017.
 79. Vagnini et al. 2009.
 80. Cucci et al. 2019.
 81. van Asperen de Boer 1968.

Three Romano-Egyptian Panel Paintings in the Ny Carlsberg Glyptotek

*Jens Stenger
Cecilie Brøns
Richard Newman
Caroline R. Cartwright*

Roman-era panel painting is mostly known by funerary mummy portraits from Roman Egypt, of which only about a thousand are preserved in museums and private collections worldwide. However, other types of panel painting on wood have also survived from the Roman period in Egypt, such as the so-called votive panels. Objects of this type are usually defined by three parameters that differ from the mummy portraits: the use of framing, their function as religious votives, and their choice of motifs. While human individuals are rendered in the mummy portraits, gods and goddesses are considered the primary subjects of the corpus of votive panel paintings from Roman Egypt. The divinities rendered on the panels derive from three distinct pantheons: the local, ancient Egyptian pantheon; the Greco-Roman pantheon; and finally, a newly defined pantheon of divine military gods from the Syro-Arabian caravan routes.¹

Panel paintings of a votive character are extremely rare, as manifested by the very few examples documented in public and private collections around the globe. Vincent Rondot assembled a corpus of fifty-five votive panel paintings, while Thomas Mathews assembled a corpus of fifty-nine examples.² Six of these panels, included in both corpora of votive paintings, have been described as lost

since their discovery.³ One of these six panels, however, is curated safely at the Ny Carlsberg Glyptotek (ÆIN 711). Mathews's corpus includes five panels that are not included in Rondot's: the famous portrait of Septimius Severus and his family;⁴ a panel depicting a goddess in mourning;⁵ a panel rendering the goddess Fortuna-Tyche;⁶ one depicting the goddess Nike, recovered at Dura-Europos;⁷ and a fragment (no. 230) from a frame in Tebtunis.

Mathews omits a painting from the corpus collected by Rondot depicting Isis and Hathor,⁸ which he believes is not a panel painting but instead part of a coffin or a type of furniture.⁹ Such a distinction might be hard to make for many of these often poorly preserved artifacts, which are frequently fragmentary, and some lack exact provenience. Indeed, the function of many of these votive panel paintings is under debate, primarily because of the contexts in which they were once used. Their find spots (where known) indicate that they had cultic functions in both temples and domestic situations, whether in neighborhood chapels or as domestic shrines.¹⁰

Scholarship on ancient panel painting differentiates between these two categories (mummy portraits and

votive panels) and a third category, funerary portraits. The latter render human individuals, but they were not intended for insertion into mummies. Rather, they were displayed in tombs or private homes, where they were probably part of an ancestral cult.¹¹ Yet, such a differentiation is not always straightforward, and there is often confusion in scholarship between these three proposed main types of Romano-Egyptian panel painting: mummy portraits, funerary portraits, and votive panel paintings. Moreover, these three categories seem to exclude portraits of living subjects and other portraits of a noncultic character, as well as other types of panel painting, such as those painted on furniture or the like, which as mentioned can be extremely hard to differentiate from other types of panel painting. This difficulty is illustrated by the four painted wooden panels on a fourth-century sarcophagus in the J. Paul Getty Museum.¹² The sarcophagus is made with cedar of Lebanon (*Cedrus libani*) wood and painted using the tempera technique with the same pigments and binders commonly used for panel paintings.¹³ In cases where only parts of these panels have been preserved—for instance, those rendering a portrait of the deceased—it would be hard, if not impossible, to discern them from funerary portraits. Thus, there is a pressing need to develop proper terminology and categories for identifying the different types of paintings created on wood and methods for discerning them.

THE THREE PANEL PAINTINGS IN THE NY CARLSBERG GLYPTOTEK

Our current study focuses on three panel paintings from the collections of the Ny Carlsberg Glyptotek, Copenhagen: two votive panels and one funerary portrait. All three paintings were acquired in Egypt by the Danish Egyptologist Valdemar Schmidt (1836–1925) (fig. 3.1). Schmidt knew the brewer and museum founder Carl Jacobsen, who was a dedicated collector of ancient Greco-Roman and Egyptian art. In fact, Schmidt became Jacobsen's personal buyer of Egyptian antiquities, and these established the Egyptian collection of the Ny Carlsberg Glyptotek. The panels were acquired in 1892, which makes them among the earliest examples of such paintings acquired for museum collections worldwide. (The earliest acquisitions were made by the Egyptian Museum in Cairo in 1889 and the British Museum in 1891.)¹⁴ Unfortunately, as with many other artifacts acquired in Egypt during the nineteenth and early twentieth centuries, the exact provenience is unknown; in line with the museum's acquisition protocols at the time, it is noted only that they are from Egypt.



Figure 3.1 Portrait of the Danish Egyptologist Valdemar Schmidt (1836–1925). Photo: Friedrich Wilhelm Schmidt. Courtesy: The Royal Danish Library

Previous publications on the three paintings are primarily based on old black-and-white photos, and this fact has inevitably resulted in some details being overlooked or misinterpreted. Moreover, one of the panels (ÆIN 711) was, for unknown reasons, considered lost and is therefore mentioned only briefly in previous studies. Additionally, these three panels have never been on display but instead safely kept in museum storage. This study aims to bring them back to light.

ÆIN 685

The first panel, ÆIN 685, consists of the left half of a votive painting (fig. 3.2), composed of two well-preserved boards of approximately the same width assembled vertically.¹⁵ On the left, top, and bottom sides of the painting is an unpainted band, which corresponds to the original wooden frame, now lost. Holes for the attachment of the frame are placed at irregular intervals along the unpainted border. Original ancient strips of fabric are glued onto the joints of the boards, to cover them and to consolidate the attachment of the two slats.



Figure 3.2 Left part of a votive panel painting depicting the goddess Nemesis and the god Harpocrates. 50.2 × 22.7 cm (19.8 × 8.9 in.). Ny Carlsberg Glyptotek, inv. no. ÆIN 685. Photo: Anders Sune Berg



Figure 3.3 Fragment of a votive panel painting rendering a female bust, a winged griffin, and two minor divinities. 53 × 18.5 × 2 cm (21 × 7.3 × 0.75 in.). Ny Carlsberg Glyptotek, inv. no. ÆIN 711. Photo: Anders Sune Berg

The woman, who is the main subject of the panel painting, has been interpreted as the goddess Nemesis, primarily due to the cubit (measuring stick) she holds in her right hand. The cubit was the attribute of Nemesis, one of the most-often-depicted deities in the corpus of Egyptian panel paintings. Based on his dress and attributes (garland and situla), the smaller, haloed male figure in the upper-left corner has been convincingly interpreted as the Hellenistic child-god Harpocrates.

ÆIN 711

ÆIN 711 is a fragment that constitutes the left part of a panel painting (fig. 3.3).¹⁶ Two adjoining boards of unequal widths are preserved and assembled vertically. The board to the right survives in its entire height and width, while only the upper left and right parts of the left board are preserved. Along the left and the upper edge is an unpainted band, corresponding to the original frame, now lost. Two pegs oriented at a 45-degree angle are preserved in the right side of the rightmost board, attesting to the

attachment of a third board to the right, which is now missing.

In the top register of the painting, two human figures are depicted. To the left is a male figure who holds a double axe and is dressed in military garb. He is probably one of the armed gods, perhaps Heron, rendered on several other votive panel paintings. The smaller female figure to the right of the armed god has a lunar crescent above her head, which might indicate her status as a goddess. In the midregister is the griffin of Nemesis, facing toward the center of the painting. Only parts of the griffin are preserved, including the head and most of the wings. At the lower register of the painting are the remains of what were probably the busts of one or two goddesses.

ÆIN 686-687

The last panel is the right section of a panel painting, consisting of three well-preserved boards of approximately the same width, assembled vertically (fig. 3.4).¹⁷ It has large irregular paint loss running vertically down the panel,



Figure 3.4 The central and right part of a funerary portrait of a man and a griffin with the wheel of Nemesis. 67.5 × 9.7/13.8 × 4 cm (25.9 × 3.8/5.4 × 1.0 in.). Ny Carlsberg Glyptotek, inv. no. ÆIN 686-687. Photo: Anders Sune Berg

separating the painting into two parts. The original panel, when complete, would probably have included two more boards to the left, indicated by the preserved dowels along the left side and the incomplete composition. On the right, top, and bottom edges of the painting is a narrow unpainted band, corresponding to the original wooden frame, now lost.

The panel depicts a half-length frontal representation of a man dressed in a white tunic and white mantle. To the right of the man's head is a winged griffin with the wheel of Nemesis. The portrait has stylistic similarities with contemporary mummy portraits, yet this panel, due to its large size, thickness, and shape, was likely never attached to a mummy but most probably functioned as a stand-alone funerary portrait, commemorating the deceased.

IMAGING METHODS

A Canon EOS 5D Mark IV camera body was modified to extend its sensitivity from the ultraviolet A (UVA) to the

near-infrared (NIR) spectral regions. For multiband imaging (MBI), this camera body was employed in combination with a Canon EF 50 mm f/2.5 Compact Macro lens. The following filters were used for image acquisition:

- ◆ XNite CC1¹⁸ for visible light (VIS) photography
- ◆ XNite CC1, PECA 918, and Tiffen Haze 2E for ultraviolet-induced visible fluorescence (UVF) imaging
- ◆ Schott RG830 for infrared-reflected imaging (IRR) and visible-induced infrared luminescence (VIL) imaging

False color infrared (FCIR) images were created by overlaying the VIS and IRR images and substituting channels in the conventional way: green to blue, red to green, and infrared to red. The subtraction of an image at 635 nm shot with a MidOpt BP635 filter from one shot at 735 nm (MidOpt BP735) uncovered information about the possible presence of indigo.¹⁹ For this imaging mode, the abbreviation MBR (multiband reflectance image subtraction) is used.

Radiation sources employed were:

- ◆ Incandescent tungsten lamps in combination with soft box diffusers for VIS and IRR
- ◆ EXC-LED RGB lamps (470 nm, 525 nm, and 629 nm) for VIL
- ◆ Hoenle UVASPOT 400/T lamps filtered with a Schott UG2A glass for UVF

The X-Rite ColorChecker Passport Photo 2,²⁰ Target-UV from UV Innovations,²¹ and a 99% Spectralon diffuse reflectance standard was included in all images.

Although multiband imaging is not an analytical tool used for chemical identification, it can reveal important characteristics and differentiate between different painting materials.

ÆIN 685 Imaging

Comparing the visible light photograph and the UVF image, it immediately becomes evident that the painter used two different red pigments (fig. 3.5A–B). In Nemesis's garment, the lighter pink areas fluoresce orange, suggesting the presence of an organic red lake pigment. Other areas exhibiting this fluorescence are in the details of her face, including chin, lips, nose, and around her eyes. Moreover, it appears that a minute amount of red lake was included in the paint used for her hairstyle (fig. 3.6A–B). Additionally, Harpocrates's sash/stole, as well as his crown/garland, emit orange fluorescence upon UV



Figure 3.5 Multiband imaging of panel ÆIN 685: (A) VIS, (B) UVF, (C) MBR, (D) IRR, (E) FCIR, (F) VIL with a small contribution from IRR. Photo: Jens Stenger

excitation (fig. 3.7A–B). Similar fluorescence characteristics are observed for the light pink object (perhaps a textile) in his proper left hand and the rendering of his proper right thigh. The other red pigment, used in the folds and shades of Nemesis’s garment, does not fluoresce under UV excitation. Further observations in the UVF image are the white to off-white fluorescence of the exposed ground, for example in Hippocrates’s face and the fibers of the textile strips used to reinforce the panel joints.

The IRR image (fig. 3.5D) suggests that carbon-based black was used for Nemesis’s staff, parts of her necklace, and hair (fig. 3.6D), for the gray background, and for Harpocrates’s sash/stole, staff, eyes, and locks of hair (fig. 3.7D).

VIL imaging is highly sensitive to Egyptian blue and its spatial distribution.²² In the VIL image of ÆIN 685, many particles appear white from the strong infrared luminescence characteristic of Egyptian blue, which indicates that it was likely used in the paint mixtures to render Nemesis’s pink garment (fig. 3.5F). In the mixture with the fluorescing red lake pigment there is much more Egyptian blue compared to the paint containing the nonfluorescing red. The blue-gray clavus running vertically across Nemesis’s garment also exhibits a high density of



Figure 3.6 Multiband imaging of a detail of ÆIN 685 rendering the head of Nemesis: (A) VIS, (B) UVF, (C) MBR, (D) IRR, (E) FCIR, (F) VIL with a small contribution from IRR. Photo: Jens Stenger

Egyptian blue particles (fig. 3.6F). The skin color of her face and the brown of her hair include far fewer particles of Egyptian blue, while the pigment is absent in the paint of the gray background and the black staff.

Very few particles of Egyptian blue are dispersed irregularly over the figure of Harpocrates (fig. 3.7F), probably indicating that their presence in this area of the panel is unintentional. FCIR images show a reddish tone in the clavus (fig. 3.5E), Nemesis’s hair, part of the necklace (fig. 3.6E), and in Harpocrates’s headgear (fig. 3.7E), suggesting the presence of indigo.

The spatial mapping of indigo was also attempted, using MBR. This tool works based on the strong signal increase when comparing the reflectance values of the spectrum of indigo at 635 nm in the visible region and 735 nm in the NIR. It can be visualized by subtracting two images captured with narrow band-pass filters at the two respective wavelengths. However, the wood in areas of paint loss also yields an MBR signal, as observed previously on mummy portraits.²³ Salas has pointed out additional



Figure 3.7 Multiband imaging of a detail of ÆIN 685 rendering the figure of Harpocrates: (A) VIS, (B) UVF, (C) MBR, (D) IRR, (E) FCIR, (F) VIL with a small contribution from IRR. Photo: Jens Stenger

shortcomings of the tool,²⁴ demonstrating that MBR cannot differentiate between indigo, Maya blue, cobalt-containing pigments, and lapis lazuli or ultramarine.

With these false positives as well as the geographic region and creation time in mind, the MBR images of ÆIN 685 were studied critically (figs. 3.5C, 3.6C, and 3.7C). Positive MBR signals were found in several parts of the painting, including the clavus of the goddess's tunic and her mantle, which is arranged horizontally across her abdomen (see fig. 3.5C). Interestingly, the MBR image exposes decoration in the shape of a cross at the uppermost part of the clavus on her proper right shoulder, which is not clearly discernible in visible light (see fig. 3.6C). The MBR image also reveals elevated counts in some parts of her hair and in the blue stones in her necklace. Moreover, the two dots on Harpocrates's forehead, his wreath/headgear, sash/stole, and the shading of his white garment near his left thigh are MBR positive (see fig. 3.7C). Additional analysis

using Fourier transform infrared spectroscopy (FTIR) detected indigo on Nemesis's gray clavus.²⁵

A detail of the raking-light image (fig. 3.8) gives a good impression of the panel's state of preservation. The most severe paint losses have occurred near the join of the two vertical slats. This was caused by the detachment, including a large loss of the textile strip that had reinforced the join. Some of the textile is preserved at the bottom of the join and on the right edge of the right slat, which can be seen at the edges of the paint losses. The paint itself shows widespread cracking, resulting in islands of paint that delaminate on the edges into concave forms, a phenomenon often described as *cupping*.

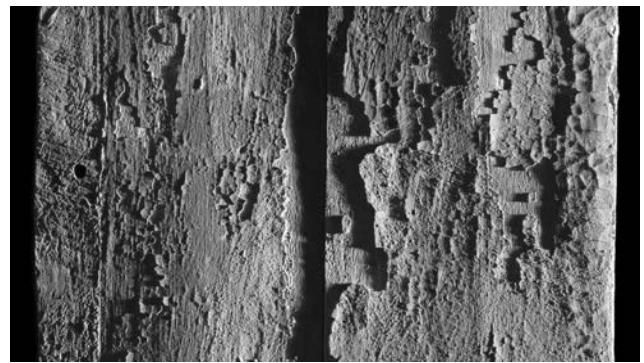


Figure 3.8 Detail of ÆIN 685 in raking light. Photo: Jens Stenger

ÆIN 711 Imaging

Approximately half of the paint is lost on panel ÆIN 711 and this, together with its fragmentary state, makes it hard to fully understand and interpret the original motif. The rendering on the lower half of the painting is particularly difficult to decipher. MBI helps in better understanding the original motif as well as the use and distribution of certain colorants.

UV-induced orange fluorescence strongly suggests the presence of an organic red lake pigment (fig. 3.9A–B). This colorant is used for highlights on the folds of the pink garment in the lower register. Its application on top of a nonfluorescing red is very similar to that in ÆIN 685, except that here the paint containing red lake exhibits two distinct fluorescence strengths, which is indicative of red paints mixed with different concentrations of red lake. Rendering of the female bust is recognizable by the right shoulder still visible at the bottom right. A gray clavus is visible on the tunic, and a whitish mantle is arranged across the figure's abdomen. Her sleeve is decorated with a white fringe at the opening. Moreover, she wears a gold

snakelike bracelet with two twisted rows. Red lake is also used for the red mantle and parts of the headgear of the armed god (only visible near his right temple) and the tunic of the neighboring smaller female figure to the right in the upper register. The UVF image (fig. 3.9B) also reveals a whitish fluorescence, which occurs in areas of paint loss where the white ground is exposed.

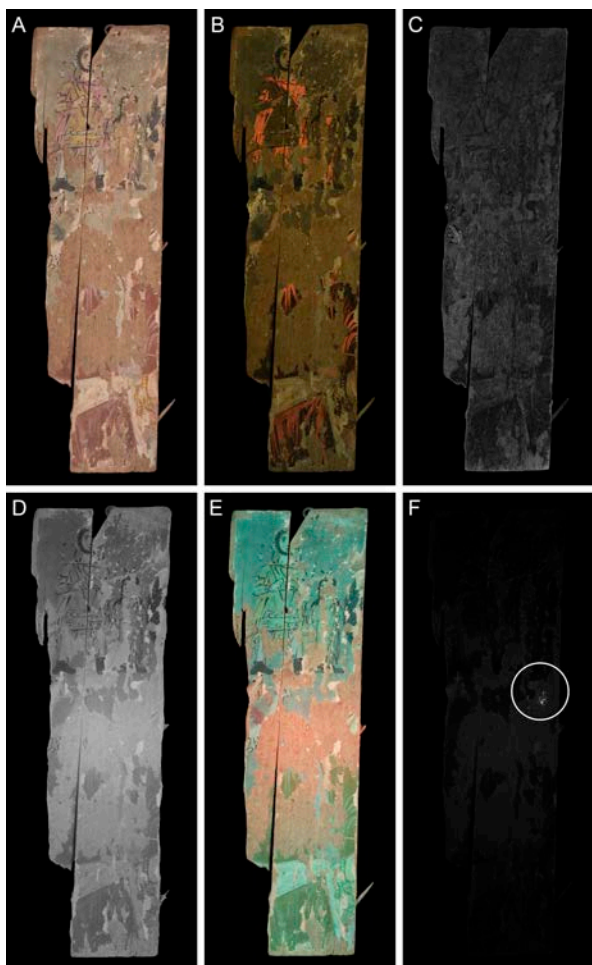


Figure 3.9 Multiband imaging of the panel ÆIN 711: (A) VIS, (B) UVF, (C) MBR, (D) IRR, (E) FCIR, (F) VIL with a small contribution from IRR. Photo: Jens Stenger

The IRR image enhances the contrast of the black line drawing, which defines the two smaller figures in the upper half of the panel, suggesting the use of a carbon black (fig. 3.9D). The elegant lines are executed with a fluid medium on top of the yellow, pink, and gray color fields. Black lines with high IR absorbance also appear in the middle-left part of the painting, which represents what is left of the outline of the teats, legs, head, and beak of the griffin (fig. 3.10). The IRR image also shows the use of carbon black for the left half of a female hairstyle, with visible strands of black hair arranged in a bun to the right

of the small female divinity. In contrast, the poorly preserved bust in the lower half of the painting does not show any carbon black or an outline in another material.

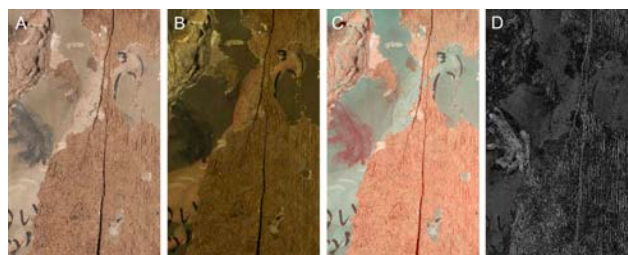


Figure 3.10 Multiband imaging of the griffin on ÆIN 711: (A) VIS, (B) UVF, (C) FCIR, (D) MBR. Photo: Jens Stenger

VIL imaging of the panel (fig. 3.9F) shows a cluster of Egyptian blue near the middle-right side of the panel. However, this concentration is outside the preserved paint and is therefore probably the result of ancient or modern contamination. The preserved original paint shows no evidence of the use of Egyptian blue. The MBR image suggests that indigo was used only to render one specific detail of this panel—the wings of the griffin (figs. 3.9C and 3.10D)—and gave weak signals in areas of exposed wood. In the FCIR image the wing is more apparent due to its false red color (figs. 3.9E and 3.10C).

A detail of the panel in raking light highlights the surface structure of the wood and its grain (fig. 3.11). It becomes clear that the support was not sanded before the application of the ground layer, in contrast to ÆIN 685, where the exposed wooden support is smooth (see fig. 3.8). The cupping is less pronounced, but there are instances of tenting, where paint slabs form a triangular, tent-like structure due to the shrinkage of the underlying support caused by environmental conditions.

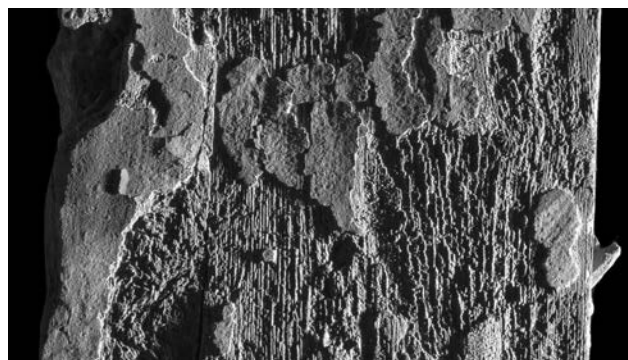


Figure 3.11 Detail of ÆIN 711 in raking light. Photo: Jens Stenger

ÆIN 686-687 Imaging

The last painting is the portrait of a man and has a very different palette from the two panels discussed previously, as is apparent in the visible light photograph showing mostly white and earth colors (fig. 3.12A). The area of the white garment has no additional paint application above the ground layer, giving it the same appearance as the painting's background.

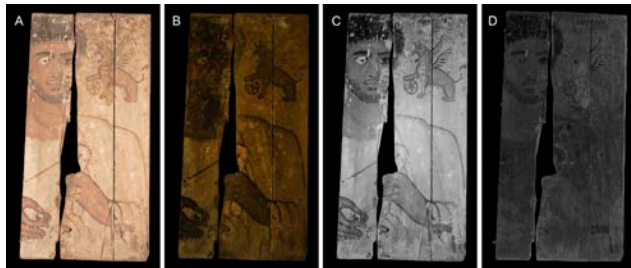


Figure 3.12 Multiband imaging of the panel ÆIN 686-687: (A) VIS, (B) UVF, (C) IRR, (D) MBR. No significant VIL signal was detected (not shown). Photo: Jens Stenger

MBI exhibits a finer and additional differentiation of colorants compared to the information obtained with only visible light. UVF imaging also detects an orange emission from a lake pigment (fig. 3.12B). But the use of the red lake here is much more selective compared to the other two panels. It occurs in the purple decorative element on the subject's mantle at the proper left cuff and in details of his face, including lips, cheeks, and around his nose. In his left hand he holds a pink floral wreath; the UVF image shows that it was also rendered with a paint containing red lake. It was applied in distinctly visible round brushstrokes that echo the warm brown marks of the outline of the wreath.

The skin tones and the griffin do not fluoresce at all, while the white garment and background emit a weak brownish fluorescence. The warm brown outlines of the garment and its folds have been changed and corrected by the artist during the painting process, as illustrated by several additional lines, which become visible under UV radiation. These compositional changes are also detected in the IRR image, though more faintly (fig. 3.12C). In contrast, the hair, beard, eyes, and eyebrows of the man, as well as the wings of the griffin, appear very dark—as expected for a carbon-based black pigment. The MBR image has very low contrast (fig. 3.12D).

Additionally, the multiband imaging reveals an inscription on the top right edge, which is easily missed in the visible light image. In particular, the IRR and MBR images make

the original inscription clearer (fig. 3.13C–D). In the infrared image the contrast is greatly enhanced, while in the MBR image the soiled background has a more flat and homogeneous appearance, improving the readability further. Unfortunately, the inscription is still unreadable, regardless of the imaging tool used. It is most probably in Greek, which appears to have been the dominant language for inscriptions on Romano-Egyptian panel paintings. However, most panels are without inscriptions, which might also relate to the often-poor preservation and the loss of the original frames. Thus, only six votive panels rendering various divinities carry extant inscriptions in Greek.²⁶ The inscriptions primarily appear to be dedicatory, mentioning the name of the dedicant and the recipient deity. Inscriptions could also be written in Demotic, as attested by a votive panel from Tebtunis depicting the god Harpocrates.²⁷ In comparison, some mummy portraits carry inscriptions, which provide the names—often Greek—of the deceased rendered in the portrait.²⁸

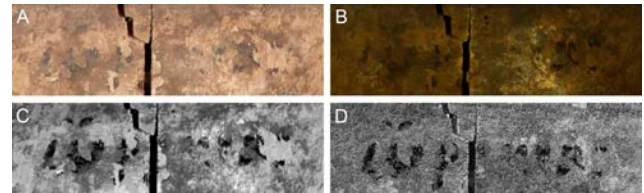


Figure 3.13 Multiband imaging of the inscription on ÆIN 686-687: (A) VIS, (B) UVF, (C) IRR, (D) MBR. Photo: Jens Stenger

MBI also reveals a significant detail of the decoration on the man's garment. In the area of the lower-right corner of the panel, at the man's left underarm, on the mantle, is a so-called gammadion (fig. 3.14A), a decorative figure composed of a capital gamma (Γ) in the shape of a right angle. The UVF image (fig. 3.14B) shows that a red lake was used to render it. The IRR image (fig. 3.14C) makes it clear that the gammadion was further ornamented with two white parallel, narrow lines at each end. The horizontal double line only becomes visible in the IRR image. The depiction of gammadia is rare but not unknown in Egyptian panel painting, as well as in mummy portraits.²⁹ Mantles with gammadia were often worn by members of the early Christian and Jewish communities, as depicted, for example, in the wall paintings of the early Christian catacombs in Rome and in the synagogue in Dura-Europos.³⁰ Gammadia are also seen on the contemporary Romano-Egyptian stucco mummy coffins, such as the second-century mummy coffin of Teuris from Tuna el-Gebel.³¹

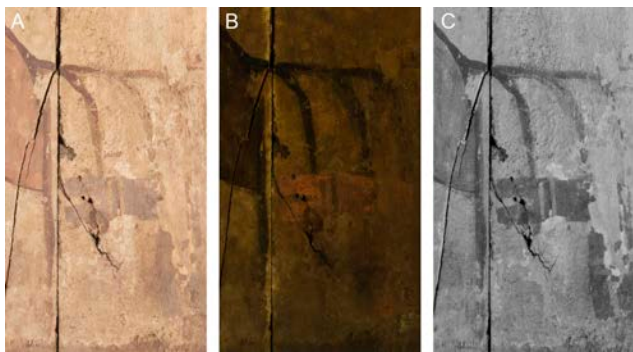


Figure 3.14 Multiband imaging of the gammadion on \AEIN 686-687: (A) VIS, (B) UVF, (C) IRR. Photo: Jens Stenger

In his right hand, the man holds a brown pine cone, a common attribute, like the funerary wreath in his other hand. Both objects are also observed in the iconography of contemporary mummy portraits.³² Centrally placed at the bottom of the panel is an unidentified object, possibly an incense burner.

For \AEIN 686-687, the VIL image (not illustrated) showed no evidence of the use of Egyptian blue, and it seems that blue was not used for this panel painting at all. Finally, the surface texture of the painting was documented in raking light (fig. 3.15). In addition to the original brushwork related to the ground application one can observe the paint lifting upward, away from the support, due to the contraction of the wood.



Figure 3.15 Detail of \AEIN 686/687 in raking light. Photo: Jens Stenger

PIGMENTS AND PAINTING TECHNIQUES

Multiband imaging provides a broader foundation for the discussion of the iconographic vocabulary and painting techniques used in Romano-Egyptian panel painting compared to what visual examination and visible light

photography alone can provide. The similarity of red lake highlights on top of red ochre in the pink garment, the gray clavus, and the very light, off-white flesh color of the female figures in \AEIN 685 and \AEIN 711 is striking.³³ Both figures also wear a bracelet on their proper right wrist in the form of a snake with yellow as the base color (fig. 3.16). Each snake makes two turns around the wrist. In both paintings the bracelet's turn toward the elbow is undulated, while the turn toward the hand is straight. On \AEIN 685 the head of the snake rests on top of the wrist, while on \AEIN 711 the head comes farther around the arm toward the center of the wrist. On the former, the yellow color is modulated by a lighter and a darker line, while on the latter the variation is applied in a dot pattern using similar colors.

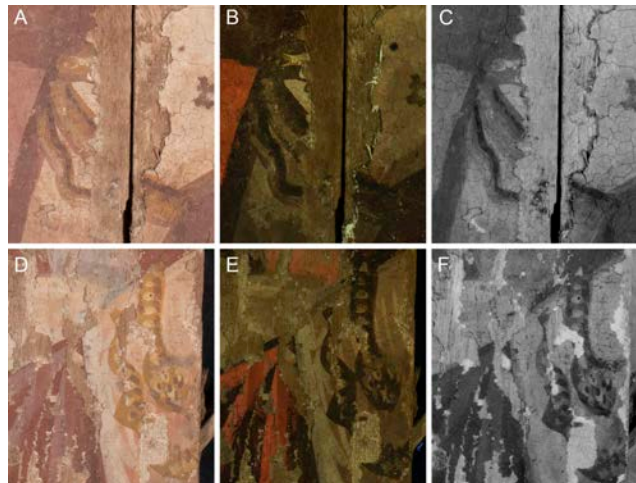


Figure 3.16 Comparison of multiband imaging of the snake bracelets on \AEIN 685: (A) VIS, (B) UVF, (C) IRR; and \AEIN 711: (D) VIS, (E) UVF, (F) IRR. Photo: Jens Stenger

When comparing the three individual panels it becomes clear that the two so-called votive panels (\AEIN 685 and 711) have several aspects in common when it comes to the pigments used. In contrast, the funerary portrait (\AEIN 686-687) employs a slightly different, somewhat simpler palette. For example, both votive panels employ indigo, which is absent on the funerary portrait.

Only \AEIN 685 uses Egyptian blue, which is somewhat surprising, considering the widespread use of this pigment during antiquity. However, Egyptian blue was reported on only 64 out of 384 panels in the APPEAR database—although it should be noted that the actual number is probably higher, as this only accounts for panels that have been analyzed.³⁴

WOOD

Each of the three paintings' supports is made from a different kind of wood (fig. 3.17). *Ziziphus spina-christi* (sidr) wood was identified for ÆIN 685, *Tamarix* sp. (tamarisk) wood for ÆIN 711, and *Ficus sycomorus* (sycomore fig) wood for ÆIN 686-687. Previously, *Ziziphus spina-christi* has been identified mostly in dowels and tenons, and occasionally for coffin panels—all used in the manufacture of pre-Romano-Egyptian coffins. Sidr is native to Egypt but is also found in southern Mediterranean Europe, the Middle East, and Arabia. It is a dense, hard, resilient wood of high quality.

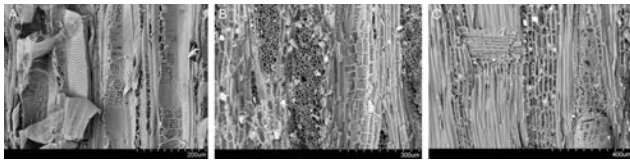


Figure 3.17 VP-SEM images of the wooden supports of ÆIN 685 (A), ÆIN 711 (B), and ÆIN 686-687 (C). Photo: Caroline R. Cartwright, Department of Scientific Research, British Museum. © The Trustees of the British Museum

Tamarisk is unlikely to have been the optimal choice of timber for painted panels, as the coarse, fibrous texture of this wood shows little resistance to attack by fungi and insects. Nonetheless, its properties include medium bending and compression strength and moderate hardness. With appropriate tools, tamarisk timber would have been easy to work and would have been readily obtainable from the vegetation of the Nile riverbank.

The choice of the indigenous sycomore fig wood for ÆIN 686-687 is rather paradoxical, since it is light, not of high quality, and very prone to insect and fungal attack.³⁵ In earlier periods, applying thick layers of gesso and pigments to cover coffins' wood planks reduced these drawbacks, and *Ficus sycomorus* is one of the relatively few local trees that grew sufficiently tall to yield the long lengths of timber suitable for such planks. Romano-Egyptian painted panels made from sycomore fig needed to be much thicker than those of other woods, and they could not easily be made to curve snugly over the mummy head in the same manner as a thin limewood panel. Indeed, the slats used for ÆIN 686-687 are 2.4 cm—much thicker than most other panel paintings.³⁶

The wood types found in this study are ones native to Egypt, perhaps because the application had a lesser demand for quality than mummy portraits. In comparison to other woods, sycomore fig, sidr, and tamarisk wood make up only a small fraction of the British Museum's

database of mummy portrait supports (see Cartwright, in this volume). The three Getty panels from the first century CE—portrait of a man, Isis, and Serapis, which have often been discussed as a triptych—are executed on sycomore fig, like ÆIN 686-687.

CONCLUSIONS

The preceding sections have presented investigations by multiband imaging of three exceptional Romano-Egyptian panel paintings, and this study has generated significant insights into the materials used for their construction that hopefully will contribute to further research into this rare corpus of ancient Egyptian art.

When comparing the votive panels to mummy portraits, it becomes clear that they are closely related, both technically and stylistically. Yet the panels examined here differ from this corpus in the use of locally sourced wood, instead of imported limewood, and by the slightly different palette employed, for example in excluding the use of green and using blue in a very limited way. However, the three panels do not express an entirely coherent palette or painting techniques and differ from one another. The two votive paintings display a slightly more extensive palette, while the funerary portrait uses fewer colors and different pigments, primarily earth pigments.

The three panels examined here, although few in number, provide insights into artistic painting from religious contexts during the Roman period, a subject about which we know, to date, very little. Moreover, despite the widespread use in various contexts of painting on wood, almost no examples are preserved from the Mediterranean littoral dating from the Roman period (or earlier).³⁷ Thus, Romano-Egyptian panel paintings can potentially provide insights into the now-vanished paintings on wood from other areas of the Roman Empire and in that way offer a better understanding of the artistic intersections between the different regions of the Empire during the first three centuries CE.

ACKNOWLEDGMENTS

The present study forms part of the interdisciplinary research project Sensing the Ancient World: The Invisible Dimensions of Ancient Art, which has been generously funded by the Carlsberg Foundation. We would like to take the opportunity to express gratitude to the Ny Carlsberg Glyptotek, especially conservator Rebecca Hast and the technical staff, for facilitating the study of the panels. Jens Stenger is also grateful for discussions with Tom Egelund

regarding the assessment of the paintings' condition with raking light imaging. Finally, we are extremely grateful to the organizers of the 2022 APPEAR conference, Marie Svoboda and Ben van den Bercken, and to the participants for their insightful comments.

NOTES

1. Rondot 2015; Mathews and Müller 2016, 11.
2. Rondot 2015, 238–39; Mathews and Müller 2016, 240.
3. Staatliche Museen, Ägyptisches Museum, Berlin, inv. no. 17957 (two door panels); Ashmolean Museum, Oxford, inv. nos. 1922.237–239.
4. Antikensammlung, Altes Museum, Berlin, inv. no. 31329.
5. British Museum, inv. no. 1975,0728.1.
6. Louvre, inv. no. AF 10878-79.
7. Yale University Art Gallery, New Haven, inv. no. 1929.288.
8. Staatliche Museen, Ägyptisches Museum, Berlin, inv. no. 12712.
9. Mathews and Müller 2016, 10, 240.
10. Mathews and Müller 2016, 20. For a thorough presentation of the find spots and archaeological sites where panel paintings have been recovered, see Rondot 2013, 28–32.
11. Sörries 2003; Parlasca 1966; Sande 2004, 82.
12. J. Paul Getty Museum, inv. no. 82.AP.75.
13. Elston and Maish 2001.
14. Rondot 2013, 21, pl. 1.
15. For previous publications of the panel, see Rondot 2013, 146–48, 274ff., 259, 284; Parlasca 2004, 329–30, fig. 8; Schmidt 1899, 413–24, no. A497; Schmidt 1908, 639–40, no. E814.
16. For previous publications of the panel, see Rondot 2013, 149–51, 317–18; Parlasca 2004, 329, n. 12, 332, fig. 9; Schmidt 1899, 415, no. A499; Schmidt 1908, 640–41, no. E816.
17. For previous publications of the panel, see Schmidt 1908, 640, no. E815; Sörries 2003, 121, no. 22; Parlasca 2004, 323, no. 22; Parlasca 1966, 67, pl. 22.3.
18. https://maxmax.com/shopper/product/15073-xnitecc152-x-nite-cc1-filter-in-52mm-diameter-x-2mm-thick/category_pathway-9217.
19. As described by Webb, Summerour, and Giaccai 2014; Bradley et al. 2020.
20. <https://www.xrite.com/categories/calibration-profiling/colorchecker-classic-family/colorchecker-passport-photo-2>.
21. <https://www.uvinnovations.com/target-uv>.
22. Verri 2009B.
23. Bradley et al. 2020.
24. Salas 2020.
25. Brøns et al. 2023.
26. Mathews and Müller 2016, 58. These include (1) a panel depicting an armed god in the Ashmolean Museum, Oxford, inv. no. 1922.237 (now lost); (2) a panel rendering the god Heron in the Rhode Island School of Design, Providence, inv. no. 59.030; (3) a panel depicting the god Sobek-Horus in the Petrie Museum, University College, London, inv. no. UC 16312; (4) a panel depicting Heron and Lykurgos in the private collection of Nicole Thierry, Etampes, France; (5) a panel rendering an enthroned goddess in the British Museum, inv. no. 1975.7-28.1 (ca. 325 BCE); (6) a panel depicting the goddess Fortuna-Tyche, Louvre, Paris, inv. no. AF 10878-79 (ca. 600 CE).
27. Phoebe A. Heart Museum of Anthropology, inv. no. 6-21387.
28. See, for example, Metropolitan Museum of Art, inv. no. 18.9.2.
29. Gammadia are depicted on a few mummy shrouds and mummy portraits rendering both men and women. Examples include two portraits in the J. Paul Getty Museum, acc. nos. 78.AP.262 and 74.AP.11.
30. Cumbo 2019.
31. Allard Pierson Museum, inv. no. 7069.
32. Interestingly, pine cones are not native to Egypt and so would have had to be imported. Modern-day Libya is the closest area where pines (e.g., *Pinus halepensis*) are native.
33. For chemical analysis of the painting materials, see Brøns et al. 2023.
34. Thiboutot 2020.
35. Cartwright 2020.
36. Thieme et al. 2017.
37. The oldest surviving panel paintings from the Greco-Roman world are the four fragmentary wooden panels recovered in a cave at Pisa, near Sicyon, Greece. The panels date to the second half of the sixth century BCE. National Archaeological Museum, Athens, inv. nos. 16464–16467. For an examination of their polychromy, see Brecolaki et al. 2019.

Between the Linen and the Overpaint: Understanding the Materials and Techniques Used on Two Romano- Egyptian Funerary Portrait Shrouds

William J. Mastandrea

Kate Clive-Powell

Evelyn (Eve) Mayberger

Richard Newman

Lawrence M. Berman

Daniel P. Kirby

This paper is a comparative technical investigation of two “Soter-type” Theban funerary portrait shrouds held at the Museum of Fine Arts (MFA), Boston. The aims of this paper are to (1) investigate the original artists’ materials and techniques used in the painted designs and textile substrates, (2) interpret historical accretions, and (3) better understand the materials and methods of subsequent restorations, with the aim that information about the objects’ manufacture, use, and museum life can be better understood. It is also the intention that this research will lay the groundwork for future investigations of other Soter-type portrait shrouds, which are historically underrepresented in conservation literature in comparison to their wood panel counterparts.

The Ancient Panel Painting: Examination, Analysis, and Research (APPEAR) project provides a framework for institutions to investigate Romano-Egyptian funerary portraits and shrouds in global collections, contextualizing

their findings against the extant oeuvre included in the database. All forms of funerary portraits (encaustic and tempera on wood panels, stucco cartonnages, and portrait shrouds) represent multifaceted ways for the inhabitants of Roman Egypt to have received a well-appointed burial in accordance with the customs and values of the times. Portrait shrouds are larger than their wood panel counterparts, covering the entire body of the deceased, rather than only a small surface area.¹ However, most Romano-Egyptian funerary portraits in the APPEAR database are of the wood panel type. At the time of publication, the database comprises a total of 417 portraits; only 16 of these are funerary portrait shrouds. Technical investigations and publications specific to portrait shrouds are largely lacking, despite there being at least 129 such shrouds in existence, as inventoried by Lissette M. Jimenez in her PhD dissertation.² To date, that is the most comprehensive study of Romano-Egyptian

portrait shrouds published in English, and it was an indispensable resource, helping to contextualize the MFA shrouds in relation to other contemporary funerary shrouds.

EGYPTIAN USE OF FUNERARY SHROUDS

Thebes, located in Upper Egypt, rose to prominence during the Middle Kingdom (2055–1550 BCE) and functioned as a southern capital of Egypt during the New Kingdom (1550–1070 BCE).³ It was a major center for cult and religion, wherein several deities, Hathor among them, were worshipped in temples at Karnak, Deir el-Bahari, Deir el-Medina, and Medinet Habu.⁴ Hathor, known as the “mistress of the West,” had at least two known cult places at Deir el-Bahari and Deir el-Medina where she was revered “as the patroness of the surrounding cemeteries of the dead”; these were later expanded under the Ptolemies.⁵

By the Ptolemaic and Roman periods, the political, economic, and religious preeminence of Thebes had changed, impacted by several revolts against both Ptolemaic and Roman overseers, as well as a reduction in the number of active temples.⁶ The population of Ptolemaic and Roman Thebes was significantly Greco-Egyptian, with immigrant Greeks having strongly assimilated to native Egyptian religious and family structures.⁷ Roman influence was not particularly significant, having little impact on local cultural practice and identity.⁸ The combination of the lack of a strong Roman cultural presence, a shift in local economic and political power, and an increasingly shrinking world for scribes, artists, and craftspeople practicing traditional forms of writing and visual representation helped to fuel the continuity and revival of longstanding funerary traditions, imagery, and practice in Thebes.⁹

The earliest extant use of mummy shrouds can be traced to the Second Intermediate Period (ca. 1675–1550 BCE), in a decorated shroud in the tomb of Sennefer at Deir el-Medina,¹⁰ and in the New Kingdom (ca. 1550–1069 BCE) as votive offerings to the goddess Hathor at the Theban necropolis at Deir el-Bahari.¹¹ This practice continued through the Third Intermediate Period (ca. 1069–664 BCE), during which time full-length shrouds depicting Osiris were affixed to mummified individuals and then concealed by an outer layer of linen cloth.¹² The tradition persisted through the Late Period (ca. 664–332 BCE), and by the Ptolemaic and Roman periods characteristic Osiris- and Hathor-shrouded individuals were interred in reused

Middle Kingdom and Late Period tombs at Deir el-Bahari, Asasif, el-Khokha, and Sheikh Abd el-Qurna.¹³ These tombs correspond to periods of Theban preeminence, and individual interment in these contexts may suggest the importance of continuity of funerary tradition.

THE MFA SHROUDS’ CONNECTION TO SOTERNALIA

The MFA shrouds are dated stylistically to the early to mid-second century CE. They bear strong resemblance to the famed Soter group, which originates from various reused Middle Kingdom and Late Period rock-cut tombs bordering the Theban necropolis.¹⁴ It is likely the distinct regional form exhibited by these objects was strongly influenced by the political, economic, and cultural factors mentioned above. However, examination of funerary practice surrounding Theban shrouded mummies and the materials utilized in their creation during the Roman period may imply a hybridization of several traditions, despite their being deeply rooted in a uniquely Theban context.

First excavated in 1820,¹⁵ these objects were some of the first Soternalia to enter European collections. With no excavation documentation, the exact findspots of the two MFA shrouds are unknown. Specific to this regional subgroup of funerary portraiture is the formulaic, nonnaturalistic depiction of the deceased as a transfigured likeness of the Egyptian deities: Hathor (for females) or Osiris (for both males and females). These representations—commonly observed in the Soter group—are part of a unique regional subset that distinguishes them from the abundant depictions of the deceased-in-life on other funerary portraits in Egypt.

The shrouds began their known journey to the MFA collection through Scottish antiquarian Robert Hay (1799–1863), who presumably acquired them during his Egyptian explorations in the late 1820s and early 1830s while based in Luxor (modern-day Thebes).¹⁶ His journeys were broadly contemporaneous with explorations of Theban tombs by Champollion, Belzoni, and J. G. Wilkinson.¹⁷ Following Hay’s death in 1863, the shrouds (with some 4,500 other Egyptian antiquities in his collection) were sold to Samuel Aids Way, a Bostonian businessman, in 1871. His son, Charles Granville Way, gifted most of this collection of Egyptian material to MFA Boston in 1872.¹⁸

Exhibition and treatment documentation for these shrouds is intermittent. The shrouds are known to have been

displayed as early as 1902 in the Egyptian galleries in the Copley Square Museum and were subsequently moved to the present-day MFA location around 1908, as evidenced by historic glass plate negatives (figs. 4.1, 4.2). Their museum life after this move is unknown until 1957, when the Hathor shroud was photo documented before conservation treatment in preparation for installation in the Egyptian galleries in 1958.¹⁹



Figure 4.1 Historic photograph showing both shrouds on display (wall case, left side) in the Copley Square Museum, ca. 1902. Photo: T. E. Marr Photography. Courtesy Museum of Fine Arts, Boston

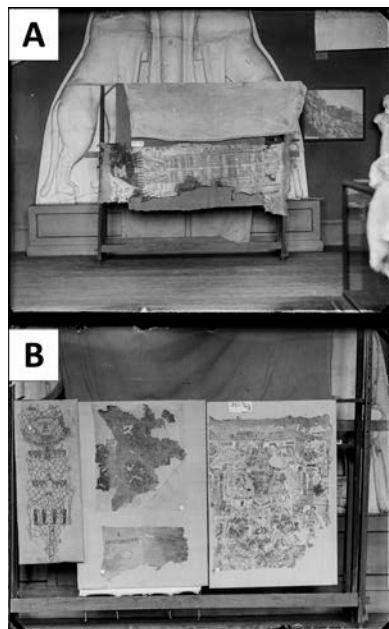


Figure 4.2 Print from glass plate negatives showing (A) Hathor shroud and (B) Osiris shroud (rightmost object) during the move from the Copley Square Museum to the current MFA location, ca. 1908. Hay Collection—Gift of C. Granville Way. Photo: © 2026 Museum of Fine Arts, Boston

Iconographic Descriptions

Hathor Shroud (72.4723)

The Hathor shroud has tasseled fringe at the top and bottom edges and is painted in thick layers of red, orange, green, pink, and black on a white ground (fig. 4.3). It bears a full-length figure of the deity Hathor, whose long hair ends in thick curls, wearing a long, striped headband and an embellished tunic under a feathered sheath dress with wide straps decorated with vines. An undecorated column runs down the center of the dress from waist to ankles. The tunic has decorated sleeves and the breasts are covered with rosettes. The figure wears various adornments, including a jeweled circlet; large hoop earrings; a long, beaded amulet; decorated pectoral; snake bracelets on either wrist; rings on both hands; and thong sandals. She is surrounded by representative hieroglyphs and mythological creatures (including Anubis jackals flanking the feet and mythical serpents in the top registers), with mourning figures and various architectural and vegetal elements at the flanks. There are considerable losses to the textile at the sides and to the paint and ground, as well as considerable staining across the face and proper right arm of the central figure.



Figure 4.3 Overall photograph of Hathor shroud: Roman Egyptian, possibly Thebes, Roman Imperial Period, possibly reign of Trajan (98-117 CE), painted linen, 218 x 104 cm (85.8 x 40.9 in.). Hay Collection—Gift of C. Granville Way, 72.4723. Photo: © 2026 Museum of Fine Arts, Boston

Osiris Shroud (72.4724)

The Osiris shroud, which has remnants of tasseled fringe at the top edge, is painted in layers of red, orange, yellow, green, red-pink, and black on a white ground (fig. 4.4); these layers are comparatively thin compared with those on the Hathor shroud. The shroud is fragmentary, and only the upper half of the shroud is extant. It bears the likeness of the deity Osiris, who wears a false beard and atef crown and wields a crook and flail. He is adorned with a colorful geometric pectoral and a large necklace with a naos pendant. He is flanked by two tall lotus bouquets and subsidiary mourning figures, and further surrounded by representative hieroglyphs, mythological creatures (including sacred winged serpents in the top registers, uraei, and a winged sun disk), and architectural and vegetal elements. There are considerable losses to the textile and paint layers, and what remains of the image is fragmentary. An odd, linear pattern of discoloration of the paint layers coincides with the wear of the paint layers, and a dark-brown stain appears on the proper left side.



Figure 4.4 Overall photograph of Osiris shroud: Roman Egyptian, possibly Thebes, Roman Imperial Period, first to third century CE, painted linen, 87 x 70 cm (34.3 x 27.6 in.). Hay Collection—Gift of C. Granville Way, 72.4724. Photo: © 2026 Museum of Fine Arts, Boston

Materials and Methods

The primary focus of the systematic approach was the identification of the original artists' materials and those of later interventions—textile substrate, pigment, ground materials, and binding media—and secondarily the

identification of unknown residues. Beginning with visual observation and documentation under magnification, all analyses thereafter proceeded from least to most destructive, including multispectral imaging (MSI), transmitted and polarized light microscopy (PLM), X-ray fluorescence (XRF), Fourier-transform infrared (FTIR) and Raman spectroscopy, fiber optic reflectance spectroscopy (FORS), excitation emission matrix spectroscopy (EEM), scanning electron microscopy with energy dispersive spectroscopy (SEM-EDS), and peptide mass fingerprinting (PMF) via matrix-assisted laser desorption/ionization time-of-flight analysis (MALDI-ToF). Sample locations are shown in figures 4.5 and 4.6. Sample lists and results are reported and summarized in figures 4.7 and 4.8.

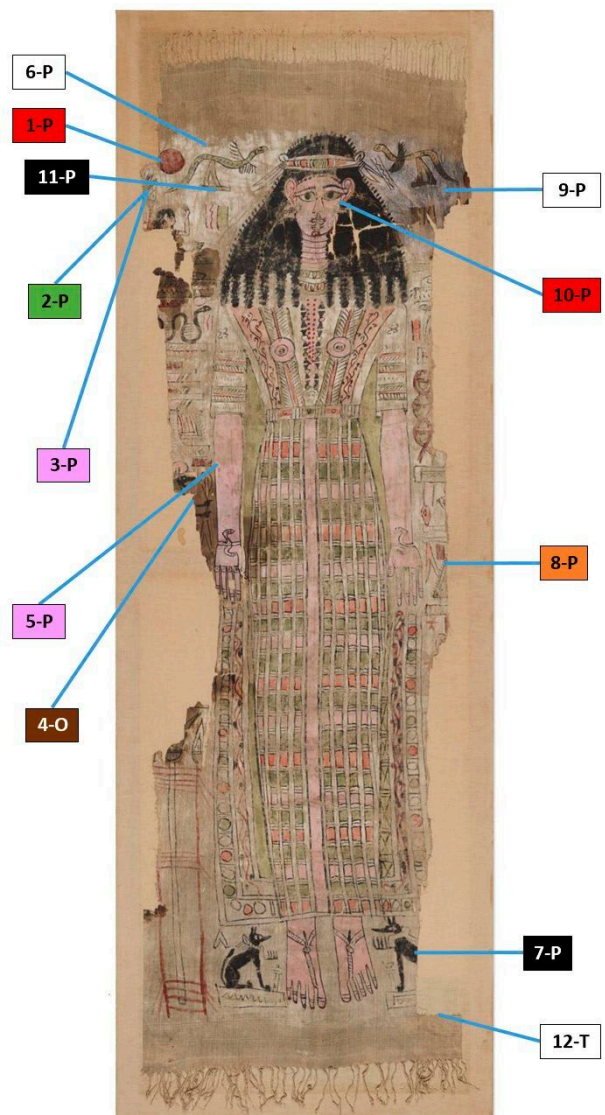


Figure 4.5 Sample locations for Hathor shroud with color-coded sample number labels and material suffixes: P = paint, T = textile, O = other. Photo: © 2026 Museum of Fine Arts, Boston

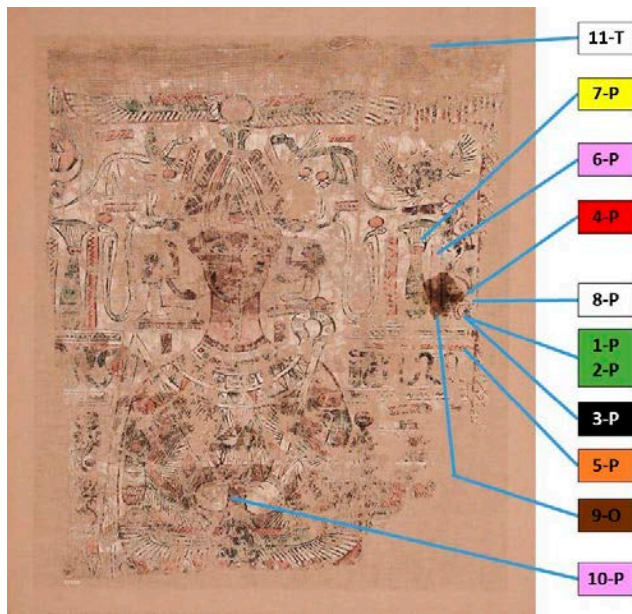


Figure 4.6 Sample locations for Osiris shroud with color-coded sample number labels and material suffixes: P = paint, T = textile, O = other. Photo: © 2026 Museum of Fine Arts, Boston

Textile Substrate Samples

Sample no. ^a	Description	Fiber	Identification method
12-T	Textile fibers from warp and weft	Undyed linen (flax)	PLM

Paint and Residue Samples

Sample no. ^a	Description	Pigments	Identification method(s)	Organic binders	Identification method(s)
6-P	White ground	Gypsum Calcite	FTIR, SEM-EDS		
1-P	Red paint	Hematite	Raman, FORS		
8-P	Orange paint	Minium Litharge	Raman	Wax, likely a contaminant Paint binder uncertain	FTIR
3-P	Pink paint	Madder on Al substrate Gypsum	MSI, FORS, EEM, SEM-EDS		
2-P	Green paint	Celadonite Unidentified silicates	FTIR, FORS SEM-EDS		
7-P	Black paint	Carbon black	Raman, SEM-EDS		
11-P	Black paint	n/a		Possibly carbohydrate binder No protein detected	FTIR MALDI-ToF
9-P	White (restoration)	Anatase Barium sulfate Zinc-containing compound (zinc oxide?)	Raman SEM-EDS		
10-P	Red (restoration)	Pigments in sample 9-P Vermilion Carbon black	Raman, SEM-EDS		
5-P	Pink (restoration)	Pigments in sample 9-P Vermilion Carbon black	Raman, SEM-EDS		
4-O	Dark-colored residue	None detected	FTIR	No protein detected	MALDI-ToF

Notes:

Pigments identified by FTIR and Raman spectroscopy are positive identifications. Other identifications utilize these and other complementary techniques to infer a most probable characterization.

Ca was detected via XRF in nearly every sample and, unless otherwise noted, is attributed to the underlying preparatory ground layer.

^a Samples include suffixes that refer to material type: T = textile, P = painting (ground and paint), O = Other material (e.g., residues or binding media). Some samples were reused.

Figure 4.7 Analytical results of material samples from the MFA Hathor shroud, 72.4723.

Textile Substrate Samples					
Sample no. ^a	Description	Fiber	Identification method		
11-T	Textile fibers from warp and weft	Undyed linen (flax)	PLM		
Paint and Residue Samples					
Sample no. ^a	Description	Pigments	ID method(s)	Organic binders	ID method(s)
8-P	White ground	Gypsum	FTIR, SEM-EDS	Possibly carbohydrate binder No protein detected	FTIR MALDI-ToF
4-P	Red paint	Hematite	Raman, FORS	Possibly carbohydrate binder No protein detected	FTIR MALDI-ToF
5-P	Orange paint	Minium	Raman		
7-P	Yellow paint	Not identified	FTIR, SEM-EDS		
6-P, 10-P	Pink paint	Madder on Al substrate Unidentified lead-containing compound	MSI, FORS SEM-EDS		
1-P, 2-P	Green paint	Celadonite	FTIR, FORS, SEM-EDS	Possibly carbohydrate binder No protein detected	FTIR MALDI-ToF
3-P	Black paint	Carbon black	Raman, SEM-EDS		FTIR MALDI-ToF
9-O	Dark-colored residue	None detected	FTIR	Carbohydrate and lipid No protein detected	FTIR MALDI-ToF

Notes:

Pigments identified by FTIR and Raman spectroscopy are positive identifications. Other identifications utilize these and other complementary techniques to infer a most probable characterization.

Ca was detected via XRF in nearly every sample and, unless otherwise noted, is attributed to the underlying preparatory ground layer.

^a Samples include suffixes that refer to material type: T = textile, P = painting (ground and paint), O = Other material (e.g., residues or binding media). Some samples were reused.

Figure 4.8 Analytical results of material samples from the MFA Osiris shroud, 72.4724.

RESULTS

Textile Substrates

The overall condition of the Hathor shroud’s fibers is good, despite significant losses. The textile maintains flexibility, and there is no evidence of powdering or fracturing of fibers. The overall condition of the Osiris shroud’s fibers is fair. There are breaks in the warps and some fracturing of

fibers. Flexibility has been compromised on both textiles in areas affected by dark brown staining.

The substrates are woven in an irregular plain weave using S-twist, single-ply threads. The quality of the weave is coarse, and the weave count is similar for both shrouds: forty-four warps and thirty wefts per inch (2.5 cm) for the Hathor shroud, and forty-six warps and twenty-five wefts per inch for the Osiris shroud. No selvage remains on either shroud. Both shrouds have tasseled fringe elements made from warp ends plied in the S direction. The Hathor shroud has a fringe at the top and bottom. Fringe survives only along the top of what remains of the Osiris shroud, and it is badly damaged, with only a few weak tassels remaining. Knots are present at the base of the tassels on the shrouds and sometimes at the ends. Both textiles have decorative bands of supplementary wefts with little to no twist (fig. 4.9). The Hathor shroud has six decorative bands—four on the bottom half and two on the top half—while the Osiris shroud has only four decorative bands on its remaining top half. These decorative patterns and a comparable weave count have been documented previously on Hathor-type shroud EA68950, currently housed in the British Museum.²⁰

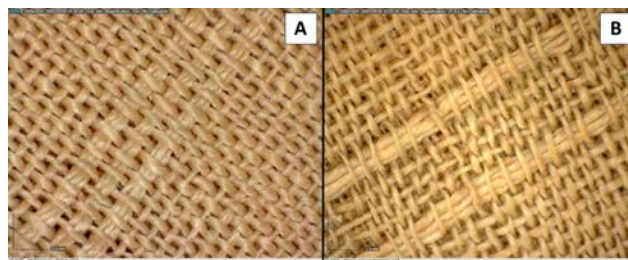


Figure 4.9 Detail of plain weave substrates with supplementary weft decorative bands from (A) Hathor shroud and (B) Osiris shroud. Photos: © 2026 Museum of Fine Arts, Boston

Fibers from both shrouds were observed via PLM and positively identified as undyed linen (flax). Morphological features include irregular, roughly cylindrical fibers with cross-shape nodes and ultimate bundles (from incomplete retting during processing). The identification was further corroborated using the modified Herzog twist test, an empirical test to determine the fibrillar orientation (Z- or S-twist) of bast fibers—specifically the helical orientation of the microfibrils of the secondary wall—that employs a polarizing light microscope and a first-order red tint plate. Fibrillar orientation is a characteristic feature, discernible from species to species, allowing for fiber identification.²¹

Ground Layers

The Hathor shroud's white preparatory layer has a uniform, coarsely ground particle size with frequent cracking through the ground layer, often along the interstices of the underlying textile. The thick application of the material appears well-adhered to the textile substrate. Where damaged, it reveals a layer characterized by small, irregular, loosely bound clumps. In contrast, the Osiris shroud's ground layer is much thinner, has a high gloss, and the particles are fine and uniform, with cracking through to the textile substrate. Damaged areas show cracking with clean, sharp breaks of even thickness, rather than irregular, loosely bound clumps.

The preparatory ground of the Hathor shroud has been identified with XRF and FTIR as a mixture of calcite (CaCO_3) and gypsum ($\text{CaSO}_4 \cdot 2\text{H}_2\text{O}$), while only gypsum was used on the Osiris shroud. The use of these calcium-based materials as a preparatory layer is consistent with the manufacture of other painted shrouds, and the presence of calcite could imply specific use as a pigment, rather than as a preparatory layer.²² However, the SEM-EDS imaging of the Hathor shroud suggested a mixture of these materials, rather than explicit layering of one atop the other, ruling out application as a pigment.

Original Pigments, Binding Media, and Residues

Features such as particle size, presence or absence of inclusions, particle luster, and the overall condition of paint layers aided in their determination as either original or a later addition. For the Hathor shroud, original paint layers are thicker, possessing a matte finish with variable particle sizes and noticeably large quartz-like inclusions (fig. 4.10). A greater number of cracks appear in the original paint and ground layers than in areas of later restoration. The paint layers of the Osiris shroud are much thinner overall but also have a matte finish with variable particle sizes—although all of the Osiris shroud's paint particles are more finely ground within the paint matrix (fig. 4.11). As with the ground layers, cracks are present along the interstices of the underlying textile weave.

Areas of original dark red in both shrouds yielded a positive result for an iron-based material such as red ochre with XRF. This result was further confirmed by Raman and FORS, which specifically identified the use of hematite (Fe_2O_3).²³ Original oranges confirmed a high concentration of lead via XRF. Using FTIR, Raman, and FORS, the presence of both litharge (PbO) and minium (Pb_3O_4) was confirmed

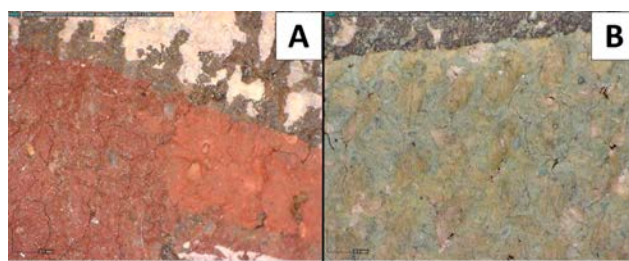


Figure 4.10 Examples of paint layers of Hathor shroud at magnification: (A) The intersection of original red (dark red), restoration red (bright red), and restoration pink (top) paint layers at figure's chin. (B) An area of green pigmentation from the winged serpent in the upper proper-right register. Photos: © 2026 Museum of Fine Arts, Boston

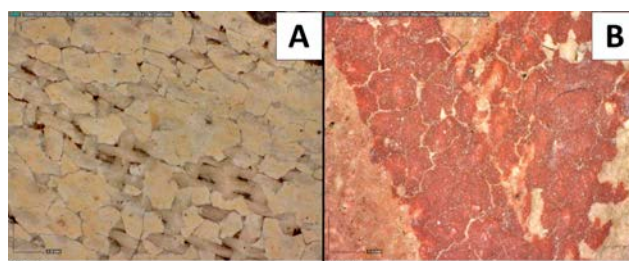


Figure 4.11 Examples of paint layers of Osiris shroud at magnification: (A) Yellow pigmentation atop the white ground from the winged serpent in the upper proper-right register. (B) Dark red pigmentation of the outline of the figure where the chin and neck meet. Photos: © 2026 Museum of Fine Arts, Boston

for Hathor but solely minium for Osiris. The yellow pigment on Osiris was hypothesized to be yellow ochre pigmented by goethite ($\text{Fe}_2\text{O}_3 \cdot 2\text{H}_2\text{O}$). As it lacked the characteristic peaks in FTIR, and in the absence of visible iron-containing particles in SEM-EDS, this pigment could not be reliably identified—likely due to its thin, limited application.

Green sections of both shrouds are of particular interest, revealing high concentrations of Fe, Mg, and K with XRF and SEM-EDS, suggestive of a green earth pigment. Transmitted FTIR yielded a good match to celadonite: one of the principal source minerals of green earth pigments. The sharp OH-stretching bands (ca. 3557, 3554, and 3602 cm^{-1}) are associated with a highly ordered distribution of Fe^{3+} , Mg, and Al in octahedral sites of the mineral. The Si-O stretching region (1200–700 cm^{-1}) also closely matches published spectra of this mineral,²⁴ although the bands here overlap major absorption bands for gypsum; a component of the ground layer was included in the samples that were analyzed (fig. 4.12). SEM-EDS analyses of both shrouds' greens indicate that other (unidentified) silicate minerals are also present, probably natural components of the green earth deposits from which the

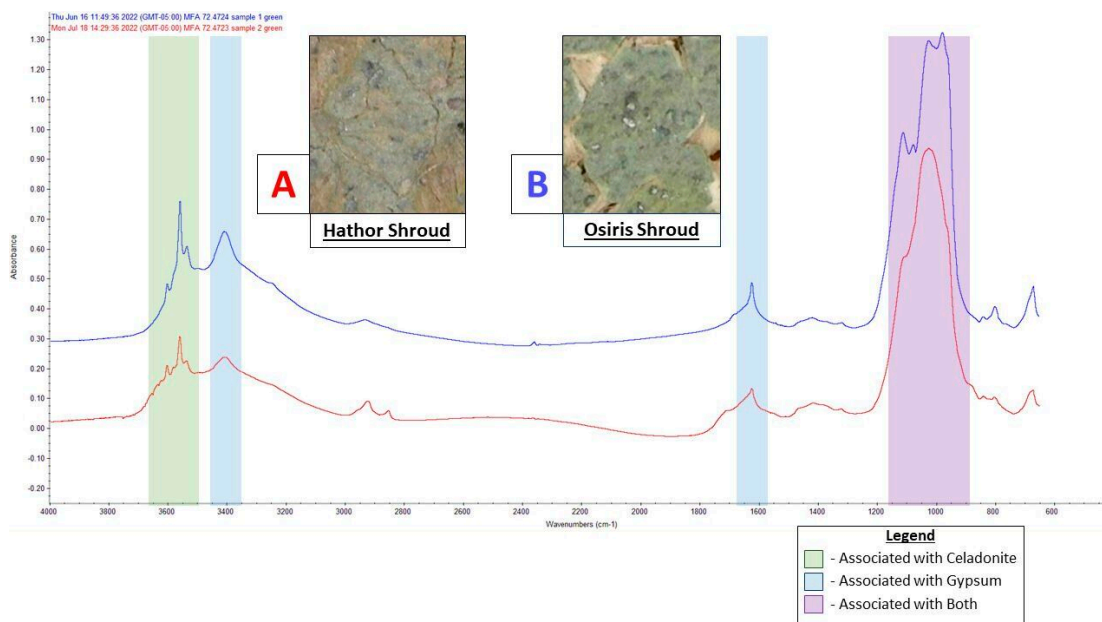


Figure 4.12 FTIR spectra of the green pigment samples from (A) Hathor shroud and (B) Osiris shroud. Areas in green are characteristic features of celadonite, those in blue are characteristic features of gypsum, and purple areas are associated with both. Photo: © 2026 Museum of Fine Arts, Boston

pigment originated. SEM images suggest that the celadonite is present mainly in the form of small, elongated crystals a few micrometers in length.

Original pink areas of Hathor bore a strong luminescent response via MSI (using green light visible-induced visible luminescence [VIVL])²⁵ and, once supported by EEM, confirmed the presence of a madder-based pigment (fig. 4.13).²⁶ This identification is further supported by (1) SEM showing the layering of red-pink material atop the mixed calcite and gypsum ground and (2) EDS revealing a high concentration of aluminum, which is necessary to form complexes with the alizarin and/or purpurin chromophores of madder-based pigments (hydroxyanthraquinones) during production.²⁷ For the red-pink of Osiris, the same luminescent response was observed, though it was less intense than Hathor's (fig. 4.14). This may be due to variable preparation methods, such as the mixing of madder pigments with a lead-based material (e.g., minium), as suggested by small Pb peaks observed with XRF. Raman spectroscopy and SEM-EDS confirmed amorphous carbon as the source of the original black pigments for both shrouds.

The paints are likely bound in a water-soluble medium. Animal glue is an often-observed medium of “tempera” for funerary portraits, whether on linen or wood. PMF via MALDI-ToF was conducted on two samples from Hathor and three samples from Osiris. The samples analyzed consisted of white ground and thin overlying paint. None

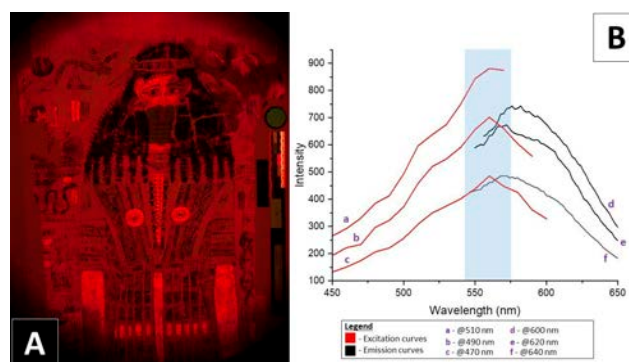


Figure 4.13 (A) VIVL image of the upper half of the Hathor shroud showing the luminescent response of madder lake (bright orange) (Canon EOS 5D Mark II [modified], CrimeScope CS-16-500W [535 nm], PECA 918, and Tiffen 23a red filter). (B) Emission and excitation spectra for an original pink paint layer from Hathor shroud. Emission spectra (black traces) at 510 (d), 490 (e), and 470 (f) nm excitation. Excitation spectra (red traces) at 600 (a), 620 (b), and 640 (c) nm emission. The range of peak excitation for madder lake is denoted in blue. Hay Collection—Gift of C. Granville Way. Photos: © 2026 Museum of Fine Arts, Boston

of these samples revealed detectable levels of protein (aside from the common contaminant keratin, unrelated to original material). While it is conceivable that protein is present beyond detection limits, it seems probable that animal glue was not a binder, at least not in the ground layers of the shrouds.

In FTIR spectra of paint and ground layers from both shrouds, C-H stretching absorbance bands in the 3000–2500 cm^{-1} region of several samples resembled

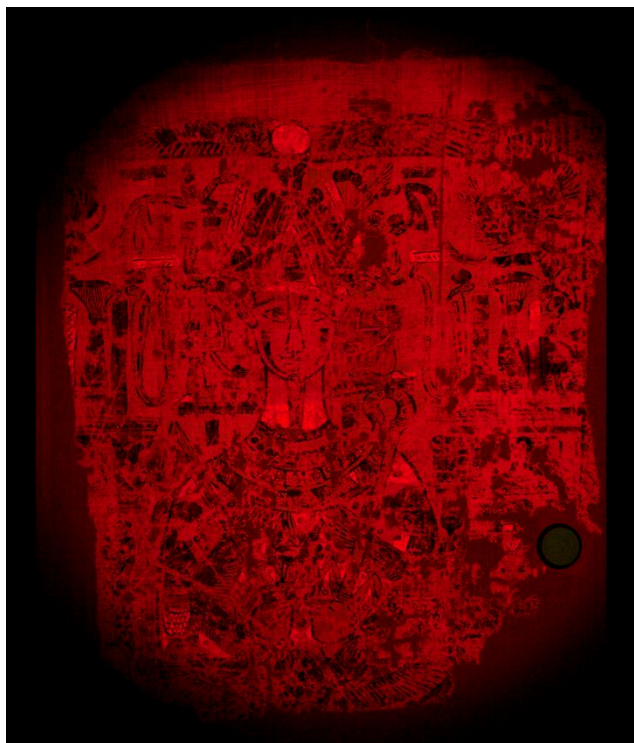


Figure 4.14 VIVL image of the upper of the Osiris shroud showing the luminescent response of madder lake (bright orange) (Canon EOS 5D Mark II [modified], CrimeScope CS-16-500W [535 nm], PECA 918, and Tiffen 23a red filter). Hay Collection—Gift of C. Granville Way. Photo: © 2026 Museum of Fine Arts, Boston

those of plant gums and gave no indications of protein. Absorbance for gums in the lower wavelength region was masked by inorganic compounds in the samples. The presence of a plant gum binder can only be considered possible, not proven. Future analysis with gas chromatography/mass spectrometry (GC/MS) may aid in the identification of these materials.

Historical Restorations: Textile Mounting and Overpainting

In 1957, both shrouds were “flattened out and mounted” by Suzanne Chapman: stitched to backing fabric affixed over wooden stretchers. This work was conducted in preparation for an exhibition of Way Collection material in the Egyptian galleries, commemorating the gift of the collection in 1872, which formed the foundations of the MFA’s Egyptian collections.²⁸

Overpainting was observed only on the Hathor shroud, having occurred after the textile had been stitched to the backing fabric, as shown by the restoration paints visible atop the stitching that fastens the shroud to its backing. Five areas were identified both visually and via MSI as

potential historical restorations emulative of the original ground, red, and pink layers. These locations coincide with areas most heavily affected by staining: the figure’s face, proper-left ear and neck, proper-right arm, and the upper, proper-left register of the shroud.

XRF of the restoration white yielded high concentrations of Ba, Zn, and Ti, in addition to the high Ca peaks from the underlying original mixed gypsum/calcite ground. Further Raman spectroscopy yielded a positive result for anatase—a natural mineral form of titanium dioxide (TiO₂)—as well as barium sulfate (BaSO₄). The analysis of the restoration red suggests the use of this restoration white as a base to which vermilion (HgS) and carbon black were likely added. Further, the restoration pink is identical in composition to the restoration red, likely mixed in a ratio to produce a pink rather than a crimson red.

DISCUSSION

Overall, the material results of the analysis are in concert with the materials and practices utilized in Roman-period Egypt. Highlights of these results and notable features of condition include applications of a shroud to an individual, wear patterns in paint layers, and the use of pigments from beyond Egypt.

Aspects of the shrouds’ condition indicate probable ways that they were secured to their individuals. Mummy shrouds were designed to cover the length of the body, with the painted figure aligning with the anatomy of the deceased.²⁹ The shrouds were loosely wrapped around the body or secured in place with linen strips.³⁰ The use of linen strips would bring attention to the face while simultaneously ensuring “the mummified body and the shroud were never separated.” This allows the funerary imagery to maintain the status of the deceased as a transfigured likeness of the respective deity, the deceased having been reborn as a god.³¹ No features of the Hathor shroud’s condition suggest that linen strips were used to secure the shroud, and the flattening treatment performed on the shroud in the 1950s removed any potentially diagnostic creasing that might have provided insight into how it was laid and/or secured to the individual.

The Osiris shroud has a stark, linear pattern of discoloration and wear in the paint layers. These features are made apparent in figures 4.15 and 4.16. The linen strips used to secure the shroud protected the underlying paint layers from exposure to dust and soot accumulation within the tomb context, though they also preferentially abraded the paint. Comparison to the wrappings used on the intact mummy of Cleopatra, daughter of Candace (ca.

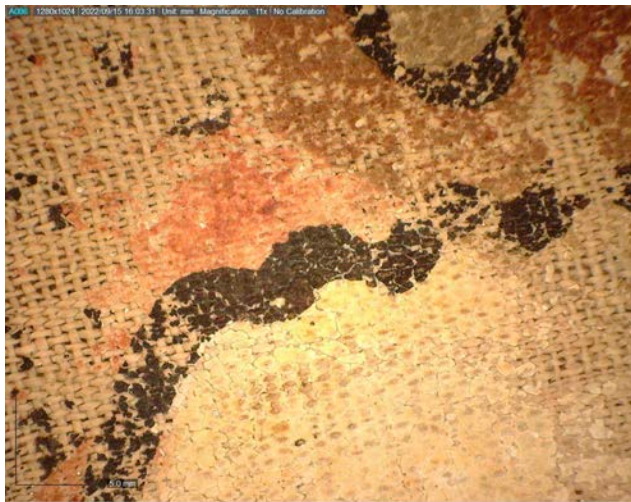


Figure 4.15 Detail of the brown discoloration of a red-pink area of paint of the Osiris shroud. Photo: © 2026 Museum of Fine Arts, Boston

100–120 CE), deriving from the Theban necropolis—and significantly identified as Soternalia—supports this hypothesis. The Cleopatra shroud is secured to the body with strips of linen in a crisscross pattern, diagonally and horizontally, over the painted image. The positioning of these strips corresponds to the nonsoiled—though abraded—areas of the Osiris shroud, suggesting a similar method of wrapping (see fig. 4.16). This manner of securing shrouds is similar to both Third Intermediate Period mummy wrappings and those of the Roman period,³² perhaps implying a hybridization of ancient Theban tradition and “new” Roman practice.

Calcium-based grounds, red ochres, madder lake, carbon black pigments, and flax for the textile substrate identified on both shrouds are materials native to Egypt and consistent with traditional Egyptian usage spanning both the Pharaonic and Greco-Roman periods.³³ However, the presence of celadonite and minium on both shrouds reflects the selection of nontraditional materials sourced from outside Egypt by Roman-Theban artisans. This suggests that artists were continuing traditional Egyptian usage of materials while also choosing newly imported pigments for their craft.

Copper-based materials were the traditional green pigments used throughout Pharaonic Egypt. Celadonite, a phyllosilicate of potassium and iron, is not native to Egypt but has two well-known sources in the Mediterranean: Italy (Verona) and the island of Cyprus.³⁴ It sees widespread use in Hellenistic Cyprus, Israel, and Greece³⁵ and has been identified on other second-century CE Roman-period painted shrouds, such as a Hathor-type shroud (EA68950),³⁶ an Osiris-type shroud (25.184.20),³⁷

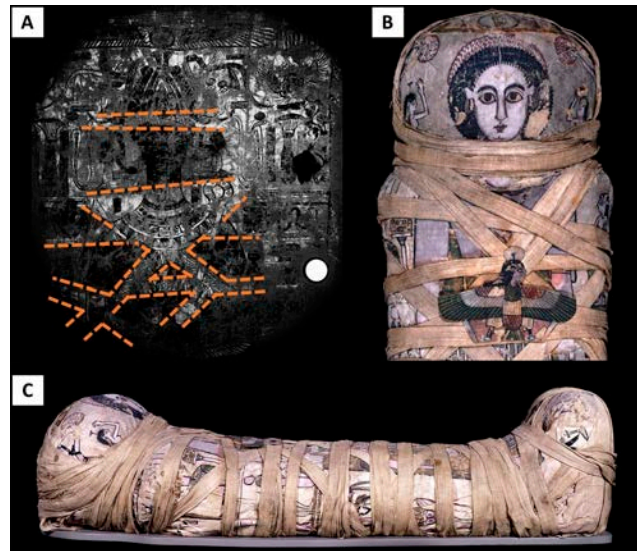


Figure 4.16 (A) High-contrast black-and-white visible image of the Osiris shroud showing the pattern of discoloration in the paint layer. Hay Collection—Gift of C. Granville Way. Photo: © 2026 Museum of Fine Arts, Boston; (B) Mummy of Cleopatra, daughter of Candace, Roman Egyptian, Sheikh Abd el-Qurna (Thebes), Roman Period, ca. 100–120 CE, mummified individual with painted linen. Image shows the intact wrapping pattern of external linen strips. Photo: © The Trustees of the British Museum; (C) Full side view of the mummy of Cleopatra, 161 cm long (63.4 in.). Photo: © The Trustees of the British Museum

and a fragment of a painted shroud (X.390).³⁸ Thus, in Egypt, celadonite is readily accepted and integrated into the existing palette of Egyptian artisans, despite being nontraditional and of foreign origin.

Similarly, the use of minium as pigment is atypical in Greco-Roman Egypt. Minium production was often a by-product of silver cupellation, a major source being the Roman silver mines at Rio Tinto, Spain.³⁹ Use of this Iberian minium was identified on the red-shrouded mummy of Herakleides, dated to the first century CE, possibly from el-Hibeh in Lower Egypt, based on stylistic similarities with other red-shroud mummies.⁴⁰

While the minium identified in the MFA shrouds was not sourced, the utilization of pigments from beyond the Egyptian sphere—such as celadonite and minium—is significant. Their use on these shrouds, and others, should prompt important questions. Perhaps the use of such costly, imported pigments in nonnaturalistic portraiture should challenge the existing perspectives and value judgments concerning “what is significant,” rather than tethering these perceptions so strongly on the degree to which an image approaches realism. Is this use of “new” materials of non-Egyptian origin a choice rooted in aesthetics, working properties, symbolism, or some combination thereof? Could the costs of these materials

potentially impact the nature or number of workshops dedicated to these shroud forms? Pursuing answers to these kinds of questions will help to untangle what is likely a complex hybridization of material usages and funerary practices, rather than a strictly local Theban practice.

CONCLUSION

Driven by a gap in existing scholarship, this paper presents a detailed material analysis of two shrouds from the MFA's collection. Through extensive imaging and analysis, most of the shrouds' materials and methods were identified, areas of later restoration were discovered, and historical accretions were interpreted. The shrouds' linen textile substrates bear similar elements of construction. The manner of securing the shroud to the deceased, suggested by the wear patterns and discoloration of the Osiris shroud, reveals the continuation of a unique, longstanding local practice that is distinct from, while also inclusive of, external mummy wrappings seen elsewhere in Roman Egypt.

Nearly all the original pigments were able to be identified on the Hathor and Osiris shrouds, and this has provided insight into the Roman-Theban color palette used for painted shrouds. Materials of non-Egyptian origin were consciously incorporated, despite longstanding local funerary tradition, even when from distant imported sources. The paints used in the twentieth-century restoration of the Hathor shroud were also characterized, providing a clearer picture of the shroud's life within the MFA collection and its original appearance.

Overall, this research shows that—as with portraits on wood panels—information gleaned from the examination and analysis of painted portraits on textiles can lead to broader interpretations and understanding of life and death in Romano-Egyptian Thebes. A future survey of weave type, count, spin direction, decorative elements, and patterns of wear of the textile substrates of other extant shrouds from Roman Egypt would be an invaluable resource in further enhancing understanding of artist choices and materials. It is hoped that other institutions will be encouraged to research and analyze the materials, construction, and condition of their Romano-Egyptian shrouds so that a more comprehensive picture of the production and use of these objects can be elucidated.

NOTES

1. Jimenez 2014.
2. Jimenez 2014.
3. Manning 2013.
4. Lajtar 2005; Lajtar 2012.
5. Lajtar 2005, 75; Lajtar 2012, 180.
6. Lajtar 2012, 173–74.
7. Clarysse 1995.
8. Lajtar 2012, 179.
9. Riggs 2006.
10. Ikram and Dodson 1998.
11. Jimenez 2014, 17, 19.
12. Jimenez 2014, 20, 22.
13. Riggs 2005, 177; Schreiber, Vasáros, and Almásy 2013, 206.
14. Schreiber, Vasáros, and Almásy 2013.
15. Riggs 2005.
16. Bierbrier 2012.
17. Bierbrier 2012, 52, 114, 579.
18. The remaining portion was gifted to the British Museum.
19. Smith 1957.
20. Hillyer 1984; Vandenbeusch 2022.
21. Haugan and Holst 2013.
22. Pagès-Camagna and Guichard 2010.
23. Special thanks to Dr. Erin Mysak, senior preventive conservation scientist at Harvard Library, for her assistance with EEM and FORS analyses.
24. Zviagina, Drita, and Dorzhieva 2020.
25. Extraneous information from the intensity of the excitation light source (CrimeScope at 535 nm) could not be fully removed from image capture via filters. While properly highlighting a madder response, this unintentional “bleeding” of nonluminescence accounts for the uncharacteristic appearance of the VIVL image.
26. The EEM instrument is set to a specific excitation wavelength; it then acquires a full emission spectrum at that excitation wavelength. Following, it sets a new excitation wavelength 10 nm higher than the previous one and collects a full emission spectrum. This is conducted for the entire range denoted in the software. With the resulting data, one may then plot the emission spectrum at any excitation wavelength, or an excitation spectrum at any emission wavelength can be extracted and plotted.
27. Newman and Gates 2020.
28. Smith 1957, 40.

29. Jimenez 2014.
30. Jimenez 2014, 4.
31. Jimenez 2014, 183.
32. Ikram and Dodson 1998, 157, 160.
33. Pagès-Camagna and Guichard 2010, 26–28.
34. Roberts 2020; Pagès-Camagna and Guichard 2010, 30; Kakoulli 2009.
35. Kakoulli 2009, 48.
36. Hillyer 1984, 8; Scott 2010. Object currently housed at the British Museum: https://www.britishmuseum.org/collection/object/Y_EA68950.
37. Object currently housed at The Metropolitan Museum of Art, New York: <https://www.metmuseum.org/art/collection/search/548243>.
38. Roberts 2020, 40. Object currently housed at The Metropolitan Museum of Art, New York: <https://www.metmuseum.org/art/collection/search/256830>.
39. Walton and Trentelman 2009.
40. Svoboda and Walton 2010.

Non-Invasive Investigations on Three Ancient Mummy Portraits at the National Archaeological Museum in Athens: Challenges and Benefits

*Peppy Tsakri
Ioannis Panagakos*

The core of the Egyptian collection of the National Archaeological Museum (NAM) in Athens consists of significant donations from two Greek expatriates from Egypt: Ioannis Dimitriou, in 1880, and Alexandros Rostovich, in 1904. The collection was further enriched with donations from the Egyptian government, in 1893, and the Greek Archaeological Society, in 1894. Among the exhibited artifacts of the Egyptian collection are five funerary portraits. Two are on fabric backings; the other three are polychromed wooden panels. The portraits lack archaeological contexts. The initial discovery sites of these works are not known and, unfortunately, are not preserved along with associated burial finds. Moreover, no further scientific examination of their state of preservation, of previous interventions, and of the manufacturing methods and materials has ever been carried out. Therefore, it soon became obvious to the NAM that a more in-depth investigation of the works was both needed and urgent; the museum's participation in the APPEAR project brought about the opportunity for further study.

For the museum's initial participation in the APPEAR project the three portraits on wooden panels were chosen.

The first depicts a young man (inv. no. 1627); the second, an older man (inv. no. 1629); and the third, a woman (inv. no. 1628; figs. 5.1–5.3). Although no analysis of the binding media was performed, the two male portraits appear to be painted in tempera and the female portrait in encaustic.¹ Macroscopically, the two male portraits appear very similar in terms of manufacture and style, while the female portrait exhibits more elaborate workmanship. Previous conservation and restoration interventions are obvious in the portraits of the young man and the woman: split wood fragments have been adhered in both.

Using instruments available at the NAM, the present study involved multiple approaches with consecutive steps. First and foremost, we employed multiband imaging (MBI) and reflectance transformation imaging (RTI) to document in detail the works' painted surface. In the next step, X-radiography investigated both surface characteristics and items of initial manufacture or later intervention. Portable X-ray fluorescence (pXRF) spectroscopy followed for the elemental analysis of the painted surface. We decided to examine many spots across the painted surface to acquire information on a larger area, which produced results

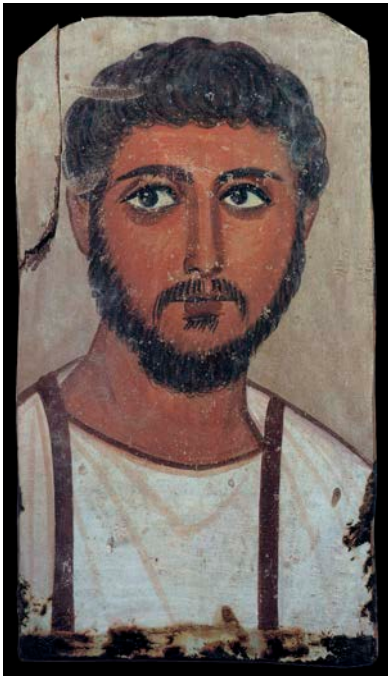


Figure 5.1 Visible light image of Mummy Portrait of a Young Man, Romano-Egyptian, 117–138 CE. Tempera on wood, 35 x 19 cm (13 3/4 x 7 1/2 in.). Athens, National Archaeological Museum, Department of Prehistoric, Egyptian Cypriot and Near Eastern Antiquities Collection, 1627. Photo: Hellenic National Archaeological Museum, Athens, Greece



Figure 5.3 Visible light image of Mummy Portrait of an Old Man, Romano-Egyptian, 138–161 CE. Tempera on wood, 36 x 11.5 cm (14 3/16 x 4 1/2 in.). Athens, National Archaeological Museum, Department of Prehistoric, Egyptian Cypriot and Near Eastern Antiquities Collection, 1629. Photo: Hellenic National Archaeological Museum, Athens, Greece

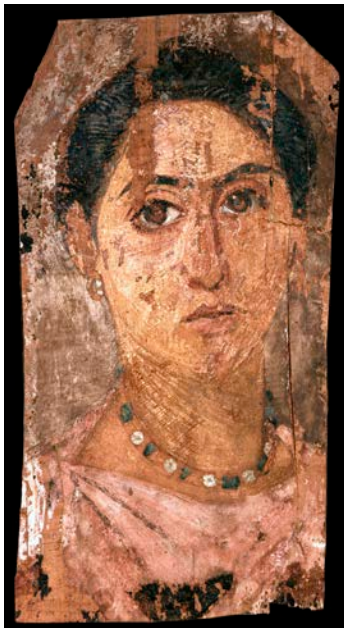


Figure 5.2 Visible light image of Mummy Portrait of a Woman, Romano-Egyptian, 138–161 CE. Encaustic on wood, 35.5 x 18 cm (14 x 7 1/16 in.). Athens, National Archaeological Museum, Department of Prehistoric, Egyptian Cypriot and Near Eastern Antiquities Collection, 1628. Photo: Hellenic National Archaeological Museum, Athens, Greece

similar to those obtained by the XRF mapping. Finally, a digital microscope, used in a handheld “scanning mode,” helped us to interpret the results obtained by some of the other aforementioned methods.

IMAGING

For imaging purposes, we used MBI and X-ray radiography. RTI is a very powerful tool that, in short, combines raking light photography with computational algorithms to digitally examine surface details. For the portraits, RTI shed light on the state of preservation of the works’ wooden supports and paint surface as well as on the methods of color application.

RTI revealed that significant warping along the grain of the wooden support is present on the male portraits; also, cracks appear both on the supports and within the paint layers. Cracking is an issue on the female portrait panel too; however, in this case the severity of the compromised paint layer has resulted in a significant loss of paint. RTI emphasized the highly textured impasto layer on the female portrait, especially on the skin, facial features, and jewelry (fig. 5.4). On the two male portraits, in contrast,



Figure 5.4 Raking light detail of fig. 5.2, highlighting the textured paint surface. Photo: Hellenic National Archaeological Museum, Athens, Greece

because all paint layers had been applied very thinly, all relief was limited to the wooden support.

MBI carried out on all three portraits consists of images captured in the visible spectrum; fluorescence in the visible region, generated by ultraviolet-induced visible fluorescence (UVF); and reflectance in the near infrared region, produced by infrared reflectography (IRR) and visible-induced luminescence (VIL). Figure 5.5 summarizes the imaging methodology used.

Technique	Camera	Light source	Filters
VIS	CANON EOS 700D	Daylight	BRAUN Blueline UV Lens Protection
UVF	CANON EOS 700D	SYLVANIA Blacklight- Blue F18W/BLB-T8 Tube (315nm–400nm)	BRAUN Blueline UV Lens Protection
IRR	CANON EOS 20D Modified	Halogen Flood light IP44 400W	LVSHI IR850nm
VIL	CANON EOS 20D Modified	LUMAX Plati LFL107 LED Flood light 4500lm, 6000K	LVSHI IR850nm

Figure 5.5 Experimental setup used for the MBI. Chart: Peppy Tsakri and Ioannis Panagakos

Fluorescence in the visible region (figs. 5.6–5.8) revealed undocumented previous interventions, some of which had never been observed before. The apparent assemblages of the separated fragments in the portraits of the young man and the woman were executed with probably a cellulose nitrate adhesive.² For the paint surface’s consolidation, which for the most part had gone undetected, UVF

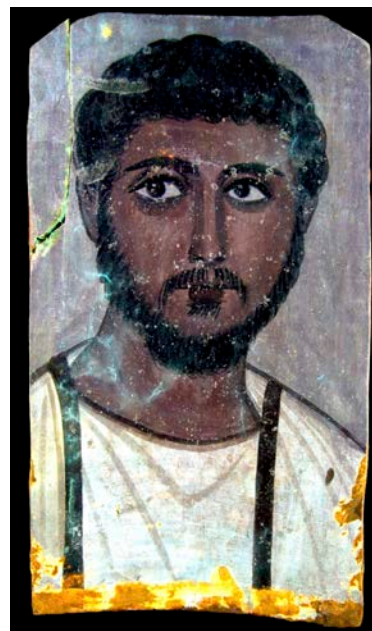


Figure 5.6 UVF results for fig. 5.1. Photo: Hellenic National Archaeological Museum, Athens, Greece

photography proved immensely valuable; it showed both the extent of the treatment and the various materials used to carry it out—most likely at different times. The two male portraits were locally treated with what appears to be, based on its characteristic fluorescence, a polyvinyl acetate (PVAc) dispersion, which was likely applied in the same manner to the female portrait as well.³ However, the latter revealed at its lower half extensive consolidation with a different material, demonstrating the greenish fluorescence of a plant-based resin, possibly dammar gum or mastic.⁴ The use of a natural resin for consolidation purposes suggests treatment at an earlier date than that of the PVAc application. Additionally, two small areas above the proper right (PR) eyebrow of the young man were treated with what appears to be shellac; however, because they are only two very small spots in an area that does not seem to have ever needed consolidation, we cannot rule out the possibility of accidental contamination when the portrait was kept in a conservation laboratory—or rather, a “mending workshop”—of that period. UVF also exposed the use of an organic lake, probably madder, on the facial features and garments of the older man (forehead, cheekbone highlights, clavus) and the woman (lips, eyes, tunic).

The VIL technique, employed for every portrait, produced positive results only for that of the female (see figs. 5.1 and 5.9). The spatial distribution of Egyptian blue on this work—apart from the obvious areas appearing in the visible spectrum with a green-blue hue—was observed in

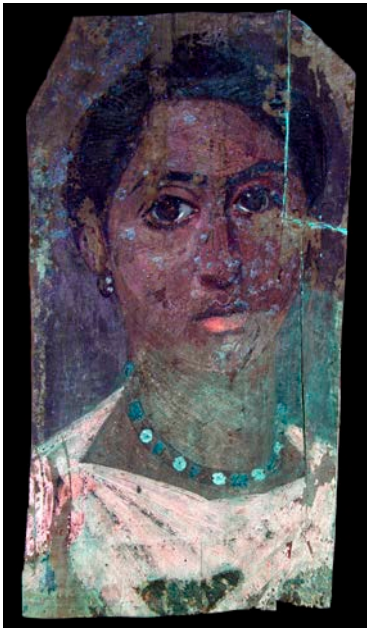


Figure 5.7 UVF results for fig. 5.2. Photo: Hellenic National Archaeological Museum, Athens, Greece

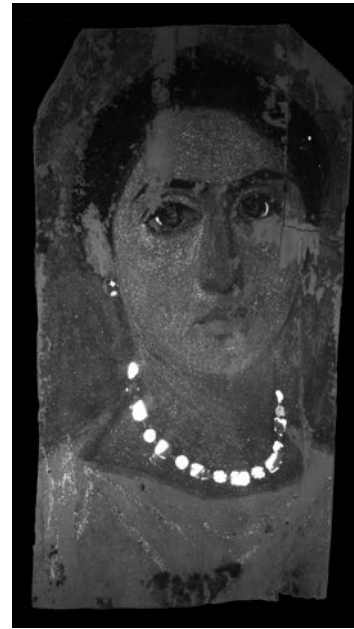


Figure 5.9 VIL image of fig. 5.2, revealing the spatial distribution of Egyptian blue. Photo: Hellenic National Archaeological Museum, Athens, Greece



Figure 5.8 UVF results for fig. 5.3. Photo: Hellenic National Archaeological Museum, Athens, Greece

more unexpected areas: the white beads of the jewelry, the skin, and parts of the tunic and eyes. A point of interest is the fact that the luminescence of Egyptian blue appears equally bright among areas that are presented in totally different hues, as if the pigment application is of equal proportion. This effect is notably manifested in the green-blue and the white beads of the necklace and earring.

A reflectance response in the IR region suggests the addition of an organic black colorant for the darker areas such as the hair, eyebrows, and outlines for all three portraits. IRR also revealed the presence of underdrawings on the female portrait (fig. 5.10). A distinct outline, a half rectangle in shape, guides the placement of each of the green-blue beads of the necklace.



Figure 5.10 Detail of IRR image of fig. 5.2, showing the underdrawing used for the placement of the green-blue beads. Photo: Hellenic National Archaeological Museum, Athens, Greece

We also digitally combined the IRR and VIS images to create infrared-reflected false color (IRRFC) images.⁵ In the case of the older man's wreath, the IRRFC image revealed a hue, mainly in the shading of the leaves, consistent with



Figure 5.11 Visible light detail of the wreath in fig. 5.3. Photo: Hellenic National Archaeological Museum, Athens, Greece



Figure 5.13 The IRRFC image of the older man's wreath generated by using the visible and IR images (inv. no. 1629). Photo: Hellenic National Archaeological Museum, Athens, Greece

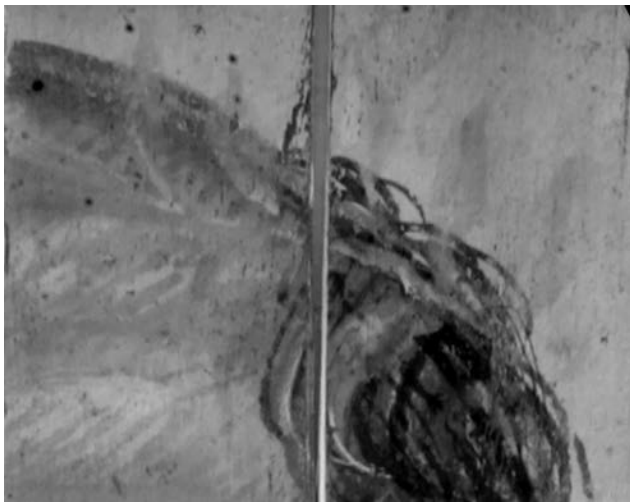


Figure 5.12 IRR image of the wreath in fig. 5.3. Photo: Hellenic National Archaeological Museum, Athens, Greece

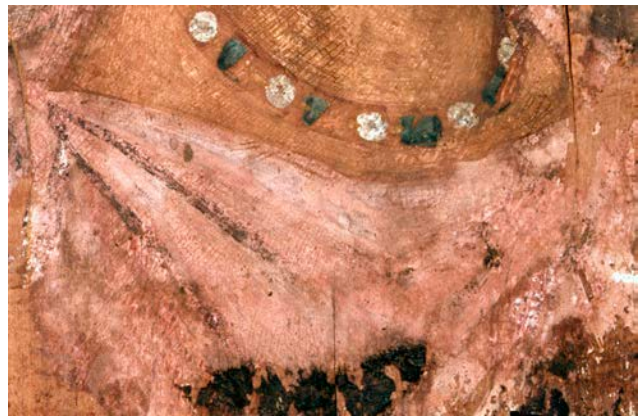


Figure 5.14 Visible image of the tunic in fig. 5.2. Photo: Hellenic National Archaeological Museum, Athens, Greece

the response of Egyptian blue, indigo, and some green earths (figs. 5.11–5.13).⁶ In the case of the woman's necklace and garment, the IRRFC image indicated that the green-blue beads and a few of the central folds corroborate the use of Egyptian blue—as seen in the VIL image. A wash of green earth or indigo is likely to have been added (figs. 5.14–5.16).⁷

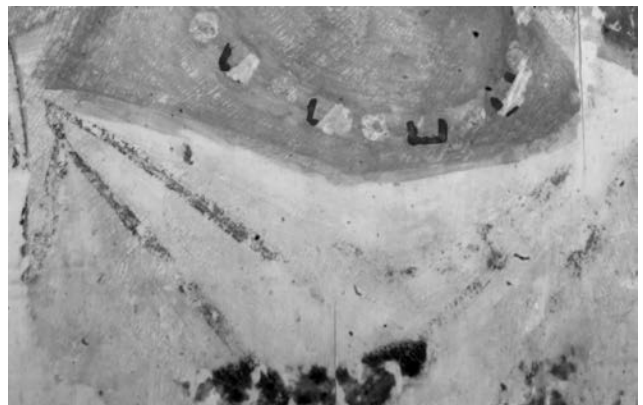


Figure 5.15 IRR image of the tunic in fig. 5.2. Photo: Hellenic National Archaeological Museum, Athens, Greece



Figure 5.16 IRRFC image of the tunic in fig. 5.2. Photo: Hellenic National Archaeological Museum, Athens, Greece

X-radiography was carried out using the in-house X-ray tube even though the equipment's setup is intended for industrial applications. The resultant images (figs. 5.17 and 5.18) indicate the application of a lead-based pigment, most probably lead white, for most of the female portrait and for the older man's wreath.



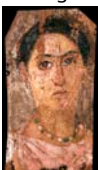
Figure 5.17 Radiograph of fig. 5.2. Photo: Hellenic National Archaeological Museum, Athens, Greece



Figure 5.18 Radiograph of fig. 5.3. Photo: Hellenic National Archaeological Museum, Athens, Greece

CHEMICAL ANALYSIS

Although imaging is a powerful tool for examining artifacts, it is regarded as a preliminary step in a scientific study; in-depth analysis is needed to obtain more precise results. For the portraits' elemental assessment, we employed readily available instruments at the NAM. The portable TRACER 5i XRF spectrometer by Bruker, equipped with a live-view camera and an 8-millimeter collimator, was used and run at two of the manufacturer's built-in applications—that is, Alloys 2 and MuddrockAir—so as to capture all possible chemical elements present on the paint surface. We also decided to examine between thirty-three and forty-five of the XRF targets' locations on each portrait to acquire information from a larger surface area and to produce results that yield a map of the elements present. In addition to this mapping attempt, we separated the paint surfaces into groups according to their hue and uniformity during data capture. The mean, median, maximum, and minimum values of the elements were calculated for different areas—the background, hair, skin, etc.—of the three portraits. Figure 5.19 summarizes the portraits' chemical elements according to their mean values.

	Group Areas	Major Elements	Minor Elements	Trace Elements
Fig. 5.1 33 targets 	Background	Ca, S	Si, Al,	Fe, Mn, K, P
	Hair	Ca, Fe, Si, S	Al, Mg	Mn, P
	Skin	Ca, S	Fe, Al, Si, Mg	Mn, K, P
	Lips	Ca, S, Fe, Si, Mg	Al	Mn, P
	Tunic	Ca, S		Fe, P, Si, Mg
	Clavi	Fe, Ca, Si	As, S, Al, Mg	Mn, K, P
Fig. 5.2 45 targets 	Background	Pb, Ca, S, Si	As, Fe, Mg	Cu, Mn, K, P, Al
	Hair	Pb, Fe, Ca, S, Si	As, Mg	Cu, Mn, K, P, Al
	Eyebrows	Pb, As, Fe, S	Ca, Si, Mg	Cu, Mn, K, P
	Skin	Pb, As, Fe, S	Hg, Ca, Si, Al, Mg	Cu, Mn, K, P
	Lips	Ca, S, Si	Pb, As, Fe, Al, Mg	Cu, Mn, K, P
	Tunic	Ca, S, Al	Pb, Si, Mg	As, Cu, Fe, Mn, K, P
	Green beads	Pb, Cu, Fe, Ca, Si, Hg	As, S, Al, Mg	Mn, K, P
White beads	Pb, As, S, Si	Cu, Fe, Ca, Mg	K, P, Al	
Fig. 5.3 35 targets 	Background	S, Al	Pb, As, Fe, Ca, Ca, Si, K, Mg	Cu, Mn, P
	Hair	Fe, S, Al	Ca, Si, Mg	Pb, As, Cu, Mn, K, P
	Skin	S, Al	Fe, Ca, Si	Pb, As, Cu, K, P, Mg

Group Areas	Major Elements	Minor Elements	Trace Elements
Wreath	Pb, As, S	Ca, Cl, Si, Mg	Cu, Fe, Mn, K, P, Al
Tunic	S, Al	Ca, Si	Pb, As, Cu, Fe, Mn, K, P, Mg
Clavus	Ca, S, Si, Al	Pb, Fe, Mg	As, Cu, Mn, K, P

Figure 5.19 Summary of the chemical elements detected via XRF in the three portraits. Chart: Peppy Tsakri and Ioannis Panagakos

Although the citation of numerous XRF results exceeds the scope of this paper, a special mention must be given to the jewelry beads in the woman's portrait, in relevance to their Egyptian blue content and how it relates to the VIL image. As previously noted, the white and the green-blue beads present a very similar, if not identical, degree of Egyptian blue luminescence in the IR spectrum. This finding raised the question of whether the proportions of Egyptian blue in the mixture of each colorant was of equal amounts. The elemental analysis performed with the XRF indicated that, when compared with the white beads, the green-blue beads have higher values of copper, silica, and calcium (the main compounds of Egyptian blue) as well as iron (fig. 5.20). The strong response of both the green-blue and the white beads with VIL suggests that the proportions of Egyptian blue present in the paint are not quantitative.

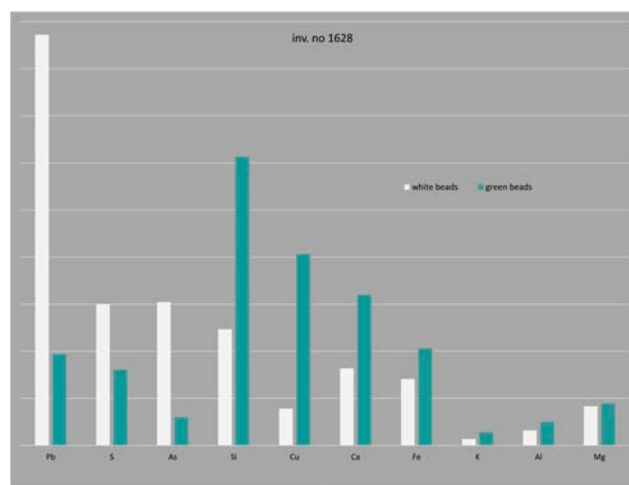


Figure 5.20 Graph of the chemical composition (mean values) of the woman's jewelry beads, according to XRF analysis. Chart: Peppy Tsakri and Ioannis Panagakos

MICROSCOPIC OBSERVATION

Microscopy could be considered an imaging technique; however, as an examination tool, it complements the other procedures used, aiding significantly to our understanding of the portraits' unique characteristics. Thus, microscopy should be mentioned separately.

We used a Leica optical microscope equipped with a digital camera to examine as much of the surface as possible. Therefore, all the XRF target locations were compared with the microscopy performed at different magnifications. Both male portraits appear to have a very thin ground layer (or none at all) applied on the wooden support; however, they have distinct differences in the style and the layering of the features of the eyes (figs. 5.21 and 5.22). In the case of the young man, the round iris was put down first, followed by the white sclera around it. The eye of the older man was painted in the opposite manner: first the sclera, then the iris, followed by the brown semicircle to form the inner pupil and on top of them the white highlights of the sclera, and lastly the dark details.

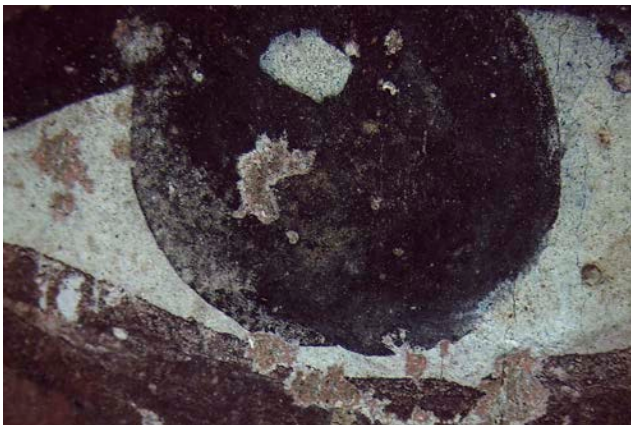


Figure 5.21 Visible image of the proper left eye in fig. 5.1. Photo: Hellenic National Archaeological Museum, Athens, Greece



Figure 5.22 Visible image of the only surviving eye in fig. 5.3. Photo: Hellenic National Archaeological Museum, Athens, Greece

In the female portrait, it is obvious, even macroscopically, that the paint surface is significantly thicker than those of the other two portraits, and under the microscope it becomes even more apparent. Specifically, some areas of skin have lost their top layer, revealing a lower pink layer (figs. 5.23 and 5.24). That same thick layering of paint is also very evident in the jewelry, and the sequence of applying the details becomes more apparent—for example, in the “gold” hoop of the earring and the “gold” links of the necklace that overlap the beads (figs. 5.25 and 5.26).



Figure 5.23 Microscopic detail image of an area on the PR cheek on fig. 5.2. Photo: Hellenic National Archaeological Museum, Athens, Greece



Figure 5.24 Microscopic detail image of an area of the forehead on fig. 5.2. Photo: Hellenic National Archaeological Museum, Athens, Greece



Figure 5.25 The overlapping of links on the earring beads in fig. 5.2. Photo: Hellenic National Archaeological Museum, Athens, Greece

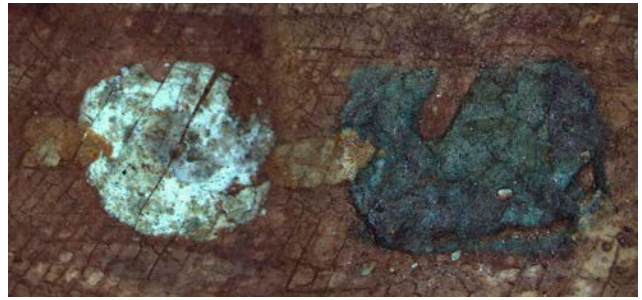


Figure 5.26 The overlapping of links on the necklace beads in fig. 5.2. Photo: Hellenic National Archaeological Museum, Athens, Greece

In terms of paint composition, various pigments were used in most instances. This fact is very clearly demonstrated in the microscopic images of a white bead on the woman's necklace and of an outer corner highlight of her PR eye (figs. 5.27 and 5.28), where granules of Egyptian blue can be observed in the white paint.

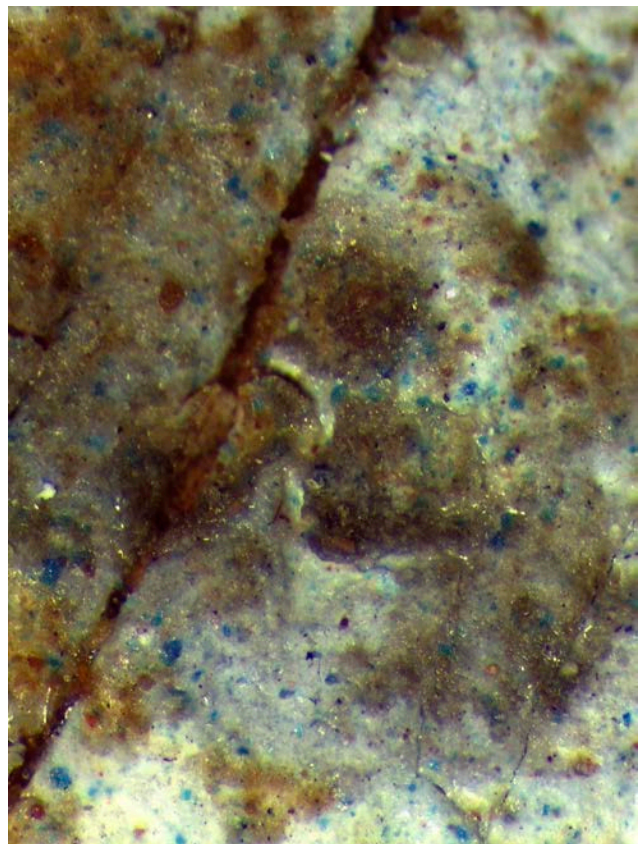


Figure 5.27 Egyptian blue particles in a white necklace bead in fig. 5.2. Photo: Hellenic National Archaeological Museum, Athens, Greece

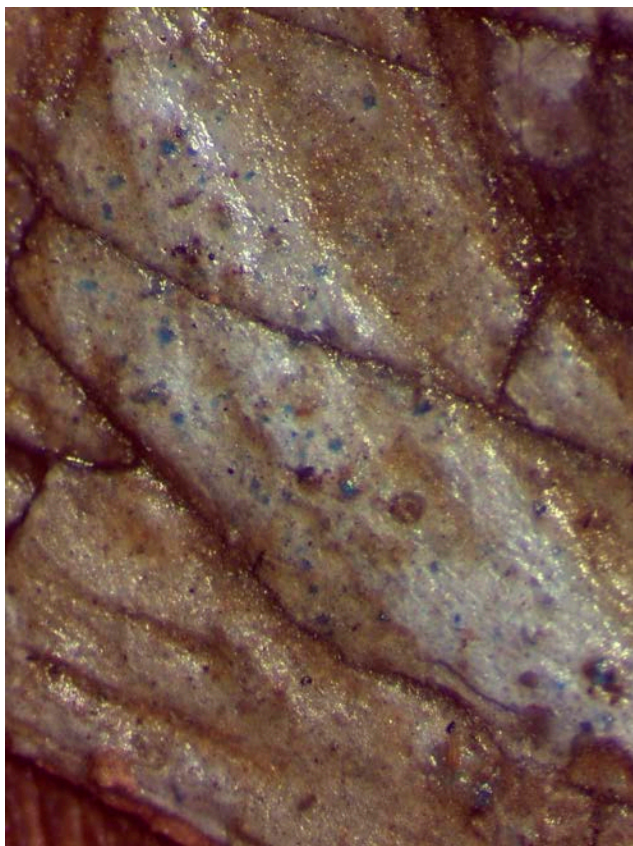


Figure 5.28 Egyptian blue particles in the sclera highlight of the PR eye in fig. 5.2. Photo: Hellenic National Archaeological Museum, Athens, Greece

CONCLUSIONS

This paper has described the scientific study of three funerary portraits in the Egyptian collection at the NAM, examined for the first time at the museum to overcome the challenge of “decoding” the portraits holistically. The methods used are part of the current infrastructure for non-invasive investigation of the Department of Conservation, Physical-Chemical Research, and Archaeometry at the NAM and were employed conjunctively.

In specific instances, XRF analysis provided the means to better understand the results of the imaging techniques for pigment identification in relation to the pigments’ unique characteristics. Specifically, we could better distinguish the pigments present in each portrait, as seen in figure 5.29, which enabled us to form robust deductions on the manufacture of the portraits and the intent of their creators. For example, the white beads of the woman’s jewelry most likely represent pearls and were painted using a mixture of mainly lead white, some orpiment, and a little Egyptian blue. The green-blue beads, however, most

likely are meant to represent emeralds. According to the XRF results, the mixture used to achieve the precious stone’s color was Egyptian blue (also verified by VIL) with possibly a green pigment and the addition of some yellows and reds. The presence of arsenic (As) and mercury (Hg) (see fig. 5.19) strongly indicates the use of realgar or orpiment and cinnabar. The addition of Egyptian blue in the mixture also shows the artist’s attempt to imitate a specific type of highly valued emerald.⁸ The fact that the jewelry is carefully rendered suggests that the portrait was intended to portray a person of wealth or a high-ranking member of society.

Colorant	No. 1627 (Young Man)	No. 1628 (Woman)	No. 1629 (Older Man)
Iron oxide (Umber or Ochre)	P	P	P
Orpiment or Realgar	P	P	P
Cinnabar		P	
Gypsum	P	P	
Kaolin			P
Lead oxide		P	P
Egyptian blue		P	
Green earth	P	P	P
Malachite		?	
Red lake		P	P
Indigo		?	?

Figure 5.29 Pigments (P) detected via XRF in each portrait. Chart: Peppy Tsakri and Ioannis Panagakos

The same cannot be said for the production of the portrait of the young man. Here, the artist took a more minimal approach, and the color palette used seems to be rather poor. It looks as though the artist chose limited pigments and made no attempt to depict shadows and highlights.

Somewhere in the middle lies the production of the older man’s likeness. The sitter has some degree of detailing, such as the addition of shadows and highlights and more ornamentation (with the wreath). His color palette has been more carefully chosen, as is evident in the formation of the wreath and clavus. IRRFC images confirm that the artist used various pigments, such as those based on lead,

arsenic, iron, and possibly green earth or indigo, for the wreath. As for the clavus, apart from madder lake, there is strong indication that realgar was also used.

Despite our initial understanding and subsequent investigation of these portraits—and the considerable new information that has been brought to light—some aspects still require investigation: the identification of the wood used for the panels and the analysis of the organic substances (colorants, varnishes, adhesives, binding media). The prospect of future work is exciting and challenging. We feel that the main benefits gained by our participation in the APPEAR project are the methods established at the NAM and the exchange of scientific investigations in the study of these precious artifacts.

ACKNOWLEDGMENTS

We would like to thank the following individuals at the NAM: Dr. Konstantinos Nikolentzos, head of the Department of Prehistoric, Egyptian, Cypriot, and Near Eastern Antiquities Collection; Dr. Georgianna Moraitou,

head of the Department of Conservation, Physical-Chemical Research, and Archaeometry; Panagiotis Lazaris, conservator in the Organic Materials, Paper, and Photo Negatives Conservation Laboratory; and Dr. Eleni Tourna, archaeologist in the Department of Prehistoric, Egyptian, Cypriot, and Near Eastern Antiquities Collection.

NOTES

1. Doxiadis 1995, 178–82, 223.
2. Measday, Walker, and Pemberton 2017.
3. Measday, Walker, and Pemberton 2017.
4. Measday, Walker, and Pemberton 2017.
5. Digital processing using Photoshop CC 2015 by Adobe.
6. Boust and Wohlgelmuth 2017.
7. Boust and Wohlgelmuth 2017.
8. In modern commercial terms, a rich bluish-green hue and a deep intense tone are considered characteristics of the more valuable emeralds. See Gemological Institute of America N.D.

Learning from Lemons: Mummy Portrait Forgeries in the Menil Collection

*Corina E. Rogge
Caroline R. Cartwright*

In 1954, art collectors John and Dominique de Menil established the Menil Foundation, a nonprofit charitable foundation in Houston, Texas, dedicated to the promotion of understanding and culture through the arts. The collecting habits of the de Menils were somewhat idiosyncratic; their collection was not encyclopedic but instead had particular strengths in antiquities and art from the Byzantine era, Africa, Oceania, the Pacific Northwest, and the twentieth century. These collecting areas correspond to art that the de Menils personally liked or to specific educational or social projects in which they engaged.¹ In 1987, the Menil Collection, a museum managed by the Menil Foundation, opened as the permanent home for their artworks. Its mission is to foster direct, personal encounters with works of art. Reflecting the ideals of the de Menils, admission is free, and the museum is dedicated to pursuing new and challenging ideas and disseminating original scholarly research.

A recent trend in the teaching of art history is object-based learning, in which students actively engage in the examination of objects and interpret and contextualize their findings to understand the means of manufacture, use, meaning, and/or history of objects.² The Collection Analysis Collaborative, a recent partnership between the Menil Collection, Rice University, and the University of Houston–Clear Lake, uses object-based learning to

enhance education, provide research opportunities, and improve understanding of the collection.³ The success of the initiative has stimulated a more holistic approach to utilizing the collection, including objects known or suspected to be forgeries.⁴

Among the antiquities in the Menil Collection are five Romano-Egyptian mummy portraits. Such portraits, which were originally integrated into the deceased individual's burial wrappings, exemplify cross-cultural exchange and integration of Greco-Roman artistic practices into ancient Egyptian funerary traditions.⁵ The period in which these objects were manufactured was relatively brief, beginning around the first century CE and ending with Emperor Theodosius's ban on the embalming of bodies in 392 CE.⁶ The limited period of manufacture, the relatively elevated socioeconomic status of individuals able to afford portraits,⁷ and the vagaries of preservation mean that only about a thousand mummy portraits are held in museum collections today.

In 2013, the J. Paul Getty Museum, recognizing a lack of scientific and technical information on mummy portraits, launched a collaborative project, Ancient Panel Paintings: Examination, Analysis, and Research (APPEAR). The Menil Collection joined this endeavor and conducted technical analyses on the five mummy portraits, which had never

been carefully studied. The analysis of two of the portraits, 1970-001 DJ (ST) and CA 5878 (ST) (figs. 6.1 and 6.2, respectively), described herein, reveals a nineteenth-century *terminus post quem* manufacture date, confirming them to be modern forgeries. These portraits, although not authentic, can facilitate a deeper understanding of the history of collecting and of the Menil Collection. They also make excellent case studies for discussing analytical approaches, sampling ethics, and the relationship between technical analysis and connoisseurship. We hope that illustrating how we utilize these forgeries will encourage other institutions to reevaluate the roles of such objects in their collections.

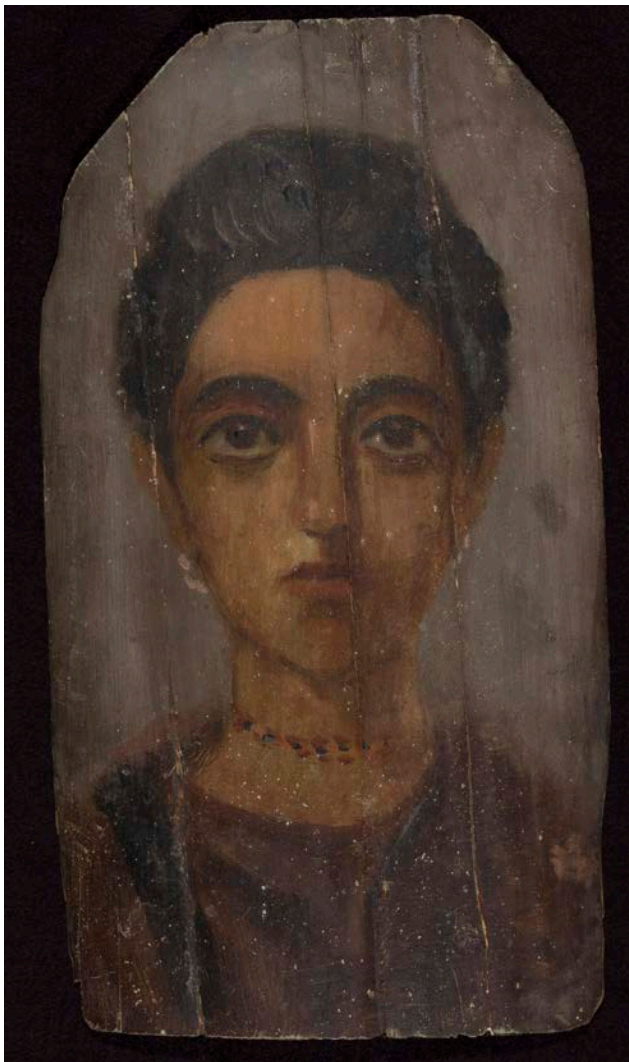


Figure 6.1 Mummy Portrait of a Woman, modern copy, second to third century CE. Encaustic on wood, 39.4 x 22.2 cm (15 1/2 x 8 3/4 in.). Although purchased as an authentic Romano-Egyptian mummy portrait, this study confirms it to be a modern forgery made with oil paint and anachronistic pigments, with a surface coating of wax meant to simulate an authentic encaustic work. The Menil Collection, Houston, 1970-001 DJ (ST). Photo: A. Neese

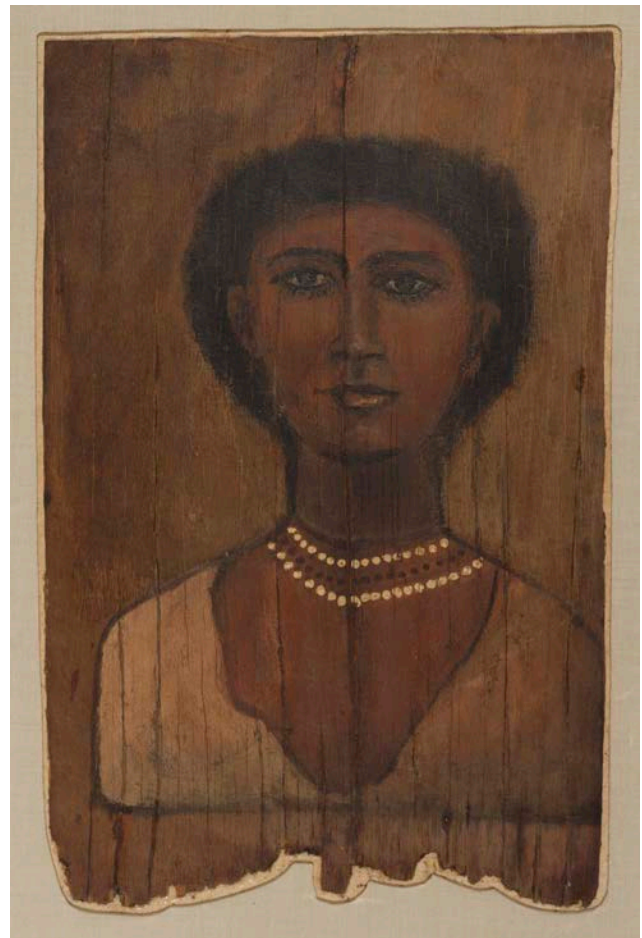


Figure 6.2 Portrait of a Woman, modern copy of Ptolemaic, 330-323 BCE. Paint and wood, 35.6 x 23.5 cm (14 x 9 1/4 in.). This work is confirmed to be a modern forgery made with oil paint and anachronistic pigments. The Menil Collection, Houston, CA 5878 (ST). Photo: A. Neese

RESULTS: TECHNICAL ANALYSIS OF THE MUMMY PORTRAITS

Mummy Portrait of a Woman, 1970-001 DJ (ST)

An unknown craftsman painted 1970-001 DJ (ST) (see fig. 6.1) on a *Pinus* sp. (pine) panel, a type of wood not hitherto found in authentic mummy portraits.⁸ A cross-sectional sample taken from the background (figs. 6.3-6.4) revealed that the artist applied a greenish-gray ground layer containing Prussian blue, barium sulfate, and zinc white onto the panel (fig. 6.5). These pigments are anachronistic; they were not introduced into artists' palettes until the early eighteenth century or later.⁹



Figure 6.3 Cross section taken from the gray background of 1970-001 DJ (ST) (fig. 6.1), showing a portion of the wooden substrate, the greenish ground that contains the modern pigments barium sulfate and Prussian blue, and the surface gray paint. Photo: C. E. Rogge

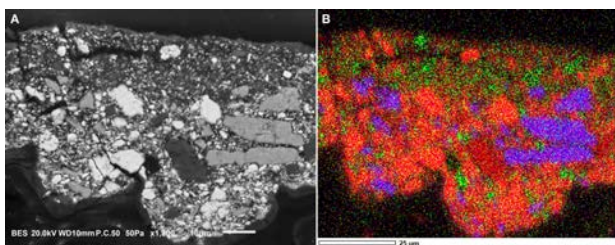


Figure 6.4 (A) Backscatter electron image of the sample shown in figure 6.3. (B) Elemental map showing lead in red, barium in blue, and zinc in green. Photo: C. E. Rogge

The red and yellow necklace beads may contain lead chromate species, first manufactured in the nineteenth century.¹⁰ The blue beads are high in cobalt, suggesting the use of cobalt blue, a species that came into widespread use in the early 1800s; however, cobalt blue has been found on painted ceramic vessels from ancient Egypt dating from 1400–1200 BCE, so it is not necessarily anachronistic—although no cobalt pigments have been found on authentic mummy portraits to date.¹¹

The binding media of the paints is a drying oil,¹² a material not used on authentic portraits, and all paints were applied with a brush. Visual inspection and Fourier-transform infrared spectroscopy (FTIR) analysis of a surface scraping reveals that a coating of wax was brushed over the finished work in an attempt to simulate the appearance of true encaustic portraits. The use of inappropriate wood and anachronistic pigments in the ground conclusively shows that this is not a pastiche or heavily restored object but a *de novo*, modern creation.

	Mummy Portrait of a Woman, 1970-001 DJ (ST)	Mummy Portrait of a Woman, CA 5878 (ST)	Analytical methods
Ground	Barium sulfate, lead white, Prussian blue, calcium carbonate, gypsum	Not present	Raman, FTIR, XRF, SEM-EDX
White	Not present	Barium sulfate, zinc white and/or lithopone, calcium carbonate	Raman, FTIR, XRF
Black	Not analyzed	Magnetite	XRF
Gray	Lead white, carbonaceous black, silicates	Not present	Raman, FTIR
Red	Vermilion, iron earth pigments, lead chromate	Not present	XRF
Pink	Vermilion, zinc white	Not present	XRF
Orange-yellow	Lead chromate, iron earth pigments, vermillion	Not present	
Blue	Cobalt blue	Not present	XRF
Skin	Iron earth pigments, lead white, zinc white, barium sulfate and/or lithopone	Iron earth pigments, calcium carbonate, barium sulfate, zinc white and/or lithopone	XRF

Figure 6.5 Pigments present in the mummy portraits.

Mummy Portrait of a Woman, CA 5878 (ST)

The second forgery, CA 5878 (ST) (see fig. 6.2) is more simply manufactured. The wood support is *Fagus sylvatica* (European beech) (fig. 6.6); this wood has not been identified to date in the more than 190 portraits analyzed and published by one of the authors (Caroline R. Cartwright), although other European species, such as *Tilia europaea* (lime), are common.¹³ The creator applied paint directly to the bare wood using a brush. X-ray fluorescence

(XRF) analysis indicates that the white paint contains either a mixture of zinc white and barium sulfate or lithopone (a mixture of zinc sulfide and barium sulfate), all components of which were introduced in the nineteenth century and so are inconsistent with the purported date.¹⁴ The red of the flesh tones is made from a mixture of earth pigments, calcium carbonate, barium sulfate, zinc white and/or lithopone. The black of the individual's hair contains high iron levels and is thus likely magnetite, a pigment not used in ancient Egypt.¹⁵ The binding medium of the paints is a drying oil.¹⁶

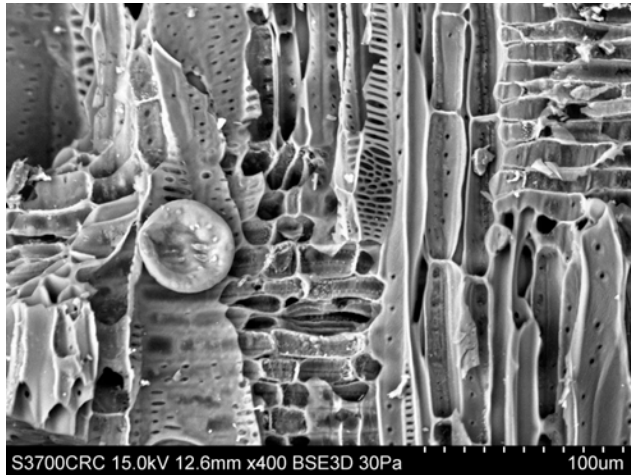


Figure 6.6 Scanning electron microscope image of a radial longitudinal section of *Fagus sylvatica* (European beech) wood from CA 5878 (ST). It shows (among other features) scalariform and reticulate perforation plates, one tylosis (of many), and rays with procumbent cells and square marginal cells. The condition of this wood is similar to modern fresh wood samples; it is unlike the condition of other mummy portrait woods. The presence of scalariform and reticulate perforation plates shows clearly that it is beech rather than oak, which has simple perforation plates. Photo: C. R. Cartwright. © The Trustees of the British Museum

DISCUSSION

After the analytical results confirmed that these two objects are forgeries, the question then became what value they held to the Menil Collection. Many institutions deaccession such objects or consign them to storage, never to be shown or discussed again. However, a few exhibitions have chosen to highlight the presence of forgeries in collections and explain the role technical analysis plays in their unveiling.¹⁷ These are popular with museum visitors, but exhibiting these forgeries and explaining their stories would require more didactics than is permitted at the Menil Collection.

While these portraits do not have ancient lives, their modern ones are instructive. Forgeries inform us about

supply and demand, about appeal and desire—and often the style of a forgery reflects contemporary fashions.¹⁸ Although not authentic objects from ancient Egypt, these portraits tell a story of the de Menils, their philosophies, collecting habits, and favored gallerists, expanding the research begun by the Collection Analysis Collaborative.¹⁹ The forgeries are also excellent pedagogical materials and can be used with almost any audience level to initiate discussions on a variety of topics, including the interplay of connoisseurship and technical investigations, the ethics of destructive sampling, and low-tech versus high-tech analytical approaches.

Fashions, Fads, and Forgeries

The French campaign in Egypt (1798–1801), the publication of *Description de l'Égypte* (1809–1829), and the deciphering of hieroglyphs by Jean-François Champollion in 1822 began a period of Egyptomania. Archaeological sites were plundered and artifacts, whether acquired legally or illegally, were exported for sale, and the popularization of antiquities inevitably led to the production of forgeries. An early collector lamented, “What, for Christ’s sakes, was to be done in order to supply antiquities to so many amateurs, interested, and curious parties? How does one find divinities, statuettes, and scarabs? How does one find them when they are not to hand? Either by looking for or by making them—the latter being the faster option.”²⁰

Forgers reacted quickly to new archaeological finds and demands of the market. As early as 1826, forgeries began to enter collections. In 1912, Dr. T. G. Wakeling published a book on forgeries of ancient Egyptian materials, interviewing forgers, discussing different “schools” of forgers, and documenting the types of objects commonly forged. He provided photographs of the forgeries in his collection and information on the types of materials and pigments to be expected in authentic objects.²¹ In 1930, Ludwig Borchardt published a paper with accompanying photographs of “ancient Egyptian” objects in collections that he believed to be inauthentic.²² Since that time, museums—including the British Museum, Metropolitan Museum of Art, Brooklyn Museum, the Louvre, the Ägyptisches Museum und Papyrussammlung, and the Staatliches Museum Ägyptischer Kunst—have discovered forgeries in their collections.²³ The creation and unmasking of forgeries of ancient Egyptian materials continue to this day, with the Bolton Museum’s Amarna Princess being an infamous example.²⁴

Mummy portraits first came to the attention of Europeans in 1615, when Pietro della Valle, an early Italian explorer, visited an excavation at Saqqara.²⁵ Della Valle fell in love

with the portraits, describing them as the “most delicate sight in the world,”²⁶ and acquired two, both of which are now in the Staatliche Kunstsammlungen Dresden collection (inv. nos. Aeg 777 and Aeg 778). The acquisition and export of mummy portraits continued when Egypt was under British administration. One of the primary responsibilities of Sir Henry Salt, the consul general of Egypt from 1816 to 1827, was to acquire antiquities for the British Museum. He also collected mummy portraits for himself, including one now in the Louvre collection (N 2733.3).²⁷ It was the Viennese antiquities dealer Theodor Graf, however, who truly popularized mummy portraits. In 1887 he began acquiring them, ultimately amassing a collection of almost three hundred, which he exhibited and sold in Europe and North America.²⁸ Ironically enough, the emergence of such a large number of portraits with little provenance raised suspicions that they might all be forgeries, but Sir Flinders Petrie’s excavations at Hawara (1888–89 and 1910–11) conclusively demonstrated that mummy portraits had been made in antiquity.²⁹

The relative scarcity and appealing nature of the mummy portraits made them attractive targets for forgers, and many forgeries date from the late 1800s to early 1900s, when they were novel and in demand. Four portraits in the Brooklyn Museum (inv. nos. 51.253.1–4) were collected in the Fayum region of Egypt around 1911³⁰ and document the quick response of forgers to Petrie’s excavations. The two Menil portraits may also date to the early 1900s, as both lack titanium white, a pigment that became ubiquitous by the mid-1900s,³¹ suggesting that it may not have been accessible to the forgers. Although absence of a material can never provide definitive proof, it is suggestive and would slot the creation of these forgeries nicely into the time frame when mummy portraits were becoming desired objects.

In addition to mimicking objects of desire and demand, forgeries may inadvertently reflect the aesthetic standards of their time of creation. Subconsciously, forgers may integrate ideals of beauty and contemporary tastes into their works. Kenneth Clark, director of the National Gallery from 1934 to 1945, first became suspicious of a “Botticelli” painting when he noticed that, as depicted, the Madonna resembled contemporaneous cinema stars.³² In figure 6.1, the portrait’s strong half-moon eyebrows, large eyes, and rosebud lips are evocative of the Edwardian beauty ideal—as is the hairstyle resembling a low pompadour—suggesting an early 1900s creation date.

Reflections of a Collection

A small number of art historians and dealers were extremely influential to the de Menils; among them was Alexander Iolas (1907–1987).³³ He was a friend of artists, including Giorgio de Chirico, Georges Braque, Max Ernst, René Magritte, Man Ray, and Pablo Picasso, and traded upon these personal associations when he became head of the Hugo Gallery in New York in 1946. This gallery was founded by Maria Hugo, a fellow émigré and one of the first friends the de Menils made in the United States. Their personal friendship with Hugo led the de Menils to invest in the gallery, beginning a forty-year relationship with Iolas. Over that period, the de Menils purchased a large number of works from Iolas, 450 paintings alone, including the majority of their Surrealist collection. Dominique trusted his judgments on contemporary art, saying, “He always kept paintings for us, and since he had a very good eye, they were the best.”³⁴ Financial support commingled with friendship; the reason that paintings were “kept” by Iolas for the de Menils was thanks to their financial underwriting: they advanced money to support collecting trips to Paris, which was repaid by their keeping “this and that” when he came back.³⁵

The “this and that” kept by the de Menils may have included CA 5878 (ST) (see fig. 6.2). Neither the Hugo Gallery nor Iolas’s later galleries specialized in antiquities, but Iolas himself collected and sold them. The de Menils acquired a variety of antiquities from Iolas, including some that were later found to be suspected or outright forgeries, and by 1963 or 1964 they had become skeptical of his trustworthiness when it came to antiquities.³⁶ The de Menils did not leave any indication of why they purchased the mummy portrait, but the unconvincing style of the portrait makes it hard to believe they thought it authentic, so perhaps by purchasing it they effectively donated funds to support Iolas’s gallery. This supposition is supported by the de Menils’ accounting records, which show no other purchases made at the same time, suggesting that the transaction could have been a one-off donation to a friend. The world-class Surrealism collection created by the de Menils and Iolas, which hangs in a dedicated gallery space in the museum, is a testament to their productive relationship—but so, in its own way, is this portrait.

Dominique de Menil purchased 1970-001 DJ (ST) in 1962, but left no information on why she chose to acquire it. The portrait was obtained from Michel Abemayor, a New York City dealer and scion of a family of well-established antiquities dealers; his grandfather founded a shop opposite Shephard’s Hotel in Cairo in 1888.³⁷ After World

War II, Abemayor relocated to the United States and established his Ancient Works of Art gallery. Objects that passed through the Abemayor family ended up in a variety of different museums, and the Archaeological Institute of America has an annual Abemayor Lecture “in recognition of Mr. and Mrs. Abemayor’s lifelong interest and enjoyment in the study of ancient cultures.” The respect paid to Michel Abemayor implies he did not have a reputation for dealing in forgeries, although the large number of forgeries in the antiquities market inevitably resulted in some passing through his gallery. The de Menils paid for two different conservation treatments of the mummy portrait, suggesting that they did not initially suspect it to be a forgery. However, by 1970 it was considered suspect on stylistic grounds, as mentioned above.

One unifying theme of the de Menils’ collection was humanism. They were strongly influenced by Father Marie-Alain Couturier, who advised and advocated for purchases of non-naturalistic modern and “primitive” art because the materials shared a purity of spirit.³⁸ Pamela Smart summarized the philosophy shared by Couturier and the de Menils, writing, “The aesthetic qualities of artworks lie not in the character of the objects themselves but are predicated on the human virtues of those who craft these objects. The art object is a trace of humanity, just as it is a means by which that very humanity might be fostered.”³⁹ The eyes of a modern viewer are drawn directly to the eyes of the individuals in mummy portraits, and a connection across time is created. This automatic recognition of humanity in mummy portraits exemplifies the type of relationship the de Menils were trying to foster between viewers, objects, and their creators. A more personal connection may have existed between the de Menils and the more stylistically convincing of our two forgeries, 1970-001 DJ (ST): a family friend noted that the portrait subject resembled Christophe de Menil, one of John and Dominique’s daughters.⁴⁰

Pedagogical Value of Forgeries

John de Menil was sanguine about the possibility of purchasing forgeries; he saw it as a learning opportunity: “So there are the fakes and the lemons and the total involvement and the engulfing passion. There is all of that but it’s worth it. . . . You learn a lot in the process of researching and cataloguing. A lot about civilizations, about men—and their yearnings and their fears.”⁴¹ The ability to learn from art, to use their collection as a means to teach, was an important part of the collecting philosophy of the de Menils. They felt that students at Rice University and the University of St. Thomas lacked access

to art, and that to understand and appreciate objects they needed the opportunity to look at and handle works of art—not just to experience them through slides or images in a book. Although the term had not yet been coined, the de Menils wanted students to engage in object-based learning. Many of the purchases made by the de Menils were intended to help establish a teaching collection. The mummy portrait forgeries make excellent case studies for illustrating critical thinking and the importance of technical studies in art history.

High-Tech versus Low-Tech Analysis

“Bigger, better, faster” is one mantra of the modern era, and it leads to the perception that high-tech approaches are most effective. When discussing with audiences how to determine whether the Menil mummy portraits are forgeries, radiocarbon dating is almost always suggested as the first approach. We have found that using this suggestion as a pivot to discuss the ethics of sampling, limitations of the method, the cost of analysis, and the value of low-tech approaches is highly effective and engaging. Until the advent of accelerator mass spectrometry, radiocarbon dating required large samples. Modern instrumentation has reduced the sample size required, but other techniques can be undertaken non-destructively or with still less material. Members of the American Institute of Conservation, including conservators and conservation scientists, abide by a code of ethics and guidelines for practice.⁴² These mandate that non-invasive methods of analysis are to be preferred, and “the choice of testing techniques, the amount of sample required, and the expected value of the information gained, must be weighed against the effect of removal of the sample upon the cultural property.”⁴³ We could have radiocarbon dated the mummy portrait panels, but many forgers utilize age-appropriate supports, and the results would not have revealed the age of the pictorial layers. Given the sample size, the cost of radiocarbon dating (often over \$400 per sample), and the incomplete information that would have been obtained, we decided to employ other approaches.

Our first approach to analysis in a museum laboratory is often X-ray fluorescence spectroscopy (XRF), a non-destructive form of elemental analysis. Although not able to conclusively identify materials, this method can provide strong suggestions for the pigments present based upon elemental signatures. In both of our forged mummy portraits, XRF clearly revealed the presence of anachronistic materials, while scanning electron microscopy (SEM) was used to detect anachronistic wood species in the two forgeries. However, many institutions do not have access to scientific equipment, or a scientist.

In the case of mummy portraits, more accessible imaging techniques, including X-radiography and visible-induced infrared luminescence (VIL), may provide the same answer. Many museums own X-radiography systems or can negotiate access to medical or veterinary units or contract with commercial companies. Comparison of the X-radiograph of 1970-001 DJ (ST) with that of an authentic mummy portrait from the Menil Collection, Mummy Portrait of a Man (CA 7013), is quite revealing (fig. 6.7). The X-radiograph of the man's portrait (fig. 6.7D) shows the individual strokes of paint quite clearly, due to the use of the radiopaque lead white pigment. In contrast, the X-radiograph (fig. 6.7B) of Mummy Portrait of a Woman shows almost no detail, because of the method of paint application and the use of an anachronistic barium sulfate-rich ground layer that is X-ray opaque. The absence of clearly defined strokes of paint in this portrait supports its identification as a modern forgery.



Figure 6.7 Top: Mummy Portrait of a Woman, modern forgery: (A) Normal light, (B) X-radiograph. Bottom: Mummy Portrait of a Man, second century CE. Encaustic paint on wood, 45.1 x 27 cm (17 3/4 x 10 5/8 in.): (C) Normal light, (D) X-radiograph. The authentic portrait clearly shows individual lead white-rich brushstrokes that are X-ray opaque and appear white in (D). The modern forgery shows only the radiopaque ground layer (B). The Menil Collection, Houston, 1970-001 DJ (ST) and CA 7013. Photo: A. Neese / X-radiographs: B. Epley

Egyptian blue, one of the first manufactured pigments, has the relatively unique property of emitting light in the infrared range when illuminated with visible light.⁴⁴ Cameras modified by removal of the manufacturer-installed infrared filter placed over the image sensor can document this luminescence.⁴⁵ Figure 6.8A shows a mummy portrait of a girl; in the VIL image (fig. 6.8B) the hazel eyes of the girl appear white, due to the luminescence of Egyptian blue. The camera modification and filter sets needed to do this type of imaging are inexpensive, and this sensitive, non-destructive technique can be used to identify Egyptian blue in museums and at archaeological sites.



Figure 6.8 Mummy Portrait of a Young Girl, 30 BCE–200 CE. Encaustic on wood, 26.8 x 15.2 cm (10 9/16 x 6 in.). (A) Normal light. Photo: Thomas R. DuBrock; (B) VIL. The eyes glow in the VIL image due to the presence of Egyptian blue. Private collection on long-term loan to the Museum of Fine Arts, Houston, TR:184-2013. Photo: VIL image by M. Golden

The identification of Egyptian blue is of key importance because, while it was the most common blue pigment in ancient Egypt, its use gradually declined until the process for making it was lost sometime after the ninth century CE, although sporadic instances of use, or perhaps reuse, continued until the sixteenth century.⁴⁶ In 1815, Egyptian blue was reintroduced to the world through Sir Humphry Davy's analysis of samples excavated at Rome and Pompeii, and by 1889 the chemical formula of the material had been determined.⁴⁷ However, it was not produced on a commercial scale until around 1893 and then was available only through a single French manufacturer.⁴⁸ It was seen as an historic curiosity rather than a useful pigment since it is coarse grained and difficult to use. Because it was not widely available during the nineteenth century, it is unlikely that many forgers at the time or in the early twentieth century would have had access to it. For this reason, a mummy portrait with Egyptian blue on it that entered a collection in the early 1900s has a good

probability of being authentic. Still, not all authentic mummy portraits use Egyptian blue, and its absence cannot be taken as proof of inauthenticity.

No techniques discussed in this section—radiocarbon dating, XRF, X-radiography, or VIL—are definitive, but the last three are non-destructive, and so, preferable. Realities of and limitations to scientific investigations are often glossed over in forensic television shows or academic papers. We want students to appreciate these factors and engage in critical thinking about why a technique was used and whether it was appropriate. Using our mummy portraits as examples, we ask students to define what the expected outcomes for each analytical test would be for authentic or inauthentic objects, to select what analytical techniques they would use, and to justify that choice. The discussion can then be broadened to include other analytical techniques or other types of artworks, if desired.

Connoisseurship and Technical Analysis in Dialogue

Traditional connoisseurship involves the gathering of visual cues from the close examination of an artwork that are then compared against a corpus of work accepted as authentic. One of the best descriptions of connoisseurship is that it “requires a wide range of intellectual qualifications; something of the astuteness of a lawyer, the diagnosis of a physician, and the research of the antiquary and historian, all combined in an art which most of us are practicing every day, more or less consciously, the art of comparison.”⁴⁹ Like provenance research or technical analysis, it is not an infallible means of establishing authenticity, but when used in conjunction these complementary methods constitute a highly effective approach.

A letter in the Menil Collection Archives dated August 31, 1970, from John de Menil to Dr. Klaus Parlasca of the Archäologisches Institut Goethe Universität Frankfurt am Main expresses concern about the authenticity of 1970-001 DJ (ST). De Menil described four main issues:

1. There was no base paint (ground) under the subject of the painting.
2. The wood has “coarse veins.”
3. It was painted with a brush instead of a spatula.
4. The ears and earrings are painted impressionistically.

Based upon these points, when the de Menils donated the painting to the Menil Foundation it was as a suspected

forgery. The letter can initiate excellent discussion among students, especially since none of the issues raised by de Menil in his letter are entirely confirmed by technical analysis. For example:

1. John de Menil incorrectly describes both this object and authentic objects: there *is* a ground layer underlying the portrait, and the use of ground layers on authentic mummy portraits is inconsistent.⁵⁰
2. The statement that the wood has “coarse veins” is ambiguous; woods do not have veins. It is likely that de Menil meant that the wood was coarse grained, and as the majority of authentic mummy portraits on panel utilize *Tilia europaea*, a fine-grained wood, a coarse-grained wood could seem suspicious.⁵¹ However, the coarse-grained genus *Quercus* was used occasionally in antiquity for mummy portraits.⁵² The actual wood was identified as *Pinus* sp., a species not encountered thus far by Cartwright in authentic portraits, which is suspicious.
3. The ancient painters used both brushes and spatulas, and often used both on a given painting, so brushstrokes are not necessarily anachronistic. A close examination of the portrait under raking light does show a stylistic anachronism, however: some of the brushstrokes do not correspond to the underlying paint application and instead arise from the surface application of wax, a coating technique not used on authentic portraits.
4. The final point of concern, the impressionistic treatment of the earrings, is a particularly engaging topic. The artist simply used three quick dashes of paint to indicate the earrings, rather than very carefully depicting the jewelry, as seen in some authentic portraits, such as the portrait of Isidora in the J. Paul Getty Museum (fig. 6.9). For ancient Egyptians, expensive accessories signaled social status, and finely executed mummy portraits tend to depict jewelry as realistically as they do the sitter, whereas the earrings and necklace of 1970-001 DJ (ST) lack such realism. That said, not all artists creating mummy portraits were highly skilled. Another example from the J. Paul Getty Museum, shown in figure 6.10, is less realistic than either the forged Menil portrait or that of Isidora. Introducing this contrast to the discussion reinforces the ideas that “crudeness” does not necessarily denote inauthenticity and that royal workshops and village craftsmen will create objects with a wide skill gamut. (At this point, we found it very effective to ask the

audience to reevaluate the other Menil forgery, CA 5878 [ST], in light of diverse artistic abilities.)



Figure 6.9 Mummy Portrait of a Woman, 100 CE. Encaustic on limewood, gilt and linen, 48 x 36 x 12.8 cm (18 7/8 x 14 3/16 x 5 1/16 in.). This portrait exemplifies the skill achievable by the ancient portraitists. Los Angeles, J. Paul Getty Museum, 81.AP.42.

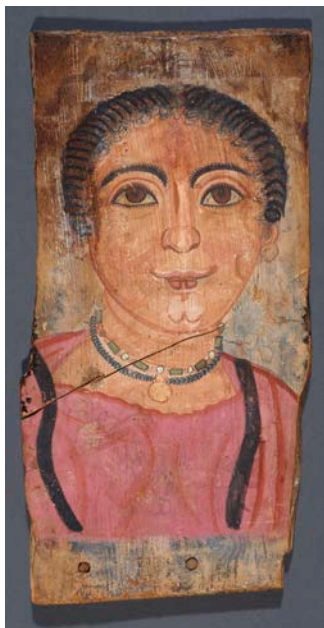


Figure 6.10 Mummy Portrait of a Woman, unknown Romano-Egyptian, ca. 175-200 CE. Tempera on wood, 28.2 x 14.5 cm (11 1/8 x 5 11/16 in.). This portrait is charming but does not exhibit the same realism shown by the portrait of Isidora (fig. 6.9). Los Angeles, J. Paul Getty Museum, 79.AP.129.

In an educational environment, this dialogue between connoisseurship and technical analysis can be turned into a Socratic lesson. Students can be asked to compare 1970-001 DJ (ST) with images of authentic mummy portraits and generate their own lists of characteristics for supporting or refuting authenticity. Their lists can then be compared with the issues voiced by John de Menil and the differences discussed. The technical analyses can be introduced into the discussion and used to address the students' concerns as well as those of de Menil. This type of discursive dialogue between the students and the object, facilitated by the instructor, is indispensable for training rigorous scholars in almost any field.

CONCLUSIONS

Thomas Hoving, a past director of The Metropolitan Museum of Art, claimed that 40 percent of all objects he looked at over a fifteen-year period were either fakes or so heavily restored as to be nonrepresentative.⁵³ Careful preacquisition screening may reduce the number of fakes and forgeries in a collection, but it is almost inevitable that some will be acquired, and to avoid falsification of history and distortion of scholarship they must be identified. Such revealed forgeries can be used to enhance scholarship by training the eyes of the public and young scholars and by serving as tools in object-based learning methods to teach critical thinking and analytical approaches. Museums should include them in collection databases and publish their characteristics so that other institutions and collectors can make comparisons with their own objects; we have contributed the technical results from the Menil Collection's mummy portrait forgeries to the Getty Museum's APPEAR database. We advocate that these objects, which John de Menil recognized as "lemons," be put to use, figuratively, to make lemonade. By illustrating the pedagogical approaches we have taken to integrate these objects into our object-based learning praxis, we hope to encourage other institutions to reevaluate the possibilities inherent in the lemons of their own collections.

APPENDIX: SCIENTIFIC METHODOLOGY

Sampling and Cross Section Preparation

Samples of the portraits were taken under magnification using a 0.5 mm Ted Pella micro-chisel. For cross sectioning, samples were embedded in Bio-Plastic resin and polished using Micro Mesh sheets (120-12000 grit). Sample images

were taken with a Zeiss AxioCam MRc 5 camera mounted onto a Nikon Labophot POL microscope and controlled by Zeiss AxioVision AC software (v. 4.5). Samples were taken from the portraits for analysis of the binding media by scientists at the Getty Conservation Institute.⁵⁴

X-ray Fluorescence Spectroscopy (XRF)

XRF spectra were collected using either a Bruker Artax 400 or Bruker Tracer III SD energy dispersive X-ray spectrometer. The Artax has a rhodium (Rh) target X-ray tube with a 0.2 mm-thick beryllium (Be) window and was operated at 40 kV and 400 mA current. The X-ray beam was directed at the artifact through a polycapillary tube. X-ray signals were detected using a Peltier-cooled XFlash silicon drift detector (SDD) with a resolution of 146.4 eV. Helium purging was used to enhance sensitivity to light elements. Spectra were collected over 180 seconds (live time). The Bruker Tracer III SD spectrometer is equipped with a Peltier-cooled XFlash SDD with a resolution of 145 eV. The excitation source was a rhodium-target X-ray tube, operated at 40 kV and 10 μ A current. Spectra were collected over 180 seconds (live time).

Fourier Transform Infrared Spectroscopy (FTIR)

Attenuated total reflectance (ATR) and transmission spectra were collected using a Bruker Lumos FTIR microscope equipped with a MCT-A detector and a motorized germanium ATR crystal with a 100 μ m tip. Transmission spectra were obtained by flattening samples in a diamond compression cell, removing the top diamond window, and analyzing the thin film on the bottom diamond window. ATR spectra were taken on cross-section samples embedded in Bio-Plastic. All spectra are an average of 64 or 128 scans at 4 cm^{-1} spectral resolution.

Dispersive Raman Microspectroscopy

Dispersive Raman spectra were collected on a Renishaw inVia Raman microscope using a 785 nm excitation laser operating at powers between 75.4 μ W and 7.41 mW at the sample, as measured using a Thorlabs PM100D laser power meter equipped with a S120C photodiode power sensor. A 50x objective was used to focus the excitation beam on the sample. Each scan was of 10 seconds duration, and the spectral resolution was 3–5 cm^{-1} across the spectral range analyzed.

Scanning Electron Microscopy–Energy Dispersive Spectrometry (SEM-EDX)

Backscatter electron images of cross-sectional samples were taken with a JEOL JSM-IT100 scanning electron microscope operating at pressures of 50–55 Pa, an accelerating voltage of 20 kV, and a probe current of 40–50 (unitless value from SEM operating software). Energy dispersive X-ray spectrometry using the integrated detector was performed under the same pressure conditions but with higher probe currents (65–75).

Wood Identification

Small samples were manually fractured to expose transverse, radial-longitudinal, and tangential-longitudinal sections and analyzed as reported by Cartwright.⁵⁵

ACKNOWLEDGMENTS

We thank Paul R. Davis, curator of collections at the Menil Collection, and David Aylsworth, collections registrar at the Menil Collection, for critical reading of the manuscript and sharing their knowledge of the de Menils and the collection; Yekatarina Barbash, associate curator of Egyptian art, and Lisa Bruno, the Carol Lee Shen chief conservator, both of the Brooklyn Museum, for kindly sharing information about the forged mummy portraits in their collection; and the Andrew W. Mellon Foundation for supporting conservation science at the Museum of Fine Arts Houston and the Menil Collection.

NOTES

1. van Dyke 2010.
2. Chatterjee and Hannan 2016.
3. Hopkins, Costello, and Davis 2021.
4. Definitions of the term *forgery* vary; here we use it to mean an object deliberately made to deceive others as to its origin and age.
5. Thompson 1982; Doxiadis 1995; Picton, Quirke, and Roberts 2018; Walker 2000B; Svoboda and Cartwright 2020.
6. Thompson 1982, 4.
7. Borg and Most 2000.
8. Cartwright 2020.
9. Feller 1986; Berrie 1997; Kühn 1986.
10. Kühn 1986.

11. Roy 2007; Shortland, Appleby Hope, and Tite 2006.
12. Mazurek, Svoboda, and Schilling 2019.
13. Cartwright 2020.
14. Kühn 1986; Eastaugh et al. 2004.
15. Lee and Quirke 2000, 108–11.
16. Mazurek, Svoboda, and Schilling 2019.
17. Examples include *Fakes and Forgeries*, Minneapolis Institute of Arts (1973); *Falsche Faraonen. Zeitung zur Sonderausstellung 400 Jahre Fälschungsgeschichte*, Staatliche Sammlung Ägyptischer Kunst (1983); *Fake? The Art of Deception*, British Museum (1990); *GeaECHTet. Fälschungen und Originale aus dem Kestner-Museum*, Kestner Museum (2001); *Unearthing the Truth: Egypt's Pagan and Coptic Sculpture*, Brooklyn Museum (2009); *The Metropolitan Police Service's Investigation of Fakes and Forgeries*, Victoria & Albert Museum (2010); *Fakes, Forgeries and Mysteries*, Detroit Institute of Arts (2019); *Russian Avant-Garde at the Museum Ludwig: Original and Fake*, Museum Ludwig (2020).
18. Jones, Craddock, and Barker 1990, 11–27; Briefel 2006; Lenain 2011.
19. Hopkins, Costello, and Davis 2021.
20. Clerc (1847) 2009, 28.
21. Wakeling 1912.
22. Borchardt 1930, appendix.
23. Cooney 1950; Schoske and Wildung 1983; Davies 1984; de Cenival 1991; Arnold and Valladas 1991; Lilyquist, Hoch, and Peden 2003; Biron and Pierrat-Bonnefois 2007; Fiechter 2009, 92–119.
24. Hardwick 2010.
25. Borg and Most 2000, 63–96.
26. Bietenholz 1962.
27. Manley and Réé 2001; Thompson 1982, 3.
28. Thompson 1982, 4.
29. Picton, Quirke, and Roberts 2018.
30. Brooklyn Museum object files, kindly communicated by Dr. Yekatarina Barbash, associate curator of Egyptian art at the Brooklyn Museum.
31. Laver 1997.
32. Jones, Craddock, and Barker 1990, 34–35.
33. Middleton 2018, 307–15.
34. Biographical interview of Dominique de Menil by Paul Winkler and Carol Mancusi-Ungaro, September 25 and 27, 1995, Menil Archives.
35. Dominique de Menil interview.
36. Davis 2021.
37. Bierbrier 2012, 3.
38. Smart 2010, 70–73, 79–86; Middleton 2018, 185–88, 251–53.
39. Smart 2010, 83.
40. Bettie Cartwright, personal conversation, October 24, 2016.
41. Typed notes held in the Menil Archives for a talk by John and Dominique de Menil entitled “The Delight and the Dilemma of Collecting,” given at the University of St. Thomas, Houston, April 9, 1964.
42. American Institute for Conservation 1994; American Institute for Conservation 2015.
43. American Institute for Conservation 2015.
44. Pozza et al. 2000; Accorsi et al. 2009.
45. Warda 2011.
46. Lee and Quirke 2000; Lazzarini 1982; Lluveras et al. 2010; Bredal-Jørgensen et al. 2011.
47. Davy 1815; Fouqué 1889.
48. Adrian 1893.
49. Eastlake 1891.
50. Ramer 1979; Salvant et al. 2018; Svoboda and Cartwright 2020.
51. Cartwright 2020.
52. Cartwright 1997A.
53. Hoving 1997, 17.
54. Mazurek, Svoboda, and Schilling 2019.
55. Cartwright 2015; Cartwright 2020.

Mummy Portraits and Painted Panels from Roman Egypt: Seeing the Wood for the Trees

Caroline R. Cartwright

It is clear that the remarkably good preservation of the cellular wood structure of mummy portraits and painted panels is due to the dry conditions that existed within sealed ancient Egyptian tombs. Such preservation has enabled the diverse research produced on these objects in the APPEAR project. At the British Museum, scanning electron microscope identifications of the chosen woods have further expanded our knowledge of wood use in Roman Egypt, and additional species have emerged, not previously published.¹

Given that we knew already² that the preference was for the selection of imported woods, principally limewood (*Tilia* sp.), it may be rewarding to unpick the reasons local Egyptian timbers were used as well. Looking back at wood use in Pharaonic Egypt, some of these elusive aspects of wood choices can be reevaluated in terms of religious, funerary, and cultural significance. At this stage of the APPEAR project, it is interesting to examine from contributions to this volume if we are any closer to finding out whether the limewood used for mummy portraits was imported into Egypt as raw timber or as prepared panels onto which the individual's image would be applied locally. Alternatively, it is possible that some of the limewood mummy portraits were entirely manufactured "to order" in what is now classified as the continent of Europe.

It is important to avoid falling into the trap of "not seeing the wood for the trees." This idiom is used to indicate when someone is missing a wider understanding of the subject as a whole because they are too immersed in the details. From the outset, the APPEAR project recognized the need to embed research results into the bigger picture in order to examine, compare, and visualize trends of wood use in mummy portraits and painted panels in association with other data, such as pigments, panel shapes, artistic styles, and (where the information exists) findspots and chronology. By updating and synthesizing such data, and by assimilating new findings revealed in other papers in this volume, we hope to formulate a better understanding of whether it might be possible to recognize workshops, specialist artisans, carpenters, and schools of artists. Integration of the many strands of research into a much larger framework of scholarship must surely be the end goal of the APPEAR project.

WOOD SAMPLING, IDENTIFICATION, AND NEW ADDITIONS TO THE SPECIES LIST

Details of the methodology of sampling wood from mummy portraits and painted wooden panels, comparison with reference collection woods, and species identifications from the British Museum using scanning electron microscopy were published in full in the first APPEAR volume, and the reader is referred to that paper for the full anatomical and taxonomic descriptions.³

Before embarking on a descriptive breakdown of the different species of woods selected, mention must be made of the terms *mummy portrait* and *painted panel*, as there seems to be some overlap or inconsistency in the use of these terms on museum, gallery, and collections websites and in publications. At the October 2022 APPEAR conference in Amsterdam, some presenters used *painted panel* in instances in which a deity was represented and reserved the use of *mummy portrait* for nondeity portraits that were (mostly) set into cartonnage over the face of a mummified person. Other presenters preferred a division into three categories: mummy portraits, funerary portraits (possibly not intended for placement over the face of the mummy), and votive panels.

Sometimes a revision of terminology has occurred, as, for example, with the so-called triptych in the J. Paul Getty Museum at the Villa, published in 2011 in the mummy portrait category.⁴ Panel 74.AP.22 represents the Egyptian goddess Isis, panel 74.AP.20 depicts a bearded man, and panel 74.AP.21 represents the Greco-Egyptian divinity Serapis. This change is reflected in this essay, where the two painted panels depicting deities are listed not as mummy portraits but as painted panels (see appendix).

There may be examples that do not fall readily into either of these categories; consequently, the percentages of wood species in this essay should be seen as indicative rather than absolute. One portrait that is difficult to categorize, as it appears to combine votive and funerary elements, is 1984-45 DJ in the Menil Collection, described as “Mummy portrait of a young man with small busts of Isis and Serapis.”⁵

The data in the appendix below reflect the status in May 2023 of 198 mummy portrait and portrait panel wood identification results. In the mummy portraits category (see fig. 7.6) imported limewood (*Tilia* sp.) still dominates (64.3%), with *Ficus sycomorus* (sycomore fig) making up the most popular native species of wood at 23.1%. Imported

Quercus sp. (oak) and native *Tamarix aphylla* (tamarisk) each contribute 3.8%, while imported *Abies* sp. (fir) and *Cedrus* sp. (cedar) contribute 1.7% each. The remainder is made up of *Taxus baccata* (yew), at 1.1%, and *Salix* sp. (willow, which could be imported or sourced locally), at 0.5%. Irrespective of whether willow is included in the imported woods percentage, we continue to see (as we did in 2020)⁶ that imported woods were preferred for mummy portraits (73.1%), with native woods accounting for the remainder (26.9%)

One of the more interesting additions to the species list is the *Salix* sp. willow from mummy portrait 128:1951 in the collection of Saint Louis Art Museum (fig. 7.1). Although the wood can be identified securely to genus level as *Salix*, it is recognized by the International Association of Wood Anatomists (IAWA) that the different species of willow cannot be distinguished on the basis of their wood anatomy. Therefore, we have to record the identification as *Salix* sp. (indicating that the species is not determined). Even just the genus-level identification of willow is interesting, however, because there is a published identification of a painted portrait on willow wood (*Salix* sp.) from a fourth-century CE grave with mummified remains in Aquincum in the Roman province of Pannonia (in the present day, part of Budapest, Hungary).⁷

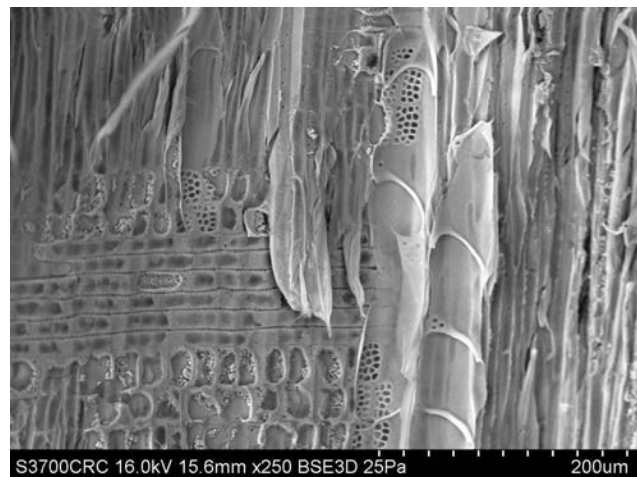


Figure 7.1 Scanning electron microscope image of a radial longitudinal section of willow wood (*Salix* sp.) from mummy portrait 128:1951, Saint Louis Art Museum (scale in microns). Photo: Caroline R. Cartwright, Department of Scientific Research, British Museum. © The Trustees of the British Museum

Willow wood used for mummy portraits or painted panels could derive from *Salix* species in Europe, including *Salix alba* and *Salix cinerea*, but could also have been sourced from *Salix mucronata* (formerly known and published as *Salix safsaf*), which is native to Egypt and has a broad

geographical distribution: southward in Africa and eastward into the Levant and Arabia. In figure 7.6, therefore, *Salix* has been placed in an intermediate category. Irrespective of the species, willow wood is light in weight, resilient, and flexible. It can be prone to rot and decay, however.

Figure 7.7 highlights the marked difference in the choice of woods for deity (or votive) painted panels, door panels, dowels, a board associated with a portrait mummy, and a panel providing a backing to a linen shroud. No limewood is present. Hard, dense native sidr (*Ziziphus spina-christi*) wood was chosen for six painted panels, including one with a frame made of the same species. Less-dense native woods are also present: sycomore fig (*Ficus sycomorus*) is represented by four examples, and tamarisk (*Tamarix aphylla*) by one example.⁸

LAYING THE GROUNDWORK FOR THE BIGGER PICTURE

To signpost where research might go for elucidation of the “bigger picture,” let us recap what is known. In Roman-period Egypt, although people maintained the traditional practice of mummification, they embraced a new fashion for funerary (mummy) portraiture that echoed Greek and Roman traditions. The excellent condition of the wood anatomy of mummy portraits enabled an unexpected revelation from their identifications—the majority were made from European timbers such as limewood rather than native Egyptian woods. In part, this may be attributable to the properties of the timbers. The anatomical structure of limewood⁹ allows for the creation of a thin panel that fits snugly over the face of the mummified individual. As noted in previous publications on mummy portraits,¹⁰ the choice to cut or split *Tilia* sp. limewood on the radial plane has ensured a fine-grained surface for the application of binding media and pigments for creating the portrait. Much more surface preparation would be needed for coarse-grained woods such as *Quercus* sp. (oak), *Ficus sycomorus* (sycomore fig), and *Tamarix aphylla* (tamarisk), to ensure even distribution of painting materials.

Mindful that there may be a number of factors involved, we can see that there appears to be more surface damage to the portraits and panels made on *Tamarix aphylla*, *Quercus* sp., or *Ficus sycomorus*—for example, the framed portrait of a woman in the British Museum collection (1889,1018.1) found at Hawara near one of the mummified individuals.¹¹ Both the panel and frame were made of *Ficus sycomorus* wood, and many areas of the paint have flaked

off. In contrast to limewood (*Tilia* sp.), from which very thin panels can be created easily, it would have been much more difficult to make thin mummy portrait panels from tamarisk (*Tamarix aphylla*) (fig. 7.2), oak (*Quercus* sp.), or sycomore fig (*Ficus sycomorus*) wood—again due to their anatomical features. However, we must recognize that making thin panels of wood for mummy portraits was not necessarily the sole objective.

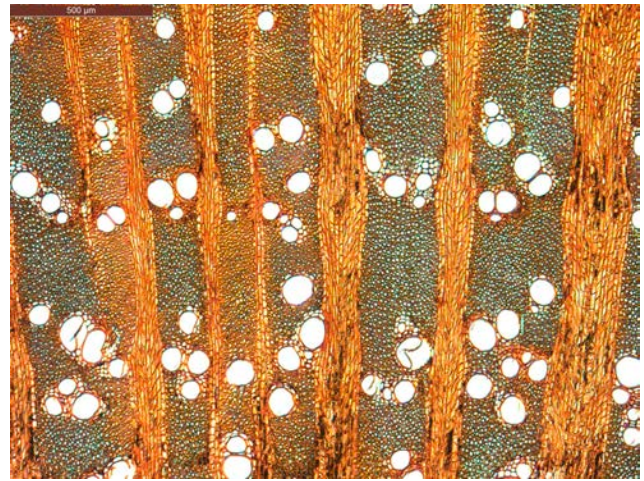


Figure 7.2 Image of a transverse thin section of *Tamarix aphylla* (tamarisk) reference specimen wood seen in transmitted light in the optical microscope. The section has been stained in the laboratory to show the cellular details (scale in microns). Note the many wide, multiseriate rays (which appear as axial orange lines in this image) and large vessels (which appear as white holes). Photo: Caroline R. Cartwright, Department of Scientific Research, British Museum. © The Trustees of the British Museum

Increasingly, as more and more samples are submitted for identification, we see that the choice of woods for the painted wooden votive or door panels favors native Egyptian woods—perhaps reflecting a carpentry trade in Egypt that was primarily engaged in producing items for household and shrine purposes. Creating and painting mummy portraits for burial with the deceased may well have had a completely different and more complex *chaîne opératoire*.

Wood properties are clearly important in the selection process, but many other factors could be considered, and it is tantalizing to try to deduce what these might be. Cultural and spiritual associations with burial and memorials may be more intangible to research than technology and materials, but they should not be completely overlooked. One small example of this can be seen with yew wood, used for mummy portraits 1902.70 (National Museums Scotland) and 1902.4 (National Museum of Ireland).¹² In 1835, Sir Thomas Browne is quoted by Lowe as saying, “the funeral pyre consisted of

sweet fuel, cypress, fir, larch, yew, and trees perpetually verdant, lay silent expressions of their surviving hopes.”¹³ Was yew selected for mummy portraits specifically because of its evergreen nature, to commemorate the deceased forever? Some were also made using cedar of Lebanon wood and fir wood—also evergreen trees.

Understanding why native woods were chosen for particular functions has been revealing for Pharaonic funerary carpentry,¹⁴ and it is now particularly useful to pay attention to Roman-period portrait and painted woods selected for dowels, tenons, and other carpentry elements when considering the following:

- ◆ Where mummy portraits and painted panels may have been made. For example, the wood identification results from the Tebtunis (and Kerke) mummy portraits in the collection of the Phoebe A. Hearst Museum of Anthropology (see fig. 7.6) have provided important new information, inasmuch as the trend toward preferential selection of limewood (*Tilia* sp.) for mummy portrait panels was reversed in favor of native fig tree (*Ficus sycomorus*) wood.¹⁵
- ◆ Whether carpentry elements are all native wood species, imported wood species, or a mixture, and what this may signify in terms of other woodworking in Egypt. It is not clear why the *Cedrus* sp. (cedarwood)¹⁶ mummy portrait 79.AP.129 in the collection of the J. Paul Getty Villa Museum has two dowels, but both are also *Cedrus* sp., suggesting they had a function at the time (now unknown), rather than indicating repair or recycling. In the same collection, we find that the batten from the *Ficus sycomorus* Serapis panel, 74.AP.21, is also made from sycomore fig wood, whereas the two dowels used to join two sections are made from *Cedrus* sp. (cedarwood). Future research may benefit from identifying associated wooden objects (where possible) from tombs known to have yielded mummy portraits or painted panels.
- ◆ Whether the wood choices were purely practical. This was the case in coffin making in Pharaonic Egypt, when wood such as sidr (*Ziziphus spina-christi*) was often chosen for the joining elements (such as dowels) because it was denser (fig. 7.3) than the wood used for coffin planks, and thereby created tight carpentry joins.¹⁷ Mummy portrait X 443 from the Kunsthistorisches Museum Vienna appears to have been made up of three panels, but only the middle and right panels have survived. Both are made from *Ficus sycomorus* (sycomore fig). Two dowels are present: one connecting the middle panel to the left

panel (now missing) and another on the top right of the middle panel. These dowels introduce a new species of wood to the discussion, acacia (*Vachellia nilotica*, formerly known as *Acacia nilotica*) (fig. 7.4).¹⁸ *Vachellia nilotica* wood is strong, shock resistant, and hard—ideal for connective carpentry.

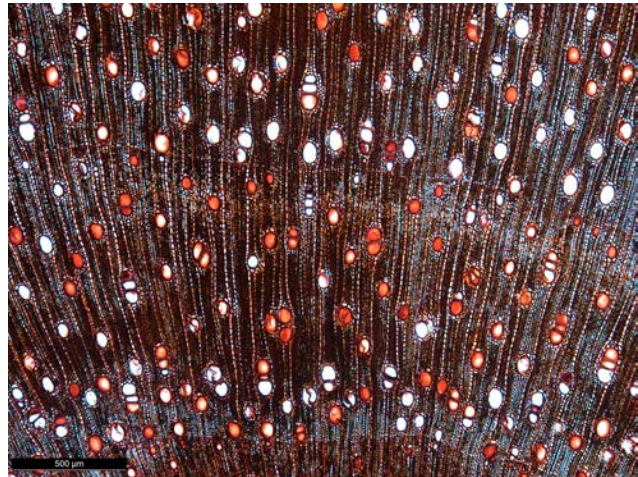


Figure 7.3 Image of a transverse thin section of *Ziziphus spina-christi* (sidr) reference specimen wood seen in transmitted light in the optical microscope. The section has been stained in the laboratory to show the cellular details (scale in microns). Note the many narrow, uniseriate rays (which appear as thin axial white lines in this image), numerous small vessels (some of which appear as white holes; others with deposits in them show in the image as reddish-brown contents), and the dense ground tissue made up of fibers and axial parenchyma. Photo: Caroline R. Cartwright, Department of Scientific Research, British Museum. © The Trustees of the British Museum

It is an understatement to say that it is extremely unfortunate that so many mummy portraits were deliberately removed from their original placement within the wrappings enclosing the mummified individual. This practice has prevented the acquisition of a great deal of important information that could assist greatly in understanding the bigger picture. Clearly a relationship existed between the outer treatment of the wrapped, mummified body and the style, size, and depiction of the associated mummy portrait. For example, the mummy EA13595, from Hawara in the British Museum collection, has a portrait of an adolescent boy. The outer covering of the body shows an intricate wrapping that creates the effect of concentric diamonds, each with a central gilded stud.¹⁹ This differs markedly from another example from Hawara (British Museum EA21810), which consists of a mummy of a Greek youth named Artemidorus in a cartonnage body case with mythological decoration in gold leaf and a limewood portrait covering the face.²⁰ Although some of the differences can be ascribed to chronological and cultural preferences, the fact that it is seldom possible

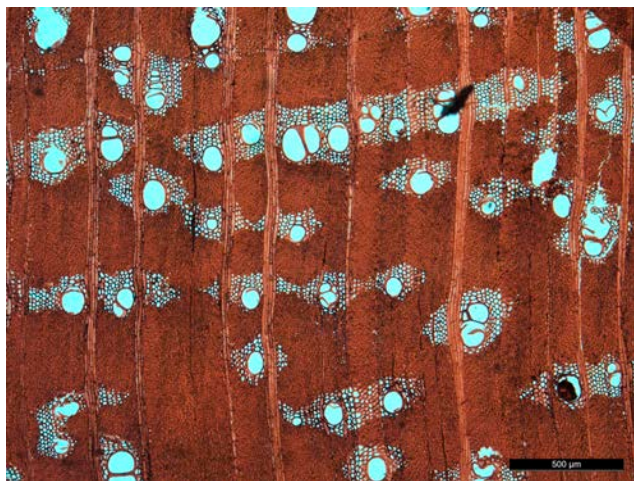


Figure 7.4 Image of a transverse thin section of *Vachellia nilotica* (acacia) reference specimen wood seen in transmitted light in the optical microscope. The section has been stained in the laboratory to show the cellular details (scale in microns). Note the many rays, one to two cells wide and four to five cells wide (which appear as axial orange lines in this image), small to medium-sized vessels (which appear as white holes), bands of parenchyma (showing as groups of white holes) in association with vessels, and extremely thick-walled fibers making up the dense ground tissue (appearing dark red in the image). Photo: Caroline R. Cartwright, Department of Scientific Research, British Museum. © The Trustees of the British Museum



Figure 7.5 Map of the Roman Empire at the time of the accession of Hadrian as Roman emperor in 117 CE. Photo: After Oppen 2008; redrafted by A. P. Simpson. © Trustees of the British Museum

to take into account all the features of the original burial (including the enclosed body) when trying to understand the phenomenon of mummy portraits within the bigger picture is a considerable drawback. Perhaps we need to embark on a different set of questions, and also look at wood use choices in the ancient Greco-Roman sphere of influence more widely.

In the longer term, the author's scientific research program includes a category of comparative information emerging from her identifications of woods selected for the ink and the stylus writing tablets from the Roman auxiliary fort at Vindolanda near Hadrian's Wall in northern England, occupied from 85 to 370 CE. Results thus far reinforce the concept of selection of particular wood species to suit specific purposes, even with reused timber. The degree to which such research can be brought directly to bear on interpretation of the selection of woods for mummy portraits and painted panels will emerge in the next few years of the project. The dominance of Roman control over much of what is now classified as Europe and Great Britain was significant at the time of Hadrian's accession as Roman emperor in 117 CE (fig. 7.5).²¹ This has undeniable implications for the sourcing and trading of timber throughout the Roman Empire, including the woods used for mummy portraits and painted panels.

CONCLUSIONS

This final set of mummy portrait and painted panel wood identifications carried out by the author at the British Museum should make it possible to incorporate information about wood choices and use more broadly within the APPEAR project. Key points can be raised in future research regarding the relationship between the properties of wood of different species in determining the choice of portrait and panel shape, as well the preparation of the wood panel surfaces for application of binding media and pigments. As part of an "object biographies" approach, it would be relevant to examine the reasons for the reuse or repurposing of both imported and local woods for portraits and panels and to explore under what circumstances and on what basis such choices may have been made. It is already a familiar concept that any reuse of timbers will have significant impact on the interpretation of radiocarbon dating of mummy portrait or painted panel woods, as does the use of wood from long-lived tree species.

Recognizing what questions to ask is integral to effectively "see the wood for the trees," in order to embed meticulous analyses into a well-rounded understanding of the bigger picture.

APPENDIX: WOOD IDENTIFICATIONS

Figure 7.6 lists the wood identifications of mummy portraits carried out in May 2023, while figure 7.7 shows analogous data on painted panels and doors, as well as various components of paintings, in the British Museum's collection.

Collection and Accession Number	Non-Native Woods Imported into Egypt					Imported/ Native	Woods Native to Egypt		
	Abies sp., fir	Cedrus sp., cedar	Tilia sp., lime	Quercus sp., oak	Taxus baccata, yew		Salix sp., willow	Ficus sycomorus, sycamore fig	Tamarix aphylla, tamarisk
Art Institute of Chicago									
1922.4798			1						
1922.4799			1						
Ashmolean Museum									
AN1888.340						1			
AN1888.341						1			
AN1888.342			1						
AN1888.1178						1			
AN1888.1179			1						
AN1890.756						1			
AN1890.757						1			
AN1896-1908.E.3755			1						
AN1911.354			1						
AN1922.240			1						
AN1922.241			1						
AN1966.1112			1						
AN1969.525			1						
British Museum, including National Gallery (NG) portraits on long-term loan									
EA5619			1						
EA6713			1						
EA13595			1						
EA21810			1						
EA29772			1						
EA63346			1						
EA63394				1					
EA63396				1					
EA63397				1					
EA65343				1					
EA65344				1					
EA65345				1					
EA65346			1						
EA74703 / NG 1260			1						
EA74704 / NG 1261			1						
EA74705 / NG 1262			1						
EA74706 / NG 1263			1						
EA74707 / NG 1264			1						
EA74708 / NG 1265			1						
EA74710 / NG 1267			1						
EA74711 / NG 1268			1						
EA74712 / NG 1269			1						
EA74713 / NG 1270			1						
EA74714 / NG 2912			1						
EA74715 / NG 2913			1						
EA74716 / NG 2914			1						
EA74717 / NG 2915	1								
EA74718 / NG 3139			1						
EA74719 / NG 5399			1						
EA74832 / NG 3932			1						
1889,1018.1 portrait and frame						2			
1890,0801.2			1						
1890,0921.1						1			
Brooklyn Museum									
41.848			1						
54.197						1			
86.226.18			1						

Collection and Accession Number	Non-Native Woods Imported into Egypt					Imported/ Native	Woods Native to Egypt		
	Abies sp., fir	Cedrus sp., cedar	Tilia sp., lime	Quercus sp., oak	Taxus baccata, yew		Salix sp., willow	Ficus sycomorus, sycamore fig	Tamarix aphylla, tamarisk
Charleston Museum									
1932.98.46			1						
Chau Chak Wing Museum: Nicholson Collection									
NM79.1								1	
Cleveland Museum of Art									
1971.137			1						
Detroit Institute of Arts Museum									
25.2									1
Fitzwilliam Museum									
E.2.1888			1						
E.102.1911			1						
E.5.1981								1	
Freud Museum									
4946									1
4947			1						
Harvard Art Museums									
1923.59			1						
1923.60									1
1924.80			1						
1939.111									1
1946.44			1						
Institute for the Study of Ancient Cultures, University of Chicago									
E2053			1						
J. Paul Getty Museum at the Villa									
71.AP.72			1						
73.AP.91			1						
73.AP.94			1						
74.AP.11			1						
74.AP.20									1
78.AP.262			1						
79.AP.129			1						
79.AP.141			1						
79.AP.142			1						
81.AP.29									1
81.AP.42			1						
91.AP.6			1						
Kunsthistorisches Museum Wien									
V 1983			1						
X 296			1						
X 297			1						
X 300									1
X 301									1
X 302									1
X 303									1
X 432									1
X 442			1						
X 443 middle panel									1
X 443 right panel									1
Landesmuseum Württemberg									
7.1			1						
7.2 portrait of Eirene			1						
7.3			1						
7.6			1						

Collection and Accession Number	Non-Native Woods Imported into Egypt					Imported/ Native	Woods Native to Egypt	
	Abies sp. fir	Cedrus sp. cedar	Tilia sp. lime	Quercus sp. oak	Taxus baccata, yew		Salix sp. willow	Ficus sycamoros, sycamore fig
Los Angeles County Museum of Art								
M.71.73.62								1
Metropolitan Museum of Art								
L.2007.4.3							1	
L.2007.4.4			1					
L.2007.4.5			1					
L.2007.4.6	1							
L.2007.4.7			1					
L.2007.4.8							1	
Michael C. Carlos Museum								
2004.048.001 portrait of Sarapion			1					
Museum of Fine Arts Budapest								
51.342			1					
51.343			1					
51.344			1					
8901			1					
8902							1	
Museum of Fine Arts Houston, and the Menil Collection								
1984-45 DJ			1					
2009.16			1					
CA 7013			1					
CA 7124							1	
TR:184-2013			1					
Myers Collection, Eton College Museum								
ECM1473			1					
ECM2149			1					
ECM2150			1					
National Gallery of Victoria, Melbourne								
1499-5							1	
1500-5								1
1501-5							1	
1502-5							1	
1504-5								1
1505-5							1	
National Museum of Denmark								
3840							1	
3891			1					
3892			1					
National Museum of Ireland								
1902.4				1				
National Museums Scotland								
A.1902.70				1				
Northwestern University								
Hawara portrait mummy No. 4			1					
Ny Carlsberg Glyptotek								
ÆIN 680			1					
ÆIN 1426			1					
ÆIN 1473			1					
ÆIN 681			1					
ÆIN 682			1					

Collection and Accession Number	Non-Native Woods Imported into Egypt					Imported/ Native	Woods Native to Egypt	
	Abies sp. fir	Cedrus sp. cedar	Tilia sp. lime	Quercus sp. oak	Taxus baccata, yew		Salix sp. willow	Ficus sycamoros, sycamore fig
ÆIN 683			1					
ÆIN 684			1					
Petrie Museum of Egyptian Archaeology								
LDUCE-UC14692								
LDUCE-UC14768	1							
LDUCE-UC19607			1					
LDUCE-UC19608			1					
LDUCE-UC19609			1					
LDUCE-UC19610			1					
LDUCE-UC19611			1					
LDUCE-UC19612			1					
LDUCE-UC19613			1					
LDUCE-UC30081			1					
LDUCE-UC30082			1					
LDUCE-UC30088			1					
LDUCE-UC30089			1					
LDUCE-UC33971			1					
LDUCE-UC36215			1					
LDUCE-UC36348			1					
LDUCE-UC38059			1					
LDUCE-UC38060			1					
LDUCE-UC38061			1					
LDUCE-UC38062			1					
LDUCE-UC38102			1					
LDUCE-UC38103			1					
LDUCE-UC38314			1					
LDUCE-UC38315			1					
LDUCE-UC38768			1					
LDUCE-UC38769			1					
LDUCE-UC38770			1					
LDUCE-UC40696			1					
LDUCE-UC40697			1					
LDUCE-UC40698			1					
LDUCE-UC40699			1					
Phoebe A. Hearst Museum of Anthropology								
5-2327							1	
6-21374							1	
6-21375			1					
6-21376							1	
6-21377							1	
6-21378							1	
6-21379							1	
6-21381							1	
6-21382							1	
6-21383							1	
Rhode Island School of Design Museum								
17.060			1					
39.025								1
39.026							1	
Sainsbury Centre								
326			1					
Saint Louis Art Museum								
128:1951							1	
Salford, City Art Gallery								
1954/9			1					

Collection and Accession Number	Non-Native Woods Imported into Egypt					Imported/ Native	Woods Native to Egypt		
	<i>Abies</i> sp., fir	<i>Cedrus</i> sp., cedar	<i>Tilia</i> sp., lime	<i>Quercus</i> sp., oak	<i>Taxus</i> <i>baccata</i> , yew		<i>Salix</i> sp., willow	<i>Ficus</i> <i>sycomorus</i> , sycomore fig	<i>Tamarix</i> <i>ophylla</i> , tamarisk
Santa Barbara Museum of Art									
1959.18							1		
Smith College Museum of Art									
SC 1932.9.1								1	
Total: 182	3	3	117	7	2	1	42	7	
Percentage*	1.7	1.7	64.3	3.8	1.1	0.5	23.1	3.8	

*Should be considered indicative, not absolute.

Figure 7.6 Wood identifications of mummy portraits, May 2023.

Collection and Accession Number	Woods Imported into Egypt		Woods Native to Egypt			
	<i>Abies</i> sp., fir	<i>Cedrus</i> sp., cedar	<i>Ficus</i> <i>sycomorus</i> , sycomore fig	<i>Tamarix</i> <i>aphylla</i> , tamarisk	<i>Vachellia</i> <i>nilotica</i> , acacia	<i>Ziziphus</i> <i>spina-christi</i> , sidr
J. Paul Getty Museum at the Villa						
74.AP.21 Greco-Egyptian divinity Serapis			1			
74.AP.22 Egyptian goddess Isis			1			
Kunsthistorisches Museum Wien						
X 443 panel dowels					2	
X 448 may be a painted panel or a door			1			
North Carolina Museum of Art						
78.1.8 wooden backing to linen portrait shroud	1					
Ny Carlsberg Glyptotek						
ÆIN 685 painted votive panel						1
ÆIN 711 painted votive panel				1		
ÆIN 687 painted panel			1			
ÆIN 1426 mummy board under body associated with mummy portrait		1				
Phoebe A. Hearst Museum of Anthropology						
6-21384 painted figure on door panel						1
6-21385 painted figure on door panel fragment						1
6-21386 painted figure on panel fragment						1
6-21387 fragments of painted panel		1				
Rhode Island School of Design Museum						
59.030 panel depicting the god Heron and frame						2
Total: 16	1	2	4	1	2	6

Figure 7.7 Wood identifications of painted panels and doors, shroud backing, mummy board, and dowels, May 2023.

ACKNOWLEDGMENTS

Grateful thanks to Antony Simpson for redrafting figure 7.5.

NOTES

1. Cartwright 2020. <https://www.getty.edu/publications/mummyportraits/part-one/2/>.
2. Cartwright 2020.
3. Cartwright 2020. For further details of some of the challenges of identifying historical timbers, see Cartwright 2015.
4. Cartwright, Spaabæk, and Svoboda 2011.
5. <https://www.menil.org/collection/objects/6487-mummy-portrait-of-a-young-man-with-small-busts-of-isis-and-serapis>.
6. Cartwright 2020.
7. Anita Kirchhof and A. Rehorovics, “A Face from the Past . . . Painted Portrait on Wood from a Mummy Grave in Aquincum,” in Bragantini 2010, 723–30.
8. Identifications of wood species used for intentional pastiches of mummy portraits have not been included in this paper as these results (carried out at the British Museum) are published separately or are archived.
9. See Cartwright 2020 for a full description.
10. See Cartwright entries in the bibliography.
11. https://www.britishmuseum.org/collection/object/G_1889-1018-1.
12. Cartwright 1997A; Cartwright 1997B; Bierbrier 1997; Cartwright and Middleton 2008.
13. Lowe 1897.
14. Cartwright 2020.
15. Salvant et al. 2018; Williams, Cartwright, and Walton 2020.
16. Presumed on geographical grounds to be *Cedrus libani*.
17. Cartwright 2020.
18. Although it is still accepted that the term *acacia* can be used internationally as a common name, the genus *Acacia* is now reserved for Australian acacias only. Depending on which species are involved (and anatomically this may not be straightforward to determine), the genera of non-Australian acacias have been reclassified as either *Vachellia* or *Senegalia*. This means that where records of occurrence of the non-Australian genus *Acacia* have been cited previously in the literature, they will now require taxonomic reclassification.
19. https://www.britishmuseum.org/collection/object/Y_EA13595.
20. https://www.britishmuseum.org/collection/object/Y_EA21810.
21. Opper 2008.

Egg on Their Faces: Investigation of an Unusual Surface Coating Observed on Egyptian Funerary Portraits

*Marie Svoboda
Daniel P. Kirby
Joy Mazurek
Lin Rosa Spaabæk
John Southon*

INTRODUCTION

The study of Egyptian mummy portraits has become an appealing and enlightening topic. These funerary portraits are not only timeless visual documents that represent the individuals who lived in Egypt between the first and third centuries CE but also valuable resources in the development and understanding of ancient painting technology. Archaeologists such as Sir William Flinders Petrie, Albert Gayet, papyrologists Bernard P. Grenfell and Arthur S. Hunt, and the prominent Viennese art dealer Theodor Graf brought many of these distinctive and evocative artifacts to light in the nineteenth century.¹ Since their discovery, most of these painted panels have been housed in museums and private collections worldwide, detached from their original contexts: their mummified bodies. This group of ancient painted artifacts also includes funerary panels depicting individuals and deities, some with their original frames or pintles still intact.

In all, these specialized works provide an important connection to the artisans, their materials, methods,

innovations, and clues for the transfer of ideas in antiquity. The excellent state of preservation of many of these works affords an unprecedented opportunity for research, increasing our understanding of ancient pigments, binding media, wood, textiles, and coatings. Throughout their histories, however, the intervention of many detached paintings involved consolidation, inpainting, flattening, backing, coatings, and alteration by combining different panels, both ancient and modern,² raising questions in the study of the materials and techniques used in their production. Fortunately, not all portraits have been disturbed and funerary paintings continue to be discovered, shedding new light on artistic practice and ancient trade in Roman Egypt.³

Unique observations and features of these paintings have come to light through the collaborative model of the J. Paul Getty's APPEAR project, which fosters examination and evaluation of funerary portraits using interdisciplinary scholarship, comparative studies, and scientific analyses.⁴ One such observation, and the focus of this paper, was that of a distinct surface coating identified on a group of

funerary panel paintings housed in five separate museum collections. A subsequent project, which evolved to investigate this unique feature, brought together a multidisciplinary team of antiquity conservators, conservation scientists with expertise in organic material studies, and a researcher specializing in radiocarbon dating (^{14}C).

Funerary Portraits

Funerary mummy portraits are images of deceased individuals painted on a wide variety of wooden panels or textile shrouds that were secured over the faces of their mummified bodies. Other types of funerary panel paintings, not attached to mummies, were likely used in private homes, possibly in a domestic shrine context, although their original functions are unknown.⁵ In this paper the terms *portrait* and *funerary portrait* are both used to describe funerary and mummy paintings. These painted artifacts, produced exclusively in Egypt,⁶ were adopted from the Greco-Roman painting tradition and incorporated into the Egyptian funerary practice. The paintings, which represented both personalized and divine images, were reserved only for those of a “certain social group.”⁷ Although the pharaonic tradition of preserving human remains spanned over five thousand years, the later practice of creating personalized portraits lasted only about four hundred years, likely because of shifting external influences and cultural diversity within Egypt. By the late fourth century CE, after the edict of Theodosius banned pagan rituals in Egypt ca. 379 CE, mummification practices were being phased out.⁸

Ancient funerary paintings were created on textile shrouds or on panels of a variety of local and imported woods. Both supports were specially prepared for their unique purpose. They were painted using an impressive palette of natural or manufactured pigments bound with organic-based media. Today, a renewed interest in ancient paintings, together with the application of sensitive and specific analytical techniques and access to multidisciplinary corroborative studies, has broadened our understanding of ancient painting technology, enabling new discoveries.⁹ For example, studies of twenty-two water-based binding media (tempera) portraits using gas chromatography/mass spectrometry (GC/MS) and enzyme-linked immunosorbent assay (ELISA) have established that animal glue was the predominant medium used in antiquity (90%), followed by plant gums (10%).¹⁰ Likewise, analyses of encaustic binding media have confirmed that their composition can involve more than just pure beeswax.¹¹

Preliminary Investigations

In 2008, a study at the J. Paul Getty Museum using ELISA confirmed the presence of an animal glue binder on the tempera funerary Portrait of a Bearded Man (74.AP.20; fig. 8.1).¹² The study also detected traces of egg in the paint, raising the question of whether it was a component of the ancient binding media or a modern conservation intervention. Subsequent analyses in 2014 using GC/MS in tandem with ultraviolet fluorescence microscopy corroborated the presence of egg on that funerary portrait as well as on two other Getty panel paintings (74.AP.21 and 74.AP.22) once associated with the bearded man portrait.¹³ Further research revealed that the egg was present as an isolated surface layer, but at that time it was noted that it “may be an artifact due to modern restoration of the portraits.”¹⁴

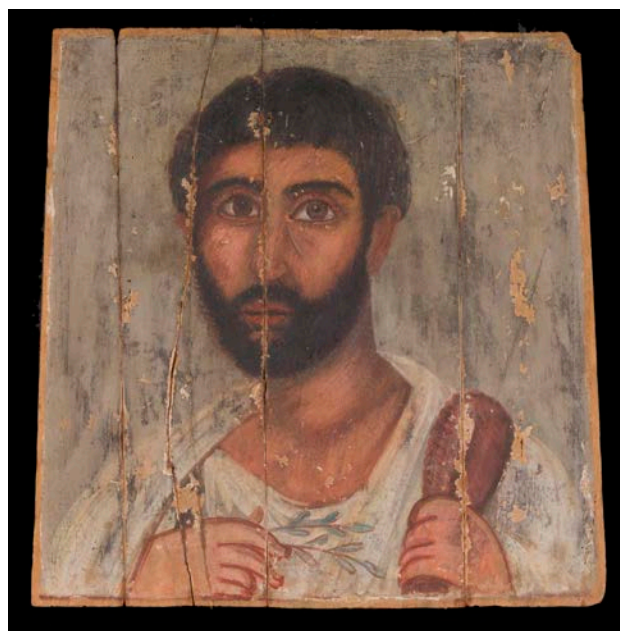


Figure 8.1 Funerary Portrait of a Man, ca.180–200 CE; ^{14}C wood date: 59–140 CE. Tempera on sycamore fig panel, 36 x 37.5 x 0.3 cm (14 3/16 x 14 3/4 x 1/8 in.). Los Angeles, J. Paul Getty Museum, 74.AP.20. Photo: Marie Svoboda

At the first APPEAR project meeting in 2013, participants from a variety of museums discussed the presence of an unusual surface deposit on the mummy portrait of a bearded man in the Getty’s collection (74.AP.11) as a possible future research topic (figs. 8.2 and 8.3). The surface feature was described as an “accretion or scum,” possibly related to the encaustic medium or the production of lead soaps.¹⁵ This open discussion led to the identification of a similar surface feature on two encaustic portraits in Copenhagen’s Ny Carlsberg Glyptotek

collection (ÆIN 681 and 684; figs. 8.4A–8.5B). GC/MS analysis of the surface accretion on the Glyptotek and Getty mummy portraits confirmed the presence of egg.¹⁶ Observation of a paint cross section from Glyptotek ÆIN 684 with ultraviolet fluorescence microscopy corroborated that the egg was present as a surface coating (fig. 8.6).¹⁷ Unlike the media commonly used to execute funerary panel paintings, such as beeswax, oil, and pine resin, or water-based media such as animal glue and plant gums, this surface coating could be visualized on the three portraits with ultraviolet radiation as an uneven, bluish fluorescence (figs. 8.7–8.9). The visible fluorescence extended only to where the linen wrappings would have covered the panel, securing it to its mummy. A further diagnostic feature could be observed with magnification: the coating appeared as yellowed “islands” of a brittle surface encrustation (see figs. 8.3, 8.4B, and 8.5B). The presence of egg was unexpected since previous analyses had shown that the paint medium of three of these four portraits was encaustic and that the medium of the other was animal glue, leaving the significance and source of the egg unclear. These initial portrait analyses provided a starting point for in-depth analysis of the egg coatings by peptide mass fingerprinting (PMF) and liquid chromatography with tandem mass spectrometry (LC-MS/MS).

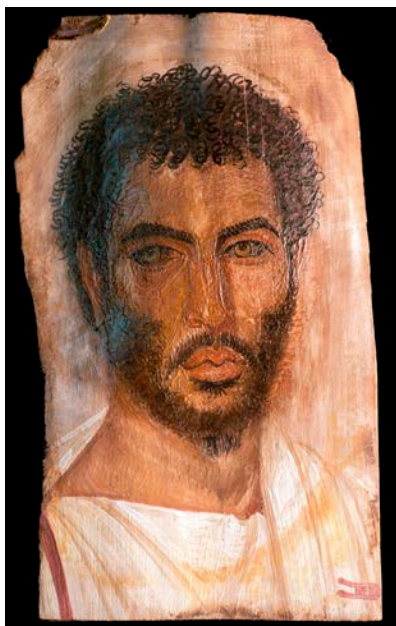


Figure 8.2 Mummy Portrait of a Man, ca. 150–170 CE; ¹⁴C wood date: 27–127 CE. Encaustic on linden wood panel, 37 x 21 x 0.2 cm. (14 9/16 x 8 1/4 x 1/16 in.). Los Angeles, J. Paul Getty Museum, 74.AP.11. Photo: Marie Svoboda

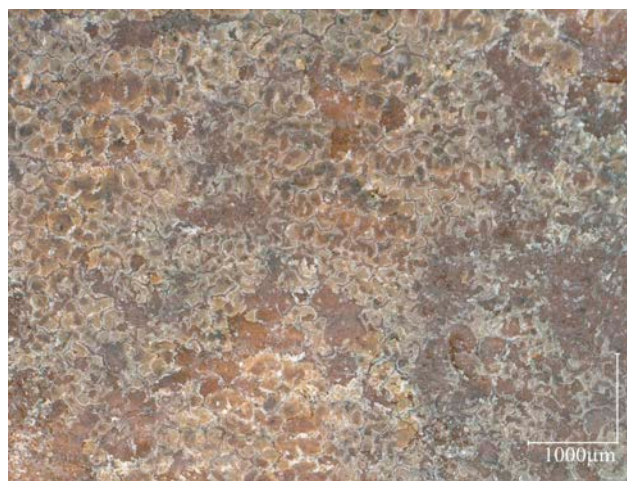


Figure 8.3 Surface detail of Mummy Portrait of a Man. Yellowed, accretion on the surface at 100x magnification. Los Angeles, J. Paul Getty Museum, 74.AP.11. Photo: Marie Svoboda

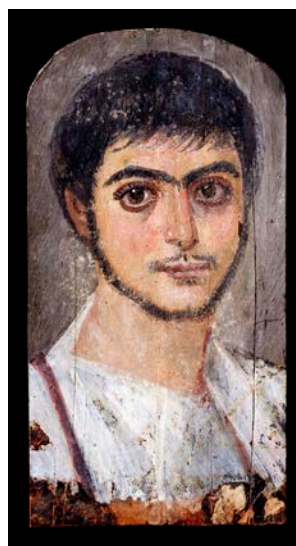


Figure 8.4A Mummy Portrait of a Young Man, ca. 125–150 CE. Encaustic on linden panel, 39.25 x 20.3 x 0.1 cm (15 1/2 x 8 x 1/25 in.). Ny Carlsberg Glyptotek, ÆIN 681. Photo: O. Haupt



Figure 8.4B Surface detail of Mummy Portrait of a Young Man. Surface accretion, at 40x magnification. Ny Carlsberg Glyptotek, ÆIN 681. Photo: Lin Rosa Spaabæk



Figure 8.5A Mummy Portrait of a Bearded Man, ca. 140–200 CE. Encaustic on linden panel, 40.7 x 7.8 x 0.1 cm (16 x 3 x 3/100 in.). Ny Carlsberg Glyptotek, ÆIN 684. Photo: O. Haupt



Figure 8.5B Surface detail of Mummy Portrait of a Bearded Man. Surface accretion, at 40x magnification. Ny Carlsberg Glyptotek, ÆIN 684. Photo: Lin Rosa Spaabæk

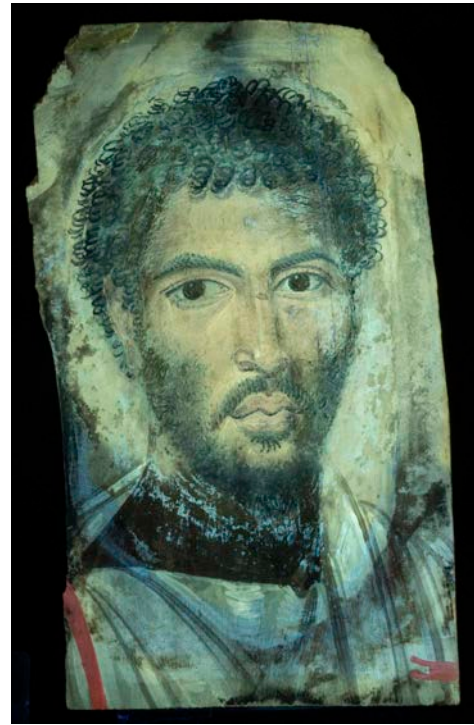


Figure 8.7 Ultraviolet-induced visible fluorescence image of Mummy Portrait of a Man; note bluish fluorescence. Los Angeles, J. Paul Getty Museum, 74.AP.11. Photo: Marie Svoboda

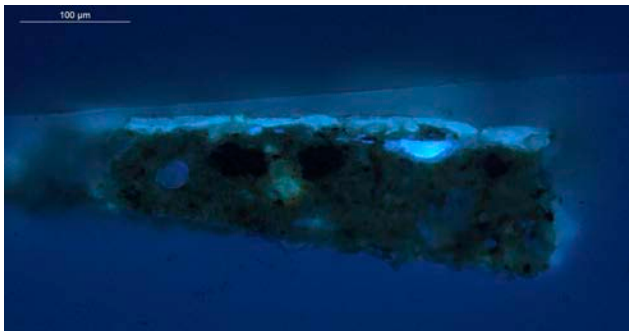


Figure 8.6 Polarized light microscopy, paint cross section under ultraviolet radiation showing characteristic fluorescence of egg on the upper layer, Mummy Portrait of a Bearded Man. Ny Carlsberg Glyptotek, ÆIN 684. Photo: Lin Rosa Spaabæk



Figure 8.8 Ultraviolet-induced visible fluorescence image of Mummy Portrait of a Young Man. Ny Carlsberg Glyptotek, ÆIN 681. Photo: Maria Louise Sargent



Figure 8.9 Ultraviolet-induced visible fluorescence image of Mummy Portrait of a Man. Ny Carlsberg Glyptotek, ÆIN 684. Photo: Maria Louise Sargent

Methods: PMF and LC-MS/MS

Advanced proteomics techniques such as PMF and LC-MS/MS, which have been adopted and adapted from biotech into cultural heritage, can provide precise identification of proteinaceous media and coatings and even determine the species of origin of those materials.¹⁸ PMF analysis involves the enzymatic digestion of proteins followed by Matrix Assisted Laser Desorption-Ionization Time of Flight Mass Spectrometric (MALDI) analysis of the resultant peptide mixture to produce a “peptide mass fingerprint.”¹⁹ Marker ions in the MALDI spectra from known reference materials are compared with those from unknown samples for identification.²⁰ LC-MS/MS with database searching is a mainstay of biotechnology. Its sensitivity is ideally matched to the minimal samples generally available from cultural objects, and its specificity allows more precise identification of proteinaceous materials than may be possible with other techniques.²¹ In the present work, LC-MS/MS was used to identify proteinaceous materials or to confirm those found with PMF.

The PMF and LC-MS/MS experimental details have been published previously and are briefly described here.²²

Samples

Samples from the Glyptotek portraits were remnants from previous analyses.²³ All other samples were obtained by conservators using sample sticks, which are polystyrene strips with adhered fiber-optic polishing film to abrade and entrap a small amount of material for analysis (fig. 8.10). All portraits had a clearly visible surface layer and characteristic visual appearance, and the UVF response guided the conservators to specific sample sites.

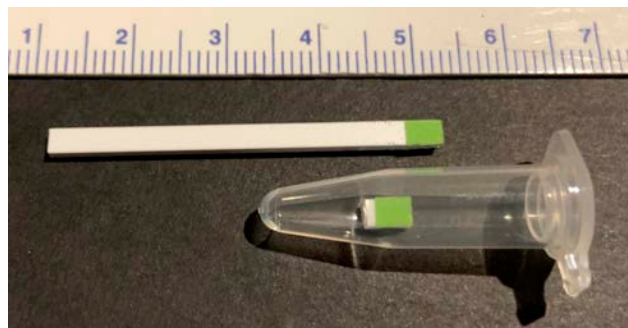


Figure 8.10 Sampling for all the PMF analyses used polystyrene support sample sticks with a micro-grit film (double-sided, 30 mm alumina grit); collected in an Eppendorf tube. Photo: Daniel Kirby

Digestion

60 μL of 50 mM ammonium bicarbonate (AMBI) was added to each sample in a 600 μL Eppendorf tube and heated to 75°C for 60 min. After cooling, 8 μL Promega Sequence Grade trypsin (0.02 $\mu\text{g}/\mu\text{L}$ in 50 mM AMBI) was added and digestion proceeded overnight at 37°C.

MALDI

2 μL of the digest were added to 20 μL 40% acetonitrile (ACN), 0.1% trifluoroacetic acid with saturated α -Cyano-4-hydroxycinnamic acid matrix; 0.65 μL of the mixture was spotted onto the MALDI plate. Spectra were obtained with an Applied Biosystems/Sciex 5800 MALDI-TOF/TOF instrument operated in positive reflector mode. Acquired spectra were exported from Applied Biosystems Data Explorer software as text files and imported into mMass,²⁴ where spectra were manually inspected for markers.

LC-MS/MS

Thermo Q Exactive-Orbitrap interfaced with an UltiMate™3000 chromatographic system. The mass spectrometer was operated in data-dependent mode (full scan 350–1800 Da, resolution 70,000; top 10 ions were

selected for fragmentation, resolution 17,500; detected ions were placed on an exclusion list for 10 sec.). LC buffers: A: 0.1% formic acid, B: 0.1% formic acid in ACN; gradient from 2–50% B over 60 min. One microliter of each of the digests analyzed by PMF was injected onto a nanocolumn: 75 μ m ID x 15 cm long, packed with Reprisil AQ C18 with 1.9 μ m beads (Dr. Maisch, Germany). LC-MS/MS data files were converted to mascot generic format (MGF), Matrix Science,²⁵ with msConvert software from ProteoWizard²⁶ and searched online through Mascot.

Results

PMF sample coating analysis on two Getty and two Glyptotek portraits (see figs. 8.1, 8.2, 8.4A, 8.5A) corroborated the previous findings of egg and, in addition, found that it is whole hen egg (yolk and white together). Figure 8.11 compares MALDI spectra for two of the portraits together with a spectrum from whole hen egg. Several of the more intense egg-related ions are labeled. Unlabeled ions are mainly contaminating keratin. The insets are examples illustrating that isotopic clusters for peptides with asparagine (N) and/or glutamine (Q) residues in the portrait spectra are shifted to higher mass due to a high degree of deamidation in the samples.²⁷ LC-MS/MS analysis of the same digests confirmed the PMF conclusions identifying proteins indicative of hen egg yolk and glair that is highly deamidated. Although the extent of deamidation can be influenced by a variety of factors, in the authors' experience it seems excessive, raising the possibility that the high degree of deamidation is the result of the preparation or application of the coating. Figure 8.12 shows the MS/MS spectra for the ions from Getty 74.AP.11, illustrated in the insets in figure 8.11. Based on these results, future analyses can be confidently done with PMF alone.

Following confirmation of the presence of whole hen egg on the four panels, the APPEAR database was searched for UV images of other portraits exhibiting the characteristic fluorescence.²⁸ Three other panels were identified based on the observed diagnostic features, one each from the collections at the Norton Simon Museum, Pasadena (F.1978.19.P), the Cleveland Museum of Art (1971.137), and the Kunsthistorisches Museum in Vienna (X 297) (figs. 8.13A–8.15B). These institutions agreed to take microsamples of the surface coating using sample sticks, as illustrated in figure 8.10, and submit them for analysis.²⁹ Both PMF and LC-MS/MS confirmed the presence of deamidated whole hen egg on the Norton Simon Museum and the Kunsthistorisches Museum portraits, and deamidated hen egg glair on the portrait from the

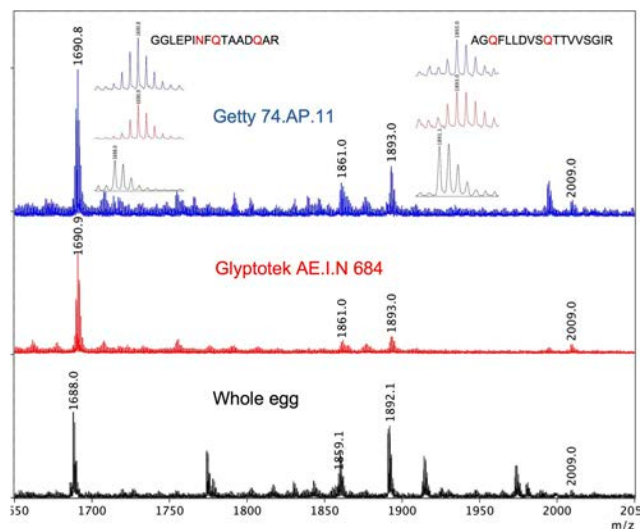


Figure 8.11 PMF spectra from a Getty (top) and a Glyptotek (center) portrait and whole hen egg reference (bottom). Several of the more intense egg-related ions are labeled; most unlabeled ions are contaminating keratin. The insets illustrate isotopic patterns for two N- and Q-containing peptides (1690.8 Da and 1893.0 Da) shifted to higher mass in the portrait samples compared to whole egg due to deamidation. All seven portraits analyzed gave similar results. Table: Daniel Kirby

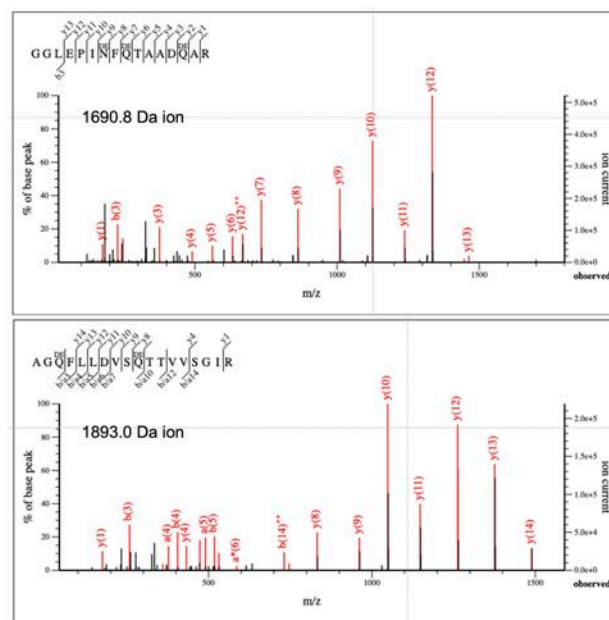


Figure 8.12 MS/MS spectra for the two ions in the insets (Figure 8.11) that confirm deamidation at N and Q residues. Labeled ions are those used to determine the peptide sequence by Mascot. Table: Daniel Kirby

Cleveland Museum of Art. Results for the seven analyzed portraits can be found in figure 8.16.



Figure 8.13A Portrait of a Man, second century CE. Encaustic on wood, 30.8 x 16.8 cm (12 1/8 x 6 5/8 in.). The Norton Simon Foundation, Gift of Mr. Norton Simon, F.1978.19.P. Photo: Yosi Pozeilov. © The Norton Simon Foundation



Figure 8.13B Ultraviolet-induced visible fluorescence image of Portrait of a Man. The Norton Simon Foundation, Gift of Mr. Norton Simon, F.1978.19.P. Photo: Yosi Pozeilov. © The Norton Simon Foundation



Figure 8.15A Portrait of a Lady, Romano-Egyptian, 117–138 CE. Encaustic on linden panel, 40 x 20 x 0.2 cm (15 3/4 x 7 7/8 x 1/16 in.). Kunsthistorisches Museum, Vienna, X 297. KHM-Museumsverband



Figure 8.15B Ultraviolet-induced visible fluorescence image of Portrait of a Lady. Kunsthistorisches Museum, Vienna, X 297. KHM-Museumsverband

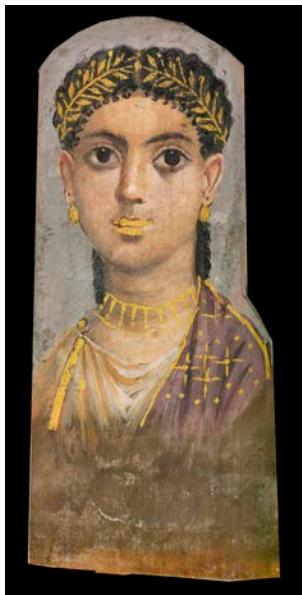


Figure 8.14A Funerary Portrait of a Young Girl, ca. 25–37 CE. Egypt, Roman Empire, late Tiberian. Encaustic on linden, 39.4 x 17.4 x 0.2 cm (15.5 x 7 x 1/32 in.). The Cleveland Museum of Art, John L. Severance Fund 1971.137. Photo: Elena Mars, courtesy of The Cleveland Museum of Art. © Joan Neubecker



Figure 8.14B Ultraviolet-induced visible fluorescence image of Funerary Portrait of a Young Girl. The Cleveland Museum of Art, John L. Severance Fund 1971.137. Photo: Elena Mars, courtesy of The Cleveland Museum of Art. © Joan Neubecker

Institution	Accession No.	Medium	ELISA	GCMS	PMF Result	LCMSMS Result
J. Paul Getty	74.AP.11	Encaustic	Egg	Egg	Whole hen egg	Whole hen egg, mammalian collagen
J. Paul Getty	74.AP.20	Tempera	Egg, glue	Glue	Whole hen egg, trace collagen	Whole hen egg, mammalian collagen
Glyptotek	ÆIN 681	Encaustic	N/A	Egg	Whole hen egg	Whole hen egg, mammalian collagen
Glyptotek	ÆIN 684	Encaustic	N/A	Egg	Whole hen egg	Whole hen egg, mammalian collagen
Norton Simon	F.1978.19.P	Encaustic	N/A	N/A	Whole hen egg	Whole hen egg, mammalian collagen
Vienna	X 297	Encaustic	N/A	N/A	Whole hen egg	Whole hen egg, mammalian collagen
Cleveland	1971.137	Encaustic	N/A	N/A	Hen egg glair	Hen egg glair, mammalian collagen

Figure 8.16 Summary of preliminary and subsequent analytical results for seven funerary portraits.

Hypothesis

To address why the observed coating does not extend to the edges of the mummy portrait panels, we initially

hypothesized that it was applied after their discovery in the late nineteenth century to protect the nearly two-thousand-year-old painted surface. This implies that the coating may have been added before the panel was removed from its mummified remains, possibly to saturate or consolidate the surface. It is probable that, when recently excavated portrait mummies reached the hands of collectors and art dealers with a desire to improve (revive or treat) their appearance, a coating may have been applied. The use of egg white (glair) as a “varnish” on paintings was a common practice in the nineteenth century.³⁰ This theory conveniently explains the egg identified on the funerary panel of a bearded man (see fig. 8.1), which had not been attached to a mummy. Another hypothesis was that this coating had been applied in antiquity, after the panels were inserted into the mummy wrappings. While applying libations as part of the funerary ritual was a well-known Pharaonic practice, the application of ritual coatings is not known on Roman Egyptian portrait mummies.³¹

Radiocarbon Dating

Radiocarbon dating (¹⁴C) was used to determine when the coatings were applied. Ancient organic materials dating is possible by measuring carbon-14 (¹⁴C) isotopes that are absorbed, via photosynthesis or consumption, by living organisms. Based on this, it is possible to determine an approximate date when an organism had died through the measurement of ¹⁴C decomposition. In 2020, the W.M. Keck Carbon Cycle Accelerator Mass Spectrometer facility at UC Irvine was contacted about the possibility of dating the egg coating.³² This facility had dated milligram-sized samples of wood and textile from eleven mummy portraits in the Getty collection in 2013, and it was now possible to obtain age data from micro samples of egg, weighing approximately one tenth of a milligram.

Two portraits were selected: the Getty’s Mummy Portrait of a Bearded Man (74.AP.11) and the Norton Simon’s Portrait of a Man (F.1978.19.P). Microsamples (approx. 0.25 mgC) were collected from the surface of each panel under magnification using a scalpel. The ¹⁴C results for the whole hen egg on the Getty portrait indicates that it was applied around 92 CE (median probability). This date is consistent with the age range of the portrait’s linden wood panel, analyzed at the same facility, and corresponding to a median probability calibrated date of 103 CE.³³ The median probability calibrated radiocarbon date for the egg coating on the Norton Simon portrait was determined to be 24 CE.

The dates acquired for both portraits indicate that the egg coatings were applied in antiquity and are not modern

additions (fig. 8.17). Although the coatings on only two of the portraits in this study have an established date of application, it is probable that the other portraits showing similar diagnostic features were also applied in antiquity. This theory is further corroborated by the confirmation of highly deamidated hen egg as established by PMF and LC-MS/MS. Although not comprehensive, the evidence of even two ancient dates for the egg coating provides new insights to artistic and/or funerary practices in Egypt between the first and second centuries CE.

Institution	Accession No.	Medium	Calibrated ¹⁴ C Date (95% confidence interval) / Median probability
J. Paul Getty	74.AP.11	Encaustic	25–128 CE / 92 CE
J. Paul Getty	74.AP.20	Tempera	
Ny Glyptotek	ÆIN 681	Encaustic	
Ny Glyptotek	ÆIN 684	Encaustic	
Norton Simon	F.1978.19.P	Encaustic	42 BCE–108 CE / 24 CE
Kunsthistorisches, Vienna	X 297	Encaustic	
Cleveland	1971.137	Encaustic	

Figure 8.17 Radiocarbon dates obtained from the egg coating on two portraits: JPM 74.AP.11 and NSM F.1978.19.P.

The egg detected is specifically from *Gallus gallus domesticus*, the domesticated chicken, exploited in antiquity for sport, prophesy, and, during Egypt’s Ptolemaic period, as an important food source. Analysis of the egg coating by PMF and LC-MS/MS indicated that it was highly deamidated, although it is uncertain whether deamidation here is related to age, burial conditions, or another type of “alteration,” possibly in preparing the egg for application.

The Chicken (*Gallus gallus domesticus*)

Although archaeological evidence for the domesticated chicken is rare and their origin is still a matter of debate, it is generally believed that the chicken originated in Southeast Asia and made its way westward into

Mesopotamia around 2000 BCE.³⁴ Shortly after the chicken's arrival in Egypt, the rooster gained popularity as a source of entertainment (cockfighting), a sport also popular in Greece and Rome.³⁵ The Romans also revered the rooster for its ability to predict the success or failure of battles.³⁶ As a result, roosters were viewed as sacred and protected, typically living long lives as a result.³⁷ In Egypt, following a mysterious period of disappearance, the chicken returned during the Ptolemaic period around 305 BCE, when unique and sophisticated egg incubators were invented, prompting the development of an industry that made chicken eggs widely available.³⁸

The ancient Egyptians documented the animals and birds they knew and used. Illustrated in hunt and banquet scenes, the more exotic species such as partridges, pigeons, ducks, geese, quail, herons, ibis, and hawks were commonly depicted, while the chicken was rarely included in the artistic repertoire.³⁹

History and Use of “Varnish” Coatings

In the early nineteenth century, the chemist Alfred Lucas was the first to identify and study the composition of coatings and varnishes (clear, pigmented, and opaque) applied on Egyptian artifacts between the first half of the Eighteenth and the Twenty-Sixth Dynasties (ca. 1549–525 BCE).⁴⁰ While Lucas's work was pivotal, in-depth investigations of these coatings today have enabled more precise identifications, expanding our understanding of their source and function.⁴¹ Believed to have been used primarily for ritual purposes, various materials such as bitumen, pistache, and pine resins (*sntr-pistacia* and *pinus*) have consistently been identified on painted funerary material.⁴²

While egg varnishes applied to artworks were common from the fourteenth through nineteenth centuries CE,⁴³ the reliable identification of egg as a coating in ancient Egypt has not been documented to date.⁴⁴ In his study of ancient Egyptian materials, Lucas discussed the identification of egg (albumin) possibly used as an ancient binder or adhesive, but states that results could not be verified.⁴⁵ Such complex investigations have significantly advanced through the development of more sensitive analytical instrumentation and techniques that enable the precise identification of aged materials.⁴⁶ Yet the question remains, why were the Roman Egyptian funerary panels coated with hen egg?

Artistic Varnishes

While various types of varnishes and glazes identified on painted artifacts were likely applied as part of religious ceremonies, their aesthetic function is also highly probable. Selectively applying a coating, sometimes pigmented, to create different striking visual impressions such as a contrasting matte and shiny surface is often described.⁴⁷ For example, coatings from a Nineteenth Dynasty (ca. 1298–1187 BCE) wall painting in the tomb of Nefertari and from Twenty-Second Dynasty (ca. 948–743 BCE) coffins contained pigmented pistacia resin to create a contrasting shiny/matte and golden-colored appearance.⁴⁸ While both natural tree resin and egg white were detected on the Nefertari wall paintings, however, traces of egg albumen could not be confirmed as ancient due to the extensive amount of modern restoration.⁴⁹

Thus far, evidence for the use of egg has not been firmly identified for rituals or as protective coatings in the funerary context in Egypt during the first to third centuries CE. Therefore, evidence presented here of a hen egg coating, confirmed as ancient on two Roman-Egyptian painted panels, reveals a unique function, potentially introducing a new practice to an enduring Egyptian funerary ritual.⁵⁰

EGG SYMBOLISM

The powerful symbolism of the egg in antiquity cannot be overlooked. Its significance was recognized in Hellenic cultures as an offering and as a symbol of rebirth.⁵¹ The egg also has deep resonance as part of the Egyptian creation myth, representing rebirth and the renewal of life.⁵² As a cosmic motif, the egg is connected to the continuation of human breath after death.⁵³ The egg embodies divinities, gods of creation such as Thoth and Amun, Isis and Osiris, and their son Horus, born as the sun god in the form of an egg.⁵⁴ It should not be surprising that the deeply symbolic egg would be selected as a material for anointing the deceased, to protect and promote rebirth in the afterlife. Its ubiquitous significance emphasizes the multicultural influences intertwined with ritual practices that make the production of portrait mummies so unique.

This study required the collaboration of a multidisciplinary team, each participant making very important contributions to the investigation. The ability to identify parallel features and acquire samples through collaborative projects, such as the APPEAR database, has enabled this study to evolve. Furthermore, characterizing

these discrete materials using various investigative techniques, such as imaging, microscopic examination, and organic analysis, has established the thread that defines a unique group of artifacts, potentially revealing a new and unique practice. The ability to confirm the egg source on seven funerary paintings using highly sensitive analytical techniques, as well as the confirmation of an ancient date by ^{14}C for the application of the coating on two mummy portraits, presents an important direction of research fostering continued corroboration.

GC/MS and/or ELISA analyses of paint collected from the Getty and Glyptotek portraits, three of which were painted with encaustic and one funerary panel with tempera, initiated the investigation into the presence of egg. This led to the identification and analyses of three other portraits from the APPEAR database with similar diagnostic features. Identifying egg in the encaustic portraits is significant as it was unexpected, resulting in the discovery that egg was not a component of the binder but was, in fact, a superficial coating. Localized investigation of the egg coating by PMF and LC-MS/MS analyses confirmed that it was whole hen egg in six of the seven portraits analyzed within this group; egg white was detected on the seventh. Furthermore, the egg on all seven was deamidated, suggesting they had undergone a type of alteration, a potential direction for future study. ^{14}C dating of two samples from the Getty (74.AP.11) and Norton Simon (F.1978.19.P) mummy portraits confirmed that the egg coatings were ancient and not modern interventions as was originally believed.

Although the ancient ^{14}C date was confirmed on only two portraits, we can deduce that, based on the identification of deamidated hen egg on seven painted panels, corroborated by their visual appearance and method of application, this may have been an Egyptian funerary practice. However, the reason for its application remains inconclusive. Was it a method to protect and saturate the surface? Was it an artistic effort to enhance the surface sheen and reflectivity, or was it a ritual practice symbolizing creation and renewal in the afterlife? These questions will remain unanswered until more ancient panel paintings are identified and studied. Foremost, this research stresses the need for more comparative studies and emphasizes the value of collaborative research to better understand ancient materials and methodology and their function.

ACKNOWLEDGMENTS

The authors would like to thank the institutions that generously allowed sampling of their portraits to make this study possible: the Norton Simon Museum; the Cleveland Museum of Art; Kunsthistorisches Museum, Vienna; Ny Carlsberg Glyptotek; and the J. Paul Getty Museum. MS graciously thanks Richard Newman, Kathlyn Cooney, Salima Ikram, Alessia Amenta, and Tamar Hodos for sharing their valuable knowledge of egg, and Susanne Gänsicke and Yosi Pozeilov for their support; DK thanks Sue Abbatiello, formerly of Northeastern University, for sharing her expertise in LC-MS/MS; JM thanks Michael Schilling; LRS is grateful to the Carlsberg Foundation, the Getty Conservation Institute, and the staff at the National Museum of Denmark and the Ny Carlsberg Glyptotek for their kind permission to examine and take samples from their mummy portraits.

NOTES

1. Barr 2020; Bierbrier 1997.
2. Jaeschke 1997.
3. Gehad et al. 2022.
4. Svoboda and Cartwright 2020.
5. Borromeo et al. 2020; Stevens 2009.
6. Anita Kirchhof and A. Rehorovics, "A Face from the Past . . . Painted Portrait on Wood from a Mummy Grave in Aquincum," in Bragantini 2010, 17–21.
7. Walker 1997.
8. Pharr, Davidson, and Pharr 2001.
9. Verri, Opper, and Deviese 2010; Verri 2014; Svoboda and Cartwright 2020.
10. Mazurek, Svoboda, and Schilling 2019; Lee et al. 2015.
11. Mazurek, Svoboda, and Schilling 2019.
12. Mazurek et al. 2008.
13. Mazurek et al. 2014; Hart 2016.
14. Mazurek et al. 2014, 82.
15. Internal notes from 2013 APPEAR meeting at the Getty Villa.
16. Spaabæk and Mazurek 2020.
17. Spaabæk and Mazurek 2020.
18. Kirby et al. 2011.
19. Henzel, Watanabe, and Stults 2003.

20. Buckley et al. 2009.
21. https://en.wikipedia.org/wiki/Liquid_chromatography-mass_spectrometry.
22. Kirby et al. 2023.
23. Spaabæk and Mazurek 2020.
24. Strohalm et al. 2010.
25. Matrix Science. <http://www.matrixscience.com>. Accessed 22 July 2022.
26. Proteowizard. <https://proteowizard.sourceforge.io>. Accessed 22 July 2022.
27. Deamidation is a chemical reaction in which an amide functional group in the side chain of asparagine or glutamine is converted to another functional group, usually a carboxylic acid.
28. Ultraviolet-induced visible fluorescence (UVF) methodology used at each institution for capturing images varied based on equipment and processing.
29. The authors would like to thank the institutions that generously allowed sampling of their portraits to make this study possible: Norton Simon Museum; Cleveland Museum of Art; Kunsthistorische Museum, Vienna; Ny Carlsberg Glyptotek; J. Paul Getty Museum.
30. Imbrogno, Nayak, and Belfort 2014.
31. Fulcher et al. 2021.
32. Southon et al. 2004.
33. Internal Report—UC Irvine AMS facility: UCIAMS-128007: 1925 ± 20 BP, corresponding to a median probability calibrated age of 103 CE, 2 sigma calibrated age range 28–204 CE.
34. Perry-Gal et al. 2015.
35. Rackham 1938–1952. Volume III, Book X: On cock fighting and omens, XXIV; on eating hens, LXXI, 139–40; on hatching, LXXV, 153.
36. Thayer 1923.
37. University of Exeter 2021.
38. Perry-Gal et al. 2015; Traverso 2019; Redding 2015.
39. Ikram 1995.
40. Lucas and Harris 1962.
41. Serpico 2000; de Vartavan 2007.
42. Serpico and White 2001; Fulcher et al. 2021; de Vartavan 2007; Edwards Howell et al. 2007.
43. Imbrogno, Nayak, and Belfort 2014; Woudhuysen-Keller and Woudhuysen-Keller 1994.
44. Imbrogno, Nayak, and Belfort 2014; Rickerby 1993.
45. Lucas and Harris 1962, 356–61.
46. Spaabæk and Mazurek 2020; Mathews and Müller 2016; Fulcher et al. 2021.
47. Gänsicke 2010.
48. de Vartavan 2009; Rickerby 1993.
49. Stulik, Porta, and Palet 1993.
50. Töpfer 2017.
51. Peruzzi 2016.
52. Omeran 2015; Dunand and Zivie-Coche 2004.
53. Maravelia 2019.
54. Wegner 2021.

Insights from a Collaborative Study of Beeswax Paint from Romano-Egyptian Mummy Portraits

Joy Mazurek
Lin Rosa Spaabæk

A study was designed to investigate the composition of beeswax and pigments from mummy portraits with the aim of improving our existing knowledge of the encaustic painting technique. This collaborative endeavor was made possible by the APPEAR project, which fosters interdisciplinary research between scientists and conservators and has resulted in new research yielding a better understanding of the inherent complexities of studying beeswax paint media. Colored paint samples were taken from nine encaustic mummy portraits (with different provenances) from two Danish museums, Ny Carlsberg Glyptotek (ÆIN) and the National Museum of Denmark (AS). Two portraits were excavated in Hawara by Sir W. Flinders Petrie, another five were bought from art dealer Theodor Graf's collection and are suggested to come from er-Rubayat, and the provenience of the last two portraits has not yet been established but according to museum records they are assumed to also derive from er-Rubayat. Dating for the nine portraits varies; the oldest are assumed to be from 25–75 CE, the youngest 150–200 CE (fig. 9.1). The research presented here complements a previous study of binding media from the same portraits.¹

The encaustic wax painting technique on some mummy portraits utilized heated and melted beeswax applied with

small metal instruments leaving behind characteristically shaped and raised tool marks. Previous researchers have distinguished between encaustic technique and a beeswax technique executed in a painterly style that appeared more blended, with subtle variations in color and less impasto.² This painterly beeswax technique has been described in the literature as “cold, modified, Punic or emulsified” and has caused misunderstanding of both the artist's intent and technique. Pliny's description of Punic wax has led to a belief among some scholars that the beeswax was (partially) saponified prior to its use in paints, allowing it to be applied cold, as an emulsion, and that various findings from analytical studies have been used to promote this idea.³ Still, the nomenclature and characterization of beeswax paint media is a source of contention and confusion.^{4,5} For example, the mummy portrait ÆIN 1425 was described as “wax used cold.”⁶

Typical beeswax is composed of 14% hydrocarbons, 35% palmitic wax esters, and 12% free fatty acids.⁷ Researchers have analyzed beeswax and paint samples from a small number of portraits executed in a painterly style (assumed to be modified or “used cold”) and concluded that a reduction in wax esters compared to hydrocarbons, the presence or absence of free fatty acids, or the detection of

Ny Carlsberg Glyptotek						National Museum of Denmark			
Provenience	Er-Rubayat (Graf collection)			Hawara (Petrie)		Presumable er-Rubayat			
	680	681	682	683	684	1425	1426	3891	3892
									
Date	100–125 CE	125–150 CE	140–160 CE	125–150 CE	140–200 CE	25–75 CE	100–125 CE	150–200 CE	150–200 CE
Flesh tone	Lead white, iron oxides, carbon black, kaolinite, goethite, minor red lead	Iron oxides, lead white, kaolinite, carbon black, red lake	Iron oxides, lead white, Egyptian blue, carbon black, quartz	Iron oxides, lead white, carbon black, red lake, quartz	Iron oxides, lead white, carbon black, kaolinite	Iron oxides, lead white, Egyptian blue, carbon black, red lake, quartz	Iron oxides, lead white, Egyptian blue, carbon black	Iron oxides, lead pigment, carbon black, calcite, gypsum	Egyptian blue, iron oxides, lead white, carbon black
Background	Lead white, iron oxides, carbon black	Iron oxides, lead white, Egyptian blue, carbon black, quartz	Iron oxides, lead white, carbon black, kaolinite	Iron oxides, lead white, carbon black, kaolinite, calcite	Iron oxides, lead white, carbon black,	Iron oxides, lead white, Egyptian blue, carbon black	Iron oxides, lead white, Egyptian blue, carbon black	Iron oxides, lead pigment, carbon black, calcite, gypsum	Iron oxides, lead white, gypsum
Chiton	Lead white, iron oxides, carbon black	Iron oxides, lead white, kaolinite, carbon black	Gypsum, red lake, bassanite, minor red lead, lead white	Blue: Indigo, gypsum, bassanite, lead white Red: iron oxides, lead pigments, carbon black	Iron oxides, lead white, carbon black, kaolinite, quartz	-	Lead white	Iron oxides, lead pigment, carbon black, calcite, gypsum	Iron oxides, lead white
Lips/red	Iron oxides, lead pigment, kaolinite	Iron oxides, lead white, red lake (lips), calcite	Iron oxides, lead white	Red lead, lead white, iron oxides, kaolinite	Iron oxides, lead white, carbon black	Vermilion, lead white, iron oxides, carbon black	Hematite	Iron oxides, lead pigment, carbon black, calcite, gypsum	Iron oxides, lead white, carbon black
Hair/black	Iron oxides, carbon black, lead white, red lake, kaolinite, quartz	Carbon black, iron oxides, lead white, quartz	Carbon black, iron oxides, lead white, quartz	Carbon black, iron oxides, lead white, quartz	Iron oxides, lead white, carbon black, kaolinite	Carbon black, iron oxides, lead white	Carbon black, red lake, lead white, iron oxides, quartz	Iron oxides, lead pigment, carbon black, calcite	Iron oxides, lead white, gypsum, carbon black
Gold imitation	-	-	Goethite	Goethite	-	-	-	-	-
Clavus	Bassanite, red lake, lead white	Gypsum, red lake, bassanite, lead white	-	Red lead, red lake (minor), lead white, gypsum	Bassanite, gypsum, lead white, red lake	Lead white, red lake, iron oxides	Gypsum (?), lead white (minor), red lake, iron oxides (minor)	Lead white, iron oxides	Lead white, red lake
Ground	-	Carbon black, iron oxides	-	Iron oxides, carbon black	-	Calcite, gypsum, carbon black	-	Iron oxides, gypsum (anhydrite), hematite	Iron oxides

Figure 9.1 The nine analyzed portraits in this study, including their provenience and age. The table is a schematic overview of the present pigment identification results together with the results from former analyses done on the portraits as part of the APPEAR project (see note 11). Ny Carlsberg Glyptotek: Young Man, AIN 680; Young Man with Beard, AIN 681; Young Woman with Jewelry, AIN 682; Woman with Blue and Red Dress, AIN 683; Man with Receding Hairline, AIN 684; Portrait of a Man on Canvas, AIN 1425; Portrait of a Man, Red Shroud Mummy, AIN 1426. Photos: Ole Haupt

fatty acid metal soaps can be used to characterize “cold” applied wax or “modified beeswax.”⁸ These conclusions seem inaccurate, as researchers within the APPEAR project have shown through the scientific analysis of over thirty wax-paint portraits that fatty acid soaps from beeswax-paint portraits are independent of painterly style.⁹ Data

also showed that they had similar beeswax profiles—the hydrocarbons had either evaporated or lesser amounts remained, fatty acid and wax ester content were consistent depending on the pigment, and they could contain significant amounts of palmitic acid lead soaps. The study showed the impact of pigments on the formation of fatty

profile of old beeswax paint is modified when compared to fresh beeswax. Lead white paint will contain significantly more palmitic acid soap, while paint samples without lead white (or metal-forming pigments) do not form lead soaps, resulting in the evaporation of fatty acids from the paint matrix.

SEM-EDX and GC/MS results for percentages of lead and palmitic acid are shown in figure 9.3, where results for each sample are described as a color with its portrait number. The percentage of lead in the paint samples was calculated based on the estimated content and sum of a variable mixture of pigments using SEM-EDX. Therefore, both values may be affected by the inhomogeneity of the paint sample and application methodology employed. Preliminary results indicate that lighter-colored samples contain significantly higher percentages of lead and palmitic acid soap, while the opposite is true for darker-colored samples. For example, the flesh tones in the ÆIN 682 portrait contain approximately 15% lead and 43% palmitic acid, while ÆIN 682 black contains 3% lead and 16% palmitic acid.

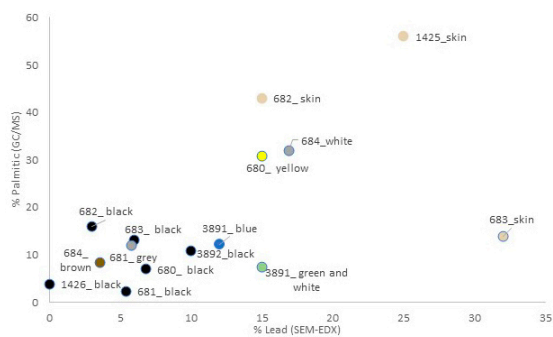


Figure 9.3 GC/MS and SEM-EDX results showing palmitic acid and lead percentages. Colored circles (with their portrait numbers) indicate the light and dark beeswax paint colors.

It should be noted that several samples were outliers and did not follow the trend of increased lead and palmitic acid content, such as the flesh tones on ÆIN 683. The variability of our data could be due to several reasons. First, the inhomogeneity of the pigment particles was evident in the area/surface of the SEM-EDX scan. When polishing the cross sections, the pigment particle size was highly variable and the size of the particles at the surface of the cross section changed with subsequent polishing. This change could impact the results of the SEM-EDX scan on a given cross section and may indicate an area of inhomogeneity that is not representative of the lead

pigment content. Second, a small cross section sample does not always represent the lead content found in larger areas of the portrait. Third, it is well known in oil-paint studies that, due to the soaps' ability and tendency to migrate throughout the paint layers, lead soaps form concentrated inclusions in areas within the paint matrix.¹⁷ This would result in variable amounts of palmitic acid detected in a small paint sample compared to an overall average in a larger paint area.

The following pigments were identified in the seven dark paint samples: carbon black, red/brown iron oxides, and, in one example, red lake. The SEM-EDX cross section scans provided information on the pigments used in the specific paint layers studied. Figure 9.4 shows an example of a cross section from a dark color, ÆIN 1426, and illustrates the complexity of pigments found in dark or black areas. The visible light image shows how the paint is composed of black, white, brown, red, and yellow pigments. There is a surprisingly high lead white content (seen as white particles in the SEM-EDX image) in many of the dark/black paint layers. The cross section also shows the presence of red lake pigment, a surprising addition to black paint. The red lake pigments can be observed as bright orange particles with or without ultraviolet radiation.

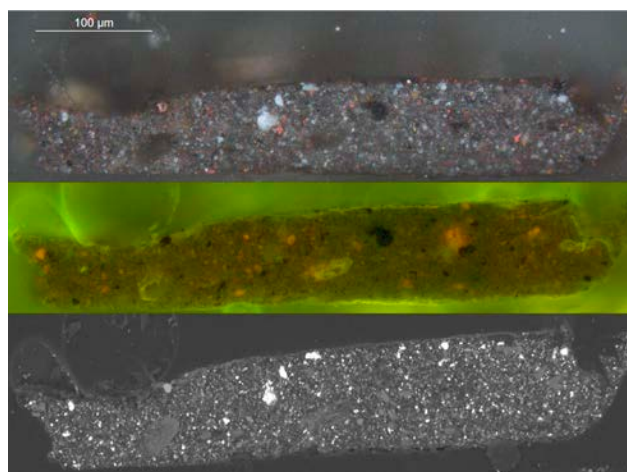


Figure 9.4 An example of a black color cross section, Portrait of a Man, inv. no. 1426. Top: visible light; center: UV-fluorescence (note that the red lake pigments appear as bright orange particles); bottom: SEM-EDX image showing lead as bright white particles. Photo: Lin Rosa Spaabæk

The cross sections also gave interesting information on the stratigraphy of the wax paint, though most samples were diminutive and thus did not contain all the layers in the paint structure. However, a cross section shows the stratigraphy of black hair (layer no. 3) on top of two layers (nos. 1 and 2) of light gray background color from ÆIN 681 (fig. 9.5). The visible light image shows how both the light

and dark colors consist of red, yellow, black, and white pigments, and in most cases yellow iron oxide as well. Calcite and quartz were present in all dark-colored samples as well as lead white in surprisingly significant amounts when compared to the dark sections of the paint. It is noteworthy that we did not detect the red pigment minium in the darker areas, however, lead white was ubiquitous in all the samples analyzed and is the only pigment present in the paint samples capable of forming lead soaps.

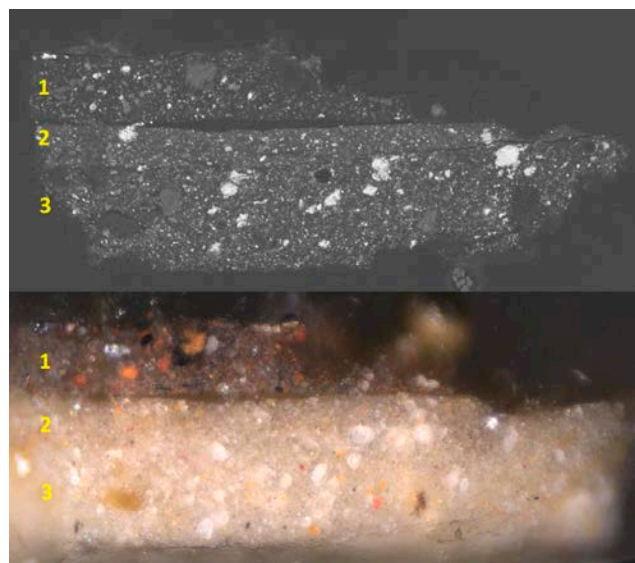


Figure 9.5 Cross section showing the stratigraphy of black hair (layer no. 1) above two layers of light gray background color (nos. 2 and 3). Mummy portrait of a bearded young man from er-Rubayat. Inv. no. ÆIN 681. Top: visible light; bottom: SEM-EDX image. Photo: Ole Haupt

Lead white, calcite, and quartz mixed with various hues of red and yellow iron oxides were observed in all six light-colored samples analyzed. The addition of Egyptian blue was also identified in two samples taken from light-colored flesh tones (see fig. 9.1). The pigments identified in this study of mummy portraits painted with beeswax-based paint revealed that the painters had an economical yet precise and conservative palette of pigments, and the results corroborate what other studies have so far reported.

CONCLUSION

The SEM-EDX results revealed that both dark and light beeswax samples taken from nine beeswax-based mummy portraits contained variable amounts of lead white. Carbon black, with the addition of red/brown iron oxides and one example of red lake, was identified in the seven dark paint samples. Lead white, calcite, and quartz mixed with various

hues of red and yellow iron oxides were observed in light-colored paints.

Through a fortuitous collaboration, evidence is presented here that allows for a better understanding of how lead soaps form in ancient beeswax and why its presence should not be used as an indication of cold applied or Punic wax. GC/MS and SEM-EDX results were compared and preliminary results show that lead is positively correlated with the formation of palmitic acid soaps. This provides further evidence that the soaps present in beeswax paint can be attributed to lead metal complexes. Therefore, differences in beeswax chemical profiles should not be used to indicate a purposeful modification of the beeswax during the preparation of the beeswax paint. Rather, the beeswax chemical profiles are different from one another because of lead content, evaporation, pigments, wax ester hydrolysis, and subsequent soap formation. The hydrolysis of wax esters occurs over time and, when palmitic acid is released, it forms a palmitic acid lead soap. This explains the variation we see in the wax ester profile, and it is hoped that these results will inspire discussion and offer a clearer understanding of the ancient beeswax painting technique.

ACKNOWLEDGMENTS

The authors are grateful to several individuals for their contribution to this study: Julie Jaeger, teaching associate professor, Royal Danish Academy for Fine Arts; Richard Newman, head of scientific research, Museum of Fine Arts, Boston; and Michelle Taube, conservation scientist, the National Museum of Denmark.

The authors would also like to thank the following entities for their support: the Carlsberg Foundation and the Getty Conservation Institute; the staff at the National Museum of Denmark and the Ny Carlsberg Glyptotek; the Molab team, led by Costanza Miliani; the APPEAR team and Marie Svoboda; and the Center for Art Technological Studies, National Gallery of Denmark.

NOTES

1. Spaabæk and Mazurek 2020.
2. Ramer 1979.
3. Kühn 1960.
4. Sutherland, Sabino, and Pozzi 2020.
5. Stacey 2011, 1749.
6. Doxiadis 1995.

7. Jiménez et al. 2004.
8. White 1978.
9. Mazurek, Svoboda, and Schilling 2019.
10. Spaabæk and Mazurek 2020.
11. Mazurek, Svoboda, and Schilling 2019.
12. S-3400N scanning electron microscope from Hitachi combined with a Bruker XFlash 6I30.
13. The pigment identifications were done by various methods: internal reports by MOLAB, led by C. Miliani (FTIR, XRF, UV-vis, SEM-EDX, Raman) (see also Miliani et al. 2010); internal report by the Danish National Museums research department, by chemist M. Taube (XRF analyses) and M. C. Christensen (amino acid and FTIR analyses); internal reports by R. Newman, MFA, Boston (FTIR, Raman, SEM); internal report by D. Buti, CATS, National Gallery of Denmark (XRF); internal report by Julie Jaeger, teaching associate professor, KADK (SEM-EDX); Nini A. Reeler, chemist, University of Copenhagen (Raman) (see also Reeler 2013). The portraits have also been studied by various analytical photographic methods: visible-induced infrared luminescence (VIL), X-radiography, and ultraviolet radiation. Figure 9.1 shows a schematic overview of pigment identification.
14. van den Berg, van den Berg, and Boon 1999.
15. Casadio et al. 2019.
16. Schilling, Carson, and Khanjian 1998.
17. Plater et al. 2003.

Calculated Viewing Angles in the Presentation of Romano-Egyptian Mummy Portraits

Jevon Thistlewood

This paper continues a discussion from “A Study of the Relative Locations of Facial Features within Mummy Portraits,” which was presented at the Getty Villa in 2018 and published in 2020.¹ This earlier study demonstrated that a mean of facial features in Roman-Egyptian mummy portraits was located higher up the face than expected, when compared with a mean of real human faces as measured from photographs. Furthermore, the apparent increase in displacement relative to distance from the bottom of the head suggested that rotation about a lower fixed position had also occurred. The images of more than two hundred painted mummy portraits in the APPEAR database were examined and measured in conjunction with this paper. Participants in the APPEAR project generously provided these images for collaborative study, and they were captured before this particular use was conceived. Understandably, therefore, they may contain inconsistencies, such as their angle of capture, which have previously not been an issue. A standardized system of capturing and recording facial feature locations among institutions holding mummy portraits would have been hugely beneficial to this study.

Romano-Egyptian mummy portraits are painted heads with shoulders, mainly executed on wooden panels that were inserted or incorporated into the wrappings of

embalmed human remains to provide an integral and recognizable human image. Whether these portraits were intended to be entirely accurate likenesses of the deceased remains contentious. In common with the majority that survive today, the works included in this study have long been separated from their mummified remains and exist in isolation from them. The measurements used here were taken from digital images of the portraits rather than from the portraits themselves. To eliminate the inherent and unaccountable errors of this method, future examination of facial features would be assisted considerably by a centralized system of standardized measurements provided by each participating APPEAR collection. Ideally, this approach would accurately locate all features on both sides of a face and allow any feasible measurements to be ascertained in the future.

A plausible explanation for the reported displacement in facial features during a portrait’s creation is that there was a difference between the plane in which human faces were presented and observed and the plane in which the likeness was recorded and painted. Figure 10.1 presents a simplified, side-on view imagines a scenario in which a body is horizontally positioned with its head supported at an angle (illustrated by the black line) while the artist works on an adjacent flat surface (the blue line). It is worth

noting that the head and working surface could be arranged in any orientation (e.g., to correlate to a vertically arranged body) as long as there is a difference in the planes of observation and execution. It is this difference that can result in the upward movement of the facial features on the human head when compared with the finished image (fig. 10.2). If the artist maintains their position, they will not realize that they are recording the positions of the facial features increasingly higher. In fact, this displacement may only be apparent when the artist changes their viewing angle. (An artist who prefers to work on a table while viewing a sitter in front of them may be aware of the progressive elongation of features and spacing in their drawing only when they stand back and view the finished work upright.) In the same vein, it will not necessarily be obvious today when viewing mummy portraits as isolated objects on walls, in display cases, or in illustration; when presented with portraits as objects in their own right, audiences naturally want to view them square-on, eye to eye (fig. 10.3).

Beyond the shoulders of mummified remains that still retain their portraits, there is often a change in angle resulting in the portrait being slightly tilted. The assumption, backed up with several CT (computed tomography) studies, is that the deceased head is angled during the embalming process, and the portrait aligns with the front of the skull. “During the embalming process, there are very practical reasons to elevate the head of the deceased at a slight angle”—not only does this position look like one of rest, but “it avoids both the disfiguring effects of blood pooling in the head and an unsightly mouth gaping open.”²

The position of the portrait may therefore simply follow the topography of the mummified remains; it may be positioned as such because the human head is not necessarily parallel to the spine. An experienced portrait painter could have known how to manipulate the relationship between these planes to best present the likeness at its intended viewing angle and distance. Awareness of, and the ability to work with, the tilting of the head is conceivable. If the relative positioning of the portraits and of their intended audience are more or less predetermined by custom or practicality—that is, a tilted portrait is viewed from a standing position near the feet of the mummified remains—then it makes sense to utilize this viewpoint or at least communicate among portrait makers a repeatable system that exploits it.

To re-create the original creator’s view, the angle between the planes of observation and execution must be calculated. For this, we require the expected positions of

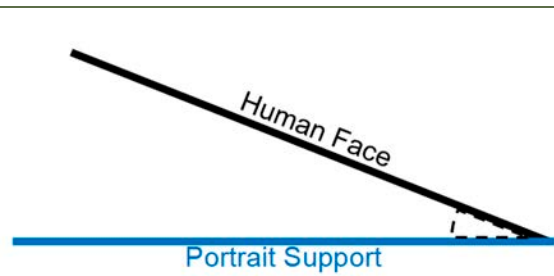


Figure 10.1 Diagram illustrating a human head (black line) and portrait support (blue line) oriented in different planes. Image: Jevon Thistlewood

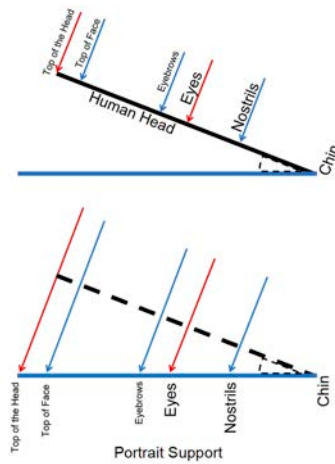


Figure 10.2 Top: Diagram illustrating sight lines when the human head is viewed straight-on. Bottom: The corresponding locations of facial features on a mummy portrait support using the same viewing location. Image: Jevon Thistlewood

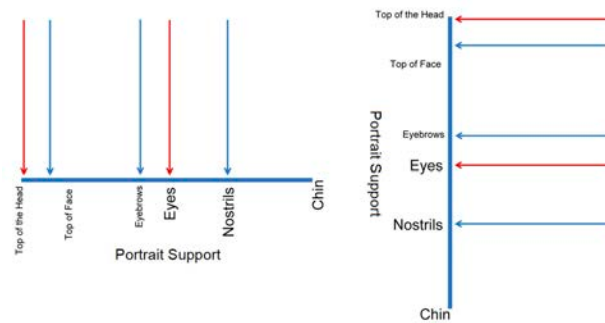


Figure 10.3 Diagrams illustrating the straight-on viewing of the resultant mummy portrait with upwardly displaced facial features, in two different orientations. Image: Jevon Thistlewood

facial features on a real human face. Ideally, they would be obtained from the very same human head on which the portrait was originally based—or one closely associated with it. However, the portraits in this study are no longer

associated with their human remains, and in many cases there is no way of tracing them. Skulls possibly exist for some that can be located, such as those collected by Flinders Petrie,³ and they could form a useful pilot study. A few skulls relating to Romano-Egyptian mummy portraits have had facial reconstruction applied,⁴ and these examples could yield further data. There are also studies, including the CT scans of mummified remains, for which skulls could be examined and measured without excessive intervention. With the appropriate ethical safeguards and considerations in place, these specimens may make an interesting future contribution, but for the purposes of this study, they were not feasible avenues to pursue.

As an alternative, many canons, guidelines, and studies exist that, however removed in time and place from Romano-Egyptian mummy portraiture, have similarly attempted to address related concerns. Such tools range in complexity and essentially communicate the basics of sizing a human head and locating key positions within it. To varying degrees, they can be used to assist in the successful rendering of a complex three-dimensional human face into a convincing two-dimensional representation via a framework of rules or steps. Such guidance presumably can be disseminated among makers of varying experience and ability so that these artists can achieve similar results. These steps potentially also facilitate efficiency and confidence in the process of making portraits, as there is less need to devise solutions to challenges that have been more collectively or previously resolved.

Among others, the information available today includes guidance attributed to Polykleitos,⁵ Lysippos,⁶ Marcus Vitruvius Pollio,⁷ Cennino d'Andrea Cennini,⁸ Francesco di Giorgio,⁹ Leonardo da Vinci,¹⁰ Albrecht Dürer,¹¹ Giorgio Vasari,¹² Dionysius of Fourna,¹³ Johann Joachim Winckelmann,¹⁴ and Avarad Fairbanks.¹⁵ These texts are sometimes challenging to interpret with regard to facial proportions, as the information concerning the face can be a minor constituent of a greater emphasis on overall human dimensions. In some cases, the relationship between the face and head is simply stated; in others, readers must ascertain this relationship from the ratio of heads and faces, which make up the height of a whole human. (This is always quoted as, or assumed to be, the height of a man, with any distinction of male and female proportions not readily evident before the twentieth century.) These approaches also have varying degrees of artistic license with respect to how closely they expect to be followed—and in some instances appear so complex as to be unworkable without more practical guidance or direction. There is also the question of the intended use of

the various guidance, as the proportion of heads making up the height of a human will have a direct result on the height of the head itself. Less head-equivalent height in the overall length of the human figure equates to a larger head overall, which may be useful if viewing from the feet of the figure.¹⁶

For the purposes of this paper, I used Vitruvian proportions as a pragmatic choice to provide the expected positions of the real-face locations:

*For the human body is so designed by nature that the face, from the chin to the top of the forehead and the lowest roots of the hair, is a tenth part of the whole height; the open hand from the wrist to the tip of the finger is just the same; the head from the chin to the crown is an eighth. . . . If we take the height of the face itself, the distance from the bottom of the chin to the underside of the nostrils is one third of it; the nose from the underside of the nostrils to a line between the eyebrows is the same; from there to the lowest roots of the hair is also a third, comprising the forehead.*¹⁷

I chose Vitruvian proportions because they predate Romano-Egyptian mummy portraits and are therefore not a more recent innovation; they are relatively simple to communicate and can be replicated consistently; and they continue to provide a good approximate framework of a recognizably realistically proportioned human head for both face creation and alteration today. In the Vitruvian system, the upper limit of the face, eyebrows, and nostrils are expected to be located at twelve-, eight, and four-fifteenths of the height of the head, respectively. Likewise, the horizontal center of the eyes is expected to align with the horizontal center of the head.

For painted portraits in this study, the current locations of the upper head limit, upper face limits, eyebrows, eyes, and nostrils were measured in respect to their distances from the lower limit of the head (fig. 10.4). These measurements were taken on the more prominently forward-facing side of each portrait. In some portraits, the lower limit of the head can be difficult to locate in a bushy beard, or the upper limit can be hard to detect in an elaborate hairstyle. Such measurements were calibrated using the associated panel heights recorded in the APPEAR database (and it is assumed that these measurements are accurate). Any future studies certainly would benefit from the direct measurement of the portraits themselves rather than measurements derived from their images. Although it is logistically difficult for one researcher to visit each portrait to undertake this work, each participating collection in APPEAR could one day collaborate in a collective resource and study of these data.

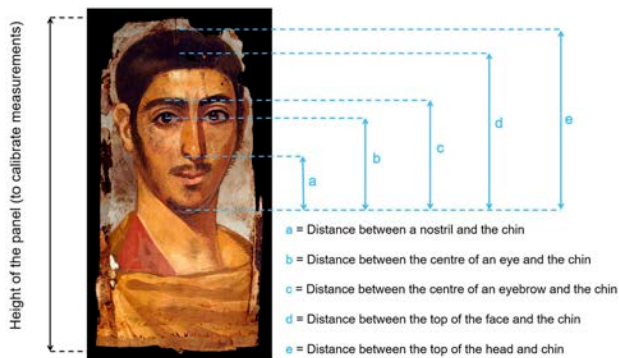


Figure 10.4 Left: Portrait of a Young Man, Romano-Egyptian, 193–235 CE. Uncovered at Tanis by Grenfell and Hunt in 1902. Encaustic paint on a limewood panel with traces of linen, 39.2 x 19.1 cm (15 7/16 x 7 1/2 in.). Oxford, Ashmolean Museum of Art & Archaeology, Egypt Exploration Fund, AN1896-1908.E.3755. Right: Locations of measurements taken from each image of a funerary portrait. Photo: © Ashmolean Museum, University of Oxford / Image: Jevon Thistlewood

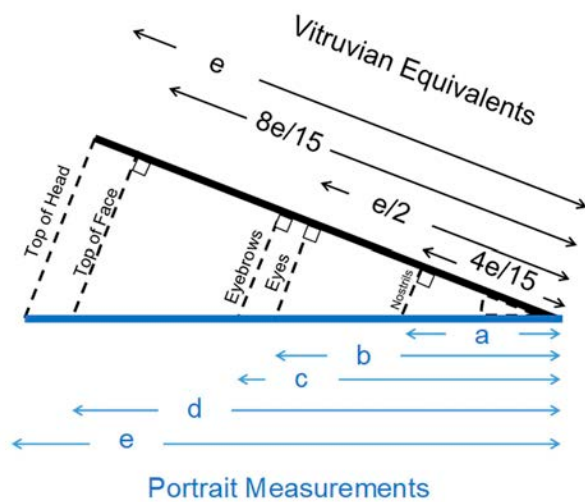


Figure 10.5 Diagram comparing the portrait measurements (fig. 10.4) with their Vitruvian equivalents. Image: Jevon Thistlewood

The Vitruvian equivalents of the facial feature locations were calculated for each portrait and again recorded as distances from the lower limit of the head. These distances were then used in conjunction with the original measurements to calculate theoretical angles between the planes of presentation of the human face and the execution of the subsequent portrait (fig. 10.5). Trigonometry determined the angles: the inverse cosine function with the portrait measurements was used as the hypotenuse, and the Vitruvian measurements were used as the adjacent.

All the facial features on each portrait were expected to correlate closely with a single angle of orientation

(allowing for an acceptable margin of error). In practice some do, but the overwhelming majority show a much more complicated situation, with variation throughout their facial features (figs. 10.6–10.9). Some of the variation is undoubtedly a natural deviation from Vitruvian proportions—and implicit error in working from images. The angle of the camera in relation to the portrait in each instance is not known; if it were, it could be factored into this study’s calculations. The variation could also relate to different working practices in the creation of the portraits. Stylistic differences in Romano-Egyptian mummy portraits suggest different creators and/or centers of production working toward common goals but not necessarily side by side. In hindsight, differences are perhaps not surprising, as the study included portraits of all styles, of various dates, and made no allowances for any with potentially substantial reconstructive restoration. Comparison of much smaller groups of stylistically similar portraits would perhaps be another, more reliable, avenue to consider.

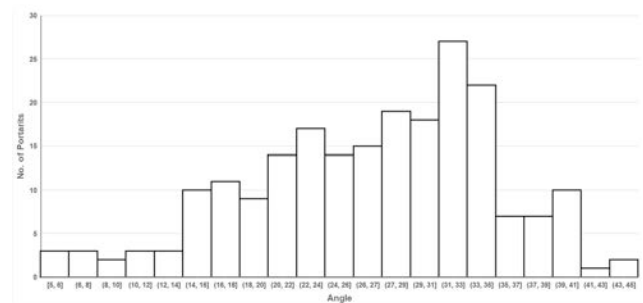


Figure 10.6 Angles generated using distances measured between a nostril and the chin. Image: Jevon Thistlewood

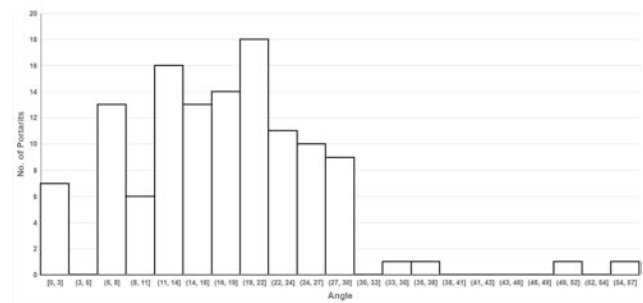


Figure 10.7 Angles generated using distances measured between the center of an eye and the chin. Image: Jevon Thistlewood

With the results of the group presented together, the range in magnitude of the calculated angles is shown in figure 10.10. It is notable that some facial features had to be excluded from the calculation—where they were measured to be in a lower (rather than higher) starting

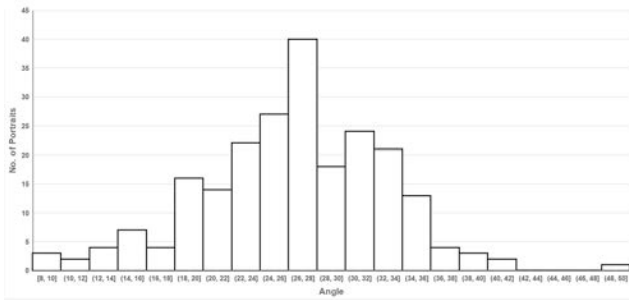


Figure 10.8 Angles generated using distances measured between the center of an eyebrow and the chin. Image: Jevon Thistlewood

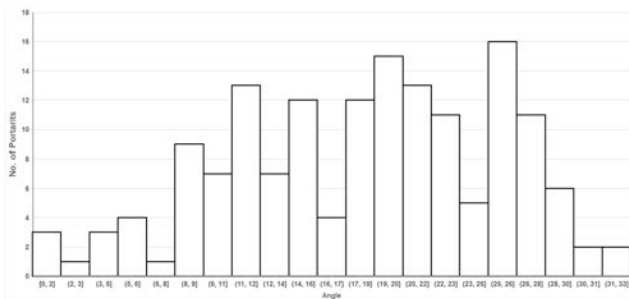


Figure 10.9 Angles generated using distances measured between the top of the face and the chin. Image: Jevon Thistlewood

position—and some facial features appear to be already positioned in their expected target locations (i.e., executed in plane with a realistically recorded human face). The exclusion rate for the eyebrow and nostril locations was very low (3 and 7 percent, respectively) compared with that of the eyes and upper limit of the face (48 and 33 percent, respectively).

	Angles generated				Portraits excluded
	Max	Min	Average	Median	
Nostril to Chin [a]	45	5	27	28	7%
Eyes (centre) to Chin [b]	57	0	17	17	48%
Eyebrows (centre) to Chin [c]	50	8	26	27	3%
Top of face [d]	33	0	18	19	33%

Figure 10.10 Minimum, maximum, average, and median values for the angles generated. Image: Jevon Thistlewood

If we look at the average and median values generated in cases where the calculation of an angle was possible, we can tentatively see a relationship emerging that suggests the horizontal center line of the eyes (which is effectively the center of the head) and upper limit of the face are similarly displaced. With the position of these two lines, we should, in principle, be able to determine the angle at

which the human face was, or the portrait is, intended to be shown. On average, these lines require between 17 and 18 degrees of angular displacement, while their median values range from 17 to 19 degrees.

In comparison, the average and median angles generated by the location of the eyebrows and nostrils suggest a much higher 26 to 28 degrees. This disparity is unexpected until we realize that there is often a lack of space to accommodate the eyebrows at the lower position that a 17- to 19-degree angle would generate. The eyes in Romano-Egyptian mummy portraits are often depicted larger than life and therefore occupy more space than they would on an actual face. It is thus possible that the incorporation of larger eyes into the portrait has necessitated further upward movement of the eyebrows in order to maintain the integrity of the overall composition.

The position of the nostrils is linked to that of the eyebrows in that both features effectively coincide with the upper and lower limits of both the nose and the ears. As such, if the eyebrows are displaced upward to accommodate a larger format of eye, you would expect the nostrils to follow suit.

From the average results, these mummy portraits appear to contain facial features in one of two planes. Possibly only one angle of viewing was inherent or intended, but accommodation of symbolically important larger-than-life eyes led to adjustments and compromises. A larger jump perhaps, and maybe more unlikely, is that two planes could also facilitate a face, or certain elements within a face, that can be convincingly presented at two different angles.

The appearance of mummy portraits often betrays the complexity they pose when attempting to understand the decisions and processes undertaken in their creation. This paper aimed to explain a theory as to how distortion of facial feature positioning could have happened in the creation of the portraits and used this theory to calculate the intended angles of orientation. More accurate references to the real-life facial positions would be an undoubted improvement on the use of Vitruvian proportions. Such data could be direct measurements from related human skulls or derived measurements from CT scans. Equally, the goal of providing accurate true-to-life facial feature proportions will already have been mastered by facial reconstruction, and this area should also be explored as a future resource for guidance and collaboration.

The question of which specifications within the production of portraits were collectively agreed upon and which were

more independently decided remains unanswered. Was there a system of proportionality and positioning that was communicated among portrait makers? A more standardized identification of the relative dates of origin and find locations of portraits across the APPEAR database would help to potentially identify subgroupings of portraits to study and compare. If the elements of error in the procedure can be minimized, will the results show tighter correlations or clarify distinct groupings? A closer agreement will point to collective decision making, while variance could suggest more localized or individual actions.

And finally, there is also the presence of outlying results, which have not been adequately considered at this time. Are they simply the exceptions? Or, with the elimination of errors, can these portraits, including those with the largest tilt or no tilt at all, be better considered alongside the debate of whether they were executed from life or after death?¹⁸ There is also the added confusion, or possible misunderstanding, of a small number of portraits that seem to contain rotation centered at the top of the head rather than at the base.

NOTES

1. Thistlewood et al. 2020.
2. Thistlewood et al. 2020, 104–5.
3. Challis 2013, 110–11, 123–25.
4. Nerlich et al. 2020; Prag 2002; Wilkinson 2002, 66–71; Picton, Quirke, and Roberts 2007, 30–31.
5. Naini et al. 2008; Tobin 1975.
6. Tobin 1975.
7. Rowland and Howe 1999, 47.
8. See Broecke 2015, 109: “Note that, before going any further, I want to give you, to the letter, the measurement of a man. . . . First, as I mentioned above, the face is divided into three sections, that is: the forehead one, the nose another and from the nose to the chin another. . . . And the whole man: eight faces and two of the three measures long.”
9. Millon 1958.
10. See Rigaud 2005, 4: “A well-proportioned and full-grown man, therefore, is ten times the length of his face.”
11. Naini et al. 2008.
12. “It is the custom of many artists to make the figure nine heads high. . . . For Vasari, a practical artist, to commit himself to the statement that figures are made nine heads high, is somewhat extraordinary, for eight heads the proportion given by Vitruvius is the extreme limit for a normal adult, and very few Greek statues, let alone living persons, have heads so small.” See Maclehorse 1960, 146.
13. “Learn, O pupil, that in the whole figure of a man there are nine faces, that is to say nine measures, from the forehead to the soles of the feet. First make the first face, which you divide into three, making the first division the forehead, the second the nose and the third the beard. Draw the hair above the face to the height of one nose-length; again measure into thirds the distance between the beard and the nose; the chin takes up two of the divisions and the mouth one, while the throat is one nose-length.” In Hetherington 1996, 12–13.
14. “The face has three parts as well, namely, three times the length of the nose; but the head is not four nose-lengths, as some very erroneously wish to teach. The upper portion of the head, namely, the distance from the hairline to the crown, measured vertically, is only three-quarters of the length of the nose, that is, this part is to the nose as nine is to twelve.” In Mallgrave 2006, 207.
15. Fairbanks and Fairbanks 2005.
16. For example, a statue on a tall plinth is to be viewed from below. Seven portraits within the APPEAR database that survive with their mummified remains were measured to compare their head heights with the overall height of the mummified remains. The ratio varied from 1:7 to 1:10; however, the group was too small from which to draw any significant conclusions.
17. Morgan 2006, bk. 3, ch.1, no. 2.
18. Amsen 2020.

The Saint Louis Painter's Artistic Circle

Branko F. van Oppen de Ruiter

ATTRIBUTION TO THE SAINT LOUIS PAINTER

In his publications on the Romano-Egyptian funerary portraits in the collection of the J. Paul Getty Museum, David L. Thompson attributed three female portraits to the same artist, whom he named the Saint Louis Painter on the basis of the portrait of an elderly woman in the collection of the Saint Louis Art Museum (appendix [hereafter app.] no. 1; fig. 11.1).¹ "The most striking feature of the style of the St. Louis Painter," in Thompson's words, "is his distinctive use of lines of hatching."² The likely provenience of these panel portraits can be traced back to the cemetery of ancient Philadelphia (conventionally referred to as er-Rubayat).³ Thompson dated the works to about 290–310 CE. He acknowledged that "a number of other portraits are related to those by the St. Louis Painter and some to each other," thus "suggesting a school of portrait artists active at er-Rubayat around A.D. 300."⁴ He did not specify any of these other portraits nor their possible number.

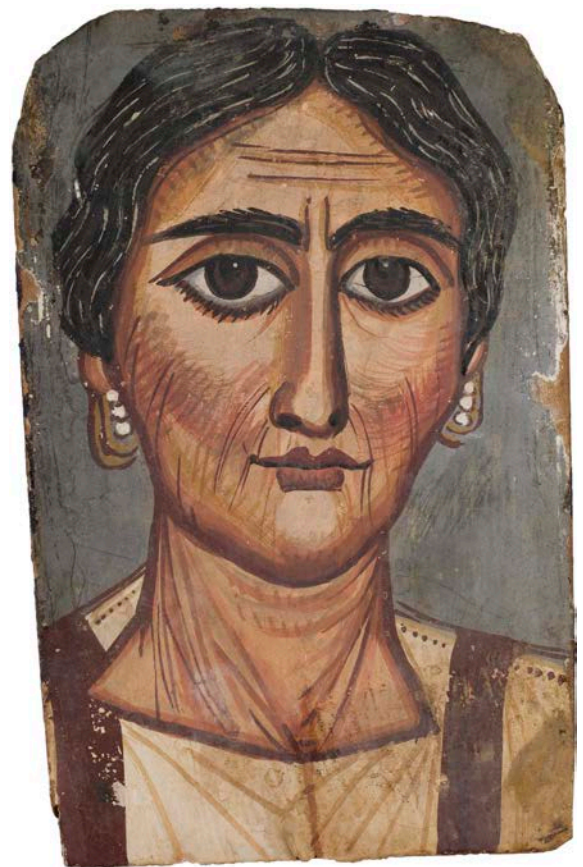


Figure 11.1 Elderly Woman with Graying Hair, Philadelphia, Fayum, Egypt, ca. second to third century CE. Tempera on willow wood panel. Saint Louis Art Museum, 128:1951. Photo: Courtesy Saint Louis Art Museum

Klaus Parlasca associated the work of the Saint Louis Painter with portraits that had been attributed to the so-called Würzburg Painter based on the portrait of the mature bearded man now at the Martin von Wagner Museum, Würzburg (app. no. 13; fig. 11.2).⁵ Parlasca also noted the artist's flat pictorial style that tends toward a definite schematism and dates some of the examples to about 300 CE, yet others to about 325–350 CE.⁶



Figure 11.2 Mature Man with Beard, Philadelphia, Fayum, Egypt, ca. second to third century CE. Tempera on wood panel. Würzburg, Martin von Wagner Museum, H 2196. Photo: C. Kiefer. © Martin von Wagner Museum der Universität Würzburg

The attribution of over a dozen portraits to the Würzburg Painter, though not by that name, may be traced to Heinrich Drerup in his 1933 dissertation on the dating of the funerary portraits.⁷ Drerup was one of the first experts to recognize that the subjects' hairstyles could offer clues for the purpose of dating the portraits.⁸ He was able to assign all specimens to the Roman Imperial age rather than the Ptolemaic period, as had been argued earlier by Georg Ebers.⁹ Drerup dated the portraits attributed to the

Würzburg or Saint Louis Painter to the early Constantinian period (324–337 CE).¹⁰ Although he explicitly mentioned portraits of the woman now at the Harvard Art Museums (app. no. 3; fig. 11.3B) and of the elderly man at the Kunsthistorisches Museum Wien (app. no. 16; fig. 11.4C), in addition to the Würzburg painting, he did not specify which other examples he had in mind.¹¹

Barbara Borg dates the Würzburg portrait significantly earlier, to about 190–210 CE, and relates its style to that of the famous tondo of the imperial family of Septimius Severus (r. 193–211 CE).¹² Borg discusses the portraits at the Pushkin State Museum of Fine Arts (app. no. 2; fig. 11.3A) and in Saint Louis among a group of female portraits with a chignon coiffure, which she dates to about 165–190 CE on account of similarities with the hairstyles of the empresses Faustina Minor, Lucilla, and Crispina.¹³ Without mentioning the Saint Louis Painter or the site of the workshop, she implicitly attributes at least nine "impressively expressive" portraits to this artist, considering them among "the last of the more naturalistic tempera portraits."¹⁴ Borg does not address the relationship between the Saint Louis Painter and the Würzburg Painter and, to reiterate, dates the relevant works to a time span of nearly half a century, from about 165 to 210 CE.

The present study is based on twenty-five portrait paintings that may be considered closely related based on stylistic features (see app.; eighteen are illustrated in this paper, figs. 11.1–11.4).¹⁵ These artistic characteristics and techniques are addressed first. The discussion will clarify the stylistic features attributed to the same workshop, if not the same painter. It will also illustrate the relative variance of identifiable characteristics. Next, an analysis is provided of the portrait features, such as basic outlines and the subjects' positions. This analysis will allow me to delve further into aspects of the paintings, particularly the subjects' physiognomy and proportions. Hairstyles, generally considered a potential dating method, as well as jewelry and clothes, will not produce firm chronological indicators. Questions about the possibility of attributing the selection of twenty-five portraits to the same artist or workshop are then addressed. The last section brings together some of the scientific examinations performed on the paintings, mostly as a result of the Getty's APPEAR project. Such analytical data is sourced to identify similarities in the materials chosen for the creation of the portraits as a means of corroborating possible attribution to an artist or workshop.¹⁶



Figure 11.3 Selection of eight female portraits, Philadelphia, Fayum, Egypt, ca. second to third century CE. Tempera on wood (see app. nos. 2–5, 8–10, 12). (A) Moscow, Pushkin State Museum of Fine Art, I.1a 5783. Photo: Courtesy Pushkin State Museum of Fine Art, Moscow. (B) Cambridge, MA, Harvard Art Museums, 1939.111. Photo: © President and Fellows of Harvard College. (C) San Jose, CA, Rosicrucian Egyptian Museum, RC-1759. Photo: Rosicrucian Egyptian Museum, San Jose, California, USA / CC BY-NC. (D) Northampton, MA, Smith College Museum of Art, SC 1932.9.1. Photo: Courtesy Smith College Museum of Art. (E) Zürich, Archäologische Sammlung der Universität Zürich, UZH-AS 3801. Photo: Frank Tomio. Courtesy Martin Bürge, used with permission. (F) Stockholm, National Museum, Ant. 2303. Photo: Courtesy of the National Museum, Stockholm. (G) London, British Museum, 1890,0921.1. Photo: © The Trustees of the British Museum. (H) New Haven, CT, Yale University Art Gallery, 2011.102.1. Photo: Courtesy Yale University Art Gallery

ARTISTIC CHARACTERISTICS AND TECHNIQUES

As Thompson recognized, one of the most characteristic features of the Romano-Egyptian portraits associated with the Saint Louis Painter that immediately catches the viewer's attention is a distinctively graphic hatching technique.¹⁷ While this may be more or less the case for about half of the examples here suggested to belong to the same workshop, in other examples the technique is admittedly less apparent or simply absent. For example, the technique is much less evident on the female portraits

at the Yale University Art Gallery, Universität Zürich, Antiken Sammlung (the Ancient Collection of the University of Zurich), and the British Museum (app. nos. 8, 9, and 12; figs. 11.3E, G, and H), as well as the male portraits at the Stockholm National Museum and the Los Angeles County Museum of Art (app. nos. 17 and 22; figs. 11.4D and H). This feature is difficult to discern on the examples sold on the art market (app. nos. 11 and 25; not illustrated). It is entirely absent on the female portrait at the Rosicrucian Egyptian Museum in San Jose, the two male portraits at the British Museum, and the paintings in Rhode Island and Vienna (app. nos. 3, 20, 21, and 23; figs. 11.3C and 11.4H).



Figure 11.4 Selection of eight male portraits, Philadelphia, Fayum, Egypt, ca. second to third century CE. Tempera on wood (see app. nos. 14–19, 21–22). (A) Leiden, Rijksmuseum van Oudheden, F 1932/3.1. Photo: Courtesy Rijksmuseum van Oudheden. (B) London, Freud Museum, 4947. Photo: Courtesy Freud Museum. (C) Vienna, Kunsthistorisches Museum Wien, AS X-300. Photo: Courtesy Kunsthistorisches Museum. (D) Stockholm, National Museum, Ant. 2309. Photo: Courtesy of the National Museum, Stockholm. (E) Berlin, Staatliche Museen zu Berlin, Antikensammlung, 31.161/38. Photo: Courtesy Staatliche Museen zu Berlin, Antikensammlung. (F) London, Freud Museum, 4946. Photo: Courtesy Freud Museum. (G) London, British Museum, 1931,0711.3/EA-63.397. Photo: © Trustees of the British Museum. (H) Los Angeles County Museum of Art, M.71.73.62. Photo: Courtesy of Los Angeles County Museum of Art

This absence might be taken as evidence that the relevant paintings were not the work of the same artist as the others. Conversely, it might indicate that the painter, his workshop, or the wider artistic circle was prone to some variation. The intermediary cases where the lines of hatching are less easily distinguished might actually represent a sliding scale of artistic variation.

The portraits exhibit little sense of perspective apart from a slight turn away from the viewer, generally indicated by a foreshortening of the proper left side of the face, and often by transverse, twisting lines in the neck. About half of the male portraits, nevertheless, are shown in full or almost frontal view. The style may best be described as expressionistic. Individualizing facial features are painted with usually fairly thin, vivid brushstrokes. These features

are applied over an initial outline drawn with broader strokes in simple contours, generally in the same dark tone as the vertical stripes of the tunic. A simplified representation of this outlining for six of the female portraits illustrates how similar these contours really are (fig. 11.5).

The parallel or crosshatched lines (often at angles of 30°, 45°, or 60°), which are applied to suggest shade and/or volume, are often found along the hairline and the side of the face, as well as on the neck, but less often elsewhere—for instance around the eyes. Occasionally, however, shades and volume have been painted in broad (gradient) tones. On two female portraits, curving lines appear to indicate shadows thrown by the locks or curls of the hair (viz. on the Yale and Zurich paintings, app. nos. 8–9; figs.

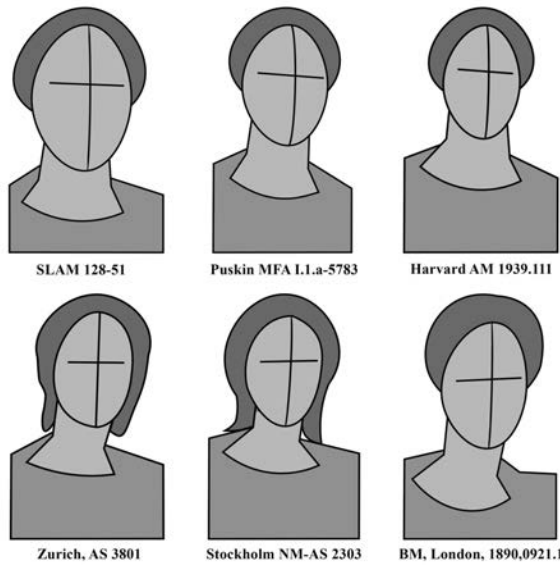


Figure 11.5 Outlines of six female portraits. Branko van Oppen

11.3E and H). On the portrait of the elderly woman in the British Museum (app. no. 12; fig. 11.3G), the painter has attempted to indicate highlights on the face—over the brows, across the nose, under the eyes, and on the chin. On the portrait of a young man sold on the art market (app. no. 25), unusual yellowish-pink highlights are drawn under the eyes, along the rim of the nose, in the nasal-labial area, and along the outline of the mouth, while the philtrum is shaded in dull brown.

FEATURES AND POSITION

Of the twenty-five panel paintings under examination, twelve portray women. Of these female portraits, half appear to depict elderly women (over sixty years old), another one shows a middle-aged woman (ca. forty-five to sixty years old), four more portray mature women (ca. thirty to forty-five years old), and just one shows a younger woman (ca. fifteen to thirty); none of them portray children (fig. 11.6). This age distribution is significant foremost because the average life expectancy at birth for women in Roman Egypt was typically low, about twenty years of age, though members of the wealthier classes may be expected to have lived longer.¹⁸ Additionally, the apparent age distribution contradicts the assumption that portraits of mummified persons represent an idealized, youthful beauty standard. In connection with this notion of beauty ideals, it should furthermore be emphasized that the portrayed women exhibit a similar complexion to their male counterparts—ranging from a soft yellowish-tan to a warm copper tone, at times with an added pinkish blush

on the cheeks—rather than the pale white skin expected for women of the Graeco-Roman upper class.¹⁹ (Compare, for instance, the difference between the skin colors of Terentius and his wife, fig. 11.10.)

Category	Age	Male	Female	Total
<i>child</i>	0–15	–	–	0
<i>young</i>	15–30	8	1	9
<i>mature</i>	30–45	2	4	6
<i>middle-aged</i>	45–60	1	1	2
<i>elderly</i>	60+	2	6	8
	Total	13	12	25

Figure 11.6 Estimated age of the subjects by gender. Branko van Oppen

In light of their represented ages, it is no surprise that the foreheads of most women are furrowed with wrinkles and/or frowns; only the younger but still mature ladies on the Harvard and San Jose portraits have smooth foreheads (figs. 11.3B and C).²⁰ They all have bushy black or brownish black eyebrows that typically curve unevenly so as to emphasize the asymmetry of the face. The eyes are, without exception, expressively stark and disproportionately large, with long eyelashes. They may occasionally be unevenly set, asymmetrically sized, and/or drooping. The eyes have large, usually brown irises with black pupils and small white dots of reflected light, all with limbal rings. In most portraits, the insides of the eyes are outlined in the same shade of gray as the background of the panel; ocular sockets are marked with semicircular folds over the eyes. The upper lids tend to pass over the lower lids at the outer corners. In only two examples is a single tear duct indicated (figs. 11.3C and G). Sagging flesh is generally drawn underneath the eyes with curved lines or darker shades of color. The ears are mostly covered by hair; what remains visible of the ear is usually no more than a curved line. If an attempt was made to draw the earlobes, they seem to be attached.

A common feature is the anatomically awkward and elongated nose. The nostrils are typically indicated with dark dots, and often the proper left nostril is barely visible due to foreshortening. Although Thompson recognized this feature as one of the hallmarks of the group of portraits in question, occasionally the nostrils are rendered more successfully (e.g., on the Harvard and Zurich portraits, figs. 11.3B and E).²¹ Cheeks may be round and full, flat, or bony and hollow. The lower face is often

creased with wrinkles and has folds from the nostrils and/or the corners of the mouth. Without exception, the mouth is full, with a Cupid-bowed upper lip and a fleshy lower lip. Occasionally the lips are pursed or puckered, and in one example (fig. 11.3C), both lips are outlined. A dimpled philtrum is indicated on three female portraits (figs. 11.3B, F, and H). The corners of the mouth are mostly rendered with short, rounded strokes, but in one example (fig. 11.3G) the proper left corner has a little dimple. The women invariably have full, round chins; their jawlines may be slanting, jutting, long, or round. Their necks suggest wrinkles or sagging flesh, while one example (fig. 11.3D) has Venus rings and in another example (fig. 11.3C) the neck is smooth.

The thirteen male portraits display a somewhat wider range of age distribution than the women (figs. 11.4 and 11.6). Only two depict elderly men (over sixty years old), and just one can be said to be middle-aged (ca. forty-five to sixty years old). Two more portray mature men (ca. thirty to forty-five years old). The remaining eight represent young men (ca. fifteen to thirty years old), of whom three seem to be adult (ca. twenty to thirty), while the remaining five may be younger (ca. fifteen to twenty) and, significantly, seem to be more distantly related to the Saint Louis and Würzburg portraits (or is that the consequence of the portrayal of their younger age?). The average male life expectancy at birth, about forty years, was higher than it was for women in Roman Egypt.²² Still, it remains notable that there are fewer middle-aged and elderly men represented than middle-aged and elderly women. The complexions of the men display a similar range to those of the women. Skin tones range from a pale yellowish to a warmer copper tan. Occasionally the complexion may shade into a darker sienna tan. In the case of the young man in the Kunsthistorisches Museum (app. no. 24), the skin tone is exceptionally pink.

The shape of the male heads is generally elongated (and occasionally more angular), at times even more so than the women's. Their foreheads are either smooth or furrowed with wrinkles and/or frowns. Like the women's brows, the men's black or brownish black eyebrows are usually thick and bushy and tend to curve or arch. Sometimes there are a few hairs on the bridge of the nose. Also much like the portraits of the women, the stark eyes are typically expressively large. Sometimes they are broadly outlined in black. If they have lashes, they are either thin and short or thick and long. The eyes have mostly large brown irises, fairly often with dark limbal ring outlines, black pupils, and normally some white dots of reflecting light. The sclera may be outlined in the same grayish tone as the background of the painting. Tear ducts

are often indicated (sometimes only in the proper right eye). In two examples, the inside corners of the eyes show red blood vessels (app. nos. 20 and 22; fig. 11.4H). Ocular sockets are invariably marked above the eyes with semicircular folds. The upper eyelids tend to pass over the lower lids at the outer corners. Below the eyes, dark shades of sagging bags may be indicated to suggest aging, fatigue, or both. At times, though, the eyes appear slightly closed, almond-shaped (app. nos. 18 and 20; fig. 11.4E), or of comparatively smaller size (app. no. 23). The irises of the portrait of the young man in the British Museum (app. no. 20) are green, and on the Rijksmuseum van Oudheden portrait (app. no. 14; fig. 11.4A) gray (not blue).

While on some male portraits the outer ears are simply depicted as curved lines, on over half an attempt has been made to depict the ear more naturalistically. In two cases, this even includes unattached earlobes (app. nos. 22 and 25; fig. 11.4H). Noses are typically elongated and usually straight, but occasionally broad or crooked. Nostrils are mostly rendered anatomically awkwardly, with dark dots for the openings, even if the proper left nostril is barely visible due to foreshortening. Some portraits do display an attempt to draw the nose in a more naturalistic manner. In nearly half the cases, a philtrum is indicated. The mouth is generally fleshy, with a Cupid-bowed upper lip and a (sometimes smaller but still) full lower lip. The mouth is occasionally pursed, puckered, or curved in a gentle smile. Corners of the mouth may be indicated with short strokes or as shadows. Because of their facial hair, many of the lower faces, cheeks, jaws, and chins remain difficult to determine. The general outline of the lower face, however, appears to range from squarish to elongated or pointed. The cheeks vary from flat or bony to round. Occasionally the face is aged with wrinkled creases, while on the younger men the skin may be described as soft and smooth.

An aspect that has little to do with artistic techniques or portrait features is the pose. The portraits are typically depicted nearly frontally, slightly turning toward the viewer's right, and with a slight foreshortening effect in the proper left side of the face, occasionally making the proper right ear nearly or fully invisible. The angles of the necks and the twisting lines on their skin further emphasize the slight turn away from the viewer. Seven subjects are portrayed even more frontally, their shoulders sloping approximately symmetrically. In the other cases, where the person is turned slightly to the viewer's right, their shoulders are generally at different levels and angles—with the proper right, near shoulder somewhat higher and the left shoulder at a more oblique angle. A notable exception is the mature bearded man at Staatliche

Museen zu Berlin, Antikensammlung (app. no. 18; fig. 11.4E), whose head is slightly turned to the viewer's left and whose shoulders are slanting as if seen frontally. The subjects' heads are nearly always upright. Only two men's heads are slightly tilted to the viewer's left (app. nos. 16-17; figs. 11.4C-D). These major similarities in the basic positioning of the portraits form yet another confirmation that this group of paintings likely derive from the same workshop.

PHYSIOGNOMIC PROPORTIONS

Since the paintings only feature disembodied heads, the general physiognomic proportion cannot be expressed in relation to the rest of the body (fig. 11.7). If we take the Pushkin portrait as a starting point (figs. 11.3A and 11.7, top left), it appears that the facial proportions follow a grid of 10 x 12 units, as proposed by Thistlewood for the Romano-Egyptian funerary portraits in general (fig. 11.8).²³ The dimensions of the general ellipse describing the face are 2:3 for width-to-height. However, the painter has adjusted the grid to achieve perspectival effects. The vertical lines are slanted at an angle of 4°—most notably at the eyes and mouth but also the brows. We find the root of the hair at the first tenth from the top of the head. The eyes are on the middle horizontal line, with the brows one-tenth above the eyes. The earlobes are in the middle of the seventh unit. The middle of the nose is at the crossing of the seventh horizontal and the central vertical. The mouth is placed on the eighth grid line, and the middle of the chin is about one-tenth from the bottom of the face.

The grid is further adjusted by using semi-elliptical curves instead of straight lines for the verticals, to suggest volume. The central vertical passes between the eyes at a shift of one unit to the (viewer's) right. The vertical lines to the (viewer's) left of the center have been shifted accordingly. We find the inner corner of the proper right eye, as well as the nostril, one unit from the center. The outer corner of the mouth is at the second grid line. The middle of the pupil, however, is drawn about a quarter unit from the third line toward the center (to better fit the iris in the eye). The outer corner of the proper right eye is on the second vertical from the outside of the face, and the end of the brow is on the first line. To indicate the effect of foreshortening due to the turning of the head, the proper left side of the face has been reduced by half a grid unit. Here we find the inner corner of the eye, as well as the nostril, on the first line from the center, and the outer corner on the first line from the outside of the face. The pupil is perfectly centered between the inner and outer

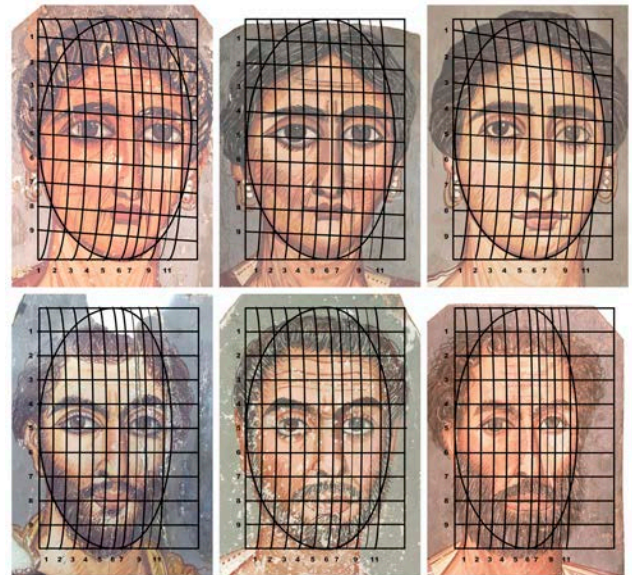


Figure 11.7 Proportional grids for six portraits. Grids overlaid by Branko van Oppen

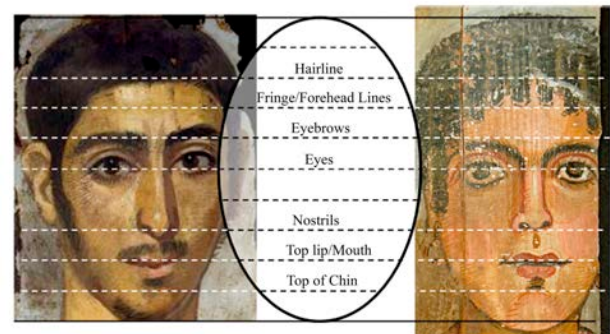


Figure 11.8 Proportional grid for two portraits. Left: Portrait of a Young Man, Romano-Egyptian, 193-235 CE. Uncovered at Tanis by Grenfell and Hunt in 1902. Encaustic paint on a lime wood panel with traces of linen, 39.2 x 19.1 cm (15 7/16 x 7 1/2 in.). Oxford, Ashmolean Museum of Art and Archaeology, Egypt Exploration Fund, AN1896-1908.E.3755. Right: Portrait of a Woman, Romano-Egyptian, 90-110 CE. Fayum. Tempera paint on a lime wood panel, 38.2 x 14.5 cm (15 x 5 11/16 in.). Oxford, Ashmolean Museum of Art and Archaeology, John Davidson Beazley (ex-Graf Collection), AN1966.1112. Photo: © Ashmolean Museum of Art and Archaeology, University of Oxford

corners of the eye; the iris falls neatly between the eighth and tenth verticals.

Comparing the Pushkin portrait with the Saint Louis painting (fig. 11.7, top center), it is obvious that the artist employed the same basic grid of 10 x 12 units to divide the general ellipse that describes the face, and at the same dimension of 2:3. However, there are some minor deviations because the Saint Louis portrait is more frontal than the Pushkin portrait. The vertical lines are slanted at

2.5° (instead of 4°), and consequently the vertical lines are less curved. The central vertical is shifted to the (viewer's) right by about one-third unit, while the outside of the face is shifted a unit to the (viewer's) left. The inner corners of both eyes and the nostrils, as well as the corners of the lower lip, all fall on the first vertical from the center. Both irises are spaced on the inner side of the eyes on the second grid line from the center, and the corners of the upper lip are drawn on the same vertical. However, while the proper left pupil is positioned nearly on the third vertical, the right pupil is centered in the middle of the third unit from the center. Notice, furthermore, that the proper left earlobe is drawn in the middle of the seventh unit, while the right earlobe is placed on the seventh grid line.

The Harvard portrait (fig. 11.7, top right) exhibits a surprising feature in the grid system of 10 x 12, for the horizontals are best understood to approximate a vanishing point of perspective to the viewer's far right of the face, in which the ninth line is perfectly horizontal while each line above is slanted at increasing increments of 1°, so that the first line below the top is at an oblique angle of 8°. The right eyebrow is drawn just above the fourth horizontal line, while the left brow curves over that line. The corners of the right eye are placed about a quarter above the fifth line, but the proper left eye is slanting inward, so that the inner corner lies neatly on the fifth line. The mouth (that is, the bottom of the upper lip) is found about a quarter below the eighth line. Also notice that the proper right earlobe is almost half a unit lower than the other. Vertically, the proper right side of the face has shifted two-thirds of a unit beyond the central line (to the viewer's right), while the outside line of the other side of the face has shifted inward by another two-thirds. On the proper right side, most features are placed where they would be expected, except that the inner corner of the eye is in the middle of the second unit from the center and the pupil is neatly centered on the third line. On the other side, the outer corner of the left eye is in the middle of the second unit from the outside rather than on the penultimate line.

If we turn to the Würzburg portrait (fig. 11.7, bottom left), it is immediately apparent that the grid of 10 x 12 has been significantly adjusted, both horizontally and, to a lesser extent, vertically. First of all, the general oval describing the face is much more elongated, at a dimension of 11:13 (instead of 2:3), and the top line of the oval falls a whole unit above the top of the head. If we follow the horizontal lines down the grid, we do find the hairline on the first horizontal, the brows on the fourth, the tip of the nose on the seventh, the mouth on the eighth, and the middle of

the chin on the ninth. The eyes, however, are aligned on the central horizontal (rather than about a quarter unit above), in such a way that the proper left eye is neatly horizontal on the fifth line, and the inner corner of the proper right eye lies also on that line, but its outer corner lies above it at an angle of 4°. Looking closer, we notice that the left brow is actually placed a little higher than the right, thus exaggerating the asymmetry. The mouth is even more slanted than the right eye, namely at an angle of 5°. Vertically, the six curved lines of the proper right side of the face (the viewer's left) are evenly spaced, without too much deviation from the expected placements, apart from the eye, which is placed just to the (viewer's) left of the third vertical (thus centered in the middle of that side of the face). The proper left side, conversely, is reduced in width—to suggest foreshortening—by a third (two whole units). The placement of the facial features nonetheless follows the established pattern.

A second male portrait, the Leiden painting (fig. 11.7, bottom right), compares very well with the Würzburg portrait. Notice, however, that the face is even more elongated. For while the central vertical has shifted just a third to the (viewer's) right, the outside of the face has shifted two whole units to the (viewer's) left, thus much reducing the width of the proper left side. Other than that, the (flattened) top of the head is again one grid line below the top of the oval describing the face, and all other vertical alignments are similar to the Würzburg painting. The eyes are slanted curiously, though, as they both droop to the (viewer's) left.

Finally, the Vienna painting (fig. 11.7, bottom center) aligns fairly well with the previous two male portraits. Starting with a clockwise rotation of 6°, the main difference from the preceding two examples is that the width of the face in this example corresponds more with that of the female portraits discussed above. The width of the proper right side has increased by a shift of half a unit, while the outside of the (viewer's) right of the face has shifted inward by one and a third unit. The top of the head is closer to the tip of the oval, but the hairline remains on the second horizontal. As on the male portraits, the eyes are drawn in the middle, on the fifth lines. On the vertical grid, the inner corner of the proper right eye falls in the middle of the second unit from the center (rather than on the first vertical from the center), while the outer corner of the left eye falls on the tenth grid line (rather than on the eleventh, as on most other paintings).

This is not the place to go into further detail about the proportions of the other specimens possibly attributable to the Saint Louis Painter's workshop or its wider circle. Nor is

it the place to compare the preceding observations with the so-called Egyptian Canon of Proportions.²⁴ Suffice to say that few conventional ancient Egyptian paintings have survived, and that on comparable two-dimensional imagery, Egyptian tradition dictated that heads were portrayed in profile, and rarely frontal, but certainly never in three-quarters view (fig. 11.9).²⁵ Moreover, no comprehensive examination of facial proportions in ancient Egyptian art exists, even for sculpture. A quick comparison with the portraits of Terentius Neo and his wife on a wall painting from Pompeii demonstrates that their proportions follow the same basic division in 10 x 12 units (fig. 11.10).²⁶ (Note, however, that the adjusted vertical lines accommodate facial features slightly differently.) Finally, it bears emphasizing that these subdivisions diverge both from the ideals expressed by Vitruvius and from actual human anatomy—neither of which prescribes such expressively large eyes or elongated heads.

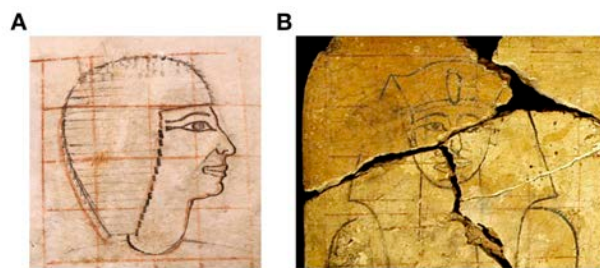


Figure 11.9 Rosters of 4 x 4 (en profile) and 4 x 5 (en face) follow evidently different proportional subdivisions for Pharaonic portraits. (A) Gridded Sketch of Senenmut; Thebes, West Bank (TT 71), Upper Egypt, ca. 1479–1458 BCE. Ink on limestone sherd, 22.5 x 18 x 3.3 cm (8 7/8 x 7 1/16 x 1 3/10 in.). New York, Metropolitan Museum of Art, 36.3.252. Photo: Courtesy The Metropolitan Museum of Art, New York. (B) Gridded Portrait of Hatshepsut or Thutmose III (detail); Thebes, West Bank (TT 11), Upper Egypt, ca. 1479–1425 BCE. Acacia wood, ca. 31 x 45.8 cm (12 3/16 x 18 in.). Luxor Museum, 1001. Photo: C. Spottorno © Proyecto Djehuty. Courtesy José M. Galán, Spanish National Research Council, used with permission

Returning to the portraits under examination, it can be safely concluded that the artist(s) creating these paintings did not employ the grid system in any hard-and-fast manner by drawing it out on the panel with a ruler. From the slight deviations and variations, it can be deduced that the grid was applied intuitively. This is significant to bear in mind for the following two reasons. In the application of the grid system of 10 x 12 units and employing a general ellipse of approximately 2:3, the portraits under question can be shown to belong to the wider Romano-Egyptian corpus of portrait paintings. Conversely, slight deviations and variations from the basic grid cannot be taken as proof that the portraits do not belong to the corpus—



Figure 11.10 Proportional grid applied to the portraits of Terentius Neo and his wife, Pompeii (House VII, 2, 6), Italy, ca. 20–30 CE. Wall painting, 58 x 53 cm (22 4/5 x 20 9/10 in.). Museo Archeologico Nazionale di Napoli, 9058. Photo: Alfredo Dagli Orti / Art Resource, NY

either of the Romano-Egyptian funerary portraits in general or of the Saint Louis Painter in particular. Such deviations are therefore no indications of suspected inauthenticity. The conventions and traditions of portrait-painting left room for individual intuition and invention.

HAIRSTYLES, JEWELRY, AND CLOTHES

The women's hair is nearly always graying brown, black, or brown-black (fig. 11.3). It is usually wavy but occasionally straight, mostly parted in the middle, and pulled to the back or bound in loose locks to the sides, often partially covering the ears. The hair falls down in loose frizzy locks or in untidy long strands to the shoulders. The hair on the portrait of the elderly woman in the British Museum (fig. 11.3G) is bound by a headband. Although female coiffures generally tend to offer significant clues for the dating of Roman portraits, the hairstyles as described above are too generic to be chronologically useful. In the two cases where the hair falls down in frizzy or untidy locks, we may consider Parlasca's suggestion that the coiffure signifies mourning.²⁷ Nonetheless, we may wonder why the deceased would be portrayed in mourning.

The men's fairly simple hairstyles are mostly short and occasionally full, usually with wavy, curly, or frizzy locks of gray or graying brown, black, or brown-black hair (fig. 11.4). It may be combed neatly forward or fall down over the forehead. Sometimes the hairline recedes above the temples. The hair may either partially conceal the ears or expose them. One of the paintings in the Freud Museum (fig. 11.4F) portrays a balding and wreathed man. One of the male subjects in the British Museum (fig. 11.4G) seems

to wear a thin headband in his short wavy hair. The young man at RISD (app. no. 23) has a golden wreath over his frizzy curls. As in other respects, the Würzburg portrait (fig. 11.2) stands apart in the hairstyle it shows, as the man is coiffed with curly dark brown hair combed in bangs, with a receding hairline over the temples and thinning to the sides. These simple hairstyles do not provide any firm chronological clues.

All of the male portraits additionally show various types of facial hair, adding distinct features to the faces. The men are shown with short and thin—or long and full—dark or graying brown, black, or brown-black, occasionally neatly groomed beards; and slanting, drooping (or handlebar), occasionally trimmed moustaches. The portrait once at Puhze (app. no. 25) has full side-whiskers. The young man at RISD (app. no. 23, RISD portrait not illustrated) has a beard but no moustache.

The only piece of jewelry worn by a man is the round brooch with pearls that fastens the mantle in the Würzburg portrait. As mentioned above, the young man at RISD (app. no. 23) wears a golden wreath with diamond-shaped leaves. His head is also crowned with a large wreath, perhaps of rose petals. The balding man in the Freud Museum (fig. 11.4F) seems to wear a kind of wreath, too.

Nearly all of the women have the very same looped ear pendants, each with three white pearls on a small vertical bar. They are mostly drawn in the same style, with ochre indicating the gold of the loops, and dark lines indicating shadow and outlining the contours. The elderly woman in the British Museum (fig. 11.3G) wears a faded terracotta-colored headband in her gray hair. Three portraits show women wearing another piece of jewelry, namely an intricately torqued golden necklace with a central medallion—perhaps decorated with a Medusa's head (app. nos. 5, 6, 11; fig. 11.3D). It is important to draw attention to the general absence of rich jewelry, as well as of fashionable coiffures; even the clothes are rather plain—often no more than a simple striped tunic. The portrayed individuals must have been among the wealthier citizens of Philadelphia for their family to afford the expense of commissioning a portrait for the deceased's mummified remains. Apart from examples such as the Würzburg portrait and the painting once offered at Christie's (app. no. 11), most individuals appear rather "middle class" instead of exhibiting the affluence of their elite status.

With the exception of the Würzburg portrait and the Yale portrait fragment (figs. 11.2 and 11.3h), the catalogued portraits depict nearly identical dress: a basic draped tunic with one or two stripes, often with dots representing

seams along one or both shoulders (sometimes only on the stripes, sometimes over the mantle, where seams would not be expected), and an accentuated, hemmed neckline, occasionally with threads in one or both corners of the neckline. About a dozen wear a mantle draped over their left shoulder. It bears emphasizing that the way in which the neck and neckline are outlined on all the portraits exhibits very little variation: on either side of the vertical outline of the neck, two diagonal lines widen toward the neckline of the tunic, which is drawn in a curve, two straight oblique lines, or a kind of downward-pointing accolade. The pleats of the tunic are generally drawn in oblique lines that follow a wide V-shape. Only a few cases have curved folds, and a single example has squiggly pleats.

Five of the portrayed women wear clothes in some shade of red, ranging from rose-taupe (light purple) and sienna (dark, moderate reddish-brown) to pale terracotta (faded orange-brown). The color is probably meant to represent the common red lake dye, madder, rather than the costly Tyrian purple dye. In all five cases the stripes on the tunics are black. All other subjects, irrespective of gender, wear clothes in shades of beige and white. The stripes on the clothes show more variation: from pale to dark, mostly desaturated, grayish or brownish shades between purple and orange. Only the Würzburg portrait (fig. 11.2) deviates from this basic costume, as the subject is here dressed in a draped white tunic with a broad black hem at the neckline and wears a fringed and draped ochre cloak, which is fastened on his right shoulder with a brooch.

WORKSHOP, MASTER, AND APPRENTICES

The possibility presents itself that the portraits themselves were painted in different stages. For instance, the stylistic differences between the often rather schematic outlines (drawn in broad, dark strokes) and the expressionistic details (painted in thinner, vivid brushstrokes) may well indicate not only two different stages of production but two different *hands*—an apprentice's and the master's, respectively. That might lead to the conclusion that the more schematic outlining that distinguishes most, if not all, of these portraits might belong to a workshop, a wider artistic circle, or even a school of portrait-painting, while the expressionistic portrait features that characterize many, though not all, could be the work of the same artist.

While there is little to no evidence to reveal where or how Romano-Egyptian portraits were created, one tantalizing clue is famously provided by a sketch drawn on the back of

a portrait from Tebtynis, now in the Phoebe A. Hearst Museum of Anthropology, University of California, Berkeley (fig. 11.11).²⁸ For on the back of the panel are written instructions in Greek, such as *σιτόχρωμος* (lit., “wheat-colored” [of the hair?], perhaps “fair-colored” [of the skin]); and *ἡδυτέρου[ς] ὀφθαλμούς* (lit., “more pleasant eyes,” probably “[paint] the eyes softer”).²⁹ Perhaps these notes should be understood as instructions from the master to a pupil or apprentice.



Figure 11.11 Portrait with a preparatory sketch and written instructions, Tebtynis (Roman tomb, cemetery VII or VIII), Fayum, Egypt, mid-second century CE. Fig wood panel, 36 x 24 x 1.4 cm (14 3/16 x 9 7/16 x 11/20 in.). University of California, Berkeley, Phoebe A. Hearst Museum of Anthropology, 6-21378a, verso. Photo: © Phoebe A. Hearst Museum of Anthropology and the Regents of the University of California

If we accept the hypothesis that the portraits attributed to the same artistic circle were produced in two stages and perhaps reveal the hands of more than one individual—a master and apprentice(s)—a further suggestion presents itself, namely that the outlines without individualizing portrait features were drawn in a kind of assembly-line process. This might imply that the workshop had a great variety of generic panels at the ready when the customer arrived to commission a portrait of their deceased family member. This would explain how nearly all twenty-five examples show nearly identical clothes, which are either white with reddish stripes or reddish with black stripes. A little under half wear a mantle (not always properly understood). The only significant exception in this respect is the Würzburg portrait (fig. 11.2), on which the bearded man wears a fringed ochre cloak, fastened with a brooch,

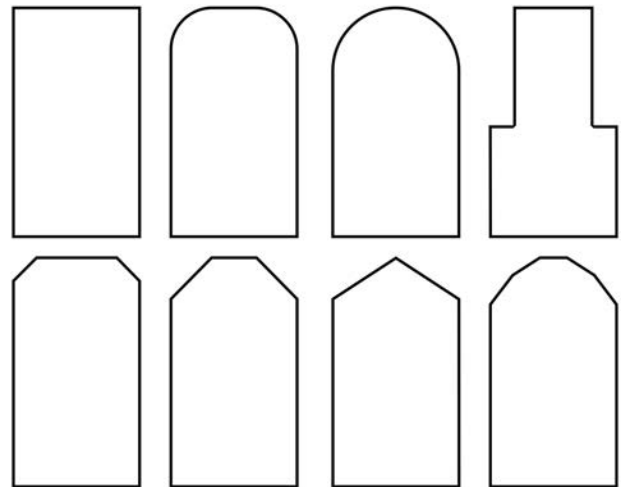


Figure 11.12 Basic types of panel shapes. Line drawings by Branko van Oppen

over a white tunic with a black-hemmed neckline. Perhaps, then, this portrait was entirely or largely painted by the master—and/or was a more expensive option at the workshop. Additionally, the color of the dress (beige-white or red lake) was apparently not—or at least not only—determined by the gender of the deceased and may have therefore been decided on the basis of considerations such as availability or expense.

MATERIALS, SHAPES, AND SIZES

The wood on which the Romano-Egyptian funerary portrait panels were painted is mostly hardwood, such as linden (lime tree). Some 75 percent of the sampled panels are proven to be a species of *Tilia*.³⁰ To the best of my knowledge, fewer than half of the panels discussed here have been examined for their wood type. The specimen in Saint Louis was made of willow (*Salix* sp.).³¹ At least four were made of fig wood (*Ficus sycomorus*), three are oak (*Quercus* sp.), another two are made of tamarisk (*Tamarix* sp.), and none of the 25 panels have thus far proven to be of linden. That is to say that if the attributed paintings are all accepted to derive from the same workshop, the artist(s) used different kinds of wood for the portraits' panels—and therefore the type of wood cannot be taken as an indication of workshop or provenience. Most of the panels measure between 27 and 37 cm in height and 15 to 22 cm in width. The mature bearded man in Berlin is exceptionally tall at 41.5 cm, while the fragmentary Yale panel measures 24.5 x 9.5 cm. The panels that have been measured are less than 1 cm in thickness.

Few panels are fully rectangular in shape. The basic panel shapes of the portraits in general can be described as rounded, angled, or stepped (fig. 11.12)—all indicating the manner in which the top edges have been cut to facilitate the portraits' eventual placement within the wrappings of the mummified person. Most of the paintings catalogued here display variations of the angled type, in which the upper edges are cut at a slanting or oblique angle. Their lower edges are straight. Eight of the examples are slightly tapered to the top. Four are unevenly or irregularly shaped. The Harvard panel (fig. 11.3B) was originally rounded at the top. The LACMA panel (fig. 11.4H), conversely, is rounded at the bottom. This variation in the panel shapes would seem to indicate that a workshop did not necessarily keep to one single type, even if the majority here are of the angled-edge type.

The plain backgrounds of the paintings display little variation among light, medium, or dark bluish- or greenish-gray. The artist used a color palette consisting of shades of red and pink; only occasionally blue, green, and orange; and additionally yellow, ochre, brown, black, gray, and white.³² For white pigments, not only calcite (e.g., calcium carbonate) or gypsum (calcium sulfate) but occasionally alum or lead white are attested. Black was mostly derived from charcoal (carbon), but also from bone char. Red could be sourced from madder or minium as well as realgar. Iron oxides such as ochre provided yellow, red, and brown pigments. Egyptian blue (calcium copper silicate) was not identified through imaging or analysis during material examinations of these portraits. Insufficient analyses have been performed to confirm if the tempera binder in the relevant examples is animal- or plant-based. The information currently provided about Romano-Egyptian painting technique—as being (hot or cold) encaustic or (wax) tempera—is confusing, misleading, and occasionally contradictory.³³

CONCLUSION

The twenty-five Romano-Egyptian portrait panels from ancient Philadelphia in the Fayum Oasis exhibit artistic characteristics that may allow their attribution to the same painter or group of painters working together. These features, foremost, include a similar expressionistic style, in addition to nearly identical portrait outlines and physiognomic proportions, as well as similar brushstrokes in just two or three different sizes, and a fairly basic palette of pigments. More individualizing portrait aspects are found in hairstyles and, in the case of the male portraits, facial hair. While the clothes are generally similar, attributes such as jewelry (in some cases) add variety to

the paintings too. In terms of panel shapes, wood types, and pigments, the group of paintings exhibit more variety than they provide indicators for attributing the portraits to the same artist or workshop.

Finally, while the attribution to either the Saint Louis Painter or the Würzburg Painter has become convention in specialized circles, it may be more appropriate to reattribute the portraits to an ancient Philadelphia painters' workshop.³⁴ Maybe there were more painters' workshops active at the same time in the area. There were certainly different painters producing portrait panels in ancient Philadelphia over time, such as the so-called Brooklyn Painter. A look at how these different painters or workshops were related would further contribute to and expand such focused studies.

ABBREVIATIONS

BM British Museum, London, U.K.

EMC Egyptian Museum, Cairo, Egypt

FREM Freud Museum, London, U.K.

HAM Harvard Art Museums, Cambridge, MA

KHM-AS Kunsthistorisches Museum Wien, Antikensammlung (Art Historical Museum, Ancient Collection), Vienna, Austria

LACMA Los Angeles County Museum of Art, Los Angeles, CA

MANN Museo Archeologico Nazionale di Napoli (National Archaeological Museum of Naples), Naples, Italy

MvWM Martin van Wagner Museum, Würzburg, Germany

PHMA Phoebe A. Hearst Museum of Anthropology, Berkeley, CA

PMFA Pushkin State Museum of Fine Arts, Moscow, Russia

REM Rosicrucian Egyptian Museum, San Jose, CA

RISD Rhode Island School of Design, Providence, RI

RMO Rijksmuseum van Oudheden (National Museum of Antiquities), Leiden, the Netherlands

SCMA Smith College Museum of Art, Northampton, MA

SLAM Saint Louis Art Museum, St. Louis, MS

SMB-AS Staatliche Museen zu Berlin, Antikensammlung
(State Museums at Berlin, Ancient Collection), Berlin,
Germany

SMME Medelhavsmuseet (The Museum of Mediterranean
and Near Eastern Antiquities), Stockholm, Sweden

SNM Ant. Nationalmuseum, Stockholm, Antikviteter
(Swedish National Museum, Antiquities), Stockholm,
Sweden

UZH-AS Universität Zürich, Antikensammlung (University
of Zurich, Ancient Collection), Zürich, Switzerland

WAMA Wadsworth Atheneum Museum of Art, Hartford, CT

YUAG Yale University Art Gallery, New Haven, CT

APPENDIX

No. 1

Saint Louis Portrait (fig. 11.1)
Title: Elderly Woman with Graying Hair
Institution: SLAM 128:51
Collection: Graf (II)
Provenience: Rubayat
Parlasca 1969–2003, III: no. 520
Dimensions: 25.7 x 14.9 x 0.8 cm (10 1/8 x 5 7/8 x 5/16 in.)
Wood: willow
Pigments: carbon, gypsum, iron oxides, lead white,
madder
Binder: “tempera”
Age: 60+

No. 2

Pushkin Portrait (fig. 11.3a)
Title: Elderly Lady in Red
Institution: PMFA I.1a 5783
Collection: Golenishchev, no. 4291
Provenience: Rubayat (?)
Parlasca 1969–2003, III: no. 519
Dimensions: 33.2 x 17.2 x 0.7 cm (13 1/16 x 6 3/4 x 1/4 in.)
Wood: fig
Pigments: carbon, gypsum, ochre
Binder: “tempera”
Age: 60+

No. 3

Harvard Portrait (fig. 11.3b)
Title: Woman with Black Hair
Institution: HAM 1939.111
Collection: Graf (II)

Provenience: Rubayat
Parlasca 1969–2003, III: no. 516
Dimensions: 32 x 19 x 0.5 cm (12 5/8 x 7 1/2 x 3/16 in.)
Wood: fig
Pigments: bone char, carbon, gypsum [bassanite and
anhydrite], red and yellow ochres, minium, madder, alum
Binder: animal glue
Age: 30–45

No. 4

San Jose Portrait (fig. 11.3c)
Title: Lady in White Tunic
Institution: REM RC-1759
Collection: Graf (II)
Provenience: Rubayat
Parlasca 1969–2003: n/a
Dimensions: 37 x 20.5 x 0.9 cm (14 9/16 x 8 1/16 x 3/8 in.)
Wood: n/a
Pigments: n/a
Binder: “tempera”
Age: 30–45

No. 5

Smith College Portrait (fig. 11.3d)
Title: Woman in Blue Tunic with Necklace
Institution: Smith College MA SC 1932.9.1
Collection: Graf (II)
Provenience: Rubayat
Parlasca 1969–2003, III: 556
Dimensions: 33 x 20.3 cm (13 x 8 in.)
Wood: n/a
Pigments: n/a
Binder: “tempera”
Age: 30–45

No. 6

Hearst Portrait
Title: Woman in Red Tunic with Necklace
Institution: PHMA 5-2327
Collection: Graf (II), no. 46
Provenience: “Kerke”
Parlasca 1969–2003, II: no. 494
Dimensions: 34.5 x 19 x 0.3 cm (13 9/16 x 7 1/2 x 1/8 in.)
Wood: fig
Pigments: gypsum, iron oxides (NB: no black?)
Binder: “tempera”
Age: 30–45

No. 7

Cairo Portrait
Title: Young Woman in Crimson

Institution: EMC CG 33.248
Collection: n/a
Provenience: Rubayat
Parlasca 1969–2003, III: no. 515
Dimensions: 35 x 19.5 cm (13 3/4 x 7 11/16 in.)
Wood: n/a
Pigments: n/a
Binder: “tempera”
Age: 15–30

No. 8

Yale Portrait (fig. 11.3h)
Title: Elderly Woman with Gray Hair
Institution: YUAG 2011.102.1
Collection: Pitt-Rivers via Chester (from Graf?)
Provenience: Rubayat?
Parlasca 1969–2003, IV: no. 856
Dimensions: 24.5 x 9.5 x 0.48 cm (9 5/8 x 3 3/4 x 3/16 in.)
Wood: oak
Pigments: n/a
Binder: “tempera”
Age: 60+

No. 9

Zürich Portrait (fig. 11.3e)
Title: Elderly Woman with Graying Hair
Institution: UZH-AS 3801
Collection: Graf (II)
Provenience: Rubayat
Parlasca 1969–2003, III: no. 518
Dimensions: 31 x 17 cm (12 3/16 x 6 11/16 in.)
Wood: n/a
Pigments: n/a
Binder: “tempera”
Age: 60+

No. 10

Stockholm Female Portrait (fig. 11.3f)
Title: Elderly Woman with Gray Hair
Institution: SNM Ant. 2303
Collection: Graf (II)
Provenience: Rubayat
Parlasca 1969–2003, III: no. 525
Dimensions: 32.5 x 19.5 cm (12 13/16 x 7 11/16 in.)
Wood: n/a
Pigments: n/a
Binder: “tempera”
Age: 60+

No. 11

Christie’s Portrait
Title: Middle-Aged Woman with Graying Hair
Institution: Christie’s, 9 December 2005, lot 85
[present whereabouts unknown]
Collection: Graf (II)
Provenience: Rubayat
Parlasca 1969–2003, III: no. 521
Dimensions: 35.2 x 18 x 0.3 cm (13 7/8 x 7 1/16 x 1/8 in.)
Wood: n/a
Pigments: n/a
Binder: “tempera”
Age: 45–60

No. 12

British Museum Portrait (fig. 11.3g)
Title: Elderly Woman with Grey Hair
Institution: BM 1890,0921.1
Collection: Chester (via Graf?)
Provenience: Faiyum District (?)
Parlasca 1969–2003, III: no. 517
Dimensions: 31.2 x 18.5 x 0.6 cm (12 1/4 x 7 1/4 x 1/4 in.)
Wood: fig (?)
Pigments: n/a
Binder: “tempera”
Age: 60+

No. 13

Würzburg Portrait (fig. 11.2)
Title: Mature Man with Beard
Institution: MvWM H2196
Collection: Graf (I), no. 44
Provenience: Rubayat
Parlasca 1969–2003, III: no. 497
Dimensions: 32.7 x 19.9 cm (12 7/8 x 7 13/16 in.)
Wood: n/a
Pigments: n/a
Binder: “tempera”
Age: 15–30

No. 14

Leiden Portrait (fig. 11.4a)
Title: Middle-Aged Man with Beard
Institution: RMO F 1932 /3.1
Collection: Graf (II)
Provenience: Rubayat
Parlasca 1969–2003, III: no. 514
Dimensions: 35.3 x 19.8 x 0.8 cm (13 7/8 x 7 13/16 x 5/16 in.)
Wood: fig (?)
Pigments: n/a

Binder: "tempera"

Age: 45–60

No. 15

Freud Portrait (fig. 11.4b)

Title: Bearded Man in White Tunic

Institution: FREM 4947

Collection: Graf (II)

Provenience: Rubayat

Parlasca 1969–2003, III: no. 500

Dimensions: 35.6 x 19.1 cm (14 x 7 1/2 in.)

Wood: n/a

Pigments: n/a

Binder: "beeswax"

Age: 30–45

No. 16

Vienna Portrait (fig. 11.4c)

Title: Elderly Man in White Tunic

Institution: KHM-AS X-300

Collection: Graf (II)

Provenience: Rubayat

Parlasca 1969–2003, III: no. 499

Dimensions: 33.2 x 22 x 0.5 cm (13 1/16 x 8 11/16 x 3/16 in.)

Wood: fig

Pigments: gypsum, iron oxides (*NB*: no black?)

Binder: "tempera"

Age: 60+

No. 17

Stockholm Male Portrait (fig. 11.4d)

Title: Bearded Man in White Tunic

Institution: SNM Ant. 2309

Collection: Graf (II)

Provenience: Rubayat

Parlasca 1969–2003, III: no. 513

Dimensions: 34.5 x 19.5 cm (13 9/16 x 7 11/16 in.)

Wood: n/a

Pigments: n/a

Binder: "tempera"

Age: 30–45

No. 18

Berlin Portrait (fig. 11.4e)

Title: Mature Man with Beard

Institution: SMB-AS 31.161/38

Collection: Graf (I), no. 72

Provenience: Rubayat

Parlasca 1969–2003, II: no. 447

Dimensions: 41.5 x 19 cm (16 5/16 x 7 1/2 in.)

Wood: n/a

Pigments: n/a

Binder: "tempera"

Age: 15–30

No. 19

Freud Portrait (fig. 11.4f)

Title: Balding Man with Graying Beard

Institution: FREM 4946

Collection: Graf (I), no. 53

Provenience: Rubayat

Parlasca 1969–2003, II: no. 482

Dimensions: 36 x 24 cm (14 3/16 x 9 7/16 in.)

Wood: n/a

Pigments: n/a

Binder: "beeswax"

Age: 60+

No. 20

British Museum Portrait

Title: Young Man with Chin Beard

Institution: BM 1931,0711.4 (EA 63397)

Collection: Graf (II)

Provenience: Rubayat

Parlasca 1969–2003, III: no. 506

Dimensions: 30.3 x 18.3 x 0.5 cm (11 15/16 x 7 3/16 x 3/16 in.)

Wood: oak

Pigments: n/a

Binder: "tempera"

Age: 15–30

No. 21

British Museum Portrait (fig. 11.4g)

Title: Mature Man with Beard

Institution: BM 1931,0711.3 (EA 63396)

Collection: Graf (II)

Provenience: Rubayat

Parlasca 1969–2003, II: no. 453

Dimensions: 31.8 x 18.5 x 0.5 cm (12 1/2 x 7 1/4 x 3/16 in.)

Wood: oak

Pigments: n/a

Binder: "tempera"

Age: 30–45

No. 22

LACMA Portrait (fig. 11.4h)

Title: Young Man with Chin Beard

Institution: LACMA M.71.73.62

Collection: Graf (II), no. 13 (?)

Provenience: Rubayat

Parlasca 1969–2003, IV: no. 915

Dimensions: 30.5 x 15.2 x 0.6 cm (12 x 6 x 1/4 in.)
Wood: Tamarisk
Pigments: n/a
Binder: "tempera"
Age: 15–30

No. 23

RISD Portrait
Title: Young Man with Golden Wreath
Institution: RISD 39.025
Collection: Graf (II)
Provenience: Rubayat
Parlasca 1969–2003, IV: no. 921
Dimensions: 34.3 x 19.7 cm (13 1/2 x 7 3/4 in.)
Wood: Tamarisk
Pigments: n/a
Binder: "tempera"
Age: 15–30

No. 24

Vienna Young Male Portrait
Title: Young Man with Chin Beard
Institution: KHM-AS X-303
Collection: Graf (II)
Provenience: Rubayat
Parlasca 1969–2003, III: no. 612
Dimensions: 35.5 x 19.3 cm (14 x 7 5/8 in.)
Wood: fig
Pigments: calcite, iron oxides, lead white, realgar
Binder: "tempera"
Age: 15–30

No. 25

Puhze Portrait
Title: Young Man with Short Beard
Institution: Galerie Puhze, *Kunst der Antike* 22 (2008), no. 213; Sotheby's, NY sale 8560, 4 June 2009, lot 103 (unsold); remained at Puhze, n.d.; private German collection, n.d.–ca. 2022/23; present whereabouts unknown
Collection: Graf (II)
Provenience: Rubayat
Parlasca 1969–2003, III: no. 607
Dimensions: 28.5 x 17 cm (11 1/4 x 6 11/16 in.)
Wood: n/a
Pigments: n/a
Binder: "tempera"
Age: 15–30

ACKNOWLEDGMENTS

As my research on the Romano-Egyptian mummy portraits began during a fellowship at the J. Paul Getty Museum in Los Angeles (spring 2017), I foremost wish to thank Mary Louise Hart and Marie Svoboda for their wholehearted encouragement, and the latter especially for all her unwavering support, advice, and genuine friendship—and for introducing me to the many colleagues at relevant institutions that hold associated mummy portraits in their collections. Furthermore, I am very grateful to Olga Vassilieva (Pushkin State Museum of Fine Arts, Moscow) for initiating the present study by our collaboration on the Pushkin portrait of the Elderly Lady in Red. For additional discussions on related Egyptological, art historical, and provenance issues, I am greatly indebted to Robert S. Bianchi (Ancient Egyptian Museum Shibuya, Tokyo), John Pollini (University of Southern California Dornsife), Kate Smith (Harvard Art Museums), Jan M. van Daal (Utrecht University), and Judith Barr (Getty Villa, Malibu). Further thanks for inspiration, background information, and/or photographs are due to (alphabetically) Ben van den Bercken (Allard Pierson), Martin Bürge (Universität Zürich), Susanne Ebbinghaus (Harvard University), Jochen Griesbach (Universität Würzburg), Laura Maccarelli (LACMA), Susan Matheson (Yale University), Irma Passeri (Yale University), Julii Piteria (Pushkin State Museum of Fine Arts, Moscow), Bjarne Purup (Museum Sydøstdanmark), Maarten Raven (formerly at the Rijksmuseum van Oudheden), Georgina Rayner (Harvard Art Museums), Yvonne Schmuhl (Staatliches Museum für Archäologie Chemnitz), Julie Scott (Rosicrucian Egyptian Museum), Jevon Thistlewood (Ashmolean Museum), Nancy Thomas (LACMA), Bettina Vak (Kunsthistorisches Museum Wien), Susan Walker (University of Oxford), Lara Weiss (formerly Rijksmuseum van Oudheden), Eman H. Zidan (formerly Ministry of Tourism and Antiquities, Cairo), as well as the speakers and attendees of both the Getty APPEAR symposia, held at the Getty Villa, Malibu, in 2018 and at the Allard Pierson, Amsterdam, in 2022.

NOTES

1. SLAM 128:1951; Thompson 1976B, 16; Thompson 1982, 20–22, figs. 35–37.
2. Thompson 1982, 22.
3. Twenty-two of the twenty-five portraits under discussion derive from the Graf collection and were unearthed "near er-Rubayat." For ancient Philadelphia in the Fayum Oasis as the site conventionally identified as er-Rubayat (variously spelled), see Walker and Bierbrier 1997, 69–87; Gehad et al. 2022, 245–64.

4. Thompson 1982, 21, fig. 37.
5. MvWM H 2196; Parlasca 1969–2003, III: no. 497, and VI: no. 856.
6. Parlasca 1969–2003, III: p. 23 (no. 497).
7. Drerup 1933, 62–63, pls. 16–17, nos. 26–28.
8. Cf. Edgar 1905, xiv (making the same point but not explored systematically).
9. Ebers 1893.
10. Drerup 1933, 63 (“der Meister [muß] seine Bilder hauptsächlich in frühconstantinischer Zeit gemalt haben”).
11. Drerup 1933, 62 (“die drei Porträts . . . wurden augenscheinlich von derselbe Hand gemalt, der mindestens noch 10 weitere Porträts zuzuweisen sind”).
12. SMB-AS 31.329; Borg 1996, 83 (“spätantoinisch-frühseverisch”), 84 (“letzte Jahrzehnt des 2. und das erste Jahrzehnt des 3. Jhs.”); cf. Parlasca 1969–2003, II: no. 390; Borg 1996, 84, further associates this work to a male portrait formerly in a Swedish private collection (Parlasca 1969–2003, no. 498).
13. Borg 1996, 51–61 (“mittel- bis spätantoinisch”); cf. Parlasca 1969–2003, nos. 519–520.
14. Borg 1996, 108, note 47.
15. Other examples not included in this study may perhaps be attributed to the same workshop, e.g., SMME 1977:005 (Parlasca 1977, II: no. 493) and WAMA 1971.52.119 (Parlasca 1969–2003, III: no. 656), though more likely are attributable to the so-called Brooklyn Painter’s workshop, also from ancient Philadelphia.
16. In this study I refrain from the conventional term *mummy portrait* to avoid objectifying the painted subjects and to show some consideration to their wish to be eternally associated with their embalmed physical remains and thus receive immortality in the hereafter.
17. Thompson 1982, 22.
18. Parkin 1992; cf. B. W. Frier in *BMCR* 1992/03.05.13 (for a critique of skepticism about the evidence’s credibility); Bagnall and Frier 1994, 75–110; Parkin in *BMCR* 1995/03.20 (for doubts about the accuracy of male life-expectancy statistics). For the representation of age and gender in Romano-Egyptian portraiture, see Purup 2019.
19. For Classical beauty ideals, see Dean-Jones 1991; Konstan 2014; Jenkins 2015; King 2016.
20. An example in Cairo (not illustrated here) similarly portrays a young woman: EMC CG 33.248 (Parlasca 1969–2003, III: no. 515).
21. Thompson 1982, 22.
22. *Supra* note 18.
23. Thistlewood 2017; Thistlewood et al. 2020; Thistlewood in this volume.
24. For the Egyptian Canon of Proportions, see especially Iversen 1955; Kielland 1955; Hanke 1961; Davis 1989; Robins 1993.
25. For the apprentice’s board from Dra Abu El-Naga, see Galán 2007.
26. MANN 9058; Gschwantler 2000, 19, fig. 5; Roberts 2013, 117, fig. 112; Jones 2019, 75, fig. 2.14.
27. Parlasca 1969–2003, nos. 521 and 525.
28. PHMA 6-21378a verso; Parlasca 1969–2003, II: 76–77, no. 432; Thompson 1976B, 12, fig. 29; Walker and Bierbrier 1997, 122–23.
29. Fournet 2004, 97–99.
30. Cartwright 1997A; Cartwright and Middleton 2008; Cartwright 2015; Cartwright 2020; Cartwright in this volume.
31. Smith et al. in this volume.
32. Pigments attested on the portrait panels under discussion are sourced from Vassilieva et al. 2021; results presented at the Harvard Art Museums’ exhibition *Facing Forward* (available online at <https://harvardartmuseums.org/exhibitions/6194/funerary-portraits-from-roman-egypt-facing-forward>); and the J. Paul Getty Museum’s APPEAR project (<https://www.getty.edu/projects/appear-project/>). For ancient painters’ pigments in general, see e.g. BM 1888,0920.23–28; Pliny the Elder 77–79 CE, 35.29–49; Petrie 1889, 11, 17; Doxiadis 1995, 98–99; Lee and Quirke 2000, 104–5; Vogelsang-Eastwood 2000, 278–79; Cartwright and Middleton 2008, 63–64, table 5; Miliani et al. 2010, 706–8; Delaney et al. 2017, 7–8; Salvant et al. 2018, 824–26.
33. Tempera is sometimes still taken to imply egg yolk as a binding medium, but yolk has not been identified in scientific analyses performed on ancient paintings.
34. A suggestion made by Egyptologist Olaf Kaper (Leiden University) at the Getty’s APPEAR conference at the Allard Pierson in 2022.

Exploring Artistic Practice in Roman Egypt: A Study of Nine Portraits at The Metropolitan Museum of Art

*Dorothy Mahon
Silvia A. Centeno
Marsha Hill
Charlotte Hale
Louisa Smieska
Clara Granzotto
Julie Arslanoglu
Anna Serotta*

The present study is focused on nine portraits at The Metropolitan Museum of Art (The Met) that are assigned dates from the mid-first through the second century CE (figs. 12.1A–I and 12.2).¹ The primary approach of this study was to consider the portraits as the production of uniquely individual artists who, in their work, exploited sophisticated techniques and materials developed in the ancient world. While there continues to be much to discover about the pigments, binding media, and other materials used, it is the way in which the artists manipulated their materials that is the focus of this paper.

The approximately 1,000 Romano-Egyptian panel portraits that exist in public and private collections display a variety of artistic productions, ranging from highly modeled and realistic to flat, mask-like, and less personalized depictions.² The portraits in The Met’s collection are all superb examples, produced by skilled artists who were able to model the subjects’ distinctive features and thus

capture the personalities of their subjects, resulting in lifelike depictions of unique individuals. All nine portraits are painted on thin wooden supports, identified as *Tilia* sp., commonly known as linden or lime, which vary in thickness from 1 to 3 mm.³ The painting technique used is characteristic of the encaustic medium, consisting of pigment mixed in beeswax, which results in a highly textured surface. Because the portraits lack an archaeological provenience, the tentative dates assigned to the portraits listed in figure 12.2 are solely based on details of costume, hairstyle, and jewelry.⁴ Stylistic similarities have been used to group the portraits with others from the Fayum and other sites along the Nile, including Antinoöpolis and Akhmim.⁵ A fully intact mummy with an inserted panel portrait of a youth was not included in this study due to its fragility (fig. 12.3). Excavated by W. M. Flinders Petrie at Hawara, Egypt, between 1910 and



Figure 12.1 Roman Egyptian portraits examined and analyzed. (A) Portrait of a thin-faced, bearded man; (B) Portrait of a man with a mole on his nose; (C) Portrait of a thin-faced man; (D) Portrait of a youth with a surgical cut in one eye; (E) Portrait of an elderly lady with a gold wreath; (F) Portrait of a young woman in red; (G) Portrait of a young woman with a gilded wreath; (H) Portrait of the Boy Eutyches; and (I) Portrait of a woman in a blue mantle. Encaustic paint on limewood. Photos: © The Metropolitan Museum of Art, Department of Egyptian Art

Title	Tentative date	Accession number	Credit line	Portrait label
Portrait of a thin-faced, bearded man	160–180 CE	09.181.1	Rogers Fund, 1909	A
Portrait of a man with a mole on his nose	130–150 CE	09.181.2	Rogers Fund, 1909	B
Portrait of a thin-faced man	140–170 CE	09.181.3	Rogers Fund, 1909	C
Portrait of a youth with a surgical cut in one eye	190–210 CE	09.181.4	Rogers Fund, 1909	D
Portrait of an elderly lady with a gold wreath	100–125 CE	09.181.5	Rogers Fund, 1909	E
Portrait of a young woman in red	90–120 CE	09.181.6	Rogers Fund, 1909	F
Portrait of a young woman with a gilded wreath	120–140 CE	09.181.7	Rogers Fund, 1909	G

1911, it is mentioned here as an example of the original context of the portraits that will be discussed.⁶

Title	Tentative date	Accession number	Credit line	Portrait label
Portrait of the Boy Eutyches	100–150 CE	18.9.2	Gift of Edward S. Harkness, 1918	H
Portrait of a woman in a blue mantle	54–68 CE	2013.438 deaccessioned 2022 and restituted to Egypt	Director's Fund, 2013	I

Figure 12.2 Portraits examined and analyzed for the present study. Images of the portraits are presented in figure 12.1. Photos: © The Metropolitan Museum of Art, Department of Egyptian Art

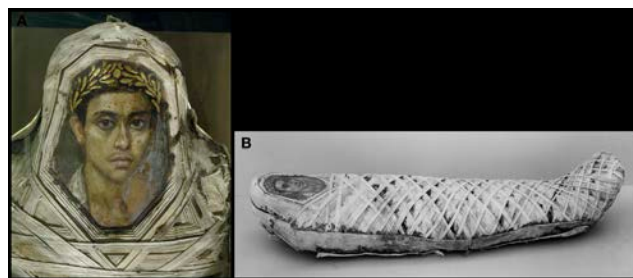


Figure 12.3 Mummy with an inserted panel portrait of a youth, encaustic paint on limewood, human remains, linen, mummification material. (A) Detail of panel portrait as exposed, 38 x 18 cm (15 x 7 1/16 in.); and (B) mummy, 169 x 45 cm (66 9/16 x 17 11/16 in.). The Metropolitan Museum of Art, Department of Egyptian Art, Rogers Fund, 1911.11.139. Photo: © The Metropolitan Museum of Art, Department of Egyptian Art

When acquired, all portraits except for Portrait I were already mounted onto laminated-wood secondary supports that extended beyond their original perimeters.⁷ Some areas of surface disruption and paint loss can be attributed to contact pressure during the initial burial, as well as ill-considered removal of mummy wrappings following excavation. Visible along the perimeter of the panel, and in some cases cutting into the paint surface, are incisions from a sharp tool used to trim and shape the portraits before attachment to the mummy bundle (fig. 12.4). All the panels show evidence of having been trimmed after painting.

Portrait I is painted on a well-preserved panel support and retains the original thickness and natural curvature resulting from attachment to the deceased (fig. 12.5).⁸ Portraits I and D differ from the others in that the paint layers originally extended to the perimeter of the wood panel. Since entering the collection, conservation treatments have been minimal.⁹ The secondary panel



Figure 12.4 Detail of Portrait of a young woman in red (Portrait F) showing that the panel was crudely trimmed with a sharp knife after painting, in preparation for attachment to the mummy bundle. The Metropolitan Museum of Art, Department of Paintings Conservation. Photo: © The Metropolitan Museum of Art, Department of Egyptian Art

supports were trimmed to the perimeter of the original supports to present the portraits closer to their historic contexts. The overall condition of each is excellent and the surfaces of only two of the portraits (Portraits H and I) show evidence of thinly applied modern coatings.



Figure 12.5 Panel painting of a woman in a blue mantle (Portrait I) is the only portrait in the study that has never been mounted. It retains the original shape and shows the exquisitely thin wooden supports used for these portraits. Photo: © Eileen Travell, The Metropolitan Museum of Art, Imaging Department.

RESULTS AND DISCUSSION

Figure 12.14 reveals that, with few exceptions, there is a striking similarity in the materials identified—such as the presence of gold leaf, copper-based pigments, and a ground preparation. The portraits differ in the way these materials were used, however, and this will be the focus of our discussion.

Visual Examination

While there are some apparent similarities in technique, none of the portraits can be identified with certainty as

having been made by the same artist. What is consistently remarkable is that all the portraits seem to have been painted rather quickly, with a sure and skillful hand. Because the encaustic medium is only workable while heated, it requires a rapid application, and the control demonstrated by these artists is particularly impressive. While passages of the encaustic were manipulated, the paint layers were never unnecessarily labored or extensively reworked. Although the nine portraits studied constitute a small number of the portraits produced at the time, they display interesting similarities as well as differences in the use of the encaustic technique.

Three of the portraits are painted directly on the unprepared wooden panel. For two of these, Portraits F and E, the artists made use of the optical brightness of the light wooden support and exploited the translucency of the wax medium to achieve delicate and bright passages in areas of the flesh where the panel is barely covered. The panel supports also served to brighten the reddish-purple garments that are painted with mixtures of largely translucent red lake pigments. A stiff brush was used to paint both portraits, judging from strokes displaying characteristic crisp furrows and tapering terminal points. Fine details, such as the eyelashes on both portraits, were painted with a small brush. Much of the surface of both portraits has a melted appearance, particularly in the flesh, where some areas have been manipulated with a heated tool. Features made with a heated tool on the surface of Portrait F include parallel marks around the nose and in the dark shadow beneath the lower lip (fig. 12.6A). The wrinkled skin texture of the elderly woman in Portrait E was created by extensive manipulation of the encaustic with a heated tool. Notable are zigzag marks along the dark contour of the head at right that extend into the hollow of the cheek (fig. 12.6B).

Although Portrait H is painted on an unprimed support like the two portraits described above, the buildup of the encaustic is different in that this artist used optically dense mixtures of paint. The use of a stiff brush to apply certain passages is evident here as well. Parallel marks indicative of manipulations with a heated tool are primarily confined to the face (fig. 12.7A). The texture of the encaustic used to construct the face reveals a change to the proper right ear, where the contour was initially larger and reduced in the final depiction. The painted inscription on the white tunic does not have the same body as the paint used for the rest of the portrait: the paint is fluid and has pooled along the edges of the lettering. Another medium seems to have been used here, perhaps chosen to more easily paint the fine details (fig. 12.7B).



Figure 12.6 Details taken in raking light illumination of (A) Portrait of a young woman in red (Portrait F) and (B) Portrait of an elderly lady with a gold wreath (Portrait E) showing the brush and tool marks in the surface of the encaustic. Photos: © The Metropolitan Museum of Art, Department of Paintings Conservation

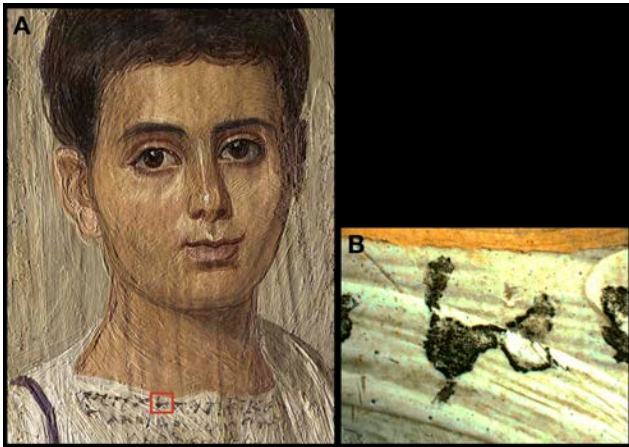


Figure 12.7 (A) Detail taken in raking light of Portrait of the Boy Eutyches (Portrait H) showing brush and tool marks in the surface of the encaustic and (B) detail of the tunic showing the reticulated edges of the inscription. The location of this detail is outlined in red in A. Photos: © The Metropolitan Museum of Art, Department of Paintings Conservation

Five of the portraits are painted on panels prepared with black grounds. Portrait G is densely painted on top of the dark preparation, resulting in a final depiction of great plasticity and a cool flesh tone. Constructed in two layers, the underpainting is done with a salmon-colored encaustic applied with crisp brushstrokes. On top of this, the final applications of encaustic have a melted appearance. Specifically, the proper left ear clearly demonstrates the layered technique. Here too, passages in the face were manipulated with a heated tool.

Portraits A, B, and C are painted on panels prepared with a black ground that is relatively thin in comparison to the black preparation in Portrait G. Although stylistic similarity

with Portraits B and A has been recognized, a later date has been suggested for the latter based on the hairstyle.¹⁰ Specific aspects of the technique and materials displayed by these two portraits, discussed below, suggest that these may have been produced in the same workshop. For Portrait C, horizontal strokes visible in an unpainted area at the bottom confirm that the black ground was applied with a stiff brush and was done using a fluid, lean medium. The face is painted with thickly applied encaustic, which was manipulated throughout with a heated tool. Applications displaying the furrows characteristic of the use of a stiff brush are present in all areas. One distinctive passage below the proper right eye shows vertical, hatched striations created by pulling through the paint with a heated stylus, which effectively softened and broadened the light pinkish strokes used to highlight the upper cheek. The highlight extending the length of the nose was done with two thin, meandering applications that twist before terminating in two separate highlights at the tip of the nose. Overall, this artist applied the paint in an animated manner, with crisscrossing strokes used to model the brow and create the final highlights (fig. 12.8).



Figure 12.8 Details of images taken under (A) ultraviolet illumination and with (B) raking light in Portrait of a thin-faced man (Portrait C) showing the distinctive application and tooling of the highlights. Photos: © The Metropolitan Museum of Art, Department of Paintings Conservation

Portrait D is painted on a panel prepared with a thick black ground and Portrait I is painted on a panel prepared with a gray ground. These two portraits differ from the other seven in that the encaustic originally extended to the perimeter of the panels. Portrait I retains the original dimensions except where the top corners have been trimmed. The perimeter of Portrait D has been trimmed except along the bottom. The encaustic used for the face, neck, costume, and background of Portrait I has a highly

textured appearance characteristic of a surface that has been manipulated throughout with a heated tool. In general, the softly rounded, swirling appearance of the surface texture suggests that the encaustic remained molten during the painting process and was possibly heated after painting. The final application of bright white paint in the tunic is riddled with small pits, possibly caused by air bubbles that erupted during or just after execution (fig. 12.9A). These are also present in the final white highlight at the tip of the nose.

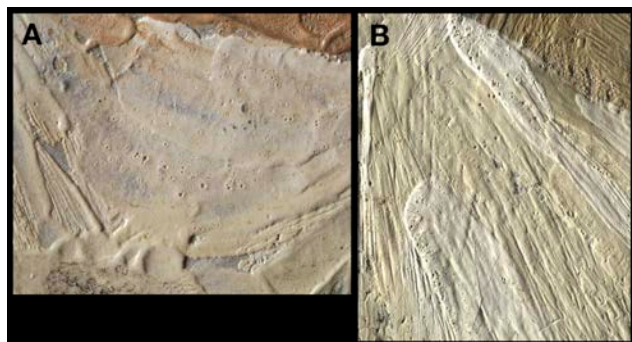


Figure 12.9 Details of (A) Panel painting of a woman in a blue mantle (Portrait I) and (B) Portrait of a youth with a surgical cut in one eye (Portrait D) showing pits in the paint, likely due to air bubbles that erupted during or just after execution. Photos: (A) © Eileen Travell, The Metropolitan Museum of Art, Imaging Department. (B) © The Metropolitan Museum of Art, Department of Paintings Conservation

The use of a brush to paint the background and figure in Portrait D is evident throughout. Furrows are visible but, in general, the surface has a fused, melted appearance. The white tunic was painted with both a brighter white and a distinctly warmer white, as well as a grayish white that was used to model the forms of the receding shoulder. There are many small pits in the surface throughout the garment, which are similar to those observed in Portrait I; these are concentrated to a greater degree in the bright white paint (fig. 12.9B). The paint depicting the flesh and facial features has been extensively manipulated with a heated tool. In the forehead and cheeks, the reworking was done using short parallel strokes. The purpose of the tool marks adjacent to the inside corner of the proper right eye is remarkable. The horizontal reddish-brown feature beneath the eye has been described as a surgical scar resulting from the treatment of an eye disease.¹¹ It could also be a wooden splint inserted into the flesh at the terminal points below the proper right eye. The point of tension where the wooden splint pulls the delicate skin at the inner corner of the eyelid is carefully indicated by the artist using a stylus to make two marks—one longer and vertical and, below, another slightly shorter and diagonal.

Infrared Reflectography

In Portraits E, F, and H, infrared reflectography (IRR) revealed a detailed underdrawing and characteristics of the medium and tools used (fig. 12.10). Due to the different spectral responses of the two cameras, IRR produced a more complete image of the underdrawing when compared to that produced using infrared photography. These three portraits are executed on panels that have no visible ground preparation, as discussed above. A clear image of the underdrawing is visible because it is executed with a carbonaceous drawing material and carbon-based black or other materials that absorb IR radiation are not present in the panel support.



Figure 12.10 Infrared reflectograms (IRR) for (A) Portrait of an elderly lady with a gold wreath (Portrait E); (B) Portrait of a young woman in red (Portrait F); and (C) Portrait of the Boy Eutyches (Portrait H). Photos: © The Metropolitan Museum of Art, Department of Paintings Conservation

Examination of the surfaces with a stereomicroscope confirmed that the drawing was done directly on the wooden panel (fig. 12.11). Additionally, the appearance of the underdrawing observed in locations where small losses are present suggests that its binding medium is not encaustic but is rather more fluid and ink-like. For Portrait E, the artist began with a bold drawing using a carbon-based black pigment, identified by *in situ* Raman spectroscopy by its characteristic broad bands at ca. 1350 and 1580 cm^{-1} ,¹² in a fluid medium applied with a brush as well as a reed pen (fig. 12.12). The characteristic markings of a reed pen with a squarely cut tip are remarkably clear, as are the more fluid tapering strokes characteristic of the use of a brush. The facial features have all been boldly drawn. Marks characteristic of the use of a brush are present throughout, particularly in the chin (fig. 12.12A). There are marks with blunt ends characteristic of the use of a reed pen throughout, especially below the proper right eye (fig. 12.12B). Additional underdrawing is present

in the neck and in the curls at right. The garment is not underdrawn. As strokes of encaustic paint containing a carbon-based black pigment also record as dark lines in IRR, it is important to distinguish painted strokes from the underdrawing through a close visual comparison of the surface with the IRR image.



Figure 12.11 Detail of Portrait of an elderly lady with a gold wreath (Portrait E). The arrows point to locations where the underdrawing of the eye, done directly on the wooden support, is visible beneath the translucent encaustic. Photo: © The Metropolitan Museum of Art, Department of Paintings Conservation



Figure 12.12 Details of infrared reflectogram for Portrait of an elderly lady with a gold wreath (Portrait E). The arrows point to (A) underdrawing on the chin done with a brush and (B) underdrawing beneath the eye done with a reed pen. Photos: © The Metropolitan Museum of Art, Department of Paintings Conservation

Observations made through examination with the stereomicroscope confirm that the lines extending across the forehead, which appear dark in the IRR (see fig. 12.10A), are not underdrawing but rather final applications of encaustic paint used to describe the wrinkling of the brow. The diagonal lines describing the muscles of the gaunt neck are also in the paint layer.

Underdrawing like that observed in Portrait E is revealed in the IRR of Portrait F, but the latter underdrawing is more fluid overall (see fig. 12.10B). The face is freely drawn with rapid strokes, using both a reed pen and a brush. The mantle is underdrawn with many sweeping brushstrokes and the collar of the tunic is drawn with the broad, bold lines of underdrawing characteristic of both a brush and a reed pen. A comparison of the underdrawings of these two portraits revealed that while both were executed with a similar carbon-based black material, they exhibit completely different characteristics and were surely made by different artists. The artist who executed the drawing for Portrait E primarily used a reed pen, and for Portrait F, most of the drawing was done with a brush and with a very fluid medium. As additional portraits from other collections are examined using IRR, it may be possible to assign groups to individual artists or workshops based on characteristics of the underdrawings.

Underdrawing is also present in Portrait H (see fig. 12.10C). In this case, it appears that the medium was fluid and applied with a finely tipped brush or pen. Noteworthy are areas of hatching in the shadows of the face: the right eye and below the cheekbone, the right of the nose, lower lip and chin, and the recess above the center of the lips. The mouth is indicated with a few short lines, including small arcs at the corners. The lines in the face are fine and appear very dark in the IRR. It is unclear whether there are lines contouring the figure, but broad lines visible in the IRR below the ear at left, and outside the contour of the face below the ear, indicate initial placements of these features. Black pigment is seen under magnification in the mid-tones and shadows in the flesh and in the drapery; these underpainted areas appear relatively dark in the reflectogram. As the paint was thickly applied, the only place underdrawing is visible when the surface is inspected under magnification is in a small gap between the flesh paint and the paint of the upper lip.

IRR did not image underdrawing in Portrait I; however, when the recesses along the contours of paint applications are examined under magnification, carbonaceous particles visible on top of the light gray ground strongly indicate the presence of one.

X-radiography

X-radiography produced bold images of the portraits, largely due to the pervasive use of the radiopaque pigment lead (Pb) white. The overall presence of lead white was inferred from the lead distribution maps obtained by macro-X-ray fluorescence spectroscopy (MA-XRF); additionally, the pigment was identified by *in situ* Raman

spectroscopy, as discussed in the following section. Because of the translucency of the wax medium, it was necessary for the artist to mix pigments with hiding power such as lead white into the colors to provide visual opacity. As these pigments are generally radiopaque, the X-radiographs reveal the overall paint handling, individual brushstrokes and tool marks, and, in some cases, the initial laying in of the ears and contours of the head and body.

The X-radiographs show that all the artists began by painting in the background color, followed by the figure, refining the contours of the head and body, and details of the hair on top. Generally, all the artists painted from light to dark, leaving darker areas such as the eyes, eyebrows, and hair in reserve, and finishing details after establishing the overall structure. In Portrait C, X-radiography shows most clearly that the gray background was painted before the figure and was brushed in with bold fluid and arching strokes, leaving the areas of the head and body in reserve (fig. 12.13A). Quickly applied sweeping strokes define the tunic and mantle. In contrast, Portraits F and D are more radiopaque overall (figs. 12.13B and C). Here too, despite the similar X-radiographic density in the flesh, each portrait clearly displays a different handling of the wax medium. The short parallel marks characteristic of the pervasive use of a heated tool present throughout Portrait D are relatively few in Portrait F. The X-radiograph of Portrait F shows that several curling strokes were used to lay in the structure of the proper left ear; these were largely concealed by dark curls of hair applied on top.

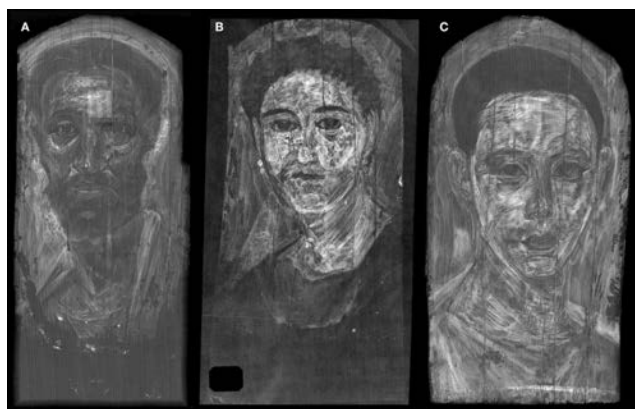


Figure 12.13 X-radiographs. (A) Portrait of a thin-faced man (Portrait C); (B) Portrait of a young woman in red (Portrait F); and (C) Portrait of a youth with a surgical cut in one eye (Portrait D). Photos: © The Metropolitan Museum of Art, Department of Paintings Conservation

Macro-X-ray Fluorescence (MA-XRF) and Raman Spectroscopy

In Raman spectra acquired in areas that have the visual appearance of an encaustic medium, bands characteristic of a wax were detected at ca. 1460, 1440, 1418, 1295, 1170, 1130, 1062, and 890 cm^{-1} , together with features due to different pigments.¹³ These results confirm the presence of the main component of the encaustic, however a chromatographic technique, and therefore the removal of samples, would be necessary to identify any possible minor components of the binding media.

MA-XRF analysis showed the presence of Pb, copper (Cu), iron (Fe), manganese (Mn), mercury (Hg), and arsenic (As) and, along with Raman spectroscopy measurements in selected paints, allowed us to identify lead white, carbon-based black/s, copper-containing blues and greens, iron ochres, most likely an umber, cinnabar, and very possibly orpiment (fig. 12.14), all pigments that have been previously reported in Romano-Egyptian portraits.¹⁴ The presence of lead white, $2\text{PbCO}_3 \cdot \text{Pb}(\text{OH})_2$, was confirmed by its characteristic Raman bands at ca. 415, 680, and 1051 cm^{-1} .¹⁵ Since Raman spectroscopy was only used to analyze selected paints in some of the portraits, and lead white and red lead (Pb_3O_4) cannot be distinguished by XRF, the presence of relatively smaller amounts of red lead in some of the portraits cannot be ruled out.¹⁶ Carbon-based blacks were identified by the very broad Raman features at ca. 1600 and 1330 cm^{-1} ; no bands at ca. 960 cm^{-1} that would indicate a bone or an ivory black were observed in the acquired spectra.¹⁷

The use of ochres was visualized in the Fe distribution maps; Raman spectroscopy analyses allowed us to identify hematite, with characteristic bands at ca. 224, 291, 411, and 611 cm^{-1} ,¹⁸ in some of the red Fe-containing paints. The artists who painted these portraits used Fe-containing pigments—ochres ranging in color from yellow to red—in very distinctive ways to model the flesh tones, hair, garments, and jewelry. The Fe distribution maps for Portraits F, D, E, and G highlight the similarities and differences of the artists' use of these pigments (figs. 12.15A–D). It is not surprising that these colors were used less liberally to paint the subject's gray hair in Portrait E in comparison to the dark hair of the more youthful subjects. Her skin tone is deeper in color and loaded with Fe, having lost its pearly tone. By contrast, the Fe-containing pigments in the flesh of the more youthful subjects is concentrated in the modeling of the contours and shadows of the head and facial features.

Ground preparations, infrared reflectograms and selected elemental distribution maps	Portrait of a thin-faced, bearded man 09.181.1	Portrait of a man with a mole on his nose 09.181.2	Portrait of a thin-faced man 09.181.3	Portrait of a youth with a surgical cut in one eye 09.181.4	Portrait of an elderly lady with a gold wreath 09.181.5	Portrait of a young woman in red 09.181.6	Portrait of a young woman with a gilded wreath 09.181.7	Portrait of the Boy Eutyches 18.9.2	Portrait of a woman in a blue mantle 2013.438 deaccessioned 2022 and restituted to Egypt
Preparatory layer	black	black	black	black	no ground	no ground	black	no ground	gray
Infrared reflectogram									
Iron map									
Lead map									
Calcium map									
Manganese map									
Copper map	-----	-----	-----						
Gold map	-----	-----		-----				-----	-----

Figure 12.14 Preparatory layers, infrared reflectograms, and selected elemental distribution maps obtained by MA-XRF in the nine portraits analyzed for the present study. Photos: © The Metropolitan Museum of Art, Department of Scientific Research

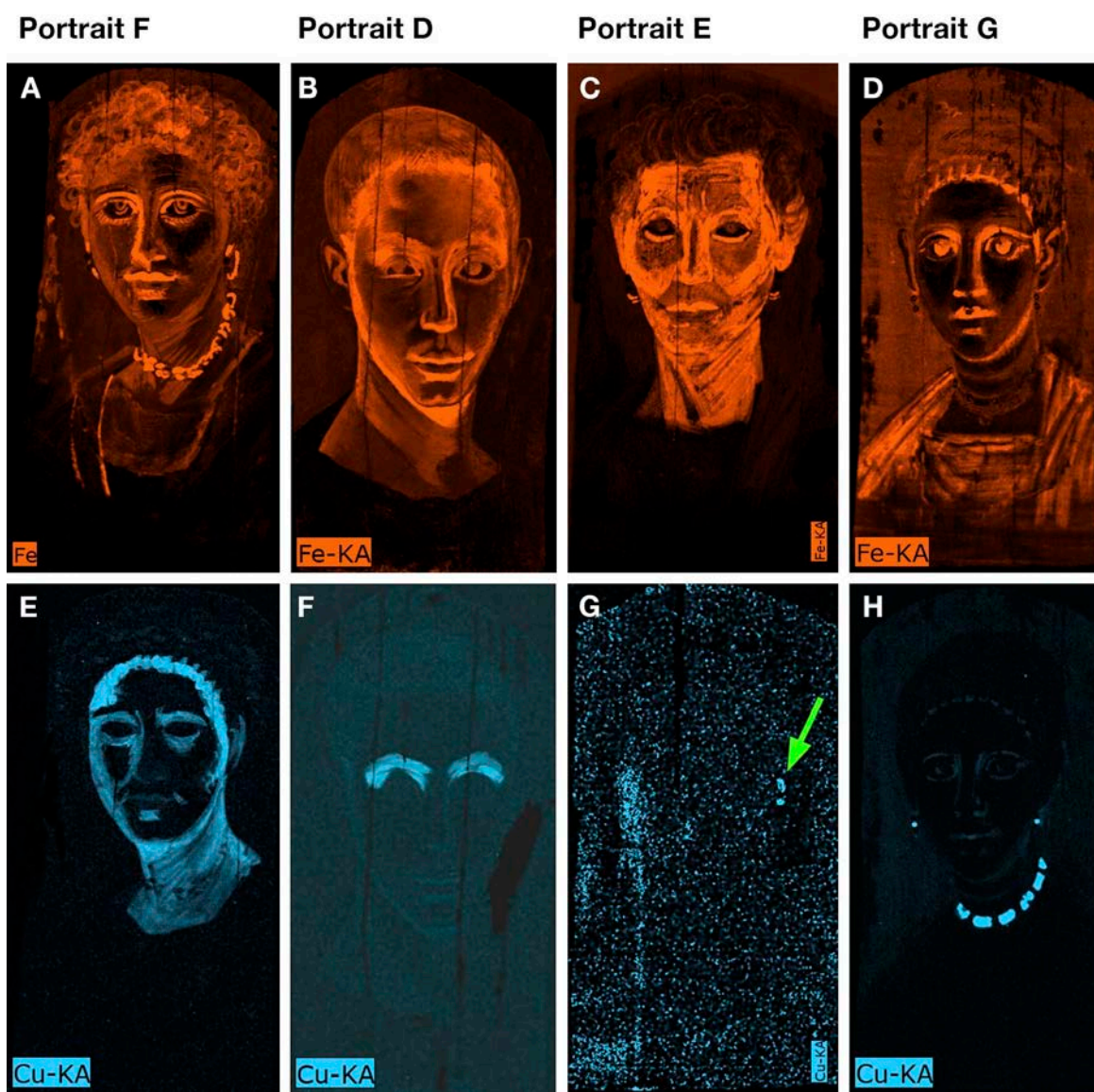


Figure 12.15 Elemental distribution maps obtained by MA-XRF: Portrait of a young woman in red (Portrait F), (A) iron (Fe) and (E) copper (Cu); Portrait of a youth with a surgical cut in one eye (Portrait D), (B) iron and (F) copper; Portrait of an elderly lady with a gold wreath (Portrait E), (C) iron and (G) copper, where the green arrow points to the copper-containing bead that is likely an emerald; and Portrait of a young woman with a gilded wreath (Portrait G), (D) iron and (H) copper. Photos: © The Metropolitan Museum of Art, Department of Scientific Research

Copper was detected by MA-XRF in the large green emeralds of the necklace and earrings in Portrait G (fig. 12.15H). The jewel located between two pearls on the earring in Portrait E has been previously described as a black bead.¹⁹ However, MA-XRF showed that a Cu-based pigment was used (fig. 12.15G) and examination under magnification confirmed that the color is greenish and achieved in two paint applications consisting of an opaque green paint layer followed by a translucent glaze, suggesting that this is an emerald. As aspects of the jewelry and hairstyle are frequently used as an aid in dating the portraits, confirming these details is critical.

Raman spectroscopy paint analysis of the green stones decorating the jewelry in Portrait G gave broad features in the $1200\text{--}1500\text{ cm}^{-1}$ range that did not allow the pigment(s) to be identified. In this case, the visual appearance is consistent with that of a verdigris, Cu resinate, or Cu oleate. Identifying these types of pigments by Raman spectroscopy in naturally aged paints is particularly difficult even if good spectra have been reported for numerous variants of these colorants in samples prepared in the laboratory.²⁰

MA-XRF mapping also revealed hidden features that contribute to the understanding of the portraits. For



Figure 12.16 Portrait of a young woman with a gilded wreath (Portrait G), elemental distribution maps obtained by MA-XRF: (A) iron (Fe), (B) lead (Pb), and (C) gold (Au). Photos: © The Metropolitan Museum of Art, Department of Scientific Research

Portrait G, the Fe and Pb distribution maps showed a crescent moon hairpin ornament, as well as details of the sitter's hairstyle, concealed by the gold (Au) leaf (figs. 12.16A–C). An important feature made more clearly visible by MA-XRF mapping is the amulet in the sitter's necklace in Portrait I (fig. 12.17). Painted mainly with an ochre pigment revealed in the Fe distribution map (figs. 12.17A and C), it can now be identified with certainty as Omphale holding the club of Herakles (fig. 12.17E).²¹ Questions have been raised as to whether the necklace was added to this portrait at a later date. That it is surely original has been confirmed by the Fe and Cu distribution maps and examination of the surface under magnification. The necklace was painted first, followed by the blue mantle, the latter painted with a Cu-containing pigment (figs. 12.17B and D). MA-XRF detected As in this necklace where the artist used a bright yellow As-containing pigment, very possibly orpiment, to enhance the highlight. This is the only instance in which As was identified in the present study. In addition, Portrait I is the only one in this study in which MA-XRF detected Hg. Here, the artist applied a tiny dab of cinnabar to redden the caruncle membrane at the inner corner of both eyes.

Another interesting use of Cu-containing pigments is in the flesh tones. In Portraits F and G, the dark undermodeling of the shadows and recesses around the facial features and along the hairline is revealed in the Cu distribution maps (see figs. 12.15E and H). The artists exploited the translucency of the wax medium by skillfully layering applications of a lighter, more delicate, rosy flesh color on top to achieve a superbly modeled, final depiction. In Portrait D, the Cu-containing pigment Egyptian blue,²² which was indicated by visible-induced luminescence (VIL) imaging, is dramatically captured in the Cu distribution

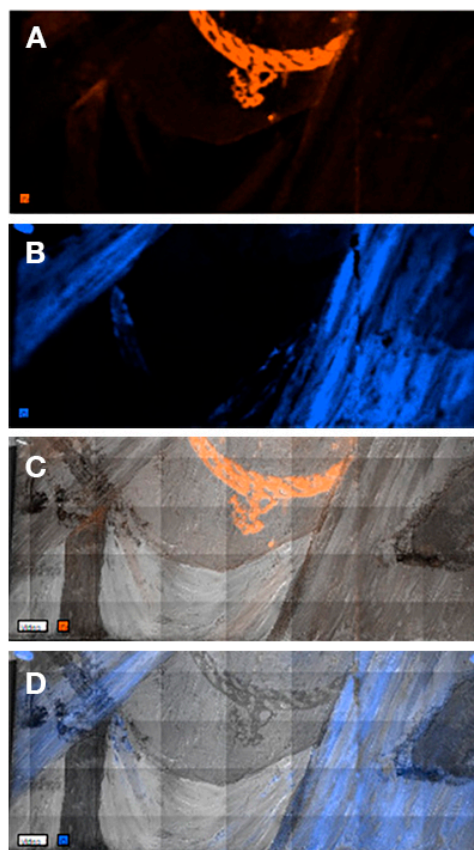


Figure 12.17 Portrait of a woman in a blue mantle (Portrait I). Details of the (A) iron (Fe) and (B) copper (Cu) distribution maps in the amulet area; (C) and (D) show the same maps as (A) and (B), respectively, superimposed to the black and white image of the area. Photos: © The Metropolitan Museum of Art, Department of Scientific Research



Figure 12.17E Amulet of Omphale. Photo: © Derek J. Content Collection, 2022.

map (fig. 12.15F). The pigment is concentrated in the upper eye socket and mixed with an Fe-containing

pigment (fig. 12.15B), apparently to achieve a sallow color suggesting ill health. Cu was also identified in the contours of the face, facial features, and neck as indicated in the MA-XRF map.

The distribution of Au leaf in the wreaths and the backgrounds of four portraits, Portraits C, E, F, and G, was visualized by MA-XRF (see fig. 12.14). Au was not identified in the other portraits. MA-XRF mapping also revealed the size and configuration of the pieces of Au leaf applied to the backgrounds. This is shown for Portrait G in figure 12.16C.

MA-XRF revealed the presence and distribution of nickel (Ni) in three of the portraits, Portraits E, G, and H (figs. 12.18A, C, and D). The Ni-containing material appears to have been deposited in a fluid form when the panels were in the upright position and extended in rivulets that pooled at the bottom. Where exposed, these areas appear grayish brown when viewed with the naked eye, and examination under magnification confirmed that the deposits are on the wooden supports beneath the paint layers and that there is a whitish material on top. In Portrait E, there is Cu in the Ni-containing areas (fig. 12.18B), but no Cu was observed in the Ni-containing areas for the other two portraits. In Portrait H, vanadium (V) was detected by MA-XRF in a distribution that does not coincide with that of Ni (fig. 12.18E). Raman analysis in the Ni-containing areas showed the presence of gypsum in the whitish material, but no other compounds were detected by this technique. These results cannot be fully explained to date. V and Ni, present in porphyrin-like complexes, are the most abundant trace metals found in almost all bitumens; the concentration and relative abundance of these elements, along with those of minor components, depend on the source of the material.²³ Bitumen could have been available to Egyptians from a number of sources,²⁴ and analysis of residues associated with mummies dating from the Greco-Roman period have identified bitumen in treatment both of the body and of the wrappings.²⁵ It has been reported that bitumen in mummies occurs with other ingredients, such as conifer resins, grease, and beeswax, and the balms show a great variety of molecular compositions.²⁶ When smeared on the exterior of mummy wrappings, bitumen may have been used as an external mechanical shield to prevent ingress by insects, fungi, bacteria, and moisture; it may also have been added as a biocidal agent to prevent the flesh from decaying.²⁷ Even though the elemental analyses in the three portraits suggest the possible presence of bitumen, to firmly identify this material GC-MS analyses are necessary.²⁸

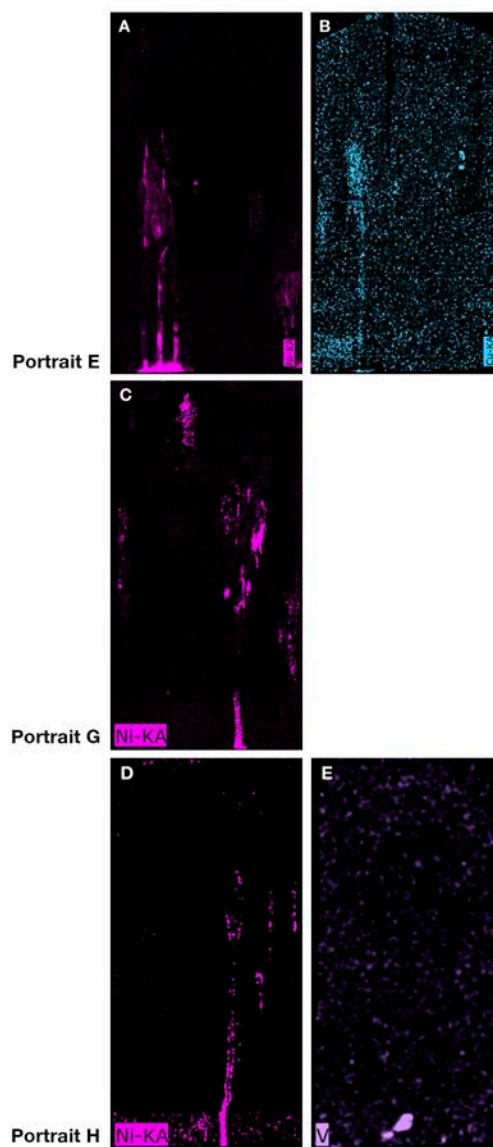


Figure 12.18 Elemental distribution maps obtained by MA-XRF: Portrait of an elderly lady with a gold wreath (Portrait E), (A) nickel (Ni) and (B) copper (Cu); Portrait of a young woman with a gilded wreath (Portrait G), (C) nickel (Ni); Portrait of the Boy Eutyches (Portrait H), (D) nickel (Ni) and (E) vanadium (V). Photos: © The Metropolitan Museum of Art, Department of Scientific Research

Visible-Induced Luminescence

VIL imaging showed the use of the pigment Egyptian blue in five portraits, Portraits C, G, D, H, and I. Egyptian blue is the earliest known synthetic pigment,²⁹ composed of an analog to the natural mineral cuprorivaite ($\text{CaCuSi}_4\text{O}_{10}$) with variable amounts of wollastonite (CaSiO_3), quartz, other phases of silicon dioxide, cuprite (Cu_2O), and tenorite (CuO).³⁰ It can vary from bright blue to nearly colorless depending on its composition, process of manufacture, and grain size.³¹

While VIL indicated Egyptian blue in Portrait C's gray background, analysis by MA-XRF showed only traces of Cu in the area in question. Furthermore, no blue particles were observed when this area was examined under magnification. Because Egyptian blue displays very high luminescence,³² VIL imaging can record relatively low amounts of this pigment. Additionally, blue particles were not observed in Portrait G's flesh under magnification, although MA-XRF analysis revealed the presence of relatively small amounts of Cu in these areas (see fig. 12.15H). This suggests that a grade of a very pale or virtually colorless form of this glassy pigment was used in both cases to increase translucency and to add bulk to the encaustic rather than for hue. Ganio et al. 2015 reported the presence of Egyptian blue with no visible blue color in panel portraits from Tebtunis and proposed that the pigment, in these cases, may have been used to impart brightness.³³ In Portrait D, VIL showed Egyptian blue primarily concentrated in the upper eye sockets. Few pale blue particles were observed when the areas were examined under magnification, but present are abundant, distinctly opaque red particles. As mentioned above, MA-XRF confirmed the presence of an Fe-containing pigment, most likely an ochre, and of Cu in these areas (figs. 12.15B and F). A pale Egyptian blue seems to have been used largely to increase translucency and to add bulk to the paint here as well. In this portrait, the paint mixture containing Egyptian blue and Fe-containing pigment(s), along with black and white pigments, was surely used to achieve dimension; the brownish tone intended to enhance a swollen appearance, emphasizing the subject's eye condition. When the surface of Portrait H was examined, large, bright blue particles of Egyptian blue mixed with a red lake to achieve the purple color of the clavus were observed. Similar large Egyptian blue particles were also used strategically to model the neck; MA-XRF confirmed the presence of Cu in these areas of Portrait H. For Portrait I, VIL showed the presence of Egyptian blue throughout the sitter's flesh, to color her beautiful blue mantle and to brighten her white tunic, and in the sclera of her eyes. Glassy, bright Egyptian blue particles were visible when the surface was examined with magnification and MA-XRF mapping detected Cu in these areas (figs. 12.17B and D).

OTHER MATERIALS AND ASPECTS OF THE PAINTING TECHNIQUE

The close relationship between Portraits B and A has long been recognized. Based on hairstyle, these portraits have been dated about a generation apart, 130–150 CE for the

former and 160–180 CE for the latter.³⁴ As mentioned above, both panels are prepared with a very thin black ground; a similarity in the handling of the paint medium is evident when the portraits are examined in raking light (figs. 12.19A and D). Under high magnification, the pigment particle sizes and mixtures containing black, white, earth colors, and transparent red lake/s used to model the flesh are remarkably similar. Also, the distributions of lead white in both portraits point to a close resemblance in handling (figs. 12.19B and E) that, if not by the same hand, surely was a product of artists trained in the same, continuous workshop tradition. Mn, which most likely indicates the use of an umber,³⁵ as mentioned above, was detected by MA-XRF in the color mixtures used to deepen the flesh tones of both subjects (figs. 12.19C and F). The attention paid by the artist when depicting individual features is revealed by a photomicrograph taken of the mole (fig. 12.20). This tiny but important feature is constructed with three applications. For texture and emphasis, the artist began with a light base color containing lead white. On top of this a quick dab of black paint was followed by a stroke of brown that curls around the black, terminating in a rounded point.

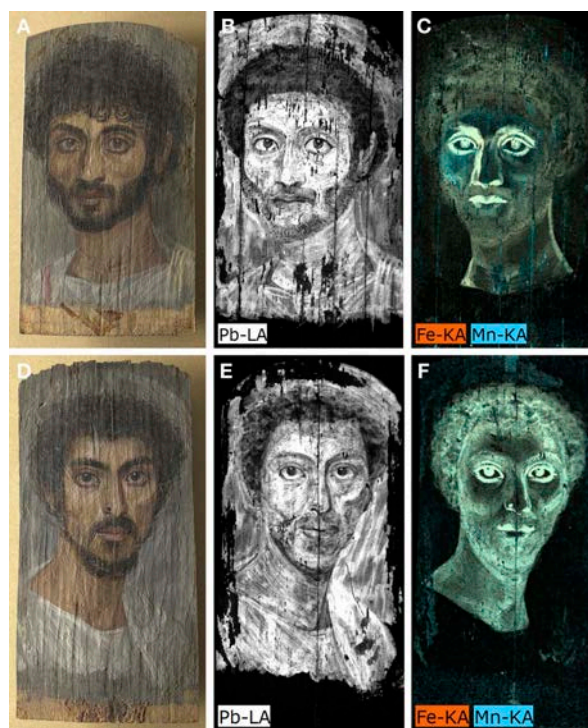


Figure 12.19 (A–C) Portrait of a thin-faced, bearded man (Portrait A) and (D–F) Portrait of a man with a mole on his nose (Portrait B): photographs taken with (A) and (D) raking light illumination; (B) and (E) lead (Pb) distribution maps obtained by MA-XRF; and (C) and (F) combined iron (Fe) and manganese (Mn) distribution maps obtained by MA-XRF. In the combined maps, the areas where Fe and Mn co-locate appear with a greenish yellow hue. Photos: © The Metropolitan Museum of Art, Department of Scientific Research



Figure 12.20 Detail of Portrait of a man with a mole on his nose (Portrait B) showing the artist's careful painting of the mole. Photo: © The Metropolitan Museum of Art, Department of Paintings Conservation

When examined under magnification, very fine black fibers were observed to be pervasive in the paints in eight of the nine portraits; photomicrographs showing these fibers in Portraits B and E are presented in figures 12.21A–F. These black fibers may be fragments of dark animal hair from the artists' brushes.

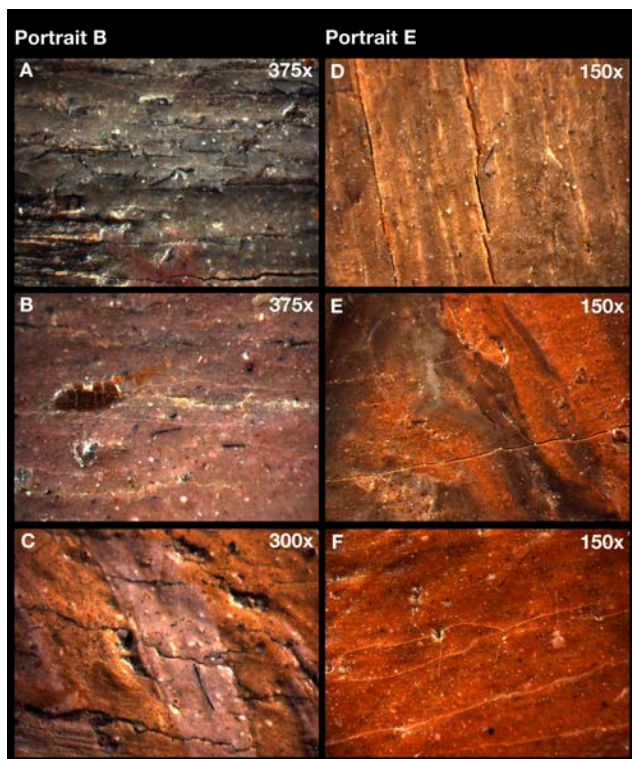


Figure 12.21 Photomicrographs showing black fibers embedded in the paint layer. (A–C) Portrait of a man with a mole on his nose (Portrait B) and (D–F) Portrait of an elderly lady with a gold wreath (Portrait E). Photos: © The Metropolitan Museum of Art, Department of Paintings Conservation

The red lakes present in the portraits investigated for this study were not identified by chemical analysis. When examined under ultraviolet radiation, all nine portraits showed transparent red lake pigment/s that display/s a bright pinkish-orange fluorescence, which may possibly indicate the presence of a madder lake.³⁶ Embedded fibers colored with a red lake were observed under magnification in all of the portraits (shown for Portraits B, F, and H in figs. 12.22A–D), which indicates that the red lake pigment/s were likely manufactured using a colorant produced from textile waste.³⁷ European sources dating to the fifteenth and sixteenth centuries describe the practice of extracting red colorants from dyed textile waste to produce red lake pigments,³⁸ and examples of this tradition have been reported in European paintings of the fifteenth and seventeenth centuries.³⁹ Our findings suggest that the knowledge and practice of preparing red lake pigments from textile waste may have originated in the ancient world. Because madder was extensively cultivated throughout the Mediterranean basin during the Roman-Egyptian period,⁴⁰ it raises the question as to why it would have been necessary to employ a thrifty practice of extracting color from textile waste. In consideration of this, it is possible that the red fibers present throughout the paint may be due to pigments produced from a mixture of red lakes extracted from textile waste dyed with the more precious insect lakes, such as kermes.⁴¹

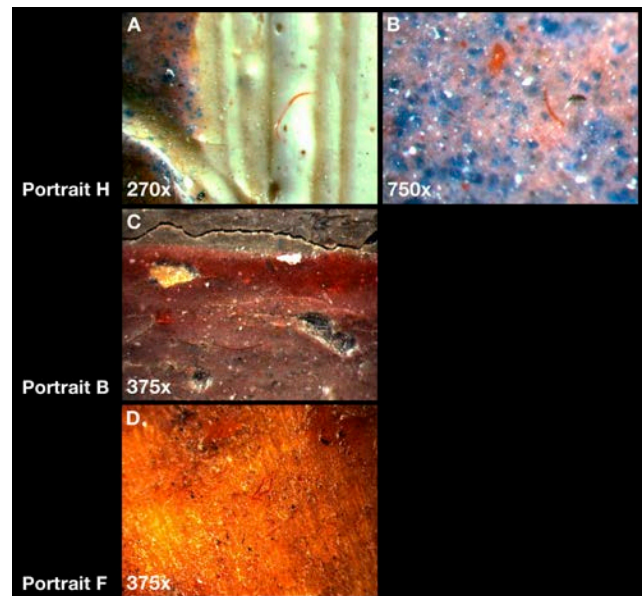


Figure 12.22 Photomicrographs showing red fibers embedded in the paint layer. (A) and (B) Portrait of a Boy Eutyches (Portrait H); (C) Portrait of a man with a mole on his nose (Portrait B); and (D) Portrait of a young woman in red (Portrait F). Photos: © The Metropolitan Museum of Art, Department of Paintings Conservation

The distinct fluorescence of the red lake/s when viewed under ultraviolet radiation draws attention to the way in which the artist used lake/s, mixed with other pigments, to emphasize facial features, model flesh, and color garments. Three remarkable examples in which ultraviolet radiation enhances the uniquely individual methods the artists employed to model and highlight the facial features using red lake/s mixed with other pigments, such as lead white, are Portraits B, C, and G (figs. 12.23A–C). For the males, the red lake/s is/are largely concentrated in the final highlights of the facial features. For the young woman, red lake is used throughout to model her subtly colored flesh. In modern times, artists have remarked on the preferred use of more delicate, transparent red lake pigments, rather than opaque red pigments such as vermilion, to achieve a more specific flesh color.⁴² Surely the lifelike depictions achieved by these ancient artists can be attributed in part to their skillful use of red lake.



Figure 12.23 Images taken under ultraviolet illumination showing the bright pink fluorescence of red lake/s. (A) Portrait of a man with a mole on his nose (Portrait B); (B) Portrait of a thin-faced man (Portrait C); and (C) Portrait of a young woman with a gilded wreath (Portrait G). Photos: © The Metropolitan Museum of Art, Department of Paintings Conservation.

Ultraviolet radiation also reveals the quick fluid strokes of what appears to be a red lake used to paint the clavi in all the male portraits, except for Portrait H, where the lake is mixed with Egyptian blue to make a purple color, as mentioned above. The tunics in Portraits B and D are decorated with two clavi. The trimming of these panels has resulted in only a sliver of this feature remaining at left, and the fragment of color is made more clearly visible under ultraviolet radiation. Red lake/s is/are used in Portraits E, F, and G to color the tunics and mantles. The clavi in Portraits I and H are purple and fluoresce under ultraviolet radiation; MA-XRF and VIL imaging indicate that this color was also made by mixing red lake with Egyptian blue.

CONCLUSION

This study celebrates the talented artists who painted the portraits, and the remarkable culture of the ancient people depicted, placing them within a larger historical context focused on artists' materials and techniques. Long considered among The Met's most esteemed collections, the portraits have been viewed and appreciated for decades by countless visitors as a palpable link that connects us with the past. These artists of the Roman period working in Egypt set a standard for the use of the encaustic technique that is unsurpassed today. The detection using IRR of extensive underdrawing on three portraits, executed with a carbonaceous black pigment in a fluid medium using both a reed pen and a brush, shows that beginning a portrait from a detailed life drawing was practiced in the ancient world. While it was of interest to confirm the use of a full range of pigments, both naturally occurring and manufactured, it is the inspired and various ways in which the artists manipulated their materials that proved most impressive.

Visual examination, IRR, VIL, and X-radiography, in combination with MA-XRF, which proved to be the most powerful analytical tool for obtaining detailed distribution maps of the pigments, provided insight into the individual painting techniques employed. The intentional and varied choice of ochres, a manganese-containing pigment (most likely umber), cinnabar, transparent and brightly colored Egyptian blue, and delicate red lake/s to depict a wide variety of nuanced flesh tones demonstrates the sophistication of these artists. This is also true of the various forms of copper-based greens as well as an arsenic-containing pigment, very possibly orpiment, used to depict the jewelry, and the strategic use of pigment mixtures to depict purple clavi. The use of lead white is ubiquitous, and this too is adjusted in sensitive ways to create modeling and nuanced hues when depicting the white garments.

The pervasive presence of fibers dyed with a red lake throughout the paint in all nine paintings suggests that the practice of producing lake pigments from textile waste dates back at least to the ancient world. The origin of the black fibers observed in eight of the paintings may be fragments of the artists' brushes. The detection of nickel on three panels and of vanadium in one of these suggests the possible presence of bitumen.

The burial practices of these ancient peoples were surely motivated by a desire to preserve themselves in the afterlife. Although the portraits were made for a quite different purpose, it is our hope that these ancient people

would be pleased that their portraits continue to be appreciated and to inspire us today.

METHODS

The paintings were photographed in normal, raking, and UV lighting conditions. In addition to examination using high magnification stereomicroscopy, technical information was gathered using imaging and non-invasive analytical techniques including X-radiography, infrared reflectography (IRR), infrared photography, visible-induced luminescence (VIL), macro-X-ray fluorescence (MA-XRF), and Raman spectroscopy.

Infrared Reflectography

Infrared reflectography (IRR) was done using an OSIRIS InGaAs near-infrared camera with a 6-element, 150 mm focal length, f/5.6–f45 lens, and spectral response in the 900–1700 nm range. The reflectograms of all paintings were recorded in one capture.

Infrared Photography

Modified Canon EOS 5D Mark II and Canon EOS 5DS cameras were used for infrared photography. The modification involved the removal of an infrared blocking filter and the addition of an infrared filter (X-nite, 830 nm). The camera is sensitive up to approximately 900 nm.

X-radiography

Digital X-radiographs were acquired for 09.181.1, 09.181.2, 09.181.3, 09.181.4, and 2013.438 using a TFI Hotshot portable industrial X-ray unit, consisting of a 603 head and 805D control. The system has a 0.5 mm focal spot and 96.5 cm radiation beam. For these portraits, the source was operated at 30 kV and 5 mA, and the exposure time was 30 s. Images were recorded onto Industrex Flex XL Blue 5537 plates and digitized with a Carestream HPX-1 scanner at 508 ppi.

For the rest of the paintings, existing film radiographs were scanned with an Epson 10000XL using Silverfast 8 software (LaserSoft Imaging) at 600 ppi. For these portraits, the acquisition conditions were as follows: 30 kV, 5 mA, and 20 s for 09.181.5; 25 kV, 5 mA, and 5 s for 09.181.6 and 09.181.7; and 35 kV, 5 mA, and 5 s for 18.9.2.

Macro-X-ray Fluorescence (MA-XRF)

Macro-X-ray fluorescence (MA-XRF) was carried out using a Bruker M6 Jetstream instrument with the X-ray source operated at 50 kV and 0.5 mA. The full paintings were mapped with a 500-micron spot size and a 500-micron step size, with a dwell time of 100 msec/pixel. The spectra were processed using the Bruker M6@ Jetstream software and open-source PyMCA tools.

Raman Spectroscopy

Non-invasive Raman spectroscopy measurements were done in situ in selected paints in some of the portraits using a Renishaw System 1000 coupled to a Leica DM LM microscope. All the spectra were acquired using a 785 nm laser excitation focused on the portraits using a long working distance 20x objective lens, with integration times between 10 and 120 s. A 1200 lines/mm grating and a thermoelectrically cooled CCD detector were used. Powers at the sample were set between 0.5 and 5 mW using neutral density filters.

Visible-Induced Infrared Luminescence (VIL)

VIL imaging was carried out with a modified Canon D60 camera (IR/UV filters removed) with a Coastal Opt UV-Vis-IR 60 mm macro lens, a X-Nite 830 filter on the lens, and red LEDs as the illumination source.

ACKNOWLEDGMENTS

The authors are indebted to the following Met colleagues: Diana Patch, Lila Acheson Wallace Curator in Charge, Department of Egyptian Art, for her continuing support of this investigation; Sara Levin, assistant conservator, Objects Conservation, for acquiring multiband images; and Evan Read, manager of technical documentation, Paintings Conservation, for photography and for acquiring and digitizing X-radiographs and IRR images. We are also grateful to Joanne Dyer, scientist at the British Museum, for suggesting bitumen as the possible origin of the Ni-containing material observed in some of the portraits studied. We thank the Andrew W. Mellon Foundation for supporting Louisa Smieska and Clara Granzotto with fellowships in The Met's Department of Scientific Research during the period of the research.

NOTES

1. Walker 2000A.

2. Walker 2000B; Walker and Bierbrier 1997.
3. Koeppen 1973.
4. Walker 2000B.
5. Walker 2000B, 105–16.
6. “Mummy with an Inserted Panel Portrait of a Youth, A.D. 80–100.” The Metropolitan Museum of Art, <https://www.metmuseum.org/art/collection/search/547697>; for accounts of excavations in the Fayum, see Petrie 1889, Petrie, 1890, and Petrie 1911; for recent evocations of the physical ambiance of one particular local that produced these portraits, see Bąkowska-Czerner and Czerner 2022; Daszewski 2008.
7. Metropolitan Museum of Art, Imaging Department Archives.
8. This portrait was acquired in 2013 by The Met and restituted to Egypt in 2022.
9. von Sonnenburg 1972.
10. Walker 2000B, 115.
11. Corcoran and Svoboda 2010, 40.
12. Burgio and Clark 2001.
13. Burgio and Clark 2001; Vandenabeele et al. 2000.
14. Delaney et al. 2017, 15509; Dyer and Newman 2020; Ganio et al. 2015; Salvant et al. 2018; Thiboutot 2020; Vak, Iannaccone, and Uhlir 2020.
15. Bell, Clark, and Gibbs 1997; Burgio and Clark 2001.
16. Eastaugh et al. 2004.
17. Bell, Clark, and Gibbs 1997.
18. Bouchard and Smith 2003; de Faria, Silva, and de Oliveira 1997.
19. Walker 2000B, 108.
20. Centeno 2016.
21. Dasen 2008.
22. Ganio et al. 2015; Eastaugh et al. 2004; Riederer 1997.
23. Nahar, Schmets, and Scarpas 2016.
24. Serpico 2000.
25. Serpico 2000.
26. Connan 1999; Serpico 2000.
27. Nissenbaum and Buckley 2013.
28. Connan 1999; Serpico 2000.
29. Riederer 1997; Eastaugh et al. 2004.
30. Ganio et al. 2015; Riederer 1997.
31. Riederer 1997.
32. Nicola et al. 2024.
33. Ganio et al. 2015.
34. Walker 2000B, 111–14.
35. Eastaugh et al. 2004.
36. de la Rie 1982; Newman and Gates 2020.
37. Kirby, Spring, and Higgitt 2005, 74–78.
38. Kirby, Saunders, and Spring 2006, 237.
39. Kirby, Saunders, and Spring 2006, 239.
40. Newman and Gates 2020; Rackham 1938–1952, Book XIX, chapter 17.
41. Eastaugh et al. 2004.
42. Northcote 1819, 18.

***Umbras dividendas ab lumine:* Pigments, Their Mixtures, and Distribution on Mummy Portraits in Relation to Primary Sources**

*Giovanni Verri
Marc Vermeulen
Alicia McGeachy
Ken Sutherland
Clara Granzotto
Federica Pozzi
Rachel Sabino
Laura A. D'Alessandro
Alison Whyte
Marc Walton*

Increasingly refined scientific investigations are bringing to light the complexities of ancient painting techniques.¹ Research on panel portraiture, in particular, is providing ever-growing evidence pertaining to the making of these complex objects, their provenience, and function.² This evidence, alongside literary, art historical, and archaeological research, sheds new light on the interpretation of the elusive nature and origins of panel portraits: a blend of different, yet intertwined, customs drawing from ancient Egyptian, Greek, and Roman traditions.

Many questions on the making and meaning of panel portraiture remain unanswered, however. Some of these questions concern the choices, preparation, and uses of

pigments to create the portraits. Advances in terms of pigment identification have been made, but fewer investigations have explored aspects of how these pigments are used and for what purpose. One possible reason for this deficiency is that a work of art is much more than the sum of its parts, and the painter's skill and the intangible qualities that went into creating the work cannot so easily be quantified. Empirical observation, however, may shed some light on artists' *modi operandi* and bring us closer to their intentions.

This paper investigates the making of a heterogeneous group of panel portraits held in Chicago-area collections. It draws some general conclusions on how a variety of pigments are used to achieve an array of often subtle tonal

variations, beginning with insights into the ways in which Egyptian blue (EB), a pigment easily characterized by means of visible-induced luminescence imaging (VIL), is used to create a variety of hues. It continues with a discussion of other pigments, which can be visualized using infrared-reflected and visible- and ultraviolet-induced luminescence imaging (IRR, VIL, and UIL, respectively; figs. 13.1–13.7) and mapping X-ray fluorescence spectroscopy (MA-XRF; fig. 13.8).

METHODOLOGY AND CASE STUDIES

In addition to archival research, visual observations with and without magnification were conducted alongside technical imaging (VIL, UIL, and IRR) using a Nikon D850 modified camera and Nikon SB80DX flashes equipped with suitable filters.³ Hyperspectral imaging (HSI) was undertaken in the 393–892 nm range, divided into 240 spectral bands, using a Resonon Pika II pushbroom camera. MA-XRF made use of a custom-made scanner developed by Northwestern University.⁴ Reflected Fourier transform infrared (R-FTIR) spectroscopy was performed using a Bruker Alpha unit equipped with an external reflectance head. A select number of microscopic samples were mounted as cross sections. Raman and transmission FTIR spectroscopy were also executed using a Jobin Yvon Horiba confocal and Bruker Hyperion microscope, respectively.

Field Museum of National History (FM 110872)

Difficult to visually appreciate due to its condition, this painting depicts a woman with dark curly hair against a gray background (fig. 13.1). She wears a white tunic with dark vertical bands and a necklace with a bright yellow pendant. According to the acquisition record, the portrait is roughly dated to the end of the second century CE and was purchased from E. A. David, Long Island City, in 1945. The painting was formerly part of the T. Graf Collection.⁵

Art Institute of Chicago (AIC 1922.4798 and AIC 1922.4799)

Gifted by Emily Crane Chadbourne in 1922, these two paintings are dated to the first half of the second century CE. The first (AIC 1922.4798; fig. 13.2) represents a man wearing a white garment with purple vertical bands and a gilded wreath with berries and leaves. The second (AIC 1922.4799; fig. 13.3) represents a man wearing a white garment with dark bands and a gilded laurel wreath. Both

figures are represented against a light gray, partially gilded background.⁶

Susan and Lew Manilow Collection (MN 0251 and MN 0252)

Figure 13.4 (MN 0251), dated to the second century CE, depicts a bearded man wearing a white garment with purple stripes and a mantle. Figure 13.5 (MN 0252), dated to the first century CE, shows a woman wearing a red garment with dark stripes, a mantle, necklace, and earrings. Both figures are represented against a gray background. They were purchased from Sotheby's, New York, in 2004.⁷

Institute for the Study of Ancient Cultures of the University of Chicago (ISAC E2053 and ISAC E9137)

The portrait of a man, ISAC E2053 (fig. 13.6), wearing a purple garment and a scarf, was likely excavated in Fag el-Gamous by Bernard Grenfell and Arthur Hunt in 1901–1902 and is dated to the end of the second century CE. He is represented against a beige background.⁸ Excavated by Flinders Petrie in Hawara in 1911 and acquired in the same year, portrait ISAC E9137 (fig. 13.7), dated to the beginning of the second century CE, represents a woman with an elaborate hairstyle, a purple tunic with purple and yellow stripes, two necklaces, and pearl earrings. She is represented against a gray background.⁹

RESULTS

Over the past decade or so, VIL imaging has revealed the use of EB in panel portraits for obvious functions, such as blue garments. Other intuitive uses include its mixture with organic and inorganic reds for purples or with yellows for greens. Less intuitive uses include its presence in varying concentrations for the representation of skin tones, in the whites of the eyes, and, in some instances, in the lower lips.¹⁰ This study provides additional clues to the functions and intended visual effects of the pigment in the case studies investigated (see figs. 13.1–13.7), with reference to the skin tones, drapery, and other features. Drawing particularly on MA-XRF data (fig. 13.8), the paper will also address instances where other pigments are used, sometimes in similar ways to EB. Finally, it will attempt to link the empirical findings within the broader framework of primary literary evidence. While this paper is necessarily focused on specific aspects of the portraits' materials and

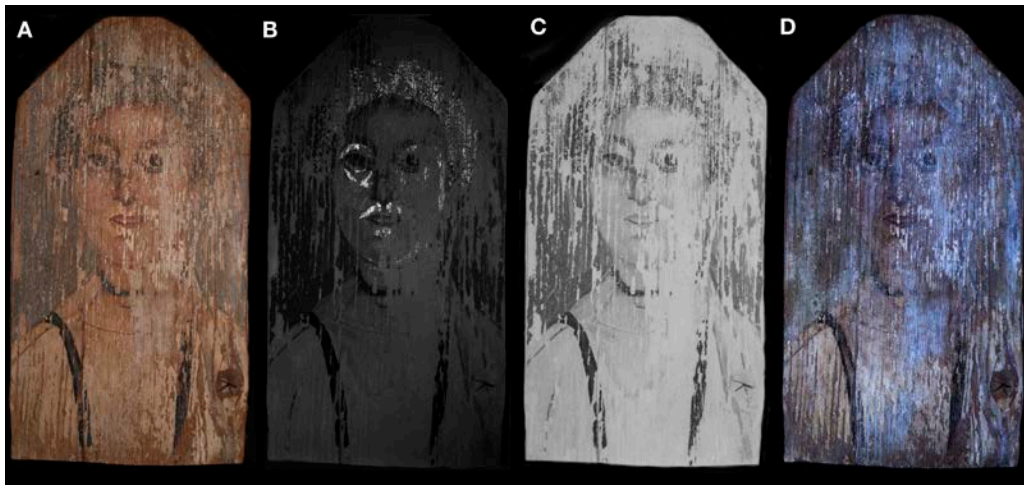


Figure 13.1 Panel portrait of a woman, Greek/Roman/Egyptian, second century CE. Wood and pigments, 28.9 x 15.3 cm (11.4 x 6 in.). From left to right, (A) visible; (B) VIL; (C) IRR; and (D) UIL images. Field Museum of Natural History, FM 110872. Photos: Giovanni Verri



Figure 13.2 Panel portrait of a man, Greek/Roman/Egyptian, second century CE. Wood and pigments, 39.4 x 22 cm (15.5 x 8.7 in.). From left to right, (A) visible; (B) VIL; (C) IRR; and (D) UIL images. Art Institute of Chicago, Gift of Emily Crane Chadbourne, AIC 1922.4798. Photos: Giovanni Verri



Figure 13.3 Panel portrait of a man, Greek/Roman/Egyptian, second century CE. Wood and pigments, 41.9 x 24.1 cm (16.5 x 9.5 in.). From left to right, (A) visible; (B) VIL; (C) IRR; and (D) UIL images. Art Institute of Chicago, Gift of Emily Crane Chadbourne, AIC 1922.4799. Photos: Giovanni Verri



Figure 13.4 Panel portrait of a man, Greek/Roman/Egyptian, second century CE. Wood and pigments, 39.4 x 21.6 cm (15.5 x 8.5 in.). From left to right, (A) visible; (B) VIL; (C) IRR; and (D) UIL images. Collection of Susan and Lew Manilow, MN 0251. Photos: Giovanni Verri



Figure 13.5 Panel portrait of a woman, Greek/Roman/Egyptian, first century CE. Wood and pigments, 36.8 x 21.3 cm (14.5 x 8.45 in.). From left to right, (A) visible; (B) VIL; (C) IRR; and (D) UIL images. Collection of Susan and Lew Manilow, MN 0252. Photos: Giovanni Verri



Figure 13.6 Panel portrait of a man, Greek/Roman/Egyptian, second century CE. Wood and pigments, 41.5 x 23.5 cm (16.3 x 9.3 in.). From left to right, (A) visible; (B) VIL; (C) IRR; and (D) UIL images. Institute for the Study of Ancient Cultures of the University of Chicago, ISAC E2053. Photos: Giovanni Verri



Figure 13.7 Panel portrait of a woman, Greek/Roman/Egyptian, second century CE. Wood and pigments, 32 x 22 cm (12.6 x 8.7 in.). From left to right, (A) visible; (B) VL; (C) IRR; and (D) UJL images. Institute for the Study of Ancient Cultures of the University of Chicago, ISAC E9137. Photos: Giovanni Verri

techniques, the broader findings from the analytical investigation are summarized in figure 13.9.

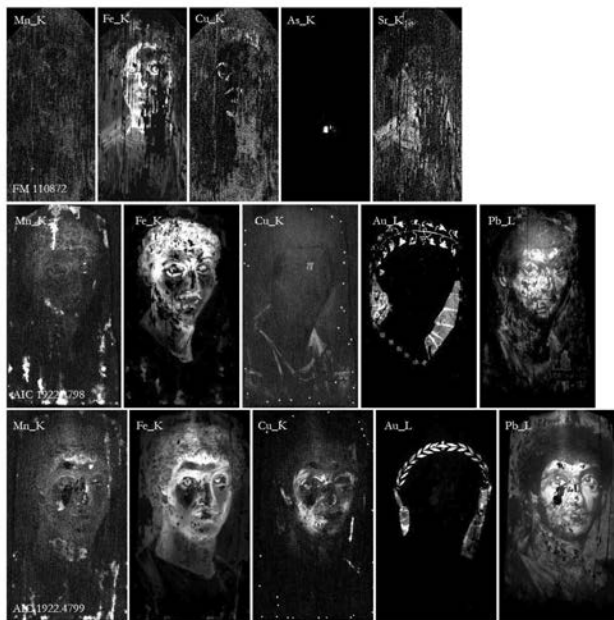


Figure 13.8A Select MA-XRF elemental maps of the panel portraits examined in this study. From top to bottom row: FM 110872, AIC 1922.4798, and AIC 1922.4799. Photos: Giovanni Verri



Figure 13.8B Select MA-XRF elemental maps of the panel portraits examined in this study. From top to bottom row: MN 0251, MN 0252, ISAC E2053 and ISAC E9137. Photos: Giovanni Verri

	Pigments	Binder
FM 110872	Gypsum (FTIR); silicates/kaolinite group (FTIR); ⁱ red ochre (HSI, MA-XRF); alunite ⁱⁱ (FTIR, Raman); umbers (MA-XRF); carbon-based black (IRR, Raman); EB (VIL, MA-XRF); arsenic-containing yellow (MA-XRF) ⁱⁱⁱ	Not determined
AIC 1922.4798	Red and yellow ochres (Raman, MA-XRF); jarosite (Raman, FTIR, MA-XRF); umbers (MA-XRF); carbon-based black (Raman); hydrocerussite (FTIR, XRF); calcite (FTIR, Raman, MA-XRF); silicates/kaolinite group (FTIR); EB (Raman, VIL); red dye of plant origin, likely madder (SERS, UIL); blue dye, likely indigo or woad (HSI); gold foil (MA-XRF)	Beeswax (GC-MS)
AIC 1922.4799	Red and yellow ochres (Raman, MA-XRF); jarosite (FTIR); umbers (MA-XRF); carbon-based black (Raman); hydrocerussite (FTIR, XRF); calcite (FTIR); gypsum (FTIR); silicates/kaolinite group (FTIR); indigo or woad (HSI, FTIR, GC-MS); gold foil (MA-XRF)	Beeswax (GC-MS)
MN 0251	Lead-based white (MA-XRF); silicates (R-FTIR); red ochre (HSI, MA-XRF); carbon-based black (IRR); EB (VIL, MA-XRF); red dye of plant origin, likely madder (HSI, UIL); blue dye, likely indigo or woad (HSI)	Wax (R-FTIR)
MN 0252	Lead-based white (MA-XRF); silicates (R-FTIR); red and yellow ochres (HSI, MA-XRF); carbon-based black (IRR); EB (VIL, MA-XRF); cinnabar (MA-XRF); red dye of plant origin, likely madder (UIL); blue dye, likely indigo or woad (HSI)	Wax (R-FTIR)
ISAC 2053	Hydrocerussite (FTIR, MA-XRF); silicates (R-FTIR); red and yellow ochres (HSI, MA-XRF); carbon-based black (IRR); EB (VIL, MA-XRF); red dye of plant origin, likely madder lake (HSI, UIL); blue dye, likely indigo or woad (HSI)	Wax (R-FTIR)

	Pigments	Binder
ISAC 9137	Hydrocerussite (FTIR, MA-XRF); red and yellow ochres (HSI, MA-XRF); EB (VIL, MA-XRF); red dye of plant origin, likely madder (UIL); carbon-based black (IRR); copper-based green (MA-XRF)	Wax (R-FTIR)

ⁱ Clay minerals from the kaolinite group are possibly associated with the ochres and umbers.

ⁱⁱ Alunite is one of a group of white-yellowish minerals of formula $AM_3(SO_4)_2(OH)_6$, where A is normally K^+ or Na^+ and M is Al^{3+} . If M is Fe^{3+} , the mineral is jarosite. While jarosite has been found used on a number of portraits (see 1922.4798 and 1922.4799), alunite is less commonly identified (see Stenger et al. and Smith et al. in same volume). In this case, Na-rich alunite was identified with FTIR through the $\nu_3(SO_4)^{2-}$ at c. 1219 and 1091 cm^{-1} , $\delta(OH)$ at c. 1028 cm^{-1} , and structural stretchings and water modes in the 3000-3800 cm^{-1} region (Bishop and Murad 2005).

ⁱⁱⁱ Arsenic is only found in the yellow pendant gem hanging from the necklace (see fig. 13.8).

Figure 13.9 Summary of the painting materials inferred from analysis using techniques indicated in parentheses. Detailed information on portraits AIC 1922.4798 and 1922.4799 can be found in Sabino et al. 2019 and Sutherland, Sabino, and Pozzi 2020. Analytical reports for all portraits are on file at the Department of Conservation and Science at AIC and relevant institutions. Table: Giovanni Verri

Skin Tones

Some questions concern the technical use of EB for the representation of skin tones: is it used only for cooler tones and shadows? Is it a “precious” pigment used in the uppermost finishing touches only? Or is it used liberally, also found beneath other paint layers? Prior to its inclusion in a paint mixture, what was the hue of the raw pigment? How was it prepared prior to mixing with other pigments and binders? Was it applied in translucent or opaque layers? The list of questions could continue to include more technical aspects related to paint application. At this stage of the research, we will mostly report on phenomenological observations aimed at understanding in more detail how technical information can supplement other means—based on style, iconography, etc.—that can help scholars in the characterization of this corpus of paintings.

FM 110872 (see fig. 13.1) shows the presence of EB in the skin tones in several locations, in two distinct concentrations, mixed with red, yellow, white, and black pigments (fig. 13.9): “low” for the shadow along the jawline and “high” elsewhere.¹¹ Figure 13.10 shows a



Figure 13.10 FM 110872. Visible (left) and VIL (right) image of a detail of the mouth showing the distribution of EB. Field Museum of Natural History. Photos: Giovanni Verri

detail of the area around the mouth. A flesh-tinted paint mixture containing EB is found in the uppermost paint layer above the upper lip, while paint containing EB is applied underneath a darker brown paint layer by the mentolabial sulcus (below the lower lip), which is intended to stress the depth of a shadow by the chin. As observed in the MA-XRF maps, the copper K spectral lines—energetic enough to penetrate through the ochre layers—confirm that the blue pigment is in fact also present on the chin but is obscured in the VIL image by subsequent layers of paint (fig. 13.8). The presence of the blue pigment in the underlayer can be seen along the margins of the damaged edges in the VIL image (fig. 13.10). Therefore, in this example, EB-containing paint was used both as a finishing layer and as part of a more complex stratigraphy.

Figure 13.11 (top) shows a microscopic sample of an area of high concentration of EB from the left of the left eye of the figure, similar to that observed on the chin. Large blue grains can be seen scattered in the uppermost translucent light-brown paint layer, revealing the ruddier skin color underneath. As observed in the VIL image of the cross section (fig. 13.11, bottom right), and as one would expect from an unsorted ground pigment, the EB particles are diverse in size (10–30 μm range).¹²

Despite the different painting style from the Field Museum's portrait, the skin tones of AIC 1922.4798 (fig. 13.2) also show two distinct concentrations of EB: high for the glabella (between the eyes) and above the upper lip, and low for the rest of the face, particularly in the neck and sternal area.¹³ In contrast to FM 110872, the EB-containing flesh paint in AIC 1922.4798 appears to have been used as the uppermost paint layer, only partially covered by very

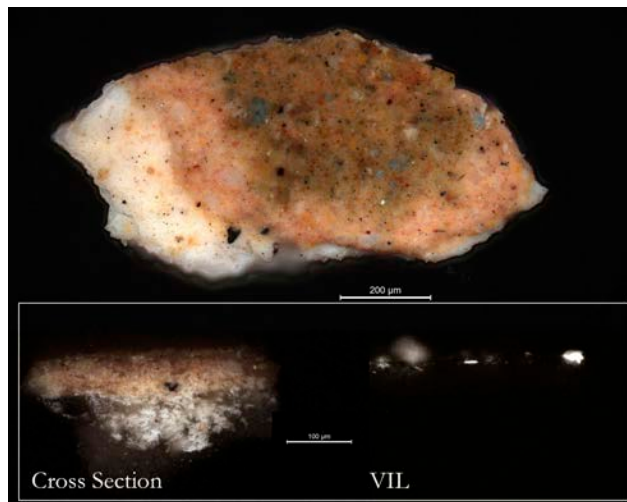


Figure 13.11 FM 110872. Sample from the area next to the left eye. Unmounted sample (top); Visible (left) and VIL (right) image of the sample in cross section (bottom). Field Museum of Natural History. Photos: Giovanni Verri

fine beige hatched lines between the eyes and black facial hairs on the upper lip. At present, this paint layer appears chalky and opaque, but this may be the result of degradation of the binding medium; calcium oxalates in the paint layers,¹⁴ as detected with FTIR, attest to processes of alteration of the binding medium.¹⁵

The skin tones of AIC 1922.4799 (fig. 13.3) are also created using at least two distinct concentrations of EB within complex mixtures of red, yellow, white, and black pigments (figs. 13.3 and 13.9). Both AIC paintings make use of luminous highlights executed with lead-based white paint (see the Pb_L map in fig. 13.8). EB is used more profusely, however, for the skin tones of AIC 1922.4799 than for AIC 1922.4798 (fig. 13.2),¹⁶ with the areas of highest concentration either in shadow or along the beard line. Areas where EB is least concentrated are those in which the white is used as a highlight, such as for the forehead, cheek, and chin. In these cases, therefore, EB is not mixed with white to modify the tone of white paint, as observed in other instances such as the sclera.¹⁷ The same low-level concentration is also observed on the neck. When observed under the microscope, the concentrated areas clearly show the presence of large blue particles, observable also at relatively low magnification (fig. 13.12, top). In cross section, the EB in the skin tones is well mixed with a lead-based white and ochres (see the Mn_K, Fe_K, and Pb_L maps in figure 13.8) and not applied only in the topmost layer; in the VIL image of the cross section, alongside the few large particles (> ca. 50 μm), several very small (< ca. 20 μm) particles can be seen across the entire stratigraphy (fig. 13.12, bottom).



Figure 13.12 AIC 1922.4799. Detail of the chin (top); cross section (middle); and VIL image of the cross section (bottom). Art Institute of Chicago, Gift of Emily Crane Chadbourne. Photos: Giovanni Verri

EB is found in the beard, neck, and eye areas of MN 0251 (figs. 13.4, 13.8, and 13.9). Figure 13.13 shows how different concentrations were used for the skin tones around the left eye, including areas in shadow and in bright light, as observed on the forehead above the eyebrow. Judging from the rather homogeneous distribution within areas of similar concentration, it seems that each color was carefully mixed with varying amounts of EB prior to its application.

The use of EB in MN 0252 (fig. 13.5) appears to be highly concentrated in some of the midtones, around the mouth, glabella, and eyes, but not in the deepest shadows such as the one on the neck below the chin. Despite a highly naturalistic appearance, no EB was found in the skin tones of ISAC E2053 (fig. 13.6).¹⁸ By contrast, a profusion of the pigment was observed in the skin tones of the female portrait ISAC E9137 (fig. 13.7), where the pigment is distinctly found on the left side of the figure in a relatively homogeneous concentration. Whether these areas are meant to represent highlights, shadows, or midtones is difficult to say, because of the discoloration of the paint layers.

It appears that, in the cases analyzed with VIL for this study, the concentration of EB in paint mixtures within a particular area is relatively constant overall, with of course some exceptions (e.g. MN 0251). Most of the tonal modulation seems instead to have been executed through

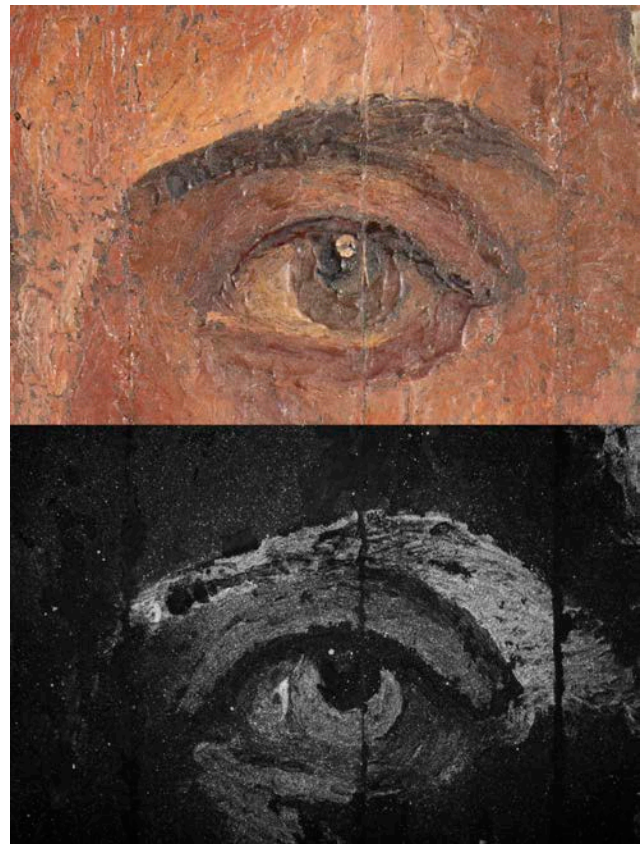


Figure 13.13 Detail of the left eye of MN 0251. Visible (top) and VIL image (bottom), showing the distribution of EB. Collection of Susan and Lew Manilow. Photos: Giovanni Verri

more nuanced distributions of other pigments, including ochres and lead-based whites, as can be observed in the elemental maps (fig. 13.8).

Whites of the Eyes: Blue, Gray, and Red

White paint containing EB has already been extensively documented for the representation of the whites of the eyes and was recently traced back to at least the fifteenth century BCE in Pharaonic Egypt.¹⁹ One explanation for the practice of adding blue to white paint is related to its possible function as an optical brightener, making off-white paint appear whiter or even distinctly bluish. Different pigment uses, however, are documented for the group investigated here, in which the whites of the eyes in most cases do not have a blue tint.²⁰

In MN 0251 and MN 0252 (figs. 13.4 and 13.5), the whites of the eyes could be described as reddish, rather than bluish, rendered with complex mixtures of EB, red ochres, and lead-based pigments in different proportions (figs. 13.8, 13.13, and 13.14). For MN 0251 (fig. 13.4), the painter has intentionally prepared different paint mixtures for the



Figure 13.14 Eye details (from top left to bottom right): FM 110872, AIC 1922.4798, ISAC E2053, AIC 1922.4799, MN 0252, and MN 0251. Photos: Giovanni Verri

bright brushstroke in the white of the eyes—where there is a high concentration of EB—and for the white dot indicating the reflected light on the cornea, in which there is no EB. These apparently idiosyncratic uses of EB bring forward the complexities and individuality of artists' techniques. A distinctive reddish tone also characterizes the whites of the eyes in AIC 1922.4799 (fig. 13.3), which were found to be composed of a lead-based white with small amounts of red ochre and no EB.

FM 110872, AIC 1922.4798, and ISAC E2053 (fig. 13.14) offer examples where a gray paint mixture was used in the white of the eye. In the IRR images, the gray paint layer absorbs infrared radiation, suggesting the likely use of a carbon-based black, as found in other parts of the figures. At this stage, it is worth noticing that EB is found elsewhere in the paintings, and was therefore clearly available, but deliberately not used for the whites of the eyes. Instead, a black pigment was used to perhaps achieve a similar effect. While the use of carbon black may create an effect reminiscent of the addition of EB to white in creating a cool tone,²¹ the use of red ochre may appear counterintuitive. However, it may well be that the intention of the artist was to replicate real-life hues.²² Evidence for the use of a red/pink tone in the whites of the eyes has been found in other contexts. A relevant comparative example is the first-century CE marble portrait bust of a young girl called Psyche at the Hellenic National Archaeological Museum, Athens (EAM 426), in which madder lake was used in the whites of the eyes. The implications of this choice, which could also be related to physiognomics, as in pseudo-

Aristotle's *Physiognomonica*,²³ and have therefore moral/ethical undertones, are still being investigated.²⁴

Drapery Shadows

EB is frequently found in drapery renditions, especially when delineating shadows. This is true for both colored garments, as in the case of the pink cloaks in ISAC E2053 (fig. 13.6) and ISAC 9137 (fig. 13.7), where EB is found in the darker areas, and for otherwise white garments, as in the case of ISAC E2053's scarf, MN 0251's cloak (fig. 13.4),²⁵ and AIC 1922.4798's mantle (fig. 13.2). ISAC E2053's scarf is made of hydrocerussite, EB, and likely a carbon-based black, as inferred through the high absorption in the infrared range (see IRR image, fig. 13.6C). Although visually similar, VIL imaging shows that the folds of the scarf are executed using very different concentrations of EB, creating subtly different levels of gray with thin and translucent gray brushstrokes (fig. 13.15). The same paint mixture seems also to have been used for finishing touches in the hair, likely to convey the idea of thin strands through which the background is clearly visible, adding an element of three-dimensionality to the painting. The application of these touches seems to belong to a somewhat separate (perhaps final) intervention, as EB is not otherwise found in the figure's hair (fig. 13.16).²⁶

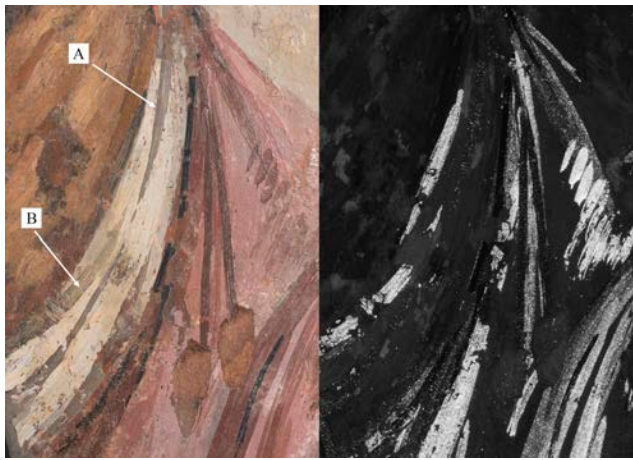


Figure 13.15 Scarf detail, ISAC E2053, visible (left) and VIL (right) image. Points (A) and (B) show gray areas that are visually similar but executed with different concentrations of EB. Institute for the Study of Ancient Cultures of the University of Chicago. Photos: Giovanni Verri

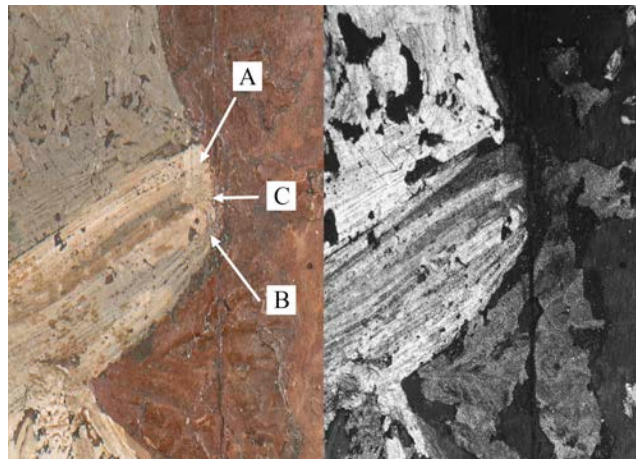


Figure 13.17 Detail of MN 0251's garment. Visible (left) and VIL (right) image: (A) white paint not rich in EB, (B) white paint rich in EB, and (C) translucent gray paint rich in EB. Collection of Susan and Lew Manilow. Photos: Giovanni Verri



Figure 13.16 Hair detail, ISAC E2053. Visible (left) and VIL (right) image showing the EB distribution. Institute for the Study of Ancient Cultures of the University of Chicago. Photos: Giovanni Verri

A similar approach was employed for MN 0251 (fig. 13.4), where different concentrations of ochres and EB were used with a lead-based white to execute the folds of the figure's ensemble. In this example, EB is mixed in both the white paint and the translucent gray layer painted over the dark shadow between two highlights (fig. 13.17). This application, which will be discussed later in more detail, is rather elaborate in the way in which it blends the darks and the highlights of the folds: the translucent gray paint layer is very subtle, although clearly visualized in the VIL image.

Green, Blue, and Pink in the Hair

Imaging techniques other than VIL can be applied to provide insights into the uses of other pigments, which are likely to be as complex and articulated as those observed for EB. In particular, MA-XRF analysis of MN 2051 reveals that a copper-containing pigment was used for hair highlights (fig. 13.8). In other features in the portrait, there is a relatively good accordance between the copper map and the VIL image where EB is present, indicating that this pigment is used mostly at the surface.²⁷ The unidentified pigment in the hair is green in color and not made of a mixture of EB and yellow pigment, as it does not show any luminescent properties in the infrared range. When observed at higher magnification, the pigment appears to be finely ground and poorly mixed within a white paint matrix, perhaps inhomogeneously redistributed by the melting and re-melting of the wax-based binding medium during the painting process (fig. 13.18).

Another example of an unexpected use of pigment can be seen in MN 0252 (fig. 13.5), where a blue dye, likely indigo or woad,²⁸ was identified in the hair. Figure 13.19 shows the infrared false-color image²⁹ of a detail of the hair, where the distribution of the dye can be clearly seen in a red hue and is therefore distinguished from the carbon-based black likely used for the rest of the hair. Finally, a red organic colorant, likely madder lake,³⁰ is also present in the hair of the same portrait (see figs. 13.5, 13.19, and 13.9). The very small amount of madder suggests that its presence is accidental. A similar example, where madder lake was instead used intentionally, and likely in



Figure 13.18 Detail of MN 0251's hair showing the presence of small amounts of a green pigment, mixed with a white pigment, in the brown hair. For a more precise location of the green pigment, see the arrow and also the Cu_K map in figure 13.8. Collection of Susan and Lew Manilow. Photos: Giovanni Verri

conjunction with indigo, was found in Brooklyn Museum's *Noblewoman* (86.226.18).³¹



Figure 13.19 Detail of the hair of MN 0252. Top: Visible (left) and infrared false-color (right) image in which a blue dye, with an absorption at ca. 660 nm, likely indigo or woad, shows as red. Bottom: Detail of the curls, showing a small amount of a pink pigment, likely madder lake (see fig. 13.9). Collection of Susan and Lew Manilow. Photos: Giovanni Verri

PRIMARY SOURCES, ANALYTICAL EVIDENCE, AND CONCLUSIONS

It is clear from this and other studies that particular pigment characteristics served specific functions, but also that similar effects could be achieved in different ways, making painting techniques more complex than just a set of recipes wherein a particular paint mixture was routinely used for a specific purpose. For example, EB appears to be used as a tone modifier for the hair of some figures examined in this study, but in one instance a green pigment was found instead, apparently used for a similar purpose. Considerable variation is found in the way in which the whites of the eyes are rendered: grays, blues, and reds are variously used to depict the whites of the eyes in the portraits studied. Are these different ways of portraying a subject the result of different schools of practice and established painting traditions or do they come from the requirements to imitate the individual physical/moral traits of the subject being represented? Or are they perhaps the idiosyncratic choices of an artist?

In considering these possibilities, it may be useful to compare the findings with the available primary literature that discusses the uses of color in antiquity and to highlight the complexities of these comparisons. For example, with the aim of explaining EB's use in cooler skin tones, Gabrielle Thiboutot compared EB and Pliny's anularian white,³² a mixture of *creta* (clay) and a pulverized *vitreis gemmis* (glassy gem) worn by the lower classes. This glassy gem, in the absence of further evidence, might have been a type of EB, and hence affordable by the lower classes.³³ Another explanation could be found in Vitruvius, according to whom *cretam anulariam* (anularian clay) is dyed with *vitrum* (woad) to imitate indigo:³⁴

*item propter inopiam coloris indici cretam selinusiam aut anulariam vitro, quod Graeci ἰσάτιν appellant, inficientes imitationem faciunt indici coloris.*³⁵

It should be remembered, however, that ἰσάτις, which is a Greek term for woad, is an interpolation; British Library's Harley MS 2767 (f. 107r)³⁶ reports in fact *insallim* as the Greek translation of *vitrum*, adding to the complication of the interpretation of the text; *insallim*, according to Leo Wiener,³⁷ is of Arabic origin (عظام, transl. 'izlim) and refers to the juice of a plant producing a color similar to indigo. Nonetheless, with the double meaning of *vitrum*—glass and woad—it could be additionally speculated that the *vitrea gemma* used for the portraits of women refers to dyed stones, affordable by the lower classes; a recipe for the preparation of a hyacinth-colored false gem in the

Stockholm papyrus calls for indigo to dye a stone (Recipe 63).³⁸

EB was also found—quite clearly in the case of MN 0251 (fig. 13.4 and fig. 13.17)—at the interface between highlights and shadows, through the application of subtle and barely noticeable brushstrokes. In addition, elegant and subtle *ton sur ton* brushwork using indigo over a carbon-based black was observed for the hair of MN 0252 (fig. 13.5) and ISAC E9137 (fig. 13.7). In a single passage, Pliny tells us two important pieces of information, as he describes one way in which artists used pigments:

*Non pridem adportari et Indicum coeptum est, cuius pretium VII. ratio in pictura ad incisuras, hoc est umbras dividendas ab lumine. Est et vilissimum genus lomenti, quod tritum vocant, quinis assibus aestimatum.*³⁹

The author remarks that indigo, a very dark blue pigment, was used by artists for incisures, or the division of shadows from light. The interpretation of the precise meaning of the term *incisura* remains speculative. Could the thin application of indigo for the hair of MN 0252 (figs. 13.5 and 13.19) and Brooklyn's 86.226.18 be a form of incisure? In addition, it is interesting to notice that in the same passage Pliny also tells us that there is a type of *lomentum*, called *tritum*, or "ground," which is the most inferior quality of *caeruleum* (blue pigment), obtained, according to its name, through grinding.⁴⁰ *Lomentum* is, according to Hillary Becker, a type of EB,⁴¹ but some of Pliny's descriptions are confusing; *lomentum* is derived from one of the *caerulea*, but which one, one of those described by Pliny?⁴² While Pliny is specifically referring to indigo for incisures, there is no reason to exclude the use of other pigments for similar purposes. In addition, it would be overly simplistic to assume that all artists followed the same directives. The gray brushstroke observed on MN 0251 (figs. 13.4 and 13.17) is found on both highlights and shadows and may correspond to an incisure, but executed with EB rather than indigo, potentially suggesting an additional element of variability in these portraits.

With its low price, *tritum*, likely intended by Pliny as a washed-out blue pigment, might have been a good option for skin tones, whites of the eyes, incisures, and shadows, where a large-grained blue pigment might not have been strictly necessary but was perhaps best preserved for creating more intense hues of blue, as well as greens and purples.

According to the study of F. Delamare, desaturated or lighter forms of EB appear to have been privileged over darker hues on the market.⁴³ Intriguingly, *lomentum*, which was a blue pigment of lighter shade, was more highly

valued (10 denarii per pound) than the blue pigment from which it was made (8 denarii per pound).⁴⁴ Based on the examples analyzed by Delamare, however, grinding was not the reason for the lighter color of the many blue pigments found in Pompeii, as all examples showed a nearly identical particle size distribution. Rather, admixtures with white pigments such as aragonite, calcite, and lead white, or the processing method, which can result in an incomplete reaction and therefore a lighter color, appear to have been some of the factors influencing the pigments' hue. Particle size may play a role, but not through grinding; instead, an intentional mixture of two distinct particle sizes with different concentrations of EB could result in different tones.⁴⁵ More recent studies, however, have highlighted additional different pathways for the creation of light-colored EB pigment in Greek contexts.⁴⁶

Looking forward, high resolution VIL imaging (fig. 13.13) may provide a means to perform granulometry of the cuprorivaite centers, which are responsible for the emission of infrared radiation in EB. As an extension of this study, computer algorithms will be employed to measure the size of the particles from VIL images and generate frequency distributions of the granulometry. This type of analysis may provide insights into the types of EB used in Roman Egypt and beyond. As VIL imaging does not, however, provide information on associated materials, such as unreacted reagents or impurities that may have originally been part of the raw pigment, the results must also be compared with complementary analysis of pigment dispersions.

Close examination of the use of pigments in panel portraits has revealed a high level of complexity. The study of this corpus of paintings is of great importance that not only sheds light on this group of objects, but also provides a useful term of comparison for the study of related materials such as sculptural polychromy, which is less well preserved and more difficult to interpret.⁴⁷ It appears reasonable to expect similar levels of complexity in works of art in diverse media, emphasizing the need for caution in the interpretation of highly fragmentary material evidence. This study revealed a variety of uses of pigments, and as more examples become available, these uses may help in distinguishing among schools of practice, practical pictorial needs, and even personal choices.

ACKNOWLEDGMENTS

The authors are grateful to Susan Manilow, who warmly welcomed us to investigate the portraits in her collection.

The authors also wish to thank William Parkinson, Jamie Kelly, J. P. Brown, and Stephanie Hornbeck for their generous support during the investigations of the portraits at the Field Museum of Natural History. Thanks are due to Joan Mertens for introducing us to the study by Elfriede R. Knauer.

NOTES

1. Verri and Brecoulaki 2023.
2. See for example Ebbinghaus et al. 2022A; Svoboda and Cartwright 2020; Salvant et al. 2018; Delaney et al. 2017; Ganio et al. 2015; Verri, Oppen, and Lazzarini 2014; Verri 2009A.
3. Verri 2009B; Verri and Saunders 2014.
4. Pouyet et al. 2020; Verri 2014.
5. Parlasca and Frenz 2003, 87, tab. 187, fig. 8.
6. Parlasca 1977, 61, tav. 90, figs. 3 and 4; Sabino et al. 2019; Sutherland, Sabino, and Pozzi 2020.
7. Parlasca 1977, 53, tab. 83, fig. 2; Parlasca and Frenz 2003, 38, tab. 1, fig. 1.
8. Parlasca 1977, 54–55, tab. 84, fig. 2; Jensen and Muhlestein 2020, 142–44, fig. 6.5.
9. Parlasca 1969, 58, tab. 27, fig. 6.
10. Verri and Brecoulaki 2023; Svoboda and Cartwright 2020; Thiboutot 2020; Salvant et al. 2018; Ganio et al. 2015; Verri, Oppen, and Lazzarini 2014, 166, fig. 10a–f; Verri 2009A.
11. In most portraits, scattered grains of EB are found throughout the face, but they are difficult to interpret and may be the result of, for example, a contaminated brush or a re-deposition of loose pigment, rather than being intentional.
12. Delamare, Monge, and Repoux 2004.
13. See note 11.
14. The presence of calcium oxalates was detected through a ν_a at ca. 1645 cm^{-1} and another sharp band at ca. 1323 cm^{-1} ; for more details on oxalate bands, see Monico et al. 2013.
15. The transformation of the binding medium and its enrichment with oxalates changes the chemical and physical characteristics of the paint layers, including the transparency of the binding medium.
16. By contrast, the white drapery of AIC 1922.4799 does not contain any EB, while that of AIC 1922.4798 is rich with it. This indicates that the pigment was deliberately chosen for particular applications.
17. Verri, Oppen, and Lazzarini 2014.
18. Luminescence from the skin tones is due to the presence of Cd-based pigments used during conservation treatments.
19. Verri and Brecoulaki 2023.
20. ISAC 9137 has undergone color change, making it very difficult to determine the original color of the eyes.
21. Generally referred to as *false* or *optical blue*, the addition of small amounts of carbon-based blacks to white pigments can give a bluish overtone. See Brill 1980, 87, 93–94.
22. The “naturalism” of panel portraiture occasionally addressed individuals affected by different conditions, including those of the eye. Medical conditions represented in panel portraits have been the subject of scholarly research; see Allen 2005, 37–38, no. 32. The reasons behind the use of bluish or reddish pigments for the sclerae can be various and include painting techniques and traditions, as well as imitation of real-life hues. However, deterioration of paint layers may also result in color change (see ISAC E9137). At present, no correspondence between bluish and reddish sclerae and medical conditions can be established; every individual case would need to be assessed with painting and medical specialists.
23. Hett 1936.
24. Verri and Brecoulaki 2023; Verri et al. 2025.
25. The bottom-left corner of the panel is not original to the painting. Another drapery is visible in the Pb_L map, suggesting that a piece from another portrait panel was used for restoring the integrity of the painting (see fig. 13.8).
26. Related findings, albeit executed likely with madder, are reported in Mayberger et al. 2020.
27. In the copper map of both MN 0251 and MN 0252, the four dots by the eyes and the neck, alongside the pins at the edges of the portrait, are related to the brass support system.
28. The presence of a blue dye, likely indigo or woad, in the hair is inferred based on a characteristic pseudo absorption at ca. 660 nm. See Aceto et al. 2014.
29. For processing false-color images see Aldrovandi et al. 2004.
30. The presence of madder lake is inferred based on its UV-induced luminescence properties in the UIL image.
31. Bradley et al. 2020, 76, figs. 7.15 and 7.16.
32. Pliny the Elder 77–79 CE, XXXV.XXX.48.
33. Thiboutot 2020.
34. The distinction here is between indigo, a pigment imported from India, and the less expensive color extracted from woad. Both indigo and woad produce indigoids.
35. “Again, for want of indigo, they dye Selinusian or anularian chalk with woad, which the Greeks call ισόαρις , and make an

- imitation of indigo,” (Morgan 1914). The Latin text reported here follows Krohn 1912; Vitruvius, *De Architectura* 7.14.2.
36. Dated to the early ninth century CE, it is the earliest extant version of Vitruvius's *De Architectura*. On the Harleian manuscript, see also Granger 1931 and Granger 1934.
 37. Wiener 1921, 333–36.
 38. Caley 2008, 63; on *vitrum*, see also Augusti 1967, 119, Knauer 1993, 23–84, and Cowell and Craddock 1995.
 39. Pliny the Elder 77–79 CE, XXXIII.LVII.163: “It is not so long since that *indicum* began to be imported, whose price is seven denarii. Painters make use of it for incisures, that is the division of shadows from light. There is also a *lomentum* of very inferior quality, known to us as *tritum*, and valued at only five asses per pound” (Bostock and Riley 1855).
 40. Pliny the Elder 77–79 CE, XXXIII.LVII.162.
 41. Becker 2021, 16–17. If *lomentum* is EB, or one of its derivatives, the subsequent section of the text is hard to understand, as it reports that it cannot be used with lime: *usus in creta; calcis inpatiens* (used for clay; intolerant to lime) (Pliny the Elder 77–79 CE, XXXIII.LVII.162).
 42. Colombo 1995, 96. The confusion, as expressed by Colombo, hinges on the interpretation of the word *usus* (it is used/ needed), and whether it refers to *lomentum* or *caeruleum*, of which there are several types. As from a syntactic standpoint it could refer to both, it generates an inevitable level of uncertainty in the interpretation.
 43. Delamare, Monge, and Repoux 2004, 107, annexe.
 44. Pliny the Elder 77–79 CE, XXXIII.LVII.162.
 45. Delamare, Monge, and Repoux 2004.
 46. Kostomitsopoulou Marketou et al. 2020.
 47. Verri, Opper, and Lazzarini 2014; Verri and Brecolaki 2023.

Insights into the Materials and Technique of a Roman Egyptian Funerary Portrait Obtained from Elemental Mapping and Luminescence Imaging

*Stephanie Spence
John Twilley*

The collection of the Nelson-Atkins Museum of Art contains a Roman Egyptian funerary portrait from Antinoöpolis stylistically dated to the second century CE. Acquired in 1937, this encaustic painting on wood panel is representative of a corpus of funerary portraits painted during the Roman rule of Egypt from the first through third centuries CE. The portrait depicts a young woman with an austere expression, dressed in a deep red tunic with a black-and-white striped collar (or undertunic), and black clavi at the shoulders (fig. 14.1). The sitter is set against a dark gray background that transitions to a light gray highlight directly behind her head. The woman's large, almond-shaped eyes are accentuated by individually painted lashes, and thick, arched eyebrows. Deep shadows and bright highlights on her olive complexion emphasize her strong features. Her jewelry, rendered in relief using gilt stucco, includes pendant earrings in the form of grape clusters, a gold necklace inset with dark blue stones modeled in painted stucco, and two hairpins that secure hair piled tightly atop her head in a thick plait. Multiple

application techniques can be observed, including the marks of a sharp, pointed instrument used to render complex shading and delicate details of the face, neck, and head, while wide, vertical brushstrokes were used in the garment and background.

One gilt stucco hairpin and the right earring are lost, revealing the wood support and stucco remnants. The necklace's painted blue stones are darkened by accretions and dirt that visually obscure the original color. The painted surface of the stone located to the proper left of the central stone is lost, leaving behind broken stucco remnants. The central blue stone in the necklace is cracked down its center, correlating to the vertical split through the center of the wood panel that was mended prior to painting and repaired by modern intervention. A clear coating applied along the central split below the large loss in the woman's hair has darkened the paint surface from the forehead to the right nostril. The paint surface near the

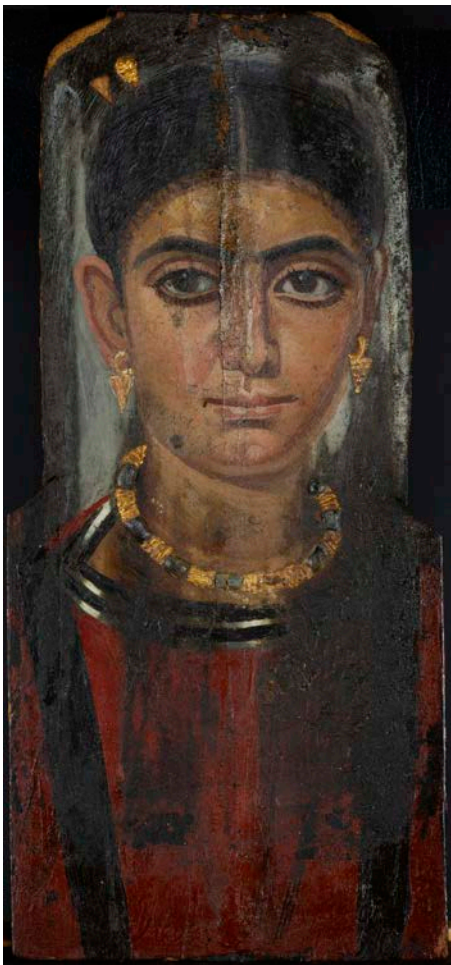


Figure 14.1 Portrait of a Woman, Romano-Egyptian, ca. 131–160 CE. Encaustic on wooden panel with gilt stucco, 44.5 x 17 cm (17 1/2 x 6 3/4 inches); panel thickness: 4 mm. Kansas City, the Nelson-Atkins Museum of Art, 37-40. Photo: S. Spence and K. Hamilton, Courtesy of the Nelson-Atkins Museum of Art

bottom of the panel is slightly sticky, with dust fibers stuck to the surface.

There are cracks in the encaustic surface throughout the portrait. The most significant paint losses are located at the top of the panel around the central crack and throughout the garment. Blanching of the paint surface has occurred in the dark background, namely along the proper left side, in smaller portions of the hair, and along the upper proper right side. Black surface deposits and staining visibly obscure a large portion of the sitter's garment and extend into the neck. The paint surface hidden below these accretions on the proper left side is damaged with some paint loss. The paint is smeared around the collar and tunic, suggesting the wax was in a softened state when this damage occurred. The black deposits terminate around the outer edges of the clavi, several inches above the bottom of the panel, suggesting

the outer edges of the panel were somehow protected from these deposits. Although there is no visual evidence of textile on the front, the well-preserved edges may indicate where the linen wrappings once secured the panel in place over the head of the mummified remains.

All that is known of the painting's provenience is based on art historical critique from visual examination. The shape of the Nelson-Atkins panel, which lacks all outer remnants of the mummy wrappings, exhibits stepped shoulders that have been recognized as a unique characteristic of works from Antinoöpolis.¹ Portraits from Antinoöpolis are cited for the depiction of solemn subjects wearing austere fashion, tightly confined hair styles, and include women often swathed in drapery.² Scholars have narrowly attributed the portrait to the early Antonine period (131–160 CE) based on her hairstyle, which is parted down the center and piled atop her head in a thick bun with a line of fine curls at the forehead.³

This paper focuses on a recent technical study that attempted to broaden our understanding of this encaustic work by clarifying the artist's working techniques and material choices not accessible through visual assessment alone. As more portraits are added to the Getty's APPEAR (Ancient Panel Paintings: Examination, Analysis, and Research) project database, comparison of the Nelson-Atkins's single example of this type of portrait with those from other collections may contribute to a better understanding of the group.

METHODS

Several non-sampling examination techniques were employed to investigate the materials, composition, and working techniques of the portrait, followed by microanalyses of a small number of samples. The structure, condition, and extent of restoration were investigated without sampling by X-radiography, multiband imaging (MBI), and surface microscopy. MBI employs technology to observe an object in wavelength ranges that extend beyond the capabilities of the human eye, from the ultraviolet (UV) to the near infrared (NIR).⁴ Images were captured using a UV-VIS-IR-modified Nikon D7000 DSLR camera with a 60mm lens and a set of UV-VIS-IR bandpass filters. While the imaging set was comprehensive, only those images with diagnostic relevance will be discussed.

Elemental mapping by X-ray fluorescence spectrometry (XRF) was conducted on the painting using a small, portable instrument built in-house following a design provided by collaborators from the Laboratoire

d'archéologie moléculaire et structurale–Centre national de la recherche scientifique (LAMS-CNRS), Paris, that has been previously published.⁵ Our instrument differs from the published design only in its use of a machined aluminum coupling component that offers improved heat dissipation for the detector's electronics and two-axis motion in only X and Y directions. The essential features and operating conditions of the instrument include a Moxtek end-window X-ray tube with Pd anode, operated at 40kV and 50 μ A, and an Amptek X123 SDD detector with 25mm² area. The tube output is collimated by a 0.7mm diameter Pd tube yielding an effective spot size of 1mm at the standoff distance of 15mm. Maps were acquired in two rectangular runs overlapping in the region where the panel width increases, one for the face and the other for the torso. The face was acquired over a 170 x 240mm area at 1mm spacings using dynamic acquisition (on the fly) with an acquisition interval of 0.5 seconds per spectrum. The torso acquisition was done over 205 x 210mm with a longer dwell time of 0.75 seconds. Acquisition control was programmed in Python and spectra were fitted using PyMca.⁶ Elemental maps output with 32-bit grayscale were rescaled to 8-bits for reproduction as standard graphics.

Microsamples from the red tunic and hazy background deposits were analyzed by polarized light microscopy (PLM) and scanning electron microscopy coupled with energy-dispersive X-ray spectrometry (SEM-EDX).

RESULTS AND DISCUSSION

Egyptian Blue

Egyptian blue, the synthetic blue pigment composed of copper calcium silicate, exhibits unique and intense photoluminescence that provides a complementary method to reflectance spectroscopy. The strong photo-induced near-infrared (NIR) luminescence emission at 910nm has been used as a characteristic marker to identify and map Egyptian blue in ancient paintings using visible-induced infrared luminescence (VIL) photography.⁷

Egyptian blue was initially discovered in the painting with VIL, showing sharply defined strokes contouring the figure's eyes, brow line, head, and neck (fig. 14.2). XRF elemental mapping showed copper concentrations in the same areas of the face and neck, confirming the use of Egyptian blue in the painting (fig. 14.3A) while also disclosing copper in another form in the dark blue stones of the necklace. The stones are rendered in stucco relief and painted with a second copper-containing pigment that has not been identified in this study. Although the painting

does not appear to visually employ Egyptian blue in the facial features, VIL and XRF uncovered the artist's use of the blue pigment in two distinct roles: (1) as a means of sketching the underdrawing and (2) in the modulations of flesh tones in the upper-layer stratigraphy.



Figure 14.2 VIL image showing the presence of Egyptian blue in the face and neck of the portrait in figure 14.1. Camera: Nikon D7000 DSLR (modified), X-Nite 830nm filter. Lighting: ADJ LED panels in red light setting- CL01. Photo: S. Spence and K. Hamilton, Courtesy of the Nelson-Atkins Museum of Art

The copper response in the facial areas does not consistently correspond to either highlights or shadows but also seems to have been a means of laying out the proportions of the face as an underdrawing. A noticeable feature of the Egyptian blue distribution is the peak in each brow line that, together, form an "M." An X-radiograph of the portrait shows the density associated with the heavier Egyptian blue applications that appear to be sketch lines above the eyes and along the nose (fig. 14.4). While lead white is also present in the face and contributes to the total radiographic density, the Egyptian blue application correlates to locations of increased density in the radiograph. When comparing the VIL image and copper map to the visible light image, the lines of Egyptian blue are in close proximity to the highlight above the eyebrows containing lead. Several blue particles are visible on the surface of the highlights when viewed under magnification, indicating the presence of some Egyptian blue in the paint mixture. A direct overlay of the elemental maps for copper and lead shows, however, some offset of the areas of maximum intensity for the two elements in the eyebrow and nose constructions. The lines for Egyptian

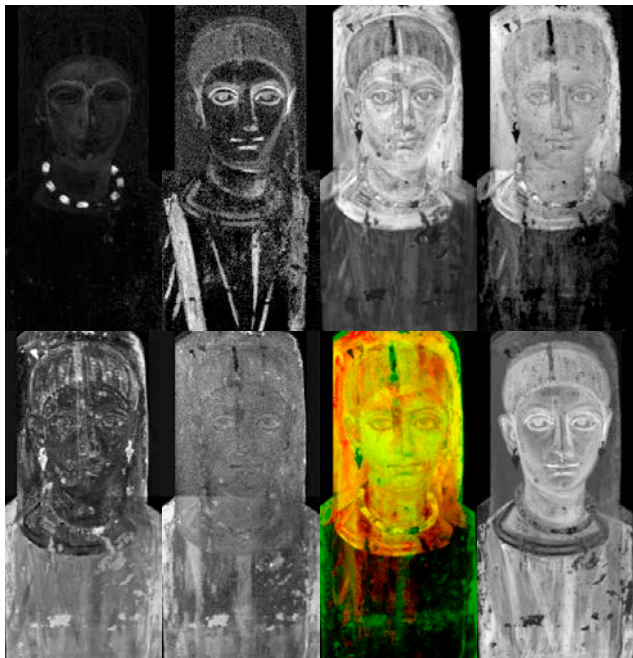


Figure 14.3 (A) Copper distribution map derived from XRF elemental mapping corroborates the Egyptian blue found in the same areas of the VIL image in figure 14.2. Higher copper concentrations in the three-dimensional necklace beads indicate that a different copper-based pigment was used there. (B) Manganese distribution map derived from XRF elemental mapping demonstrating a pronounced difference in manganese content between the two dark vertical stripes that reveals the artist's adjustment of the pigment mixture in accordance with the illumination direction. (C) Lead distribution map based on the Pb L-lines shows the selective use of lead pigment in the upper portion of the panel. (D) Lead distribution map based on the lower energy Pb M-lines also corroborates the selective application of lead in the portrait. (E) Calcium distribution map showing the muted response of calcium in much of the upper portion of the panel where Ca emissions from the preparation layer are absorbed by overlying lead paint. (F) The sulfur distribution map also shows a muted response in the upper region, suggesting that the presence of both S and Ca is indicative of a gypsum layer applied below the upper paint layers containing Pb. (G) False-color RGB image in which Pb M-lines and Cl K-lines have been assigned to the red and green channels, respectively. The resulting yellow color is indicative of the correlation of these two elements and corresponds closely to the distribution of haze formations around the head. (H) Iron map demonstrating the important role of iron pigments throughout the composition. Photos: J. Twilley, Courtesy of the Nelson-Atkins Museum of Art

blue fall slightly below and to the left of surface highlights that correspond to the lead map above the eyebrows and along the nose, respectively.

Underdrawings detected in a small number of portraits to date have more often relied on carbon black or madder than on Egyptian blue.⁸ The prominent role of Egyptian blue in this painting and its use in sketchwork are not apparent in normal viewing. In the absence of historical accounts of artists' techniques from the period, a possible explanation could be that the pigment's coarse texture allowed the sketch to remain perceptible beneath successive paint applications as an increased roughness



Figure 14.4 X-radiograph revealing greater radio-opacity associated with the M-shaped lines of Egyptian blue seen in the VIL image (fig. 14.2) and the greater thicknesses of the relief decorations, including those visible in the Cu distribution map (fig. 14.3A). Settings: 60kV; 3mA; 5 second exposure; film. Photo: J. Rogers, Courtesy of the Nelson-Atkins Museum of Art

until the work was nearly complete. A portrait of a woman excavated from the site of Tebtunis in the collection of the Phoebe A. Hearst Museum of Anthropology (PAHMA #6-21375) shows another example of Egyptian blue identified in the face that appears to be employed as an underdrawing, also discovered through VIL and complementary XRF methods.⁹ Much like that of the Nelson-Atkins's sitter, VIL reveals Egyptian blue in outlines along her face and on the "M" above the sitter's eyebrows.

The more common role of Egyptian blue—mixed with other pigments to enhance their colors¹⁰—is also seen in the Nelson-Atkins's portrait. Egyptian blue was used to modulate flesh tones in both highlights and shading around the eyes, ears, nose, neck, and forehead. While a blue hue is imperceptible in these areas, examination of the paint surface under a stereomicroscope revealed particles of Egyptian blue in corresponding areas of highlights and shading as suggested in the VIL image and copper distribution map (fig. 14.5). Along with unproven examples, portraits from Hawara and Saqqara have been found to utilize Egyptian blue in this manner.¹¹ A VIL study of Egyptian blue in Roman Egyptian funerary portraits from the Cantor Arts Center at Stanford University¹² confirmed the pigment was used in idiosyncratic ways in the flesh tones, garments, and eyes, but its use for underdrawing is noticeably absent from those findings.



Figure 14.5 Photomicrograph showing blue particles visible in the paint surface of the highlight under the sitter's right eye, corresponding to the regions with VIL responses for Egyptian blue (fig. 14.2) and XRF responses for copper (fig. 14.3A), as seen in the stereobinocular microscope with fiber optic illumination. Photo: S. Spence, Courtesy of the Nelson-Atkins Museum of Art

Umber

Elevated levels of manganese in dark areas of the painting were identified with elemental mapping. Manganese is elevated in shadows of the garment folds and shading of the facial features, both presumably using some form of umber (fig. 14.3B). Umber is known to be used in varying proportions with iron-earth pigments, carbon black, and lead white to achieve variations in brown tones in mummy portraits.¹³ A reflected infrared (IRR) image serves to differentiate nuances in dark brown and black passages when compared to the distribution of manganese derived from XRF mapping by revealing the distribution of carbon blacks not detectable with XRF (fig. 14.6). The IRR image demonstrates that carbon black was utilized in areas such as the hair, eyes, eyebrows, clavi, striped collar, and dark shading in the tunic.

It is clear from this comparison that manganese and carbon black play distinct roles in the depiction of dark details in the portrait. The hair is painted overall with carbon black, iron, and a small amount of manganese. The central "V" folds and the drapery on the proper right sleeve rely heavily on manganese and very little carbon black, while the clavi on the garment are treated differently on the right and left. The proper right clavus contains more manganese than the proper left, even though the two seem to contain equivalent applications of carbon black, as evidenced by IRR. This differing treatment of the garment's symmetrical components could have contributed to a more naturalistic depiction, with illumination falling from the sitter's right side, and may

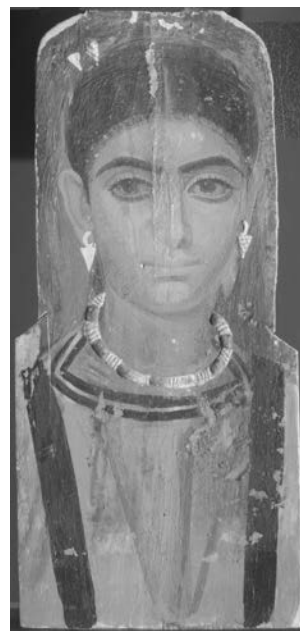


Figure 14.6 IRR image in which light absorption by carbon black is the predominant feature, providing a useful comparison for the distribution of carbon black with that of umber pigments mapped by XRF. Camera: Nikon D7000 DSLR (modified), Kodak 87C filter. Lighting: Minipro LEE Colortran tungsten light. Photo: S. Spence and K. Hamilton, Courtesy of the Nelson-Atkins Museum of Art

have once been more evident than it is today in its stained state.

Lead White

XRF mapping shows the presence of lead pigment in paint mixtures and its selective application to the region above the shoulders, including the gray background around the head, but it is noticeably absent from the torso (figs. 14.3C and D). The X-radiograph shows surprisingly little difference in density between the lead-containing background behind the head and the torso (see fig. 14.4). While this contrast is controlled by conditions of their radiography, the low contrast between the upper region and torso suggests that the lead pigment application is a thin one.

Comparison of the lead maps to XRF maps for calcium and sulfur helped to suggest the order of application of ground layers (figs. 14.3E and F). The distribution of calcium in the portrait is primarily indicative of the ground layer. The calcium map demonstrates that the heavier pigments in the upper part of the panel, such as lead, suppress the response from the relatively weaker calcium X-rays. In contrast, calcium X-rays are evident in the lower panel, especially in areas of paint loss and in the areas where the stucco earring and hairpin are missing in the upper panel.

From these findings, a calcium-based preparatory layer can be presumed to lie beneath the lead pigment on the upper panel.

The sulfur map further distinguishes the calcium-based preparatory layer identified above. With the XRF mapping apparatus employed in this study, the distribution of sulfur can be well differentiated from the overlapping response for lead M-lines, allowing calcium associated with sulfur in the form of one of the gypsum minerals to be distinguishable. This leads us to believe that a calcium sulphate ground layer was applied underneath the lead white. Additionally, this ability to separately resolve sulfur from the overlapping low-energy lead peak allows the lead response from the upper surface to be differentiated from that arising deeper in the paint layer, allowing for the comparison of the roles of lead pigment in different regions.

Lead Chloride Formation

Irregular white hazy patches obscure the darker passages of the gray background toward the outer edges of the panel (fig. 14.7). The blanching is heavily concentrated along the background behind the sitter's proper left, with some encrustations partially covering the left ear and hairline. Additional areas of blanching are present at the crown of the head and to the proper right of the hairpins. Under magnification, much of the blanching appears as a superficial crust comprised of fine, yellowish white grains of varying sizes (fig. 14.8).

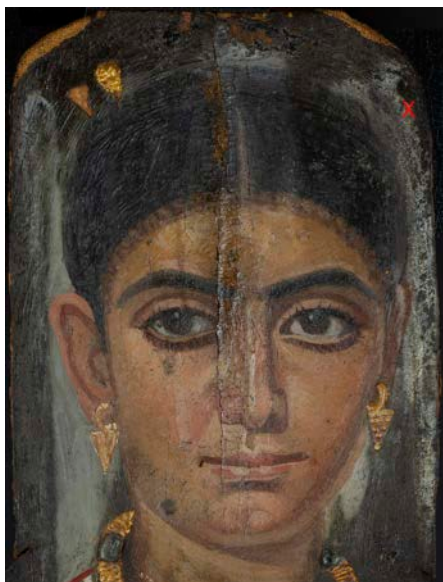


Figure 14.7 Reference image for the location (X) of the photomicrograph in figure 14.8. Photo: S. Spence, Courtesy of the Nelson-Atkins Museum of Art

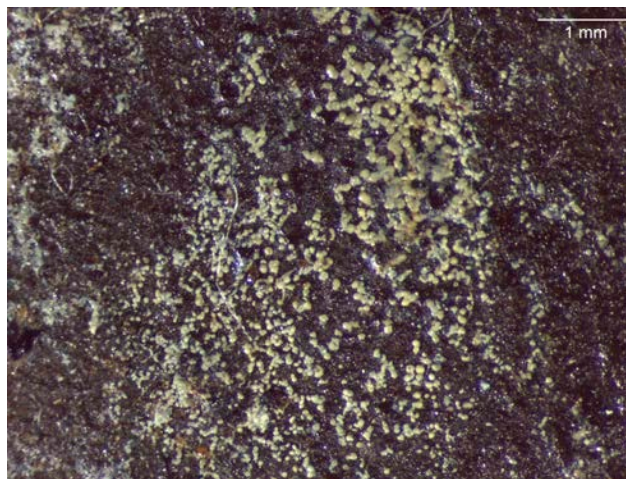


Figure 14.8 Photomicrograph of the Pb-Cl-rich white crust that has formed on the upper proper left side of the paint surface as seen in the stereobinocular microscope using fiber optic illumination. This detail shows the formation of individual yellowish white granules of varying size that appear to sit on top of the paint surface. Photo: S. Spence, Courtesy of the Nelson-Atkins Museum of Art

The element chlorine is also readily mappable with this XRF apparatus and appears to explain the blanched appearance of parts of the painting where its distribution follows that of the lead at the surface (fig. 14.3G). High levels of chlorine are visible along the proper left edge of the panel, coinciding with the heaviest concentration of the crust in the background. A microsample of this white material from the surface of the proper left side of the black background, adjacent to the sitter's hair, was further analyzed by SEM-EDX and found to consist of lead chloride without other detectable elements. This encrusted matter contained some beeswax medium identified by Fourier-transform infrared spectroscopy (FTIR) and had a gummy consistency. Unaltered lead pigment, when present in the sample, was distinguished by a finer particle size and lack of chloride. The implication of these white formations is that chloride salt, nearly ubiquitous in Egyptian artifacts from various sources and often derived from groundwater salinity or the burial environment, has interacted with the lead pigment to form lead chloride on the paint surface. Lead chloride is insoluble and thus favored to form in the interaction of most lead pigments with sodium chloride. This is a well-known phenomenon impacting not only wall paintings, but also easel paintings and lead-based architectural paints on masonry surfaces containing chlorides.¹⁴

A cross section from the forehead of a Tebtunis portrait (#6-21378b) in the PAHMA collection also contained a lead chloride compound as the main constituent in a white crust layer.¹⁵ A specific identification of the crust-forming

compound as KPb_2Cl_5 was obtained in that case by synchrotron-based micro X-ray diffraction mapping of the cross section. Therefore, while the two cases are closely related, the end product is different.

Iron-Based Pigments Including Red Ochre

The map for iron shows the extensive use of iron earths in the artist's palette (fig. 14.3H). Virtually every component of the composition relies upon iron in some form, including the red garment, all of the skin tones, and even the black in the hair. The overall red of the garment as well as its folds are rendered as variations in the distribution of this element. The rounding of the facial features in the later stages of painting that contrasts with their angularity in the Egyptian blue underdrawing is exemplified by their shapes in the iron map. The iron map also resolves pigment strokes in the hair more clearly than any other single element. It discloses the texture of the hair that could be interpreted as rows of braids at the front of the head, as well as a distinct boundary between the volume of the top of the head and that of the tightly braided hair bun in the back.

The depth of the tunic's red color suggested that this area might make use of organic lake pigment in addition to the iron-based pigment found there with elemental mapping. Ultraviolet-induced visible fluorescence (UVF) imaging showed, however, no evidence of the distinctive pink/orange fluorescence of lake pigments, such as madder (fig. 14.9). The irregular, dull orange fluorescence visible with UVF in much of the red garment also extends into most areas of the portrait, with the exception of the face. A thin strip of the red tunic and striped collar next to the inner edge of the proper right clavus is also devoid of this orange fluorescence. It is more likely that this fluorescence corresponds to a clear surface coating that was not identified in this study. The tunic also appears dark in the false-color ultraviolet (FCUV) image, corroborating the presence of red ochre without the addition of a lake pigment (fig. 14.10).¹⁶

A microsample from the red tunic near the bottom edge of the panel was examined by polarized light microscopy (PLM) and SEM-EDX to determine whether the inorganic elements detected in the garment fully accounted for its red color. PLM shows that the sample only contains a dilute amount of very fine red iron oxide particles that have been well dispersed in an excess of wax medium, causing it to function like a colored varnish and deepening its color by reducing light scattering from the surface (fig. 14.11). It is not known if red lead has been incorporated into the painting's composition elsewhere, but the lead



Figure 14.9 The UVF image does not show a response attributable to any lake pigments in the red tunic, but does show areas of restoration in the portrait, particularly down the center of the face, that correspond to the split in the wood panel. Camera: Nikon D7000 DSLR (modified), BG38 + PECA 918 + Kodak 2E filters. Lighting: Wildfire Viostorm VS-60 with a visible-cut filter. Photo: S. Spence and K. Hamilton, Courtesy of the Nelson-Atkins Museum of Art



Figure 14.10 The dark appearance of the red tunic in the FCUV image indicates the color is attributable to red ochre. This image was created through digital post-processing by combining visible and ultraviolet reflectance images. Photo: S. Spence and K. Hamilton, Courtesy of the Nelson-Atkins Museum of Art

map suggests a sparse presence of lead of unknown type in the upper regions of the red tunic (see figs. 14.3D and G). None was found in the PLM sample.

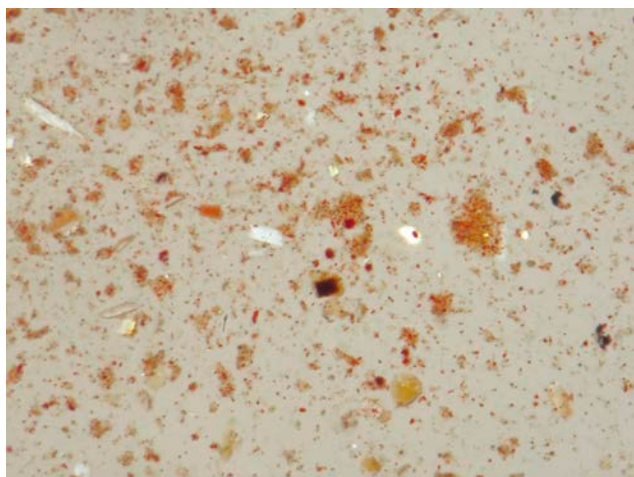


Figure 14.11 Pigment particle dispersion from the bottom edge of the red tunic confirming the presence of very fine particles of red iron oxide dispersed in an excess of medium, partially crossed polars, 100x. Photo: J. Twilley, Courtesy of the Nelson-Atkins Museum of Art

RESTORATIONS

A vertical split down the center of the panel shows evidence of both ancient and modern interventions. The paint has been consolidated in the worst areas of damage along the split in the head with a clear, glossy coating. UVF shows this coating has a milky, white fluorescence, but additional testing has not been carried out to identify it (see fig. 14.9). Due to the obvious presence of restoration coatings along the split, especially around the areas of paint loss in the head, it was assumed that repairs to the portrait occurred well after its completion, possibly at the time of excavation. However, no treatment documentation exists prior to or after its acquisition into the Nelson-Atkins collection.

The X-radiograph revealed further information about repairs to the lower half of the split hidden below the surface. While the split becomes invisible on the surface below the mouth, a narrow strip of plain-weave fabric beneath the paint layers was identified in the X-radiograph. Its texture becomes visible at the mouth and extends to the bottom of the panel (see fig. 14.4). The red tunic exhibits cracking that follows the fabric texture in some spots, but further disruptions to the paint surface that could indicate this textile was applied as a later repair, such as reworking of the wax or inpainting, are absent from the lower half of the portrait. Other splits in the panel

have not been bridged by fabric in this manner. The verso of the wood panel also has visible repairs along the crack. A dark brown resinous coating and sporadic patches of textile fragments are applied along the entirety of the vertical split (fig. 14.12). These textile fragments bear visual similarities to linen wrappings applied around funerary portraits when attached over the face of a mummy. This evidence suggests that the split in the panel was mended in preparation for painting.



Figure 14.12 Repairs to the vertical split in the panel visible from the back include a dark, resinous fill material with six fabric patches applied along the break. The patches bear visual similarities to mummy wrappings used to attach funerary portraits atop the heads of mummified remains. Photo: S. Spence and K. Hamilton, Courtesy of the Nelson-Atkins Museum of Art

CONCLUSIONS

From the time of its acquisition in 1937 until the undertaking of this technical study, the Nelson-Atkins's Roman Egyptian funerary portrait had been interpreted exclusively by means of art historical inquiry. Analysis by XRF elemental mapping and complementary imaging techniques, augmented by microanalytical techniques when necessary, has revealed hitherto unknown aspects of material usage and artist's practices. They reveal the use of Egyptian blue as an underdrawing, placing this painting within a larger corpus of funerary portraits that employed Egyptian blue as an additive to encaustic mixtures for flesh tones. The proportioning of carbon black and umber in the rendering of otherwise symmetrical dark passages of the painting reveal the painter's attempt to render the illumination of the sitter. The painter's choice of confining

the use of lead white to the upper half of the portrait is an unusual one for which no definitive explanation exists. The ability to map the distribution of chlorine by XRF demonstrated a correlation of this element with highly visible haze formations on the dark background. Confirmation of the alteration of lead white to lead chloride in SEM-EDX of haze samples, and the lack of chloride in paint not similarly affected, strongly suggests that exposure of this lead pigment to environmental chlorides over the lifetime of the portrait is the underlying cause of blanching of the dark passages behind the figure's head.

The analyses reported here have significantly furthered our understanding of the palette and working techniques in the Nelson-Atkins portrait. They have allowed us to explore both similarities and differences between this work and those investigated by other researchers, including some whose provenance is securely known. As a group, their working techniques are highly diverse and trends or groupings are only beginning to come into focus. Mineralogical analysis of the widely used earth pigments in the painting could advance our understanding of the individual pigments found in mixtures. The medium, which has not been investigated beyond FTIR confirmation that it is based upon beeswax, could provide further information about the painting through analysis by gas chromatography/mass spectrometry (GC/MS) methods. The wood and restoration materials remain yet to be identified as well. Future research of these materials will continue to broaden our knowledge of this portrait and its place within the history of Roman Egyptian funerary portraiture.

ACKNOWLEDGMENTS

The authors would like to thank Kasey Hamilton for her contributions in imaging our portrait.

NOTES

1. Doxiadis 1995; Parlasca 1966; Walker and Bierbrier 1997.
2. Walker and Bierbrier 1997.
3. Taggart 1959; Vermeule 1964; Doxiadis 1995.
4. Dyer and Newman 2020.
5. De Viguerie et al. 2018.
6. Solé et al. 2007.
7. Verri 2009A; Accorsi et al. 2009.
8. See Mahon et al., this volume; Mayberger et al. 2020.
9. Ganio et al. 2015.
10. Thiboutot 2020.
11. Dyer and Newman 2020; Park et al. 2019; Sabino et al. 2019.
12. Thiboutot 2020.
13. Park et al. 2019.
14. Ordonez and Twilley 1998.
15. Salvant et al. 2018.
16. Dyer and Newman 2020.

Linked Histories: Understanding the Making and Remaking of a Roman Egyptian Portrait at the Detroit Institute of Arts Through Comparison to a Funerary Portrait at the Walters Art Museum, Baltimore

*Christina Bisulca
Ellen Hanspach-Bernal
Aaron Steele*

Among the Egyptian antiquities in the Detroit Institute of Arts (DIA) is a Roman-period funerary portrait (fig. 15.1A).¹ Little is known about this portrait's archaeological provenience. Records at the DIA indicate only that the object was given to the museum in 1925² by Julius Haass (1869–1931),³ who, at an unknown time, had purchased it from the art dealer Dikran Kelekian (1867–1951).⁴

Despite the lack of archeological information on the DIA panel, the similarities in style and provenance with another funerary portrait now housed in the collection of the Walters Art Museum in Baltimore (fig. 15.1B)⁵ have been known since David Lowell Thompson's 1972 thesis.⁶ Most notable are the nearly identical high-relief coin pendant necklaces (figs. 15.2A and B), which (to date) are unique to these two portraits. Both portraits are believed to have originated from Antinoöpolis⁷ and their sale to American

collectors was facilitated by the Kelekian Gallery in both instances.⁸

The APPEAR project initiated the independent examination of these two portraits in recent years. Because of the resulting wealth of information, a close comparison between the materials and techniques of the two panels promised further insights into the original makers as well as later alterations to the objects.

The Detroit portrait was examined by close visual observation, using primarily non-destructive instrumentation relying heavily on point analysis with visible near-infrared fiber optics reflectance spectroscopy (vis-NIR FORS), X-ray fluorescence (XRF) spectroscopy, and various imaging techniques. Samples were removed from the edge of the panel to yield further information about

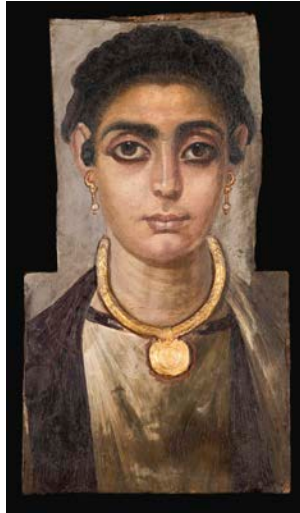


Figure 15.1A Head of a Woman, Egyptian (Antinoöpolis?), late second-third century CE. Encaustic with gilded stucco on tamarisk panel, 44.8 x 24.8 x 1.5 cm (17 5/8 x 9 3/4 x 5/8 in.). Detroit Institute of Arts, gift of Julius H. Haass, 25.2.

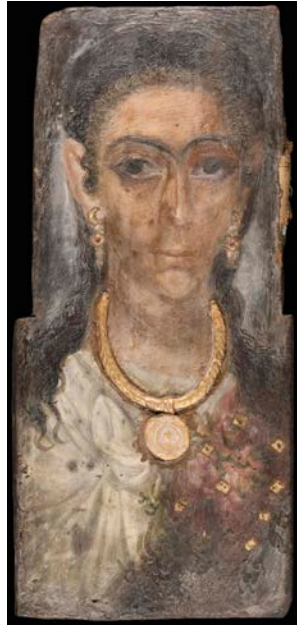


Figure 15.1B Panel Portrait of a Woman, Egyptian (Antinoöpolis), ca. 130–200 CE. Encaustic with gilded stucco on beech wood, 45.7 x 20.6 x 0.64 cm (18 x 8 1/8 x 1/4 in.). The Walters Art Museum, Baltimore, acquired by Henry Walters, 1912, 32.4.



Figure 15.2A Raking light image of figure 15.1a, showing distinct paint application marks and dimensionality of high relief necklace. Detroit Institute of Arts, gift of Julius H. Haass, 25.2.



Figure 15.2B Raking light image of figure 15.1b, showing distinct paint application marks and dimensionality of high relief necklace. The Walters Art Museum, Baltimore, acquired by Henry Walters, 1912, 32.4.

the binding media and pigment components of select colors. For technical information on the corresponding panel, we relied on the extensive research that was undertaken by the Walters Museum’s Department of Conservation and Technical Research.⁹

MAKING THE FUNERARY PORTRAITS

The Panels and Their Preparation

The wood from which the Detroit panel was cut was identified as native tamarisk (*Tamarix aphylla*) by Caroline R. Cartwright of the British Museum.¹⁰ Within the known body of wooden mummy portrait supports, the choice of this native wood is unusual.¹¹ Tamarisk is not of particularly high quality and panels made from this material needed to be of a thicker cut to maintain stability, reflected in the 1.5 cm depth of this board (see fig. 15.6A). Though comparable in size and shape, the Walters panel was made from a different wood, beech (*Fagus* sp.), and at 0.6 cm it is half as thick as the Detroit portrait. The different thickness in the boards could point to adjustments that were made by the carpenters in response to different woodworking characteristics or to prior use.

Panels believed to have originated from Antinoöpolis generally show a wide range of different wood species: native sycamore fig (*Ficus sycomorus*) or cedar of Lebanon (*Cedrus libani*),¹² for example, have also been identified. Compared to the very thin panels made from linden wood (*Tilia* sp.)—speculated to have been flexible enough to follow the contours of the mummy’s face—most of the Antinoöpolis boards are also of substantial thickness, some measuring up to 2 cm.¹³ In this context the Detroit and even the Walters panels may not be such outliers. They may fit well within local artistic traditions and preferences in how these panels were prepared and later enclosed within the wrapped shroud.¹⁴

Much of both panels’ reverse surfaces (figs. 15.3A, 15.4A, 15.4B) are coated with a dark, glossy material, identified as a terpenoid resin,¹⁵ assumed to have been added during mummification. In addition, both panels include resin-soaked textile fragments from the mummy wrapping adhered to the reverse.¹⁶ Today, these fragments remain the most tangible connection of the portraits to their original function and larger mummy assemblage.



Figure 15.3A Verso of figure 15.1A. Brushed-on calcium carbonate preparations, an ancient intervention, indicated by various blue circles. Filled or plugged holes, an ancient intervention, indicated by various yellow/orange circles. Note corresponding locations in figure 15.3B. Also note the modern repairs such as fills and a fabric patch. A resinous coating and shroud fragments from the mummy wrapping have remained. Detroit Institute of Arts, gift of Julius H. Haass, 25.2.

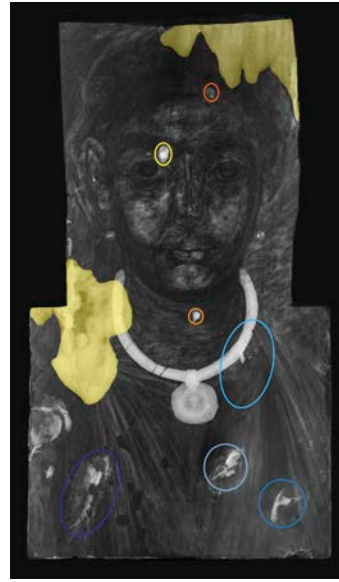


Figure 15.3B X-radiograph of figure 15.1A. Ancient wood preparations indicated by various yellow/orange and blue circles. Note corresponding locations in figure 15.3A. Large areas of modern restoration along left step and upper-right corner are indicated in light yellow. Detroit Institute of Arts, gift of Julius H. Haass, 25.2.



Figure 15.4A Verso of figure 15.1B. Drilled and filled holes, an ancient intervention, indicated by various yellow/orange circles. Note corresponding locations in figure 15.4B. Traces of possible white preparations visible in the bottom half. Also note opened insect tunnels. A resinous coating and shroud fragments from the mummy wrapping have remained. The Walters Art Museum, Baltimore, acquired by Henry Walters, 1912, 32.4.

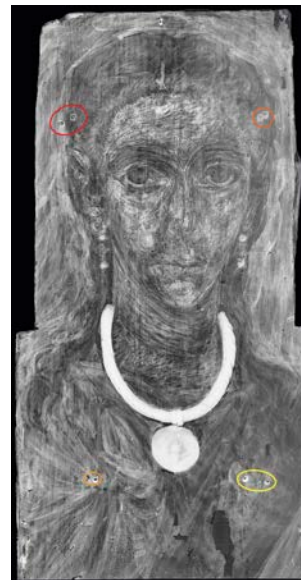


Figure 15.4B X-radiograph of figure 15.1B. Drilled and filled holes, an ancient intervention, indicated by various yellow/orange circles. Note corresponding locations in figure 15.4A. The Walters Art Museum, Baltimore, acquired by Henry Walters, 1912, 32.4.



Figure 15.5A Detail of figure 15.3A showing brushed-on calcium carbonate preparation with resinous coating residue and a filled hole from a removed knot. Detroit Institute of Arts, gift of Julius H. Haass, 25.2.



Figure 15.5B Detail of figure 15.4A showing a plugged and a filled drill hole as well as resinous coating residue. The Walters Art Museum, Baltimore, acquired by Henry Walters, 1912, 32.4.

The wood grain of the Detroit panel is irregular and includes numerous small defects, some of which appear to have ancient repairs. On the back of the panel, just below the center, a thick white coating containing calcium carbonate¹⁷ was loosely brushed over knots in the wood (fig. 15.5A). Similar applications, near the bottom edge, are now mostly covered by a modern repair comprising polyvinyl acetate (PVA) and sawdust (see fig. 15.3A).¹⁸ The calcium carbonate preparations can also be observed as amorphous shapes in corresponding areas in the X-radiograph (fig. 15.3B). They are identified as ancient because they are covered by the terpenoid resin coating associated with the attachment of the panel to the mummified body. Also detectable in the X-radiograph taken from the back are additional small round fills and possibly dowels (see fig. 15.3B). These repairs were inserted from the front, suggesting that holes left from removed knots or of other origin were plugged prior to ground and paint application.

The Walters's wood, in contrast, is speculated to have been reused. The boards have open insect tunneling on the reverse. Some of this tunneling is filled with pine resin that was applied with the textile wrapping. This suggests that an older board, already insect damaged, was cut and prepared for painting (fig. 15.4A).¹⁹ Drill holes with no direct function to the portrait are also present (figs. 15.4A,

15.4B, and 15.5B). Both boards show evidence of similar wood preparations, such as holes that were filled or plugged as well as brush-applied fill material.²⁰

A rectangular area on the back of the Detroit panel (see fig. 15.3A)—located parallel to the top edge—is noticeable because it is not fully coated with resin. It appears as if an external piece (e.g., a strip of wood or fabric) had once covered this section. This feature could either indicate an element attached for the initial preparation of the panel or a post-excavation modification, perhaps for mounting. No such evidence can be observed on the back of the Walters panel.

Examination of the panels also suggests that both boards were sawed into their distinct stepped shape only after painting was completed. No ground or paint layers overlap onto the sides of the narrower top section (fig. 15.6A) and a distinct tool cut can be observed in each panel where the horizontal step is placed.²¹ Paint from the front still extends over the sides of the wider bottom half on the Detroit panel, indicating that these are the initial edges of the board (fig. 15.6B). Some of the edges on the reverse of each panel were also beveled: specifically, the top edge of the Walters panel and the bottom left edge of the Detroit portrait (see figs. 15.3A and 15.4A). The changes to the boards' dimensions after painting suggests that the final



Figure 15.6A Left edge (seen from back) of figure 15.1A, detail showing cut edge after paint application; note gum residue and fabric fragment. Detroit Institute of Arts, gift of Julius H. Haass, 25.2.



Figure 15.6B Left edge with overlapping paint layer, note beveled edge. Detroit Institute of Arts, gift of Julius H. Haass, 25.2.

shape of these panels is closely tied to the process of including the portrait within the mummy wrappings. Small textile fragments as well as dark brown residue have remained on the trimmed edges of the Detroit panel (see fig. 15.6A). The residue was identified as a polysaccharide,²² possibly a plant gum. A similar residue was not observed on the edges of the wider section of the panel.

Modern repairs in the Detroit panel indicate structural insecurities in the board. Cracks needed to be stabilized, and parts of the wood are now supported by fills and a fabric patch; these later additions are made with a polyvinyl acetate (PVA) adhesive and were likely added during an undocumented treatment.²³ Structural post-excavation interventions were not needed for the Walters panel.

The Paint Layers

A dark brown ground was thinly applied across the surface to prepare both panels for painting. This layer contains large particles in the Detroit work and is composed of a variety of materials including sand grains, calcite, red ochre, and various clay minerals.²⁴ The black pigment in the Walters's ground has a high calcium and phosphorus content suggesting bone black—a pigment that was not used in the portrait's pictorial layers.²⁵ Phosphorus and calcium were also detected in small particles of the Detroit ground in scanning electron microscopy/energy-dispersive X-ray spectrometry (SEM/EDS). However, these particles were only a very minor component and, given the inhomogeneous nature of the ground, could not be clearly characterized. It is therefore inconclusive whether bone black or some other mineral phosphate is present in the Detroit ground layer. However, the selective use of bone black in the ground layer could provide further insight into workshop practices if confirmed in other portraits.

Palette and pigment distribution are very similar in both works (fig. 15.7) but are also aligned with techniques observed on other funerary portraits of the Roman period.²⁶ The white tunics, for example, are composed of lead white and natrojarosite, with Egyptian blue added in the highlights.²⁷ Although a blue tint is not perceptible, the scattered blue pigment particles can be seen under magnification. The presence of Egyptian blue in white garments or flesh tones has been found in a number of other examples.²⁸

Regions	Color	Colorants identified - DIA	Techniques	Colorants identified - Walters (Radpour et al. 2021)
Head [KP1]	Flesh tones	Red ochre, yellow ochre, lead white, Egyptian blue	Vis-NIR FORS; XRF	Red ochre, yellow ochre, lead white
Tunic (Walters) Shawl (DIA)	White	Lead white, natrojarosite, Egyptian blue	Vis-NIR FORS; XRF; VIL	Lead white, natrojarosite, Egyptian blue
Shawl (Walters) Tunic (DIA)	Purple	Indigo, madder lake	Vis-NIR FORS; XRF; UV	Madder lake
Red outline, necklace and earrings, bole	Red	Red ochre	XRF; vis-NIR FORS	Red ochre, yellow ochre, natrojarosite

Figure 15.7 Palette and pigment distribution of Detroit and Walters mummy portraits based on published and unpublished results from independent examinations at both institutions.

Madder lake²⁹ was confirmed in the purple fabrics for both works. Red madder was combined with indigo in the Detroit panel to create the dark purple tones in the tunic.³⁰ Indigo was not detected in the purple garment depicted in the Walters panel, which could explain the overall lighter hues compared to the Detroit paints. The use of madder

lake mixed with indigo in purple garments is consistent with finds of other funerary portraits, for example Portrait of a Woman (Harvard Art Museums), also believed to be from Antinoöpolis.³¹

The binder was identified as wax—most likely beeswax—in the pictorial layers of both works.³² As a consequence, the paint application techniques are analogous. In both paintings the artist employed a stiff, narrow tool that left fine concave marks in areas where complex shading was required, e.g. in the faces. In sections of uniform color, such as the background and the garments, they utilized brushes of various widths for longer, even marks (see figs. 15.2A and B).³³ A detail that indicates how close the painting techniques align is the transition from forehead to the dark braid that is modeled with brown and marbled paints in both portraits. The use of multiple application techniques within one painting has been well noted in other mummy portraits.³⁴

The Necklace

One of the most interesting and unusual features of the Detroit and Walters portraits is the high-relief, collar-like gold necklace with coin pendant (see figs. 15.2A and B). Both depict a mounted Roman coin (aureus), which became a fashionable accessory in the Roman Egyptian colonies by the third century CE (figs. 15.8A–C).³⁵ This is consistent with the radiocarbon date of the Detroit portrait.³⁶ Gold necklaces in low relief or other forms of gilt stucco are not uncommon in funerary portraits from Antinoöpolis, as seen, for example, on two painted shrouds now at the Musée du Louvre, Paris,³⁷ or a panel at the Nelson-Atkins Museum of Art in Kansas City.³⁸ The Detroit and Walters gilt stucco elements are, however, distinctive in that they are of a much higher relief than these other examples.

The necklace in the DIA portrait is made of a stucco consistent with calcium carbonate bound in a proteinaceous glue from which a moldable compound was made.³⁹ Based on visual observation, a similar white material is likely for the Walters necklace (see figs. 15.8B and 15.9B). The X-radiographs of both portraits (see figs. 15.3B and 15.4B) show that the necklaces are similar in construction and are uniform in composition. The artists applied a preparatory layer of red bole to both necklaces to receive the gold leaf (see figs. 15.8B and 15.9B). The gilding is a gold alloy that contains minor amounts of silver in both.⁴⁰ While difficult to discern because of the numerous repairs that occurred to the necklaces post-excavation, the gold leaf may cover the encaustic paint layer, which would indicate that gilding occurred directly

on the panel and after painting was completed. In a final step, the gilt necklaces were outlined in a red iron oxide pigmented wax paint. In the case of the Walters portrait, this wax outline also contains yellow ochre as well as traces of natrojarosite and is of a duller brown overall.⁴¹ The outlines form a scalloped edge around each pendant, perhaps to mimic the gold settings used to mount the coin (see figs. 15.8B and C).⁴² A white haze and reddish crust can be observed over the gilding in both necklaces.

More pronounced in the Detroit necklace is a surface texture (fig. 15.9A) that resembles the imprinted weave of a textile, possibly to mimic woven gold chains found in similar necklaces (see fig. 15.8A).⁴³ The majority of the Walters's necklace surface is smooth (see fig. 15.9B), although some areas show similar—albeit much fainter—impressions, especially in the pendant (see fig. 15.8C). Despite these differences the distinct surface texture could indicate that a textile was pressed into the surface during construction. Both necklaces also have designs that appear to be made with a straight tool impressed into the surface on both sides of the collar to create a V pattern, presumably to depict the twists of gold chains (see figs. 15.8A, 15.9A, and 15.9B). The Walters pendant and collar are smaller in size to accommodate the more delicate neck and generally smaller dimension of the portrait. This precludes the possibility that an identical mold was used in both works. Rather, the precise placement and proportional size of each necklace indicates they were individually constructed for each portrait.

The gilded stucco necklace of the Walters portrait is believed to have been attached with pitch that was removed during a past repair.⁴⁴ Evidence for the initial attachment technique of the Detroit necklace could not be found as the necklace was reattached at least three times since its excavation.⁴⁵ Fine holes are located along the periphery of this necklace. These holes could indicate where pins were once the initial attachment or during one of the more recent repairs. Similar pin marks were not noticed around the Walters necklace. It is not entirely clear when exactly in the painting process the necklaces were added. While a placement directly on the completed encaustic layer makes the most sense technically and compositionally, only the dark ground is visible in the void as seen in a historical picture of the Walters panel with the necklace removed.⁴⁶ However, paint could have been removed from this area when the necklace detached and was readhered in the past. The sequence of application could possibly illuminate whether there was a separation of labor between those who painted these portraits and those responsible for the stucco and gilding.



Figure 15.8A Necklace with Pendant Coins. Roman Empire, early third century. Gold, 47 x 2.4 cm (18 11/16 x (D) 15/16 in.). The Walters Art Museum, Baltimore, museum purchase (formerly part of the Walters Collection), 1941, 57.1600.



Figure 15.8B Detail of figure 15.1A, coin pendant made of gilded stucco. Detroit Institute of Arts, gift of Julius H. Haass, 25.2.



Figure 15.8C Detail of figure 15.1B, coin pendant made of gilded stucco. Both this and figure 15.8C show a nubby surface texture, color differences in the scalloped outline, and a reddish, milky crust. The Walters Art Museum, Baltimore, acquired by Henry Walters, 1912, 32.4.



Figure 15.9A Detail of 15.1A, necklace hoop, right of pendant, showing surface preparation and nubby surface texture. Detroit Institute of Arts, gift of Julius H. Haass, 25.2.



Figure 15.9B Detail of 15.1B, necklace hoop, left of pendant, showing surface preparation and smoother surface compared to the Detroit necklace. The Walters Art Museum, Baltimore, acquired by Henry Walters, 1912, 32.4.

POST-ANCIENT TREATMENTS

The panels depart drastically from one another in their post-ancient treatments. Little aesthetic intervention can be noted on the Walters panel where past treatments prioritized preservation. In contrast, examination of the DIA portrait revealed large areas of restoration that took place after the piece's excavation. Large losses with associated repairs are located along the left edge and the upper right corner (see fig. 15.3B). Further additions of overpaint, glues, and coatings can be observed throughout. The quality of these repairs—executed over gypsum fills in wax paint that carefully match the original technique—suggests that they were done by a restorer

who specialized in paintings and had the ability to closely match colors and brushstrokes (see fig. 15.1A). That treatment aimed to render the portrait pristine, with little visible signs of damage or loss.⁴⁷

It has not been possible to determine by whom and when this extensive restoration was completed. Photographs of the portrait taken at the time of its acquisition already document these major changes, indicating that the repairs were completed prior to its arrival at the DIA in 1925. Many early twentieth-century galleries employed restorers, which could suggest that the Kelekian Gallery arranged for the treatment of the DIA portrait prior to acquisition. A review of other mummy portraits sold through Kelekian,

however, reveals that they did not all receive the same level of restoration. One example was found to have been assembled from at least three different portraits,⁴⁸ while others show little evidence of restoration, such as, for example, the four portraits in the Walters collection.⁴⁹ With the extensive repairs present in the DIA panel, especially as they extend beneath the necklace, one even wonders if the necklace could be a modern addition, crafted after the Walters version to make the work more appealing on the market. If this was the case—at this point the necklace is still considered authentic to the painting—the Kelekian Gallery could be further indicated as having initiated the extensive reconstructions in the pictorial layer of the Detroit panel. Considering that we do not know how Kelekian acquired the DIA portrait, it is possible that the restoration was completed prior to its arrival at his gallery or that Haass had the work restored prior to donation to the DIA.

CONCLUSION

Material evidence gained directly from the Detroit mummy portrait has allowed us to bridge some of the gaps resulting from missing physical and archival information. Even though we still do not know where and when the mummy with its attached portrait was excavated, the technical information roots the work firmly in antiquity. Further, specific techniques and materials as well as stylistic features strongly suggest its production and possible deposition in Roman Egypt's Antinoöpolis.

While we are not yet equipped to determine whether the Walters and Detroit funerary portraits originated in the same or in associated workshops, the close comparison provides a more tangible context in which to interpret observations. The technical evidence gathered on the wooden boards contributes further information to the larger understanding of questions such as regional access to wood, possible uses of the portraits prior to mummification,⁵⁰ or workshop attributions based on distinct wood preparation techniques. The necklaces add complexity to the manufacture of these portraits and trigger questions about workshop organization and the relationship between the artists responsible for painting and those working on the mummy.

Through material evidence, we were also able to trace the panels' transformation from part of a mummy into a portrait painting displayed in a fine arts museum. The separation of these portraits from the human remains coupled with the absence of an archaeological context contributes to the erasure of the deceased person's

identity, as well as a loss of knowledge about the material, cultural, and religious practices that surrounded these objects.⁵¹ In the case of the DIA's funerary portrait, this technical investigation also clarified the panel's evolving functions and its modern identity as a dissociated fragment.⁵² Despite the many remaining gaps, the palpable human traces of its unknown makers and the material connection to an individual's funerary rite add important context to the research, care, and presentation of these complex ancient objects today.⁵³

EXPERIMENTAL DETAILS

XRF spectroscopy was performed using a Bruker Artax XRF spectrometer at 50 kV, 700 μ A, 0.65 mm collimator, and 180-second acquisition time. Vis-NIR FORS was performed with an ASD FieldSpec 4 HR spectroradiometer (350–2500 nm, spectral resolution 3 nm @ 700 nm and 8 nm @ 1400/2100 nm) using the ASD contact probe (~8 mm spot size) or a small-diameter bifurcated probe (~2 mm spot size). For Fourier transform infrared (FTIR) spectroscopy small samples were removed and analyzed on a Thermo iS20 spectrometer equipped with an ATR attachment, 4000–400 cm^{-1} , 4 cm^{-1} resolution, 32 scans. Transmission X-radiographs were taken with a Hamamatsu Microfocus unit (130 kV, 300 μ A, ~130 in. to subject, 9-minute exposure, 10-micron spot size); 2 exposures via Carestream HR 50-micron CR 14 x 17 in. plates. SEM/EDS was performed on a Joel JSM-7800FLV SEM with an Oxford XMaxX EDS system, 20 keV, at the Electron Microbeam Analysis Lab, University of Michigan. Further experimental details, data, and references have been uploaded to the APPEAR database.

ACKNOWLEDGMENTS

Colleagues at the Walters Art Museum, Baltimore, have been incredibly generous with sharing their knowledge and information about the mummy portrait housed in their collection. The authors extend special gratitude to Angie Elliott, Terry Drayman-Weisser Head of Objects Conservation and William B. Ziff, Jr. Conservator of Objects at the Walters Art Museum, for her support. We are grateful to Hae Min Park, Kaitiaki Taonga Conservator of Paintings, Museum of New Zealand Te Papa Tongarewa, and Lisa Anderson-Zhu, associate curator of Art of the Mediterranean, for being so generous with their expertise and time during our visit. We thank Roxanne Radpour and Glenn Gates as well as Geneva Griswold, on whose excellent published and unpublished research on the Walters portrait we heavily relied. Caroline R. Cartwright of

the British Museum, London, completed the wood identification of our panel; we are grateful for her work and her insightful, extensive analytical report. We also thank Katherine Aguirre, then graduate student in the Art Conservation Department at Buffalo State College, for her sharp observations on the Detroit portrait and her thorough research. Marie Svoboda of the J. Paul Getty Museum, Los Angeles, was always generous with her knowledge and experience, even beyond the APPEAR project's framework. We thank Caroline Roberts, Kelsey Museum of Archeology, University of Michigan, Ann Arbor, for her many insightful comments. At the DIA we are especially grateful to Christopher Foster, Katherine Kasdorf, and Marisa Szytman. Travel for the research of this paper was supported by funds from the Andrew W. Mellon Foundation.

NOTES

1. Head of a Woman, Egyptian (Antinoöpolis?), late second–third century CE. Encaustic with gilded stucco on tamarisk panel, 44.8 x 24.8 x 1.5 cm (17 5/8 x 9 3/4 x 5/8 in.). Detroit Institute of Arts, Gift of Julius H. Haass, 25.2.
2. See File 25.2, Registration Department, Detroit Institute of Arts.
3. Julius Haass was a Detroit banker, a prominent art collector, and served as a museum trustee in the mid-1920s.
4. Kelekian was a successful dealer of Islamic art and Egyptian antiquities with galleries in Cairo, New York, and Paris, from which he sold to major museums and collectors around the world. See also “Dirkan Garabed Kelekian (1868–1951),” Bliss-Tyler Correspondence, Dumbarton Oaks Museum, Washington, DC, accessed May 7, 2021, <https://www.doaks.org/resources/bliss-tyler-correspondence/annotations/dikran-garabed-kelekian>.
5. Panel Portrait of a Woman, Egyptian (Antinoöpolis), ca. 130–200 CE. Encaustic with gilded stucco on beech wood, 45.7 x 20.6 x 0.64 cm (18 x 8 1/8 x 1/4 in.). The Walters Art Museum, Baltimore, acquired by Henry Walters, 1912, 32.4.
6. Thompson 1972, 34–36.
7. Based mostly on the distinct “stepped” contour of the wood panel. For further information, see Thompson 1972.
8. Provenance as published on museum’s website, accessed December 29, 2022, <https://art.thewalters.org/detail/30478/mummy-portrait-of-a-woman-from-fayum-egypt/>.
9. Radpour et al. 2022; <https://doi.org/10.1186/s40494-021-00639-5>; File 32.4, Department of Conservation and Technical Research, Walters Art Museum, Baltimore; APPEAR database entry for Walters Art Museum, Panel Portrait of a Woman, 32.4, accessed December 28, 2022, <https://www.appeardatabase.org/portrait/531/>; Griswold 2014.
10. Cartwright 2022.
11. Cartwright 2020, 16–23.
12. Spaabæk 2012, 66–67; review of data available on APPEAR database, accessed December 28, 2022, <https://www.appeardatabase.org>: Of the fourteen panels here believed to be from Antinoöpolis (with wood identifications), 64% are a wood other than linden (five sycamore fig, two cedar of Lebanon, one tamarisk, one beech).
13. Review of data available on APPEAR database, accessed December 28, 2022, <https://www.appeardatabase.org>.
14. Spaabæk 2012, 67; Cartwright, Spaabæk, and Svoboda 2011, 57.
15. Fragments were analyzed with Fourier transform infrared spectroscopy (FTIR). The sample correlates with a diterpenoid resin, with a highest correlation to exudates from Pinaceae. See Tappert et al. 2011, 120–38.
16. These textile pieces are of various thread weights and weave densities and are saturated with a dark, resinous material (see note 15). In the Detroit panel there appear to be at least eight and possibly up to ten layers present. Based on identification with polarized light microscopy, the analyzed fibers are linen.
17. A small sample was removed and identified with FTIR and spectral correlation to known references.
18. A small sample was removed and identified as PVA by FTIR and spectral correlation. Wood dust was identified by polarized light microscopy.
19. For all information on the Walters board see Walters Conservation File 32.4 and the Walters APPEAR database entry.
20. Walters APPEAR database entry.
21. Seen from the front, the saw cut is located on the right side of the Detroit panel and on the left side of the Walters portrait.
22. Identification based on FTIR and spectral correlation to known reference samples.
23. Identification based on FTIR and spectral correlation to known reference samples.
24. Identification based on SEM/EDS analysis of a sample of the ground in cross section. In point analysis, red areas were consistent with iron oxide and silica and calcite grains were also noted. A significant portion of the ground was identified as clay based on the characteristic 2:1 ratio of Si:Al with varying amounts of K/Mg/Na. Small particles with calcium and phosphorus are also noted, indicating a geological apatite/phosphate mineral or possibly bone black.
25. Radpour et al. 2022, 8.
26. For example: review of data available on APPEAR database, accessed December 28, 2022, <https://www.appeardatabase.org>; Ebbinghaus et al. 2022C; and Park et al. 2019.

27. The use of Egyptian blue was inferred through visible-induced NIR luminescence alone. For further information on the Walters identification see Radpour et al. 2022; Verri et al. 2010; and Ganio et al. 2015.
28. Thiboutot 2020, 48–50; Ganio et al. 2015, 9.
29. Confirmed as a plant-based red lake through vis-NIR FORS; Newman and Gates 2020, 24–33.
30. Indigo was deduced through vis-NIR FORS by visible spectra with a sharp increase in reflectance at ~690 nm, with an inflection point at ~725 nm, consistent with indigo. See Ichimiya 2021, 97–99. The depiction of a white and purple bichromatic shawl is most likely not authentic to the painting. Because of the large loss over the proper right shoulder, the second purple stripe on the white tunic was misinterpreted as part of the scarf during a past restoration. The scarf most likely just covered the proper left shoulder. For further information see Bisulca et al. 2021, 12–14.
31. Egyptian, probably from Antinoöpolis, Portrait of a Woman, ca. 130–50 CE. Encaustic on native sycamore fig, 35.3 x 22.5 x 2 cm (14 x 9 x 7/8 in.). Harvard Art Museums/Arthur M. Sackler Museum, 1923.60. Ebbinghaus et al. 2022B.
32. Identification through vis-NIR FORS and FTIR for DIA painting (see APPEAR database). For wax identification in the Walters painting see Radpour et al. 2022, 8–9; Ramer 1979, 6–7; and Mazurek 2020, 142–47.
33. For a more detailed description of the painting materials and techniques used in the Walters funerary portrait see Radpour et al. 2022, 6–14. All technical information listed here is based on the findings published in this article. For further information on the making of the Detroit portrait see Bisulca et al. 2021, 6–19.
34. Review of data available on APPEAR database. See also Thompson 1976A, 115–19.
35. Bruhn 1993, 30–32.
36. The wood from the DIA panel was radiocarbon dated at the Accelerator Mass Spectrometry Laboratory, University of Arizona. The results are a calendar date range of 132 calCE to 335 calCE (95%), 214 calCE to 315 calCE (68%). See Bisulca et al. 2021, 11.
37. Shroud, Egyptian (Antinoöpolis), 200–299 CE. Encaustic on linen, 115 x 62 cm (45 1/4 x 24 1/2 in.). Musée du Louvre, Paris, AF 6486. Painted Shroud, Mummy Portrait, Egyptian (Antinoöpolis), 200–249 CE. Tempera and encaustic with gilt stucco on linen, 81 x 45 cm (32 x 17 3/4 in.). Musée du Louvre, Paris, AF 6487.
38. Portrait of a Woman, Egyptian (Antinoöpolis), 130–161 CE. Encaustic on wood with gilt stucco, 44.45 x 17.15 cm (17 1/2 x 6 3/4 in.). The Nelson-Atkins Museum of Art, Kansas City, Purchase: William Rockhill Nelson Trust, 37-40.
39. The gesso is consistent with calcium carbonate in a proteinaceous binder based on vis-NIR FORS. Gessos made with calcium carbonate appear to be common in ancient Egyptian artefacts, possibly more so than gypsum. See Hatchfield and Newman 1991, 34–38.
40. Radpour et al. 2022, 9.
41. Radpour et al. 2022, 8.
42. Bruhn 1993, 10–16.
43. Bruhn 1993, 32. Bruhn notes the modeling of the necklace could also indicate an embossed gold neck ring.
44. This material was removed during a treatment in the 1970s. See Walters Conservation File 32.4, Walters APPEAR database entry.
45. Today, the Detroit necklace is held in place with a clear modern glue, applied likely during a 1970s repair after an incident. No conservation record has been preserved. See Registration file for 25.2 (also see note 2). A note in the conservation file mentions that a portion of the raised stucco necklace was replaced in 1947 by conservator William Suhr. See File 25.2, Conservation Department, Detroit Institute of Arts.
46. For the historic image, see <https://art.thewalters.org/detail/30478/mummy-portrait-of-a-woman-from-fayum-egypt/>.
47. For more on the restoration and the resulting misrepresentation of the garment see Bisulca et al. 2021, 12–14.
48. Stein and Corcoran 2020, 128–31.
49. Henry Walters purchased altogether four Roman Egyptian funerary portraits from Kelekian in 1912. Walters Art Museum, Baltimore 32.4, 32.5, 32.6, 32.7.
50. Cartwright 2022.
51. Riggs 2012, 664.
52. Kersel 2021, 263–64; and Hopkins, Costello, and Davis 2021, 1–25.
53. See also introductory text panels “Facing Forward” and “Statement from the Curators” to the exhibition *Funerary Portraits from Roman Egypt: Facing Forward*, held at the Harvard Art Museums, August 27–December 30, 2022.

Mummy Portrait of a Boy from the National Museum in Warsaw: Investigation of Its History and Technology

*Agnieszka Kijowska
Aleksandra Sulikowska-Belczowska
Magdalena Wróbel-Szypula
Barbara Wagner
Justyna Kwiatkowska*

HISTORY OF THE MUMMY PORTRAIT

The only mummy portrait in the collection of the National Museum in Warsaw (NMW) (fig. 16.1) was purchased in Egypt, most likely in 1898, by eminent Kraków architect Józef Pakies (1858–1923), who acquired it from a museum in Giza.¹ The work was kept at the Czartoryski Museum in Kraków. Georgius Werner included its first known photograph (fig. 16.2) in his article “De imaginibus Graeco-Aegyptis in colonia cui El-Fayum nomen est, repertis et Cracoviae asservatis observationes,” published in the Lviv periodical *Eos* in 1909. Werner recognized the representation as a girl and noted the significant damage to the board onto which the portrait was painted.² In 1939, the work was acquired for the NMW from Dr. Władysław Kahl for 1,500 Polish zlotys, a modest sum both then and now (approximately \$283 in 1939).

The portrait was entered into the museum’s inventory in May of the same year (the invoice, dated 22 May, also

described the sitter as a girl). During World War II, the very existence of the object was seriously threatened.

According to the account of prominent conservator Bohdan Marconi, it was “privately” stolen in late 1939 by Theo Diesel (SS-Untersturmführer, who led the confiscation of works of art at the museum in 1939–1940) and kept in Diesel’s room in the Bristol Hotel, but soon returned to the museum. Removed from Poland by the Nazis presumably in 1944, the work returned to the National Museum through restitution efforts. In October 1946, the portrait was discovered in one of the crates brought from Fischhorn Castle in Austria that contained items looted during the war.³ There is no documentation to show how storage conditions between 1939 and 1946 affected the portrait’s state of preservation. However, its condition in the 1946 post-war photo (fig. 16.3) is nearly identical to that in the 1909 photo. In his article published in 1966, archaeologist Janusz Ostrowski discussed the



Figure 16.1 Mummy Portrait of a Boy, second half of the second century CE. Encaustic on linden, 37 x 18 cm (14.5 x 7 in.), 236767 MNW. Photo shows the work in its current condition, 2020. The National Museum in Warsaw. Photo: Jakub Płoszaj



Figure 16.3 Photo showing the portrait's condition after World War II. The National Museum in Warsaw. Photo: J. Mizerska



Figure 16.2 Mummy Portrait of a Boy. An illustration in Georgius Werner's 1909 paper "De imaginibus Graeco-Aegyptis in colonia cui El-Fayum nomen est, repertis et Cracoviae asservatis observationes," *Eos*, vol. 15, f. III.

authenticity of several parts of the portrait.⁴ This was the first time that the work was described as depicting a boy.⁵

DESCRIPTION OF THE PORTRAIT

The portrait dates to the second half of the second century CE. It shows a youth's face with regular features and large eyes looking straight ahead. His dark hair is pulled back and cinched behind the ear. The boy wears a white tunic with a vertical pink clavus over his right shoulder. On his neck is an amulet, a container for an apotropaic text, and above his right shoulder is a rearing horse painted in dark rose, a rare motif in funerary portraits whose meaning requires further research. The "lock of youth" and *bulla*, an amulet protecting the wearer from the evil eye, are the attributes of a boy of early age.⁶

The portrait appears to be painted in encaustic. The board is 37 x 18 cm and the upper corners are cut at an angle, which some scholars believe to be characteristic of the local tradition in er-Rubayat.⁷ The support is very thin, about 1–2 mm. The NMW laboratory identified the wood as linden after analyzing thin sections of wood through the optical microscope in transmitted light.⁸ The bottom of the board is left unpainted, with visible traces of a black layer. This thin black primer can also be detected in some places where the painting layer is slightly translucent.

For the most part, the paint was thickly and vividly applied in a well-practiced formula. The upper edges of the panel seem to have been cut after painting. Evidence for this is visible at the top of the panel, below where it was trimmed, where an incised line for marking (or guiding) the shaping

of the panel is still evident in the paint. The background, which was likely painted first,⁹ outlines the figure, a practice also observed on other mummy portraits.¹⁰ Observations in raking light show a variety of textures and methods of paint application suggesting the use of brushes and other tools, possibly hard and pointed. Parallel brushstrokes are clearly visible on the painted surface of the gray background and, especially, on the boy's white tunic. The face, neck, and hair texture reveals a modelling method that creates various patterns, likely the result of the use of metal tools in the paint's application.¹¹ Additionally, there are striking differences in highlights and shadows in the figure's face and neck that give the work a beautiful, expressive appearance.

The panel is split both vertically and horizontally in several places and is slightly deformed and concave. Approximately nine separate pieces have been joined and glued to a cardboard backing. A vertical section that includes the boy's right eye is a later addition—an element most likely originating from a similar ancient mummy portrait. The added fragment is raised above the surface because the left edge overlaps with the adjoining piece. The paint exhibits a craquelure pattern in irregular angular shapes in the white tunic and the gray background. In the darker areas, the cracks assume simple shapes and tend to be smaller. The blistering of the paint layer in the upper part of the pink clavus is consolidated with an adhesive. The wooden panel has deformed due to changes in relative humidity, causing movement of the split panel and the cardboard backing and resulting in a straight or bent concave shape (cradle) of both the entire portrait and the individual splits.

NON-INVASIVE EXAMINATION: TECHNICAL IMAGING AND SPECTROSCOPY

The portrait was examined using non-invasive technical imaging methods—ultraviolet-induced visible fluorescence (UVF), infrared reflectography (IRR), X-radiography, computed tomography (CT), X-ray fluorescence spectroscopy (XRF), and Fourier transform infrared spectroscopy (FTIR)—to gather more information about its overall condition. The images were made after dirt and overpaint removal. The research aimed to establish whether the paint layer is homogeneous and whether all of the sections mounted on cardboard come from the same object.

UV imaging (fig. 16.4)¹² shows clear differences between the fluorescence of the paint layers on the fragment with



Figure 16.4 UVF imaging after removal of dirt and overpainting. The National Museum in Warsaw. Photo: Anna Lewandowska

the right eye and the rest of the composition. Other fluorescent areas include: a green color in areas of modern retouching; a slight difference in the luminosity on the left side of the face, which ends along the horizontal crack across the neck; a bright orange-to-pink area, characteristic of the type usually emitted by red lake pigments, in the area of the head and the tunic (on the clavus, evidence for the use of madder has been corroborated by FTIR analysis); and a light orange fluorescence above the right side of the hair and background, presumably a trace of shellac that was also confirmed by an analytical examination. Additionally, in the IRR image,¹³ the striking outline of the right eye, the eyebrow, and the hairline above the right eye is visibly different from the adjacent composition (fig. 16.5).

The portrait was further examined by X-radiography and computed tomography.¹⁴ X-ray images revealed information about the painting process and the uniformity of the paint layers. More importantly, X-radiography was able to detect the continuity of brushstrokes between separate split pieces (fig. 16.6). This was possible due to the strong X-ray absorption of lead pigments used in the paint layers, identified during analytical testing. Technological differences between the fragment with the right eye and the rest of the portrait were also confirmed. The hidden fragment of the panel under the board with the right eye was visualized along with the irregular shape (line) of the damaged edge of the panel at this location (fig. 16.7). Computed tomography enabled us to penetrate



Figure 16.5 IRR imaging following the removal of dirt and overpainting. The National Museum in Warsaw. Photo: Anna Lewandowska



Figure 16.7 Detail of figure 16.1 showing the hidden fragment of the broken panel near the right eye, now covered by the transplanted board. Image: Łukasz Kownacki, MD, PhD



Figure 16.6 X-radiograph showing the painting technique and direction of the brushstrokes. The image reveals a clear difference in the paint layer between the transplanted board with the right eye and the rest of the painting. Image: Łukasz Kownacki, MD, PhD

the work, making it possible to recognize the state of preservation, structure, and materials, and retrace the artist's creative process.¹⁵ The interpretation of the obtained multi-layered cross section is still pending analysis.

Microscopic observation brought several important findings to light that will require further research. The surface of the encaustic paint of the portrait was especially varied in terms of composition and texture. We documented some deposits inside the paint, likely connected with the process of painting with encaustic. A piece of reed or wood was noticed, alongside numerous short black hairs and one fragment of a red thread. Cavities from air bubbles were also observed on the surface.

Another finding was the observation of the white particles firmly attached to the paint surface. These individual white deposits, resembling scattered crumbs, were visible on the surface of the gray background (fig. 16.8). Different minor white spots in the form of clusters were noticed on the right side of the painting (fig. 16.9) (see following section).



Figure 16.8 Detail of the portrait showing the white particles (dots) on the surface of the gray background (20x). The National Museum in Warsaw. Photo: Agnieszka Kijowska



Figure 16.9 Detail of the portrait showing the irregular clusters of white deposits at the border of the forehead and hair (40x). National Museum in Warsaw. Photo: Agnieszka Kijowska

PIGMENT INVESTIGATION AND ELEMENTAL ANALYSIS USING PORTABLE X-RAY FLUORESCENCE SPECTROSCOPY (P-XRF)

All measurements were performed using an XRF Tracer III-SD spectrometer (Bruker) equipped with a silicon drift detector (SDD detector).¹⁶ The system enables elemental analysis in the Mg–Pu range. A primary X-ray radiation lamp with an Rh anode with variable 2–25 μA current and maximum voltage up to 45 kV was used. All XRF spectra were acquired from areas of ca. 0.5cm^2 , and no subtle variabilities between the analyzed areas could be detected. The following instrumental settings and data acquisition parameters were used: voltage 45 kV; current 23.1 μA ; spectra acquisition time 60 s; pressure < 60 Tr.

XRF spectra were registered using S1PXRF software and then compiled in Excel. The presence of Pb was detected in all samples. The presence of barium was also detected in all analyzed areas by recognition of $\text{BaK}\alpha_1$ at 32.19 keV, $\text{BaK}\alpha_2$ at 31.82 keV and $\text{BaK}\beta_1$ at 36.38 keV. The information about Ba versus Ti was selected after careful examination of the presence of their signals at the characteristic energies ($\text{TiK}\alpha_1/\text{K}\alpha_2$ at 4.50/4.51 keV; $\text{TiK}\beta_1$ at 4.93 keV; $\text{BaL}\alpha_1/\text{L}\alpha_2$ at 4.47/4.45 keV; and $\text{BaL}\beta_1$ at 4.83 keV), bearing in mind that they are difficult to distinguish while using p-XRF. The highest Zn signals accompanied Ba

in the same areas. The interpretation of these results is not obvious, but barite (BaSO_4) is a relatively common mineral. It is typically found as an opaque white heavy mineral in sedimentary rocks such as limestone. It can be also associated with sulfide secondary minerals, like galena (PbS) or sphalerite (ZnS). It is possible that the mineral barite might be used as a filler in the painting.

The XRF results allow us to make some conclusions about the presence of lead white (basic lead carbonate) and iron oxides in brown, yellow, and red (lips) areas. The red horse was probably painted with organic pigments, which could not be identified by means of XRF (fig. 16.10).

ORGANIC ANALYSIS USING FOURIER TRANSFORM INFRARED SPECTROSCOPY (FTIR)

The spectra obtained from the samples were recorded by attenuated total reflection Fourier transform infrared (ATR-FTIR) spectrometer (Alpha, Bruker Optics, Germany USA-MA) equipped with a diamond crystal. The spectra were collected in the $4000\text{--}400\text{ cm}^{-1}$ range with a resolution of 4 cm^{-1} . The characteristic bandwidths were interpreted and compared with literature data¹⁷ and reference spectra collected in the laboratory.

One microsample was taken for analysis by FTIR-ATR spectrometry. The material was collected from an area on the pink clavus (near the lower edge of the painting from an area of loss) where we suspected the presence of an organic dye. Peaks characteristic of wax ($2918, 2846, 1736, 1457, 1169, \text{ and } 721\text{ cm}^{-1}$) were visible in the sample's spectrum. Other peaks at $1091, 721, 674, \text{ and below } 600\text{ cm}^{-1}$ were also identified. Their presence resembles spectra of a plant-based red containing anthraquinone, a commonly used pigment in antiquity and a component of madder lake.¹⁸

A second microsample from the black ground layer was taken to identify organic binder. The spectra with characteristic peaks at $2918, 2851, 1631, 1421, \text{ and } 1379\text{ cm}^{-1}$ correlate a reference spectrum for bitumen, also commonly used in antiquity in the production of mummified human remains.¹⁹

OTHER INVESTIGATIONS USING FTIR-ATR

We used an FTIR-ATR spectrometer to examine a sample of the single white deposit from the gray background layer,

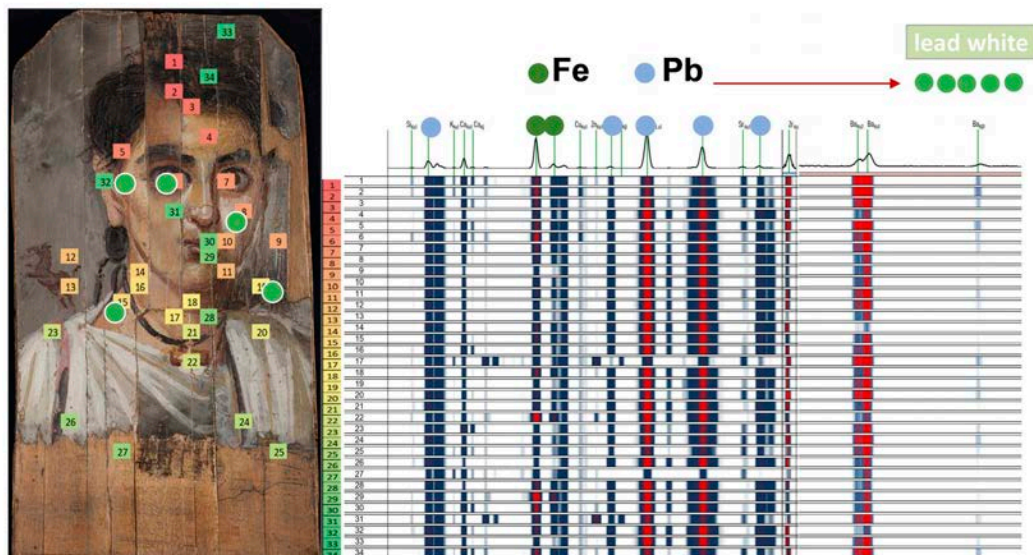


Figure 16.10 Schematic visualization of the XRF results with thirty-four measurement spots. The dimensions of the spots are shown against the size of the entire object. Recorded spectra are presented in the form of a colorful matrix. The scale (min | max) reflects the relative variation in the intensity of the signals from the lowest (white) to the highest (red). In all analyzed spots, the signals of two elements were observed: iron (Fe, lines K α and K) and lead (Pb, lines L α , L β , L γ , and M). Such elemental information is consistent with the presence of lead white pigment. Bright green dots over the portrait indicate spots of FTIR. Chart: Barbara Wagner

comparing the results with the different-looking clusters of white spots within the brown background layer. Wax was identified in the sample taken from the gray area at the left edge near the boy's shoulder. The peaks at 2922, 2851, 1736, 1461, 1167, and 718 cm^{-1} correspond to the reference spectra for beeswax. The presence of lead white, evidenced by peaks at 1403 and 681 cm^{-1} , was also identified. Consequently, the results obtained for this sample aligned with the measurements taken with the portable spectrometer. An unusual signal appeared at 1515 cm^{-1} , which did not correspond to any pure standard reference samples typically used in ancient Egypt. Signals recorded for the brown sample from the area of the upper edge (2920, 2849, 1738, 1463, 1421, 1171, 1026, and 723 cm^{-1}) correlate with the reference spectrum for resin, most likely shellac from previous conservation treatments, confirming observations made with UV radiation. There is also a signal at 1519 cm^{-1} , similar to the gray area sampled from the left panel edge in the boy's shoulder.

Peaks between 1550 and 1510 cm^{-1} come from amide II band stretching, mainly showing N-H motion. These signals are attributed to protein deformation in the literature concerning protein interactions with pigments²⁰ and the investigation of funerary masks.²¹ In the case of the current portrait, they may also indicate either the use of egg or reactions caused by a series of factors such as the presence of fungi or an interaction with substances

used in the mummification process. Experiments concerning reactions with fungi have already been explored but need to be continued, considering the artificial aging process in such a complex environment.

FTIR BINDING-MEDIA ANALYSIS

The binding media used to paint the NMW's mummy portrait were identified using FTIR. This method allows the determination of the material groups used and the identification of possible interventions to the object. The analysis was performed using an ALPHA (Bruker) portable spectrometer equipped with a module for non-invasive analysis. The module, with 4 mm diameter openings, was placed against representative points on the surface of the painting. The selected spots were analyzed with the use of a transmitted infrared beam. Consequently, we were able to obtain molecular information about a wide range of painting materials. The characteristic bandwidths produced by individual bonds and functional groups were also identified.

The exemplary FTIR reflectance spectra from the skin area at the center of the proper right cheek are shown in figure 16.11. The presence of wax (2932 cm^{-1} , 1746 cm^{-1} , and 1704 cm^{-1}), oil (2960 cm^{-1}), protein (1554 cm^{-1}), and lead white (1479 cm^{-1} , 694 cm^{-1}) was identified. It was possible to

identify the presence of wax and protein in the nine analyzed points. Oil was identified in all areas except the temple near the proper right ear. The presence of lead white, whose high-intensity signals often make it difficult to distinguish bandwidths characteristic of other substances, interfered with the analysis.

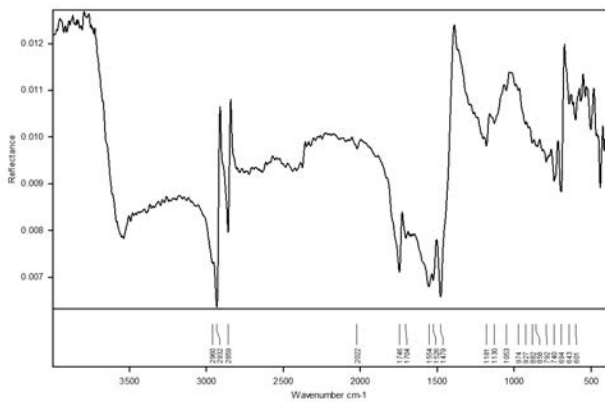


Figure 16.11 Sample FTIR reflectance spectrum from the skin at the center of the figure's right cheek. The National Museum in Warsaw. Chart: Justyna Kwiatkowska

CONSERVATION

The portrait, cracked and broken into individual narrow sections, was most likely mounted onto cardboard when it was still in Egypt. It is also likely that this was when an antiquities dealer replaced a destroyed fragment of the right eye with a section originating from another mummy portrait. There is no evidence of conservation treatment between the time that the portrait was acquired for the NMW and 1998, when an analytical report was published describing the reduction of a white bloom that appeared on the painting's surface. The decision was made to stabilize the portrait in 2004, when the paint layer began to flake and crack and the portrait's cardboard backing continued to detach from the panel. During the conservation treatment, dirt and overpaint were removed from the surface of the painting, the flaking paint layer was consolidated, and the cardboard was stabilized. Even before conservation treatment, in 2005,²² there were visible differences between the portrait's fragments (fig. 16.12). After the surface was cleaned, the section containing the proper right eye appeared more distracting. It was determined that this area had been overpainted to hide various anomalies: the eye painted on the board that was originally larger, the brow was higher, and the hairline inconsistent with the rest of the portrait (fig. 16.13). The



Figure 16.12 Detail of the portrait before dirt and overpainting removal. The National Museum in Warsaw. Photo: Zbigniew Doliński



Figure 16.13 Detail of the portrait after dirt and overpainting removal. The National Museum in Warsaw. Photo: Piotr Ligier

examination also proved the use of different techniques for the added section.

After the removal of dirt and overpainting, the portrait's new appearance was poorly received by viewers. However, the decision was made against changing the addition of later sections or removing the cardboard backing,

considering that such manipulations could damage the paint layer and wood.²³ Following the curatorial request, the inserted section was retouched with (reversible) watercolor paint in the form of minute *tratteggio* (hatching) lines to minimize the visual difference between the added piece and the rest of the composition.

Following our investigation, a digital rendering of the presumed original appearance of the portrait was made. The images of matching pieces (fig. 16.14) as well as the separate section with the eye (fig. 16.15) were prepared based on the assumption that the latter probably originated from another mummy portrait, and a hypothetical reconstruction of the portrait (fig. 16.16) was made. According to the observations, neither the shape nor the size of the transplanted section fit in with the rest of the work and this is why its left edge is slightly raised on the neighboring board. We noticed that the edge where the portrait cracked horizontally was inconsistent in color with the neighboring paint layers. This inconsistency is visible in the imaging examination (see figs. 16.6 and 16.7). Additionally, the vertical cracks do not run in one line, suggesting that the left side of the portrait should be shifted toward the center, and a small fragment on the left edge was not positioned correctly. In our digital reconstruction, we corrected the position of the sections and made a color reconstruction of the missing part. Fig. 16.16 shows a completed face of the boy and, additionally, a separate fragment of another portrait (see fig. 16.15).



Figure 16.14 Computer reconstruction of the presumed original configuration of the boards. The National Museum in Warsaw. Photo: Jakub Płoszaj. Reconstruction: Agnieszka Kijowska



Figure 16.15 Detail of fig. 16.13, transplanted board with the right eye. The National Museum in Warsaw. Photo: Piotr Ligier. Reconstruction: Agnieszka Kijowska



Figure 16.16 Computer reconstruction of missing elements in the paint layer. The National Museum in Warsaw. Photo: Jakub Płoszaj. Reconstruction: Agnieszka Kijowska

OBSERVATION SUMMARY

The wood panel was identified as linden over the course of our research. The vertical section with the boy's proper right eye (see fig. 16.15) was recognized as an element most likely originating from another ancient mummy portrait. UVF, X-radiography, and IRR show clear differences between the response of the paint layers on this added fragment and the rest of the object. X-radiography provided information about the painting process and the uniformity of the paint layers, allowing us to detect the continuity of brushstrokes between the other separated sections. Wax, oil, lead white, earth compounds, madder, and bitumen were detected using a variety of analytical methods. Based on the XRF results the presence of lead white (basic lead carbonate) and iron oxides in the brown, yellow, and red (lips) areas is suggested.

CONCLUSIONS

The materials identified during the examination of the object are consistent with mummy portrait production in second-century Egypt. The portrait from the NMW may come from one of the known Egyptian sites²⁴ (based on the shape of the original panel, possibly er-Rubayat) and made its way to Giza before being purchased by the Polish architect Józef Pakies. The object's condition, combined with our investigations and analyses, prove that the portrait underwent conservation treatment before 1909, when it was photographed and analyzed by Georgius Werner. Fragments of the cracked portrait of the boy were mounted on cardboard and the damaged part of the face was reconstituted from an ancient panel removed from a different mummy portrait. It was then overpainted to unify the added board with the rest of the composition. The artifact could have been part of a group of works discovered in Egypt and restored for the antiquities market at the end of the nineteenth century by creating a pastiche of better-preserved sections of similar portraits.²⁵ In recent years, following the removal of the modern overpainting, *tratteggio* was used to unify and improve the appearance for display in the Ancient Art Gallery in the National Museum in Warsaw.

NOTES

1. Werner 1909, 132. Fig. 16.1: Inv. no. 23676 MNW (former inv. no. 127191 MNW).
2. Werner 1909, 132.
3. Marconi 1967, 271. Maria Ludwika Bernhard, "Sprawozdanie do Kroniki za mc. październik 1946 r. Zbiory Sztuki Starożytnej" (The Report for the Chronicle to October 1946). The Archive of the National Museum in Warsaw, no. PL/304/1/0/859, 132. We are grateful to Kacper Laube (Department of Ancient Art, National Muzeum Warsaw) for turning our attention to this archival document; see also Bernhard 1947, 302–9, and Michałowski 1957, 120.
4. Ostrowski 1966, 19.
5. Ostrowski 1966, 16–17.
6. Laes and Strubbe 2014, 55; Montserrat 1993, 216–17; Wiedemann 2014, 114–16.
7. Doxiadis 1995, 129–33; Freccero 2000, 6.
8. *Tilia* sp. The wood was identified by Iwona Pannenko in 2006.
9. van Daal 2019, 62.
10. Thompson 1982, 7; Salvant et al. 2018, 13.
11. Bostock and Riley 1855, XXXV, 41.
12. Canon 5D Mark II camera, Canon Macro fixed focal 100 mm lens, UV wavelength 300–400 nm. Image by Anna Lewandowska.
13. Canon 6D camera, modified to IR wavelength range of above 1000 nm, Canon EF 50 mm f/1.8 lens, 830 nm and 1000 nm filters. Image by Anna Lewandowska.
14. The painting was imaged using a Philips Digital Diagnost X-ray system and Neusoft NeuViz 64 En 64-slices computed tomography scanner, thanks to a collaboration between the NMW and the European Health Centre Otwock (EHC). The imaging was performed by Łukasz Kownacki, MD, PhD, in the Department of Diagnostic Imaging, EHC, in 2017.
15. As part of a long-term project between the NMW and the EHC directed by Łukasz Kownacki and Dorota Ignatowicz-Woźniakowska (senior conservator for specialized diagnostic imaging at the NMW) in cooperation with scientists working in this area of research.
16. We would like to thank Olga Syta, PhD, for her contribution to the XRF investigation.
17. Zaffino et al. 2015; Rosi et al. 2019; Hofko et al. 2017.
18. Scott 2016; Nicholson and Shaw 2000.
19. Scott 2016; Nicholson and Shaw 2000.
20. Duce et al. 2012; Socrates 2001, 143–44.
21. Schiavon et al. 2021.
22. The cleaning and adhesive lining were done by Agnieszka Kijowska from the NMW Ancient Art Conservation Workshop.
23. In 2005, we discussed the risks of removing the secondary support by email correspondence with conservators specializing in the subject of mummy portraits: Marie Svoboda

(J. Paul Getty Museum, Los Angeles), Jane Williams (Phoebe A. Hearst Museum of Anthropology/Fine Arts Museums of San Francisco), Britta Nilsson (Nationalmuseum, Stockholm), and Nicola Newman (British Museum).

24. Aubert 2000, 88.

25. Thompson 1981; Thompson 1973, tab. 88.

Funerary Portraits from Roman Egypt: Facing Forward—An Exhibition and Inter-Institutional Collaboration Looking for the Artists of Ancient Philadelphia

Kate Smith
Susanne Ebbinghaus
Katherine Eremin
Georgina Rayner
Jen Thum
Courtney Books
Richard Hark
Irma Passeri
Marcie Wiggins

In 2014, when the Harvard Art Museums (HAM) agreed to participate in the APPEAR project, analytical findings about the Romano-Egyptian funerary portraits in the care of the museums and new questions emanating from the research became a rich resource in teaching undergraduate and graduate courses in art history, chemistry, ancient studies, and beyond. Students of all disciplines are fascinated by these alluring fragmentary depictions and by the collaborative research of the curatorial, conservation, and scientific departments at the museums. What we know about these portraits and how we come to know it can be shared not just with students or specialist groups but with any audience we welcome through our doors; with this in

mind we launched our exhibition, *Funerary Portraits from Roman Egypt: Facing Forward* (August 27–December 30, 2022). In the following, we give a brief overview of the exhibition and its goals, and then focus on a particular topic that was explored in the display: What can the scientific study of materials and techniques contribute to the identification of individual painters or workshops?

EXHIBITION

The exhibition centered around the profound connection the ancient portraits evoke in modern viewers, the

scientific investigations undertaken to better understand the painting techniques, and our responsibility, in stewarding these fragments, to honor the memory of the long-dead people depicted in the portraits by acknowledging the desecration of their burials. The show was team-curated by Susanne Ebbinghaus, curator of ancient art; Georgina Rayner, conservation scientist; Kate Smith, paintings conservator; and Jen Thum, Egyptologist and museum educator.¹ In a new model of co-curation for the Harvard Art Museums, we each brought a particular lens to the work, enriching the truly collaborative presentation.

In a welcome departure from our usual practices, we invited students and faculty, along with Harvard community members of Egyptian heritage and identity, to join us for Community Conversations designed to shape the exhibition early in the process. As a result, we changed our minds about some things—for example, we had already intuited that using the word “mummy” to refer to a person was a form of objectification (many other museums are moving away from this term now, too) and thought we might say “mummified remains,” but Harvard community members of Egyptian heritage asked us to avoid the word “remains” as well. We also heard helpful suggestions about how to frame the exhibition for people not very familiar with ancient Egyptian culture, such as the inclusion of a label describing the funerary rituals surrounding the portraits’ use. These conversations helped us think more clearly about how to discuss provenance, identity, and the troubling legacy of the modern “mummy” paint in the gallery space, both in label texts and in gallery talks and virtual events.

The exhibition’s introductory room (fig. 17.1) was dedicated to contextualizing the portraits by addressing what they are, their cultural functions, and their paths into the museum. Our curators’ statement at the start of the show reminded viewers to keep the sensitive and problematic nature of these collections in mind. In the absence of actual mummified bodies, we borrowed the burial shroud of Tasheret-Horudja from the nearby Museum of Fine Arts, Boston (MFA 54.993), to contextualize the portraits and suggest human scale. We also borrowed inscribed wooden “mummy labels” from the MFA and the Brooklyn Museum (BKM) to present visitors with the identities and personhood of real ancient people—not those depicted in the portraits on view, but others (such as Plenis and Hor, who are only known today through their labels)—to show how those buried in this manner were meant to be remembered, as people, with bodies, likenesses, and names.²



Figure 17.1 Installation shot from the Harvard Art Museums, Gallery 3600, *Funerary Portraits from Roman Egypt: Facing Forward*. © President and Fellows of Harvard College. Photo: Mary Kocol

The second, central space (fig. 17.2) focused on eight funerary portraits (five from the HAM collection joined by three loans), our analytical investigation, and what new understanding was gleaned from the materials we identified. An electromagnetic spectrum displayed with a corresponding set of technical images derived from infrared through radiographic bandwidths illustrated the various imaging techniques and what they can tell us. Brief video loops near the portraits presented technical imaging and pigment analysis results, inviting the viewer to join us as we investigated each painting.



Figure 17.2 Installation shot from the Harvard Art Museums, Gallery 3600, *Funerary Portraits from Roman Egypt: Facing Forward*. © President and Fellows of Harvard College. Photo: Mary Kocol

We showed two of the eight panel portraits in the round so that both sides of the portraits could tell their stories of ancient construction and modern dismantling. The back of an encaustic portrait of a woman (HAM 1923.60) retains linen wrappings and resins from the funerary equipment, a stark and intimate reminder of the panel’s original placement above a deceased woman’s face. The back of a tempera portrait of another woman (HAM 1939.111) reveals a modern restoration of the perimeter, as well as

stamps and labels that permit at least a partial reconstruction of its provenance.

We took a new approach to what was conveyed by the labels accompanying the objects in the exhibition, providing more specific information than usual. The media line was expanded from the basic description into a rich cataloguing of identified materials, from the wood species of the panel to individual pigments used in the paint mixtures. We also included what is known of the portraits' provenance, their modern history after they were taken from the burial context. Most museum visitors are unfamiliar with the concept of provenance. The information offered in HAM's online database is difficult to parse, comprising short phrases separated by semicolons, with terms that may themselves be unfamiliar (what, for example, is a bequest?). By stringing the information available for each object into a cohesive and easy-to-follow narrative, we gave visitors the opportunity to better understand the trajectory that each object took before entering the museum where it now resides. Anecdotal evidence suggests that these efforts were well received.

We confronted the damage and desecration inherent in collecting these portraits by showing fragmentary portraits along with early twentieth-century tubes of the brown paint known as "mummy" (fig. 17.3). Valued by artists for centuries for its handling properties and transparent brown tone, the powdered pigment for this oil paint was made from mummified ancient Egyptian individuals.³ Edward Forbes, second director of the Harvard Art Museums, collected two tubes from the London artist supplier Charles Robeson in 1915 for his renowned pigment collection.



Figure 17.3 Fragmentary portraits 1946.44 and 1924.80 with a tube of "mummy pigment" in the far-right case. Installation shot from the Harvard Art Museums, Gallery 3600, *Funerary Portraits from Roman Egypt: Facing Forward*. © President and Fellows of Harvard College. Photo: Mary Kocol

The portrait subjects were not the only ancient people we engaged with while studying the paintings. In identifying the pigments, binders, and wood panels the portrait painters chose, we felt both the presence and absence of the ancient artists. The last area of the exhibition (fig. 17.4) evoked an artists' studio. A horizontal, table-like case showed pigments in their plant and mineral sources and as prepared colored powders along with beeswax and animal-skin glue binding media, all of which were used in antiquity. Visitors could touch panels painted with these materials to feel the difference between encaustic and tempera paint. The Harvard Art Museums have always been a place for the study of artworks from a material perspective, where students are taught historical techniques through making copies (fig. 17.5). In 1931, a student named Muriel Mussels chose the fragmentary portrait of a man (1924.80) to copy in an encaustic technique for a research project. Her copy (1938.GNRA.1) has lived in our collection ever since. In preparation for and coinciding with the run of our exhibition, we invited Francisco Benitez, a contemporary encaustic painter who focuses on replicating ancient techniques,⁴ to offer workshops for students and visitors to try their hand at encaustic painting. A current Harvard student, Namirah Quadir, lent her copy to the exhibition. It was displayed next to the 1931 student copy alongside the artist materials, a testament to a century of learning through making at our teaching museum.



Figure 17.4 Installation shot from the Harvard Art Museums, Gallery 3600, *Funerary Portraits from Roman Egypt: Facing Forward*. Artist materials from the Forbes Pigment Collection displayed with student copies of funerary portraits and touchable paint outs for a tactile visitor experience. © President and Fellows of Harvard College. Photo: Mary Kocol



Figure 17.5 Edward Waldo Forbes (third from right) with students from his *Methods and Processes of Italian Painting* course, Fogg Museum, ca. 1932. Harvard Art Museums Archives, HC 22, folder 3.187. Photo: © President and Fellows of Harvard College

A Workshop Active in Ancient Philadelphia (Fayum)

Three exhibition portrait loans gave us an opportunity to compare a group of panel portraits that had been attributed through visual analysis to the hand of a single artist, or possibly a workshop or “school,” which painted funerary portraits exclusively in a tempera technique (fig. 17.6). The attribution to this artist of the only tempera portrait in HAM’s collection, representing a woman with graying hair in a white tunic (fig. 17.6B), goes back almost a century to the study of German scholar Heinrich Drerup. In 1933 he named the painter after a portrait of a bearded man in the collection of Würzburg University, Germany, which he admired, although he thought that the portrait of a woman now at Harvard was painted in a “rough and careless” manner. Among the characteristics of his “Würzburg Painter,” Drerup noted the “whiplash determination and elegance” of the lines as well as the “flourishing polychromy basking in unbroken colors.”⁵ Almost fifty years later, David Thompson baptized the same artist or “extensive school” as the “Saint Louis Painter” after a portrait of a woman now residing at the Saint Louis Art Museum (SLAM 128:1951; fig. 17.6A), who looks like an older sister of the woman depicted in the portrait at HAM.⁶ Most recently, Branko van Oppen de Ruiter assembled a group of more than twenty portraits that he associated with a single workshop based on shared features such as the elongated nose, lip shape, and earrings, as well as the hatching technique used to suggest volume and shading in the flesh tones (fig. 17.7).⁷

Many portraits in this group are remarkable for showing wrinkles and strands of gray or whitish hair. Such signs of advanced age are comparatively rare among Egyptian funerary portraits overall.⁸



Figure 17.6 (A) Portrait of a woman, Egypt, probably from Philadelphia (near er-Rubayat), second half of the second century CE. 25.7 x 14.9 cm (10 x 6 in.). Saint Louis Art Museum, Gift of Mrs. Max A. Goldstein, 128:1951. Photo: Courtesy Saint Louis Art Museum. (B) Portrait of a woman, Egypt, probably from Philadelphia (near er-Rubayat), second half of the second century CE. 32 x 19 x 0.5 cm (12 1/2 x 7 1/2 x 1/4 in.). Harvard Art Museums/Arthur M. Sackler Museum, Gift of Mrs. John D. Rockefeller Jr., 1939.111. Photo: © President and Fellows of Harvard College. (C) Portrait of a woman, probably from Philadelphia (near er-Rubayat), Egypt, second half of the second century CE. 24.5 x 9.5 cm (10 x 4 in.). Yale University Art Gallery, Ruth Elizabeth White Fund, 2011.102.1. Photo: Courtesy Yale University Art Gallery. (D) Portrait of a woman, Egypt, probably from Philadelphia (near er-Rubayat), second half of the second century CE. 33 x 20.3 cm (13 x 8 in.). Smith College Museum of Art, Purchased with the Drayton Hillyer Fund, SC 1932.9.1. Photo: Courtesy Smith College Museum of Art

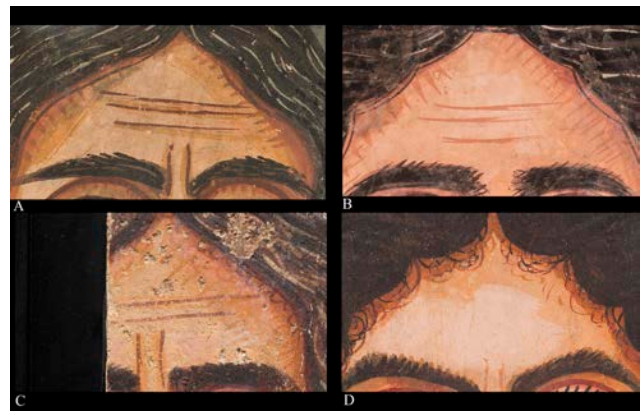


Figure 17.7 Details of the hairline of each portrait illustrating the contour and hatch line technique used for shading and volume. (A) Saint Louis Art Museum. Photo: Courtesy Saint Louis Art Museum. (B) Harvard Art Museums. Photo: © President and Fellows of Harvard College. (C) Yale University Art Gallery. Photo: Courtesy Yale University Art Gallery. (D) Smith College Museum of Art. Photo: Courtesy Smith College Museum of Art

We borrowed the eponymous portrait from SLAM to join the HAM example, along with another, fragmentary painting attributed to the Saint Louis Painter that is now in the care of the Yale University Art Gallery (YUAG 2011.102.1; fig. 17.6C) and a portrait not previously

connected with this painter, which now resides at the Smith College Museum of Art (SCMA 1932.9.1; fig. 17.6D). An investigation into the portraits' provenance, based on museum and other archival records as well as the labels and stamps preserved on the reverse of some of the panels, suggests that all four were part of a cache of over three hundred portraits amassed in the late 1880s by Theodor Graf (1840–1903), an Austrian businessman active in Cairo who also dealt in rugs, papyri, and ancient textiles. Graf stated that the portraits came from er-Rubayat in the northeastern Fayum, and "er-Rubayat" is the location with which the portraits attributed to the Saint Louis Painter have tended to be associated in art historical scholarship. However, a brief report by the Austrian surveyor P. Stadler, who sold portraits to Graf, indicates that while er-Rubayat was the nearest modern settlement, the panels were in fact found closer to the ruins of Philadelphia, some six miles to the east.⁹ Current excavations in the cemetery area outside this ancient city have brought to light complete as well as fragmentary panel portraits associated with burials in tombs of various architectural forms, including masonry-built catacombs.¹⁰

The ongoing (and future) excavations of the cemeteries of ancient Philadelphia hold the promise of providing context for the dissociated and dispersed fragments that were part of Graf's stock as well as information about the date of the portraits attributed to the Saint Louis Painter. Originally assigned to the fourth century CE based on stylistic traits considered to be late antique, they are now more often thought to reflect Roman hairstyles current in the late second and the beginning of the third centuries CE.¹¹ However, many of the hairstyles in the Egyptian portraits are quite simple and therefore difficult to place. Perhaps they are shaped more by the painting style than by the fashion of the time. Proponents of a later date thought that the portraits were indicative of a switch in the Fayum from the encaustic to the tempera technique, following the assumption that tempera was quicker and easier to use. Even well over a century after the discovery of these portraits, there still is much to discover about them, including a better understanding of which stylistic and technical features are owed to the chosen binding medium, which ones might be a sign of the times (or region, for that matter), and which might be characteristic of a painter or workshop.

Hallmarks of the Workshop

Having several examples of portraits attributed to the Saint Louis Painter in physical proximity at HAM allowed us to closely observe and analytically compare various features. Details such as the earrings and manner of building

volume in the faces reveal what appears to be a range of approaches to a common visual goal, implying a workshop environment rather than an individual artist.

The earrings in each of these four portraits are remarkably alike at first glance (fig. 17.8): gold loops expressed with ochre pigments and decorated with three white beads each. Nine of the eleven female portraits currently proposed as products of this ancient Philadelphia "school" wear these exact earrings. Close inspection of the jewelry reveals a range of finish and detailing from portrait to portrait. The SLAM portrait's double loops and bead outlines (fig. 17.8A) are described with interrupted lines, and there is no piercing mark on the earlobes. The portrait at HAM (fig. 17.8B) shows piercing marks, and the double loops and bead outlines are painted in continuous lines. In the example at YUAG (fig. 17.8C), there is a single loop each of yellow and red, and piercing, while the beads are simply underlined. And in the SCMA portrait (fig. 17.8D) there are double loops of red ochre only, no piercings are indicated, and the three beads are separated by two red ochre dots between them, rather than surrounded by ochre.

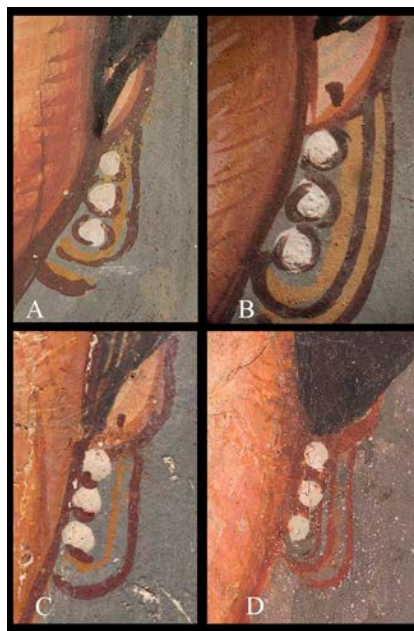


Figure 17.8 Details of the earrings from each portrait illustrating the similarities and subtle differences among them. (A) Saint Louis Art Museum. Photo: Courtesy Saint Louis Art Museum. (B) Harvard Art Museums. Photo: © President and Fellows of Harvard College. (C) Yale University Art Gallery. Photo: Courtesy Yale University Art Gallery. (D) Smith College Museum of Art. Photo: Courtesy Smith College Museum of Art

Volume and shadow in the flesh tones are suggested by shaping the face, neck, ears, and nose with bands of paint

that narrow in width and darken in color toward the outer contours. Hatch marks often perpendicularly cross these contouring bands either everywhere in the flesh or in particular places like the cheeks, further animating these surfaces. A subtle technique in all but the SCMA example is that the lightest flesh tones were applied earliest, and the contouring details applied last. The SCMA portrait, by contrast, has the highlight tone applied in a final swirl of paint visible at the center of the forehead, with the earliest color field visible in the mid-tone (see fig. 17.7D).

We pursued technical imaging and materials analysis to deepen the investigation of these formal relationships, revealing many shared material features and significant differences.¹² We also interrogated panel wood species, ground layers, preparatory sketches, and pigments to establish patterns of material choices and application techniques.¹³

Wood Species

Three of the four portraits were sampled for wood identification, and a variety of wood types were found: native sycomore fig (*Ficus sycomorus*) for HAM, willow wood (*Salix* sp.) for SLAM, and tamarisk (*Tamarix aphylla*) for SCMA, all native to Egypt. This diversity could suggest that in a wood-scarce region, Egyptian artists and workshops used what materials were at hand or available at a given time.

Priming Layer

For the tempera painting technique, a priming layer appears to be a typical¹⁴ preparation for the wood surface to accept the thin, matte paint produced with animal glue. SLAM and HAM have white calcium sulfate priming, with some ochre inclusions observed in cross sections of minute samples (fig. 17.9). YUAG's portrait was not sampled, but close visual examination through a microscope paired with elemental information from scanning X-ray fluorescence spectroscopy (XRF) implies a similar method, though with much coarser texture, likely due to a larger pigment particle size than in the priming layers of the other portraits. The SCMA priming layer is gray to the naked eye where visible; in cross section the priming layer is also calcium sulfate but toned with carbon-containing particles. The choice of priming color may have impacted the painting process, lending tone to the final paint layers and affecting the degree of contrast as the design was developed. The color and elemental makeup of the priming may well be a marker of individual painters or methods within a workshop.

Preparatory Sketch

Once the ground layer was in place, a loose preparatory sketch was made in liquid black paint on the SLAM, HAM, and YUAG portraits, with broad strokes visible in infrared reflectography (IR) and in some cases detectable with the naked eye through the thin surface paint (fig. 17.10). No infrared or visible evidence of sketching was detected in the SCMA example. While there may in fact be no preparatory sketch, it is also possible that the carbon content in the ground obscures a carbon-based sketch. It might also be that the artist sketched an initial design with another material not detected with IR.

Paint Stratigraphy

The HAM paint layers are markedly thicker than in the other two sampled portraits (see fig. 17.9) at SLAM and SCMA (fig. 17.11). There is a white layer for the tunic and a pink layer for the clavus (shoulder stripe) over the calcium sulfate ground, and both paint layers are substantial. In the SLAM portrait the white ground was left exposed to stand as the white of the tunic without additional paint, and the clavus was laid directly onto that surface in a single thin layer of red ochre. The SCMA sample has two paint layers over a gray ground: the tunic color followed by the dark stripes describing folds. The two layers together are still thinner than even one of the layers from the portrait at HAM. While the thickness of paint applied can certainly vary among a single artist's body of work, it seems unlikely that an artist would make economic use of the priming in one portrait but then paint a white tunic over a white ground in another; these differences imply the presence of more than one artist, each accomplishing a similar visual goal with different approaches.

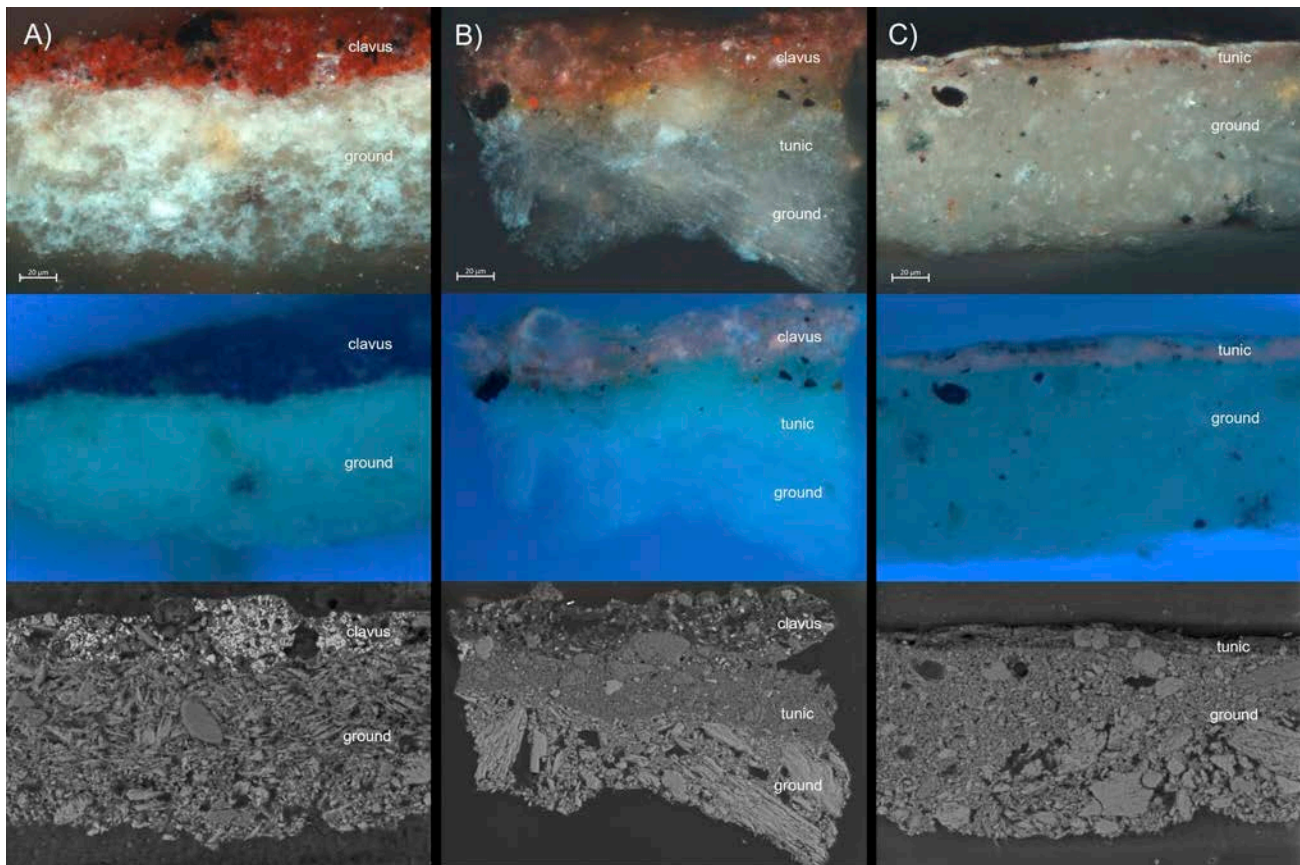


Figure 17.9 Cross sections prepared from the tunic in normal radiation (top), ultraviolet radiation (middle), and the backscattered electron image (bottom). (A) Saint Louis Art Museum. Photo: Courtesy Saint Louis Art Museum. (B) Harvard Art Museums. © President and Fellows of Harvard College. (C) Smith College Museum of Art. Courtesy Smith College Museum of Art

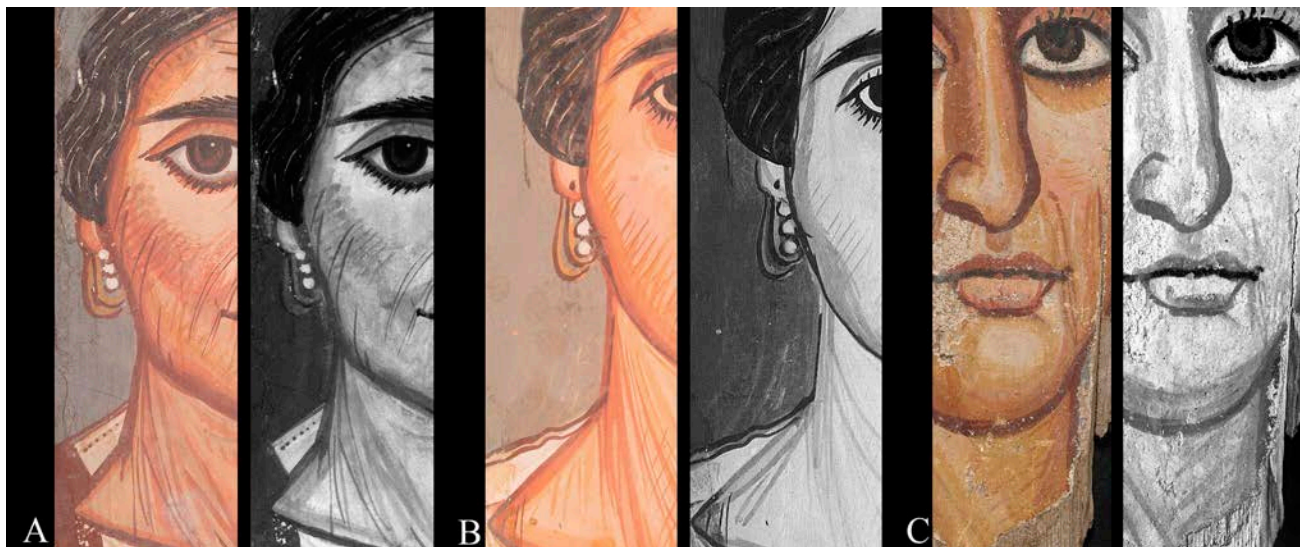


Figure 17.10 Details of infrared reflectograms compared with normal-light details illustrating evidence of preparatory sketches. (A) Saint Louis Art Museum. Photo: Courtesy Saint Louis Art Museum. (B) Harvard Art Museums. Photo: © President and Fellows of Harvard College. (C) Yale University Art Gallery. Photo: Courtesy Yale University Art Gallery

Layer	Saint Louis Art Museum	Harvard Art Museums	Smith College Museum of Art
Clavus	About 30 μm thick Red: ochre (iron rich plus clay), trace gypsum, unidentified black (likely carbon)	About 25 μm thick. Madder, ochre (iron oxide), gypsum, alunite, unidentified black (likely carbon)	
Tunic		About 35 μm thick. Alunite* (a mixture of fine grained with some coarse particles), small amounts of gypsum and ochre (iron oxide), unidentified black (likely carbon)	About 12 μm thick. Madder, possible Al-based mordant, gypsum, possible clay (Al, Si)
Ground	At least 95 μm thick. Gypsum (much finer particle size than HAM and SCMA) with possible clay, one particle of alunite much finer ground in comparison.	At least 60 μm thick. Gypsum (very coarse and variable)	At least 10.5 μm thick. Gypsum (very coarse but with a higher proportion of fine material compared to HAM), trace ochre (iron oxide and clay), unidentified black (likely carbon)

Note: Layer thickness varies across the individual layers in the sample. Measurements given in the table above are an average. Cross sections did not capture the wooden panel, so the true thickness of the lowest layer (ground) is unknown.

*Some of the alunite contained jarosite.

Figure 17.11 Layers present and pigments detected in the cross sections prepared from the tunic of the Saint Louis Art Museum, Harvard Art Museums, and Smith College Museum of Art portraits.

Use of Red Lead

In all but the SCMA example, the lips were painted with a lead-based pigment. Lead's high density makes it visible as a light area in X-radiographs (fig. 17.12), whereas most of the other pigments used in the tempera medium are less dense and therefore penetrated by X-rays, which means that they are less visible in the X-radiograph. The YUAG portrait was not X-radiographed, but its XRF elemental distribution map for lead shows that the lips of the portrait were painted with a lead-containing pigment (fig. 17.12C). In the HAM and SLAM examples (fig. 17.12B and A), red lead is suggested by XRF detection of elemental lead in the context of the presenting red color, although it is not the brilliant color typical of red lead, but instead closely resembles the iron ochre reds used elsewhere in the facial features. In situ Raman spectroscopy of the lips of the HAM portrait, in the X-ray opaque area, conclusively identified a mixture of red lead and hematite (red ochre). However, red lead can discolor to a duller brown color when suspended in a porous, aqueous medium such as animal glue because oxygen can interact with the pigment (fig. 17.13).¹⁵ Did the choice of a more expensive, synthetic,¹⁶ brilliant red color for the lips have a symbolic significance in its ancient context, or was it simply an aesthetic choice that has altered over time?

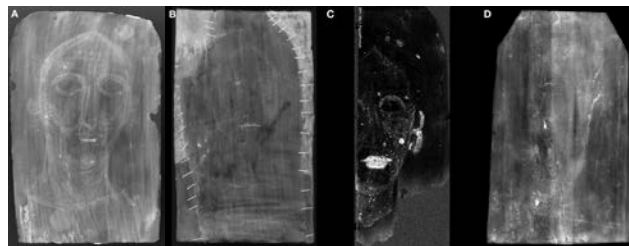


Figure 17.12 (A) X-radiograph of Saint Louis Art Museum. Photo: Courtesy Saint Louis Art Museum; (B) X-radiograph of Harvard Art Museums. Photo: © President and Fellows of Harvard College; (C) Elemental lead L α XRF scanning map of Yale University Art Gallery. Photo: Courtesy Yale University Art Gallery; (D) X-radiograph of Smith College Museum of Art. Photo: Courtesy Smith College Museum of Art



Figure 17.13 Jar of red lead from the Forbes Pigment Collection showing darkening caused by light exposure. Harvard Art Museums/Straus Center for Conservation and Technical Studies, Forbes Pigment Collection, Straus, 1707. Photo: © President and Fellows of Harvard College

Common Features and Outliers

The portraits now residing at SLAM, HAM, and YUAG align in many material ways: all have a similar panel shape, white priming layer, underdrawings, and red lead in the lips. But the SCMA portrait is different in these particulars as well as in formal analysis of its content: the woman portrayed in this painting wears a necklace painted with an arsenic-containing pigment, possibly orpiment or realgar; her neck is described with horizontal instead of diagonal brush strokes; and her tunic is painted with a mixture of indigo and red lake. Are these differences an indication that the SCMA portrait does not belong to this group, despite its visual connections to the other paintings? Or is it part of a subset that could reveal itself through examination of the larger group?

Use of Madder Lake

Ultraviolet-induced visible fluorescence (UVF) images (fig. 17.14) reveal the orange-pink fluorescence characteristic of organic red madder lake in the HAM, YUAG, and SCMA examples. In these portraits, the artist used madder lake in finishing strokes on the surface in a markedly similar way, hatching along the bridge of the nose, eyes, lips, chin, earlobes, and cheeks, as well as in the extant clothing where it is used as the color of the clavus in the HAM example and mixed with indigo for the tunic in the SCMA example. In the SLAM portrait, the result is unclear; red

lake may be present in the lower layers of the flesh tones, as a slight fluorescence is faintly visible between surface strokes, but even if the pigment was used on this portrait, it is not applied in the manner so strikingly similar in the other three examples.



Figure 17.14 Ultraviolet-induced visible fluorescence images of (A) Saint Louis Art Museum. Photo: Courtesy Saint Louis Art Museum; (B) Harvard Art Museums. Photo: © President and Fellows of Harvard College; (C) Yale University Art Gallery. Photo: Courtesy Yale University Art Gallery; (D) Smith College Museum of Art. Photo: Courtesy Smith College Museum of Art

Alunite

Because the grounds of all four portraits were pigmented with calcium sulfate, we anticipated that the white pigment elsewhere in the panels would be the same. However, the HAM portrait is unique within this group; the UVF image suggests a distinction between the ground layer and the white tunic color (see fig. 17.14). The tunic's white paint has a dull brownish color in UV, while the calcium sulfate ground fluoresces with a different, faintly blue-white color. This separate layer for the tunic can be seen clearly in cross section (see fig. 17.9B) and primarily contains an alunite mineral with similar proportions of sodium and potassium, referred to here as alunite. Alunite was confirmed analytically in samples taken from other areas of the portrait in both the gray background and the pink clavus. While a trace of alunite was identified in the white layer of the SLAM cross section, it does not appear to have been used in any substantial way for that portrait.

Alunite has not been suggested as a typical pigment in the Egyptian palette,¹⁷ although recent studies have identified it in a selection of tempera portraits.¹⁸ Of particular interest is its identification in the flesh tones, gray background, and white tunic of the portrait of a bearded man¹⁹ in the collection of the Martin von Wagner Museum at Würzburg University, mentioned above as a portrait by the artist now commonly referred to as the Saint Louis Painter.

CONCLUSION

In some respects, the portrait of a woman in our care at HAM is materially similar to the one at YUAG, in others to that at SLAM, and often to neither. The SCMA example, not previously associated with the Saint Louis Painter, bears remarkable visual and material similarities to the other three; for this reason, it should perhaps also be included in this artistic grouping. The formal similarities combined with the range of materials and techniques across these paintings suggest multiple hands working toward a common template or visual type in a workshop setting. The possibility of multiple artists working simultaneously or even sequentially over several generations could also explain the absence or presence of features such as the hatched use of madder lake, the use of alunite as a white pigment, or the application of a gray priming color. Whatever the case, if these paintings were made in a larger workshop environment, we are left with the question of how the faces were rendered so similarly. Was there a template or model of some kind? If so, how was it communicated, and over what period? Our present study sets the groundwork for future technical examinations of panels attributed to the Saint Louis Painter from collections around the world. This will eventually give us a clearer picture of the work of the artists who provided ancient Philadelphians with the portraits required to care for and memorialize the dead.

To date, the group of paintings discussed above has been named after the modern, Western collections where a particular example is held: Würzburg, Germany, or Saint Louis, Missouri. These names have also implied a single painter, while our study suggests the existence of a group of artists working toward a similar visual goal. We propose a new name for this group that emphasizes the original site of creation, rather than the location of the modern collections that benefit from the desecration and fragmentation of the burials that once contained the portraits. The term “Ancient Philadelphia Workshop” lacks sufficient specificity, as another group of paintings attributed to “the Brooklyn Painter” were also made in ancient Philadelphia, but in a markedly different style.²⁰ We therefore propose the name “Ancient Philadelphia Workshop of the Hatch Mark Style,” taking our cue from the long-observed application technique employed across the group. It is our hope that this renaming will be the first of many changes in museums’ approaches to funerary portraits as we seek to consider these remarkable paintings in their original cultural context and aim to pay respect to both those portrayed and those who portrayed them.

NOTES

1. The exhibition was accompanied by a digital research tool with the same title; see Ebbinghaus et al. 2022A (<https://harvardartmuseums.org/tour/770>).
2. Thum 2022A.
3. Woodcock 1996.
4. Benitez 2018.
5. Drerup 1933 (with antisemitic stereotypes that were unfortunately rather common at the time).
6. Thompson 1976B, 16; Thompson 1982, 22.
7. See van Oppen de Ruiter, this volume.
8. Matheson 2022.
9. Ebbinghaus et al. 2022D.
10. Gehad et al. 2022.
11. Borg 1996; Borg 1998.
12. Our colleagues at Yale University and the Saint Louis Art Museum performed extensive analysis on their own portraits in support of this study and they, along with staff at the Smith College Museum of Art, allowed us to do additional imaging prior to the exhibition in order to obtain consistent conditions where possible.
13. SLAM infrared reflectography carried out with an Opus Osiris camera InGaAs-array detector, 900–1700 nm operating wavelength.

Technical imaging at HAM was carried out with a Canon Mark III 5D DSLR camera and Zeiss 50mm Makro-Planar ZE lens. The internal camera filtration was removed to allow for full bandwidth response at the detector. External filters and light sources per technique: PECA 918 and Wratten 2E filters with Elinchrom Style RX 1200 strobes for visible and with UV Systems Triple Bright 3 for ultraviolet-induced visible fluorescence photography, Tiffen 87A filter with Lowell Pro tungsten lights for infrared reflected photography, and with Sylvania LED 13 PAR 30LN bulbs for visible-induced infrared luminescence photography. Infrared reflectography for HAM and SCMA was carried out with Xenics Tigris imager (InSb detector) filtered to the 1.5–1.8 micron range. Computed X-radiography was carried out with a Comet MXR-320/26 tube and Carestream Industrex Flex HR detector plate.

A Bruker Artax XRF spectrometer with a Silicon Drift Detector (SDD) and a rhodium anode X-ray tube was used for point analysis. The primary X-ray beam is collimated to give a spot size of 0.65mm. Using the Bruker Artax (version 7.6) software, spectra were acquired for 100 seconds live time at 50kV and 600 μ A. A helium flux was used to increase the detection efficiency for light elements (atomic number of potassium and lower).

Elemental distribution maps were generated using a Bruker M6 Jetstream scanning XRF spectrometer equipped with a Rh target and operated at 50 kV and 600 μ A. The Yale portrait was imaged using a 200 μ m nominal spot size, 150 μ m pixel spacing, a dwell time of 50 ms per pixel, and He purge of 0.6 L/min. The data were processed in PyMca and DataMuncher.

Samples for cross-section analysis were embedded in Bio-Plastic liquid polyester casting resin (Ward's Natural Science). Mounted samples were ground to exposure using a Buehler Handimet 2 roll grinder with CarbiMet abrasive paper rolls ranging in grit from 240 to 600. Samples were then polished using a Buehler Metaserv 2000 polisher with 6 μ m and 1 μ m Buehler MetaDi Monocrystalline Diamond Suspension.

Cross sections were observed using a Zeiss Axio Imager.M2m upright microscope equipped with four objectives (5x, 10x, 20x, and 50x) and a Zeiss Axiocam 512 Color digital camera. Images were captured using the Zeiss Zen 2.6 (blue edition) software. Visible light and bright field conditions utilized a halogen lamp and either an EPI-polarization filter cube or an EPI-Bright Field cube respectively. Ultraviolet conditions utilized a mercury vapor lamp and either a DAPI filter cube (excitation BP 450–490, beam splitter FT 510 and emission BP 515–565) or a FITC filter cube (excitation BP 450–490, beam splitter FT 510 and emission LP515).

The cross sections were analyzed using a JEOL JSM-IT500LV SEM (tungsten filament) with an Oxford Instruments X-MaxN SDD, 80 mm² detector (resolution Mn K α , 126 eV) running the Oxford Instruments AZtec software (version 4.2 SP1). The SEM was operated in low vacuum mode at a chamber pressure of 70 Pa, with an operating voltage of 20 kV, beam current optimized for dead time of analysis and working distance of 10 mm. The cross sections were not coated prior to analysis.

FTIR in transmission mode was performed using a Bruker Vertex 70 infrared bench spectrometer coupled to a Bruker Hyperion 3000 infrared microscope. Samples were compressed onto a diamond cell with a stainless-steel roller prior to analysis. Using the Bruker OPUS (version 6.0) software, spectra were recorded between 4000 and 600 cm^{-1} at 4 cm^{-1} spectral resolution and 32 scans per spectrum. The collected spectra were compared to in-house and IRUG databases.

Raman analysis was conducted using a Bruker Optics Senterra dispersive Raman microscope with an Olympus BX51M microscope equipped with 20x and 50x long working distance objectives and using the Bruker OPUS (version 7.5) software. The Raman spectrometer has three laser sources, 532 nm, 633

nm, and 785 nm. The optimum laser source depends on the pigment analyzed, but in general, blue and green pigments were predominantly analyzed with the 532 nm laser at 2 mW or 5 mW power and other colors with the 785 nm laser at 10 mW power. Spectra were compared with reference libraries, particularly the RRUFFTM database, using the Opus software.

The following procedures were carried out by Caroline Cartwright in the laboratory of the Department of Scientific Research at the British Museum. Because of the three-dimensional nature of wood anatomy, each wood sample, irrespective of its size, was fractured manually to show transverse, radial longitudinal, and tangential longitudinal sections (TS, RLS, and TLS). Each TS, RLS, and TLS wood section was then mounted onto aluminum stubs. Examination of the wood samples and comparative reference specimens (prepared and mounted using the same method) was undertaken in a variable-pressure scanning electron microscope (VP SEM), Hitachi S-3700N, using the backscattered electron (BSE) detector at 15 kV, with the SEM chamber partially evacuated (40Pa). Magnifications ranged from 35x to 1000x. The preferred working distance was ca. 14 mm but was raised or lowered from 10.6 mm to 16.5 mm (as required). With the BSE detector, 3D mode (rather than Compositional) was preferentially selected for maximum topographical information and to maximize the potential for revealing diagnostic features for identification. Further details on wood identification methods and techniques can be found in Cartwright 2015, Cartwright 2020, and Cartwright in this volume.

14. "APPEAR Ancient Panel Painting Examination, Analysis, and Research Database," J. Paul Getty Trust, 2022: <https://www.appeardatabase.org/login>. Sorting the database entries by binding medium and reviewing all tempera portraits, we find most employ a priming between the wood substrate and the paint layer.
15. FitzHugh 1986.
16. Walton and Trentelman 2009.
17. Lee and Quirke 2000; Scott 2016.
18. Dietemann et al. 2017; Freccero 2000; Brøns et al., this volume; and Verri et al., this volume.
19. Dietemann et al. 2017.
20. Thompson 1976B, 16; Parlasca 1966, 25; Walker 2000B, 84–86.

Glossary

Akhmim (Greek: *Panopolis*). A city in upper Egypt on the east bank of the Nile River. With a long history dating back to the pre-dynastic period, this site has important ties to the Graeco-Roman and Roman periods.

Alunite. A white mineral recently identified as a pigment used for painting mummy portraits. As a source of alum, it was also used as a mordant for fixing organic dyes on textiles and for producing lake pigments. Chemical formula: $KAl_3(SO_4)_2(OH)_6$

Animal glue. A collagen-based adhesive made by boiling animal skin, bones, or tendons in water. The proteinaceous glue is used as a binding medium that is mixed with pigments for painting; it can also be used for sizing or sealing wood, for applying gilding, and for joining or bonding. Glues can be made from many types of animals including cow, rabbit, horse, or fish and has been identified on thirty-six percent of painted panels (at the time of publication).

Antinoöpolis. An ancient Roman city south of Cairo and the Fayum basin, on the east bank of the Nile. The mummy portraits believed to have been discovered at this site exhibit a characteristic austere style and the wooden panels a unique stepped shape. The city was founded in 130 BCE when the emperor Hadrian named it in honor of Antinous, his lover who drowned in the Nile.

Antonine period (138–192 CE). The era that encompasses the reigns of the emperors Antoninus Pius (138–161 CE), Marcus Aurelius (168–180 CE), and Commodus (180–192 CE). Provincial elite populations flourished in the Antonine period, and the distinctive, Hellenized hairstyles of members of the imperial court were seen on coins and in widely disseminated portraits, largely of stone and bronze. For women, a bun of braids coiled at the crown of the head

and gradually draped to the nape of the neck; men adopted a bearded appearance with long, tousled hair. Closely imitated, these specific hairstyles help scholars propose a rough chronology of Roman portraiture and art.

Balteus. A sword strap, typically depicted on painted portraits as a diagonal red band, sometimes with gold or silver studs, worn over the tunic. Its presence suggests that the deceased was in the military.

Beeswax. A natural wax produced by honeybees (*Apis* sp.) that is primarily composed of hydrocarbons, fatty acids, esters, and long-chain alcohols. Egyptians used beeswax for the mummification process, in cosmetics, to retain the permanency of wig curls, and to create painted portraits (encaustic). The material has been identified on sixty-two percent of painted panels (at the time of publication).

Binding media. Organic materials that hold pigments together, enabling them to be applied as a cohesive film. Ancient binding media are based on natural materials, including wax, plant gums, and proteins such as animal glues. The physical properties of the medium strongly influence the handling and visual characteristics of the paint.

Bitumen. A naturally occurring petroleum-based black resinous material used throughout antiquity as an adhesive, waterproof sealant, and for decorative effect. It was commonly used for its ritual and preservative properties in the production of mummies.

Bulla (pl. bullae). A type of amulet, similar to a locket, worn around the neck of a boy. An indication of free birth, a bulla was used for protection as well as an official status symbol.

Calcium carbonate (chalk, lime, calcite). A chemical compound used to create a stable white pigment with limited hiding power (opacity); this pigment is used to make grounds (preparation layers) for painting. Chemical formula: CaCO_3

Carbon black. A pigment made by charring wood or other organic materials in a reducing environment (restricted air supply). It is also known as vine black (charred, desiccated grape vines and stems) or lamp black (soot collected from oil lamps). Due to the pigment's tendency to absorb infrared radiation, infrared imaging can be used to reveal artists' sketches and underdrawings made in carbon black that may not otherwise be visible beneath the painted layer.

Cauterium (cautarium). Similar to a spatula or a palette knife, a metal tool that, after being heated, was used to blend the wax colors in encaustic painting.

Cestrum. A pointed graver, possibly metal, used for adding incised details in encaustic. The cestrum would have been heated and used to draw into wax.

Chiton (tunic). A simple garment that covered the upper body, starting at the shoulders and ending at a length somewhere between the hips and the ankles. The English word *chiton* originates from the Latin *chiton*, which means "mollusk"; that, in turn, is derived from the Greek word *khitōn*, meaning "tunic." The tunic was a basic garment worn by both men and women during the Roman empire. Citizens and noncitizens alike wore chitons (usually white for men and red for women). Citizens might wear the garment under the toga, especially on formal occasions. Its length and the presence or lack of stripes (clavi), as well as width and ornamentation, indicated the wearer's status in Roman society.

Cinnabar. An orange-red pigment with excellent hiding power (opacity) and good permanence. It has been used from antiquity to the present. Chemical formula: Mercuric sulfide, HgS

Clavus (pl. clavi). A vertical stripe or ribbonlike ornament, placed in pairs, that adorned the shoulders of a tunic. In Rome some clavi of specific width and/or color distinguished members of a particular rank or status, but the significance of the clavus in an Egyptian context remains undetermined.

Computerized tomography or computerized axial tomography (CT, CAT). An imaging technique combining computer technology with X-rays to create cross-sectional images enabling detailed and layered viewing through an object.

Conifer resin. A sticky and aromatic exudate that is produced by coniferous trees such as cedar and pine. This resin was used in antiquity as a medical unguent, perfume, and for religious and ritual applications.

Consolidate. To strengthen or stabilize a material by adding another impregnating material, such as an adhesive (consolidant). For example: *The paint on the surface was consolidated using gelatin.*

Copper greens. Green pigments based on the element copper. They can include, but are not limited to, synthesized pigments such as verdigris ($\text{Cu}(\text{CH}_3\text{COO})_2$), copper resinate (copper salts of resin acids), copper (II) oleate (copper and fatty acid), Egyptian green ($\text{CaOCuO}(\text{SiO}_2)_4$), and naturally occurring mineral pigments such as malachite ($\text{Cu}_2\text{CO}_3(\text{OH})_2$).

Dura-Europos. An ancient city, in what is now Syria, that borders the Euphrates River. A strategic site that served as a crossroads for different cultures, language, and religions. With a long and complex history, the site is best known from the excavations sponsored by Yale University and the French Academy in the 1920s and 1930s.

Earth pigments. Naturally occurring minerals colored by metal oxides, principally of iron and manganese, mixed with clays and silicates. Earth pigments have been used since prehistoric times and their primary forms are ochres (iron oxide-based) and umbers (iron and manganese-based).

Egyptian blue (Roman: caeruleum, mineral: cuprorivaite). A pigment manufactured and used by Egyptians possibly as early as 3100 BCE. Considered to be the first synthetic pigment, Egyptian blue was traditionally made by mixing copper with a calcium compound (typically lime) together with silica/quartz and a flux. The mixture was heated to a very high temperature (900°C) and the resulting glassy product was then ground to a powder. Chemical formula: Calcium copper silicate, $\text{CaCuSi}_4\text{O}_{10}$ or $\text{CaOCuO}(\text{SiO}_2)_4$

el-Hibeh (el-Hiba). An archaeological site on the east bank of the Nile, south of Cairo. Remains at the site date from the late Pharaonic, Graeco-Roman, Coptic, and early Islamic periods—approximately 1100 BCE to roughly 700 CE.

ELISA (enzyme-linked immunosorbent assay). An analytical technique that employs antibodies to identify proteins in binding media such as animal glue, egg, and milk, as well as polysaccharides in plant gums. ELISA can also often characterize the biological source of the protein (e.g., rabbit-skin vs. fish glue).

Encaustic. A wax-based painting technique. From the Greek word *enkaustikos* (“burned in”), the term in its most literal sense refers to the use of molten beeswax combined with pigments; once solidified, the paint can be further manipulated using heated tools. The term is also often used, however, to describe any painting technique in which wax is the major component of the medium.

er-Rubayat (er-Rubayyat, er-Rubiyat, er-Rubayet, el-Rubaiyat). An archaeological site on the west bank of the Nile within the Fayum basin, also known as the cemetery near ancient Philadelphia. This location is where many portraits acquired by the Viennese art dealer Theodor Graf were found.

Excitation-emission matrix (EEM) fluorescence spectroscopy. A non-destructive analytical technique in which emission spectra are collected across a range of excitation wavelengths and plotted together, creating a 3D contour plot (the excitation-emission matrix) from which the wider fluorescence behavior of the material under investigation can be measured. EEM has a high sensitivity and is most often used to detect trace materials present in foodstuffs, water, and biological samples. The excitation-emission matrix can often serve as a unique indicator of the material present.

Fag el-Gamous. A large ancient Graeco-Roman cemetery located within the Fayum, Egypt, approximately 90 km south of Cairo. It was first excavated by Bernard Grenfell and Arthur Hunt in 1901–1902; more recent excavations by Brigham Young University have discovered nearly 2,000 burials.

False-color infrared (FCIR) / infrared-reflected false color (IRRFC). Images created through digital post-processing by combining visible and near-infrared images. The false colors produced can help in characterizing materials or in distinguishing between visually similar substances.

False-color ultraviolet (FCUV) / ultraviolet-reflected false color (UVRFC). Images created through digital post-processing by combining visible and ultraviolet reflectance (UVR) images. The false colors produced can help in characterizing materials or in distinguishing between visually similar substances.

Fatty acid metal soaps (lead soaps). Products created by the saponification of an oil (such as a drying oil, which hardens due to oxidation) promoted by a lead-based pigment, such as lead oxide. The soaps formed by interaction between fatty acids in the oil and lead ions from the pigment can manifest as insoluble white

aggregates within the paint layer or as a white haze (efflorescence) on the surface. Soaps can also form in wax-based paints. Beeswax is composed of wax esters that contain palmitic acid (fatty acid) and a long-chain alcohol. Hydrolysis of the wax ester produces free palmitic acids and alcohols, and if lead pigment (or another metallic ion) is present, a fatty acid soap (such as lead palmitate) can form.

Fayum (Faiyum, El Faiyûm, Al-Fayoum, Fayyum, Fayoum). A fertile desert basin immediately to the west of the Nile River, south of Cairo. Roman mummies were discovered there in several ancient cemeteries and archaeological sites, including Hawara and er-Rubayat. The Fayum was a very prosperous region and a vibrant cultural center during the Ptolemaic and Roman periods.

Fiber optics reflectance spectroscopy (FORS), also visible near-infrared fiber optics reflectance spectroscopy (VIS-NIR-FORS). A non-invasive analytical technique in which reflectance spectra are collected using two fiber optics: one to illuminate the area of interest and one to collect the spectrum. The illumination source is typically white light with reflectance spectra collected across the visible and into the near-infrared regions of the electromagnetic spectrum. FORS is most often used in the identification of pigments and dyestuffs.

Fibula. A decorative pin or brooch, usually made of metal such as bronze, silver, or gold, used to gather and secure the folds of a garment.

Flavian period (69–96 CE). The era that encompasses the reigns of Vespasian (69–79 CE) and his sons Titus (79–81 CE) and Domitian (81–96 CE). Although Vespasian encouraged a return to traditional Roman values of austere modesty, the rule of Domitian saw new levels of extravagance, especially in the dress and coiffure of imperial women. As imperial fashions became known through the dissemination of coins and sculptured busts and statues, the elaborate hairstyles were imitated, with tiers of curls requiring hairpieces to achieve the required height and mitred shape above the brow; men copied the look of balding emperors Vespasian and Titus.

Fluorescence / luminescence / photoluminescence. The response of certain materials when exposed to a high-energy radiation source. When these materials absorb high energy, they become unstable and, as they return to a more stable state, release energy (i.e., fluorescence / photoluminescence / luminescence). This response is captured with a sensor (such as a camera or an analytical instrument) and it allows for the identification of the

response as a unique signature of that material. *See also* UVF/UVL, VIL, and XRF.

Fourier transform infrared spectroscopy (FTIR). An analytical method used for characterization and identification based on the absorption of discrete wavelengths of infrared radiation to excite molecular vibrational modes. Analysis can be performed in Reflectance or Attenuated Total Reflectance (ATR) mode. This is a primary technique for the characterization of organic and some inorganic materials.

Galena. A natural mineral form of lead sulfide used as a gray/black pigment and as a cosmetic in antiquity. Chemical formula: PbS

Gammadion (pl. gammadia). A symbol composed of four Greek capital letters gamma (Γ) placed at right angles to form a decorative cross figure. Originally an ancient cosmic or religious symbol thought to bring good luck, this symbol has been found in many ancient contexts associated with Byzantium, Rome, and Graeco-Roman cultures.

Garland. A floral necklace used in religious rituals and for festive occasions. The Egyptians placed garlands on their mummified bodies as a sign of celebration in entering the afterlife; this practice developed at the beginning of the New Kingdom and continued into the Roman period. The rose was specifically associated with the goddess Isis.

Gas chromatography/mass spectrometry (GC/MS). An analytical technique used for the precise identification of organic binding materials such as proteins, oils, waxes, resins, and gums. The gas chromatograph separates complex mixtures of organic compounds using a capillary column housed in a temperature-controlled oven and, in combination with the mass spectrometer, can facilitate identification and quantification of the individual components.

Gilding. A term that describes the various decorative techniques for applying a very thin layer of gold leaf or gold powder to a solid surface such as wood, stone, or metal to give the appearance of being made of solid gold. Gold leaf, typically between 18 and 22 karats, is hammered into extremely thin sheets (leaves) or ground into a powder, and then applied with an adhesive.

Graeco-Roman Egypt / Greco-Roman Egypt (332 BCE to 395 CE). A period in ancient Egypt that lasted over 700 years. During this time, Egypt was ruled by the Greeks (332–30 BCE), also known as the Ptolemaic period, and the Romans (30 BCE–395 CE), when it became a far-reaching and wealthy province of the Roman Empire.

Green earth (terre verte). A naturally occurring Fe, Mg, Al, K hydrosilicate mineral pigment colored by glauconite or celadonite, with other associated minerals.

Ground (preparation layer). A primary layer applied to a substrate to form a smooth surface on which to paint. Typically, ground layers were composed of a white material such as gypsum, although they can range in color and composition.

Gum. A water-soluble, polysaccharide exudate obtained from woody plants or other natural sources and used as a binder for pigments. Acacia gum was the most commonly used plant binder in antiquity.

Gypsum (calcium sulfate dihydrate). A soft sulfate-based mineral found in nature. Often mixed with water to form plaster, it is used in the preparation of substrates, such as wood panels for painting. Also used as a white pigment, gypsum was identified in Tutankhamen's paint box. Chemical formula: $\text{CaSO}_4 \cdot 2\text{H}_2\text{O}$

Hadrianic period (117–138 CE). The era that encompasses the reign of Hadrian, who was known for his interest in Greek culture. The visual legacy in the portraiture of this period is exemplified in the Hellenization of male features (a short Greek beard reminiscent of that of the Athenian general and politician Pericles, and a full head of curly hair) and the classicization of female features (modest clothing and coiffures made of braids wrapped around the head).

Hawara. A Roman site in Egypt located in the Fayum basin. The necropolis at this site is well known for the systematic and well-documented excavations by British Egyptologist Sir Flinders Petrie.

Himation (pallium in Latin). A mantle worn by both men and women in the Greek world. It consisted of a square piece of cloth worn over the shoulder (typically the left), with the excess cloth draped over to the opposite shoulder. (*See* pallium.)

Horus lock. A distinctive Egyptian hairstyle depicted on the gods Horus/Harpocrates, worn by children (typically male) and sometimes by adult males. It appears as a single lock of hair (a sign of youth) on the right side of the head, above the ear.

Huntite. A white carbonate-based mineral used as a pigment throughout the ancient Mediterranean. Chemical formula: $\text{Mg}_3\text{Ca}(\text{CO}_3)_4$

Hyperspectral imaging (HSI). A spectral imaging technique in which images of the same spatial area are recorded at a series of different wavelengths across the

electromagnetic spectrum. HSI systems typically utilize a dispersion element to enable the collection of hundreds of images over a set of wavelengths. Depending on the instrument, this range typically includes the visible through the near infrared (400–1000 nm) but is sometimes extended further into the infrared (up to 2500 nm). The stack of images collected at each wavelength is called a hyperspectral data cube, where each pixel contains spectral information that can help detect or characterize the materials present.

Indigo. A natural blue dye derived from the plant *Indigofera tinctoria* and related species growing in the Mediterranean, India, and Asia, among other locations. It is believed that originally the dye woad (*Isatis tinctoria*), rather than indigo, was used in antiquity. Indigo has better lightfast properties than woad. Chemical formula: $C_{16}H_{10}N_2O_2$

Infrared reflectography (IRR). An imaging technique in which an object is irradiated with short-wave infrared radiation (SWIR; 1000–3000 nm). A specialized infrared-sensitive camera detects and captures the contrast between materials that reflect the infrared, such as lead white, and those that absorb it, such as carbon-containing pigments. Because infrared radiation has longer wavelengths than visible light, it can penetrate low-absorbing materials, revealing hidden underdrawings, artist's modifications and methodology, or modern interventions.

Iron oxide pigments (hematite, ochres, sienna, umber). Also referred to as earth pigments and made from minerals containing oxides and hydroxides of iron. Iron oxide pigments can occur in many different colors, most commonly yellow, orange, red, brown, and black. Approximately sixteen known iron oxides and oxyhydroxides were widely sourced and processed (calcined) for use as pigments.

Jarosite (natrojarosite). A yellow-to-brown mineral within the alunite group used as a pigment in Egypt. It is composed of basic hydrous sulfate of potassium and ferric iron (Fe-III). Natrojarosite is the sodium analog of jarosite. Chemical formula: $KFe_3(SO_4)_2(OH)_6$ / $NaFe_3(SO_4)_2(OH)_6$

Julio-Claudian period (27 BCE–68 CE). The era that saw the establishment of imperial rule at Rome by five successive members of a single family: Augustus (27 BCE–14 CE); Tiberius (14–38 CE); Gaius, often known as Caligula (38–41 CE); Claudius (41–54 CE); and Nero (54–68 CE). Augustus developed a clean-shaven look of somewhat short, neatly cut hair with a fringe of locks above the brow. Later Julio-Claudian court hairstyles were longer and more

elaborate, with coiled corkscrew ringlets in front of the ears and tightly wound curls around the face. Wealthy provincial men and women imitated Roman imperial court style, which was rigorously disseminated across the empire, notably on coins and in portraits in many media.

Kermes. An insect-derived ancient red dye/colorant, source of the word *crimson*. Early Egyptians made this red dye from the dried bodies of a female wingless scale insect—either *Kermes ilices* or *K. vermilio*, both of which live on certain species of Mediterranean oaks and produce a powerful, permanent scarlet dye and organic colorant. Chemical formula: kermesic and flavokermesic acid, $C_{16}H_{10}O_8$

Lake. A pigment manufactured by precipitating a dye onto an inorganic substrate/mordant (such as the metallic ions aluminum or calcium).

Lead white. A white pigment, both found as a naturally occurring mineral known as hydrocerussite and produced synthetically by exposing metallic lead to an acid (e.g., vinegar). Lead white has been widely used since antiquity and in Egypt from around 400 BCE. Chemical formula: Basic lead (II) carbonate, $2PbCO_3 \cdot Pb(OH)_2$

Linen (flax). A textile derived from the flax fiber, commonly used in but not originally native to Egypt, dating back to the Neolithic period (about 4000 BCE). Two types of flax were cultivated in predynastic Egypt: *Linum bienne* (synonym *Linum angustifolium*) and *Linum usitatissimum*. To produce linen thread, flax was dried, retted (soaked), beaten to separate the bast fibers from the stems, spliced, and spun. Although rarely done, linen thread could then be dyed (using ochre or organic colorants) before being woven into cloth. Women, men, and children were involved in linen production, but weaving is most closely associated with women. Linen cloth was very valuable and sometimes used as currency. Egyptian mummies were wrapped in linen because it symbolized wealth, light, and purity.

Liquid chromatography with diode array detection and mass spectrometry (LC/DAD/MS). An analytical technique typically employed for the study of natural dyes, which consist of multiple chemical compounds. The sample is placed in a liquid solution and the individual components are separated by passing through a chromatography column, then detected using the DAD and MS detectors.

Litharge and Massicot (from Greek *lithargyros*, *lithos* “stone” + *argyros* “silver” λιθάργυρος). A red-colored pigment that is one of the natural mineral forms of lead

(II) oxide, having a tetragonal crystal structure, t-PbO. The orthorhombic form, o-PbO, is yellow in color and known as massicot.

Lomentum (Tritum). Ancient literary sources describe various shades and grades of the Roman pigment caeruleum (Egyptian blue) based on its production. According to Pliny, washing and grinding caeruleum was used to produce a refined, fine-particle sized, and thus paler, blue pigment called lomentum. While more expensive than caeruleum, tritum was an even paler and lower-quality (cheaper) version.

Macro-X-ray fluorescence spectroscopy (MA-XRF). A mode of X-ray fluorescence spectroscopy (see XRF) wherein spectra are collected over a wide area, producing images showing the distribution of individual elements over the area. The distribution, or combination, of elements not only can inform researchers about the identity of pigments or other materials present but can also help unravel the artistic process. XRF maps can reveal, for example, initial composition, artist changes, or even the order in which materials may have been applied, down to individual brushstrokes.

Madder. A dyestuff derived from the root of the madder plant (*Rubia tinctorum*), which is native to the eastern Mediterranean and Persia. Likely introduced to Egypt by the Greeks or Romans, madder was used throughout antiquity for coloring textiles and as a pigment. Chemical name: alizarin (1,2-dihydroxyanthraquinone), purpurin (1,2,4-trihydroxyanthraquinone)

Malachite. A naturally occurring green copper-based mineral. It can be ground to produce pigments of varying green hues, with finer grinds producing lighter green hues. Found on Egyptian tomb paintings, malachite is perhaps one of the oldest known green pigments. Chemical formula: Basic copper (II) carbonate, $\text{Cu}_2\text{CO}_3\cdot\text{Cu}(\text{OH})_2$

Minium. See red lead.

Modified wax. Beeswax that has been modified by the addition of other materials—such as resin, glue, or oil—or treated with an alkali to make it water soluble and cold paintable. Some scholars have proposed that modified wax was used as a paint medium in ancient Egypt.

Morellian method. Developed by nineteenth-century art historian Giovanni Morelli, this technique explores and assists in identifying an artist's "hand" by analyzing a painting's details and minutiae through an iterative procedure.

Multiband imaging (MBI), also broadband imaging. A technical imaging protocol that uses a modified full-spectrum silicon sensor camera, filters, and lighting to capture images in broad spectral bands (such as those within the near-ultraviolet [UV] and near-infrared [IR] regions). The technique is used to enhance, compare, and reveal features that are beyond the visible region of the electromagnetic spectrum.

Multiband reflectance subtraction imaging (MBR). A digital post-processing technique that subtracts a near-infrared image from a visible light image, thus enabling the visible characterization of certain materials, specifically indigo.

Multispectral imaging (MSI). The creation of a series of images, each recording reflectance and luminescence within a different, limited, narrow-band range of wavelengths. This process involves using a series of band-pass camera filters or a set of narrow-band illumination sources; thus, it records variations in the absorption of materials at different wavelengths. Comparing or combining these images can help to characterize materials or to distinguish between materials that may appear similar.

Orchil. A violet/purple dye extracted from certain lichen (*Roccella*) through a fermentation process. Used in antiquity, orchil has been identified as a dye on textiles and in manuscript paintings. It is often used as a substitute for Tyrian purple, a rare and expensive dye obtained from a sea mollusk.

Orpiment. From the Latin *auripigmentum* (*aurum* "gold" + *pigmentum* "pigment"). A naturally occurring bright yellow arsenic sulfide mineral. When ground into a pigment, it has large, sharply faceted particles and a glittering quality. Sourced from the Red Sea and Asia Minor, and mentioned by Pliny and Vitruvius as well as in Egyptian works of the Pharaonic period, orpiment was widely traded by the Romans. Chemical formula: Arsenic trisulfide, As_2S_3

Pallium. A large, draped rectangular cloth, worn as a cloak or mantle with no undergarment, often associated with Greek intellectual activities. To the Romans, the pallium was a distinctly Greek form of dress, and so it was worn only in specific contexts. (See himation.)

Panel. Painting support made from various woods, including lime, sycomore fig, and cedar of Lebanon, among others. The shape of the upper portion of mummy portrait panels may indicate the region in which the mummy was buried: stepped panels are associated with

Antinoöpolis, round-topped panels with Hawara, and angled panels with er-Rubayat.

Pastiche. An artwork that incorporates several different styles or is composed of parts drawn from a variety of sources (e.g., a complete panel that is made of two or more components).

Penicillum. A paintbrush with bristles made from plant fibers or animal hair.

Peptide mass fingerprint (PMF). An analytical technique that involves the enzymatic digestion of proteins followed by Matrix Assisted Laser Desorption-Ionization Time of Flight mass spectrometric (MALDI) analysis of the resultant peptide mixture. PMF is currently applied extensively to collagen- and keratin-based materials, and can be used to determine the sources of, for example, leather, bone, parchment, animal and fish glues, ivory, horn, hoof, hair, baleen, and silk. In cultural heritage and art, materials such as egg and casein can similarly be identified to a specific source with PMF.

Pharaonic Egypt (3000–332 BCE). An era during ancient Egyptian history that lasted over 3,500 years and is known for important developments in art, architecture, and writing, and for contributions to science and technology. The Pharaonic period ended with Alexander the Great's conquest of Egypt in 332 BCE.

Philadelphia. An ancient cemetery near the archaeological site of er-Rubayat on the west bank of the Nile and within the Fayum basin, where many portraits acquired by the Viennese art dealer Theodor Graf were discovered. The site is often listed as the find spot for mummy portraits.

Photometric stereo imaging. A computational imaging technique that separates color from shape data to generate a high-resolution composite image that estimates surface topography.

Pigment. A colorant either derived from natural sources—mineral, plant, or insect—or produced synthetically. Typically, pigments are crushed into a fine powder and mixed with a binder, resulting in a suspension that becomes insoluble when dry; a dye produces a lake pigment when attached to an inorganic substrate or mordant.

Pistacia resin. An aromatic resin obtained from the mastic tree (*Pistacia lentiscus*).

Plant resin. A water-insoluble exudate obtained from plants, particularly coniferous trees such as pine, cedar, or fir. Composed of chemical compounds known as terpenes,

plant resins are used to produce varnishes and adhesives and for mummification processes. Many resins have an aromatic quality that also acts as a preservative (biocide).

Polarized light microscopy (PLM). A form of optical microscopy in which a sample is observed under polarized light, often used to examine the crystalline properties of materials. Pigments may be characterized by their isotropic and anisotropic characteristics when viewed under polarized light, which can provide information about their crystallographic structure.

Polychrome. The application of multiple colors to an object to produce a decorative effect.

Polysaccharide gums. Complex long chains of carbohydrate molecules of natural origin, typically in the form of a plant gum. Gum acacia is a polysaccharide gum.

Polyvinyl acetate (PVA, PVAc). Developed in the 1950s, PVA is a synthetic resin and/or emulsion. It is widely available in artist-grade paints and is also used as an adhesive. Due to reversibility challenges with emulsion preparations and the potential for the release of volatile compounds, such as acetic acid, PVA adhesives are not typically used in conservation today, although they have been identified on historical treatments.

Provenance. The ownership history of an artifact.

Provenience. The geographic origin of an artifact and its context.

Ptolemaic period (323–30 BCE). The Ptolemies were an ancient Greek dynasty in Egyptian history that began with Alexander the Great's defeat of the Persians and were the longest and final rulers of ancient Egypt until its incorporation into the Roman Empire in 30 BCE.

Punic wax. Described by both Pliny and Dioscorides, the precise nature and composition of Punic wax have been much debated, with the source texts variously interpreted as describing the preparation of a purified or clarified beeswax, or one that has been partially or completely saponified by the addition of an alkali. In the latter case the product is presumed by some to be water miscible and amenable to application in a cold state.

Radiocarbon dating (carbon14, C-14, ¹⁴C). A scientific method for dating organic materials or objects containing organic materials. All living things take up the radioactive carbon isotope carbon-14, and when the plant or animal dies, the amount of carbon-14 it contains begins to decay at a known rate. Measuring the amount of carbon-14

remaining in a sample can be used to estimate the time that has elapsed since the plant or animal died.

Raking light. Illumination by a light source positioned at an oblique angle or almost parallel to an object's surface. It is used to provide information about the surface topography.

Raman spectroscopy. An analytical technique that can be used to identify the molecular components of materials. Most frequently used for the analysis of pigments, Raman spectroscopy uses laser light (typically directed onto the sample through a microscope objective, allowing the interrogation of single particles) to generate a spectrum that is uniquely characteristic of the material under study (a "fingerprint" spectrum). Identification is often made by comparing spectra to reference spectral databases, although the examination of specific bands can also provide information about the functional groups present. Raman spectroscopy is a complementary spectroscopy to Fourier transform infrared spectroscopy (*see* FTIR).

Realgar. Closely related to orpiment, realgar is a naturally occurring red-orange arsenic sulfide pigment that was widely traded in the Roman Empire and used throughout ancient Egypt and Mesopotamia. When exposed to light, realgar alters to pararealgar, a more yellow-orange compound with the same elemental composition but different crystalline structure. Chemical formula: Arsenic sulfide, As_4S_4

Red lead (minium). A bright red-orange pigment that was one of the first to be synthetically produced. It is also referred to as *minium*, the naturally occurring form of the pigment named after the river Minius, located in northwest Spain. Chemical formula: Lead (II,IV) oxide, Pb_3O_4

Red ochre. A brownish red earth pigment colored by anhydrous iron oxide, or hematite (from the Greek *hema*, meaning "blood"), along with clays and silicates. Used since prehistory as pigments, ochres may vary widely in shades and transparency depending on the composition. *See also* earth pigments. Chemical formula: Anhydrous iron (III) oxide, Fe_2O_3

Reflectance transformation imaging (RTI). A computational imaging technique that reveals surface topography, details, and textures, thus enabling the study of tool and brush marks, etc. To perform RTI a light source is positioned at a constant radius from the subject and images are collected at different angles creating a hemisphere of image captures. The final processed file determines all possible light positions within the virtual

hemisphere and generates a polynomial texture map, or pseudo three-dimensional image of an object or surface.

Reflected near-infrared (NIR) photography. An imaging technique that records radiation responses in the near-infrared region (700–1100 nm), thus capturing the contrast between materials that reflect the infrared and those that absorb it, such as carbon-containing pigments. Because infrared is of longer wavelength than visible light, some low-absorbing materials may also allow the infrared to be transmitted through them, revealing hidden underdrawings, artist's modifications and methodology, or modern interventions.

Romano-Egypt or Roman Egypt (30 BCE to ~305 CE). The era when Egypt was a province of the Roman Empire. This period followed the defeat of Marc Antony and Cleopatra in the battle at Actium by the later emperor Augustus.

Sagum. A long, dark-colored (red, blue, or purple) outer cloak worn by Roman soldiers. The sagum was fastened on the shoulder with a fibula (brooch).

Scanning electron microscopy and energy dispersive X-ray spectroscopy (SEM-EDS / SEM-EDX). SEM is an analytical imaging technique in which a narrow beam of high-energy electrons is directed onto the surface of a sample in a raster pattern, and detectors are used to collect electrons either scattered (backscatter electrons [BSE], related to the average atomic number of the sample) or produced as a result of an ionization process (secondary electron [SE], sensitive to the surface topography). The addition of an energy-dispersive X-ray detector can collect fluorescence emission spectra that enable the identification of the elemental composition of the sample (*see* X-ray fluorescence).

Severan period (193–235 CE). An era characterized by, among other things, a fashion for short military beards and hair cropped close to the head for men and center-parted and pulled back for women. These distinctive styles help scholars to propose a rough chronology of Roman portraiture and art, as images with these coiffures appear on dated materials such as coins and busts.

Shroud. A cloth used to cover or protect another object. The term is most often used to refer to a cloth that covers or envelops a corpse. Many mummy shrouds were painted before being placed over the mummy's head or enveloping the entire body.

Specular light. Light that behaves as if it has been reflected by a mirror—that is, a ray of incoming light (incident ray) that strikes a surface and is reflected in a single outgoing direction.

Stucco. A fine plaster made of either gypsum or calcite that is used for coating surfaces or that is molded into decorative shapes. The mixture is applied wet and shaped/molded; it is typically painted after drying. Funerary masks made of stucco are found in Egypt from the First Dynasty to at least the third century CE.

Tebtunis or Tebtynis. A settlement in the lower Fayum region, known for its rich source of ancient literary, astronomical, magical, medical, and religious texts. An important regional center during the Ptolemaic period, the site was first excavated by British archaeologists Bernard Grenfell and Arthur Hunt in 1899/1900.

Tempera. In the context of ancient art, this term generally refers to a fast-drying, water-miscible painting medium such as animal glue or plant gum. The term *tempera* originates from the Latin *temperare* (“combining, blending”).

Terpenoid resin. A major component of conifer (cone-bearing seed trees and bushes) oleoresin. This natural plant resin is used as a defense from insects and pathogens and was an ingredient used for ritual mummification in ancient Egypt, with a primary function as a biocide to help preserve the body from decay.

Thebes. Located on the east bank of the Nile, south of Cairo, Thebes was the ancient capital of Egypt during the Middle and New Kingdoms. Today occupied by the modern city of Luxor, the site of ancient Thebes was one of the richest and most important cities in ancient Egypt, functioning as the religious capital of the country with temples and palaces at Karnak and the necropolises of the Valley of the Kings and the Valley of the Queens.

Trajanic period (98–117 CE). The era that corresponds to the reign of Trajan. This period is exemplified by a distinctive women’s hairstyle consisting of a “nest” of braids placed at the back of the head and rolls of curls arranged into a tall diadem (crown or headpiece) towering over the forehead. These distinguishing styles help scholars to propose a rough chronology of Roman portraiture and art, as images with these coiffures appear on dated materials such as coins and busts.

Tuna el-Gebel. Known as the “City of the Dead” in Egypt, this site mainly houses funerary monuments ranging in date from the New Kingdom up to and including the Graeco-Roman period. The majority of those buried at the necropolis during the Roman period were Egyptian, yet their burial style was Greek.

Tunic. See chiton. A simple garment that covered the upper body, starting at the shoulders and ending at a

length somewhere between the hips and the ankles. The English word *chiton* originates from the Latin *chiton*, which means “mollusk”; that, in turn, is derived from the Greek word *khitōn*, meaning “tunic.” The tunic was a basic garment worn by both men and women in ancient Rome. Citizens and noncitizens alike wore chitons (usually white for men and red for women). Citizens might wear a chiton under the toga, especially on formal occasions. The length of the garment and the presence or lack of stripes (*clavi*), as well as their width and ornamentation, indicated the wearer’s status in Roman society.

Ultraviolet-induced visible fluorescence (UVF) / UV-visible fluorescence / Ultraviolet-induced visible luminescence (UVL) (historically UV/VisFL) / Ultraviolet-induced luminescence (UIL). An imaging technique and diagnostic examination method, based on characteristic responses of materials to ultraviolet (UV) radiation (~185–400 nm, commonly the narrow band at 365 nm) in the form of fluorescence, in which radiant energy in the UV region is absorbed to create an unstable high-energy state and then reemitted as lower-energy visible light to regain stability. The fluorescence revealed by the technique is used to assist in the general characterization or differentiation of materials—such as pigments, coatings, binders, and adhesives—and to diagnose the condition of an object (e.g., to detect areas of restoration). The term *luminescence* also encompasses the possibility of a phosphorescent response to UV radiation in which there is a delay in the reemission of the absorbed energy by some materials, so that emission might even continue for a period after the UV excitation source is turned off. While *luminescence* encompasses all the emission processes that may occur, the term *fluorescence* is by far the dominant phenomenon being observed and has historically been used in describing this technique in conservation (as well as in medicine, non-destructive testing, and forensics). *Luminescence* is an equally appropriate descriptor. (See also fluorescence / photoluminescence / luminescence.)

Ultraviolet reflectance or ultraviolet reflected (UVR) imaging / reflected ultraviolet (RUV) imaging. An imaging technique that records variations in reflection and absorption of ultraviolet (UV) radiation by the surface of a subject. This imaging technique primarily aids in the characterization or differentiation of materials. Also, because UV radiation exhibits very limited surface penetration, the technique can also help in characterizing surface sheen.

Umbers (raw and burnt umber). Natural earth pigments colored by iron and manganese oxides and hydroxides. Used throughout history as earth-tone pigments, umbers

range in color from cream to brown, depending on the amount of iron and manganese oxides present. Chemical formula: Iron (III) oxide, partly hydrated + manganese oxide, $\text{Fe}_2\text{O}_3 \cdot (\text{H}_2\text{O}) + \text{MnO}_2 \cdot (n\text{H}_2\text{O})$

Visible-induced infrared luminescence / visible-induced luminescence (VIL). An imaging technique in which visible light is used to induce the emission of infrared radiation (primarily in the near-infrared [NIR] region [700–1100 nm]) by certain materials. It has been used to identify historical blue pigments (principally Egyptian blue, Han blue, and Han purple) as well as many cadmium pigments and some natural dyes. These materials may show a very strong IR emission when excited by visible light. The setup for VIL imaging is relatively simple, only requiring an excitation source emitting visible light with no IR component, a detector with sensitivity to NIR (such as an IR-modified digital camera), and a lens filter that absorbs all visible light and transmits NIR.

Visible-induced visible luminescence (VIVL). A method of recording a photo-induced emission of light in the visible region (500–700 nm) when the object is illuminated within a narrow band of visible light of higher energy (400–500 nm). The technique requires careful control of the illuminating source and imager lens filtration to ensure the range of wavelengths imaged do not include those in the excitation source.

Vitruvian proportions. Based on the work of the ancient architect Vitruvius (first century BCE), the ideal proportions, measurements, and scale of the human body as delineated in his *Ten Books on Architecture*. Leonardo da Vinci (1452–1519) was the first to successfully illustrate Vitruvius's description with his drawing, *Vitruvian Man*.

Woad (*Isatis tinctoria*). Known as “dyers woad” and used since the Neolithic period, this plant was grown as an important source of a blue dye that was extracted from the leaves. Although a different plant than *Indigofera tinctoria* (indigo), the chemical extracted from woad is the same dye extracted from “true indigo,” but in a lower concentration and thus not as lightfast.

Wreath. An assortment of flowers, leaves, fruits, twigs, or other materials constructed to resemble a loop. Typically worn on the head in ceremonial events, wreaths have much history and symbolism associated with them. In the

Graeco-Roman world, wreaths were used as adornments that could represent a person's occupation, rank, achievements, or status.

X-radiography. An imaging technique used to reveal the internal structure of an object by using X-rays to record variations in the densities of its constituent materials. X-rays are transmitted, absorbed, or scattered in varying degrees by the materials present; the radiation that passes through the object is then captured on photographic film or a digital receptor placed behind the subject, thereby creating the radiograph. Dense materials and/or those containing elements of high atomic number, such as metal and lead white paint, strongly absorb X-rays and will appear white or light in tone; less dense materials, such as wood or other organic matter, readily transmit X-rays and appear dark in the resulting image.

X-ray diffraction (XRD). An analytical method that can give information about the structure of crystalline materials, from which the identity of the materials may be inferred. This technique is most used to examine mineral pigments, stone, and corrosion products.

X-ray fluorescence (XRF) spectroscopy. A non-invasive technique that provides a means to identify the chemical elements present in a sample or area of study. The technique employs a focused beam of X-rays that excite the atoms in the irradiated area. As the atoms relax back to their initial state, they emit fluorescent X-rays at specific energies that are unique to the element. XRF spectrometers employed in conservation applications typically can detect the elements present in metals, mineral-based pigments, and other inorganic materials, but cannot detect light elements such as carbon, oxygen, or nitrogen, found in organic materials. The identification of the main elements may allow researchers to infer the identity of the materials present, but a molecularly specific technique, such as Raman spectroscopy or XRD, is necessary to provide a definitive identification.

Yellow ochre. A naturally occurring mineral consisting of silica and clay colored by the iron oxide mineral goethite. Found throughout the world, yellow ochre has many shades and hues. Chemical formula: Iron oxyhydroxide, $\text{FeO}(\text{OH})$

Bibliography

Accorsi et al. 2009

Accorsi, Gianluca, Giovanni Verri, Margherita Bolognesi, Nicola Armaroli, Catia Clementi, Costanza Miliani, and Aldo Romani. 2009. "The Exceptional Near-Infrared Luminescence Properties of Cuprorivaite (Egyptian Blue)." *Chemical Communications*, no. 23, 3392–94. <https://doi.org/10.1039/B902563D>.

Aceto et al. 2014

Aceto, Maurizio, Angelo Agostino, Gaia Fenoglio, Ambra Idone, Monica Gulmini, Marcello Picollo, Paola Ricciardi, and John K. Delaney. 2014. "Characterisation of Colourants on Illuminated Manuscripts by Portable Fibre Optic UV-Visible-NIR Reflectance Spectrophotometry." *Analytical Methods* 6 (5): 1488–1500. <https://doi.org/10.1039/c3ay41904e>.

Adrian 1893

Adrian, Louis Alphonse. 1893. *Exposition internationale de Chicago, 1893, compte rendu des groupes 87 et 88, Comité 19: Produits chimiques et pharmaceutiques, matériel de la peinture, parfumerie*. A. Hennuyer.

Aldrovandi et al. 2004

Aldrovandi, Alfredo, Ezio Buzzegoli, Annette Keller, and Diane Kunzelman. 2004. "Indagini su superfici dipinte mediante immagini UV riflesse in falso colore." *OPD Restauro*, no. 16, 83–87, 197–99. <http://www.jstor.org/stable/24392513>.

Allen 2005

Allen, James, ed. 2005. *The Art of Medicine in Ancient Egypt*. The Metropolitan Museum of Art.

Allen 2019

Allen, Ruth. 2019. "'Eye-Like Radiance': The Depiction of Gemstones in Roman Wall Painting." *Arts* 8 (2): 60. <https://doi.org/10.3390/arts8020060>.

American Institute for Conservation 1994

American Institute for Conservation. 1994. "Code of Ethics and Guidelines for Practice; Commentaries." <https://www.culturalheritage.org/docs/default-source/administration/governance/code-of-ethics-and-guidelines-for-practice.pdf>.

American Institute for Conservation 2015

American Institute for Conservation. 2015. "Commentaries to the Guidelines for Practice of the American Institute for Conservation of Historic & Artistic Works." <https://www.culturalheritage.org/docs/default-source/administration/governance/commentaries-to-the-guidelines.pdf>.

Amsen 2020

Amsen, Eva. 2020. "Facial Reconstruction Suggests that Some Egyptian Mummy Portraits Were Painted after Death." *Forbes*, September 27. <https://www.forbes.com/sites/evaamsen/2020/09/27/facial-reconstruction-suggests-that-some-egyptian-mummy-portraits-were-painted-after-death/>.

Anderson 2019

Anderson, Jaynie. 2019. *The Life of Giovanni Morelli in Risorgimento Italy*. Officina Libraria.

Apostolaki 2005

Apostolaki, Chrsi. 2005. "Study of Roman Mortars and Wall Painting Colourants from Ancient Corinth." Master of

Science thesis, Technical University of Crete. <http://purl.tuc.gr/dl/dias/64FA6667-B23B-486A-A5FF-4291AB79E3B6>.

Arnold and Valladas 1991

Arnold, Maurice, and H el ene Valladas. 1991. "Datation carbone 14 de la t ete de harpe en bois." *La Revue du Louvre et des mus ees de France* 1: 7. <https://agorha.inha.fr/ark:/54721/b06e9134-528f-4f27-836d-8ff2190104fa>.

Asensi Amor s and D etienne 2008

Asensi Amor s, Victoria, and Pierre D etienne. 2008. "Les bois utilis es pour les portraits peints en Egypte   l' poque romaine." In Aubert and Cortopassi 2008.

Asensi Amor s et al. 2001

Asensi Amor s, Victoria, Sylvie Colinart, Madeleine Fabre, Catherine Gras, H el ene Guichard, Daniel Jaunard, and Sylvie Watelet. 2001. "Survivre au-del  de la mort: Les portraits fun raires  gyptiens du mus e des Beaux-Arts de Dijon." *Techn *, nos. 13–14, 119–30.

Aubert 2000

Aubert, Marie-France. 2000. "Portraits from Antinoopolis and Other Sites." In Walker 2000A.

Aubert and Cortopassi 2008

Aubert, Marie-France, and Roberta Cortopassi. 2008. *Portraits fun raires de l' gypte romaine*. Volume 2. R union des mus ees nationaux and  ditions Kheops.

Augusti 1967

Augusti, Selim. 1967. *I colori Pompeiani*. De Luca.

Bagnall and Frier 1994

Bagnall, Roger S., and Bruce Frier. 1994. *The Demography of Roman Egypt*. Cambridge University Press.

B kowska-Czerner and Czerner 2022

B kowska-Czerner, Grażyna, and Rafa  Czerner. 2022. "Marina El-Alamein as an Example of Painting Decoration of Main Spaces of Hellenistic-Roman Houses in Egypt." *Arts* 11 (1): 2.

Barr 2020

Barr, Judith. 2020. "From All Sides: The APPEAR Project and Mummy Portrait Provenance." In Svoboda and Cartwright 2020.

Barr et al. 2019

Barr, Judith, Clara M. ten Berge, Jan M. van Daal, and Branko F. van Oppen de Ruiter. 2019. "The Girl with the Golden Wreath: Four Perspectives on a Mummy Portrait." *Arts* 8 (3): 92–122.

Becker 2021

Becker, Hilary. 2021. "Pigment Nomenclature in the Ancient Near East, Greece, and Rome." *Archaeological and Anthropological Sciences* 14 (20). <https://doi.org/10.1007/s12520-021-01394-1>.

Bell, Clark, and Gibbs 1997

Bell, Ian M., Robyn J. H. Clark, and Peter J. Gibbs. 1997. "Raman Spectroscopic Library of Natural and Synthetic Pigments (pre- ≈ 1850 AD)." *Spectrochimica Acta Part A: Molecular and Biomolecular Spectroscopy* 53 (12): 2159–79. [https://doi.org/10.1016/S1386-1425\(97\)00140-6](https://doi.org/10.1016/S1386-1425(97)00140-6).

Benitez 2018

Benitez, Francisco. 2018. "Francisco Benitez." <http://www.franciscobenitez.com/>.

Bernhard 1947

Bernhard, Maria Ludwika. 1947. "Zbiory Sztuki Starożytniej w Muzeum Narodowym w Warszawie w latach 1939–1946." *Archeologia* 1: 302–9.

Berrie 1997

Berrie, Barbara. "Prussian Blue." 1997. In vol. 3 of *Artists' Pigments: A Handbook of Their History and Characteristics*, edited by Elizabeth FitzHugh. National Gallery of Art.

Bierbrier 1997

Bierbrier, Morris. 1997. "The Discovery of the Mummy Portraits." In Walker and Bierbrier 1997.

Bierbrier 2012

Bierbrier, Morris L. 2012. *Who Was Who in Egyptology*. 4th ed. Egyptian Exploration Society.

Bietenholz 1962

Bietenholz, Peter G. 1962. "Pietro Della Valle 1586–1652." *Studien zur Geschichte der Orientkenntnis und des Orientbildes im Abendlande* 85: 205–8.

Biron and Pierrat-Bonnefois 2007

Biron, Isabelle, and Genevi ve Pierrat-Bonnefois. 2007. "La t ete  gyptienne en verre bleu du mus e du Louvre." *L'actualit  chimique*, nos. 312–313 (October–November): 47–52.

Bishop and Murad 2005

Bishop, Janice, and Enver Murad. 2005. "The Visible and Infrared Spectral Properties of Jarosite and Alunite." *American Mineralogist* 90 (7): 1100–1107.

Bisulca et al. 2021

Bisulca, Christina, Ellen Hanspach-Bernal, Aaron Steele, and Caroline Roberts. 2021. "Deconstructing an Ancient Egyptian Mummy Portrait." *Bulletin of the Detroit Institute of Arts* 95 (1): 12–14.

Borchardt 1930

Borchardt, Ludwig. 1930. "Ägyptische 'Altertümer', die ich für neuzeitlich halte." *Zeitschrift für Ägyptische Sprache und Altertumskunde* 65 (1): unnumbered appendix.

Borg 1996

Borg, Barbara. 1996. *Mumienporträts: Chronologie und kulturelle Kontext*. Philipp von Zabern.

Borg 1997

Borg, Barbara. 1997. "The Dead as a Guest at Table: Continuity and Change in the Egyptian Cult of the Dead." In *Portraits and Masks: Burial Customs in Roman Egypt*, edited by Morris L. Bierbrier. The British Museum.

Borg 1998

Borg, Barbara. 1998. "Der zierlichste Anblick der Welt..." In *Ägyptische Porträtmumien*. Phillip von Zabern.

Borg and Most 2000

Borg, Barbara E., and Glenn W. Most. 2000. "The Face of the Elite." *Arion: A Journal of Humanities and the Classics*, 3rd ser., 8 (1): 63–96. <http://www.jstor.org/stable/20163786>.

Borromeo et al. 2020

Borromeo, Georgina E., Ingrid A. Neuman, Scott Collins, Catherine Cooper, Derek Merck, and David Murray. 2020. "Framing the Heron Panel: Iconographic and Technical Comparanda." In Svoboda and Cartwright 2020.

Bostock and Riley 1855

Bostock, J., and H. Riley, trans. 1855. *The Natural History (Naturalis Historia)*. By Pliny the Elder. Taylor and Francis; Henry G. Bohn.

Bouchard and Smith 2003

Bouchard, Michel, and David C. Smith. 2003. "Catalogue of 45 Reference Raman Spectra of Minerals Concerning Research in Art History or Archaeology, Especially on Corroded Metals and Coloured Glass." *Spectrochimica Acta Part A: Molecular and Biomolecular Spectroscopy* 59 (10): 2247–66. [https://doi.org/10.1016/S1386-1425\(03\)00069-6](https://doi.org/10.1016/S1386-1425(03)00069-6).

Boust and Wohlgelmuth 2017

Boust, Clotilde, and Anne Wohlgelmuth. 2017. "Database: Pigments under UV and IR Radiations." Scientific Imaging for Cultural Heritage/Images scientifiques pour le

patrimoine. *Hypotheses*, August 18. Accessed June 30, 2021. <https://copa.hypotheses.org/552>.

Bradley et al. 2020

Bradley, Lauren, Jessica Ford, Dawn Kriss, Victoria Schussler, Federica Pozzi, Elena Basso, and Lisa Bruno. 2020. "Evaluating Multiband Reflectance Image Subtraction for the Characterization of Indigo in Romano-Egyptian Funerary Portraits." In Svoboda and Cartwright 2020.

Bragantini 2010

Bragantini, Irene. 2010. *Atti del X Congresso internazionale dell'AIPMA, Associazione internazionale per la pittura murale antique, Napoli 17-21 Settembre 2007 / a cura di Irene Bragantini. Annali di Archeologia e Storia Antica. Quaderni / Dipartimento di Studi del Mondo Classico e del Mediterraneo Antico*, no. 18. Napoli: Università degli Studi di Napoli "L'Orientale."

Brecoulaki 2014

Brecoulaki, Harikleia. 2014. "'Precious Colours' in Ancient Greek Polychromy and Painting: Material Aspects and Symbolic Values." *Revue Archéologique*, no. 1, 3–35. <http://www.jstor.org/stable/24751260>.

Brecoulaki et al. 2019

Brecoulaki, Hariclia, Giovanni Verri, Brigitte Bourgeois, Francesco Paolo Romano, Andreas G. Karydas, Claudia Caliri, Elena Martín González, and Giorgos Kavvadias. 2019. "The 'Lost Art' of Archaic Greek Painting: Revealing New Evidence on the Pitsa *Pinakes* through MA-XRF and Imaging Techniques." *Technè* 48: 34–54. <https://doi.org/10.4000/techne.2046>.

Bredal-Jørgensen et al. 2011

Bredal-Jørgensen, Jørn, Jana Sanyova, Vibeke Rask, Maria Louise Sargent, and Rikke Hoberg Therkildsen. 2011. "Striking Presence of Egyptian Blue Identified in a Painting by Giovanni Battista Benvenuto from 1524." *Analytical and Bioanalytical Chemistry* 401: 1433–39. <https://doi.org/10.1007/s00216-011-5140-y>.

Briefel 2006

Briefel, Aviva. 2006. *The Deceivers: Art Forgery and Identity in the Nineteenth Century*. Cornell University Press.

Brill 1980

Brill, Thomas B. 1980. *Light: Its Interaction with Art and Antiquities*. Plenum.

Broecke 2015

Broecke, Lara, trans. 2015. *Cennino Cennini's Il Libro Dell'arte: A New English Translation and Commentary with Italian Transcription*. Archetype.

Brøns et al. 2023

Brøns, Cecilie, Jens Stenger, Richard Newman, Caroline Cartwright, Fabiana Di Gianvincenzo, Anna Katerinopoulou, Luise Ørsted Brandt, Negar Haghipour, and Laura Hendriks. 2023. "'A Lost Chapter of Ancient Art': Archaeometric Examinations of Panel Paintings from Roman Egypt." *Studies in Conservation* 69 (7): 557–95. <https://doi.org/10.1080/00393630.2023.2256132>.

Bruhn 1993

Bruhn, Jutta-Annette. 1993. *Coins and Costume in Late Antiquity*. *Dumbarton Oaks*.

Buckley et al. 2009

Buckley, Michael, Matthew Collins, Jane Thomas-Oates, and Julie C. Wilson. 2009. "Species Identification by Analysis of Bone Collagen Using Matrix-Assisted Laser Desorption/Ionisation Time-of-Flight Mass Spectrometry." *Rapid Communications in Mass Spectrometry* 23 (23): 3843–54. <https://doi.org/10.1002/rcm.4316>.

Burgio and Clark 2001

Burgio, Lucia, and Robyn J. H. Clark. 2001. "Library of FT-Raman Spectra of Pigments, Minerals, Pigment Media and Varnishes, and Supplement to Existing Library of Raman Spectra of Pigments with Visible Excitation." *Spectrochimica Acta Part A: Molecular and Biomolecular Spectroscopy* 57 (7): 1491–521. [https://doi.org/10.1016/S1386-1425\(00\)00495-9](https://doi.org/10.1016/S1386-1425(00)00495-9).

Caley 2008

Caley, Earle Radcliffe. 2008. *The Leyden and Stockholm Papyri*. Oesper Collections in the History of Chemistry, University of Cincinnati.

Cardon et al. 2018

Cardon, Dominique, Witold Nowik, Adam Bülow-Jacobsen, Renata Marcinowska, Katarzyna Kusiak, and Marek Trojanowicz. 2018. "La pourpre en Egypte romaine: Récentes découvertes, implications techniques, économiques et sociales." In *Les arts de la couleur en Grèce ancienne... et ailleurs*, edited by Philippe Jockey. École française d'Athènes.

Cartwright 1997A

Cartwright, Caroline R. 1997. "Egyptian Mummy Portraits: Examining the Woodworkers' Craft." In *Portraits and*

Masks: Burial Customs in Roman Egypt, edited by Morris Bierbrier. The British Museum.

Cartwright 1997B

Cartwright, Caroline R. 1997. Wood identifications for Walker and Bierbrier 1997, multiple pages.

Cartwright 2015

Cartwright, Caroline R. 2015. "The Principles, Procedures and Pitfalls in Identifying Archaeological and Historical Wood Samples." *Annals of Botany* 116 (1): 1–13. <https://doi.org/10.1093/aob/mcv056>.

Cartwright 2020

Cartwright, Caroline R. 2020. "Understanding Wood Choices for Ancient Panel Painting and Mummy Portraits in the APPEAR Project through Scanning Electron Microscopy." In Svoboda and Cartwright 2020. <https://www.getty.edu/publications/mummyportraits/part-one/2>.

Cartwright 2022

Cartwright, Caroline R. 2022. "Identification of the Wood Used for the Mummy Portrait 25.2 in the Collection of the Detroit Institute of Arts, Michigan." Internal Document, Department of Scientific Research, The British Museum.

Cartwright and Middleton 2008

Cartwright, Caroline R., and Andrew P. Middleton. 2008. "Scientific Aspects of Ancient Faces: Mummy Portraits from Egypt." *The British Museum Technical Research Bulletin* 2: 59–66.

Cartwright, Spaabæk, and Svoboda 2011

Caroline R. Cartwright, Lin Rosa Spaabæk, and Marie Svoboda. 2011. "Portrait Mummies from Roman Egypt: Ongoing Collaborative Research on Wood Identification." *The British Museum Technical Research Bulletin* 5: 49–58.

Casadio et al. 2019

Casadio, Francesca, Katrien Keune, Petria Noble, Annelies Van Loon, Ella Hendriks, Silvia A. Centeno, and Gillian Osmond. 2019. *Metal Soaps in Art*. Springer International.

Centeno 2016

Centeno, Silvia A. 2016. "Identification of Artistic Materials in Paintings and Drawings by Raman Spectroscopy: Some Challenges and Future Outlook." *Journal of Raman Spectroscopy* 47 (1): 9–15. <https://doi.org/10.1002/jrs.4767>.

Challis 2013

Challis, Debbie. 2013. *The Archaeology of Race*. Bloomsbury.

Chatterjee and Hannan 2016

Chatterjee, Helen J., and Leonie Hannan. 2016. *Engaging the Senses: Object-Based Learning in Higher Education*. Routledge.

Christie's New York 2005

Christie's New York. 2005. "An Egyptian Painted Wood Mummy Portrait of a Woman." Auction Catalogue (Sale 1584). December 9. Accessed August 13, 2019. <https://www.christies.com/lotfinder/lot/an-egyptian-painted-wood-mummy-portrait-of-4617234-details.aspx>.

Christie's New York 2011

Christie's New York. 2011. "An Egyptian Painted Wood Mummy Portrait of a Woman." Auction Catalogue (Sale 2450). June 9. Accessed August 13, 2019. <https://www.christies.com/lotfinder/Lot/an-egyptian-painted-wood-mummy-portrait-of-5443249-details.aspx>.

Clarysse 1995

Clarysse, Willy. 1995. "Greeks in Ptolemaic Thebes." In *Hundred-Gated Thebes: Acts of a Colloquium on Thebes and the Theban Area in the Graeco-Roman Period*, edited by Sven P. Vleeming. Brill.

Clementi et al. 2008

Clementi, Catia, Brenda Doherty, Pier Luigi Gentili, Costanza Miliiani, Aldo Romani, Bruno G. Brunetti, and Antonio Sgamellotti. 2008. "Vibrational and Electronic Properties of Painting Lakes." *Applied Physics A* 92 (1): 25–33. <https://doi.org/10.1007/s00339-008-4474-6>.

Clerc (1847) 2009

Clerc, Alfred. 1847. "Lettre à M. De Saulcy sur Quelques Antiquités Égyptiennes et sur le Boeuf Apis." *Revue Archéologique* 3 (2): 649–67. Translated in Fiechter 2009. Flammarion.

Colinart and Grappin-Wsevoljsky 1999

Colinart, Sylvie, and Sibille Grappin-Wsevoljsky. 1999. "La cire punique: Étude critique des recettes antiques et de leur interprétation; Application aux portraits du Fayoum." In *ICOM-CC 12th Triennial Meeting, Lyon*, vol. 1, edited by Janet Bridgland and Jessica Brown. James & James.

Colinart et al. 2001

Colinart, Sylvie, et al. 2001. "Masques funéraires égyptiens de l'époque romaine." In *Le plâtre: L'art et la matière*, edited by Georges Barthe. Créaphis.

Colombo 1995

Colombo, L. 1995. *I colori degli antichi*. Nardini.

Connan 1999

Connan, Jacques. 1999. "Use and Trade of Bitumen in Antiquity and Prehistory: Molecular Archaeology Reveals Secrets of Past Civilizations." *Philosophical Transactions of the Royal Society B: Biological Sciences* 354 (1379): 33–50. <http://doi.org/10.1098/rstb.1999.0358>.

Cooney 1950

Cooney, John D. 1950. "A Reexamination of Some Egyptian Antiquities." *Brooklyn Museum Bulletin* 11 (3): 11–26. <http://www.jstor.org/stable/26458610>.

Corcoran 1995

Corcoran, Lorelei H. 1995. *Portrait Mummies from Roman Egypt (I-IV Centuries AD): With a Catalog of Portrait Mummies in Egyptian Museums*. Oriental Institute of the University of Chicago.

Corcoran and Svoboda 2010

Corcoran, Lorelei H., and Marie Svoboda. 2010. *Herakleides: A Portrait Mummy from Roman Egypt*. J. Paul Getty Museum.

Cosentino 2013

Cosentino, Antonino. 2013. "Infrared False Color for Art Examination." Cultural Heritage Science Open Source. February 13. Accessed June 20, 2020. <https://chsopencsource.org/photoshop-for-multispectral-imaging-speeding-up-workflow/>.

Cosentino 2014

Cosentino, Antonino. 2014. "Identification of Pigments by Multispectral Imaging: A Flowchart Method." *Conservation Heritage Science* 2 (8): 1–12. <https://doi.org/10.1186/2050-7445-2-8>.

Cowell and Craddock 1995

Cowell, M. R., and P. T. Craddock. 1995. "Addendum: Copper in the Skin of Lindow Man." In *Bog Bodies: New Discoveries and New Perspectives*, edited by R. C. Turner and R. G. Scaife, 74–75. British Museum Press.

Cucci et al. 2019

Cucci, Costanza, E. Keats Webb, Andrea Casini, Marina Ginanni, Elena Prandi, Lorenzo Stefani, Tatiana Vitorino, and Marcello Picollo. 2019. "Short-Wave Infrared Reflectance Hyperspectral Imaging for Painting Investigations: A Methodological Study." *Journal of the American Institute for Conservation* 58 (1–2): 16–36. <https://doi.org/10.1080/01971360.2018.1543102>.

Cumbo 2019

Cumbo, Cristina. 2019. *Le c.d. gammadiae nelle catacombe cristiane di Roma: Censimento, confronti ed ipotesi interpretative*. BAR Publishing.

Cuní et al. 2012

Cuní, Jorge, Pedro Cuní, Brielle Eisen, Rubén Savizkyc, and John Bové. 2012. "Characterization of the Binding Medium Used in Roman Encaustic Paintings on Wall and Wood." *Analytical Methods* 4 (3): 659–69. <https://doi.org/10.1039/C2AY05635F>.

Dandrau 1999

Dandrau, Alain. 1999. "La peinture murale minoenne, I. La palette du peintre égéen et égyptien à l'Âge du Bronze: Nouvelles données analytiques." *Bulletin de Correspondance Hellénique* 123 (1): 1–41. https://www.persee.fr/doc/bch_0007-4217_1999_num_123_1_7209.

Dasen 2008

Dasen, Véronique. 2008. "Le secret d'Omphale." *Revue Archéologique* 46 (2): 265–81. <http://www.jstor.org/stable/23911294>.

Daszewski 2008

Daszewski, Wiktor Andrzej. 2008. "Graeco-Roman Town and Necropolis in Marina El-Alamei." *Polish Archaeology in the Mediterranean* 20: 421–56.

Davies 1984

Davies, W. Vivian. 1984. *The Statuette of Queen Tetisheri: A Reconsideration*. The British Museum.

Davis 1989

Davis, Whitney M. 1989. *The Canonical Tradition in Ancient Egyptian Art*. Cambridge University Press.

Davis 2021

Davis, Paul R. 2021. "The Twentieth-Century Life of a 'Hellenistic' or 'Imperial Roman' Statue of a Bull." In Hopkins, Costello, and Davis 2021.

Davy 1815

Davy, Humphry. 1815. "Some Experiments and Observations on the Colours Used in Painting by the Ancients." *Philosophical Transactions of the Royal Society of London* 105: 97–124. <https://www.jstor.org/stable/107361>.

Dean-Jones 1991

Dean-Jones, Lesley. 1991. "The Cultural Construct of the Female Body in Classical Greek Science." In *Women's History and Ancient History*, edited by Sarah B. Pomeroy. University of North Carolina Press.

de Cenival 1991

de Cenival, Jean-Louis. 1991. "La fin de la tête de harpe." *La Revue du Louvre et des musées de France* 1: 6–7.

de Faria, Silva, and de Oliveira 1997

de Faria, Dalva L. A., S. Venâncio Silva, and M. T. de Oliveira. 1997. "Raman Microspectroscopy of Some Iron Oxides and Oxyhydroxides." *Journal of Raman Spectroscopy* 28 (11): 873–78.

Delamare, Monge, and Repoux 2004

Delamare, François, Gabriel Monge, and Monique Repoux. 2004. "À la recherche de différentes qualités marchandes dans les bleus égyptiens trouvés à Pompéi." *Rivista di Studi Pompeiani* 15: 89–107. <http://www.jstor.org/stable/44291046>.

Delaney et al. 2017

Delaney, John K., Kathryn A. Dooley, Roxanne Radpour, and Ioanna Kakoulli. 2017. "Macroscale Multimodal Imaging Reveals Ancient Painting Production Technology and the Vogue in Greco-Roman Egypt." *Scientific Reports* 7 (1): 15509. <https://doi.org/10.1038/s41598-017-15743-5>.

de la Rie 1982

de la Rie, E. René. 1982. "Fluorescence of Paint and Varnish Layers (Part I)." *Studies in Conservation* 27 (1): 1–7.

de Vartavan 2007

de Vartavan, Christian T. 2007. "Pistacia Species in Relation to Their Use as Varnish and 'Incense' (Sntr) in Pharaonic Egypt." *Bulletin of Parthian and Mixed Oriental Studies*, no. 2, 63–92.

de Vartavan 2009

de Vartavan, Christian T. 2009. "Labeling Ancient Egyptian Complex-Media Varnish as 'Imperial.'" *Journal of Ancient Egyptian Interconnections* 1 (2): 26–28.

De Viguerie et al. 2018

De Viguerie, Laurence, Sophie Rochut, Matthias Alfeld, Philippe Walter, Sophie Astier, Valérie Gontero, and Florence Boulc'h. 2018. "XRF and Reflectance Hyperspectral Imaging on a 15th-Century Illuminated Manuscript: Combining Imaging and Quantitative Analysis to Understand the Artist's Technique." *Heritage Science* 6: 11. <https://doi.org/10.1186/s40494-018-0177-2>.

Dietemann et al. 2017

Dietemann, Patrick, Heike Stege, Ursula Baumer, Andrea Obermeier, Christoph Steuer, Luise Sand, Catharine Bländsdorf, Elisabeth Fugmann, and Kristian Kaiser. 2017.

"Pigmente und Bindemittel antiker Mumienporträts." In *Inkarnat und Signifikanz: Das menschliche Abbild in der Tafelmalerei von 200 bis 1250 im Mittelmeerraum*, edited by Yvonne Schmuhl and Esther Pia Wipfler. Zentralinstitut für Kunstgeschichte.

Doxiadis 1995

Doxiadis, Euphrosyne. 1995. *The Mysterious Fayum Portraits: Faces from Ancient Egypt*. Thames & Hudson.

Drerup 1933

Drerup, Heinrich. 1933. *Die Datierung der Mumienporträts*. Ferdinand Schönigh.

Drimmer 2022

Drimmer, Sonja. 2022. "Connoisseurship, Art History, and the Paleographical Impasse in Middle English Studies." *Speculum* 97 (2): 415–68.

Duce et al. 2012

Duce, Celia, Lisa Ghezzi, Massimo Onor, Iliara Bonaduce, Maria Perla Colombini, Maria Rosaria Tine', and Emilia Bramanti. 2012. "Physico-Chemical Characterisation of Protein-Pigment Interactions in Tempera Paint Reconstructions: Casein/Cinnabar and Albumin/Cinnabar." *Analytical and Bioanalytical Chemistry* 402 (6): 2183–93.

Dunand and Zivie-Coche 2004

Dunand, Françoise, and Christiane Zivie-Coche. 2004. *Gods and Men in Egypt: 3000 BCE to 395 CE*. Cornell University Press.

Dyer and Newman 2020

Dyer, Joanne, and Nicola Newman. 2020. "Multispectral Imaging Techniques Applied to the Study of Romano-Egyptian Funerary Portraits at the British Museum." In Svoboda and Cartwright 2020.

Dyer, Verri, and Cupitt 2013

Dyer, Joanne, Giovanni Verri, and John Cupitt. 2013. *Multispectral Imaging in Reflectance and Photo-Induced Luminescence Modes: A User Manual*. The British Museum.

Eastaugh et al. 2004

Eastaugh, Nicholas, Valentine Walsh, Tracey Chaplin, and Ruth Siddall. 2004. *Pigment Compendium: A Dictionary and Optical Microscopy of Historical Pigments*. Butterworth-Heinemann.

Eastaugh et al. 2008

Eastaugh, Nicholas, Valentine Walsh, Tracey Chaplin, and Ruth Siddall. 2008. *Pigment Compendium: A Dictionary and*

Optical Microscopy of Historical Pigments. 3rd ed. Butterworth-Heinemann.

Eastlake 1891

Eastlake, Elizabeth. 1891. "Giovanni Morelli: Patriot and Critic." *Quarterly Review* 173: 235.

Ebbinghaus et al. 2022A

Ebbinghaus, Susanne, Georgina Rayner, Kate Smith, and Jen Thum. 2022. "Funerary Portraits from Roman Egypt: Facing Forward." Harvard Art Museums. Accessed September 2, 2022. <https://harvardartmuseums.org/tour/770>.

Ebbinghaus et al. 2022B

Ebbinghaus, Susanne, Georgina Rayner, Kate Smith, and Jen Thum. 2022. "Portrait of a Woman." Harvard Art Museums. Accessed December 28, 2022. <https://harvardartmuseums.org/tour/funerary-portraits-from-roman-egypt-facing-forward-2/slide/12405>.

Ebbinghaus et al. 2022C

Ebbinghaus, Susanne, Georgina Rayner, Kate Smith, and Jen Thum. 2022. "Results of Technical Studies." Harvard Art Museums. Accessed December 28, 2022. <https://harvardartmuseums.org/tour/funerary-portraits-from-roman-egypt-facing-forward/stop/2609>.

Ebbinghaus et al. 2022D

Ebbinghaus, Susanne, Georgina Rayner, Kate Smith, and Jen Thum. 2022. "Tracing the Path to the Museum." Harvard Art Museums. Accessed September 2, 2022. <https://harvardartmuseums.org/tour/funerary-portraits-from-roman-egypt-facing-forward-2/slide/12413>.

Ebers 1893

Ebers, Georg. 1893. *Antike Portraits: Die hellenistischen Bildnisse aus dem Fajjûm*. Leipzig.

Edgar 1905

Edgar, Campbell C. 1905. *Graeco-Egyptian Coffins and Portraits: Catalogue général des antiquités Égyptiennes du Musée du Caire*. Imprimerie de l'Institut français d'archéologie orientale.

Edwards Howell et al. 2007

Edwards Howell, G. M., Ben Stern, Susana E. Jorge Villar, and A. Rosalie David. 2007. "Combined FT-Raman Spectroscopic and Mass Spectrometric Study of Ancient Egyptian Sarcophagal Fragments." *Analytical and Bioanalytical Chemistry* 387 (3): 829–36.

El-Rifai, Mahgoub, and Ide-Ektassabi 2016

El-Rifai, Ibrahim, Hend Mahgoub, and Ari Ide-Ektassabi. 2016. "Multi-Spectral Imaging System (IWN) for the Digitization and Investigation of Cultural Heritage." In *Digital Heritage. Progress in Cultural Heritage: Documentation, Preservation, and Protection: 6th International Conference, EuroMed 2016, Nicosia, Cyprus, October 31–November 5, 2016, Proceedings, Part I*. Springer. https://doi.org/10.1007/978-3-319-48496-9_19.

Elston and Maish 2001

Elston, Maya, and Jeffrey Maish. 2001. "Technical Investigation of a Painted Romano-Egyptian Sarcophagus from the Fourth Century A.D." In vol. 2 of *Studia Varia from the J. Paul Getty Museum*. J. Paul Getty Museum.

Fairbanks and Fairbanks 2005

Fairbanks, Avarad T., and Eugene F. Fairbanks. 2005. *Human Proportions for Artists*. Fairbanks Art and Books.

Feller 1986

Feller, Robert. 1986. "Barium Sulfate." In vol. 1 of *Artists' Pigments: A Handbook of Their History and Characteristics*, edited by Robert Feller. National Gallery of Art.

Fiechter 2009

Fiechter, Jean-Jacques. 2009. *Egyptian Fakes: Masterpieces That Duped the Art World and the Experts Who Uncovered Them*. Flammarion.

FitzHugh 1986

FitzHugh, Elisabeth West. 1986. "Red Lead and Minium." In vol. 1 of *Artists' Pigments: A Handbook of Their History and Characteristics*, edited by Robert Feller. National Gallery of Art.

Fouqué 1889

Fouqué, Ferdinand. 1889. "Sur le bleu égyptien ou vestorien." *Comptes-rendus hebdomadaires des séances de l'Académie des sciences* 108: 325–27.

Fournet 2004

Fournet, Jean-Luc. 2004. "Deux textes relatifs à des couleurs: 1. Liste mentionnant des teintures (P. Société Fouad inv. 99); 2. Un portrait avec des indications destinées au peintre (Phoebe Hearst Museum [Berkeley] inv. 6/21378b)." In *Gedenkschrift Ulrike Horak (P. Horak)*, edited by Hermann Harrauer and Rosario Pintaudi. *Papyrologica Florentina* 34. Gonnelli.

Freccero 2000

Freccero, Agneta. 2000. *Fayum Portraits: Documentation and Scientific Analysis of Mummy Portraits Belonging to Nationalmuseum in Stockholm*. Acta Universitatis Gothoborgensis.

Fulcher et al. 2021

Fulcher, Kate, Margaret Serpico, John H. Taylor, and Rebecca Stacey. 2021. "Molecular Analysis of Black Coatings and Anointing Fluids from Ancient Egyptian Coffins, Mummy Cases, and Funerary Objects." *PNAS: Proceedings of the National Academy of Sciences of the United States of America* 118 (18): e2100885118. <https://doi.org/10.1073/pnas.2100885118>.

Galán 2007

Galán, José M. 2007. "An Apprentice's Board from Dra Abu el-Naga." *JEA (Journal of Egyptian Archaeology)* 93 (2007): 95–116.

Ganio et al. 2015

Ganio, Monica, Johanna Salvant, Jane Williams, Lynn Lee, Oliver Cossairt, and Marc Walton. 2015. "Investigating the Use of Egyptian Blue in Roman Egyptian Portraits and Panels from Tebtunis, Egypt." *Applied Physics A* 121 (3): 813–21. <https://doi.org/10.1007/s00339-015-9424-5>.

Gänsicke 2010

Gänsicke, Susanne. 2010. "The Conservation of Decorated Organic Egyptian Surfaces: A Literature Review." In *Decorated Surfaces on Ancient Egyptian Objects: Technology, Deterioration, and Conservation; Proceedings of a Conference Held in Cambridge, UK, on 7–8 September 2007*, edited by Julie Dawson, Christina Rozeik, and Margot M. Wright. Archetype.

Gehad et al. 2022

Gehad, Basem, Lorelai H. Corcoran, Mahmoud Ibrahim, Ahmed Hammad, Mohamed Samah, Abd Allah Abdo, and Omar Fekry. 2022. "Newly Discovered Mummy Portraits from the Necropolis of Ancient Philadelphia–Fayum." *BIFAO* 122, 245–64. <https://journals.openedition.org/bifao/11727>.

Gemological Institute of America N.D.

Gemological Institute of America. n.d. "Buyer's Guide." Accessed September 9, 2022. <https://www.gia.edu/emerald/buyers-guide>.

Granger 1931

Granger, Frank, trans. 1931. *On Architecture; Volume I: Books 1–5*. By Vitruvius. Harvard University Press.

Granger 1934

Granger, Frank, trans. 1934. *On Architecture; Volume II: Books 6–10*. By Vitruvius. Harvard University Press.

Griswold 2014

Griswold, Geneva. 2014. "Light as a Feather, Stiff as a Board: Highlights from the Objects Lab at the Walters Art Museum." Unpublished document. Walters Art Museum.

Gschwantler 2000

Gschwantler, Kurt. 2000. "Graeco-Roman Portraiture." In Walker 2000A.

Halleux 1981

Halleux, Robert. 1981. *Les alchimistes grecs. Tome I. Papyrus de Leyde. Papyrus de Stockholm. Fragments de recettes. Texte établi et traduit par Robert Halleux*. Les Belles Lettres.

Hanke 1961

Hanke, Rainer. 1961. *Untersuchungen zur Komposition des ägyptischen Flachbildes*. PhD diss. Kramer.

Hardwick 2010

Hardwick, Tom. 2010. "A Group of Art Works in the Amarna Style." In *Offerings to the Discerning Eye: An Egyptological Medley in Honor of Jack A. Josephson*, edited by Sue D'Auria. Brill.

Hart 2016

Hart, Mary Louise. 2016. "A Portrait of a Bearded Man Flanked by Isis and Serapis." In *Icon, Cult and Context: Sacred Spaces and Objects in the Classical World*, edited by Maura K. Heyn and Ann Irvine Steinsapir. UCLA Cotsen Institute of Archaeology Press.

Hatchfield and Newman 1991

Hatchfield, Pamela, and Richard Newman. 1991. "Ancient Egyptian Gilding Methods." In *Gilded Wood: Conservation and History*, edited by Deborah Bigelow et al. Sound View Press.

Haugan and Holst 2013

Haugan, E., and Bodil Holst. 2013. "Determining the Fibrillar Orientation of Bast Fibers with Polarized Light Microscopy: The Modified Herzog Test (Red Plate Test) Explained." *Journal of Microscopy* 252 (2): 159–68. <https://doi.org/10.1111/jmi.12079>.

Henzel, Watanabe, and Stults 2003

Henzel, William J., Colin Watanabe, and John T. Stults. 2003. "Protein Identification: The Origins of Peptide Mass Fingerprinting." *Journal of the American Society of Mass Spectrometry* 14 (9): 931–42. [https://doi.org/10.1016/S1044-0305\(03\)00214-9](https://doi.org/10.1016/S1044-0305(03)00214-9).

Hetherington 1996

Hetherington, Paul, trans. 1996. *The "Painter's Manual" of Dionysius of Fournà*. By Dionysius of Fournà. Oakwood.

Hett 1936

Hett, W., trans. 1936. *Minor Works: On Colours, On Things Heard, Physiognomics, On Plants, On Marvelous Things Heard, Mechanical Problems, On Indivisible Lines, The Situations and Names of Words, On Melissus, Xenophanes, and Gorgia*. By Aristotle. Harvard University Press.

Hillyer 1984

Hillyer, Lynda. 1984. "The Conservation of a Group of Painted Mummy Cloths from Roman Egypt." *Studies in Conservation* 29 (1): 1–9.

Hofko et al. 2017

Hofko, Bernhard, Mohammad Zia Alavi, Hinrich Grothe, David Jones, and John Harvey. 2017. "Repeatability and Sensitivity of FTIR ATR Spectral Analysis Methods for Bituminous Binders." *Materials and Structures* 50 (3): 1–15.

Hopkins, Costello, and Davis 2021

Hopkins, John N., Sarah K. Costello, and Paul R. Davis, eds. 2021. *Object Biographies: Collaborative Approaches to Ancient Mediterranean Art*. Yale University Press.

Horie 1987

Horie, Charles V. 1987. *Materials for Conservation*. Butterworth-Heinemann.

Hoving 1997

Hoving, Thomas. 1997. *False Impressions: The Hunt for Big-Time Art Fakes*. Touchstone.

Ichimiya 2021

Ichimiya, Yae. 2021. "FORS Identification of Azurite, Indigo, and Prussian Blue in Chinese Paintings." In *Scientific Studies of Pigments in Chinese Paintings*, edited by Blythe McCarthy and Jennifer Giaccai. Archetype.

Ikram 1995

Ikram, Salima. 1995. "Food for Eternity: What the Ancient Egyptians Ate and Drank, Part 1: Meat, Fish Fowl." *KMT: A Modern Journal of Ancient Egypt* 5 (1): 24–33.

Ikram and Dodson 1998

Ikram, Salima, and Aidan Dodson. 1998. *The Mummy in Ancient Egypt: Equipping the Dead for Eternity*. Thames & Hudson.

Imbrogno, Nayak, and Belfort 2014

Imbrogno, Joseph, Arpad Nayak, and Georges Belfort. 2014. "Egg Varnishes on Ancient Paintings: A Molecular Connection to Amyloid Proteins." *Angewandte Chemie* 53 (27). <https://doi.org/10.1002/anie.201400251>.

Iversen 1955

Iversen, Erik. 1955. *Canon and Proportion in Egyptian Art*. Sidgwick and Jackson.

Jaeschke 1997

Jaeschke, Richard L. 1997. "Mechanical Cleaning and the Conservation of Portraits from the Petrie Museum of Egyptian Archaeology." In *Portraits and Masks: Burial Customs in Roman Egypt*, edited by Morris Bierbrier. The British Museum.

Jenkins 2015

Jenkins, Ian, ed. 2015. *Defining Beauty: The Body in Ancient Greek Art*. The British Museum.

Jensen and Muhlestein 2020

Jensen, Bethany, and Kerry Muhlestein. 2020. "The Mummy Portraits of Fag el-Gamous." In *Excavations at the Seila Pyramid and Fag el-Gamous Cemetery*, edited by Kerry Muhlestein, Bethany Jensen, and Krystal V. L. Pierce. Brill.

Jimenez 2014

Jimenez, Lisette Marie. 2014. "Transfiguring the Dead: The Iconography, Commemorative Use, and Materiality of Mummy Shrouds from Roman Egypt." PhD diss., University of California, Berkeley. ProQuest (Jimenez_berkeley_0028E_14840).

Jiménez et al. 2004

Jiménez, Juan J., José L. Bernal, S. Aumente, María Jesús del Nozal, María Teresa Martín, and José Bernal Jr. 2004. "Quality Assurance of Commercial Beeswax. Part I. Gas Chromatography–Electron Impact Ionization Mass Spectrometry of Hydrocarbons and Monoesters." *Journal of Chromatography A* 1024 (1–2): 147–54.

Jones 2019

Jones, Nathaniel B. 2019. *Painting, Ethics, and Aesthetics in Rome*. Cambridge University Press.

Jones, Craddock, and Barker 1990

Jones, Mark, Paul T. Craddock, and Nicolas Barker. 1990. *Fake? The Art of Deception*. University of California Press.

Kakoulli 2009

Kakoulli, Ioanna. 2009. *Greek Painting Techniques and Materials: From the Fourth to the First Century BC*. Archetype.

Kersel 2021

Kersel, Morag M. 2021. "Telling Stories of Objects." In Hopkins, Costello, and Davis 2021.

Kielland 1955

Kielland, Else Christie. 1955. *Geometry in Egyptian Art*. Tiranti.

King 2016

King, Helen. 2016. *The One-Sex Body on Trial: The Classical and Early Modern Evidence*. Routledge.

Kirby et al. 2011

Kirby, Daniel P., Narayan Khandekar, Julie Arslanoglu, and Ken Sutherland. 2011. "Protein Identification in Artworks by Peptide Mass Fingerprinting." In *ICOM Committee for Conservation, 16th Triennial Meeting, Lisbon, Portugal, 19–23 September 2011*, edited by Janet Bridgland. Critério Artes Gráficas.

Kirby et al. 2023

Kirby, Daniel P., Marie Svoboda, Joy Mazurek, Lin Rosa Spaabæk, and John Southon. 2023. "Characterization of an Unusual Coating on Funerary Portraits from Roman Egypt circa 100–300 AD." *Heritage Science* 11: 1–18.

Kirby, Saunders, and Spring 2006

Kirby, Jo, David Saunders, and Marika Spring. 2006. "Proscribed Pigments in Northern European Renaissance Painting and the Case of Paris Red." In *The Object in Context: Crossing Conservation Boundaries*, edited by David Saunders, Joyce H. Townsend, and Sally Woodcock. International Institute of Conservation.

Kirby, Spring, and Higgitt 2005

Kirby, Jo, Marika Spring, and Catherine Higgitt. 2005. "The Technology of Red Lake Pigment Manufacture: Study of the Dyestuff Substrate." *National Gallery Technical Bulletin* 26: 71–87.

Knauer 1993

Knauer, Elfriede R. 1993. "Roman Wall Painting from Boscotrecase: Three Studies in the Relationship Between Writing and Painting." *Metropolitan Museum Journal* 28: 13–46.

Knudsen 2017

Knudsen, Sandra. 2017. "Cats. 155–156: Two Mummy Portraits." In *Roman Art at the Art Institute of Chicago*, edited by Katharine A. Raff. Art Institute of Chicago. <https://publications.artic.edu/roman/reader/romanart/section/1965/1965>.

Koeppen 1973

Koeppen, R. C. 1973. "Report Sent to Hubert Von Sonnenburg, Dated January 31, 1973." Center for Wood Anatomy Research, Forest Service, United States of Agriculture.

Konstan 2014

Konstan, David. 2014. *Beauty: The Fortunes of an Ancient Greek Idea*. Oxford University Press.

Kostomitsopoulou Marketou et al. 2020

Kostomitsopoulou Marketou, Ariadne, Fabrizio Andriulo, Calin Steindal, and Søren Handberg. 2020. "Egyptian Blue Pellets from the First Century BCE Workshop of Kos (Greece): Microanalytical Investigation by Optical Microscopy, Scanning Electron Microscopy-X-ray Energy Dispersive Spectroscopy and Micro-Raman Spectroscopy." *Minerals* 10 (12): 1063. <https://doi.org/10.3390/min10121063>.

Krohn 1912

Krohn, F., ed. *On Architecture*. By Vitruvius. B. G. Teubner.

Kühn 1960

Kühn, Hermann. 1960. "Detection and Identification of Waxes, Including Punic Wax by Infrared Spectrography." *Studies in Conservation* 5 (2): 71–81. <https://doi.org/10.2307/1504955>.

Kühn 1986

Kühn, Hermann. 1986. "Zinc White." In vol. 1 of *Artists' Pigments: A Handbook of Their History and Characteristics*, edited by Robert Feller. National Gallery of Art.

Laes and Strubbe 2014

Laes, Christian, and Johan Strubbe. 2014. *Youth in the Roman Empire: The Young and the Restless Years?* Cambridge University Press.

Lajtar 2005

Lajtar, Adam. 2005. *Deir el-Bahari in the Hellenistic and Roman Periods: A Study of an Egyptian Temple Based on Greek Sources*. Institute of Archaeology, Department of Papyrology, Warsaw University.

Lajtar 2012

Lajtar, Adam. 2012. "The Theban Region Under the Roman Empire." In *The Oxford Handbook of Roman Egypt*, edited by Christina Riggs. Oxford University Press.

Larsen, Coluzzi, and Cosentino 2016

Larsen, Randolph, Nicolette Coluzzi, and Antonino Cosentino. 2016. "Free XRF Spectroscopy Database of

Pigments Checker." *International Journal of Conservation Science* 7 (3): 659–68.

Laver 1997

Laver, Marilyn. 1997. "Titanium White." In vol. 3 of *Artists' Pigments: A Handbook of Their History and Characteristics*, edited by Elisabeth FitzHugh. National Gallery of Art.

Lazzarini 1982

Lazzarini, Lorenzo. 1982. "The Discovery of Egyptian Blue in a Roman Fresco of the Mediaeval Period (Ninth Century AD)." *Studies in Conservation* 27 (2): 84–86. <https://doi.org/10.1179/sic.1982.27.2.84>.

Lee and Quirke 2000

Lee, Lorna, and Stephen Quirke. 2000. "Painting Materials." In Nicholson and Shaw 2000.

Lee et al. 2015

Lee, Hae Young, Natalya Atlasevich, Clara Granzotto, Julia Schultz, John Loike, and Julie Arslanoglu. 2015. "Development and Application of an ELISA Method for the Analysis of Protein-Based Binding Media of Artworks." *Analytical Methods* 7 (1): 187–96.

Lehmann 2012

Lehmann, Ann-Sophie. 2012. "How Materials Make Meaning." *Netherlands Yearbook for History of Art* 62 (1): 6–27. <https://doi.org/10.1163/22145966-06201002>.

Lehmann 2014

Lehmann, A. S. 2014. "Stil und Material: Ein beschaenktes Verhaeltnis." *kritische berichte – Zeitschrift für Kunst- und Kulturwissenschaften* 42 (1): 127–36.

Lenain 2011

Lenain, Thierry. 2011. *Art Forgery: The History of a Modern Obsession*. Reaktion.

Lilyquist, Hoch, and Peden 2003

Lilyquist, Christine, James E. Hoch, and A. J. Peden. 2003. *The Tomb of Three Foreign Wives of Tuthmosis III*. The Metropolitan Museum of Art.

Lliveras et al. 2010

Lliveras, Anna, Anna Torrents, Pilar Giráldez, and Marius Vendrell-Saz. 2010. "Evidence for the Use of Egyptian Blue in an 11th-Century Mural Altarpiece by SEM-EDS, FTIR and SR XRD (Church of Sant Pere, Terrassa, Spain)." *Archaeometry* 52 (2): 308–19.

Longoni et al. 2022

Longoni, Margherita, Beatrice Genova, Alessia Marzanni, Daniela Melfi, Carlotta Beccaria, and Silvia Bruni. 2022. "FT-NIR Spectroscopy for the Non-Invasive Study of Binders and Multi-Layered Structures in Ancient Paintings: Artworks of the Lombard Renaissance as Case Studies." *Sensors* 22 (5): 2052.

Lowe 1897

Lowe, John. 1897. *The Yew-Trees of Great Britain and Ireland*. Macmillan.

Lucas and Harris 1962

Lucas, Alfred, and J. R. Harris. 1962. *Ancient Egyptian Materials and Industries*. Histories & Mysteries of Man.

Maclehose 1960

Maclehose, Louisa S., trans. 1960. *Vasari on Technique*. By Vasari. Dover.

Mallgrave 2006

Mallgrave, Harry, trans. 2006. *Johann Joachim Winckelmann: History of the Art of Antiquity*. Getty Research Institute.

Manley and Rée 2001

Manley, Deborah, and Peta Rée. 2001. *Henry Salt: Artist, Traveller, Diplomat, Egyptologist*. Libri.

Manning 2013

Manning, Joseph. 2013. "Thebes (Diospolis Magna), Ptolemaic and Roman Periods." In *The Encyclopedia of Ancient History*, edited by Roger S. Bagnall, Kai Brodersen, Craige B. Champion, Andrew Erskine, and Sabine R. Huebner. Blackwell.

Maravelia 2019

Maravelia, Alicia. 2019. "The Conception of the Cosmic Egg in the Ancient Egyptian and in the Orphic Cosmology." *The Oriental Studies* (83): 25–52.

Marconi 1967

Marconi, Bohdan. 1967. "Wspomnienia z lat 1939–1945." *Rocznik Muzeum Narodowego w Warszawie* 11: 269–77.

Matheson 2022

Matheson, Susan. 2022. "Individuality and Old Age in the Painted Funerary Portraits of Roman Egypt." Harvard Art Museums. Accessed December 29, 2024. <https://harvardartmuseums.org/tour/770/slide/12398>.

Mathews 2016

Mathews, Thomas F. 2016. "Appendix B – Media Analysis." In Mathews and Müller 2016.

Mathews and Müller 2016

Mathews, Thomas F., and Norman E. Müller. 2016. *The Dawn of Christian Art in Panel Paintings and Icons*. J. Paul Getty Museum.

Mayberger et al. 2020

Mayberger, Evelyn (Eve), Jessica Arista, Marie Svoboda, and Molly Gleeson. 2020. "Invisible Brushstrokes Revealed: Technical Imaging and Research of Romano-Egyptian Mummy Portraits." In Svoboda and Cartwright 2020.

Mazurek 2020

Mazurek, Joy. 2020. "Characterization of Binding Media in Roman-Egyptian Funerary Portraits." In Svoboda and Cartwright 2020.

Mazurek et al. 2008

Mazurek, Joy, Michael Schilling, Giacomo Chiari, and Arlen Heginbotham. 2008. "Antibody Assay to Characterize Binding Media in Paint." In *ICOM Committee for Conservation 15th Triennial Meeting, New Delhi, India, 22–26 September 2008*, edited by Janet Bridgland. Allied.

Mazurek et al. 2014

Mazurek, Joy, Marie Svoboda, Jeffrey Maish, Kazuki Kawahara, Shunsuke Fukakusa, Takashi Nakazawa, and Yoko Taniguchi. 2014. "Characterization of Binding Media in Egyptian Roman Portraits Using Enzyme-Linked Immunosorbent Assay and Mass Spectrometry." *e-Preservation Science* 11: 76–83.

Mazurek, Svoboda, and Schilling 2019

Mazurek, Joy, Marie Svoboda, and Michael Schilling. 2019. "GC/MS Characterization of Beeswax, Protein, Gum, Resin, and Oil in Romano-Egyptian Paintings." *Heritage* 2 (3): 1960–85. <https://doi.org/10.3390/heritage2030119>.

Measday, Walker, and Pemberton 2017

Measday, Danielle, Charlotte Walker, and Briony Pemberton. 2017. "A Summary of Ultra-Violet Fluorescent Materials Relevant to Conservation." *AICCM National Newsletter*, no. 137. Accessed April 26, 2021. <https://aiccm.org.au/national-news/summary-ultra-violet-fluorescent-materials-relevant-conservation>.

Metropolitan Museum of Art N.D.

Metropolitan Museum of Art. n.d. "Mummy with an Inserted Panel Portrait of a Youth, A.D. 80–100." Accessed April 8, 2022. <https://www.metmuseum.org/art/collection/search/547697>.

Michałowski 1957

Michałowski, Kazimierz. 1957. "Galeria Sztuki Starożytnej w Muzeum Narodowym w Warszawie." *Rocznik Muzeum Narodowego w Warszawie* 2: 101–38.

Middleton 2018

Middleton, William. 2018. *Double Vision: The Unerring Eye of Art World Avatars Dominique and John de Menil*. Knopf.

Miliani et al. 2010

Miliani, Costanza, Alessia Daveri, Lin R. Spaabæk, Aldo Romani, Valentina Manuali, Antonio Sgamellotti, and Brunetto G. Brunetti. 2010. "Bleaching of Red Lake Pigments in Encaustic Mummy Portraits." *Applied Physics A* 100 (3): 703–11. <https://doi.org/10.1007/s00339-010-5748-3>.

Millon 1958

Millon, Henry. 1958. "The Architectural Theory of Francesco di Giorgio." *The Art Bulletin* 40 (3): 257–61.

Monico et al. 2013

Monico, Letizia, Francesca Rosi, Costanza Miliani, Alessia Daveri, and Brunetto G. Brunetti. 2013. "Non-Invasive Identification of Metal-Oxalate Complexes on Polychrome Artwork Surfaces by Reflection Mid-Infrared Spectroscopy." *Spectrochimica Acta Part A: Molecular and Biomolecular Spectroscopy* 116: 270–80.

Montserrat 1993

Montserrat, Dominic. 1993. "The Representation of Young Males in 'Fayum Portraits.'" *The Journal of Egyptian Archaeology* 79: 215–25.

Montserrat 1998

Montserrat, Dominic. 1998. *Changing Bodies, Changing Meanings: Studies on the Human Body in Antiquity*. Routledge.

Moreau et al. 2023

Moreau, Raphaël, Lucile Brunel-Duverger, Laurent Pichon, Brice Moignard, Didier Gourier, and Thomas Calligaro. 2023. "Application of a MA-XRF/RIS/PL Scanner to Paintwork Studies." *European Physical Journal Plus* 138: 16.

Moreau et al. 2024

Moreau, Raphaël, Thomas Calligaro, Laurent Pichon, Brice Moignard, Sorin Hermon, and Ina Reiche. "A Multimodal Scanner Coupling XRF, UV-Vis-NIR Photoluminescence and Vis-NIR-SWIR Reflectance Imaging Spectroscopy for Cultural Heritage Studies." *X-Ray Spectrometry* 53 (2): 271–81. <https://doi.org/10.1002/xrs.3364>.

Morgan 1914

Morgan, M., trans. 1914. *The Ten Books on Architecture*. By Vitruvius. Harvard University Press.

Morgan 2006

Morgan, Morris Hicky, trans. 2006. *Vitruvius Pollio: The Ten Books on Architecture*. Adamant Media.

Nahar, Schmets, and Scarpas 2016

Nahar, Sayeda, Alexander Schmets, and Athanasios Scarpas. 2016. "Probing Trace-Elements in Bitumen by Neutron Activation Analysis." *CROW InfraDagen* (2016): 1–13. <https://repository.tudelft.nl/record/uuid:133aed5b-45ed-4893-8cbf-6d56e3799022>.

Naini et al. 2008

Naini, F. B., M. T. Cobourne, F. McDonald, and A. N. A. Donaldson. 2008. "The Influence of Craniofacial to Standing Height Proportion on Perceived Attractiveness." *International Journal of Oral and Maxillofacial Surgery* 37 (10): 877–85.

Nerlich et al. 2020

Nerlich, Andreas G., Lukas Fischer, Stephanie Panzer, Roxane Bicker, Thomas Helmberger, and Sylvia Schoske. 2020. "The Infant Mummy's Face—Paleoradiological Investigation and Comparison between Facial Reconstruction and a Mummy Portrait of a Roman-Period Egyptian Child." *PLoS ONE* 15 (9): e0238427. <https://doi.org/10.1371/journal.pone.0238427>.

Newman and Gates 2020

Newman, Richard, and Glen Alan Gates. "The Matter of Madder in the Ancient World." In Svoboda and Cartwright 2020.

Nicholson and Shaw 2000

Nicholson, Paul T., and Ian Shaw. 2000. *Ancient Egyptian Materials and Technology*. Cambridge University Press.

Nicola et al. 2024

Nicola, Marco, Claudio Garino, Sophia Mittman, Emanuele Priola, Luca Palin, Marta Ghirardello, Vamshi Damagatla, Austin Nevin, Admir Masic, Daniella Comelli, and Roberto Gobetto. 2024. "Increased NIR Photoluminescence of Egyptian Blue via Matrix Effect Optimization." *Materials Chemistry and Physics* 313: 128710.

Nissenbaum and Buckley 2013

Nissenbaum, Arie, and Stephen Buckley. 2013. "Dead Sea Asphalt in Ancient Egyptian Mummies—Why?"

Archaeometry 55 (3): 563–68. <https://doi.org/10.1111/j.1475-4754.2012.00713.x>.

Northcote 1819

Northcote, James. 1819. *The Life of Sir Joshua Reynolds*. Volume 1. Printed for Henry Colburn, Conduit-Street.

Omaran 2015

Omaran, Wahid. 2015. "The Egg and Its Symbolism in the Graeco-Roman Period." *Journal of Faculty of Tourism and Hotels* 9 (1): 173–85.

Opper 2008

Opper, Thorsten. 2008. *Hadrian: Empire and Conflict*. The British Museum.

Ordonez and Twilley 1998

Ordonez, Eugena, and John Twilley. 1998. "Clarifying the Haze: Efflorescence on Works of Art." *Analytical Chemistry* 69 (13): 416A–22A. Reprinted without color illustrations in *WAAC Newsletter* 20 (1). <https://cool.culturalheritage.org/waac/wn/wn20/wn20-1/wn20-108.html>.

Ostrowski 1966

Ostrowski, Janusz. 1966. "Portret fajumski ze zbiorów Muzeum Narodowego w Warszawie." *Rocznik Muzeum Narodowego w Warszawie* 10: 13–22.

Pagès-Camagna and Guichard 2010

Pagès-Camagna, Sandrine, and Hélène Guichard. 2010. "Egyptian Colours and Pigments in French Collections: 30 Years of Physiochemical Analyses on 300 Objects." In *Decorated Surfaces on Ancient Egyptian Objects: Technology, Deterioration, and Conservation; Proceedings of a Conference Held in Cambridge, UK, on 7–8 September 2007*, edited by Julie Dawson, Christina Rozeik, and Margot M. Wright. Archetype.

Park et al. 2019

Park, Hae-Min, Amaris Sturm, Glenn Gates, and Lisa Anderson-Zhu. 2019. "Findings from an Examination of Two Mummy Portraits." *The Journal of the Walters Art Museum* 74. <https://journal.thewalters.org/volume/74/note/the-walters-portrait-mummies/>.

Parkin 1992

Parkin, Tim G. 1992. *Demography and Roman Society*. Johns Hopkins University Press.

Parlasca 1966

Parlasca, Klaus. 1966. *Mumienporträts und verwandte Denkmäler*. Steiner.

Parlasca 1969

Parlasca, Klaus. 1969. Vol. 1 of *Repertorio d'arte dell'Egitto: Greco-Romano serie B; Ritratti di mummie*. Banco di Sicilia Fondazione Mormino.

Parlasca 1969–2003

Parlasca, Klaus. 1969–2003. *Repertorio d'arte dell'Egitto: Greco-Romano serie B; Ritratti di mummie*. 4 vols. Officine Tipo-Litografiche I.R.E.S.

Parlasca 1977

Parlasca, Klaus. 1977. Vol. 2 of *Repertorio d'arte dell'Egitto: Greco-Romano serie B; Ritratti di mummie*. L'Erma di Bretschneider.

Parlasca 2004

Parlasca, Klaus. 2004. "Kaiserzeitliche Votivgemälde aus Ägypten." *Chronique d'Egypte* 79 (157–158): 320–35.

Parlasca and Frenz 2003

Parlasca, Klaus, and Hans G. Frenz. 2003. Vol. 4 of *Repertorio d'arte dell'Egitto: Greco-Romano serie B; Ritratti di mummie*. L'Erma di Bretschneider.

Perry-Gal et al. 2015

Perry-Gal, Lee, Adi Erlich, Ayelet Gilboa, and Guy Bar-Oz. 2015. "Earliest Economic Exploitation of Chicken outside East Asia: Evidence from the Hellenistic Southern Levant." *PNAS: Proceedings of the National Academy of Sciences of the United States of America* 112 (32): 9849–54.

Peruzzi 2016

Peruzzi, Bice. 2016. "Eggs in a Drinking Cup: Unexpected Uses of a Greek Shape in Central Apulian Funerary Contexts." In *The Consumers' Choice: Uses of Greek Figure-Decorated Pottery*, edited by Thomas H. Carpenter, Elizabeth Langridge-Noti, and Mark Stansbury-O'Donnell. Archaeological Institute of America.

Petrie 1889

Petrie, William Matthew Flinders. 1889. *Hawara, Biahmu, and Arsinoe, with Thirty Plates*. Field & Tuer.

Petrie 1890

Petrie, William Matthew Flinders. 1890. *Kahun, Gurob, and Hawara*. Kegan Paul, Trench, Trübner and Co.

Petrie 1911

Petrie, William Matthew Flinders. 1911. *Roman Portraits and Memphis (IV)*. School of Archaeology in Egypt, University College.

Pharr, Davidson, and Pharr 2001

Pharr, Clyde, Theresa Sherrer Davidson, and Mary Brown Pharr, trans. 2001. *The Theodosian Code and Novels, and the Sirmundian Constitutions*. The Lawbook Exchange.

Picton, Quirke, and Roberts 2007

Picton, Janet, Stephen Quirke, and Paul C. Roberts, eds. 2007. *Living Images: Egyptian Funerary Portraits in the Petrie Museum*. Left Coast Press.

Picton, Quirke, and Roberts 2018

Picton, Janet, Stephen Quirke, and Paul C. Roberts. 2018. *Living Images: Egyptian Funerary Portraits in the Petrie Museum*. Routledge.

Plater et al. 2003

Plater, M. John, Ben De Silva, Thomas Gelbrich, Michael B. Hursthouse, Catherine L. Higgitt, and David R. Saunders, 2003. "The Characterisation of Lead Fatty Acid Soaps in 'Protrusions' in Aged Traditional Oil Paint." *Polyhedron* 22 (24): 3171–79. [https://doi.org/10.1016/S0277-5387\(03\)00461-3](https://doi.org/10.1016/S0277-5387(03)00461-3).

Pliny the Elder 77–79 CE

Pliny the Elder (Gaius Plinius Secundus). 77–79 CE. *Naturalis Historia*. https://la.wikisource.org/wiki/Naturalis_Historia.

Pouyet et al. 2020

Pouyet, Emeline, Nicholas Barbi, Henry Chopp, Owen Healy, Aggelos Katsaggelos, Sophia Moak, Rick Mott, Marc Vermeulen, and Marc Walton. 2020. "Development of a Highly Mobile and Versatile Large MA-XRF Scanner for In Situ Analyses of Painted Works of Art." *X-ray Spectrometry* 50 (4): 263–71.

Pozza et al. 2000

Pozza, Giorgio, David Ajò, Giacomo Chiari, Franco De Zuane, and Marialuisa Favaro. 2000. "Photoluminescence of the Inorganic Pigments Egyptian Blue, Han Blue and Han Purple." *Journal of Cultural Heritage* 1 (4): 393–98.

Prag 2002

Prag, A. J. N. W. 2002. "Proportion and Personality in the Fayum Portraits." *British Museum Studies in Ancient Egypt and Sudan* 3: 55–63.

Purup 2019

Purup, Bjarne B. 2019. "A Social Approach to the Sex and Age Distribution in the Mummy Portraits." In *Family Lives: Aspects of Life and Death in Ancient Families*, edited by Kristine Bøggild Johannsen and Jane Hjarl Petersen. Acta Hyperborea 15. Museum Tusculanum Press.

Rackham 1938–1952

Rackham, H., trans. 1938–52. *The Natural History (Naturalis Historia)*. By Pliny the Elder. Loeb Classical Library. Harvard University Press.

Radpour et al. 2022

Radpour, Roxanne, Glenn A. Gates, Ioanna Kakoulli, and John K. Delaney. 2022. "Identification and Mapping of Ancient Pigments in a Roman Egyptian Funerary Portrait by Application of Reflectance and Luminescence Imaging Spectroscopy." *Heritage Science* 10 (8). <https://doi.org/10.1186/s40494-021-00639-5>.

Ramer 1979

Ramer, Brian. 1979. "The Technology, Examination and Conservation of the Fayum Portraits in the Petrie Museum." *Studies in Conservation* 24 (1): 1–13.

Redding 2015

Redding, Richard W. 2015. "The Pig and the Chicken in the Middle East: Modeling Human Subsistence Behavior in the Archaeological Record Using Historical and Animal Husbandry Data." *Journal of Archaeological Research* 23: 325–68.

Reeler 2013

Reeler, Nini Elisabeth Abildgaard, Ole Faurskov Nielsen, Lin Spaabæk, Mogens Jørgensen, and Henrik Grum Kjaergaard. 2013. "Pigments and Binding Material in Fayum Mummy Portraits Determined by NIR-FT-Raman Microscopy." *Asian Chemistry Letters* 17: 1–12.

Rickerby 1993

Rickerby, Stephen. 1993. "Original Painting Techniques and Materials Used in the Tomb of Nefertari." In *Art and Eternity: The Nefertari Wall Paintings Conservation Project 1986–1992*, edited by Miguel Angel Corzo and Mahasti Afshar. Oxford University Press.

Riederer 1997

Riederer, Josef. 1997. "Egyptian Blue." In vol. 3 of *Artists' Pigments: A Handbook of Their History and Characteristics*, edited by Elisabeth FitzHugh. National Gallery of Art.

Rigaud 2005

Rigaud, J. F., trans. 2005. *A Treatise on Painting*. By Leonardo da Vinci. Dover.

Riggs 2005

Riggs, Christina. 2005. *The Beautiful Burial in Roman Egypt: Art, Identity and Funerary Religion*. Oxford University Press.

Riggs 2006

Riggs, Christina. 2006. "Archaism and Artistic Sources in Roman Egypt: The Coffins of the Soter Family and the Temple of Deir el-Medina." *BIFAO: Bulletin de l'Institut français d'archéologie orientale* 106: 315–32.

Riggs 2012

Riggs, Christina, ed. 2012. *The Oxford Handbook of Roman Egypt*. Oxford University Press.

Roberts 2013

Roberts, Paul. 2013. *Life and Death in Pompeii and Herculaneum*. The British Museum.

Roberts 2020

Roberts, Caroline. 2020. "Green Pigments: Exploring Changes in the Egyptian Color Palette through the Technical Study of Roman-Period Mummy Shrouds." In Svoboda and Cartwright 2020.

Robins 1993

Robins, Gay. 1993. *Proportion and Style in Ancient Egypt*. University of Texas Press.

Rondot 2013

Rondot, Vincent. 2013. *Derniers visages des dieux d'Égypte: Iconographies, panthéons et cultes dans le Fayoum hellénisé des II-III siècles de notre ère*. Éditions du Louvre.

Rondot 2015

Rondot, Vincent. 2015. "Graeco-Roman Fayum Pantheons as Documented by 2nd-Century Painted Wooden Panels." In *Von der Pharaonenzeit bis zur Spätantike: Kulturelle Vielfalt im Fayum, Akten des 5. Internationalen Fayum-Konferenz, 29. Mai bis 1. Juni 2013, Leipzig*, edited by Nadine Quenouille. Harrassowitz.

Rosi et al. 2019

Rosi, Francesca, Laura Cartechini, Diego Sali, and Costanza Miliani. 2019. "Recent Trends in the Application of Fourier Transform Infrared (FT-IR) Spectroscopy in Heritage Science: From Micro- to Non-Invasive FT-IR." *Physical Sciences Reviews* 4: n.p.

Rowland and Howe 1999

Rowland, Ingrid D., and Thomas Noble Howe, eds. 1999. *Ten Books on Architecture*. By Vitruvius. Cambridge University Press.

Roy 2007

Roy, Ashok. 2007. "Cobalt Blue." In vol. 4 of *Artists' Pigments: A Handbook of Their History and Characteristics*, edited by Barbara H. Berrie. National Gallery of Art.

Sabino et al. 2019

Sabino, Rachel C., Ken Sutherland, Emeline Pouyet, Federica Pozzi, and Marc Walton. 2019. "Surprise Encounters with Mummy Portraits at the Art Institute of Chicago." *AIC Paintings Specialty Group Postprints* 31.

Salas 2020

Salas, Megan Elizabeth. 2020. "Evaluating the Effectiveness of In-Situ Non-Invasive Photophysical Characterization Methods for Distinguishing Indigo from Other Blue Colorants." Master's thesis, University of California, Los Angeles.

Salvant et al. 2018

Salvant, Johanna, Jane Williams, Monica Ganio, Francesca Casidio, Céline Daher, Ken Sutherland, Letizia Monaco, Frederik Vanmeert, Steven de Meyer, Koen Janssens, Caroline R. Cartwright, and Marc Walton. 2018. "A Roman Egyptian Painting Workshop: Technical Investigation of the Portraits from Tebtunis, Egypt." *Archaeometry* 60 (4): 815–33. <https://doi.org/10.1111/arcm.12351>.

Sande 2004

Sande, Siri. 2004. "Pagan Pinakes and Christian Icons: Continuity or Parallelism?" *Acta ad archaeologiam et artium historiam pertinentia* 18: 81–100.

Sand et al. 2017

Sand, Luise, Elisabeth Fugmann, Ina Reiche, Agnes Schwarzmaier, Stefan Rohrs, Sabine Schwerdtfeger, Heike Stege, and Andrea Obermeier. 2017. "Tabellarischer Überblick zu den Farbmitteln der Mumienporträts und des Severertondos." In *Inkarnat und Signifikanz: Das menschliche Abbild in der Tafelmalerei von 200 bis 1250 im Mittelmeerraum*. Veröffentlichungen des Zentralinstituts für Kunstgeschichte.

Schiavon et al. 2021

Schiavon, Nick, Carlo Emmanuele Bottaini, Sara Valadas, Cristina Barrocas Dias, Ana Manhita, and Antonio Candeias. 2021. "A Multi-Analytical Study of Egyptian Funerary Artifacts from Three Portuguese Museum Collections." *Heritage* 4 (4): 2973–95.

Schilling, Carson, and Khanjian 1998

Schilling, Michael R., David M. Carson, and Herant P. Khanjian. 1998. "Evaporation of Fatty Acids and the Formation of Ghost Images by Framed Oil Paintings." *WAAC Newsletter* 21 (1). <https://cool.culturalheritage.org/waac/wn/wn21/wn21-1/wn21-106.html>.

Schmidt 1899

Schmidt, Valdemar. 1899. *Det gamle glyptotek på Ny Carlsberg. Den ægyptiske samling*. N.p.

Schmidt 1908

Schmidt, Valdemar. 1908. *Ny Carlsberg Glyptotek: Den ægyptiske samling*. Nielsen og Lydiche.

Schneede 2021

Schneede, Uwe M. 2021. *Paula Modersohn-Becker: Die Malerin, die in die Moderne aufbrach*. C. H. Beck.

Schoske and Wildung 1983

Schoske, Sylvia, and Dietrich Wildung. 1983. *Falsche Pharaonen: Zeitung zur Sonderausstellung, 400 Jahre Fälschungsgeschichte*. Staatliches Museum Ägyptischer Kunst.

Schreiber, Vasáros, and Almásy 2013

Schreiber, Gábor, Zsolt Vasáros, and Adrienn Almásy. 2013. "Ptolemaic and Roman Burials from Theban Tomb -400-." *Mitteilungen des Deutschen Archäologischen Instituts Abteilung Kairo* 69: 187–225.

Scott 2010

Scott, David A. 2010. "Greener Shades of Pale: A Review of Advances in the Characterisation of Ancient Egyptian Green Pigments." In *Decorated Surfaces on Ancient Egyptian Objects: Technology, Deterioration, and Conservation; Proceedings of a Conference Held in Cambridge, UK, on 7–8 September 2007*, edited by Julie Dawson, Christina Rozeik, and Margot M. Wright. Archetype.

Scott 2016

Scott, David A. 2016. "A Review of Ancient Egyptian Pigments and Cosmetics." *Studies in Conservation* 61 (4): 185–202. <https://doi.org/10.1179/2047058414Y.0000000162>.

Serpico 2000

Serpico, Margaret. 2000. "Resins, Amber and Bitumen." In Nicholson and Shaw 2000.

Serpico and White 2001

Serpico, Margaret, and Raymond White. 2001. "The Use and Identification of Varnish on New Kingdom Funerary Equipment." In *Colour and Painting in Ancient Egypt*, edited by W. V. Davies. The British Museum.

Shortland, Appleby Hope, and Tite 2006

Shortland, Andrew J., Colin Appleby Hope, and M. S. Tite. 2006. "Cobalt Blue Painted Pottery from 18th Dynasty

Egypt." *Geological Society, London, Special Publications* 257 (1): 91–99. <https://doi.org/10.1144/GSL.SP.2006.257.01.07>.

Smart 2010

Smart, Pamela G. 2010. *Sacred Modern: Faith, Activism, and Aesthetics in the Menil Collection*. University of Texas Press.

Smith 1957

Smith, William Stevenson. 1957. "Department of Egyptian Art." *Annual Report for the Year ... (Museum of Fine Arts, Boston)* 82 (1957): 38–44. <http://www.jstor.org/stable/43473833>.

Smith and Ólafsson 2023

Smith, Kevin P., and Guðmundur Ólafsson. 2023. "All That Glitters Is Not Gold: Multi-Instrumental Identification of Viking Age Orpiment (As₂S₃) from Surtshellir Cave, Iceland." *Journal of Archaeological Science: Reports* 47: 103724. <https://doi.org/10.1016/j.jasrep.2022.103724>.

Socrates 2001

Socrates, George. 2001. *Infrared and Raman Characteristic Group Frequencies. Tables and Charts*. 3rd ed. John Wiley & Sons.

Solé et al. 2007

Solé, V. Armando, Emmanuel Papillon, Marine Cotte, Philippe Walter, and Jean Susini. 2007. "A Multiplatform Code for the Analysis of Energy-Dispersive X-Ray Fluorescence Spectra." *Spectrochimica Acta Part B: Atomic Spectroscopy* 62 (1): 63–68.

Sörries 2003

Sörries, Reiner. 2003. *Das Malibu-Triptychon: Ein Totengedenkbild aus dem römischen Ägypten und verwandte Werke der spätantiken Tafelmalerei*. Christliche Archäologie 4. J. H. Röhl.

Sotheby's New York 2009

Sotheby's New York. 2009. "Old Master Paintings, European Sculpture & Antiquities." Auction Catalogue (Sale 8560). June 4. Accessed October 21, 2019. <https://www.sothebys.com/en/auctions/2009/old-master-paintings-european-sculpture-antiquities-n08560.html>.

Southon et al. 2004

Southon, John, Guaciara Santos, Kevin Druffel-Rodriguez, Ellen Druffel, Sue Trumbore, Xiamei Xu, Sheila Griffin, Shahla Ali, and Maya Mazon. 2004. "The Keck Carbon Cycle AMS Laboratory, University of California, Irvine: Initial Operation and a Background Surprise." *Radiocarbon* 46 (2): 41–49.

Spaabæk 2012

Spaabæk, Lin Rosa. 2012. "Mummy Portrait Supports." In *Conservation of Easel Paintings*, edited by Joyce Hill Stoner and Rebecca Rushfield. Routledge.

Spaabæk and Mazurek 2020

Spaabæk, Lin Rosa, and Joy Mazurek. 2020. "Binding Media and Coatings: Mummy Portraits in the National Museum of Denmark and the Ny Carlsberg Glyptotek." In Svoboda and Cartwright 2020.

Stacey 2011

Stacey, Rebecca J. 2011. "The Composition of Some Roman Medicines: Evidence for Pliny's Punic Wax?" *Analytical and Bioanalytical Chemistry* 401 (6): 1749–59.

Stamm 2007

Stamm, Rainer, and Paula Modersohn-Becker. 2007. *Paula Modersohn-Becker und die ägyptischen Mumienportraits: Eine Hommage zum 100. Todestag der Künstlerin* (exhibition catalogue). Hirmer Verlag.

Stein and Corcoran 2020

Stein, Renée, and Lorelei H. Corcoran. 2020. "Scrutinizing 'Saparon': Investigating a Mummy Portrait of a Young Man in the Michael C. Carlos Museum, Emory University." In Svoboda and Cartwright 2020.

Stevens 2009

Stevens, Anna. 2009. "Domestic Religious Practices." In *UCLA Encyclopedia of Egyptology*, edited by Willeke Wendrich and Jacco Dieleman. University of California, Los Angeles. <http://escholarship.org/uc/item/7s07628w>.

Strohalm et al. 2010

Strohalm, Martin, Daniel Kavan, Petr Novák, Michael Volný, and Vladimír Havlíček. 2010. "MMass 3: A Cross-Platform Software Environment for Precise Analysis of Mass Spectrometric Data." *Analytical Chemistry* 82 (11): 4648–51. <https://doi.org/10.1021/ac100818g>.

Stulik, Porta, and Palet 1993

Stulik, Dusan C., Eduardo A. Porta, and Antonio Palet. 1993. "Analyses of Pigments, Binding Media, and Varnishes in the Tomb of Nefertari." In *Art and Eternity: The Nefertari Wall Paintings Conservation Project 1986–1992*, edited by Miguel Angel Corzo and Mahasti Afshar. Oxford University Press.

Sutherland, Sabino, and Pozzi 2020

Sutherland, Ken, Rachel C. Sabino, and Federica Pozzi. 2020. "Challenges in the Characterization and

Categorization of Binding Media in Mummy Portraits." In Svoboda and Cartwright 2020.

Svoboda and Cartwright 2020

Svoboda, Marie, and Caroline R. Cartwright, eds. 2020. *Mummy Portraits of Roman Egypt: Emerging Research from the APPEAR Project*. J. Paul Getty Museum.

Svoboda and Walton 2010

Svoboda, Marie, and Marc Walton. 2010. "Material Investigation of the J. Paul Getty Museum's Red-Shrouded Mummy." In *Decorated Surfaces on Ancient Egyptian Objects: Technology, Deterioration, and Conservation; Proceedings of a Conference Held in Cambridge, UK, on 7–8 September 2007*, edited by Julie Dawson, Christina Rozeik, and Margot M. Wright. Archetype.

Taggart 1959

Taggart, Ross E., ed. 1959. *Handbook of the Collections in the William Rockhill Nelson Gallery of Art and Mary Atkins Museum of Fine Arts*. 4th ed. William Rockhill Nelson Gallery of Art and Mary Atkins Museum of Fine Arts.

Tappert et al. 2011

Tappert, Ralf, Alexander P. Wolfe, Ryan C. McKellar, Michelle C. Tappert, and Karlis Muehlenbachs. 2011. "Characterizing Modern and Fossil Gymnosperm Exudates Using Micro-Fourier Transform Infrared Spectroscopy." *International Journal of Plant Sciences* 172 (1): 120–38. <https://doi.org/10.1086/657277>.

Thayer 1923

Thayer, Bill, trans. 1923. *De Divinatione*. By Cicero. Book 1, XXXIV, 74. Loeb Classical Library. https://penelope.uchicago.edu/Thayer/e/roman/texts/cicero/de_divinatione/1*.html.

Thiboutot 2020

Thiboutot, Gabrielle. 2020. "Egyptian Blue in Romano-Egyptian Mummy Portraits." In Svoboda and Cartwright 2020.

Thieme et al. 2017

Thieme, Cristina, Anna Rommel-Mayet, and Luise Sand. 2017. "Bilder von Göttern und Menschen der römischen Kaiserzeit – eine kunsttechnische Betrachtung." In *Inkarnat und Signifikanz. Das menschliche Abbild in der Tafelmalerei von 200 bis 1250 im Mittelmeerraum*, edited by Yvonne Schmuhl and Esther Pia Wipfler, 121–50. Zentralinstitut für Kunstgeschichte.

Thistlewood 2017

Thistlewood, Jevon. 2017. "Drawing the Face of a Mummy Portrait." Unpublished Research Seminar Paper. Ashmolean Museum of Art and Archaeology.

Thistlewood et al. 2020

Thistlewood, Jevon, Olivia Dill, Marc S. Walton, and Andrew Shortland. 2020. "A Study of the Relative Locations of Facial Features within Mummy Portraits." In Svoboda and Cartwright 2020.

Thomas and Brunel-Duverger 2023

Thomas, Caroline, and Lucile Brunel-Duverger. 2023. "Les tableaux culturels d'Égypte romaine: Étude matérielle des deux panneaux du musée du Louvre (Dioscure MND 193 – E 10815; Hèrôn et Lycurgue RFML.AE.2020.8.1)." *Techne* 55: 118–27. <https://doi.org/10.4000/techne.17881>.

Thompson 1972

Thompson, David L. 1972. "The Classes and Hands of Painted Funerary Portraits from Antinoopolis [sic]." PhD diss., University of Michigan.

Thompson 1973

Thompson, David L. 1973. "A Patchwork Fayum in Toledo." *American Journal of Archaeology* 77 (4): 438–39.

Thompson 1976A

Thompson, David L. 1976. "A Painted Funerary Portrait from Roman Egypt." *Boston Museum Bulletin* 74 (370): 115–19.

Thompson 1976B

Thompson, David L. 1976. *The Artists of the Mummy Portraits*. J. Paul Getty Museum.

Thompson 1981

Thompson, David L. 1981. "A Lost Patchwork 'Fayum Portrait.'" *American Journal of Archaeology* 85 (4): 491–92.

Thompson 1982

Thompson, David L. 1982. *Mummy Portraits in the J. Paul Getty Museum*. J. Paul Getty Museum.

Thum 2022A

Thum, Jen. 2022. "The People behind the Portraits." Harvard Art Museums. <https://harvardartmuseums.org/tour/770/stop/2623>.

Thum 2022B

Thum, Jen. 2022. "Speak Their Names." Harvard Art Museums. <https://harvardartmuseums.org/tour/770/slide/12399>.

Tobin 1975

Tobin, Richard. 1975. "The Canon of Polykleitos." *American Journal of Archaeology* 79 (4): 307–21.

Töpfer 2017

Töpfer, Susanne. 2017. "Theory and Practice/Text and Mummies: The Instructions of the 'Embalming Ritual' in the Light of Archaeological Evidence." In *Burial and Mortuary Practices in Late Period and Graeco-Roman Egypt: Proceedings of the International Conference Held at the Museum of Fine Arts, Budapest, 17–19 July 2014*, edited by K. A. Kóthay. Museum of Fine Arts, Budapest.

Totelin 2016

Totelin, Laurence M. V. 2016. "Pharmakopōlai: A Re-Evaluation of the Sources." In *Popular Medicine in Graeco-Roman Antiquity: Explorations*, edited by William V. Harris. Brill.

Tourna et al. 2008

Tourna, E. et al. 2008. *The Egyptian Collection, National Archaeological Museum*. Hellenic Ministry of Culture and Sports, Fund of Archaeological Proceeds.

Traverso 2019

Traverso, Vittoria. 2019. "The Egyptian Egg Ovens Considered More Wondrous than Pyramids." Atlas Obscura. <https://www.atlasobscura.com/articles/egypt-egg-ovens>.

Tzachou-Alexandri 1995

Tzachou-Alexandri, Olga, ed. 1995. *The World of Egypt in the National Archaeological Museum*. Kapon.

University of Exeter 2021

University of Exeter. 2021. "Ancient Chickens Lived Significantly Longer than Modern Fowl Because They Were Seen as Sacred, Not Food." *Science Daily*. <https://www.sciencedaily.com/releases/2021/06/210607161043.htm>.

Vagnini et al. 2009

Vagnini, Manuela, Costanza Miliani, Laura Cartechini, P. Rocchi, Bruno Brunetti, and A. Sgamellotti. 2009. "FT-NIR Spectroscopy for Non-Invasive Identification of Natural Polymers and Resins in Easel Paintings." *Analytical and Bioanalytical Chemistry* 395 (7): 2107–18.

Vak, Iannaccone, and Uhlir 2020

Vak, Bettina, Roberta Iannaccone, and Katharina Uhlir. 2020. "Nondestructive Studies of Ancient Pigments on Romano-Egyptian Funerary Portraits of the

Kunsthistorisches Museum, Vienna." In Svoboda and Cartwright 2020.

van Asperen de Boer 1968

van Asperen de Boer, J. R. 1968. "Infrared Reflectography: A Method for the Examination of Paintings." *Applied Optics* 7 (9): 1711–14.

van Daal 2019

van Daal, Jan. 2019. "Ancient Incarnations: Depicting Human Flesh in Mummy Portraits from Roman Egypt." Master of Science thesis, University of Amsterdam.

Vandenabeele et al. 2000

Vandenabeele, Peter, Bernhard Wehling, Luc Moens, Howell Edwards, Martine de Reu, and Guido van Hooydonk. 2000. "Analysis with Micro-Raman Spectroscopy of Natural Organic Binding Media and Varnishes Used in Art." *Analytica Chimica Acta* 407 (1): 261–74.

van den Berg, van den Berg, and Boon 1999

van den Berg, Jorrit D. J., Klaus Jan van den Berg, and Jaap J. Boon. 1999. "Chemical Changes in Curing and Ageing Oil Paints." In *ICOM Committee for Conservation 12th Triennial Meeting Lyon 29 August–3 September 1999*. James & James.

Vandenbeusch 2022

Vandenbeusch, Marie. 2022. "A Soter (Re)connection: Five Fragments of Shrouds from Roman Egypt at the British Museum." *Mitteilungen des Deutschen Archäologischen Instituts Abteilung Kairo* 76/77.

van Dyke 2010

van Dyke, Kristina. 2010. "Losing One's Head: John and Dominique de Menil as Collectors." In *Art and Activism: Projects of John and Dominique de Menil*, edited by Josef Helfenstein and Lauren Schipsi. Yale University Press.

Vassilieva, Piteria, and Nilova 2021

Vassilieva, Olga A., Julii V. Piteria, and Maya V. Nilova. 2021. "Portrait of an Elderly Lady in Red." *Kermes* 121: 33–38.

Vermeule 1964

Vermeule, Cornelius. 1964. "Greek and Roman Portraits in American Collections Open to the Public: A Survey of Important Monumental Likenesses in Marble and Bronze Which Have Not Been Published Extensively." *Proceedings of the American Philosophical Society* 108 (2): 99–134.

Verri 2009A

Verri, Giovanni. 2009. "The Application of Visible-Induced Luminescence Imaging to the Examination of Museum Objects." *Proceedings SPIE 7391, O3A: Optics for Arts,*

Architecture, and Archaeology 2: 739105–12. <https://doi.org/10.1117/12.827331>.

Verri 2009B

Verri, Giovanni. 2009. "The Spatially Resolved Characterisation of Egyptian Blue, Han Blue and Han Purple by Photo-Induced Luminescence Digital Imaging." *Analytical and Bioanalytical Chemistry* 394 (4): 1011–21.

Verri 2014

Verri, Giovanni. 2014. "Roman Sculpture and Colour: The 'Treu Head'" (Ancient Greek and Roman Color/ Polychromy). Video, 9 min., 6 sec. <https://www.youtube.com/watch?v=gRMPYh2QdSM>.

Verri and Brecoulaki 2023

Verri, Giovanni, and Hariclia Brecoulaki. 2023. "'From the Face and the Expression of the Eyes': Multidisciplinary Studies of Pigments in Ancient Greek and Roman Painted Surfaces." *Technai: An International Journal for Ancient Science and Technology* 14: 51–69.

Verri and Saunders 2014

Verri, Giovanni, and David Saunders. 2014. "Xenon Flash for Reflectance and Luminescence (Multispectral) Imaging in Cultural Heritage Applications." *The British Museum Technical Research Bulletin* 8: 83–92.

Verri et al. 2010

Verri, Giovanni, David Saunders, Janet Ambers, and Tracey Sweek. 2010. "Digital Mapping of Egyptian Blue: Conservation Implications." In *Conservation and the Eastern Mediterranean: Contributions to the 2010 IIC Congress, Istanbul*, edited by Christina Rozeik, Ashok Roy, and David Saunders, 220–24. Archetype.

Verri et al. 2023

Verri, Giovanni, Hero Granger-Taylor, Ian Jenkins, Tracey Sweek, Katarzyna Weglowska, and William Thomas Wootton. 2023. "The Goddess' New Clothes: The Carving and Polychromy of the Parthenon Sculptures." *Antiquity* 97(395): 1173–92. <https://doi.org/10.15184/aqy.2023.130>.

Verri et al. 2025

Verri, Giovanni, Hariclia Brecoulaki, Ioanna Mennenga, and Despina Ignatiadou. 2025. "Evoking Enargeia (ἐνάργεια): The Investigation and Reconstruction of the Portrait Bust of Psyche from Melos." In *Chroma: Sculpture in Color from Antiquity to Today*, edited by Seán Hemingway, Vinzenz Brinkmann, and Mark B. Abbe. The Metropolitan Museum of Art.

Verri, Opper, and Devière 2010

Verri, Giovanni, Thorsten Opper, and Thibaut Devière. 2010. "The 'Treu Head': A Case Study in Roman Sculptural Polychromy." *The British Museum Technical Research Bulletin* 4: 39–52.

Verri, Opper, and Lazzarini 2014

Verri, Giovanni, Thorsten Opper, and Lorenzo Lazzarini. 2014. "*In picturae modum variata circumlitio?* The Reconstruction of the Polychromy of a Roman Ideal Female Head (Treu Head)." In *Diversamente bianco: La policromia della scultura romana*, edited by Paolo Liverani and Ulderico Santamaria. Quasar.

Vogelsang-Eastwood 2000

Vogelsang-Eastwood, Gillian. 2000. "Textiles." In Nicholson and Shaw 2000.

von Sonnenburg 1972

von Sonnenburg, Hubert. 1972. *Examination and Treatment Reports*. The Metropolitan Museum of Art, Department of Paintings Conservation.

Wakeling 1912

Wakeling, T. G. 1912. *Forged Egyptian Antiquities*. Adam & Charles Black.

Walker 1997

Walker, Susan. 1997. "Mummy Portraits in Their Roman Context." In *Portraits and Masks: Burial Customs in Roman Egypt*, edited by Morris L. Bierbrier. The British Museum.

Walker 2000A

Walker, Susan, ed. 2000. *Ancient Faces: Mummy Portraits from Roman Egypt*. 2nd ed. The Metropolitan Museum of Art.

Walker 2000B

Walker, Susan. 2000. "A Note on Dating Mummy Portraits." In Walker 2000A.

Walker and Bierbrier 1997

Walker, Susan, and Morris Bierbrier, with Paul Roberts and John Taylor. 1997. *Ancient Faces: Mummy Portraits from Roman Egypt*. A Catalogue of Roman Portraits in the British Museum 4. The British Museum.

Walton and Trentelman 2009

Walton, Marc S., and Karen Trentelman. 2009. "Romano-Egyptian Red Lead Pigment: A Subsidiary Commodity of Spanish Silver Mining and Refinement." *Archaeometry* 51 (5): 845–60.

Warda 2011

Warda, Jeffrey. 2011. *The AIC Guide to Digital Photography and Conservation Documentation*. 2nd ed. American Institute for Conservation of Historic and Artistic Works.

Webb, Summerour, and Giaccai 2014

Webb, E. K., R. Summerour, and J. Giaccai. 2014. "A Case Study Using Multiband and Hyperspectral Imaging for the Identification and Characterization of Materials on Archaeological Andean Painted Textiles." *Postprints of the Textile Specialty Group of the American Institute for Conservation of Historic and Artistic Works* 24: 23–35.

Wegner 2021

Wegner, Jennifer Houser. 2021. "Ancient Egyptian Creation Myths: From Watery Chaos to Cosmic Egg." *Glencairn Museum News*, no. 5. <https://www.glencairnmuseum.org/newsletter/2021/7/13/ancient-egyptian-creation-myths-from-watery-chaos-to-cosmic-egg>.

Werner 1909

Werner, Georgius. 1909. "De imaginibus Graeco-Aegyptis in colonia cui El-Fayum nomen est, repertis et Cracoviae asservatis observations." *Eos* 15: 130–37.

White 1978

White, Raymond. 1978. "The Application of Gas-Chromatography to the Identification of Waxes." *Studies in Conservation* 23 (2): 57–68. <https://doi.org/10.2307/1505796>.

Wiedemann 2014

Wiedemann, Thomas. 2014. *Adults and Children in the Roman Empire*. Routledge.

Wiener 1921

Wiener, Leo. 1921. *Contributions towards a History of Arabo-Gothic Culture*. Vol. 4. Innes & Sons.

Wilkinson 2002

Wilkinson, Caroline M. 2002. "The Facial Reconstruction of the Marina el-Alamein Mummy." *Polish Archaeology in the Mediterranean* 14: 66–71.

Williams 2010

Williams, Jane. 2010. "The Conservation Treatment of the Roman Egyptian Paintings in the Hearst Museum of Anthropology, University of California, Berkeley." In *Decorated Surfaces on Ancient Egyptian Objects: Technology, Deterioration, and Conservation; Proceedings of a Conference Held in Cambridge, UK, on 7–8 September 2007*, edited by

Julie Dawson, Christina Rozeik, and Margot M. Wright. Archetype.

Williams, Cartwright, and Walton 2020

Williams, Jane L., Caroline R. Cartwright, and Marc S. Walton. 2020. "Defining a Romano-Egyptian Painting Workshop at Tebtunis." In Svoboda and Cartwright 2020.

Woodcock 1996

Woodcock, Sally. 1996. "Body Colour: The Misuse of Mummy." *The Conservator* 20 (1): 87–94.

Woudhuysen-Keller and Woudhuysen-Keller 1994

Woudhuysen-Keller, Renate, and Paul Woudhuysen-Keller. 1994. "The History of Egg White Varnishes." *Hamilton Kerr Institute Bulletin* 2: 90–141.

Zaffino et al. 2015

Zaffino, Chiara, Vittoria Guglielmi, Silvio Faraone, Alessandro Vinaccia, and Silvia Bruni. 2015. "Exploiting External Reflection FTIR Spectroscopy for the In-Situ Identification of Pigments and Binders in Illuminated Manuscripts. Brochantite and Posnjakite as a Case Study." *Spectrochimica Acta: Part A, Molecular and Biomolecular Spectroscopy* 136 (B): 1076–85.

Zviagina, Drits, and Dorzhieva 2020

Zviagina, Bella B., Victor A. Drits, and Olga V. Dorzhieva. 2020. "Distinguishing Features and Identification Criteria for K-Dioctahedral 1M Micas (Illite-Aluminoceladonite and Illite-Glaucanite-Celadonite Series) from Middle-Infrared Spectroscopy Data." *Minerals* 10 (2): 1–29.

APPEAR Participants

Allard Pierson Museum, Amsterdam
Ägyptisches Museum und Papyrussammlung, Berlin
Antikensammlung, Staatliche Museen zu Berlin
ArtAncient Ltd, London
Art Institute of Chicago
Ashmolean Museum of Art and Archaeology, Oxford
British Museum, London
Brooklyn Museum of Art
Cantor Arts Center, Stanford, California
Cleveland Museum of Art
Detroit Institute of Arts
The Fitzwilliam, Cambridge, UK
Goucher College, Maryland
Harvard Art Museums, Cambridge, Massachusetts
Icon Museum and Study Center, Clinton, Massachusetts
Institute for the Study of Ancient Cultures, Chicago
The J. Paul Getty Museum and Getty Conservation Institute, Los Angeles
Johns Hopkins Archaeological Museum, Baltimore
Kelsey Museum of Archaeology, Ann Arbor, Michigan
Kunsthistorisches Museum, Vienna
Los Angeles County Museum of Art
Manchester Museum, UK
The Menil Collection, Houston
The Metropolitan Museum of Art, New York
Michael C. Carlos Museum, Atlanta
Musée du Louvre, Paris
Museo Egizio, Turin
Museum August Kestner, Hannover, Germany
Museum für Kunst und Gewerbe Hamburg
Museum of Fine Arts, Boston
Museum of Fine Arts, Budapest
The Museum of Fine Arts, Houston
National Archaeological Museum, Athens, Greece
National Gallery, London
National Gallery of Victoria, Melbourne, Australia
National Museum in Warsaw

The National Museum of Denmark, Copenhagen
The Nelson-Atkins Museum of Art, Kansas City, Missouri
Nicholson Museum, Sydney University Museums
Norton Simon Museum, Pasadena, California
Ny Carlsberg Glyptotek, Copenhagen
Paul and Alexandra Canelopoulos Museum (CAMU), Athens, Greece
The Petrie Museum of Egyptian Archaeology, London
Phoebe A. Hearst Museum of Anthropology, Berkeley, California
Reiss-Engelhorn-Museen, Mannheim, Germany
Rhode Island School of Design Museum, Providence
Rijksmuseum van Oudheden, Leiden, Netherlands
Rosicrucian Egyptian Museum, San Jose, California
Royal Museum of Mariemont, Belgium
Royal Ontario Museum, Toronto
San Antonio Museum of Art, Texas
Santa Barbara Museum of Art, California
Saint Louis Art Museum, Missouri
Seattle Art Museum, Washington
The Egypt Centre, Museum of Egyptian Antiquities, Swansea, UK
The State Pushkin Museum of Fine Arts, Moscow
University of Georgia (Lamar Dodd School of Art), Athens
University of Heidelberg
University of Pennsylvania Museum of Archaeology and Anthropology, Philadelphia
Virginia Museum of Fine Arts, Richmond
Wadsworth Atheneum Museum of Art, Hartford, Connecticut
The Walters Art Museum, Baltimore

Contributors

Caroline R. Cartwright

Caroline R. Cartwright is the wood anatomist and a senior scientist in the Department of Scientific Research at the British Museum. Her primary areas of scientific expertise cover the identification and interpretation of organic materials, including wood, charcoal, fibers, and macro-plant remains from all areas and time periods, mainly using scanning electron microscopy. Cartwright has led many teams of environmental scientists on archaeological projects in various parts of the world including the Middle East, Africa, the Caribbean, and Europe. Reconstructing past environments, charting vegetation and climate changes, and investigating bioarchaeological evidence from sites and data also form important aspects of her research. Before joining the British Museum, she was a lecturer in archaeological sciences at the Institute of Archaeology, University College London. Cartwright is the author or coauthor of more than 310 publications.

Marie Svoboda

Marie Svoboda is a conservator in the Antiquities Conservation Department at the J. Paul Getty Museum. She received an MA from the Art Conservation program at the State University of New York at Buffalo, majoring in artifacts and minoring in paintings conservation. Focusing on the study of ancient materials, Svoboda joined the Getty in 2003. She is actively involved in various in-depth studies that pertain to her interest in ancient technology and pigment studies. She manages the APPEAR project, an international collaboration on the study of ancient funerary paintings.

Maria Victoria Asensi Amorós

Maria Victoria Asensi Amorós is an Egyptologist and wood anatomist who works with private collections, public museums, and international archaeological teams to identify wooden artifacts from different civilizations. Based in Paris, France, she is a scientific director of the Xylodata company, involved in wood anatomy identifications, and is an officeholder at IUFRO (International Union of Forest Research Organizations; 5.15.01, Wood Culture). Her involvement for the past twenty-five years in several archaeological programs in Egypt has made her an expert on wood from the Pharaonic to the beginning of the Islamic period, which led to the development of Xyloteca for the IFAO (French Institute of Oriental Archaeology, Cairo).

Christine Andraud

Christine Andraud is a physicist in the service of conservation sciences. She is a professor at the Muséum National d'Histoire Naturelle (MNHN) and director of the Centre de Recherche sur la Conservation (CRC), a national organization carrying out research for the preservation of museum collections that is funded by the French Ministry of Culture, the Centre National de la Recherche Scientifique (CNRS), and the MNHN. Andraud is a specialist in optics, with expertise in complex optical processes generated by light on heterogeneous surfaces; she is a master of optical modeling and optical measurements.

Julie Arslanoglu

Julie Arslanoglu is a research scientist in the Department of Scientific Research at The Metropolitan Museum of Art (The Met). She investigates the identification, interaction, and degradation of natural and synthetic organic materials including paints, coatings, and adhesives using mass-spectrometric, imaging, immunological, and DNA techniques. She is co-founder of Art Bio Matters, a coalition of scientists, conservators, historians, and curators focused on biological materials used to create cultural heritage, and of Art and Cultural Heritage: Natural Organic Polymers by Mass Spectrometry (ARCHE), a partnership between The Met and the University of Bordeaux, studying the material dimension of museum collections on a molecular level using mass spectrometry.

Lawrence M. Berman

Lawrence M. Berman is John F. Cogan Jr. and Mary L. Cornille Chair, Art of Ancient Egypt, Nubia, and the Near East at the Museum of Fine Arts (MFA), Boston. He received his PhD in Egyptology from Yale University in 1985. Before coming to the MFA in 1999, he was curator of Egyptian and Ancient Near Eastern Art at the Cleveland Museum of Art. He has worked on numerous exhibitions and gallery reinstallations and has written many books and articles. His latest book is *Faces of Ancient Egypt* (MFA Publications, 2022).

Christina Bisulca

Christina Bisulca is the Andrew W. Mellon conservation scientist at the Detroit Institute of Arts (DIA). She has a PhD in materials science and engineering through the heritage conservation science program at the University of Arizona, an MS in objects conservation through the Winterthur/University of Delaware Program in Art Conservation, and a BA in chemistry from Rutgers University. Prior to the DIA she worked in conservation at various institutions, including the Arizona State Museum (University of Arizona), the Department of Conservation and Scientific Research at the Freer Gallery of Art (Smithsonian Institution), and the Bernice Pauahi Bishop Museum in Honolulu, Hawaii.

Courtney Books

Courtney Books is associate painting conservator at the Saint Louis Art Museum and serves on the editorial

board of *Materia: Journal of Technical Art History*. She maintains a strong interest in bio-art, mural and large-format paintings, and paintings on atypical substrates.

Cecilie Brøns

Cecilie Brøns is a senior researcher and curator at the Ny Carlsberg Glyptotek in Copenhagen. She is the director of an interdisciplinary research project on the polychromy of ancient art, "Sensing the Ancient World: The Invisible Dimensions of Ancient Art," financed by the Carlsberg Foundation. She received her PhD in classical archaeology in 2015 from the National Museum of Denmark and the Danish National Research Foundation's Centre for Textile Research (CTR) at the University of Copenhagen. In 2017–18 she was a research fellow at the Harvard Center for Hellenic Studies, Washington, DC. Her research concentrates on the polychromy of ancient art, architecture, and textiles, particularly in relation to ancient sculpture, as well as on the effect of the senses on our perception of ancient art.

Lucile Brunel-Duverger

Lucile Brunel-Duverger is a physical chemist with a background in chemistry and archaeometry, specializing in the study of painting materials and craft-making practices developed during her work in laboratories and museums and, as part of her PhD, conducted at the Centre de Recherche et de Restauration des Musées de France (C2RMF) on the polychromy of the Louvre "yellow coffins." She acquired new skills in non-invasive techniques, such as hyperspectral imaging, while working on the FAYOUM Project and in her subsequent postdoctoral position at the Laboratoire d'Archéologie Moléculaire et Structurale (LAMS) (CNRS, University of Pierre and Marie Curie [UPMC]). She joined the C2RMF Research Department in March 2024.

Thomas Calligaro

Thomas Calligaro is a physicist and research engineer at the French Ministry of Culture. He specializes in the development of new methods for the study of cultural heritage materials and, more particularly, analysis and imaging techniques by ion beams, X-radiography, luminescence, and reflectance. Part of the team who built the particle accelerator for the C2RMF, AGLAE, Calligaro currently works on its evolution through the development of a new line dedicated to PIXE imaging for

large objects (PIXXL project; Equipex+ ESPADON). His research interests were initially focused on the composition and provenance study of gems and stones (ruby, emerald, garnet, quartz, obsidian, and more); he is now lending his expertise to the study of pigments on a variety of supports.

Silvia A. Centeno

Silvia A. Centeno is a research scientist in the Department of Scientific Research at The Met, where she is responsible for investigating artists' materials and techniques and deterioration processes in paintings, photographs, and works of art on paper. She has conducted research in a variety of topics, including heavy-metal soap deterioration in oil paintings; early pigment- and platinum-based photographic processes; daguerreotypes; and old master, modern, and contemporary paintings. She received a PhD in chemistry from Universidad Nacional de La Plata, Argentina, and started at The Met as an L. W. Frohlich Fellow, studying unusual gilding techniques in pre-Columbian metalwork.

Kate Clive-Powell

Kate Clive-Powell is the project textile conservator at the University of Washington Libraries. She received her MPhil in Textile Conservation from the University of Glasgow. She completed a one-year ICON Textile Conservation internship at the Bowes Museum and St. Fagans National Museum of History, and a three-year Sherman Fairchild Textile Conservation Fellowship at the MFA, Boston.

Laura A. D'Alessandro

Laura A. D'Alessandro has been head of the conservation laboratory at the Institute for the Study of Ancient Cultures, University of Chicago, since 1986. She holds a bachelor's degree in Greek and Roman civilizations from the State University of New York at Albany and a degree in archaeological and ethnographic conservation from the Institute of Archaeology, University of London. D'Alessandro has served as project manager for various reinstallations of large-scale architectural sculptures, including oversized Assyrian reliefs and a sixteen-foot statue of Tutankhamun. She currently manages a multi-year project involving the stabilization, conservation, analysis, and display of

eighth-century BCE glazed bricks from the Sin Temple at Sargon II's palace at Khorsabad, Iraq. Her interests include the study of ancient glazes and pigments.

Susanne Ebbinghaus

Susanne Ebbinghaus is the George M. A. Hanfmann Curator of Ancient Art and head of the Division of Asian and Mediterranean Art at the Harvard Art Museums. She received MPhil and DPhil degrees from the University of Oxford. Her research focuses on the art and archaeology of ancient Greece and the Middle East, with special interests in cross-cultural interaction, feasting, sculptural polychromy, and bronzes. She organized the exhibitions *Gods in Color: Painted Sculpture of Classical Antiquity* (2007) and *Animal-Shaped Vessels from the Ancient World: Feasting with Gods, Heroes, and Kings* (2018) and participates in the Archaeological Exploration of Sardis (Türkiye).

Katherine Eremin

Katherine Eremin is the Patricia Cornwell Senior Conservation Scientist at the Straus Center for Conservation and Technical Studies, Harvard Art Museums. She has a PhD in geology from the University of Cambridge. She has been at the Straus Center since 2004, and previously worked at the National Museum of Scotland (1994–2003). Eremin focuses on the identification of inorganic materials in works of art, including Chinese jade and glass, wall paintings, and manuscripts.

Clara Granzotto

Clara Granzotto is assistant conservation scientist in the Conservation and Science Department at the Art Institute of Chicago (AIC). She received her PhD in chemical sciences from the University of Venice, Italy, and the University of Lille, France. Granzotto conducted postdoctoral research at the Center for Scientific Studies in the Arts at Northwestern University in Evanston, Illinois, the scientific department of The Met, and the University of Copenhagen, Denmark. She specializes in the analysis of traditional binding media in works of art by mass spectrometry, with a focus on polysaccharides and proteins.

Charlotte Hale

Charlotte Hale is a conservator who received her training in the conservation of paintings at the Courtauld Institute of Art, London. In 1987 she joined the Department of Paintings Conservation at The Met, where she has focused on the technical examination and treatment of European nineteenth-century paintings. Recent publications include studies of works by Gauguin, Cézanne, Seurat, and van Gogh.

Ellen Hanspach-Bernal

Ellen Hanspach-Bernal is a 2006 graduate of the art conservation program at the University of Fine Arts, Dresden. From 2006 to 2009 she was the Andrew W. Mellon Fellow in painting conservation at the Menil Collection in Houston, Texas. She has worked for the Klassik Stiftung Weimar and for the Conservation Centre for the Museums of the City of Erfurt, Thüringen, in Germany. Hanspach-Bernal has been the paintings conservator at the DIA since 2015, where her work focuses on preserving, researching, and treating the paintings of the collection from the antiquities to the present. She also supervises and teaches postgraduate fellows to prepare a new generation of conservators for work in a museum environment. Most recently she has published on a Roman-period funerary portrait, Pieter Bruegel the Elder, Max Ernst's Surrealist painting techniques, and Pablo Picasso's use of non-artist paints.

Richard Hark

Richard Hark is a conservation scientist at the Institute for the Preservation of Cultural Heritage (IPCH), Yale University. After earning degrees in chemistry, Hark served as a chemistry professor for twenty-five years before moving to Yale in 2017 to focus his efforts on the scientific analysis of cultural heritage objects. He has worked on diverse projects involving the Vinland Map and its sister manuscripts, Tudor and Stuart portraiture, the Gutenberg Bible and related incunables, fifteenth-century *tarocchi* cards, portolan charts, wood analysis of early American mahogany furniture, and William Henry Fox Talbot's *The Pencil of Nature*.

Marsha Hill

Marsha Hill is an art historian, Egyptologist, and curator emerita in the Department of Egyptian Art at The Met. There she was concerned with the galleries of First

Millennium BCE Egypt, and organized installations and exhibitions dealing with that period, including co-curating with Dorothea Arnold the 2000 New York version of Susan Walker's exhibition *Ancient Faces*, originally held at the British Museum in 1997.

Agnieszka Kijowska

Agnieszka Kijowska graduated from the Art Conservation Department of the Academy of Fine Arts in Warsaw. She is employed at the Conservation Workshop of Ancient Art and Stone Architecture of the National Museum in Warsaw, where she works on ancient artifacts of polychromed wood, ceramics, and wall painting. She has participated in archaeology-conservation missions in Egypt (Sakkara and Wadi Natrun) and is coauthor of articles about the conservation of wall paintings from the Faras Cathedral.

Daniel P. Kirby

Daniel P. Kirby turned his interests to conservation after a career as an analytical chemist in semiconductor electronics, pharmaceuticals, and academic research. He currently works both in private practice and as a volunteer in the Scientific Research Lab at the MFA, Boston, specializing in applications of mass spectrometry in art and cultural heritage, with a particular interest in protein identification.

Justyna Kwiatkowska

Justyna Kwiatkowska is a graduate in chemistry at Warsaw University and authored the MA thesis "LA-ICP-MS in the Study of Heterogeneous Historic Objects." Since 2016 she has been a conservation assistant in the laboratory of the Conservation Department at the National Museum in Warsaw. From 2016 to 2019 Kwiatkowska participated in the project *Henryk Siemiradzki's Corpus of Painting Works*. She conducts Oddy tests and physicochemical analyses of works of art using technological layer stratigraphy, microchemistry, and infrared reflection spectroscopy (FTIR-ATR).

Anne-Solenn Le Hô

Anne-Solenn Le Hô is senior conservation scientist at the National Center for Research and Restoration in French Museums (C2RMF/IRCP, PSL University, Paris). In charge of the painting group, she has extensive experience in interdisciplinary research on the characterization of

painted materials and their interactions and alteration mechanisms. Her research interests are in the use of color and technical processes in paintings, polychrome objects, and lacquerware. She is also an associate editor, scientific member, and contributor to journals and books about cultural heritage, archaeometry, and art history.

Dorothy Mahon

Dorothy Mahon is a conservator in the Department of Paintings Conservation at The Met, where she has examined and conserved paintings spanning the collection since joining the staff in 1981. Recent publications focus on Rembrandt, Vermeer, Jacques-Louis David, and John Singer Sargent. Mahon received her master's degree in the history of art and a Certificate of Advanced Study in Conservation from the Institute of Fine Arts, New York University.

William J. Mastandrea

William J. Mastandrea is currently working as an assistant conservator for the Ancient Near East and Cypriot Gallery renovation at The Met. Prior to joining the objects conservation department, he was the inaugural Gale R. Guild and Henry R. Guild Fellow for Advanced Training in Objects Conservation at the MFA, Boston. William received his MSc in Conservation for Archaeology and Museums from University College London. Combining his background in both conservation and archaeology, his research interests include the multi-band imaging, in-depth investigation, and treatment of archaeological objects and their pigments, binders, and other constituent materials.

Evelyn (Eve) Mayberger

Evelyn (Eve) Mayberger holds a BA from Wesleyan University and MA and MS degrees in art history and conservation from the Institute of Fine Arts, New York University, where she specialized in objects conservation. She has worked in the conservation departments of Olin Library at Wesleyan University, Smithsonian American Art Museum, Historic Odessa Foundation, Small Collections Library at the University of Virginia, National Museum of the American Indian, Worcester Art Museum, University of Pennsylvania Museum of Archaeology and Anthropology, and MFA, Boston. In addition to museum work, she has participated in excavations at Sardis (Türkiye), Selinunte

(Sicily), Abydos (Egypt), and el Kurru (Sudan). Currently, Mayberger is an assistant conservator at the MFA, Boston.

Joy Mazurek

Joy Mazurek is an associate scientist at the Getty Conservation Institute. She specializes in the identification of binding media in paint using gas chromatography/mass spectrometry, the characterization and degradation of plastics, and the application of biological methods to study artwork. She obtained her MS in microbiology from California State University, Northridge, and her BS in biology from the University of California, Davis.

Alicia McGeachy

Alicia McGeachy joined the Scientific Research Partnership (SRP) at The Met as an associate research scientist in May 2022. She received her PhD in chemistry from Northwestern University and a BS in chemistry from Spelman College. She was Andrew W. Mellon postdoctoral fellow in the Department of Scientific Research (2018–20), where her primary research focused on the analysis of eighteenth-century English ceramics with the goal of reconstructing the practices employed at the Chelsea Porcelain Manufactory. She continued her postdoctoral training (2020–22) with the Northwestern University–Art Institute of Chicago Center for Scientific Studies in the Arts (NU-ACCESS). In her role with SRP, McGeachy applies her wide technical experience to the study of works in partnering cultural institutions to inform treatment and research and, more broadly, the stories that we can tell about ourselves. She has coauthored numerous articles.

Michel Menu

Michel Menu, physicist, was director of the Research Department of C2RMF from 2001 to 2021. Today he is the director of the Science and Technology in Archaeology and Culture Center (STARC) of the Cyprus Institute (Nicosia, Cyprus). Its main research focus is the color and appearance of painted works, considered to be “augmented art objects,” by the integration of data collected by a variety of disciplines.

Anne Michelin

Anne Michelin is an assistant professor at the MNHN in Paris and conducts research in the CRC. Her research focuses on the characterization of ancient materials and on the understanding of their alteration processes. She works on a team dedicated to the study of color and visual appearance of museum artifacts and develops non-destructive techniques such as hyperspectral imaging analysis. Her latest projects concern the analysis of ancient manuscripts with two objectives: to improve the legibility of the writing when the documents are faded or altered, and to characterize the material constituents to investigate the techniques involved in a manuscript's creation.

Raphaël Moreau

Raphaël Moreau joined the Cyprus Institute as a PhD student in August 2020 after graduating with a master's degree in analytical chemistry (2019) and a bachelor's degree in physics and chemistry (2017). His work focuses on the use and development of analytical devices, combining several spectroscopic techniques such as X-ray fluorescence, photoluminescence, and optical reflectance. The treatment and understanding of the large amount of data gathered with such devices is another central point of his work, as these provide clues that lead to a deeper understanding of the stakes of cultural heritage material comprehension.

Richard Newman

Richard Newman is the head of scientific research at the MFA, Boston, where he has worked as a research scientist since 1986. He holds a BA in art history from Western Washington University and an MA in geology from Boston University, and he completed a three-year apprenticeship in conservation and conservation science at the Straus Center for Conservation and Technical Studies. He has carried out research on a wide range of cultural artifacts, from the stone sculpture of the Indian subcontinent to the paintings of Diego Velázquez. A coauthor of the chapter on adhesives and binders in *Ancient Egyptian Materials and Technology* (Cambridge University Press, 2000), Newman has collaborated with conservators and curators on numerous projects involving ancient Egyptian and Nubian art.

Ioannis Panagakos

Ioannis Panagakos is a conservator of antiquities, specializing in stone artifacts, at the Sculpture Conservation Lab of the National Archaeological Museum in Athens. He earned his degree at the University of West Attica and furthered his studies with the completion of the postgraduate course in digital arts (MA) at the Athens School of Fine Arts. He is especially interested in the study of polychromed artifacts, 3D digital modeling, and virtual reassembly.

Irma Passeri

Irma Passeri is the Susan Morse Hilles Chief Conservator at the Yale University Art Gallery (YUAG). Passeri studied painting conservation at the Scuola di Alta Formazione at the Opificio delle Pietre Dure (OPD) in Florence, Italy, where she received her degree in the Conservation of Easel Paintings in 1998. She joined the conservation staff of the YUAG in 2000. Passeri has worked at the OPD and the Philadelphia Art Museum, among other institutions. She has published articles on materials and techniques of Italian paintings and different approaches to the restoration treatment of loss compensation.

Laurent Pichon

Laurent Pichon has been a research engineer at the French Ministry of Culture since 1999. He works as an electronic and computer science engineer on the particle accelerator at the C2RMF, AGLAE. His work concerns the development of new analysis techniques and data processing software that are specially dedicated to the characterization of artworks. Initially, his field of expertise was ion beam applications, but he now works in service to the design and realization of innovative portable instruments, such as the XRF/RIS/PL/SWIR scanning device used in the study of the Fayum portraits from the Louvre collection.

Federica Pozzi

Federica Pozzi is the director of scientific laboratories at the Centro per la Conservazione ed il Restauro dei Beni Culturali "La Venaria Reale," Turin, Italy. She earned her PhD in chemical sciences in 2012 from the University of Milan. Prior to her current appointment, Pozzi held positions at The Met, City University of New York (CUNY), the American Institute of Conservation (AIC), and the Solomon R. Guggenheim Museum. She was recently

awarded Professional Membership of the AIC and a Fellowship of the IIC in recognition of her professional achievements and contributions to the conservation science profession.

Georgina Rayner

Georgina Rayner is the associate conservation scientist at the Straus Center for Conservation and Technical Studies, Harvard Art Museums. She holds a PhD in chemistry from the University of Warwick, UK. Rayner specializes in the identification of organic materials at the Straus Center. She has worked on many technical investigations studying the materials used in artworks, including a survey identifying the plastics present in objects in the collection; John Singer Sargent's paint palettes; and the pigments and binders used by Aboriginal artists in traditional bark paintings.

Corina E. Rogge

Corina E. Rogge is a conservation scientist and director of conservation at the Menil Collection, Houston. She earned a BA in chemistry from Bryn Mawr College, a PhD in chemistry from Yale University, and held postdoctoral positions at the University of Wisconsin-Madison and the University of Texas Health Sciences Center. Before joining the Menil Collection in 2023 Rogge served as the Andrew W. Mellon Research Scientist at the Museum of Fine Arts, Houston (MFAH) and the Menil Collection (2013–23), and the Andrew W. Mellon Assistant Professor in Conservation Science in the Department of Art Conservation at State University of New York Buffalo (2010–13). She is the vice president and fellow of the American Institute for Conservation and an associate editor for the *Journal of the American Institute for Conservation*. She works on materials across all cultures, media, and ages, and is a coauthor of *Franz Kline: The Artist's Materials* (GCI, 2022).

Rachel Sabino

Rachel Sabino is director of Objects and Textiles Conservation at the AIC, where she has been a staff member since 2011. A specialist in structural issues related to large-scale objects, Sabino has previously held positions at the MFAH, the National Gallery London, and the Chicago Conservation Center; internships at The Met and the J. Paul Getty Museum; and a sabbatical at the Corning Museum of Glass. She received her training at

West Dean College of Arts and Conservation, UK, and is a fellow of the International Institute of Conservation and the American Institute for Conservation of Historic and Artistic Works.

Anna Serotta

Anna Serotta is an associate conservator in the Department of Objects Conservation at The Met, specializing in the care and study of archaeological materials. Her primary role is as conservator for the Egyptian art collection. Serotta is also a lecturer at the NYU Institute of Fine Arts Conservation Center, a fellow of the American Academy in Rome, and has worked as a field conservator on archaeological sites in Egypt, Greece, Italy, and Türkiye.

Louisa Smieska

Louisa Smieska leads the Functional Materials Beamline at the Cornell High Energy Synchrotron Source in Ithaca, New York. She is especially interested in applications of synchrotron radiation for the study of material cultural heritage. In 2016–17 she held an Andrew W. Mellon Foundation postdoctoral fellowship in the Department of Scientific Research at The Met, where she examined paintings and other objects with the museum's Bruker XRF scanner.

Kate Smith

Kate Smith is conservator of paintings and head of the paintings lab at the Straus Center for Conservation and Technical Studies at the Harvard Art Museums. She received an MA in conservation from SUNY Buffalo in 2001 and previously worked at the MFA, Boston, and the Isabella Stewart Gardner Museum. Smith studies and preserves the Harvard paintings collection, with works spanning from ancient Roman to modern and contemporary periods. She specializes in technical examination using radiography, infrared reflectography, and fluorescence imaging to investigate artists' materials and techniques.

John Southon

John Southon is a researcher in the Earth System Science Department, University of California, Irvine (UCI), and co-director of UCI's W. M. Keck Carbon Cycle Accelerator Mass Spectrometry (AMS) Laboratory. Prior to taking up the position at UCI, Southon helped design the AMS

spectrometer at Lawrence Livermore National Laboratory (LLNL) in the mid-1980s and was head of the natural radiocarbon group at LLNL's Center for AMS from 1989 to 2001. His interests include the development of AMS technology and applications of the technique in fields including archaeology, paleontology, paleoclimate, and paleoceanography.

Lin Rosa Spaabæk

Lin Rosa Spaabæk is a conservator at the Agency for Culture and Palaces in Copenhagen. She previously held a position at the Ny Carlsberg Glyptotek, where she restored and studied their collection of mummy portraits. Spaabæk obtained her bachelor's degree in paintings conservation and completed her master's thesis on the study of mummy portraits at the Royal Academy of Fine Arts, School of Conservation, Copenhagen. She has recently completed a study of mummy portraits, materials, and painting techniques, supported by the Carlsberg Foundation.

Stephanie Spence

Stephanie Spence is the assistant objects conservator at the Nelson-Atkins Museum of Art in Kansas City, Missouri. She earned her MA in art conservation, specializing in objects conservation, from the Patricia H. and Richard E. Garman Art Conservation Department at SUNY Buffalo in 2017. She completed her third-year internship at the Nelson-Atkins, and was the conservation fellow at the Toledo Museum of Art.

Aaron Steele

Aaron Steele has been the imaging specialist and photographer for the Conservation Department at the DIA since 2014. He has more than twenty years of experience in cultural heritage, museum, and art conservation imaging. He recently co-curated the 2019–20 DIA exhibition *Bruegel's The Wedding Dance Revealed*, and contributed to the associated technical publication on the painting *The Wedding Dance*. His undergraduate and graduate education was at Indiana University focusing on art, art librarianship (visual resources), and art education. Prior to his current position at the DIA, he worked as associate photographer at the Northeast Document Conservation Center (NEDCC), as conservation department photographer and imaging specialist at the Indianapolis

Museum of Art (IMA), and as photographer for the Lilly Rare Books Library at Indiana University. Steele has also worked at the Indiana University Art Museum (IUAM) in the curatorial, registration, and education departments.

Jens Stenger

Jens Stenger is a senior scientist at the Ny Carlsberg Glyptotek in Copenhagen, where he conducts research on the polychromy of ancient artifacts. He earned his PhD in physics at Humboldt-Universität zu Berlin and was a postdoctoral researcher at the University of California, Berkeley. He has held positions at the Straus Center for Conservation and Technical Studies at the Harvard Art Museums, the Institute for the Preservation of Cultural Heritage at Yale University, the Swiss Institute for Art Research, and the Cologne Institute of Conservation Sciences.

Aleksandra Sulikowska-Bełczowska

Aleksandra Sulikowska-Bełczowska is a curator of the Collection of Ancient Art and the Collection of Eastern Christian Art at the National Museum in Warsaw, where she oversees Nubian, Coptic, and Ethiopian collections, as well as the Collection of Icons and Byzantine Crafts. She is also a professor in the Institute of Art History at the University of Warsaw. Sulikowska-Bełczowska has authored books and papers on the cult of images in late antique and eastern Christian art and the iconography of the icons and wall paintings in Orthodox art.

Ken Sutherland

Ken Sutherland is Andrew W. Mellon Director of Scientific Research in the Department of Conservation and Science at the AIC. His primary research interests concern the characterization of organic materials in works of art to inform an understanding of their technique, condition, and appearance. He held previous positions at the Philadelphia Museum of Art and the National Gallery of Art, Washington, DC. He received a PhD in chemistry from the University of Amsterdam, a diploma in the conservation of easel paintings from the Courtauld Institute of Art, London, and a BSc in biochemistry from University College, London. His previous publications include "Challenges in the Characterization and Categorization of Binding Media in Mummy Portraits," coauthored with Rachel Sabino and Federica Pozzi, in

Mummy Portraits of Roman Egypt: Emerging Research from the APPEAR Project (J. Paul Getty Museum, 2020).

Jevon Thistlewood

Jevon Thistlewood is the conservator of paintings at the Ashmolean Museum of Art and Archaeology, University of Oxford, and is an accredited member of the Institute of Conservation (ICON). He graduated from the University of Leeds with degrees in chemistry and sculpture studies, and he has a master's degree in the Conservation of Fine Art (Easel Paintings) from the University of Northumbria. Thistlewood's research interests are wide and varied, and often relate to paintings from antiquity to the present.

Caroline Thomas

Caroline Thomas is curator for Egyptian art at the Louvre Museum in Paris, where she oversees the Graeco-Roman, Egyptian, and Sudanese collections. In addition to her work on mummy portraits and panels of gods, her research focuses on First Millennium BCE cartonnages, coffins, and funerary practices. Before joining the Louvre in 2018 she worked for the C2RMF, where she developed her expertise in conservation sciences. She trained at the École du Louvre, Sorbonne University (Paris), and Lille University in art history, Egyptology, and museology.

Jen Thum

Jen Thum is associate director of Academic Engagement and Campus Partnerships and research curator at the Harvard Art Museums. She holds a PhD in Archaeology and the Ancient World from Brown University and an MPhil in Egyptology from the University of Oxford. Thum creates interdisciplinary learning experiences for students across the university, teaches about museum pedagogy for the Harvard Graduate School of Education, delivers programs and workshops about object-based learning, and researches and teaches with the museums' ancient Egyptian collection. She is committed to celebrating the learning potential of art and artifacts for students and the public.

Aurélie Tournié

Aurélie Tournié obtained a PhD in physical chemistry in January 2009 from the Laboratoire de Dynamique, Interactions et Réactivité at CNRS and University of Pierre and Marie Curie (UPMC; Paris 6). She held three

postdoctorate positions from 2009 to 2012, during which she acquired expertise in the characterization, by vibrational spectroscopies (Raman and IR), of inorganic and organic materials in the laboratory and on-site. She is currently research engineer at the CRC where her main projects develop optical and spectroscopic methods, in particular hyperspectral imaging applied to cultural heritage objects and materials.

Peppy Tsakri

Peppy Tsakri is a conservator of antiquities and works of art in the Department of Conservation and Physical-Chemical Research and Archaeometry at the National Archaeological Museum, Athens, Greece. She received an MSc in conservation science from De Montfort University in the United Kingdom.

John Twilley

John Twilley is the Mellon Science Advisor to the Nelson-Atkins Museum of Art, Kansas City. His work has focused on the application of microanalytical techniques to the history of artists' materials, their alterations by time and environmental effects, artwork attributions, and the development of treatment methods.

Jan M. van Daal

Jan M. van Daal currently works for the Dutch Tax and Customs Administration. He obtained his BAs in Archaeology and Prehistory and Latin Language and Culture, and his MSc in Technical Art History from the University of Amsterdam. In May 2025 he obtained his PhD from Utrecht University after completing a dissertation on long-term investments and risk analysis in medieval west European art production, as part of the ERC-DURARE project. He has fulfilled several voluntary board functions in the humanities and cultural sector and continues to do so. Van Daal's main research interests lie with painted portraits from Roman Egypt, medieval Latin, and art technological source research.

Branko F. van Oppen de Ruiter

Branko F. van Oppen de Ruiter is the Richard E. Perry Curator of Greek and Roman Art at the Tampa Museum of Art, Florida. He received his PhD in ancient history from the City University of New York (2007), where he specialized in queenship during the period from Alexander the Great to Cleopatra. Before coming to

Tampa, van Oppen worked for five years at the Allard Pierson Museum, Amsterdam. His academic interests include clay seal impressions, animals in ancient material culture, and Romano-Egyptian funerary portraits, as well as ancient religion and art history in general.

Marc Vermeulen

Marc Vermeulen is the head of Heritage Science and Conservation Research at the National Archives (TNA). He earned his PhD in chemistry from the University of Antwerp in 2017, specializing in the study of arsenic sulfide pigments. Before joining TNA, he worked at the Center for Scientific Studies in the Arts (NU-ACCESS), where he contributed to various projects, including the material characterization of Fayum portraits. Vermeulen has coauthored thirty-five peer-reviewed scientific papers concerning heritage science and conservation techniques, pigment and colorant analysis, analytical methodologies and data processing, and material characterization and degradation studies. His research integrates scientific analysis and cultural heritage preservation, advancing the understanding and conservation of historical materials.

Giovanni Verri

Giovanni Verri has been a conservation scientist in the Department of Conservation and Science at the AIC since 2019. He holds a PhD in physics from the University of Ferrara, Italy, and an MA in the conservation of wall paintings from the Courtauld Institute of Art in London. In 2007, he developed an imaging technique called visible-induced luminescence imaging, through which it is possible to map the presence of Egyptian blue, a very commonly used blue pigment in antiquity, even when otherwise invisible to the naked eye. His research interests include the development and application of investigative techniques for the analysis of color. With a focus on the ancient Mediterranean, Verri also studies how materials and techniques are shared across different media and their relationship with primary written sources.

Barbara Wagner

Barbara Wagner is a chemist and professor in the Laboratory of Theoretical Aspects of Analytical Chemistry at the Faculty of Chemistry, University of Warsaw. She received her master's from the Faculty of Conservation

and Restoration of Works of Art at the Academy of Fine Arts in Warsaw with highest honors. As head of the Interdisciplinary Laboratory of Archaeometric Research at the University of Warsaw Biological and Chemical Research Centre, she is actively involved in the Polish Distributed Research Infrastructure for Heritage Science project (<http://www.e-rihs.pl/>). She has authored papers about the use of micro- and non-destructive spectral methods in the analysis of cultural heritage objects.

Marc Walton

Marc Walton joined the Museum Studies program at the University of Hong Kong in the fall of 2024 as a professor. Prior to this, he held senior leadership positions at Hong Kong's M+ (head of conservation and research) and worked in academia as co-director of NU-ACCESS, where he was also research professor of materials science. He led multiple scientific projects investigating art objects in collaboration with cultural heritage institutions representing a broad range of disciplines at NU-ACCESS, from anthropology to contemporary art, with broad geographical reach. Walton's areas of research have focused primarily on the manufacture and trade of archaeological objects and on developing imaging technologies in the field of conservation science. He has more recently delved into sustainable collections care. These efforts have resulted in over one hundred peer-reviewed articles.

Alison Whyte

Alison Whyte is senior conservator of objects at the Institute for the Study of Ancient Cultures at the University of Chicago where she has specialized in the preservation of archaeological material from West Asia and North Africa since 2001. A professional associate of the American Institute for Conservation, she is a graduate of the Queen's University Master of Art Conservation Program and holds a BA in anthropology from the University of British Columbia and an MA in ancient studies from the University of Toronto.

Marcie Wiggins

Marcie Wiggins is an assistant conservation scientist and the Diana Luv Chen Fellow in the Technical Studies Lab working on material characterization for Yale's collections. She received her PhD in analytical chemistry at the University of Delaware in 2019, studying copper-

based pigments via spectroscopic methods and collaborating with Winterthur Museum. Marcie has held internships at the Library of Congress, the Smithsonian's Museum Conservation Institute, and the Rijksmuseum. She started at the Institute for the Preservation of Cultural Heritage in 2019 as a postdoctoral associate focused on large-scan X-ray fluorescence mapping and data processing.

Magdalena Wróbel-Szypula

Magdalena Wróbel-Szypula works in the Department of Conservation laboratory of the National Museum in Warsaw. She specializes in the analysis of organic compounds present in historical artifacts using FTIR spectroscopy. She obtained her PhD in physical chemistry from the University of Leeds and an MSc in chemistry, with specialization in analytical chemistry, from the University of Silesia in Katowice.

Acknowledgments

Marie Svoboda
Caroline R. Cartwright

The APPEAR project has grown significantly since its formation in 2013: today it represents sixty-three institutions, bringing together scholars with diverse areas of expertise for the collaborative research, analyses, and exploration of ancient funerary paintings. This cooperative venture to develop a collective data platform has involved considerable international communication and meetings, two conferences, two publications, and many journal articles. None of this would have been possible without the generosity, insight, and guidance of many people. We are grateful to the J. Paul Getty Trust, and to those who have supported the project over the past twelve years, especially Timothy Potts, Robin Weissberger, and Richard Rand, as well as former Getty President and CEO James Cuno, who was instrumental in championing APPEAR from the outset.

The editors would not only like to thank the British Museum for their support over more than two decades but wish to recognize the invaluable participation of other collaborating institutions and their teams—they have provided the foundation for APPEAR and aided in its progress by enabling comparative surveys, open discussion, and inspiration to advance the study of ancient paintings. In supporting the project's mission by making visible and analytical data accessible, these institutions have helped build a rich platform for collective growth and study. As a result, APPEAR has encouraged research, enabled discoveries, and provided a deeper connection to the ancient world by improving our understanding of materials and technology within Roman Egypt and beyond. Volumes 1 and 2 of *Mummy Portraits of Roman Egypt: Emerging Research from the APPEAR Project* are a testament to this significant research.

Any dedicated, multifaceted scholarly work requires a team of committed, knowledgeable individuals. Within the Getty we acknowledge the many people who have contributed to the success of APPEAR, particularly Brenda Podemski, Alexandra Bancroft, Neal Johnson, Wesley Walker, Jennifer Tanglao, Matthew Hrudka, David Newbury, Tina Priestley, and Susanne Gänsicke. We also want to express gratitude to all the dedicated participants included in this volume, our over 200 APPEAR members, and the supportive colleagues at the Allard Pierson Museum who made the 2022 conference possible: Ben van den Bercken, Els van der Plas, Rogier Rompen,

and Pètra Huijgen. We thank the APPEAR steering committee and Caroline Roberts, Yosi Pozeilov, Karen Trentelman, Joy Mazurek, Daniel Kirby, Ben van den Bercken, and Lisa Bruno. Most especially, we are grateful to Julie Unruh, who developed and carefully maintains the online Tableau visualization that statistically summarizes the APPEAR database. This new and improved database would not have been possible without the expert team at Ace Workflow, specifically Garrett Houghton, Tim Rodgers, and Andy Wood.

The editors would also like to acknowledge the tremendous work put into the production of this digital publication. We express gratitude to the many people in Getty Publications who brought this book to fruition: Greg Albers, Rachel Barth, Danielle Brink, Nola Butler, Jeffrey Cohen, Clare Davis, Michelle Woo Deemer, Erin Dunigan, Victoria Gallina, Alex Hallenbeck, Kara Kirk, Elizabeth S. G. Nicholson, Jenny Park, and Leslie Rollins. We thank Katrina Posner, Amanda Sparrow, Courtney Johnson Thomas, Leslie Tilley, and Anne Canright for their meticulous editorial work and guidance. Additionally, we are grateful to the peer reviewers for their contributions and thoughtful assessments. We hope projects like APPEAR continue to fuel a passion for ancient materials, object biographies, and technology; a curiosity to explore; and collaboration that will enhance and open the possibility for more artistic connections and discoveries.